OE 4651
Volume I

Handbook of Bottom Founded Offshore Structures

by

Prof dr. ir. J.H. Vugt

HANDBOOK OF BOTTOM FOUNDED OFFSHORE STRUCTURES

GLOBAL CONTENTS

1 GENERAL INTRODUCTION

2 A CLASSIFICATION OF OFFSHORE STRUCTURES

3 MODELS AND MODELLING

4 THE OFFSHORE ENVIRONMENT AND ENVIRONMENTAL LOADING

5 DESIGN

6 FIXED STEEL SPACE FRAME STRUCTURES – QUASI-STATIC BEHAVIOUR

7 FIXED STEEL SPACE FRAME STRUCTURES – MEMBER AND JOINT DESIGN CHECKS

8 FIXED STEEL SPACE FRAME STRUCTURES - FATIGUE

9 THE DYNAMICS OF STRUCTURES

10 RESPONSE ANALYSIS IN RANDOM SEAS / NOT AVAILABLE (YET)

11 FABRICATION, TRANSPORTATION AND INSTALLATION OF STEEL SPACE FRAME STRUCTURES / NOT AVAILABLE (YET)

12 INSPECTION, MAINTENANCE AND REPAIR / NOT AVAILABLE (YET)

13 DECOMMISSIONING

14 SELF-ELEVATING PLATFORMS OR JACK-UPS

15 COMPLIANT STRUCTURES

APPENDIX A NOTATIONS

1 GENERAL INTRODUCTION 1-1

1.1 INTRODUCTORY REMARKS 1-1
1.2 OFFSHORE TECHNOLOGY 1-3
1.3 INTERACTIONS WITH OTHER ENGINEERING FIELDS 1-6
  1.3.1 Civil engineering and naval architecture/shipbuilding 1-6
  1.3.2 Mechanical engineering 1-6
  1.3.3 Petroleum engineering 1-7
  1.3.4 Relationships with other disciplines and engineering fields in general 1-8
1.4 TYPICAL OFFSHORE CONTRIBUTIONS TO TECHNOLOGY DEVELOPMENT 1-11
1.5 SPECIAL FEATURES OF OFFSHORE STRUCTURES 1-13
  1.5.1 The offshore environment 1-13
  1.5.2 Stages in the life cycle 1-13
  1.5.3 Safety 1-16
1.6 REFERENCES 1-20
1.7 BIBLIOGRAPHY 1-21

2 A CLASSIFICATION OF OFFSHORE STRUCTURES 2-1

2.1 MAIN CLASSIFICATION 2-1
2.2 CLASSIFICATION OF SUPPORT STRUCTURES 2-3
2.3 THE WORLDWIDE POPULATION OF OFFSHORE STRUCTURES 2-13

3 MODELS AND MODELLING 3-1

3.1 INTRODUCTION 3-1
3.2 MODELLING 3-4
3.3 MAIN MODEL CHARACTERISTICS 3-11
3.4 REFERENCES 3-14
ANNEX A – A GENERIC APPROACH TO THE SOLUTION OF A PROBLEM 3-15
ANNEX B – A FEW WORDS ON MECHANICS 3-17
  B.1 Definition and classification 3-17
  B.2 Mechanics of solids 3-18
  B.3 Mechanics of fluids 3-20
  B.4 Mechanics of Soils 3-22
ANNEX C – USE OF MODELS IN PRACTICAL APPLICATIONS 3-23

4 THE OFFSHORE ENVIRONMENT AND ENVIRONMENTAL LOADING 4-1

4.1 A GENERAL DISCUSSION OF THE OFFSHORE ENVIRONMENT 4-1
4.2 WIND MODEL 4-4
4.3 CURRENT MODEL 4-8
4.4 WAVE MODELS 4-10
4.4.1 General introduction 4-10
4.4.2 Periodic wave models 4-12
4.4.3 Random wave model 4-15
4.4.4 Comparison of the main features of both wave models 4-18
4.4.5 Wave spectra 4-18
4.4.6 Waves in the presence of a current or a ship at forward speed 4-29
4.5 AERO- AND HYDRODYNAMIC LOAD MODELS 4-37
4.5.1 General 4-37
4.5.2 Steady flow conditions 4-37
4.5.3 Unsteady flow conditions 4-38
4.5.4 Arbitrary flow conditions 4-41
4.5.5 Classification of wave load calculation methods 4-44
4.6 HYDRODYNAMIC LOADS ON SLENDER MEMBERS 4-46
4.6.1 General discussion 4-46
4.6.2 Hydrodynamic loads at a particular point 4-51
4.6.3 Correlation between loads at spatially separated points 4-54
4.6.4 Global loads on a structure 4-57
4.7 SPECIAL LOADS 4-66
4.8 REFERENCES 4-68
ANNEX A – AN ALTERNATIVE WIND MODEL 4-71
ANNEX B – AIRY WATER WAVE FORMULAE 4-73
B.1 General observations 4-73
B.2 Complex number notation 4-76
B.3 Summary of a consistent set of equations in the direction of wave propagation for all waterdepths 4-77
B.4 Summary of a consistent set of equations in the direction of wave propagation for deep water 4-79
ANNEX C – SUMMARY OF MAIN CONCLUSIONS FROM THE LABORATORY MEASUREMENTS PERFORMED FOR THE NETHERLANDS MARINE TECHNICAL RESEARCH PROGRAMME (MATS, [4.4-11]) 4-80
ANNEX D – GUIDANCE FOR MODELLING A STRUCTURE AS AN EQUIVALENT VERTICAL STICK 4-81
D.1 Introduction 4-81
D.2 Vertical members 4-83
D.3 Members in a vertical plane perpendicular to the wave direction 4-86
D.4 Members in a vertical plane parallel to the wave direction 4-89
D.5 Members in a horizontal plane 4-91
D.6 Arbitrarily inclined members 4-93
D.7 Waves and current 4-95
D.8 Variable submergence of members around the still water line 4-95
D.9 The influence of marine growth 4-95
D.10 Complete stick model 4-97

5 DESIGN 5-1
5.1 A FEW WORDS ON DESIGN IN GENERAL 5-1
5.2 DIFFERENCES BETWEEN STRUCTURES ON LAND AND AT SEA 5-1
5.2.1 General aspects 5-1
5.2.2 Main technical differences 5-1
5.2.3 Cost differences 5-6
5.3 CONCEPTUAL DESIGN 5-7
5.3.1 Historical overview 5-7
5.3.2 General design considerations for bottom founded structures 5-7
5.3.3 Design of the superstructure 5-12
5.3.4 Design of the foundation 5-14
5.3.5 Design of the substructure 5-30
5.3.6 Design for fabrication, transportation and installation 5-38
5.4 PRELIMINARY DESIGN OF THE SUPPORT STRUCTURE 5-39
5.5 DESIGN LOADS AND DESIGN SITUATIONS 5-45
5.6 ALLOWABLE STRESS AND PARTIAL FACTOR DESIGN METHODS 5-48
5.7 MATERIALS 5-58
5.8 OFFSHORE STRUCTURES STANDARDS 5-58
5.9 REFERENCES 5-58
ANNEX A – JACKET PLATFORMS [5.3-1] 5-60
ANNEX B – FOUNDATIONS [5.3-1] 5-63
ANNEX C – DEFINITIONS OF FIXED STRUCTURE, JACKET AND TOWER STRUCTURES [5.3-7] 5-66
ANNEX D – SELECTION OF BAY HEIGHTS 5-67

6 FIXED STEEL SPACE FRAME STRUCTURES – QUASI-STATIC BEHAVIOUR 6-1

6.1 INTRODUCTION 6-1
6.2 A TWO-DIMENSIONAL IDEALISATION OF IN-PLACE STRUCTURAL BEHAVIOUR UNDER EXTREME STORM LOADING 6-4
6.3 MODELLING OF THE APPLIED LOADS. 6-8
6.3.1 General.......... 6-8
6.3.2 Permanent and variable superstructure loads 6-8
6.3.3 Wind loads on the superstructure.......... 6-12
6.3.4 Hydrodynamic loading on the frame.......... 6-13
6.3.5 More general modelling of hydrodynamic loads.......... 6-18
6.3.6 Permanent and variable substructure loads.......... 6-18
6.3.7 Total applied loading in extreme storm conditions 6-21
6.4 THE SUPPORT REACTIONS FOR THE FRAME.......... 6-26
6.4.1 Introduction.......... 6-26
6.4.2 Reactions at the sea floor 6-26
6.4.3 Reactions at the sea floor for vertical chord members and vertical piles 6-35
6.4.4 Reactions at the sea floor due to hydrodynamic loads only 6-36
6.4.5 Some notes on shear take-out.......... 6-37
6.5 SUPPORT REACTIONS FOR MULTIPLE PILE FOUNDATIONS 6-41
6.5.1 General conditions 6-41
6.5.2 Two-dimensional frame supported by multiple piles.......... 6-41
6.5.3 Three-dimensional structure supported by multiple piles 6-48
6.5.4 Equivalence of the procedures in sections 6.4 and 6.5 6-53
6.6 A MODEL FOR THE PILE SUPPORT OF THE FRAME AT THE SEA FLOOR.......... 6-54
6.6.1 Review of the assumptions made 6-54
6.6.2 Justification of equal pile forces at the top of the piles 6-54
6.6.3 Relationship between pile moments and lateral pile forces 6-58
6.7 THE INTERACTION BETWEEN FRAME AND PILES 6-64
6.7.1 General.......... 6-64
6.7.2 The tower.......... 6-64
6.7.3 The jacket 6-65
6.7.4 Hybrid structure types.......... 6-69
6.7.5 The internal forces and stresses in the piles.......... 6-70
6.8 MECHANICAL MODELS FOR FRAME BEHAVIOUR 6-71
6.8.1 General.......... 6-71
6.8.2 A mechanical model for the tower.......... 6-71
6.8.3 A mechanical model for the jacket 6-74
6.9 DEFORMATIONS OF STEEL SPACE FRAME STRUCTURES 6-78
6.10 FRAME LOADING AND SECTIONAL FORCES OVER THE HEIGHT OF THE FRAME 6-79
6.11 THE INTERNAL FORCES IN THE MEMBERS OF THE FRAME 6-90
6.11.1 General.......... 6-90
6.11.2 Individual leg and brace forces for diagonal bracing due to horizontal loading by the environment.......... 6-93
6.11.3 Individual leg and brace forces for other bracing patterns due to horizontal loading by the environment.......... 6-97
6.11.4 Further consideration of leg forces over the height of a frame due to horizontal loading by the environment.......... 6-100
6.11.5 Real and apparent differences between a tower and a jacket frame 6-102
6.11.6 Individual leg and brace forces due to vertical loading.......... 6-106
6.11.7 Total individual leg and brace loads.......... 6-108
6.12 EXAMPLES OF COMPUTER CALCULATIONS 6-109
6.13 REFERENCES.......... 6-111
ANNEX A – GRAPHICAL DETERMINATION OF AXIAL AND LATERAL PILE REACTION FORCES 6-112
ANNEX B – EXAMPLE ONE: A SMALL STRUCTURE FOR THE CENTRAL NORTH SEA IN 70 M WATERDEPTH ... 6-116
ANNEX C – EXAMPLE TWO: A FRAME FROM A DEEP WATER TOWER STRUCTURE IN 750 M WATERDEPTH 6-129

1 GENERAL INTRODUCTION

1.1 Introductory remarks

This handbook deals with offshore structures and more particularly with those that are founded on the bottom of the sea. It intends to provide insight into the various aspects that control the behaviour of these structures and the interrelationships between these aspects. To put the subject into context, this general introduction first defines the term Offshore Technology, clarifies the relationship between Offshore Technology and other engineering disciplines, and highlights some features that are special for offshore structures. This is followed in chapter 2 by a general classification of offshore structures, of which the bottom founded variety is only one type.

Wherever possible the handbook considers structures irrespective of type, thus providing an introduction to offshore engineering in general including specific detail where useful and relevant. Where the discussion of a subject requires this it focuses on the bottom founded class and the steel space frame type in particular. Chapter 3 on ‘Models and modelling’ and Chapter 4 on ‘The offshore environment and environmental loading’ are essentially applicable to all offshore structures; only section 4.6 deals more specifically with the hydrodynamic loads on slender members that are typical of steel structures.

Chapter 5 presents an overview of offshore structure design. This includes a discussion of many general considerations, but is in the main aimed at fixed steel space frame structures with piled foundations. These after all represent more than 90 per cent of all offshore structures worldwide. Chapter 6 then treats the quasi-static behaviour of this specific type of structure. Member and joint design checks in chapter 7 and fatigue in chapter 8 are similarly more particularly concerned with fixed steel space frame structures. However, the treatment of dynamics in chapter 9 and response analysis in random seas in chapter 10 once more allows a more general discussion of these topics, largely irrespective of structure type. [1]

The first 10 chapters of this handbook therefore give a consistent and fairly comprehensive description of offshore structures engineering, including the design and analysis of steel space frame structures that have always been and still are the ‘workhorse’ of the offshore industry. These chapters are followed by chapter 11 on the fabrication, transportation and installation, and chapter 12 on the in-service management (inspection, maintenance and repair) of steel space frame structures. Treatment of the subject matter is concluded by a general discussion of decommissioning issues.

Finally, two special structure types that also belong to the bottom founded variety are discussed. Chapter 14 deals with self-elevating platforms or jack-ups. These are very interesting structures that are in fact counted under the temporary or mobile structures according to the classification presented in chapter 2. In elevated condition jack-ups resemble fixed steel space frame structures in many respects; however, it is especially the differences that make their discussion really interesting. Last but not least, chapter 15 presents an overview and discussion of the main issues associated with compliant towers.

---

[1] At the time of writing this (January 2001) several chapters have not yet been completed, while other ones are subject to further review and possible changes. When applicable this is indicated or will be clear form the text.

The co-ordinate systems and notations that are used throughout this handbook are summarised in Appendix A.

1.2 Offshore Technology

Offshore Technology, or Offshore Engineering as it is also called, is a relatively young branch of engineering; it dates from after the Second World War. Many people use the term rather casually and a definition is not easily found. Few users of the words will actually know with any degree of precision what they mean when talking about offshore technology; some would even contest altogether that it is a separate branch of engineering. These circumstances illustrate the importance of defining what we mean with offshore technology so that we all talk about the same things. In general terms it may be described as follows:

> "Offshore technology concerns the technology for stationary man-made structures *on*, *in* or *under* the sea, that are used for the exploitation of natural resources or the support of a public utility. It thus relates to 'hardware' in the widest sense of the word. The environment in which these man-made structures exist and the nature of the application for which they are used both have a profound impact on their design and operation."

The origin and principal applications of offshore technology until now are the exploration and production of oil and gas. These industrial activities, of course, include many other essential elements than structures, such as the processes (e.g. drilling of wells) and the equipment (e.g. oil treatment facilities) involved. These elements clearly have a profound impact on the associated man-made structures as well, but they are not considered to belong to offshore technology as defined in here.

Offshore technology is further increasingly used for applications or planned applications of man-made structures that are not associated with oil or gas. Examples are deep-sea research; the launching of space satellites; offshore wind energy; floating plants, airfields or cities; and energy derived from waves or from the thermal capacity of the oceans. Typical marine activities that are associated with ships sailing the seas, such as merchant shipping, fishing and naval vessels, are outside the scope of offshore technology.

A more precise definition than the general description given above is centred on the three words *technology***,** *applications* and *man-made structures***,** and features five distinctive characteristics. This definition reads as follows:

Offshore Technology concerns *technology*, i.e.

1. the systematic application of science and other organised knowledge for practical purposes [2],

where the *applications of the technology* are aimed at structures that are

2. situated at sea off the coast,

and are

3. centred at a more or less fixed location *on*, *in* or *under* the sea,

whereas the practical purposes concern *man-made structures (hardware)* that

---

[2] This definition of 'technology' is due to the American economist John Kenneth Galbraith; see Van Dale, 'Groot Woordenboek der Nederlandse Taal', 10th edition, 1976, part II.

4. by design and construction are strongly influenced by the environmental conditions at the intended location, while accepting the natural state of the environment at the location as given,

and that serve for

5. the exploitation of natural resources *on*, *in* or *under* the sea, or the support of a public utility.

As it is rather long-winded wording to keep referring to *man-made structures* [3] we will often use *structures* only for short, but it is important to recognise that this is used as a generic term. It refers to man-made structures of all types and not only to platforms that rise above the water. The above definition of offshore technology defines the applications and the practical purposes involved more precisely in order to distinguish this branch of engineering from such well-established fields as shipbuilding, shipping, fishing and coastal engineering. Except for the last named one, offshore technology distinguishes itself from these other marine fields in that it is always associated with structures that are in essence stationary, while activities like shipping, fishing and the navy are invariably concerned with structures that sail the sea. Several aspects of the technologies involved in the various applications will of course be closely related, but in other respects they will differ distinctly.

Offshore technology and coastal engineering both deal with stationary structures at a fixed location, but the waterdepth and distance to the coast are usually markedly different. However, the more pertinent key to distinguishing these two engineering fields lies in the purpose of the man-made structures involved and in the impact they have on the environment. Any structure placed in flowing water affects the flow, while conversely the flow affects the structure; these two aspects are inseparably linked. However, with a view to the intended applications in both engineering fields the two aspects are not necessarily equally important. In offshore technology the environment is accepted as given. Offshore technology is concerned with the impact of the environment on design, construction and operation of the structures, but not vice-versa. It uses knowledge of the environment, but there is no attempt to influence the natural environment as it exists. Coastal engineering, on the other hand, is specifically concerned with both the pre-existing ocean environment and the changes to the environment that are caused by the structure once in place; changes that are often deliberately intended. That is a characteristic difference between the two engineering fields.

A further distinction lies in the purpose of the structures. In coastal engineering man-made structures serve to protect the coast and the land that lies behind it, or to intentionally interfere with the natural situation for the benefit of e.g. transportation, industry or recreation. In offshore technology the structures are intended to assist in the search for and the production of natural resources at sea. Examples of such natural resources are oil and gas, but also wind energy *on* the sea, thermal energy *in* the sea and manganese nodules *under* the sea. The man-made structures may further serve to support a public utility. Examples of which are navigational aids for sea or air traffic, a floating airport, an offshore fish farm, an offshore waste incineration plant, a floating platform for the launching of satellites, a bridge across a wide and deep strait, etc.

---

[3] There is no real equivalent in Dutch for the English term man-made structures; the best translation is '*kunstwerken'*. In Van Dale's 'Groot Woordenboek der Nederlandse Taal', 10th edition, 1976, part I, a 'kunstwerk' is described as '*a product of human activity, for which other materials than just soil and sand have been used'*. Therefore dikes, dams and sand islands, that are entirely or predominantly made of soil and sand, are excluded from man-made structures in the present context.

The five features in the above definition are believed to be characteristic and exclusive. They truly distinguish offshore technology from other fields of engineering. Only when each and all of these five distinctive characteristics are met can we refer to offshore technology.

The hardware involved may concern a component, an entire installation or a complete system, while the material from which the hardware is made may be steel, concrete, timber or a synthetic material such as GRE (glass fibre reinforced epoxy). The definition further implies no restriction to the technical activities associated with the structures other than restrictions that may be due to the nature of their application and their purpose. Offshore technology therefore covers all aspects related to the design and construction of man-made structures at sea that fall under the definition.

Offshore technology excludes the subsurface, i.e. the ground below the sea floor. With the exception of the top layers of the sea floor that serve as the founding material for the structures, offshore technology relates to engineering activities above ground level, where ground level is the sea floor rather than the water surface. The subsurface proper is the domain of the geologist, the geophysicist and the petroleum engineer. Offshore technology also excludes the technology and the mechanical equipment for the industrial processes that are performed on a platform. There will clearly be many interfaces and overlaps with other engineering fields, and it is especially the interfaces that are always very important and possibly causes of concern. For offshore technology it is notably the interfaces with petroleum engineering and with mechanical engineering that matter; see also the next section.

1.3 Interactions with other engineering fields

1.3.1 Civil engineering and naval architecture/shipbuilding

The first offshore platforms for the oil industry were nothing else than little artificial islands on legs. They merely served to support the normal onshore exploration and production operations by keeping equipment and people above water at an offshore location. The operations were actually land-based operations performed over water. The separation between the offshore engineering activities and the oil business was virtually complete. In creating these platforms two groups of engineers played a key role: the civil engineers for the platform substructure (which resembles a building standing in water) and the naval architects/shipbuilders for the floating support vessels (transportation barges and floating work platforms) that were needed to enable working at sea. In this type of work there is a natural co-operation between these two groups of engineers, as is also apparent from e.g. the delta works along the Dutch coast.

Bottom founded and floating platforms have historically developed along rather different paths. Floating structures are a natural application and extension of shipbuilding practice. However, their subsequent *use* for oil industry applications (other than as support vessels) required the adaptation of oil industry operations (such as drilling) from a land-based activity to one performed from a moving platform. In other words, land based operations over water had to be converted into real water based operations. This integration of floating vessels with oil industry processes has only become possible through the active involvement of the oil industry itself. However, the marine *design* and *construction* of the floating platforms have largely remained the domain of the naval architect and shipbuilder.

Contrary to this, bottom founded structures at sea were a new development and from the very beginning the oil industry has far more closely been involved with these; not only with their use but also with their design and construction. This accorded best with the activities of the civil engineer with his background of building on land and along the coast. From the outset the civil engineer was therefore more closely involved with the development of bottom founded structures for the oil industry than any other type of engineer.

Civil engineering and naval architecture/shipbuilding have jointly shaped offshore technology. The engineers of these two fields have worked closely together; their interest and activity spheres overlapped and, of course, eventually influenced one another. Yet it has never come to a real integration of their technologies with the objective of educating a true offshore engineer. The interfaculty offshore engineering programme at Delft University of Technology is as far as known the first to pursue this.

1.3.2 Mechanical engineering

Besides the part played by civil engineers and naval architects/shipbuilders there have been substantial contributions to offshore technology from mechanical engineering. Without the active participation of mechanical engineers offshore technology and oil and gas field operations in general, as these exist today, would not have been possible. In this respect the offshore is not different from the onshore: in virtually all industrial activities mechanical engineering is omnipresent. The contributions from mechanical engineering to offshore technology are so plentiful and important that some further elaboration is warranted. The mechanical contributions may logically be grouped into three main parts, i.e. power generation, the thermal side and the truly mechanical side of mechanical engineering.

Power generation concerns equipment such as diesel engines, electric motors and gas turbines. Power generation is naturally accompanied by power distribution, which includes high and low voltage systems and three-phase currents. In this area mechanical engineers co-operate closely with electrical engineers.

The thermal side of mechanical engineering includes aspects of physical/chemical process technology for oil and gas production and the associated equipment. Examples are separation of oil, gas and water; removal of CO_2 and H_2S; drying/cooling/heating of product streams; pressure regulation and compression. The mechanical engineers share these tasks with physicists and chemical engineers.

The truly mechanical engineering side covers numerous and diverse aspects such as:
- drilling equipment items (including the storage and treatment of drilling mud and cement, pipe handling and storage);
- well heads, blow-out preventers (BOP's), control valves, down hole equipment as well as other drilling and production equipment;
- heating and ventilation systems;
- smoke and gas detectors, fire fighting and other safety equipment;
- jacking mechanisms for jack-up platforms;
- anchor winches and ballast systems for floating platforms;
- motion compensators and other equipment for drilling and production risers;
- constant tension winches, offshore cranes for fixed and floating platforms;
- subsea equipment (e.g. valves, swivels, connectors, hydraulic or electrical control systems);
- remotely operated vehicles (ROV's) for under water support services.

This is undoubtedly an incomplete but yet impressive list. However, these mechanical engineering contributions concern predominantly special applications and adaptations of existing equipment items that find more widespread use, although the adaptation may make them rather unconventional or of an unprecedented size. These items are indispensable, but do not characterise the offshore scene. The mechanical engineering contributions are, of course, also subject to the special circumstances and demands of offshore applications, such as the corrosive environment, limitations in space and weight, and the effect of vessel motions on the operation of equipment items on board. These essential contributions and the special considerations involved have not always received the attention of the offshore industry that they deserve. Active co-operation in a multi-disciplinary effort is again what is usually called for. However, the components and equipment items concerned are considered to remain to belong to the field of mechanical engineering, rather than being an integral part of offshore technology.

1.3.3 Petroleum engineering

It goes without saying that the historical relationship between the offshore and the oil industry also means a close relation with the subsurface engineers (geologists, geophysicists, petroleum engineers). The offshore engineer must therefore have a good understanding of what the activities associated with exploring and appraising a reservoir involve. However, as already stated in section 1.2, the subsurface domain remains excluded from his territory, except for the geotechnical issues related to the foundation of the structures.

1.3.4 Relationships with other disciplines and engineering fields in general

Offshore hardware and its applications require contributions from many individual disciplines from many different engineering fields. The terms ‘discipline’ and ‘engineering field’ are generally used rather loosely and not too well defined. However, there is a distinction in the broadness implied. A discipline may be seen as a relatively narrow branch of learning (e.g. mathematics, hydrodynamics, structural mechanics), while an engineering field is much broader and may be seen as an entire sphere of technical activities (e.g. chemical, civil or mechanical engineering). A discipline will therefore be a subset of an engineering field, which in its scope of activities will make use of several disciplines. Conversely, a particular discipline will tend to be used in markedly different engineering fields. Further to the discussion in the preceding sections, important contributions are also made, for example, by geology, geophysics, geodetic surveying, oceanography, hydrodynamics, geotechnical engineering, materials and corrosion engineering, welding, electrical engineering, control theory, reliability and risk analysts, communications technology and so on and so forth.

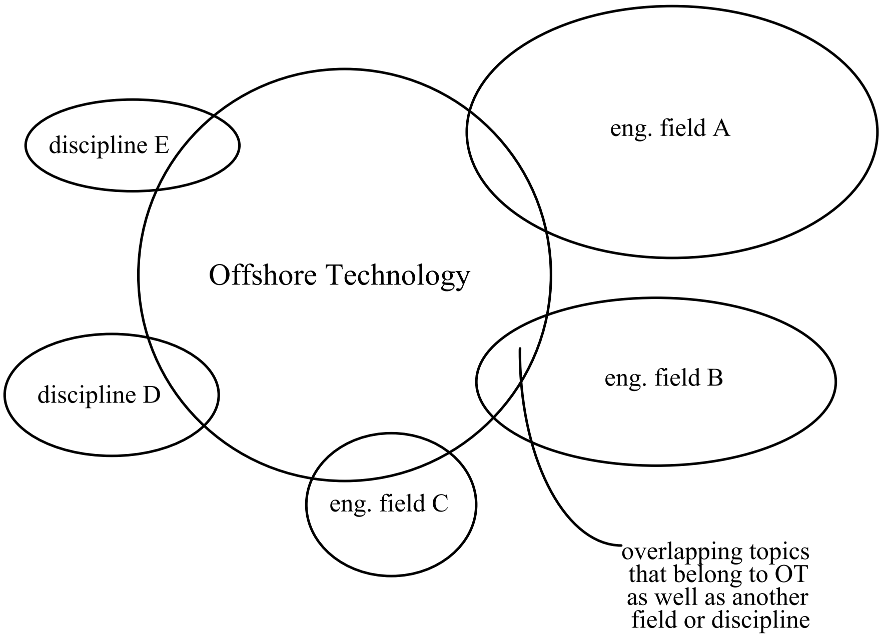

Figure 1.1. Illustration of the relationship between offshore technology and other disciplines or engineering fields

The situation can be depicted in a very general manner as schematically shown in figure 1.1. A picture like this relates in fact to any scientific or engineering field; there are always interactions and overlaps with neighbouring fields. It is entirely natural to use existing knowledge and experience from other areas wherever possible and relevant to one's own sphere of interest. Such knowledge and experience will frequently need to be customised to the particular circumstances and requirements of the problem under consideration. Furthermore, a particular offshore problem may require a different formulation of the problem and a different approach than traditionally followed, which may in turn lead to new developments in related fields.

It belongs to the domain of offshore technology to identify what the overlapping areas with neighbouring fields are, to incorporate these into offshore applications and to customise the knowledge and results involved. In some cases the customisation or further development for application to an offshore problem may be so extensive that the special application should preferably be seen to have become part of offshore technology. In other cases it simply remains a special application of knowledge from another discipline. There will obviously always be a wide range of gradual transitions and hence of the 'ownership' of the knowledge involved.

In a material sense, offshore technology for the man-made structures involved combines four major sub-areas. These are:

- the man-made structure proper,

that exists in an environment in which three domains can be distinguished:

- the atmosphere, that consists of the medium air, a gas,
- the sea, that consists of the medium water, a fluid,
- the ground or sea floor, that consists of the medium soil or rock, a solid material.

The boundaries and interactions between these sub-areas often require special attention, literally and figuratively, in which the multi-disciplinary nature of offshore technology clearly manifests itself. Furthermore, the expansion of offshore developments over the past 50 years has been so strong and the technical advancements so rapid that on many occasions unknown territory had to be explored and new ground had to be broken; see section 1.4 for a few examples. In all cases the essence of the matter is integration of diverse knowledge and experience and synthesis of various contributions into solutions for the particular offshore application under consideration. This is unquestionably a task of offshore technology itself. It includes promotion of research and development efforts in overlapping areas. The special *topics* involved in the overlaps with other disciplines or technical fields should therefore rightly be considered to belong to offshore technology. However, it would be presumptuous to claim that the *entire discipline or technical field* would be a part of offshore technology.

1.4 Typical offshore contributions to technology development

The technical developments in response to the requirements for offshore applications have been enormous. The necessity to find solutions for technical problems associated with offshore developments, combined with the financial and technical resources of the oil industry, have led to unprecedented deepening in certain areas. Examples are the knowledge of oceanography, wave loading, static and dynamic analysis of large structures, fatigue of steel and concrete. This expansion of knowledge has clearly had implications for the more traditional areas of application as well; these have of course equally benefited from the advancements. Furthermore, offshore developments required new areas to be opened up that were previously hardly of any practical significance. Examples of such developments are large tubular space frame structures, tubular joints, marine applications of very large concrete structures, behaviour of soils and foundations under continual cyclic loading, soil investigations in deep water.

In respect of the exploitation of hydrocarbons we can further point at the need to drill deviated or even horizontal wells from a restricted location at the surface, at the development of mobile drilling units, at drilling methods and equipment to enable drilling from floating vessels, and at the rapid development of three-dimensional seismic that started at sea. Similar developments have taken place with regard to mechanical equipment. The continual problems of weight and space limitations on offshore installations have promoted this equipment to be made lighter and more compact. Equipment also needed to be more reliable because maintenance and repair offshore are very difficult and costly. Furthermore, the safety of industrial processes in confined spaces needed to be assured. Logistic difficulties and the very high costs of working offshore have led the way to doing as much prefabrication onshore as possible. This in turn resulted in the appearance of very large floating cranes and heavy lift vessels for offshore use, far exceeding the capacity of cranes on land.

Against this background of a considerable extension in depth and breadth of knowledge, and especially the integration and synthesis of radically different traditional fields of engineering, we may safely conclude that offshore technology has developed into a distinctly separate engineering field of its own. It is not only strongly multidisciplinary, it even transgresses the traditional boundaries of a number of firmly established engineering fields. Civil engineering and naval architecture/shipbuilding have shaped offshore technology, while its relationships with the mechanical and petroleum engineering fields are historical and deep-rooted. These last two fields contribute significantly to the functional requirements and often provide, literally, the boundary conditions for the man-made structures that are at the very heart of offshore technology. Therefore a good appreciation of these two engineering fields is an important requirement for an offshore engineer. When future uses of offshore technology may be focused on new applications, such as offshore wind energy, similar relationships will need to be developed with aerodynamicists and power system engineers.

main or driver activities in offshore engineering	Planning	Design	Fabrication	Transportation	Installation	Management during operation	Abandonment
	identification feasibility study basis of design design specs. selection of concept execution strategy	preliminary design global design detailed design	procurement construction	load-out offshore tow	launching upending setting on bottom founding lifting	monitoring inspection maintenance repair	
stages in an offshore project	Identification phase and definition phase	Execution phase				Operational phase	Planning Execution
parties involved	▪Public sector ▪Intended owner	▪Consultants ▪Contractors ▪Public sector ▪(Future) owners	▪Contractors			▪Owners ▪Users	▪Owners ▪Consultants ▪Contractors ▪Authorities

Figure 1.2. The generic main activities associated with man-made structures, the phases in which typical projects may be distinguished and the different parties that may be involved

1.5 Special features of offshore structures

1.5.1 The offshore environment

The offshore environment is alien and hostile to men. The nature of the environment and the difficult logistics result in special demands on offshore operations and on the design and construction of offshore structures. Typical differences between structures on land and at sea will be discussed in chapter 5. A further factor is that offshore structures are often of an unparalleled size, which naturally brings its own complexities.

By implication, offshore structures are during their entire life exposed to the vagaries of the ocean environment. In the majority of cases this includes exposure to waves, two typical properties of which are their time varying nature and their unpredictability, i.e. waves are dynamic and random or stochastic. Thus, the dynamic and stochastic aspects exemplify many problems associated with offshore structures.

1.5.2 Stages in the life cycle

Between the initial plans for and the eventual decommissioning of a structure there is a series of related but yet clearly different activities associated with their creation and upkeep. A useful classification distinguishes main or driver activities, sub- or execution activities and supporting activities. The main or driver activities are described below. Sub- or execution activities relate to tasks that need to be performed in executing a main activity. Supporting activities are e.g. data collection, data management, computing, drafting, procurement, etc.

The main activities can be divided into logical and consecutive steps in the life cycle of the hardware. In different fields of engineering the grouping and the terminology may differ but these differences are essentially variations of the same generic classification. It is further noteworthy that there are generally different parties involved in the various main activities.

In offshore engineering it is common to distinguish the following seven main activities which suit all types of structure (see figure 1.2):

- **P**: **planning**
- **D**: **design**
- **F**: (onshore) **fabrication**
- **T**: **transportation**
- **I:** (offshore) **installation**
- **O**: management during **operation** (e.g. structural maintenance, modifications, repair)
- **A**: **abandonment** (nowadays usually more correctly referred to as decommissioning).

Fabrication, transportation and installation may be collectively identified as construction or (project) execution. However, the distinction in 3 separate activities for the man-made structures that are of interest here reflects the special circumstances of offshore application. Fabrication now refers to the onshore phase of the construction process, which is followed by transportation of the whole structure or of very substantial pre-fabricated parts from the onshore fabrication site to the offshore location, where the structure is subsequently installed.

Figure 1.2 gives a broad overview of the main activities related to this generic classification. It also indicates the stages in which the overall process may be divided for a typical offshore project. It further illustrates the different parties that are normally involved in the example cases. The generic breakdown in main activities and the terminology for describing them introduced above will be adopted in further discussions throughout this handbook.

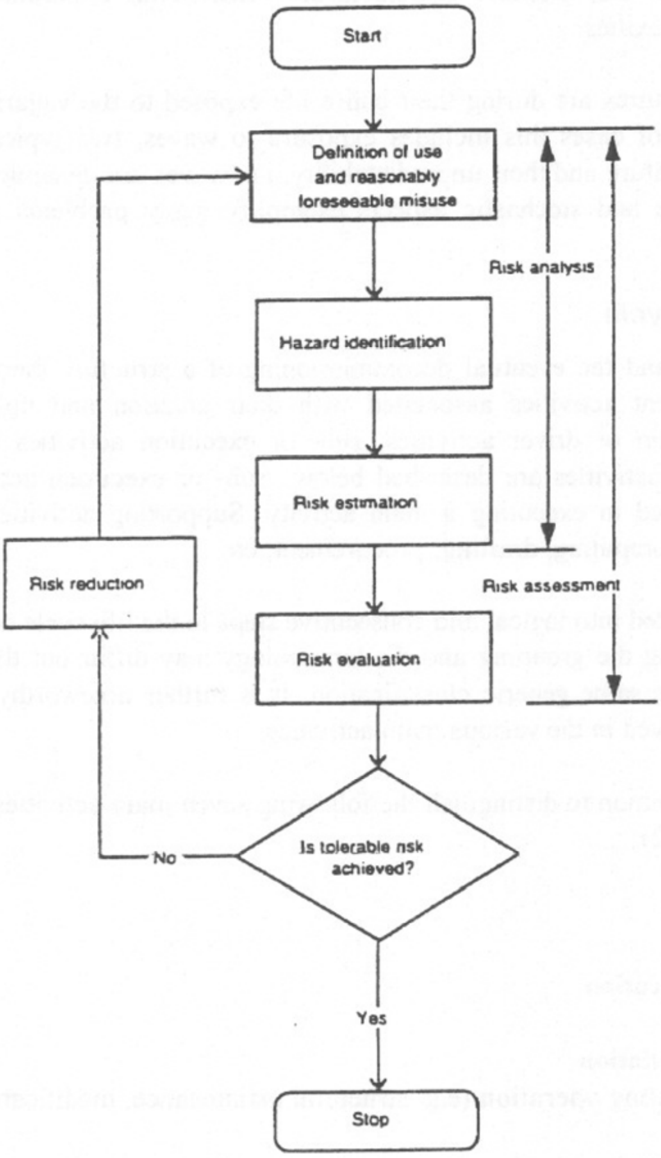

Figure 1.3. The iterative process of risk assessment and risk reduction (from [1.1])

1.5.3 Safety

Safety is a vitally important consideration in all activities undertaken by people. In the offshore environment it only deserves extra attention due to the difficulties associated with heavy industrial processes in confined spaces, the problems of escaping from the danger area if an incident occurs, the hostile environment and the difficult logistics. Safety is not limited to a consideration of the risks that are inherent in a particular design or the risks that are involved with a particular operation. It is an all-embracing concept that needs to include all aspects that are somehow related to the entire system under consideration. Safety is invariably aimed at three objectives, in the order as they are given below:

(1) protection of the people directly or indirectly involved;
an example of the first group of people is personnel on board the platform, while examples of the second group are those living or working in the neighbourhood (e.g. on adjacent platforms) or those associated with the transportation of goods and people to the platform;
(2) protection of the environment against pollution of air, water or soil;
(3) protection of the assets and the flow of products these assets deliver.

Safety is a very common word; however, in the context of industrial activities it is a term with a specific meaning. *Safety* is often defined as “freedom from unacceptable risk”, see ref. [1.1]. This definition highlights, and correctly so, that safety is always a relative concept; there is no such thing as complete freedom from risk. *Risk* is another term with a specific meaning that is defined in the same document as “combination of the probability of occurrence of harm and the severity of that harm”. It is, in other words, the product of the probability of an incident to occur and the consequences that result from that incident when it happens. A risk may be expressed in any unit that is appropriate for the situation under consideration, e.g. days of unavailability of a product, fatal injuries, or monetary loss. However, when many different types of risk must be combined and subsequently compared with the resources that are required to reduce the risk, there is often little alternative to using money as the common denominator for expressing both costs and benefits; this implies a necessity to attach a value to human life. *Tolerable risk* is further defined as “risk which is accepted in a given context based on the current values of society”, while *residual risk* is “risk remaining after protective measures have been taken.” Figure 1.3, which is figure 1 from ref [1.1], illustrates the iterative process of risk assessment and risk reduction. Other relevant and useful terms described in this document are:

- harm: physical injury or damage to the health op people, or damage to the environment or property;
- hazard: potential source of harm;
- risk analysis: use of available information to identify hazards and to estimate the risk;
- risk evaluation: judgement, on the basis of risk analysis, of whether a tolerable risk has been achieved;
- risk assessment: overall process of risk analysis and risk evaluation.

Over the years the study of safety and how to improve safety has become a specialist field on its own. This has resulted in a variety of techniques and analysis procedures to investigate safety, to ensure that hazards are identified, to quantify the risks involved and to implement measures to control risks. Formal Safety Assessment or FSA is actively promoted where necessary and possible. FSA is a complex process in which 5 steps may be distinguished:

- hazard identification
- estimation of the risks involved
- study of options to control the risks
- assessment of costs and benefits that are associated with these options
- making decisions by weighing the costs against the benefits of risk reduction measures.

This breakdown in 5 steps is entirely similar to the process of figure 1.3, where the last three steps above are covered by the box of risk evaluation. The FSA methodology is normally carried out by a team of experts and unavoidably involves subjective judgements. As already noted, it is a complex process that is not really suitable for routine assessments. Its main application will therefore be limited to major projects and to the development of general rules for inclusion in design or operational guidelines.

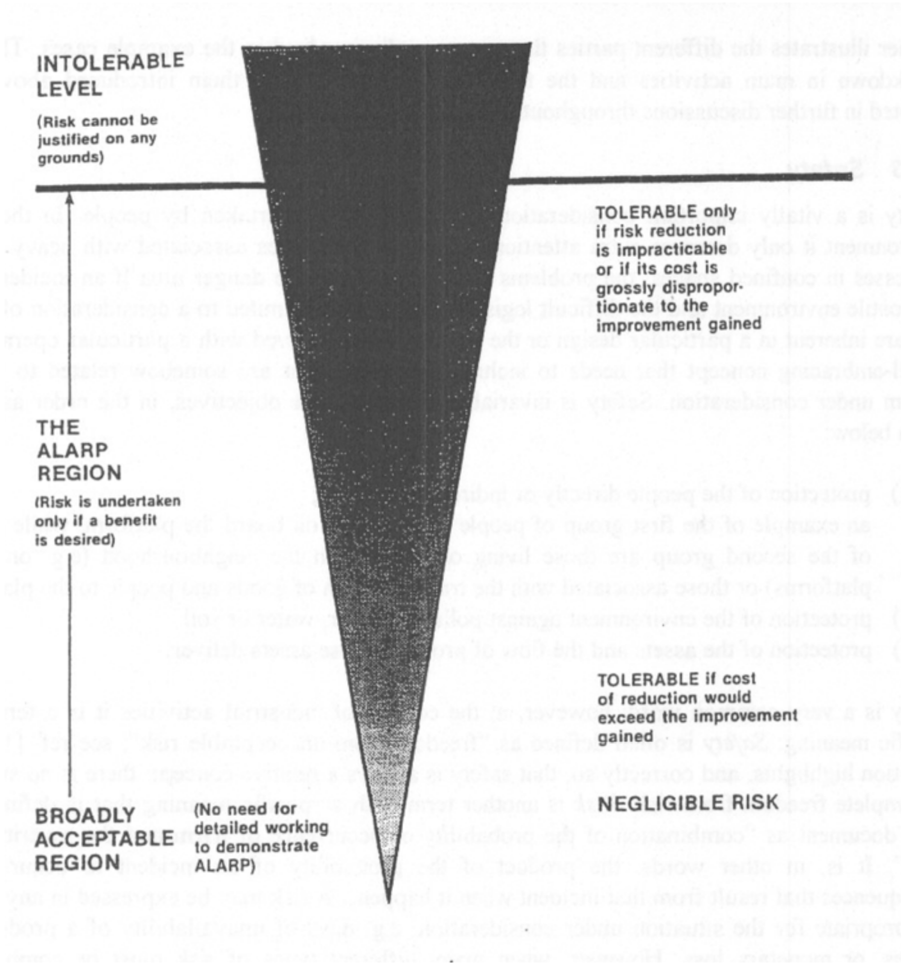
INTOLERABLE LEVEL
(Risk cannot be justified on any grounds)
TOLERABLE only if risk reduction is impracticable or if its cost is grossly disproportionate to the improvement gained
THE ALARP REGION
(Risk is undertaken only if a benefit is desired)
TOLERABLE if cost of reduction would exceed the improvement gained
NEGLIGIBLE RISK
BROADLY ACCEPTABLE REGION
(No need for detailed working to demonstrate ALARP)

Figure 1.4. Levels of risk and ALARP (from [1.2])

Levels of fatal risk
(average figures, approximated)

per annum	per annum	
1 in 1000	10^{-3}	Risk of death in high risk groups within relatively risky industries such as mining
1 in 10 000	10^{-4}	General risk of death in a traffic accident
1 in 100 000	10^{-5}	Risk of death in an accident at work in the very safest parts of industry
1 in 1 million	10^{-6}	General risk of death in a fire or explosion from gas at home
1 in 10 million	10^{-7}	Risk of death by lightning

Table 1.1. General levels of risk, which individuals appear to accept for personal benefit or which they appear to regard as negligible (from [1.2])

Setting criteria to judge risks is a difficult task, especially when potential injury to people is involved. Such judgements are not universal either; they are culturally and time dependent, as is clearly indicated by the definition of tolerable risk on the previous page. A concept proposed by the Health and Safety Executive in the United Kingdom for the setting of criteria for the safety of workers has been found to be very useful and is widely accepted [1.2]. It divides risk levels into three bands, see figure 1.4. The top band includes risks that are intolerable under any circumstance. The lowest band includes risks that are negligible, so that no further precautions are deemed necessary. The middle band represents risks that may be acceptable if the benefits that flow from it are large enough. This is the range where risks must be managed and risk reduction measures should be taken to make the risk 'As Low As Reasonably Practicable', bearing the benefits in mind and accounting for the costs associated with any further reduction of the risk. This so-called ALARP principle is a sensible and powerful concept. The difficulty lies, of course, in attaching numbers to the boundaries of the bands. Suggested numbers that have been discussed extensively, and that indeed appear reasonable to many people as well as many authorities, are a risk with a frequency of fatal injury (death) to an individual worker of 1 in 1.000 per annum as the upper limit and of 1 in 1 000 000 per annum as the lower limit of the ALARP region. Table 1.1 may serve as general guidance and reference to set these risk levels in context.

Looking at these risk levels in relation to the frequency with which structures fail (collapse) we can say the following. The first offshore structure was installed in 1947 and there are now (1998) of the order of 7 000 structures worldwide; nearly all of these are fixed steel structures; see chapter 2, section 2.3. The total exposure of the population of structures is approximately 100 000 unit-years. If we interpret the per annum risk levels of table 1.1 in terms of the average frequency of failure of a structure per unit-years of exposure, the level of 10^{-3} would mean that 100 structures should have failed in these 50 years; similarly the level of 10^{-5} would mean that only one structure should have failed in the entire offshore history. Data for the Gulf of Mexico indicate that the number of platform failures in 1950 stood at 0.06 to 0.07 (approximately 6.5 times 10^{-2}) per unit-year of exposure [1.3]. In 1974 this had dropped to 0.003 per unit-year (3 times 10^{-3}). In connection with this it should be noted that platforms in the Gulf of Mexico are evacuated at the approach of a hurricane, so that there is no direct risk to people when the environmental design event occurs; this is in contrast with platforms in e.g. the North Sea where evacuation is not realistically possible and structures are thus permanently manned. More recent worldwide data [1.4] indicate that the frequency of failure for modern structures is between 1 in 10 000 and 1 in 100 000 per unit-year (between 10^{-4} and 10^{-5}). One may conclude from this that after an understandably somewhat difficult start the frequency of platform failure has decreased by a factor of 10 in the first 25 years of offshore history, to decrease by another factor of 50 over the second 25 years.

These desired low frequencies per annum and their 'validation' against actual experience should be treated with great caution. The experience base of some 100 000 unit-years is in actual fact too low to provide adequate statistical reliability for risk levels of the order of 10^{-5} per unit-year, even without considering that he population that we are dealing with is obviously far from homogeneous. Notwithstanding this, it will be clear that the failure risk of well-designed fixed steel structures is very low. This warrants a collective tribute to all concerned in the industry, in oil companies, consultants, contractors, classification societies, warranty surveyors and authorities alike.

1.6 References

1.1 ISO/IEC Guide 51, ***Safety aspects – Guidelines for their inclusion in standards;*** draft dated January 1998.

1.2 Health and Safety Executive, ***The tolerability of risk from nuclear power stations***; HSMO publiction, London, 1987; ISBN 0 11 883982 9.

1.3 Vugts, J.H. and Edwards, G., ***Offshore structural reliability assessment- from research to reality?***; Proceedings of the 6th international conference on the Behaviour of Offshore Structures (BOSS '92), London, 1992, volume 3 (Supplement).

1.4 Veritas Offshore Technology Services A/S, ***Worldwide Offshore Accident Data Bank (WOAD)***; statistical report, Det norske Veritas, Oslo, latest edition.

1.7 Bibliography

The general literature on offshore technology for educational purposes is very limited. Most of the written material publicly available has been published at technical conferences and is of a rather specialised nature. Books are rare, and most of those that exist are rather outdated. Specific references that are relevant to particular subjects are given in the chapters concerned. In this section a number of books and other publications are listed that cover a wider range than a single subject and may serve as background reading for those interested.

B.1 Veldman, H.E. and Lagers, G.H.G., ***50 Years Offshore***; Foundation for Offshore Studies, Delft, 1997; distributed by Veldman Bureau voor Bedrijfsontwikkeling, Sittard; ISBN 90-803677-1-0.

B.2 Barltrop, N.D.P. and Adams, A.J., ***The dynamics of fixed marine structures***; Butterworth Heinemann Ltd., London, 3rd edition 1991; ISBN 0 7506 1046 8.

B.3 Clauss, G.; Lehmann. E. and Östergaard, C., ***Offshore Structures***;
Volume 1: Conceptual design and hydrodynamics, Springer Verlag, Berlin, 1992.
Volume 2: Strength and safety for structural design, Springer Verlag, Berlin, 1993.

B.4 Gerwick, B.C., ***Construction of offshore structures***; A Wiley - Interscience Publication in the Wiley series of Practical Construction Guides; John Wiley & Sons, 1986; ISBN 0-471-29705-4.

B.5 Graff, W.J., ***Introduction to offshore structures - design, fabrication, installation***; Gulf Publishing Company, Houston, 1981; ISBN 0-87201-694-5. (rather old and mainly descriptive, but one of the few books of a general and introductory nature)

B.6 Visser, W., ***The structural design of offshore jackets***; Published by the Marine Technology Directorate Limited, London; publication 94/100, 1994; ISBN 1 870553 16 0.

B.7 Vugts, J.H., ***Bottom founded platforms: an overview***; Paper presented at the Deep Offshore Technology Conference, 16 October 1989, Marbella, Spain;
(the paper is not included in the conference proceedings, but was separately published in Oil Gas - European Magazine, international edition in the English language of Erdöl Erdgas Kohle, volume 15, no. 4, 1989, p. 16-24)

B.8 Veritas Offshore Technology Services A/S, ***Worldwide Offshore Accident Data Bank (WOAD)***; statistical report, Det norske Veritas, Oslo, latest edition.

B.9 ***Offshore standards*** from several organisations, such as:
the International Standards Organisation (ISO), the American Petroleum Institute (API), the classification societies (e.g. Lloyds Register of Shipping, Det Norske Veritas, Bureau Veritas (Paris), Germanischer Lloyd, American Bureau of Shipping).

2 A CLASSIFICATION OF OFFSHORE STRUCTURES

To facilitate discussion of man-made structures for offshore use and to put bottom founded structures in context we will in this chapter present a classification of offshore structures.

2.1 Main classification

Two major clusters of structures may be distinguished, i.e. permanent and temporary installations. *Permanent installations* are intended to stay on location for an extended period of time, usually many years. In the oil industry such structures are typically associated with the *production* of oil and gas. They are therefore to remain on station for the full economic life of a producing field. This can range from a few years to 50 years or more, but it is usually some 20 to 30 years. If the installation is to support a public utility the time scales involved are likely to be at least similar or even longer.

Temporary installations, on the other hand, are intended to *perform a specific task* during a *limited period of time*. In the oil industry temporary installations are typically associated with one of three activities: the search for offshore oil and gas reservoirs, i.e. exploration (e.g. seismic investigation or exploration drilling); offshore construction (e.g. offshore installation activities, the lifting of heavy loads, pipe laying); or providing support services (e.g. floating hotel accommodation, the transportation of personnel and material). These temporary installations move from one location to the next and perform a similar activity at each location during periods that typically range from days to several months. Because of their mobility these structures are also called *mobile units*.

Each of these two clusters may be divided further into a number of different groups, sub-groups and types as shown in figures 2.1 and 2.2. The groups and sub-groups relate logically to the technical disciplines (not to be confused with academic disciplines) into which the oil industry has historically developed and organised itself. By implication this reflects the way in which the engineering in many companies associated with the offshore industry is organised and in which business is done. It thus provides a practical division of the field in coherent technical sub-fields and a firm basis for dialogue and exchange of technology. The further distinction of (sub)groups into types relates to individual classes of structure that are distinguishable on the basis of function, geometry or some other major characteristic.

The sub-group ‘support structures’ under the ‘platforms’ group of the permanent installations (see figure 2.1) distinguishes five structure types. This distinction is based on a rational classification of the mechanisms by which the environmental loads are accommodated as will be discussed in section 2.2. A similar distinction into two types applies to the ‘platforms’ group of the temporary installations (figure 2.2).

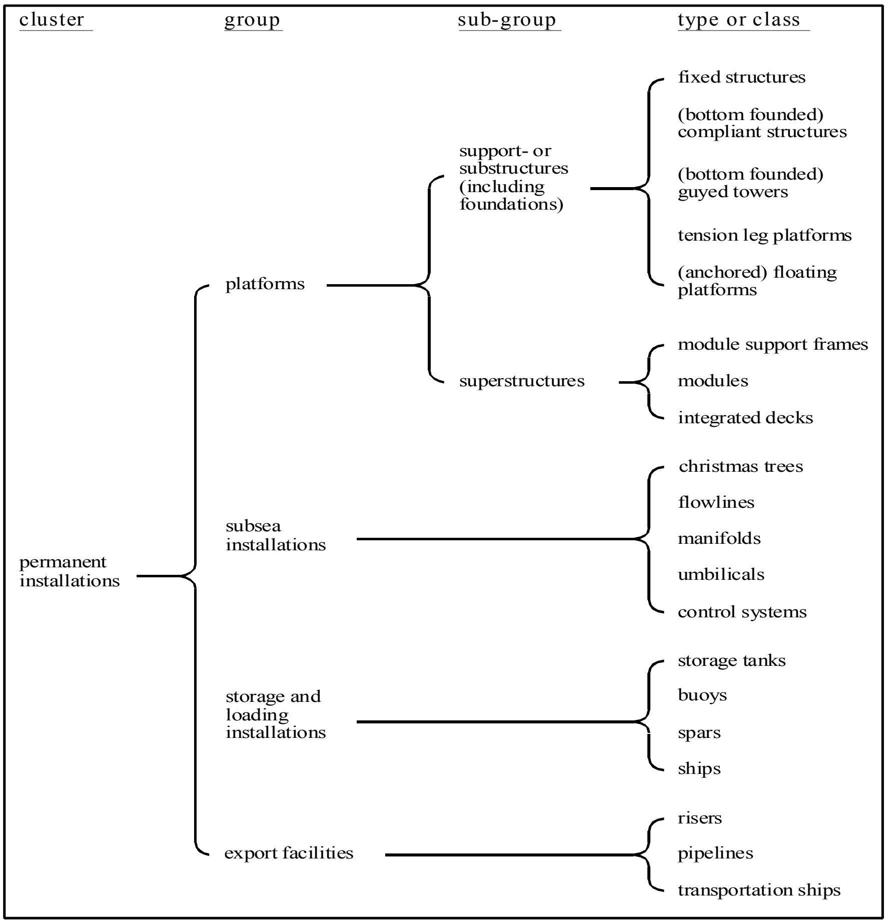

Figure 2.1. Cluster of permanent structures

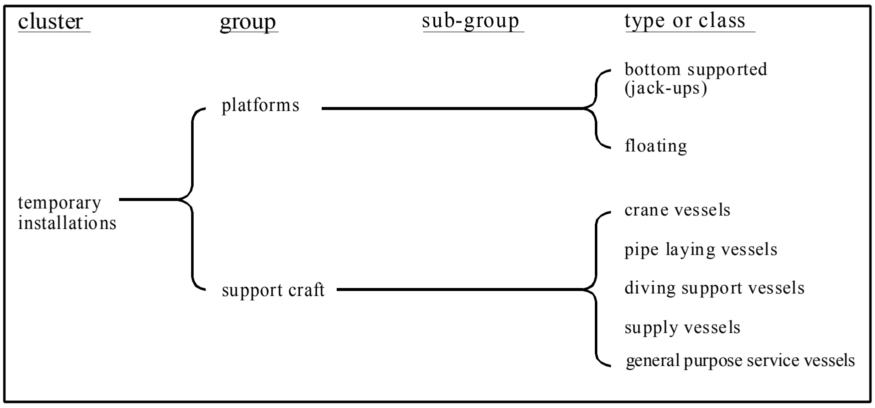

Figure 2.2. Cluster of temporary structures

2.2 Classification of support structures

Support- or substructures used for the exploration for or the production of oil and gas may be grouped into specific categories according to a number of distinguishing features. Without claiming completeness five possible distinctions are:

- their function
  (e.g. drilling, production, compression, flaring, accommodation platforms)
- their degree of permanency
  (e.g. permanent v. temporary or mobile structures)
  Note that instead of permanent the word fixed is also often used to indicate the opposite of mobile; however, the term fixed structure will get a specific meaning in the classification scheme that will be presented and should therefore be avoided as the counterpart of mobile.
- the material from which they are constructed
  (steel v. concrete structures)
- the type of foundation supporting them
  (deep and piled v. shallow and bearing foundations)
- the way in which the loads on the structures are accommodated
  (e.g. bottom supported v. floating structures).

Classifications of the first and the second type are closely related to the purpose that the structures are intended to serve. The second type combines this with aspects that have a major impact on their design. In the previous section we have chosen this very feature to distinguish two main clusters of man-made structures. Classifications of the third and fourth type are associated with the civil and marine engineering aspects of their design and construction.

Classification according to the fifth and final type of distinction is on the other hand based on the structural mechanics features of their behaviour in service. Categorisation on the basis of load carrying mechanisms is a very useful and robust one and is our preferred choice for the classification of substructures. The loads on offshore structures are very large and the way in which these loads are accommodated must therefore be a major distinguishing feature.

The other options to distinguish the various types can, of course, also be used whenever these are considered useful to highlight particular aspects for a particular purpose. Using these options will naturally result in different classification schemes that are, however, equally valid. It should further be recognised that, whatever scheme is chosen, distinctions will not always be pure. In several cases there will be combinations and overlaps of features. If this is the case, then the predominant feature should be used for the classification.

The loads on an offshore structure derive from its function, from its own weight including all the facilities and equipment that it carries, and from the environment. All loads are either vertical or horizontal (which is also called lateral), and they may be essentially constant (i.e. static) or they vary appreciably as a function of time (i.e. they are dynamic). In this regard, variations in time

TYPE OF SUPPORT / RESISTANCE	**TYPE OF LOAD**			
	STATIC		DYNAMIC	
	VERT.	HOR.	VERT.	HOR.
BUOYANCY		▨		▨
PARTLY BUOYANCY PARTLY SEABED		▨		▨
SEABED				
CABLES, OR SIMILAR CONSTRAINTS				
BALANCED BY INERTIAL FORCES	▨	▨		

Figure 2.3. Full matrix of possibilities to accommodate load types by support types

TYPE OF SUPPORT / RESISTANCE	**TYPE OF LOAD**			
	STATIC		DYNAMIC	
	VERT.	HOR.	VERT.	HOR.
BUOYANCY		▨		▨
PARTLY BUOYANCY PARTLY SEABED		▨		▨
SEABED				
CABLES, OR SIMILAR CONSTRAINTS				
BALANCED BY INERTIAL FORCES	▨	▨		

Figure 2.4. Matrix after excluding impossible combinations of load and support types

are usually measured with reference to the periods of the waves, which are between some 2-3 and some 25 seconds, because waves tend to be the predominant dynamic loading source on an offshore structure. The static vertical loads on the structure due to weights always act downwards, while buoyancy forces always act upwards.

In view of the definition of offshore technology, all structures are associated with an approximately fixed location. Therefore, they must be in a state of equilibrium. The equilibrium can be a static equilibrium or a dynamic equilibrium. In the case of static equilibrium all applied loads must be transmitted through the structure to "supports", where they are resisted by reaction forces through spring actions. In the case of dynamic equilibrium the applied loads can also be balanced by mass inertial forces, which are self-generated as a result of induced movements. The net effects of the applied loads and the mass inertial forces together (the resultant of which may either be larger or smaller than the applied loads) are then similarly resisted by the "supports", again through spring actions. Clearly, static loads will always need to be balanced by static reaction forces in a static equilibrium. Dynamic loads, on the other hand, may be balanced either by dynamic reaction forces at the supports, or by mass inertial forces, or by a combination of the two. The distribution between dynamic reaction and mass inertial forces depends on the dynamic characteristics of the structure and the effectiveness of the "supports". In practice, a combination of static and dynamic equilibrium is often found, e.g. depending on the frequency content of the environmental loads.

In the above, the term "supports" is used in a generic sense. For example, for a structure standing on the sea floor the foundation is an obvious support. However, in a very similar manner the surrounding water provides a buoyancy force equal to the weight of the displaced volume of water for both floating structures and structures standing on the sea floor. This is also a "support" in the generic sense of the word. Other supporting elements are e.g. cables or struts, which may be attached to the structure and thus provide a reactive force. Such elements are components of the total structural *system*, but they do not form an inherent part of the *structure itself*. The structure may be thought of as an organised assembly of connected elements that provide some measure of rigidity. These elements can normally not be separated without severely affecting the rigidity of the structure, up to the point that this is likely to damage or even destroy the original assembly. However, the removal of one or more supports will, of course, affect the equilibrium when external loads are present, but it will not damage or destroy the rigidity of the assembly of elements making up the structure proper.

All reaction forces to the applied loads must eventually, directly or indirectly, be transmitted via one or more of the supports to earth, which provides the only fixed point they can go to.

As the applied **static** *vertical* loads always act downwards they can only be supported by the sea floor or by buoyancy, or by a combination of the two. Cables or similar slender constraints in tension can additionally resist a resultant upward vertical force that may exist in some special cases. The applied static *lateral* loads can also be resisted by the sea floor; alternatively, lateral restraint can be provided by cables or similar slender elements acting in tension and anchoring the structure in a fixed average position relative to earth. There is one possible extension to these options. That is when thrusters, mounted on a floating platform, provide the counteractive force to keep the platform in position instead of cables. Although such a system is called 'dynamic positioning', the thrusters can only be expected to resist the (quasi-) static lateral loads. This is a result of both the magnitude of the dynamically applied loads and the time constant of the dynamic positioning system.

The applied **dynamic** loads arise from the environment, with waves being the predominant cause. They can act both horizontally and vertically, the latter perhaps being less commonly appreciated. The best examples of dynamic vertical loads are the heave excitation of floaters and the fluctuating vertical loads on the base (the caisson) of a concrete gravity structure. The variable vertical wave pressures on the top of the caisson also create a dynamic moment, which is an additional contribution to the overturning moment that is often wrongly associated with the existence of lateral loads on the vertical columns and the vertical sides of the caisson only. For steel structures the variable vertical wave pressures on horizontal members are much smaller but have in principle the same effect.

The dynamic loads can be resisted by the sea floor, by cables or by similar constraints to which the structure may be attached, or they may be balanced by inertial forces resulting from structure movements. These are the only three possibilities, and although strictly speaking combinations are usual, one of these three is invariably the most important mechanism.

In summary, there are 4 different types of loads and 5 different types of supports, together forming a matrix of 20 possible combinations; see figure 2.3. Not all these combinations are physically possible, however. For example, buoyancy always acts vertically and can therefore never accommodate horizontal loads. Similarly, inertial forces can never balance static loads. These boxes must therefore be excluded and are shaded in the matrix in figure 2.4.

Following these principles, figures 2.5 (a) and 2.5 (b) can be constructed. In this way five different types of structure are distinguished. These are:

- the fixed structure
- the compliant tower
- the guyed tower
- the tension leg platform (TLP)
- the (catenary) anchored floater (CAF or AF).

The first three of these are bottom founded, the last two are floating structures.

Using the principles underlying this classification system we can conclude the following. If all four load categories are transmitted to the sea floor the structure is a fixed platform. If inertial forces balance the dynamic *lateral* loads the platform is called compliant. However, the mechanisms that are associated with the dynamic *vertical* loads create different types. For instance, when these too are balanced by inertial forces due to vertical motions the platform is a floater (catenary anchored or dynamically positioned). On the other hand, when cables or tethers resist them, thus suppressing the tendency of the platform to move up and down, it is a tension leg platform (TLP). If the dynamic vertical loads are transmitted to the sea floor the structure is a bottom founded compliant platform.

Similarly, the basic distinction between a guyed tower and other bottom supported compliant towers is the way in which the *static horizontal* loads are accommodated. For the guyed tower these are mainly transmitted to the guylines, whereas for other types of compliant towers these are transmitted to the sea floor.

Inspection of figures 2.5 (a) and (b) will show all the differences between the five basic types of structure thus distinguished. One note of clarification concerning the static vertical loads should be added. Submerged members of all structures will experience buoyancy forces. Therefore, the static (downward) vertical forces will always be supported by a combination of buoyancy and the sea floor. This is true for fixed structures as well as for compliant and guyed towers. Fixed structures will mainly transmit the vertical loads to the sea floor. Compliant and guyed towers are invariably much more slender and will in many cases need greater buoyancy support. That is the reason that in figure 2.5 (a) (and the subsequent figures 2.6 (a), (b) and (c) to be discussed hereafter) the fixed structure is marked as transferring the static vertical loads to the sea floor while the compliant and guyed towers are shown to transfer the loads partly to buoyancy and partly to the sea floor. However, as explained, this is a soft rather than a hard distinction.

It is believed that this breakdown with respect to load carrying mechanisms is complete and that any proposed structure concept, now or in the future, will belong to one of the five types identified.

Projecting the appropriate combinations of load and load carrying mechanism onto the matrix scheme results in the figures 2.6 (a) to (e), one for each type of structure. Superimposing these five figures onto one schematic gives figure 2.7. This contains 4 empty boxes which, if filled, could potentially result in additional structure types. However, it is easily argued that this is very unlikely ever to occur. The reasoning goes as follows.

Flexible cables or similar slender constraints cannot take up (downward) static vertical loads.

In what manner the dynamic vertical loads are reacted will depend on the relative stiffnesses involved. Bottom founded structures will transmit these to the sea floor, because the structure and the foundation represent much stiffer springs than the surrounding water. A TLP will transmit them to the taut and vertical anchoring system for the same reason. The vertical motions of a more or less free floating structure (a CAF) will hardly be affected by the soft spring action of a catenary anchoring system and, therefore, the dynamic vertical loads will be entirely balanced by inertial forces.

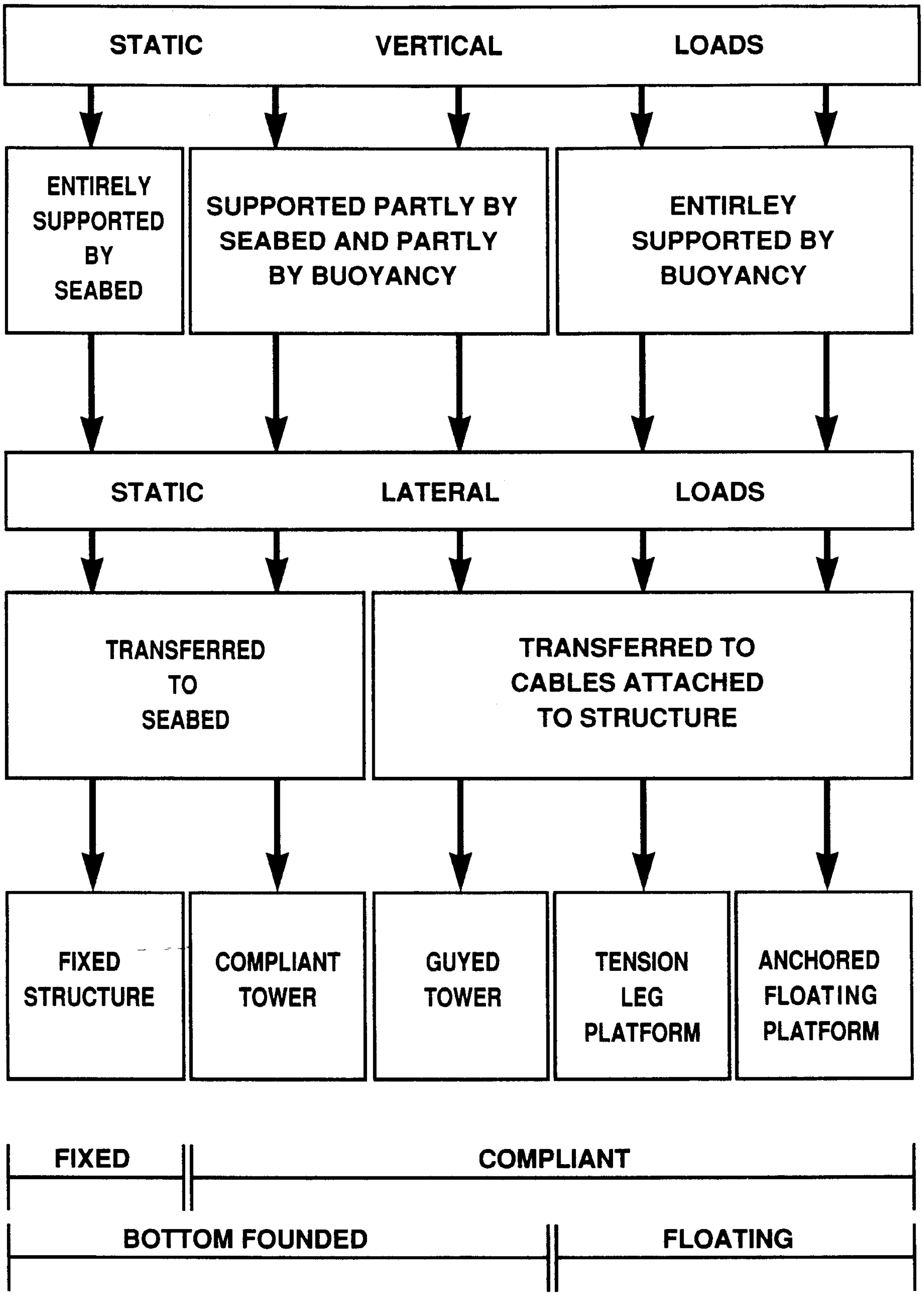
STATIC VERTICAL LOADS
ENTIRELY SUPPORTED BY SEABED
SUPPORTED PARTLY BY SEABED AND PARTLY BY BUOYANCY
ENTIRLEY SUPPORTED BY BUOYANCY
STATIC LATERAL LOADS
TRANSFERRED TO SEABED
TRANSFERRED TO CABLES ATTACHED TO STRUCTURE
FIXED STRUCTURE
COMPLIANT TOWER
GUYED TOWER
TENSION LEG PLATFORM
ANCHORED FLOATING PLATFORM
FIXED
COMPLIANT
BOTTOM FOUNDED
FLOATING

Figure 2.5(a). Classification of offshore structures by load transfer of static loads

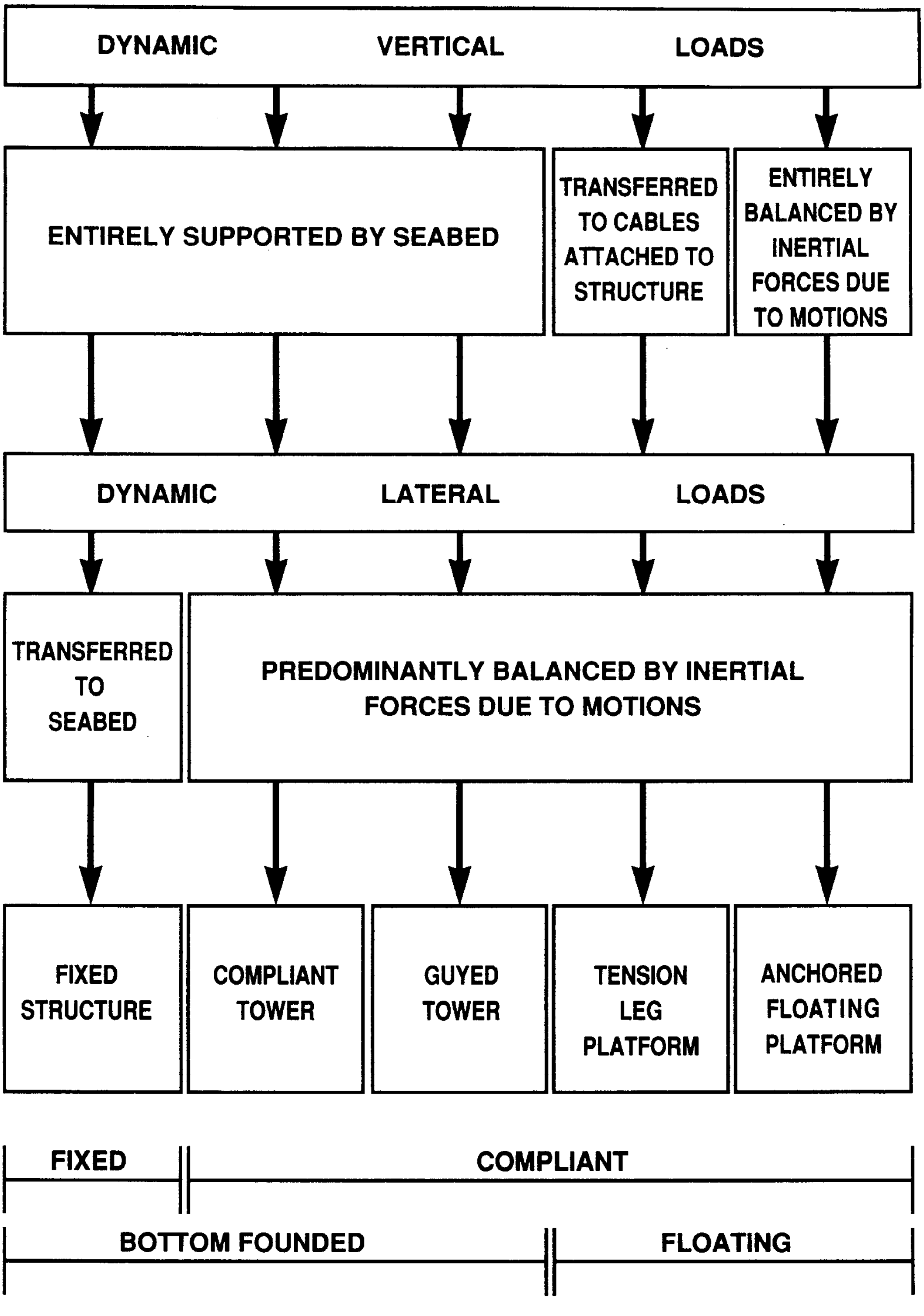
DYNAMIC VERTICAL LOADS
ENTIRELY SUPPORTED BY SEABED
TRANSFERRED TO CABLES ATTACHED TO STRUCTURE
ENTIRELY BALANCED BY INERTIAL FORCES DUE TO MOTIONS
DYNAMIC LATERAL LOADS
TRANSFERRED TO SEABED
PREDOMINANTLY BALANCED BY INERTIAL FORCES DUE TO MOTIONS
FIXED STRUCTURE
COMPLIANT TOWER
GUYED TOWER
TENSION LEG PLATFORM
ANCHORED FLOATING PLATFORM
FIXED
COMPLIANT
BOTTOM FOUNDED
FLOATING

Figure 2.5(b). Classification of offshore structures by load transfer of dynamic loads

TYPE OF SUPPORT/ RESISTANCE	TYPE OF LOAD			
	STATIC		DYNAMIC	
	VERT.	HOR.	VERT.	HOR.
BUOYANCY		■		■
PARTLY BUOYANCY PARTLY SEABED		■		■
SEABED	FS	FS	FS	FS
CABLES OR SIMILAR CONSTRAINTS				
BALANCED BY INERTIAL FORCES	■	■		

Figure 2.6 (a). Fixed Structures

TYPE OF SUPPORT/ RESISTANCE	TYPE OF LOAD			
	STATIC		DYNAMIC	
	VERT.	HOR.	VERT.	HOR.
BUOYANCY		■		■
PARTLY BUOYANCY PARTLY SEABED	CT	■		■
SEABED		CT	CT	
CABLES OR SIMILAR CONSTRAINTS				
BALANCED BY INERTIAL FORCES	■	■		CT

Figure 2.6 (b). Compliant Towers

TYPE OF SUPPORT/ RESISTANCE	TYPE OF LOAD			
	STATIC		DYNAMIC	
	VERT.	HOR.	VERT.	HOR.
BUOYANCY		■		■
PARTLY BUOYANCY PARTLY SEABED	GT	■		■
SEABED			GT	
CABLES OR SIMILAR CONSTRAINTS		GT		
BALANCED BY INERTIAL FORCES	■	■		GT

Figure 2.6 (c). Guyed Towers

TYPE OF SUPPORT/ RESISTANCE	TYPE OF LOAD			
	STATIC		DYNAMIC	
	VERT.	HOR.	VERT.	HOR.
BUOYANCY	TLP	■		■
PARTLY BUOYANCY PARTLY SEABED		■		■
SEABED				
CABLES OR SIMILAR CONSTRAINTS		TLP	TLP	
BALANCED BY INERTIAL FORCES	■	■		TLP

Figure 2.6 (d). Tension Leg Platforms

TYPE OF SUPPORT/ RESISTANCE	TYPE OF LOAD			
	STATIC		DYNAMIC	
	VERT.	HOR.	VERT.	HOR.
BUOYANCY	AF	■		■
PARTLY BUOYANCY PARTLY SEABED		■		■
SEABED				
CABLES OR SIMILAR CONSTRAINTS		AF		
BALANCED BY INERTIAL FORCES	■	■	AF	AF

Figure 2.6 (e). Anchored Floaters

TYPE OF SUPPORT/ RESISTANCE	TYPE OF LOAD			
	STATIC		DYNAMIC	
	VERT.	HOR.	VERT.	HOR.
BUOYANCY	TLP AF	■		■
PARTLY BUOYANCY PARTLY SEABED	CT GT	■		■
SEABED	FS	FS CT	FS CT GT	FS
CABLES OR SIMILAR CONSTRAINTS		GT TLP AF	TLP	
BALANCED BY INERTIAL FORCES	■	■	AF	CT TLP GT AF

Figure 2.7. Superimposition of figures 2.6 a-e

Similar reasoning clarifies the situation with respect to the dynamic horizontal loads. For bottom founded structures the structural stiffness and the foundation stiffness represent two horizontal springs in series. As long as the combined spring action is stiff enough, the dynamic horizontal loads are transmitted through these springs to the sea floor. However, when the combined spring becomes weak, significant motions with the associated inertial forces will develop, creating a largely self-balancing system in a state of dynamic equilibrium; any differential dynamic horizontal force will be accommodated by the sea floor. For floating structures and practical designs of anchoring systems, either of the vertically taut or the catenary type, the horizontal springs are always weak and hence these structures will tend to be self-equilibrating in a state of dynamic equilibrium.

Consequently, the empty boxes in figure 2.7 are almost certain to remain empty forever. They are effectively excluded from the range of possibilities on practical grounds, as opposed to the shaded boxes that are excluded as a matter of principle.

Permanent installations

Platforms

Structure type	Fixed Structure	Compliant Tower	Guyed Tower	Tension Leg Platform	Anchored Floater	Total
USA – Gulf of Mexico	4000	2	1	5		4000
USA – West Coast	45					45
Central/South America	340				8	360
Europe – North Sea	400			3	20	425
Europe/Africa – Medit.	100				3	100
Africa – West Coast	380				9	390
Middle East	700					700
Asia	950				19	975
Australia/New Zealand	30				7	40
Total	~ 7000	2	1	8	66	~ 7000

Table 2.1. Approximate numbers of different types of structure in the platforms group of the permanent installations (1999)

Temporary installations

Platforms

		Number
Jack-ups		460
	Drilling Submersibles	25
Floaters	Drilling Semi-submersibles	200
	Drill Ships	50
	Drill Barges	35
Total		770

Tabel 2.2. Approximate numbers of different types of structure in the platforms group of the temporary installations (situation around 1998)

2.3 The worldwide population of offshore structures

Structures (in the narrower sense of the word) form part of the platform groups of the permanent and temporary or mobile installations (see figures 2.1 and 2.2). A snapshot of the approximate worldwide population for each type of structure is shown in tables 2.1 and 2.2. Additionally, for the structures belonging to the permanent installations a rough distribution over geographical areas is included.

From these tables it is obvious that there are about 10 times as many permanent as mobile platforms. It is further obvious that fixed offshore structures form the overwhelming majority of permanent structures. The next size group is the anchored floating (production) platforms, which are on the increase; they are particularly well suited for application in remote areas, for marginal fields and for deep water. However, their total number is only about 1% of the fixed structures population. And even though they have lately attracted a lot of attention and their number is rapidly rising, relatively speaking, they will remain a small group by comparison.

The other floating platform type, the vertically anchored Tension Leg Platform (TLP), currently comprises 8 units. The first TLP was installed by Conoco in the Hutton field in the central North Sea in 1984 in some 150 m waterdepth, followed in 1989 by the Jolliet Tension Well Leg Platform or TWLP in the Gulf of Mexico in 536 m waterdepth, also by Conoco. The TLP type of structure is a prime contender as a production platform in waterdepths from about 800 to some 2000 m. In the 1990s six further TLPs have been installed; four in the Gulf of Mexico by Shell Oil Company, all steel, and two in the North Sea off the Norwegian coast, one steel (Snorre, by Saga) and one concrete (Heidrun, by Conoco). The record holding waterdepth for a TLP is now (1998) 1158 m (Ursa, Gulf of Mexico). As for the anchored floating (production) platforms, the number of TLPs is also bound to increase in the future but they too will forever remain a small group in comparison with the fixed structures.

The one and only Guyed Tower was installed by Exxon on the Lena field in the Gulf of Mexico in 300 m of water in 1983. Although this was a successful project and the platform performs well, it is unlikely that more guyed towers will ever arrive on the scene. The concept does not have sufficient benefits in comparison with the regular fixed steel structure or the compliant tower. Until 1998 the only compliant structures in existence were a few articulated loading and flare towers and one control tower on the Frigg field of Norway (decommissioned in the 1990s). The two compliant towers in table 2.1 were both installed in the Gulf of Mexico in 1998, the first by Amerada Hess on the Baldpate field in 503 m waterdepth and the second by Texaco on the Petronius field in slightly deeper water of 535 m.

The fixed structures group comprises in total some 7000 structures. The great majority of these are steel space frame structures in waterdepths ranging from some 10 to 410 m. In the very shallow waterdepth areas along the coasts of the states of Louisiana and Texas in the Gulf of Mexico there are an appreciable number of steel single column structures as well, supporting one or a few producing wells. These single column structures are also called caissons. The single column structures or caissons form a subgroup of the fixed structures; they are suitable for

Operator	**Field**	**Design**	**Waterdepth**	**Yr of install.**
Existing Fixed Structures (28)				
Phillips	Ekofisk	Doris	73 m	1973
Mobil	Beryl A	Condeep	118 m	1975
Shell	Brent B	Condeep	140 m	1975
Total	Frigg CDP1	Doris	104 m	1975
Shell	Brent D	Condeep	140 m	1976
Elf	Frigg TP1	Sea Tank	104 m	1976
Total	Frigg MCP01	Doris	94 m	1976
Shell	Dunlin A	Andoc	153 m	1977
Elf	Frigg TCP2	Condeep	104 m	1977
Mobil	Statfjord A	Condeep	145 m	1977
Shell	Cormorant A	Sea Tank	149 m	1978
Chevron	Ninian Central	Doris	141 m	1978
Shell	Brent C	Sea Tank	141 m	1978
Mobil	Statfjord B	Condeep	145 m	1981
Phillips	Maureen ALC	EMH	92 m	1982
Texaco	*Schwedeneck A*	*Doris*	*25 m*	*1983*
Texaco	*Schwedeneck B*	*Doris*	*16 m*	*1983*
Mobil	Statfjord C	Condeep	145 m	1984
Statoil	Gullfaks A	Condeep	135 m	1986
Statoil	Gullfaks B	Condeep	141 m	1987
Norsk Hydro	Oseberg A	Condeep	109 m	1988
Statoil	Gullfaks C	Condeep	216 m	1989
Phillips	Ekofisk Barrier	Doris	75 m	1989
Hamilton Br.	Ravenspurn N.	Ove Arup	43 m	1989
Shell	F3	HBW/VSCI	42 m	1992
Shell	Draugen	Condeep	250 m	1993
Statoil	Sleipner A	Condeep	82 m	1993
Shell	Troll (gas devt.)	Condeep	302 m	1995
Planned Fixed Structures (4)				
Esso	*West Tuna*	*Kinhill/Doris*	*61 m*	*1996*
Esso	*Bream B*	*Kinhill/Doris*	*61 m*	*1996*
Ampolex	*Wandoo*	*......*	*80 m*	*1996*
Mobil	*Hibernia*	*Doris*	*80 m*	*1997*
Existing Floating Structures (3)				
Arco	*Ardjuna (LPG-FSO)*	*SBM*	*42 m*	*1974*
Conoco	Heidrun (TLP)	Condeep	345 m	1995
Norsk Hydro	Troll Oil Devt. (semi)	KDOC	325 m	1995
Planned Floating Structures (1)				
Elf	*Nkossa*	*Bouygues Offshore*	*170 m*	*1996*
Existing concrete Gravity Base (Storage) Tank (1)				
BP	Harding	Costain-Taylor Woodrow	109 m	1995

NB - the 8 structures not located in the North Sea are printed in *italics*

Figure 2.8. The 37 existing or planned concrete structures (1995)

waterdepths up to some 25 m and are hardly seen anywhere else. Another subgroup is formed by concrete as opposed to steel structures. Concrete structures are without exception of the gravity base type. In total they number less than 30, but most of them are very big structures supporting major production capacities; they are mainly found in the (northern) North Sea. A list of all existing and planned concrete structures (1995) is presented in figure 2.8; the list includes a few concrete floating structures as well.

Finally, it is noteworthy to observe that the total number of bottom founded structures in waterdepths greater than 200 m, worldwide, is less than 20. This includes 3 concrete gravity structures; the guyed tower and the two compliant bottom founded structures.

3 MODELS AND MODELLING

3.1 Introduction

Models play a crucial role in the description of situations, in the thinking about processes and in the solution to problems. This is irrespective of whether the subject concerns the technical, the economic or the social order of things. In relation to the behaviour of offshore structures we need to be able to formulate the questions we have as clearly as possible and to represent the physical reality accordingly in an adequate manner. It should be clearly understood that models merely serve as tools in an approach towards the answering of questions. A generic procedure for the solving of a problem is described in Annex A to this chapter.

The concept of a 'model' can be described in various ways. Some examples from dictionaries and encyclopaedia are:

- "A model is a simplified description of a system etc. to assist calculations and predictions."[1]
- (according to modern scientific opinion): "Empirical interpretation of a mathematical-logical system." [2]
- "M is a model of A in as far as one can use M to answer questions about A; M and A do never correspond completely." [3]

Or perhaps more simply, but very usefully:

- "A model is a manageable, understandable, schematic image of a part of reality." [4]

The last one of these descriptions is a very usable formulation, but one important element is missing; that is that a model is invariably constructed with a particular purpose in mind. By adding this aspect we get the following description or definition of a model that we will adopt in this handbook:

- "A model is a manageable, understandable, schematic image of a part of reality that serves a particular purpose."

It follows from the above that all models are incomplete and imperfect representations of reality. It is very important to be continually aware of this. In modelling it is often as important, or even more important, to carefully consider what can be omitted than what must be included. The incomplete and imperfect state of a model is of no particular concern as long as the user is fully aware of the model's limitations. *What matters, therefore, is that a model serves to obtain reliable information regarding those aspects that a user seeks to acquire information about using his model, to the level of detail and the degree of accuracy required for the problem considered.* Thus, models should be judged on their adequacy and their effectiveness in describing what is needed rather than on their 'truth'. Their 'correctness' is a relative and not an absolute attribute. However, this does not make it less necessary that models should, wherever possible, be tested to demonstrate their validity in the sense required.

---

[1] The Concise Oxford dictionary, 7th edition, 1982/83.

[2] VanDale Groot Woordenboek der Nederlandse Taal, 12th edition, 1992.

[3] Grote Winkler Prins Encyclopedie, 8th edition, 1982.

[4] Prof. dr. ir. H.J. de Vriend, 'Onzekerheid troef?', inaugural address, Technical Univerity of Twente, Enschede, 1995.

Models are indispensable and powerful tools in an engineer's toolkit. However, they also have an inherent danger as is very well expressed by the following statement:

- "One of man's greatest gifts is his ability to construct mental models. However, one of his greatest handicaps is his tendency to mistake these models for reality." [5]

For technical applications we must be able to describe the physical environment and the relevant physical phenomena around us, and on that basis to predict situations that arise therefrom. The science that aims to do this for many technical applications, including those that are of interest to offshore engineering, is mechanics; mechanics in its various forms of the mechanics of solids, fluids and soils, see Annex B. Using a limited set of basic principles, a number of coherent theories have been developed over many years that are indeed able to explain and predict many phenomena. These theories are nothing else than generalised models.

Modelling thus plays a very important role, whether it involves the intelligent use of existing theories or the development of new tailor-made models to suit a particular set of circumstances. Every description or calculation is based on a representation of reality, i.e. a model, whether we are explicitly aware of this or not. An entire process is usually broken into a number of sequential or parallel sub-processes that are modelled separately. Therefore we need to ensure that the models of the sub-processes are tuned to one another and can be joined together. This relates among other things to e.g. the bases of the descriptions, the degree of detailing and their intended accuracy. In other words, the models of the various sub-problems need to be compatible. We often use existing models that have proven their usefulness for a wide range of circumstances. The validity of such models for the particular application contemplated should nonetheless be critically assessed; it should never be taken for granted that a model suits the purpose. In some cases existing models can only be used after suitable adjustment, while in other cases models need to be specially developed for the circumstances under consideration.

An effective treatment of a problem always requires that two translations are made, i.e.:

- a translation from the physical reality into the artificial world of the model, and
- a translation of the results obtained by solving the problem in the artificial world of the model back into the real world.

The first step involves analysis of the problem and understanding of the real world; it is associated with such notions as schematisations, approximations and problem formulation. The second step involves synthesis of the solutions of the individual parts of the problem and an evaluation of the overall results. This step is associated with such notions as an estimation of the uncertainties involved and the effect of the approximations made, discussion of the use of the results in practice, as well as an assessment of the potential consequences and risks that may be associated with the overall solution.

---

[5] Klaus G. Müller, proposition with a doctoral thesis in The Netherlands in the early 1970s.

Both steps are of paramount importance. Poor understanding or poor formulation of the problem in the real world is frequently the source of choosing a wrong approach, of frustration and dissatisfaction with the model. It may even be worse when a perfectly adequate model is used beyond its range of validity, leading to erroneous and possibly dangerous results. Furthermore, an excellent solution to the right problem has still little value if it cannot be explained in terms and implications that the engineer who has to use the solution can understand. For technical problems the engineer is normally the only one who can perform both translations. If solutions involve the assistance of specialists he must be the intermediary between the various parties joining in: the specialists, his colleagues, those who actually perform the work, the users of the results, the client, the supervising authorities and whoever else. All this puts high demands on the engineer in terms of teamwork, the depth and breadth of his knowledge and his communication skills.

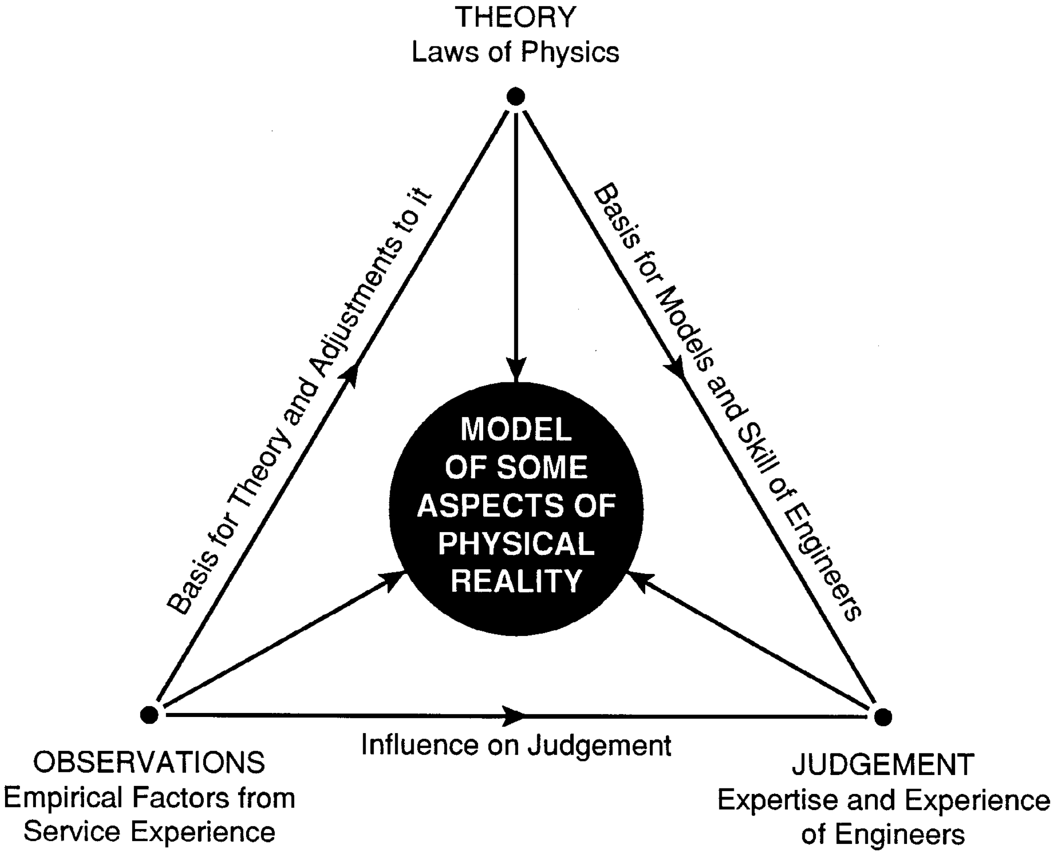

Figure 3.1. Schematic illustrating the process of creating models for the design or assessment of structures

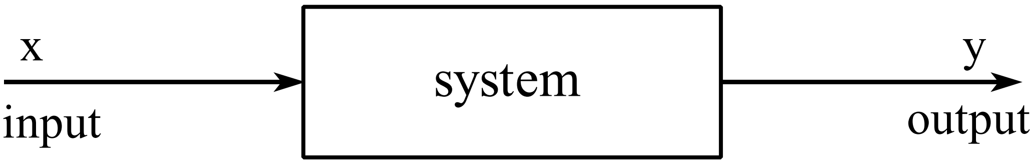

Figure 3.2. Most elementary form of a block diagram

3.2 Modelling

The making of models is based on a combination of theory, observations and the judgement of highly skilled engineers. The process is illustrated schematically in figure 3.1. Models can take many different forms, such as scale models of a building or a city district providing a three-dimensional impression of a new design; scale models for testing in laboratories (which are also called physical models); analogue models that use a different medium, such as an electrical circuit, to simulate processes that are governed by similar laws of physics; mental models that help us in discussing highly complex issues like a view of the world; and mathematical models that serve to do calculations. The two most common model forms used in engineering are scale models and mathematical models. Scale models are used for testing a scaled-down simulation of the physical reality in a laboratory. The information required is obtained through measurements. In mathematical models the physical reality is represented by means of mathematical descriptions of the processes involved. The information required is obtained through calculations. The calculations are either carried out using theoretically derived relationships between known causes and unknown consequences, or using a numerical simulation of what is envisaged to happen in the real world. With the advances in computer technology, calculations using mathematical models have in many cases become a very practical, powerful, versatile and relatively cheap alternative to laboratory testing. In actual practice several different ways of modelling will often be used. These vary from a simple, crude mathematical model enabling an approximate but quick estimate of an order of magnitude by hand, to a sophisticated model necessitating extensive numerical calculation with the aid of a large computer. In some cases such calculations are supplemented with laboratory testing for final confirmation of the results of the calculations, or for direct measurement of those aspects that are not (yet) properly understood and hence cannot be formulated mathematically. Guidance for modelling structures in laboratory testing is e.g. given in ref. [3.1].

The emphasis in this handbook will be on mathematical modelling and numerical simulation. This means that all processes at work must be described in mathematical terms. The resulting models are referred to by various names: mathematical models, theoretical models, or mental models to distinguish them from the physical scale models. More in general, models used for engineering purposes may also be called engineering models, a term which tends to indicate that the models are only a relatively crude and approximate representation of reality.

As noted before, in making a suitable model of a problem it is often practical to break the problem into a number of more easily manageable sub-problems, each of which is described by a separate model which are subsequently linked together. Schematics or block diagrams can be very helpful in this respect. The most elementary form of a block diagram is shown in figure 3.2. The block represents a system with known properties. The input to the system is a variable x, the output a variable y. The input is the cause that something happens, the output is the effect if the cause acts on the system; x is also called the *action* while y is called the *action effect* or the *response* of the system. Block diagrams can be a great help in visualising and clarifying the problem, in focusing the thinking and in deriving a correct mathematical formulation. In linear [6] problems the answer does not depend on the route we follow to get

---

[6] linear means that the following two relationships between input and output are valid:

input:	$a \cdot x$	output:	$a \cdot y$
input:	$x_1 + x_2$	output:	$y_1 + y_2$

there. In other words, we can sub-divide the problem in any way we like, superimpose the solutions for each part and invariably arrive at the correct final solution. This implies that a block diagram is not a unique representation. For a non-linear problem there is no such freedom. The ultimate solution now depends on the route followed so that it is very important to depict the interrelationships between phenomena and the sequence in which these occur in the correct manner and construct the block diagram accordingly.

An example of a block diagram for a linear(ised) problem is shown in figure 3.3, see ref. [3.2]. It relates to the problem of the interaction between the fluid and a body, when the body moves in an unsteady fluid flow. The body movement may be a rigid body motion, a structural deformation or a combination of these. We can represent this problem as the sum of two problems, i.e. firstly a body that is at rest in the moving fluid and secondly a body that is moving while the fluid is at rest. The first sub-problem is shown in figure 3.3a. The input to this problem is the velocities and accelerations of the fluid particles; the output is the fluid excitation forces experienced by the body at rest in its undisplaced and undeformed position. The second sub-problem is shown in figure 3.3b. The input is now the movements of the body and the output is the fluid reaction forces experienced by the body when it is forced to move through the fluid at rest. The full problem is shown in figure 3.3c and is the combination of the two previous figures. The resulting mathematical formulation is also shown. Block diagrams clearly depict the interdependencies that exist between the various parts of the problem and the links that must be maintained to make them fit together.

As noted, the model maker must know what he wants to achieve with his model, so that he can include those aspects that are relevant while omitting other aspects that are of no significance to his objectives. Some simple examples may illustrate this. Forces on an object are classified as point forces, surface forces and volume forces. Examples of point forces are concentrated loads and the force with which a cable pulls on an object. These are fully determined by their *magnitude*, *direction* and *point of application*. However, what causes the concentrated load or what the cable is made of is of no concern to the resulting load case. Typical surface forces are

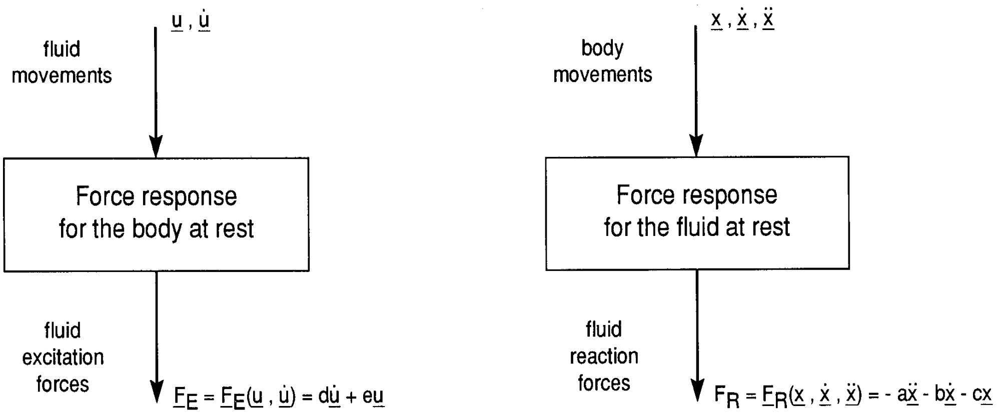
$\underline{u}, \dot{\underline{u}}$
fluid movements
Force response for the body at rest
fluid excitation forces
$\underline{F}_E = \underline{F}_E(\underline{u}, \dot{\underline{u}}) = d\dot{\underline{u}} + e\underline{u}$
$\underline{x}, \dot{\underline{x}}, \ddot{\underline{x}}$
body movements
Force response for the fluid at rest
fluid reaction forces
$\underline{F}_R = \underline{F}_R(\underline{x}, \dot{\underline{x}}, \ddot{\underline{x}}) = - a\ddot{\underline{x}} - b\dot{\underline{x}} - c\underline{x}$

A) FLUID EXCITATION FORCES

B) FLUID REACTION FORCES

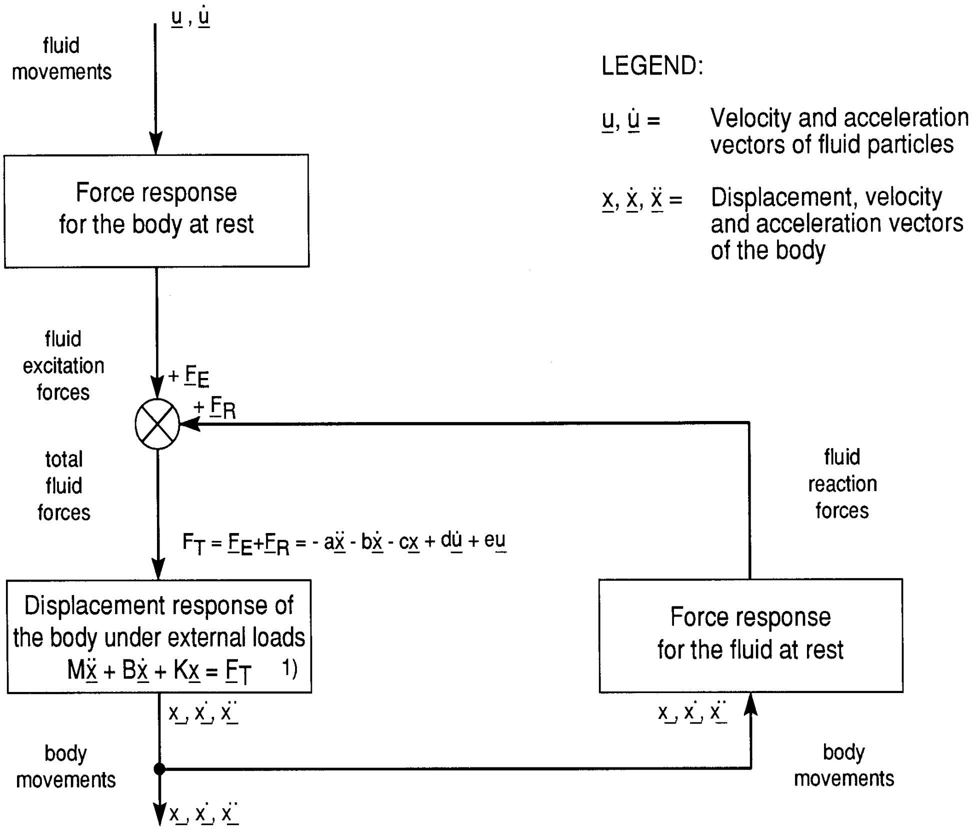
$\underline{u}, \dot{\underline{u}}$
fluid movements
Force response for the body at rest
fluid excitation forces
$+\underline{F}_E$
$+\underline{F}_R$
total fluid forces
$F_T = \underline{F}_E + \underline{F}_R = - a\ddot{\underline{x}} - b\dot{\underline{x}} - c\underline{x} + d\dot{\underline{u}} + e\underline{u}$
Displacement response of the body under external loads
$M\ddot{\underline{x}} + B\dot{\underline{x}} + K\underline{x} = \underline{F}_T$ 1)
fluid reaction forces
Force response for the fluid at rest
$\underline{x}, \dot{\underline{x}}, \ddot{\underline{x}}$
body movements
body movements
$\underline{x}, \dot{\underline{x}}, \ddot{\underline{x}}$
$\underline{x}, \dot{\underline{x}}, \ddot{\underline{x}}$
LEGEND:
$\underline{u}, \dot{\underline{u}}$ = Velocity and acceleration vectors of fluid particles
$\underline{x}, \dot{\underline{x}}, \ddot{\underline{x}}$ = Displacement, velocity and acceleration vectors of the body

1) re-writing this equation it becomes the well-known equation of motion

$$(M+a)\ddot{\underline{x}} + (B+b)\dot{\underline{x}} + (K+c)\underline{x} = d\dot{\underline{u}} + e\underline{u}$$

C) FLUID EXCITATION AND REACTION FORCES COMBINED INTO TOTAL EXTERNAL FORCES

Figure 3.3. Example of a block diagram: Schematic illustration of fluid-structure interaction in a linear(ised) problem

pressure forces and friction forces. For an accurate representation of these the *shape*, the *orientation* and the *area* of the surface are important, but nature and size of surface irregularities do not need to be described. Typical volume forces are gravity and inertial forces. For their representation it usually suffices to include the *volume* or the *mass* of the object, together with the *centre of mass*, while the precise shape of the object is of no consequence, not to mention the internal molecular structure of the object.

Another illustration is a steel beam spanning an opening in a masonry wall to support the loads above it. The end conditions of the beam are uncertain; depending on the way in which the supports are actually constructed and on the workmanship of the brick layers each support may vary from close to pinned to nearly fixed. We may size the beam conservatively on the maximum moment that may be experienced. Therefore, for this design purpose a model of a pinned-pinned beam with length L and a concentrated load F at mid-span may be assumed. In this model the maximum moment will be $FL/4$ at the centre, decreasing to zero at the ends. However, it would be potentially dangerous to use this information to refine the design of the beam to have a variable cross section over its length, unless we make very sure that the real supports are indeed pinned. If in reality they would be closer to fixed, the end moments would be equal to the moment at mid-span and have the value $FL/8$. In that case the ends of the beam would clearly be underdesigned to carry the load F.

A few further examples that are more related to offshore problems are discussed below.

We all know Archimedes' principle that a body immersed in a fluid is subject to an upward force equal in magnitude to the weight of the fluid it displaces. While perfectly true, it should be recognised that this principle is a particular formulation of the underlying physical phenomena and is only valid for problems associated with hydrostatic equilibrium. It expresses that an integration of the hydrostatic pressure distribution over the wetted part of the surface of a floating or fully submerged body results in a net upward force of the given magnitude. However, it says nothing about the hydrostatic pressures in any other direction than the vertical, or about dynamic pressures when the fluid is not at rest. Horizontal components of the pressure forces on a body in a still fluid are always in balance and do not produce a net horizontal force. They thus do not affect the static equilibrium. However, the body will still have to accommodate the pressure forces by its internal structure. Therefore, for structural design Archimedes' principle is of no use; we will have to resort to pressures as the basic physical cause of the loads on a body.

Let us next consider slender, hollow steel cylindrical members that are so extensively used in offshore structures under water. Their structural design can normally be based on simple beam theory. If this is the case we only need to know the distribution of the hydrodynamic forces along the length of the member that act perpendicular to the member's axis. The pressure distribution around the circumference is of no particular interest. Hence, a global scale (macroscopic) representation of the fluid flow in terms of the velocities and accelerations perpendicular to the member's axis is all that is required; we do not need to be concerned with the detailed scale (microscopic) description of the fluid flow in terms of vortices, boundary layers, etc. If, however, the diameter to thickness ratio of the cylinder is large and we would need to design or check the

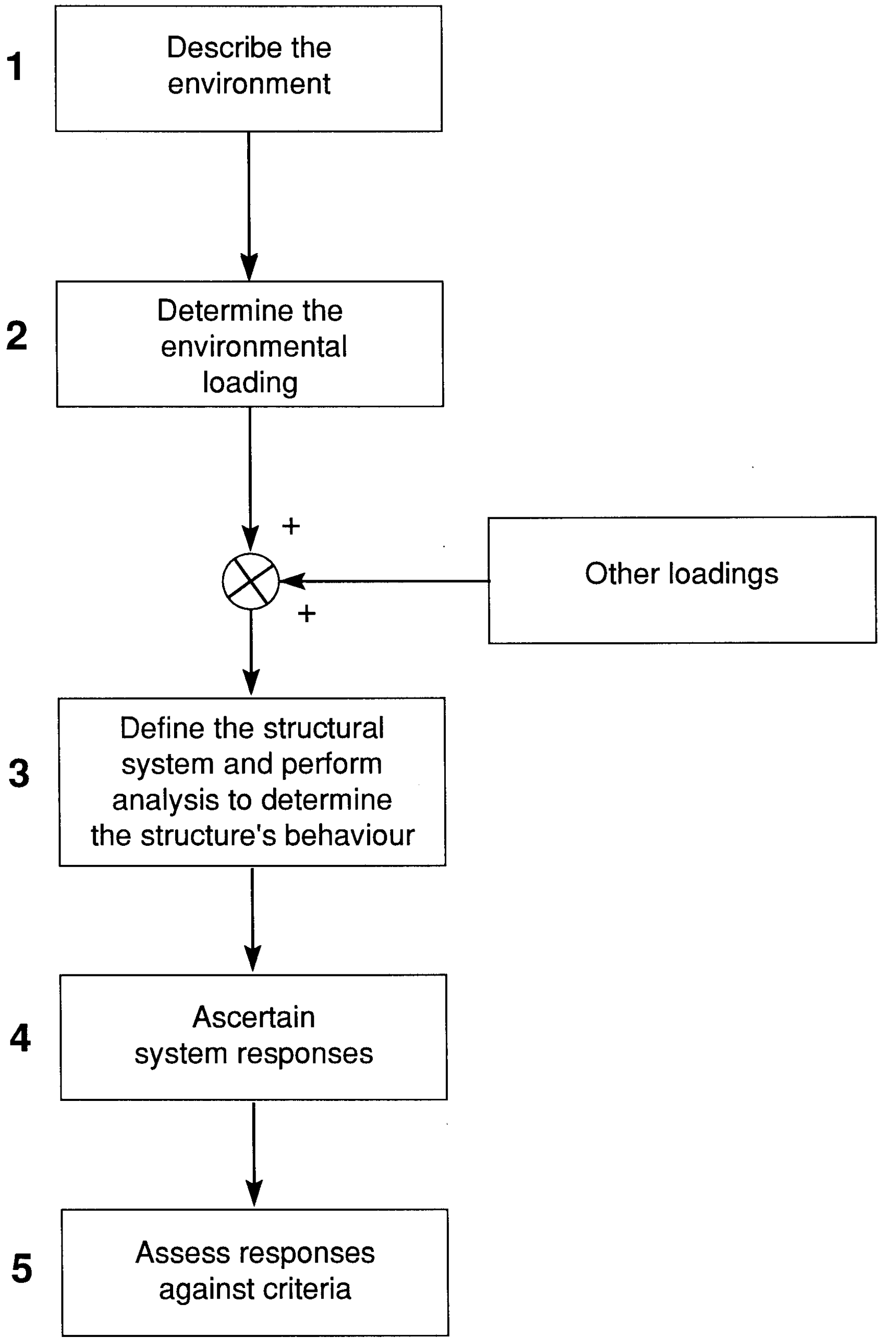
1
Describe the environment
2
Determine the environmental loading
+
+
Other loadings
3
Define the structural system and perform analysis to determine the structure's behaviour
4
Ascertain system responses
5
Assess responses against criteria

Figure 3.4. Schematic representation of the main steps involved in the design or assessment of a structure

stiffened or unstiffened cylindrical shell in detail, then the pressure distribution around the cylinder is also needed.

As a final example we will consider the motions of a floating semi-submersible in waves. The motions depend on the wave loads and moments on the structure, together with the hydrostatic and hydrodynamic characteristics of the semi-submersible. These characteristics are usually expressed in terms of added masses, damping coefficients and hydrostatic restoring actions. The damping coefficient has a very great influence on resonant motions, but is irrelevant for motions at frequencies well away from resonance. For semi-submersibles the natural frequencies of the angular motions roll and pitch are generally very low and well outside the wave frequency range; therefore, these motions can usually be accurately determined without any knowledge of their damping. However, for ships and barges the angular motions have much higher natural frequencies that usually fall within the frequency range of wave excitation. In these cases, therefore, knowledge of the damping coefficients of the motions concerned is very important. The natural frequency of the heave motion normally falls in a frequency range that damping is a significant parameter for all floating vessels.

All this means that engineers, regardless whether they are model makers or model users, must have a very good overview of the problem area involved and an in-depth understanding of the physical reality underlying it. This requires profound knowledge and extensive experience, but also some engineering intuition. The determination of the right model(s) is the decisive step in problem formulation and its subsequent solution. An error that should be avoided but is often made is that models of the various parts of the problem are incompatible, thus preventing them from being adequately linked together. Another frequent error is that they are unbalanced as to their impact on the accuracy and reliability of the ultimate result.

Referring to figure 3.2, the responses of a structure are governed by the cause(s) of (a) disturbance(s) (i.e. the input) and the properties of the system. Both these aspects need to be considered in a coherent manner. They will jointly determine how a problem should be modelled. Offshore structures spend their lifetime in a harsh environment comprising the atmosphere, the ocean and the seabed. Although winds and currents may in some cases play a significant role, waves are usually the dominant environmental influence. Consequently, waves are likely to feature prominently in most models involving environmental actions. The general procedure for the design or assessment of an offshore structure may be depicted as a number of separate but related steps as shown in figure 3.4. In chapter 4 the offshore environment and the associated environmental loading will be discussed in some detail. In a general sense, problems related to offshore structures belong to the class of structural systems that are subject to time-varying random excitation. With very few exceptions the parameters of the structural system may be considered as time-invariant and are hence constants. In the next section the general characteristics and areas of application of different types of model will be discussed following ref. [3.3].

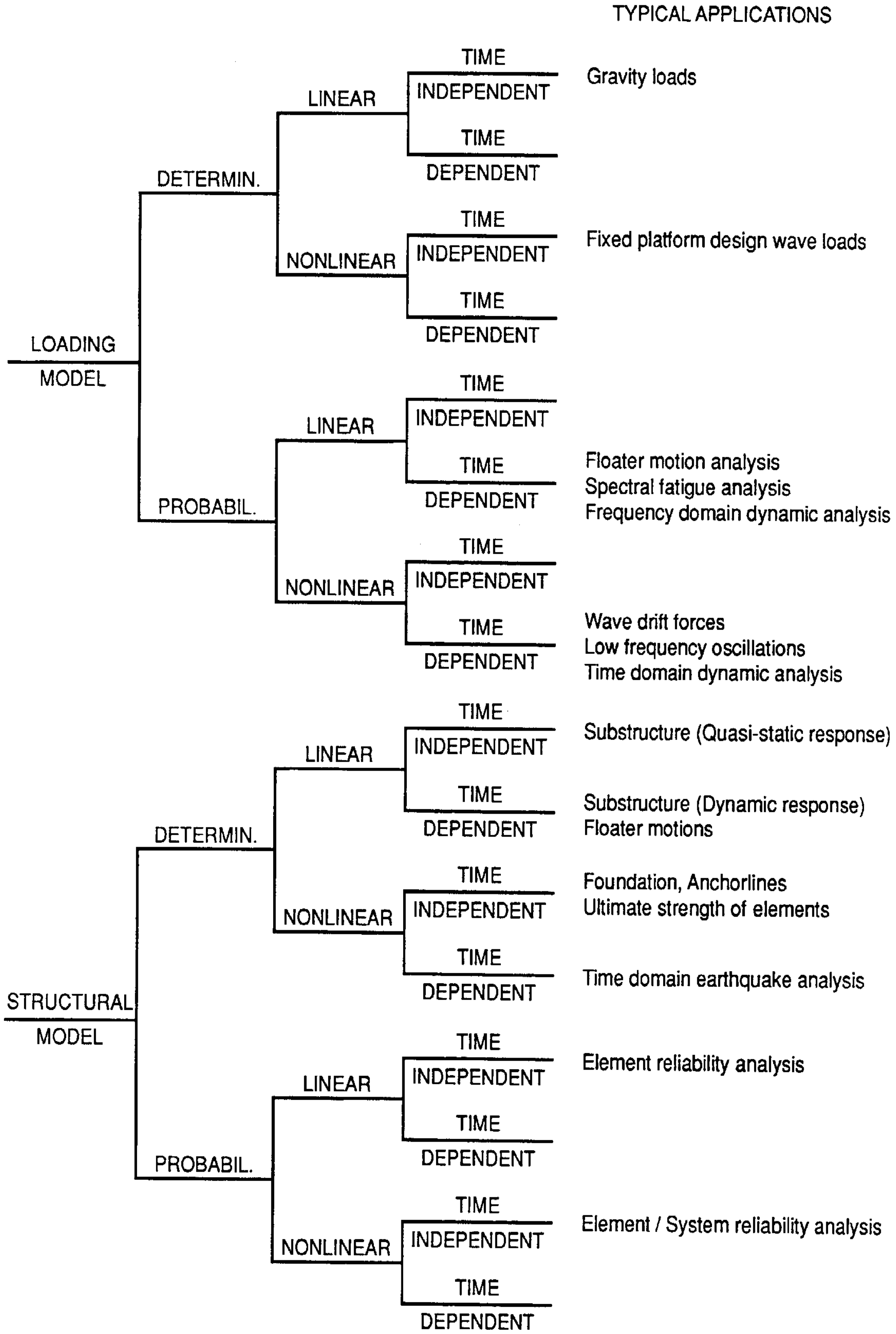

Figure 3.5. Main characteristics of loading and structural models with typical examples of field of application

3.3 Main model characteristics

The two models that are central to all questions of the design or assessment of offshore structures are the load model and the structural model, i.e. models for blocks 2 and 3 in figure 3.4. A description of the environmental loads is so closely interrelated with a description of the environment itself that it is commonplace to refer to a combination of blocks 1 and 2 as the environmental load model. This practice will be followed here too. In applications all loads should be considered; however, for the present discussion we will focus on the environmental loads and more particularly on the wave and current loads. The second model, the structural model, relates to all system properties, i.e. mass, spring and damping characteristics, as well as to the system's boundary conditions (e.g. its foundation or anchoring system).

Model attributes
Each of the two models may be identified by three main characteristics or attributes, i.e. they are deterministic or probabilistic (*D* or *P*); they are linear or non-linear (*L* or *NL*); and they are time dependent or time independent (*TD* or *TI*). When we refer to a structural model as time dependent we mean that it includes mass and damping properties, either as a rigid body or as an elastic system, enabling it to exhibit dynamic response. This terminology is perhaps somewhat unusual, but by introducing it we are able to make common distinctions for both models.

Combining 2 choices for each of 3 model attributes leads to 8 different possibilities for each model, as illustrated in figure 3.5. Hence there are 8 x 8 = 64 different combinations in a joint application of the two models. A number of these combinations are in everyday use, other ones only find application in special cases, while some of them are rather hypothetical; see the typical applications that are also indicated in figure 3.5. However, all 64 possibilities do exist and the most appropriate choice for each and every application should be consciously made, keeping the state-of-the-art of the technology and the (im)practicality of the particular model(s) for the intended purpose firmly in mind.

Examples of choices to suit applications
Let us by way of example consider a few applications. A fixed offshore structure is normally designed using a design wave procedure, i.e. an extreme single, periodic wave is selected and 'frozen' at different times in its passing through the structure. The *load model* usually chosen for this event is deterministic, non-linear and time independent (*D,NL,TI*). The wave is selected by the designer and any possible variation of this selection is treated as a separate load case; hence the model is deterministic. For a single periodic wave non-linear features can easily be retained so that it presents no difficulties to use a non-linear formulation for the wave and the associated wave loading. Finally, although several wave positions may be considered in succession, each of these is independent of time. The usual choice for the *structural model* is either (*D,L,TI*) or (*D,NL,TI*), mainly depending on the properties of the foundation and whether structure and foundation are integrally or separately modelled.

For a fatigue or a dynamic analysis of a structure the time varying nature of the loading is an essential feature and must be retained. As long as the structural response may be treated as quasi-static the structural model does not need to include time dependent properties to enable it to exhibit dynamic response. However, when the response is truly dynamic time dependency is an important element and must be incorporated. For fatigue as well as for dynamic problems it is generally necessary to include the random nature of the environment in a realistic manner. If a spectral approach is used the loading must be linearised and the load model is chosen as (*P,L,TD*). In case of time domain simulations the non-linearity may be retained and the *load model* can consequently be (*P,NL,TD*). The *structural model* normally remains deterministic and satisfies (*D,L* or *NL, TI* or *TD*). The choice of *L/NL* depends on the use of a spectral or a time domain simulation approach, while the choice *TI/TD* depends on the quasi-static or dynamic response of the structure as discussed before.

As a final example, the vertical motions of a semi-submersible due to heave, pitch and roll can usually be determined while ignoring the anchoring system. As these vertical motions are time dependent, the random nature of the environment must be retained and a spectral approach has become the norm since many years. Consequently, the *load model* is chosen as (*P,L,TD*) and the *structural model* as (*D,L,TD*). Applications concern e.g. the assessment of downtime of floating drilling rigs. For the horizontal motions of anchored floaters low frequency drift forces play an important role. These forces are non-linear with the wave environment; therefore time domain simulation would seem to be called for, but in various cases reasonable results have been obtained by second order spectral methods in the frequency domain. The *load model* would correspondingly be chosen to be (*P,NL,TD*) while the *structural model* remains (*D,L,TD*).

A more systematic overview of combinations used in practical applications is shown in figures C.1 to C.3 in Annex C. These illustrate the current state of affairs and the future development required. Each of these figures is a two-dimensional representation of a really three-dimensional picture.

Probabilistic v. deterministic models

All science and engineering has probably begun by developing deterministic models. In marine and offshore technology the prime source of randomness is the ocean environment, as is illustrated by a saying of Lord Rayleigh towards the end of the last century: “The basic law of the seaway is the apparent lack of any law”. The advent of probabilistic models in oceanography dates back to the days of World War II when attempts at modelling the ocean surface more realistically than by periodic waves began to have success and a modern era of oceanography emerged. Probabilistic environmental loading models combined with a deterministic model of the structure have been used since the early fifties for studying ship motions. They were introduced jointly by a naval architect (St Denis) and an oceanographer (Pierson) in a famous paper for the Society of Naval Architects and Marine Engineers in New York [3.4]. They introduced their work under the heading “In a broad sense the laws of nature are Gaussian”. A very valid and useful statement. The fact that it is not strictly true and that in may instances we are now looking for refinements and improvements on it is only an indication of the degree of progress we have made over the last forty plus years. Since then spectral analysis techniques and statistical treatment of problems based on Gaussian random processes have been widely used. An example of a discussion of some basic aspects of the methodology and some applications in wind and water may be found in ref. [3.5].

In the offshore arena analogous applications of *probabilistic loading* and *deterministic structural* models have gradually become common practice for assessing most aspects related to the motion behaviour of floating offshore craft. Examples are motion downtime predictions, lifting operations of crane barges and the analysis of marine risers. For fixed structures similar model choices were introduced in the early seventies for spectral fatigue analyses for the then new generation of northern North Sea structures (see e.g. [3.6]). Such methods are now fairly routinely applied to large and important structures, especially if dynamic behaviour is to be incorporated. An extension of this situation by also introducing probabilistic structural models is the ultimate challenge of structural reliability analysis. These probabilistic structural models should then account for such things as tolerances on dimensions, geometrical or material imperfections, variations in yield stress and distribution of residual stresses. However, this is largely still beyond the present state-of-the-art.

Generally speaking, the offshore industry has been somewhat slow in adopting random analysis procedures. This is probably due to a lack of familiarity with these techniques as well as a failure to recognise the essential probabilistic nature of the environment (and hence of the environmental loading) amongst most engineers in the early days of offshore developments. However, this has now been largely overcome. What remains and forms a serious complication for the load model is the problem of loading non-linearities. Such non-linearities are e.g. due to the wave kinematics around the free water surface (which cannot be predicted well by linear wave theory), drag forces of viscous origin, and time dependent lengths of structural members that are subjected to wave forces. However, this difficulty cannot be solved by adopting a model that includes non-linearities at the expense of reducing wave loading to a deterministic and periodic phenomenon. To avoid misunderstanding, a deterministic and periodic load model is generally quite suitable as an abstraction of reality for designing fixed structures; it has proven its worth for this purpose. However, it is so great an over-simplification that it loses realism and is inadequate for a rational debate of the occurrences in nature.

The use of probabilistic models is nearly always more suited to analysis than to design. The design process is generally based on simplified deterministic load cases, drawing heavily on the experience of the design engineer. The use of such simplified procedures is likely to remain the norm for practising engineers in the everyday routine of design applications. There is nothing wrong with this, provided the engineer is aware of the simplifications involved and can revert to other approaches when circumstances demand it.

3.4 References

3.1 Chakrabarti, S.K., ***Offshore Structures Modelling***; series on Advances in Ocean Engineering, volume 9; World Scientific Publishing, 1994, Singapore

3.2 Vugts, J.H., ***A review of hydrodynamic loads on offshore structures and their formulation***; Proceedings of the 2nd international conference on the Behaviour of Off-Shore Structures (BOSS '79), London, 1979; volume 3, paper 54.

3.3 Vugts, J.H., ***Environmental forces in relation to structure design or assessment-a personal view towards integration of the various aspects involved***; keynote paper presented at the international conference on Environmental Forces on Offshore Structures, the Society for Underwater Technology (SUT), London; 28-29 November 1990.

3.4 St Denis, M. and Pierson, W.J., ***On the motions of ships in confused seas***; Transactions of the Society of Naval Architects and Marine Engineers, Vol. 61, New York, 1953, pp 280-357.

3.5 Constructies in wind en water - Stochastiek en dynamica in de civiele techniek;
een vijftal lezingen gegeven op de Vreedenburghdag, Delft, 18 november 1971:
Bouma, A.L. : ***Het dynamisch gedrag van constructies***
Dorrestein, R. : ***Lineaire systemen en stochastische signalen***
Battjes, J.A. : ***Statistische eigenschappen van stationaire Gaussische systemen***
Vugts, J.H. : ***De analyse van constructies onder invloed van de stochastische golfbelasting***
Koten, H. van : ***Een lichtmast als voorbeeld voor het berekenen van een eenvoudige door wind belaste constructie***
De Ingenieur, jaargang 84, nummers 27 (7 juli 1972) en 28/29 (14 juli 1972).

3.6 Vugts, J.H. and Kinra, R.K., ***Probabilistic fatigue analysis of fixed offshore structures***; Offshore Technology Conference, Houston, 1976, paper OTC 2608.

Annex A – A generic approach to the solution of a problem

This annex presents a generic approach to the solution of a problem in eight different steps. These steps, their interdependencies and the feedback loops are visualised in figure A.1. The eight steps are:

1. Recognition

The phase in which someone becomes aware that there is a problem and what the most important aspects of the problem are.

2. Analysis

The phase in which one charts the problem, begins to understand its structure, divides it into manageable sub-problems, determines the relationships between the parts or the absence thereof, and the like.

3. Schematisation

In this step deliberate and well-considered simplifications are introduced by making approximations or deleting aspects that are irrelevant to the problem under consideration. The purpose of these measures is to make the problem more tractable without changing its essence for the intended purpose.

4. Modelling

The various parts of the problem are captured in (mental) models. These are often existing models or models that are transferable from other technical areas; sometimes entirely new models need to be purposely developed for the case under consideration.

5. Formulation

Developing a description of the mental model, either in words or in mathematical terms.
There is no sharp separation between modelling and formulation; they merge smoothly into one another and interact strongly. Many people will therefore consider these two steps probably as one. However, it is nevertheless useful to distinguish them formally as two steps: given a particular mental (sub)model more than one formulation may still be possible.

6. Solution

A step that speaks for itself; each sub-problem is solved, either by reasoning or by solving the mathematical equations. Normally a quantitative solution is required, but sometimes a qualitative solution suffices.

7. Synthesis

The solutions of the parts are combined into one whole to obtain the overall solution to the original problem.

8. Evaluation

The step in which the results are assessed and interpreted, both in respect of the various parts of the overall problem and of the problem as a whole.

The eight steps discussed above are usually not fully independent of one another; often there are feedbacks possible or even necessary. In many cases the approach to the problem is also an iterative process in which case (parts of) the diagram in figure A.1 are passed through a couple of times before a satisfactory model is obtained.

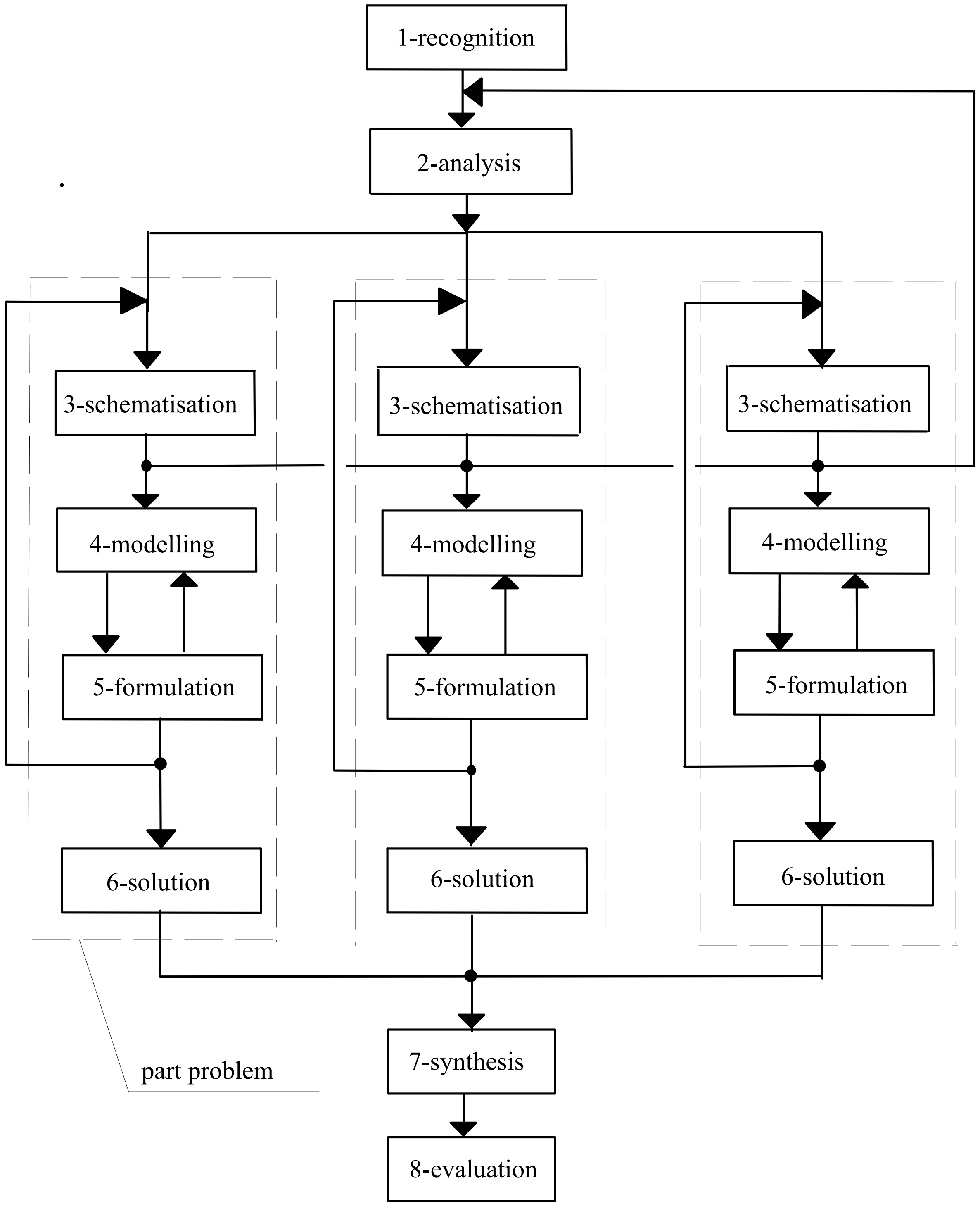

Figure A.1. A generic approach to the solution of a problem

Annex B – A few words on Mechanics

B.1 Definition and classification

Mechanics is the basis of most engineering fields, including Offshore Engineering. Mechanics may be defined [7] as " the science that describes and predicts the conditions of rest or motion of bodies under the action of forces", where motion is a change of position as a function of time.

The subject matter is largely treated mathematically and some people therefore consider mechanics to be a part of mathematics. Others, however, consider mechanics to be a part of engineering [7]:

quote

> Mechanics is a physical science, since it deals with the study of physical phenomena. However, some associate mechanics with mathematics, while many consider it is an engineering subject. Both these views are justified in part. Mechanics is the foundation of most engineering sciences and is an indispensable prerequisite to their study. However, it does not have the *empiricism* found in some engineering sciences, i.e., it does not rely on experience or observation alone; by its rigor and the emphasis it places on deductive reasoning it resembles mathematics. But, again, it is not an *abstract* or even a *pure* science; mechanics is an *applied* science. The purpose of mechanics is to explain and predict physical phenomena and thus to lay the foundations for engineering applications.

unquote

The mechanics we are talking about here is the so-called classical or Newtonian mechanics. During the early part of the twentieth century it was found that classical mechanics did not correctly predict phenomena at velocities close to the speed of light, nor at the microscale of the atom. These observations have led to the formulation of two new forms of mechanics in modern physics, i.e. relativistic mechanics and quantum mechanics, respectively. However, these two new forms of mechanics do not play a role in engineering.

Classical mechanics is a large field that can be subdivided into a number of different parts, each of which has over time developed along different paths making it seem as if they are altogether separate branches of science or engineering. However, this is not really so. The diagram shown in figure B.1 overleaf gives an overview of the whole field of classical mechanics.

Kinematics (Dutch: 'kinematica') is a part of mechanics that deals with the study of motions without regard to their causes. Kinetics (Dutch: 'kinetica'), on the other hand, deals with motions under the influence of forces.

Forces may be classified as point forces (these are idealised representations of actual forces), surface forces (these are distributed forces that act over a two-dimensional surface and are proportional to an area, i.e. the square of a dimension) and volume forces (these are distributed

---

[7] From "Vector Mechanics for Engineers", 3rd edition, 1977, by F.P. Beer and E.R. Johnson

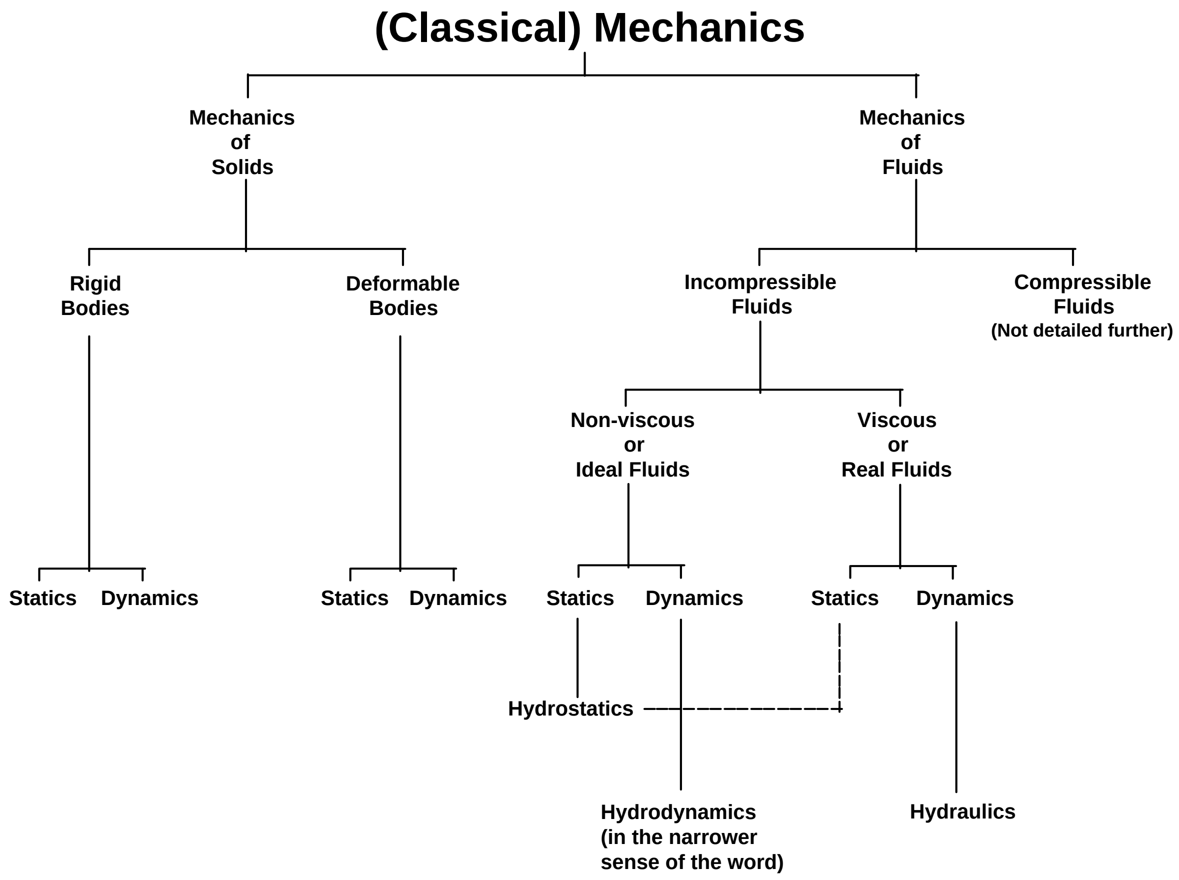

Figure B.1. An overview of classical mechanics

forces that act over a three-dimensional space and are proportional to a volume, i.e. the cube of a dimension). All forces that we will normally encounter are the result of some mechanical action. Electromechanical forces (electrical or magnetic forces) play no role in offshore engineering. Hereafter the word forces will be used in a more general sense to include moments as well.

B.2 Mechanics of solids

Solids are subdivided into rigid bodies and deformable bodies. The mechanics of rigid bodies is sometimes also called ‘theoretical mechanics’, while the mechanics of deformable bodies is then by contrast called ‘applied mechanics’.

In the *mechanics of rigid bodies* there are only external forces. These may be divided into applied forces and reactions (e.g. support reactions). The mechanics of rigid bodies can be divided into statics and dynamics. In statics (Dutch: 'statica') the external forces are collectively always in equilibrium and the body is at rest. In dynamics (Dutch: 'dynamica') the external forces are not in equilibrium. The resultant or net force causes the body to accelerate (or decelerate) and thereby to change its state of motion. The motion can be a rectilinear or a rotational motion, or both.

In the *mechanics of deformable bodies* there are external as well as internal forces. The internal forces arise as a result of the resistance of a body to deformation, i.e. resistance to the relative movement of one part of the body to another. These internal forces are generally called elastic forces, regardless of whether they remain within the elastic region or are well into the plastic regime. The resistance of a body to deformation depends on the material from which it is made and is studied in the mechanics of materials. This and the theories of elasticity and plasticity are all parts of the mechanics of deformable bodies.

The mechanics of deformable bodies is formulated using a number of basic hypotheses, of which the assumption that plane sections remain plane during deformation is a very important one. It can again be divided into statics and dynamics. In *statics* the body as a whole as well as all parts of the body are at rest and the forces are once more in equilibrium.
Considering the *body as a whole*, there must be equilibrium of the applied forces and the (support) reaction forces, just as in the case of rigid bodies. The difference is that for deformable bodies the reaction forces cannot always simply be obtained from the equilibrium equations (3 if the forces all act in one plane, 6 in the general case of a body in space). It may be necessary to supplement the equilibrium equations with *global* relationships derived from the deformation of the body. This distinguishes statically determinate (Dutch: 'statisch bepaalde') from statically indeterminate (Dutch: 'statisch onbepaalde') problems.
Considering a *part of the body*, there must be equilibrium between the applied forces and the internal or elastic forces. The internal forces may again be found from the equilibrium equations, where necessary supplemented with *local* relationships associated with the deformation of the part(s) concerned, depending on the static (in)determinacy of the problem.

In *dynamics of deformable bodies* a part of the body moves with respect to another part of the body. As for rigid bodies, there is now no equilibrium and the resultant or net force causes the relevant part of the body to accelerate and change its state of motion. As the part concerned is connected with other parts of the body, these other parts are forced to participate to a greater or lesser degree in the motion of the first part; thereby the parts exert forces on one another and influence what happens to them.

In dynamic problems of deformable bodies the body as a whole may or may not move with respect to its average position in space. In most cases of practical interest in Offshore Engineering the body will be supported by or be connected to earth in some manner so that its average position is fixed. In some cases the body may be subject to global motions as well as local deformations. In these cases the local deformations are nearly always small compared to the global displacements and therefore they may be neglected for determining the global motions. Under these circumstances the overall problem can conveniently be divided into two separate sub-problems, i.e. the body can be treated as a rigid body in solving for the global motions and as a deformable body in solving for the local motions about a time dependent mean position of the rigid body in space.

In general, dynamics are due to the fact that the applied forces vary with time. Time variation of forces should then be understood to refer to their magnitude, their direction or the location at which they act; usually it is the magnitude of the force(s) that is (are) a function of time. These problems belong to the class of forced oscillations. However, bodies may also be in a state of motion without any applied forces being present. In these cases the reaction forces and the internal forces in a deformable body vary with time and are able to sustain the motion, after an initial disturbance from equilibrium causes it to start. There is no energy supplied to the system and if there are no energy losses (no damping) there is a continuous exchange from potential into kinetic energy of (parts of) the body and vice versa. These motions are called ‘eigen motions’. They can only occur at certain frequencies (the ‘eigen’ or natural frequencies) and in certain patterns (the ‘eigen’ or natural modes). There are as many natural frequencies and natural modes as there are degrees of freedom for the body.

If (a part of) a body is in motion there are two types of additional forces being generated as a result of the motion. These are inertial forces and damping forces. In some cases the motions are so slow that the inertial and damping forces are very small compared to the other forces present (i.e. the applied forces, the reaction forces and the elastic forces, where applicable, all of which vary with time), so that they may be neglected. The problem is then said to be quasi-static.

B.3 Mechanics of fluids

The mechanics of fluids concern both fluids and gases. Fluid is often used as a general word to describe non-solid media. The difference between what we normally call a fluid in a narrower sense and a gas lies in only its compressibility. Fluid mechanics, therefore, includes hydromechanics and aeromechanics.

We may thus divide fluids into *incompressible* and *compressible* fluids, the latter being what we normally refer to as gases. However, in many problems of practical interest the compressibility is an insignificant feature and may be neglected. Gases then behave in exactly the same manner as fluids. As compressible fluids hardly play a role in Offshore Engineering these will not be discussed any further. Within the group of incompressible fluids we may further distinguish *non-viscous or ideal fluids* and *viscous or real fluids*. Both classes can next be subdivided again into statics (hydrostatics, and more generally also aerostatics) and dynamics (hydrodynamics, aerodynamics).

Viscosity only plays a role when a fluid is in motion, i.e. in dynamics. Therefore the *statics* of ideal fluids and of real fluids are the same. However, the dynamics of ideal and real fluids differ substantially. The *dynamics of ideal fluids* are commonly called hydrodynamics in the narrower sense of the word, while the *dynamics of real fluids* are often referred to as hydraulics. The relationship between these two branches of fluid mechanics and the historical development of each is very clearly described by Prandtl and Tietjens [8]:

quote
Although in classical and medieval times there was a certain amount of interest in hydrodynamics and more especially in hydrostatics, as is testified by the existence of the law of Archimedes, and although this knowledge was advanced by the work of Stevin, Galileo, and Newton, it is Leonhard Euler who is justly recognised as the father of hydromechanics. To him we owe our clear ideas on fluid pressure, and it was through his grasp of this fundamental concept that he later propounded the equations of motion bearing his name. He was a great theoretical mathematician, yet he brought his genius to bear on such technical matters as the construction of turbines.

But the great growth in technical achievement which began in the nineteenth century left scientific knowledge far behind. The multitudinous problems of practice could not be answered by the hydrodynamics of Euler; they could not even be discussed. This is chiefly because, starting from Euler's equations of motion, the science had become more and more a purely academic analysis of the hypothetical frictionless "ideal fluid". This theoretical development is associated with the names of Helmholtz, Kelvin, Lamb, and Rayleigh.

---

[8] From the Introduction in “Fundamentals of Hydro- and Aeromechanics”, by L. Prandtl and O. Tietjens, Dover Publications Inc, New York; reprinted in 1957 as an unaltered reproduction of the first edition of 1934.

The analytical results obtained by means of this so-called "classical hydrodynamics" usually do not agree at all with the practical phenomena. To such extremely important questions as the magnitude of the pressure drop in pipes, or the resistance of a body moving through the fluid, theoretical hydrodynamics can only answer that both pressure drop and resistance are zero. Hydrodynamics thus has little significance for the engineer because of the great mathematical knowledge required for an understanding of it and the negligible possibility of applying its results. Therefore the engineers - such as Bernoulli, Hagen, Weissbach, Darcy, Bazin, and Boussinesq - put their trust in a mass of empirical data collectively known as the "science of hydraulics", a branch of knowledge which grew more and more unlike hydrodynamics.

While the methods of classical hydrodynamics were of a specially analytical character, those of hydraulics were mostly synthetic. Hydrodynamics began with certain simple principles and, having made certain assumptions about the mechanical properties of fluids, attempted to formulate the behaviour of the whole fluid mass from that of its elements. Hydraulics proceeded quite differently; it started out from the simple facts of experience and tried to explain complicated processes in terms of these. Hydrodynamics was built up on simplified natural laws, hydraulics on natural phenomena.

This difference in the outlook and method of the two sciences is connected with the difference in their purposes. In classical hydrodynamics everything was sacrificed to logical construction; hydraulics on the other hand treated each problem as a separate case and lacked an underlying theory by which the various problems could be correlated. Theoretical hydrodynamics seemed to lose all contact with reality; simplifying assumptions were made which were not permissible even as approximations. Hydraulics disintegrated into a collection of unrelated problems; each individual problem was solved by assuming a formula containing some undetermined coefficients and then determining these so as to fit the facts as well as possible. Hydraulics seemed to become more and more a science of coefficients.

Toward the end of the nineteenth and the beginning of the twentieth century a new critical spirit appeared in both sciences. The rapid growth of aeronautics and turbine engineering created a demand for more fundamental knowledge than "hydraulics" could provide. On the other hand, there grew up, among the physicists, a more realistic attitude associated especially with the great name of Felix Klein, having for its object a restoration of the unity between pure and applied science. Under these two influences, great progress was made in the synthesis of hydrodynamics and hydraulics.

It will be clear from these remarks about the evolution of hydrodynamics in what manner the subject will be treated here. The relation between theory and practice will always be kept in the foreground. Theory will not be detached from the facts of experience but will be put in its proper relation to them. Experimental results, on the other hand, will be considered in their relation to the fundamental laws and underlying theory.
unquote

B.4 Mechanics of Soils

Soils are granular materials. They consist of discrete particles that are relatively free to move with respect to one another. Much more so than in a solid where the particles (e.g. the crystals in a metal) are strongly bonded together, but on the other hand much less so than the elements in a fluid. The soil particles themselves are solid material (rigid or deformable bodies, as the case may be) while the pores between the particles are filled with a fluid. Thus, soil mechanics has to deal with a system of solids (which is sometimes referred to as a *particulate system*) with a fluid in the pores between the solids. The deformation of a soil mass will be partly due to the deformation of individual particles and partly to sliding of the particles along one another, followed by their rearrangement within the soil mass as a whole. The effect of rearrangement is generally by far the more important of the two contributions. As this is an irreversible process, deformation under loading is a non-linear phenomenon.

In the formulation of soil mechanics concepts from both solid mechanics and fluid mechanics are used. Due to the particulate structure of a soil mass with its associated non-linear behaviour and the two phases involved (solids and a fluid), it can easily be appreciated that soil mechanics is the youngest branch of mechanics. The basis was developed and formulated by Terzaghi in the 1920s; Terzaghi is often called the 'father of soil mechanics'. It is still a very empirical science, its development having distinct similarities with the development of hydraulics as described by Prandtl and Tietjens in section B.3.

Soil mechanics is clearly also a branch of mechanics, but its place in the diagram presented in figure B.1 cannot so simply be identified. As regards the distinction of statics and dynamics, soil mechanics is in practice nearly exclusively dealt with in a static or quasi-static manner.

Annex C – Use of models in practical applications

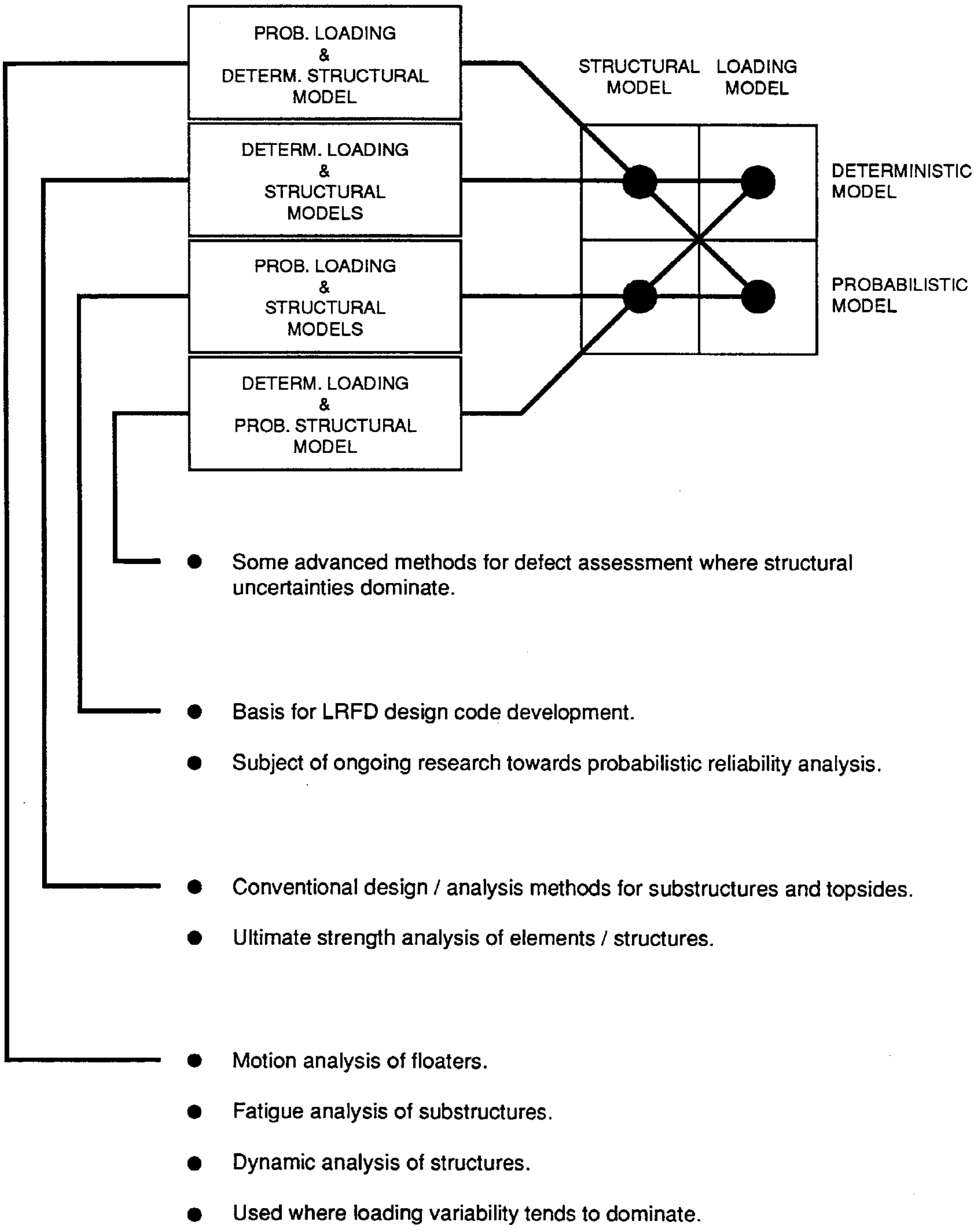
PROB. LOADING & DETERM. STRUCTURAL MODEL
DETERM. LOADING & STRUCTURAL MODELS
PROB. LOADING & STRUCTURAL MODELS
DETERM. LOADING & PROB. STRUCTURAL MODEL
STRUCTURAL MODEL
LOADING MODEL
DETERMINISTIC MODEL
PROBABILISTIC MODEL

- Some advanced methods for defect assessment where structural uncertainties dominate.

- Basis for LRFD design code development.
- Subject of ongoing research towards probabilistic reliability analysis.

- Conventional design / analysis methods for substructures and topsides.
- Ultimate strength analysis of elements / structures.

- Motion analysis of floaters.
- Fatigue analysis of substructures.
- Dynamic analysis of structures.
- Used where loading variability tends to dominate.

Figure C.1. Use of deterministic and probabilistic models in practical applications

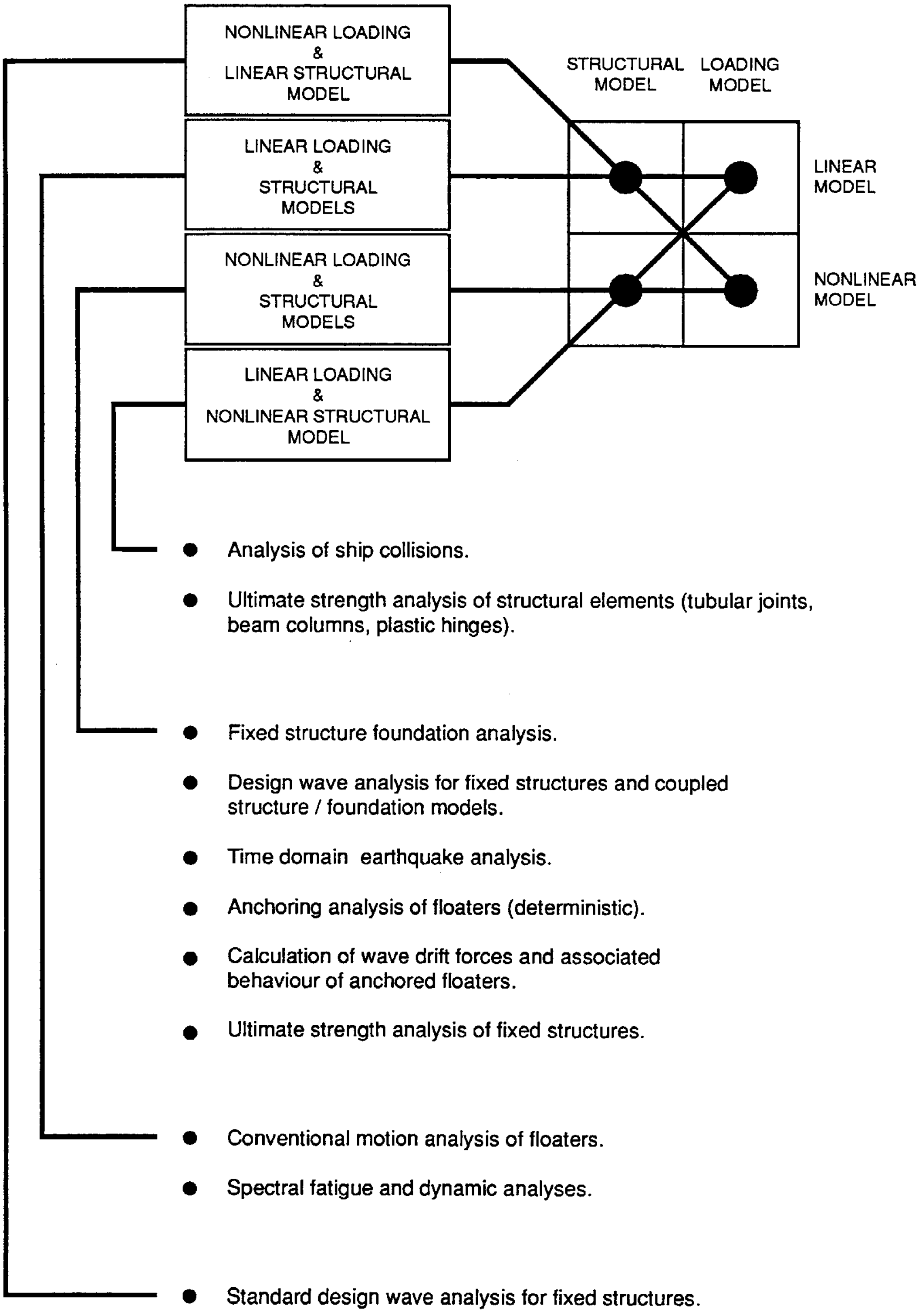
NONLINEAR LOADING & LINEAR STRUCTURAL MODEL
LINEAR LOADING & STRUCTURAL MODELS
NONLINEAR LOADING & STRUCTURAL MODELS
LINEAR LOADING & NONLINEAR STRUCTURAL MODEL
STRUCTURAL MODEL
LOADING MODEL
LINEAR MODEL
NONLINEAR MODEL

- Analysis of ship collisions.
- Ultimate strength analysis of structural elements (tubular joints, beam columns, plastic hinges).

- Fixed structure foundation analysis.
- Design wave analysis for fixed structures and coupled structure / foundation models.
- Time domain earthquake analysis.
- Anchoring analysis of floaters (deterministic).
- Calculation of wave drift forces and associated behaviour of anchored floaters.
- Ultimate strength analysis of fixed structures.

- Conventional motion analysis of floaters.
- Spectral fatigue and dynamic analyses.

- Standard design wave analysis for fixed structures.

Figure C.2. Use of linear and non-linear models in practical applications

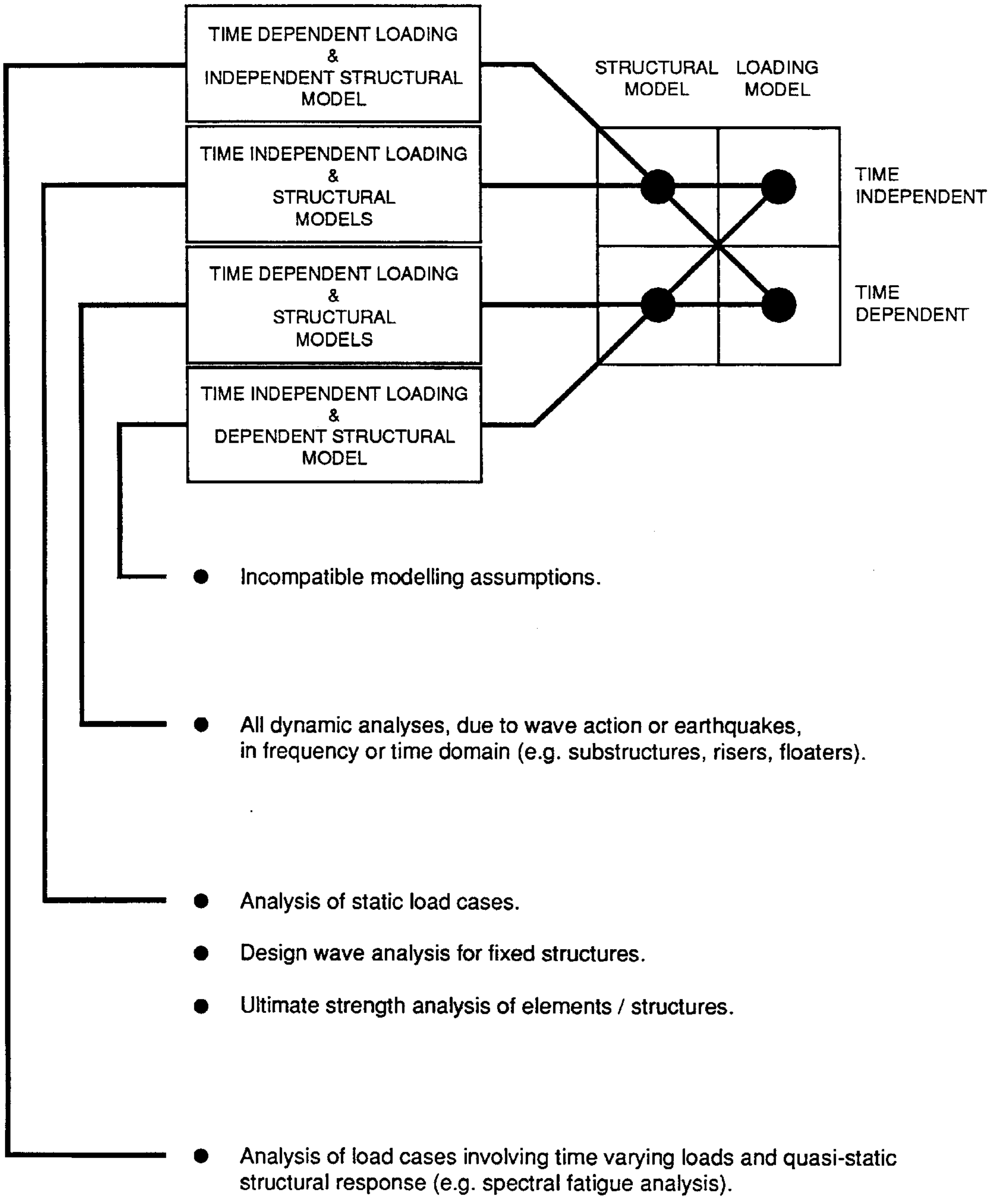
TIME DEPENDENT LOADING & INDEPENDENT STRUCTURAL MODEL
TIME INDEPENDENT LOADING & STRUCTURAL MODELS
TIME DEPENDENT LOADING & STRUCTURAL MODELS
TIME INDEPENDENT LOADING & DEPENDENT STRUCTURAL MODEL
STRUCTURAL MODEL
LOADING MODEL
TIME INDEPENDENT
TIME DEPENDENT

- Incompatible modelling assumptions.
- All dynamic analyses, due to wave action or earthquakes, in frequency or time domain (e.g. substructures, risers, floaters).
- Analysis of static load cases.
- Design wave analysis for fixed structures.
- Ultimate strength analysis of elements / structures.
- Analysis of load cases involving time varying loads and quasi-static structural response (e.g. spectral fatigue analysis).

Figure C.3. Use of time (in)dependent models in practical applications

4 THE OFFSHORE ENVIRONMENT AND ENVIRONMENTAL LOADING

4.1 A general discussion of the offshore environment

The three different parts of the environment are the atmosphere, the ocean and the sea floor. The two interfaces between these three layers merit special consideration. Especially the interface between the atmosphere and the ocean at which surface gravity waves develop is of very great importance.

The *sea floor* is the only part of the environment that consists of solid material and represents 'fixed earth'. It provides the foundation for bottom-supported structures and a fixed point of attachment for the anchoring of floating structures. This is the domain of offshore geotechnical engineering, a rather specialised branch of mechanics for which reference is made to e.g. [4.1-1] to [4.1-3]. Where appropriate, some general discussion of geotechnical and foundation issues will be included at relevant places in this handbook. For the present discussion it suffices to summarise the most important factors that are associated with the sea floor and are important for the design and assessment of offshore structures:

- soil type, parameters and stratigraphy;
- geological faults;
- active geological processes (e.g. earthquakes, mud slides, shallow gas deposits);
- sediment transport at the surface (e.g. sand ridges);
- surface erosion (scour) around an object;
- (reservoir) subsidence;
- obstacles (e.g. boulders, anchors, pipelines, wrecks).

The *atmosphere* and the *ocean* consist of a gas (air) and a fluid (water). When the air and the water are at rest, density controls the pressures that provide the loads governing static equilibrium of an object placed in either medium; both for a rigid and for a deformable body. However, in the usual situation the atmosphere and the ocean are not at rest. The flow condition is then an important additional factor in governing the mechanical actions that affect the behaviour of offshore structures. Meteorological and oceanographic (together often abbreviated to metocean) conditions that are important for the design or assessment of offshore structures are:

- wind velocity and its variation in time and space (particularly over height);
- water depth;
- tides;
- storm surge;
- current velocity and its variation in time and space (particularly over depth);
- waves and their variation in time and space;
- marine growth;
- air and water temperature (normally only for material selection);
- snow and ice.

The air and water temperature are important for material selection as the properties of steel and most other materials (such as their yield strength and brittleness) depend on temperature. An example of the problems that can develop in this respect are the brittle fractures of allied forces Liberty and Victory ships, some of which suddenly broke into two when they were en route to Murmansk, a harbour in the north of Russia, during the second World War. A relatively high water temperature further increases corrosion rates, thus having an influence on corrosion protection requirements, while warm water is also more oxygen rich than cold water, which promotes marine growth.

All offshore structures are exposed to the environmental actions of wind, current and waves, albeit to different degrees. These conditions produce substantial environmental loadings on the structure that nearly always need to be carefully considered and accounted for in their design. In many situations the directions of wind, current and waves are clearly related to one another. Wind seas are e.g. generated by the local wind and the waves would thus tend to propagate more or less in the mean wind direction. Similarly, strong winds will produce a wind driven current component, which will again proceed in the general direction of the wind. However, other current components (e.g. due to tide) have no relationship to the local wind whatsoever. Furthermore, various local circumstances such as the presence of a coastline, bottom topography and general ocean circulations exert their influence. Generally therefore, wind, current and wave directions are not collinear, even though this may be assumed to be the case in design conditions by lack of better information, or simply for convenience. It should expressly be noted that the directions by which these environmental conditions are indicated are subject to age-old and different conventions. The wind direction is denoted by the direction *from* which the wind is blowing, while current and waves are denoted by the direction *towards* which they proceed. For example, a northerly wind blows from north to south, whereas a northerly current and northerly waves proceed form south to north! This is a difference that engineers must be very much aware of to avoid potential errors in the interpretation and use of data presented to them.

In some cases other phenomena than wind, current and waves also need to be considered. The most common of these are earthquakes in seismically active areas; mud slides on sloping sea floors, e.g. in certain parts of the Gulf of Mexico; sea ice at high latitude locations, especially on the northern hemisphere; and the possible accumulation of snow and ice on the superstructure.

In sections 4.2, 4.3 and 4.4 wind, current and wave models are described, respectively. These descriptions focus on a discussion of the main features of the environmental conditions in relation to the global environmental loadings experienced, together with the associated global responses of the structure due to these loadings. This is followed by a discussion of the mechanisms of aero- and hydrodynamic loading in sections 4.5 and 4.6. The aim of these discussions is to promote understanding of the environmental phenomena and their influences, so that appropriate models can be chosen or developed for any practical application. There will be only limited discussion of the detailed physical and / or mathematical formulations of the respective models; for such details the reader is referred to the available textbooks.

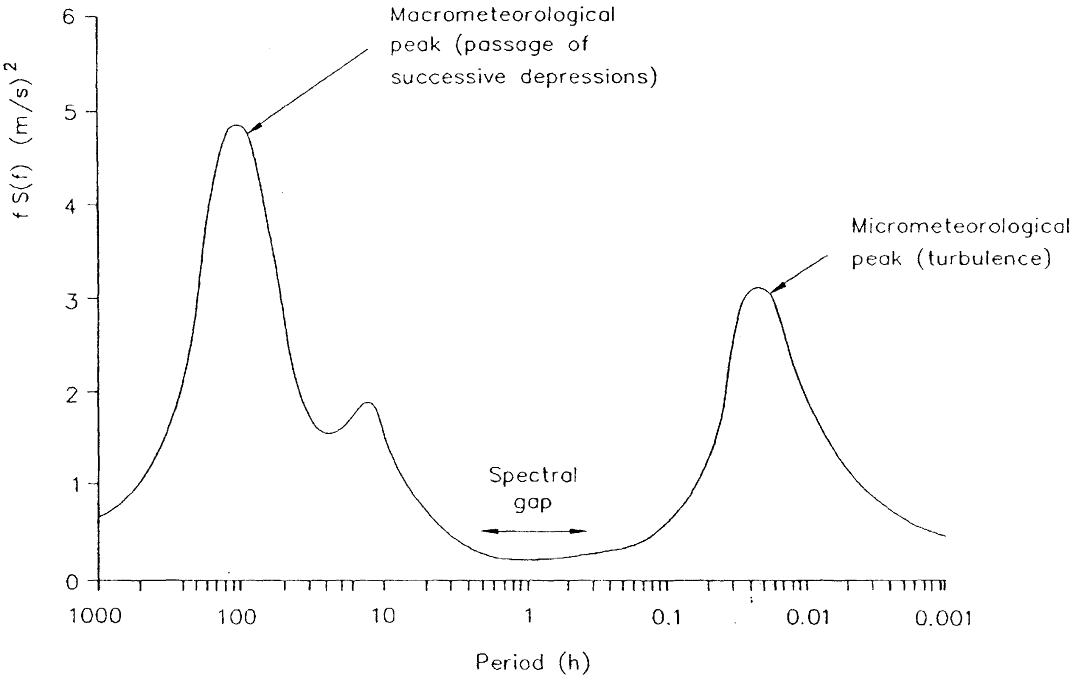

Figure 4.2-1. Energy spectrum of wind velocity after Van der Hoven (from [4.2-1])

4.2 Wind model

Wind is a turbulent flow of air; wind speed and direction vary in space and time. At a particular point in space wind may be considered to consist of a steady mean flow with an associated mean direction, and speeds that vary in time and direction around this mean. The velocity can thus be written in the form of the following vector equation:

$$\underline{U_{wi}}(x,y,z;t)=\underline{U_w}(x,y,z)+\underline{u_w}(x,y,z;t) \tag{4.2-1}$$

where: $\underline{U_{wi}}$ = local and instantaneous wind velocity vector

$\underline{U_w}$ = mean wind velocity vector at point (x,y,z), which is constant in magnitude and direction over a period of time that is long compared to the time t

$\underline{u_w}$ = turbulent wind velocity vector around the mean velocity $\underline{U_w}$ at point (x,y,z); $\underline{u_w}$ varies in magnitude and direction as a function of time, while the time average of $\underline{u_w}$ is by definition zero.

There is normally insufficient data available to describe the spatial and time variations in great detail, while for most applications this is also unnecessary. Therefore, descriptions of the wind field are usually substantially simplified in that wind parameters are described in statistical terms such as the mean and the standard deviation of the speed as well as the direction. For the definition of such statistical parameters both length scales and time scales are needed.

Let us first consider the variation in time. When very long records of wind velocity are analysed it turns out that there are short-period variations due to turbulence, with periods ranging mainly from a few seconds to some 6 minutes, and long-period variations with periods ranging from several hours to many days. Figure 4.2-1 shows a typical power spectrum of the wind velocity determined by Van der Hoven [4.2-1] that clearly shows both variations. The long-term variations show a lower peak at around 12 hours associated with the daily thermal cycle and a higher peak at some 100 hours or 4 days, due to the succession of pressure systems passing the measurement station at the time that the measurements were taken. The figure further shows that the two variations are clearly separated by a spectral gap, i.e. a range of low wind energy, around a period of 1 hour. Therefore 1 hour is a suitable period for averaging of wind speeds (and directions). The long period variations will then manifest themselves as slow changes of the mean velocity $\underline{U_w}(x,y,z)$, while the short-period variations are rapid fluctuations $\underline{u_w}(x,y,z;t)$ about $\underline{U_w}(x,y,z)$.

As to the spatial variation, observations show that on length scales that are typical of an offshore structure (even the largest ones) the mean and standard deviation of the wind speed and direction, averaged over durations of the order of an hour or so, do not vary horizontally. However, vertically they differ with elevation above the ground or above mean sea level (MSL). Therefore, the mean velocity vector $\underline{U_w}(x,y,z)$ can conveniently be described as a scalar quantity $U_w(z)$ in the mean wind direction θ_w. This is called the steady state wind velocity at elevation z.

Due to its variability in space and time a wind velocity value is only meaningful if it is qualified by its elevation as well as the duration over which it is averaged. With regard to time averages wind velocities are classified as either:

- sustained wind velocities, which are averages over 1 minute or longer;
- wind gust velocities, which are averages over less than 1 minute.

The mean velocity determined by averaging the wind velocity $\underline{U_{wi}}(x,y,z;t)$ at a height of 10 m above MSL over a duration of 1 hour is used as a standard reference value U_{w0}. For shorter averaging durations than 1 hour there will clearly be periods in which the mean wind velocity is higher. Examples are the 10 min. sustained wind, the 1 min. sustained wind and the 3 s wind gust velocity.

The fluctuating velocity $\underline{u_w}(x,y,z;t)$ for t appreciably shorter than the averaging duration is usually referred to as a wind gust. It reflects the local turbulence in the atmospheric conditions. Detailed information about the full structure of the turbulent wind field will rarely be available. Therefore the spatial variation of $\underline{u_w}(x,y,z;t)$ is generally assumed to be similar to that of the sustained wind. In other words, $\underline{u_w}(x,y,z;t)$ is assumed to be a horizontal velocity in the same direction as the mean wind with a vertical profile, i.e. it reduces to the scalar quantity $u_w(z;t)$. As a function of time $u_w(z;t)$ varies randomly about a zero mean in an approximately gaussian manner. Further and more detailed information about mean and gust wind may e.g. be found in references [4.2-2] to [4.2-4].

The importance of wind for the global environmental loading on offshore structures differs with the type of structure and the nature of a structure's response (quasi-static or dynamic). Fixed structures are usually rather stiff and tend to respond quasi-statically to the environmental actions. Furthermore, wind loads form only a small contribution to the total environmental loads on these structures, typically less than some 15%. Hence a very simple wind model and a sustained velocity $U_w(z)$ are adequate characterisations of the wind field for calculating global wind loads on these structures. The 10 min or even the 1 hr sustained wind is usually an appropriate wind velocity to determine wind loading that is concurrent with the dominant wave and current loading. In case of doubt, or where a fixed structure experiences some dynamic response, the 1 min sustained wind may conservatively be used. For the quasi-static design of parts of the superstructure it should be observed that the three-dimensional spatial scales of wind turbulence in gusts varies with the duration of the gusts. For example, a 15 s gust is coherent over larger distances and thus affects larger elements than a 3 s gust. Local loads should hence be calculated using a shorter averaging duration than global loads. For individual structural members a 3 s gust velocity should preferably be used, while for parts of the superstructure with horizontal dimensions less than some 50 m the 5 s gust velocity is more appropriate. For larger parts the 15 s gust velocity can be considered to be adequate.

Fore compliant bottom founded structures, floating structures and mobile offshore units the response to wind action should be considered much more carefully and in much greater detail where appropriate . For floating structures mean wind loads are clearly important for their station keeping ability. These mean loads must be compensated by anchorline forces or the forces produced by thrusters; they determine the (static) equilibrium position of the floater. In view of the long natural periods of the horizontal motions of floating structures the 10 min

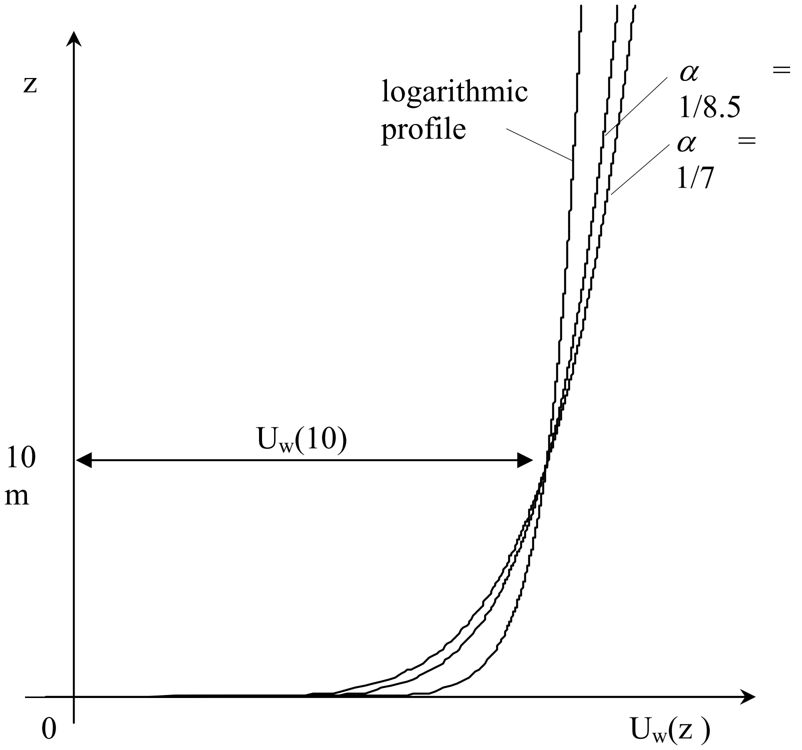

Figure 4.2-2. Vertical profile of steady wind velocity, according to equations 4.2-2 and the logarithmic profile in Annex A.

sustained wind will usually be an appropriate choice for such applications. Finally, for structures that respond truly dynamically to wind action the time and spatial variation of the wind speed and its direction can be very important, especially when the wind field contains energy at frequencies close to a natural frequency of the structure. Therefore, the wind model to be used in such cases will likely need to be much more detailed to account for such variation. This requires knowledge of turbulence intensity, wind spectra and spatial coherence.

Structure types that may exhibit *global* dynamic response include compliant bottom founded structures and floating structures, i.e. 4 of the 5 types distinguished in chapter 2. Individual structural elements and structural parts such as masts and flare or communication towers may be subject to *local* dynamic response. The design of such elements and parts will therefore generally need to be based on their dynamic response to wind action.

The vertical profile of the mean wind speed has traditionally been expressed in the form of a power law:

$$U_w(z) = U_w(10) \cdot \left(\frac{z}{10} \right)^{\alpha} \tag{4.2-2}$$

where:

$U_w(z)$	=	mean (sustained or gust) wind speed at z m above MSL	[m/s]
$U_w(10)$	=	mean (sustained or gust) wind speed at 10 m above MSL (both averaged over the same time interval)	[m/s]
z	=	vertical distance above MSL	[m]
α	=	an exponent depending on the roughness of the terrain over which the wind is blowing	[-]

For onshore conditions the exponent α is of the order of 1/7 (0.14). At sea the terrain is flatter than on land so that the wind profile is steeper with a correspondingly lower value of α of the order of 1/8.5 (0.12).

A theoretically preferred and more correct description of the vertical profile is based on a logarithmic function; see Annex A. For illustration, the wind profiles according to the power law profile of equation 4.2-2 (for both exponents of α) and the logarithmic profile of Annex A are shown in figure 4.2-2. As a result of the empirical nature of the wind field description, adjustments to the wind profile at a particular location or under certain conditions may be made when specific measured data from offshore locations are available.

As discussed, in many applications the time varying component $u_w(z;t)$ is an unnecessary sophistication and can be ignored, reducing the wind model to the steady wind with a vertical profile only. There are three main reasons why such a gross simplification is often entirely adequate. These are:

1) The mean wind velocity and hence the steady mean wind load is usually rather large compared to the fluctuating velocity and the fluctuating load. Additionally, the steady load is correlated over the full exposed area as opposed to the fluctuating load, where the degree of correlation depends on the relative dimensions of the object and the atmospheric turbulence. As a result, the fluctuating loads on separate parts of the exposed area will tend to partly cancel one another, thus being of more local than global importance.
2) The time varying wind loads are small compared to the time varying wave loads, which is mainly due to the density of air being roughly a factor 800 times smaller than the density of water.
3) The periods contained in the fluctuating wind velocities and hence in the fluctuating wind loads range from a few seconds to several minutes, with most energy concentrated around a few minutes (see figure 4.2-1). The wind energy is therefore mainly concentrated at rather low frequencies that are generally outside the practical range of interest for most offshore structures. Exceptions to this may be long periodic motions of anchored floating vessels and the rigid body motions of compliant bottom supported structures. In these cases the wind load excitation may be an additional and important source of excitation, resulting in significant resonant response of a lightly damped system.

4.3 Current model

Currents are created by astronomical forces (resulting in tides), by the wind stress on the ocean surface (causing wind drift currents) and by both horizontal and vertical density gradients due to differences in temperature or salinity. The horizontal density gradients are caused by the variation in solar heating of the ocean between the equator and the higher latitudes nearer to the poles. The forces on the water masses caused by these density gradients, together with the Coriolis forces due to the earth's rotation, are the joint primary forcing mechanism for the large-scale ocean circulations. An example of such a circulation is the Gulf Stream, but there are many other ones. Due to differences in the horizontal velocities within and along the edges of such streams, large scale eddies may be formed, which cause more or less circular patterns of secondary horizontal flow deviating from the global circulation. In areas where these occur the magnitude and direction of current velocities may be markedly different from the main stream velocity and may further differ from one location to another. Vertical density gradients have the same effect and may also manifest themselves in (potentially highly variable) currents of different magnitude and direction, depending on the strength and scale of the circulation patterns developing. Additionally, local topography, river outflows and local wind stress can create perturbations to the general current flow in an area.

In principle, current velocities also vary in space and time as wind velocities do. However, the horizontal length scales as well as the time scales of the variations in current velocity are much larger than those for wind. They are also large compared to the horizontal dimensions of an offshore structure and compared to the range of periods of interest for determining a structure's behaviour. Therefore currents may generally be considered as a horizontally uniform flow field of constant velocity, which is only a function of the vertical co-ordinate z. In most cases this is a realistic description rather than a fairly crude approximation of actual conditions, as is the case for wind. The vertical profile of the current velocity over the water depth depends on the relative importance of the various factors that contribute to the current. The resulting profile is empirical and can look rather strange, even involving counter currents at a certain depth. At different locations in the same geographical area the current profile can also be rather different. A reliable determination of the current velocity and direction over depth requires measured data and expert knowledge; for a particular location of interest it can therefore best be specified by an oceanographer.

Currents contribute to the hydrodynamic loading and can thus be important for the structural design of fixed structures and especially for the design of risers. They may further affect the location and orientation of appurtenances, such as boat landings and fenders. Additionally, they may cause sea floor scouring, which must be accounted for in the design of the foundation of a structure. As was the case for wind, current loads on floating structures must be counteracted by anchorlines or thrusters to stay on location. However, the most important influence of currents is often associated with their effect on marine operations, performed on or under the water surface. Examples of operations that can suffer severely from current action are drilling in deep water; the stabbing of piles in pile guides; the deployment of subsea equipment and risers; and operations by Remotely Operated Vehicles (ROV's).
By lack of more specific information for a particular site, current models for structural design will usually define a simple current profile over depth. Typical current profiles $U_c(z)$ used in practice are:

- a power law analogous to equation 4.2-2 from the sea floor upwards and an exponent of 1/7. The power law profile can be formulated as follows:

$$U_c(z) = U_{c0}\left(\frac{z'}{d}\right)^{\alpha} = U_{c0}\left(\frac{z+d}{d}\right)^{\alpha} \quad (4.3\text{-}1)$$

where: z' = the vertical co-ordinate, measured positively upwards from the sea floor
z = the vertical co-ordinate, measured positively upwards from mean sea level
$(z = z' - d)$
d = the storm mean water depth
$U_c(z)$ = the current velocity at elevation $0 \le z' \le d$ or $-d \le z \le 0$
U_{c0} = the current velocity at the water surface for $z' = d$ or $z = 0$
α = an exponent

- a linear distribution between the surface velocity U_{c0} and a bottom current equal to one half the surface current;
- a bilinear distribution with parameters determined for the location.

Currents and waves usually occur together. Their flows may thus influence one another, which is a topic of interest in oceanography and hydrodynamics that will not be discussed here any further. There are two main interactions between current and waves that need to be taken into account for structural design. The first is the effect of their co-existence on the hydrodynamic loading due to the combined current and wave orbital velocities impacting on a structure. This will be discussed further in sections 4.5 and 4.6. The second is the shift in wave period or frequency in stationary and moving frames of reference due to the Doppler effect. This will be discussed in section 4.4.6.

4.4 Wave models

4.4.1 General introduction

There are many forms of waves in nature. Focusing on disturbances of the ocean surface, waves can be classified by their frequency of oscillation as shown in figure 4.4-1 reproduced from [4.4-1]. The waves of greatest interest for offshore structures are the gravity waves in the frequency range of approximately 0.03 to 1 Hz (periods of 1 to 30 s). Of the three environmental effects wind, current and waves, waves are normally by far the most important for offshore structures. They produce very large loads and contain a wide range of frequencies that have a significant influence on the quasi-static or dynamic behaviour of structures, fixed and floating alike.

An observer at a high vantage point above the sea looking down at the sea surface can take snapshots that provide a picture of the surface elevation as a function of (x,y) location, or he can focus on a fixed point and watch the surface elevation as a function of time. Combining these two pieces of information it will readily occur to him that there are three types of parameters to describe the surface. These are, firstly, the water surface elevation or height above the mean still water level; secondly, the distance between corresponding elevations in a snapshot (such as peaks or crossings of the still water level), or alternatively the time between the passing of equal elevations at a fixed point; and thirdly, the direction in which crest lines appear to propagate. All three parameters will in general be functions of (x,y) position as well as time t. The challenge is to formulate an appropriate model that describes the sea surface and also serves to derive the corresponding velocities and accelerations (the kinematics) of the water particles in the entire fluid domain.

Observations of the sea surface have long defied attempts to discern patterns that would lend themselves to any form of description at all. Physicists have therefore traditionally worked with highly idealised waveforms that are periodic in time and space. These form a well-researched two-dimensional problem in classical hydrodynamics that has been extensively discussed in many textbooks. The theory dates back to the 19th century and deals with propagating gravity waves on the surface of an ideal fluid that has no viscosity (no friction) while the flow is irrotational. These idealisations enable the introduction of a velocity potential from which the entire flow field can be derived. The fluid domain is bounded by two boundaries, i.e. the sea floor and the free surface. The boundary condition at the sea floor states that the water particle velocity normal to the bottom must be zero. At the free water surface there are two boundary conditions, i.e. a kinematic and a dynamic condition. The kinematic condition states that fluid particles on the surface will follow its movement and stay on the surface, so that the velocities of the particle and the surface must at all times be the same. The dynamic condition states that the pressure at the free surface is everywhere equal to the atmospheric pressure and hence a constant. These two boundary conditions are non-linear, but they are often linearised after which they can be combined into one linearised free surface condition that needs to be satisfied on the mean still water level instead of on the actual time varying free surface.

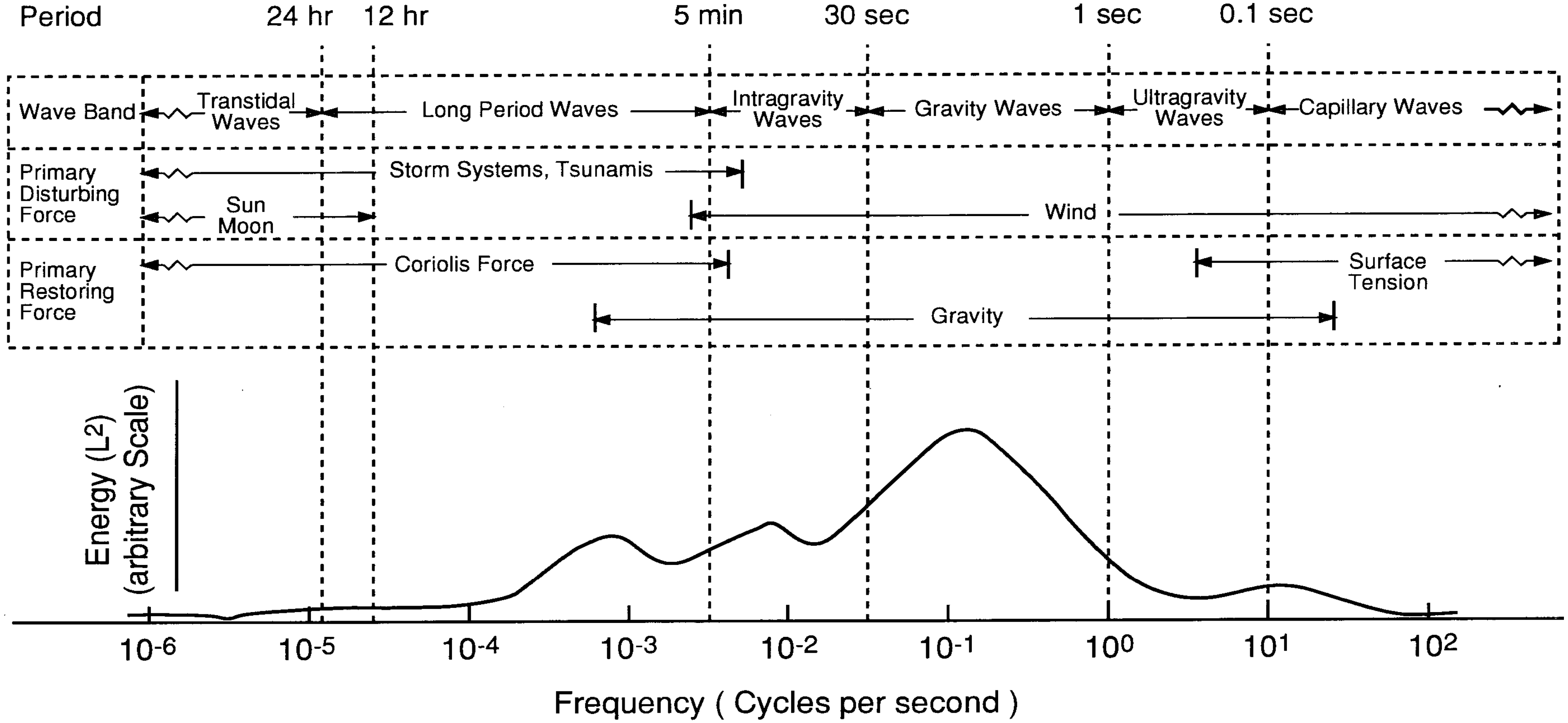

Figuur 4.4-1. Approximate distribution of ocean surface energy illustrating the classification of surface waves by wave band, primary disturbing force and primary restoring force (from [4.4-1])

It was only during and after the Second World War that an entirely new approach to waves emerged. This approach is based on the application of random noise theory, a statistical theory that was developed by Rice [4.4-2] to describe noise affecting the transmission of electrical signals. Application of this theory to gravity waves proved capable of giving a much more detailed description of the "chaos" of real waves at sea.

Following the above, there are two basic models to describe waves: a *periodic model*, which is deterministic, and a *random model*, which is statistical or probabilistic. Both models are in common use; each has its own advantages and disadvantages, and the choice for the most appropriate model in each application depends on circumstances and the intended purpose of a particular analysis.

4.4.2 Periodic wave models

The *periodic wave model* is based on idealised waveforms and dates back to the 19th century. Several theories have been developed, depending on the ratio of wave height to wave length (i.e. the wave steepness, which is an important parameter for linearisation) and on the ratio of water depth to wave length. For water depth to wave length ratios greater than 1/2 = 0.5 waves are deep water waves; for ratios smaller than 1/20 = 0.05 they are shallow water waves. For intermediate values the waves are in a transitional water depth range. Further information may be obtained from many textbooks, including e.g. [4.4-3] and [4.4-4]. The various theories have in common that they are all periodic in the wave period T and that they are two-dimensional. The theories differ in the fact that the theory is either linearised with respect to the free surface boundary condition or includes non-linear terms up to a particular order. As the theories are all periodic, the waveform and the associated kinematics field repeat themselves every T seconds. The wave model thus contains one single base frequency in the form of the wave frequency $\omega = 2\pi / T$. In case of a linear theory this is the only frequency present, in case of a non-linear theory there are higher harmonics with multiple frequencies $n\omega = n(2\pi) / T$ included as well. As periodic theories are two-dimensional, this further means that they all describe waves that have infinitely long crests and propagate in one direction.

Linearised periodic waves are sinusoidal in shape and thus symmetric with respect to a vertical line through the wave crest as well as the horizontal line of the mean still water level; they are called Airy waves after the British mathematical physicist who developed the theory first. Strictly speaking the Airy theory only applies to waves of infinitesimally small amplitude; it can be used in all water depths. The water particles describe closed orbits that are circular for deep water waves and elliptical for waves in intermediate water depths. The radius of the circle and the axes of the ellipse (long axis horizontal, short axis vertical) both decrease with depth below the free surface; see section 4.6. As the linearised free surface boundary condition is applied on the mean still water line the theory is not capable of predicting the kinematics up to the wave crest. A consistent set of formulae from the Airy water wave theory is given in Annex B to this chapter. For further discussion and more details reference is made to one of the many textbooks on water waves and their applications (e.g. [4.4-1, 3, 4, 5, 6, or 4.2-3]).

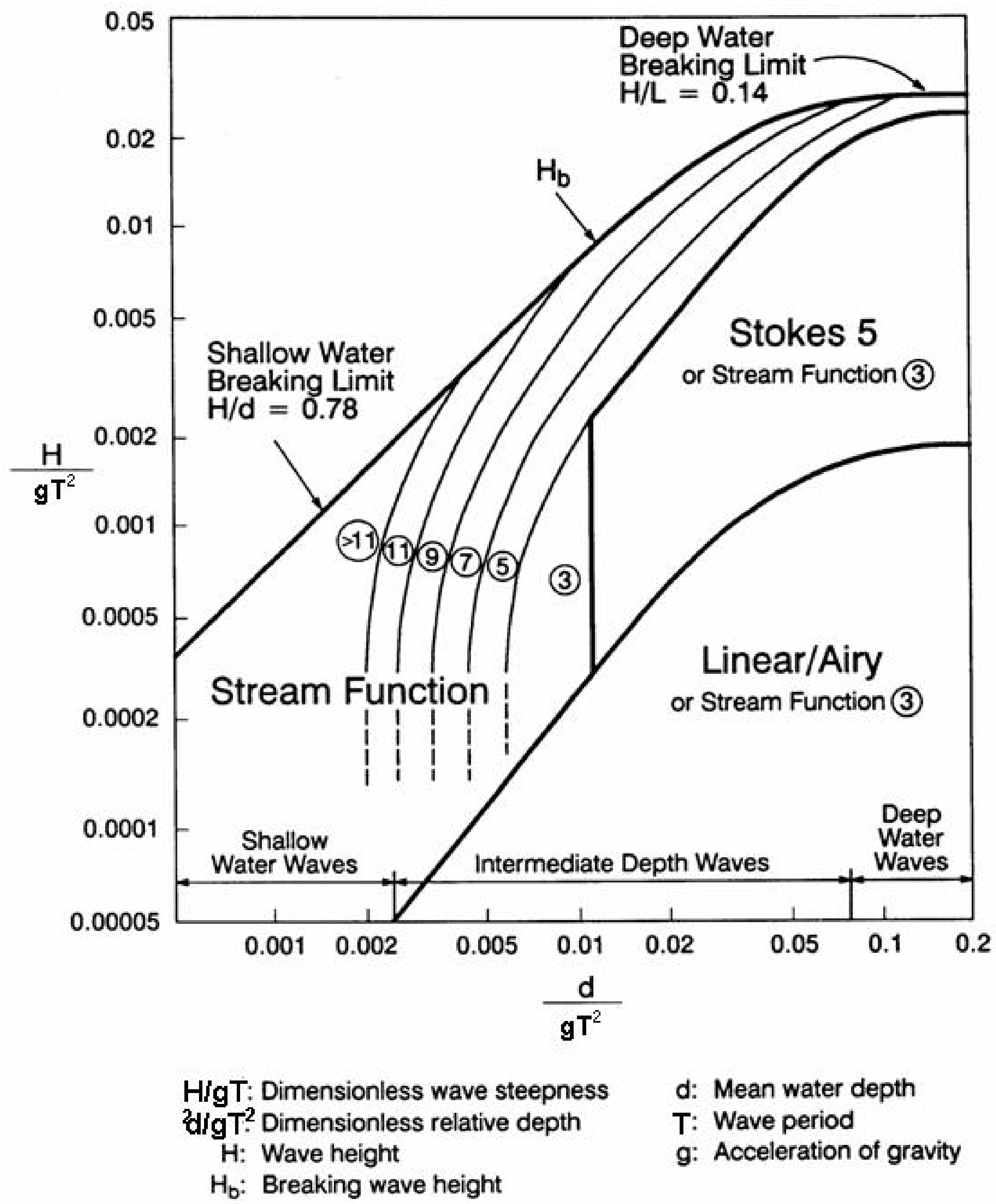

Figure 4.4-2. Diagram for the selection of an appropriate periodic wave theory (adapted from [4.4-7])

Non-linear periodic waves in deep or intermediate water depths are often described by one of the Stokes' higher order theories (e.g. up to the fifth order). These theories approximate the non-linear boundary conditions at the free surface in a much better way than the linear Airy theory does and are therefore capable of representing periodic waves of relatively large heights. The wave shape is now asymmetrical with respect to the mean still water level, with higher and more peaked crests and lower and flatter troughs. Symmetry with respect to a vertical line through the wave crest is maintained. There are several other non-linear theories than those of Stokes in practical use, for example Dean's range of stream function theories. The non-linear theories differ in their objective of which of the free surface boundary conditions by preference is satisfied best, and in the manner in which this is achieved. Stokes e.g. uses a 3rd or a 5th order expansion about the mean water level to satisfy both free surface boundary conditions as well as possible. Stream function theory on the other hand satisfies the kinematic boundary condition exactly, while minimising the errors in the dynamic boundary condition. Stream function theory is particularly suitable for relatively high and periodic waves in fairly shallow water; the order of the stream function theory is chosen on the basis of wave height and period in relation to water depth. Under the conditions described above Stokes theory is not very suitable and Dean's stream function theory is preferred. For (very) shallow water depths special wave models have been developed, such as cnoidal waves and solitary waves. Within the constraints of idealised, periodic and two-dimensional waveforms, an appropriately selected non-linear theory is in principle capable of a rather precise representation of the physical occurrences, such as the wave shape, the kinematics in the entire fluid domain, the speed of wave propagation, etc.

A wave theory selection diagram for periodic waves is presented in figure 4.4-2 [1] reproduced from [4.4-7]. Note that the parameter gT^2 that is used as a normalising factor on both axes is equivalent to the wave length λ . The general relationship is:

$$\frac{\lambda}{\tanh(2\pi d / \lambda)} = \frac{gT^2}{2\pi} \tag{4.4-1}$$

For a particular water depth, the wave period T is easily determined for any given wave length λ. However, the reverse is not true. For a given period T, equation 4.4-1 is an implicit relationship from which the wave length λ can only be determined by iteration using numerical procedures such as the Newton-Raphson method.

For deep water conditions $(d / \lambda > 0.5)$ the hyperbolic tangent approaches 1.0 ($\tanh \pi = 0.996$) so that:

$$\lambda \approx \frac{gT^2}{2\pi} \tag{4.4-2}$$

---

[1] For waves occurring on still water, or on a stationary current where the reference frame is moving with the current, the wave period is called the intrinsic wave period. The wave period that is observed by a stationary observer in the presnce of a curent is usually called the apparent wave period. These periods are different; see section 4.4.6. In some works these terms are unfortunately interchanged, which may cause considerable confusion and error. Regrettably, this is also the case in ref. [4.4-7]. However, figure 4.4-2 on the opposite page has been corrected for this and is therefore different from the same figure in [4.4-7]. The wave period in figure 4.4-2 is the intrinsic period $T = T_i$.

For shallow water conditions $(d / \lambda < 0.05)$ the hyperbolic tangent approaches $2\pi d / \lambda$ ($\tanh(0.1\pi) = 0.097\pi$) and:

$$\lambda^2 \approx gT^2 d \qquad \text{or} \qquad \lambda \approx T\sqrt{gd} \tag{4.4-3}$$

For the two limiting cases of deep and shallow water the relationship thus becomes explicit and the wave length follows directly from the wave period and the water depth using equations. 4.4-2 or 4.4-3, respectively. For the often occurring intermediate water depths the full relationship of equation 4.4-1 must be used, however.

The horizontal scale in figure 4.4-2, which is linear in d / gT^2, hence changes gradually from left to right from a quadratic scale in $(d / \lambda)^2$ to a linear scale in d / λ. A similar transformation applies to the vertical scale, which is logarithmic in H / gT^2

4.4.3 Random wave model

The linear *random wave model* dates from the 1940s and has only begun to be applied in engineering practice since the 1950s, both in ship hydromechanics (ship motions) and in coastal engineering. The theory may conceptually be envisaged as a superimposition of an infinite number of sine wave components, each with their own amplitude, frequency and direction and a random phase angle; see figures 4.4-3 (reproduced from [4.4-8]) and 4.4-4. The component waves, which are the building blocks of this model, are in themselves periodic waves described by a classic wave theory. In view of the superimposition, the component waves must be linear or Airy waves. As discussed before, these waves do not satisfy the non-linear boundary condition at the free surface and are strictly speaking only valid for waves with infinitesimally small amplitudes. Correspondingly, the wave kinematics field is only specified in the fluid domain between the sea floor and the mean still water surface. Wave kinematics under crests above mean still water are hence not covered in this model and require a separate assumption in the form of an empirical extension. As the component waves are sine waves and symmetric with respect to the mean still water level, there is no difference between crests and troughs in the random model. A synthetic record of the water surface elevation can thus be turned upside down and remains equally valid; the random wave model cannot describe the asymmetry of large real ocean waves. However, all this does not mean that the theory cannot be applied very usefully and realistically to describe severe storm conditions with substantial wave heights. It only means that in doing so there is an approximation involved and that under these conditions the theory loses some of its accuracy and detail. The random wave model and some typical offshore applications will be discussed a bit further in chapter 10. For more details the reader is referred to the text books (e.g. [4.4-3, 5, 6, 8, 9, 10, or 4.2-3].

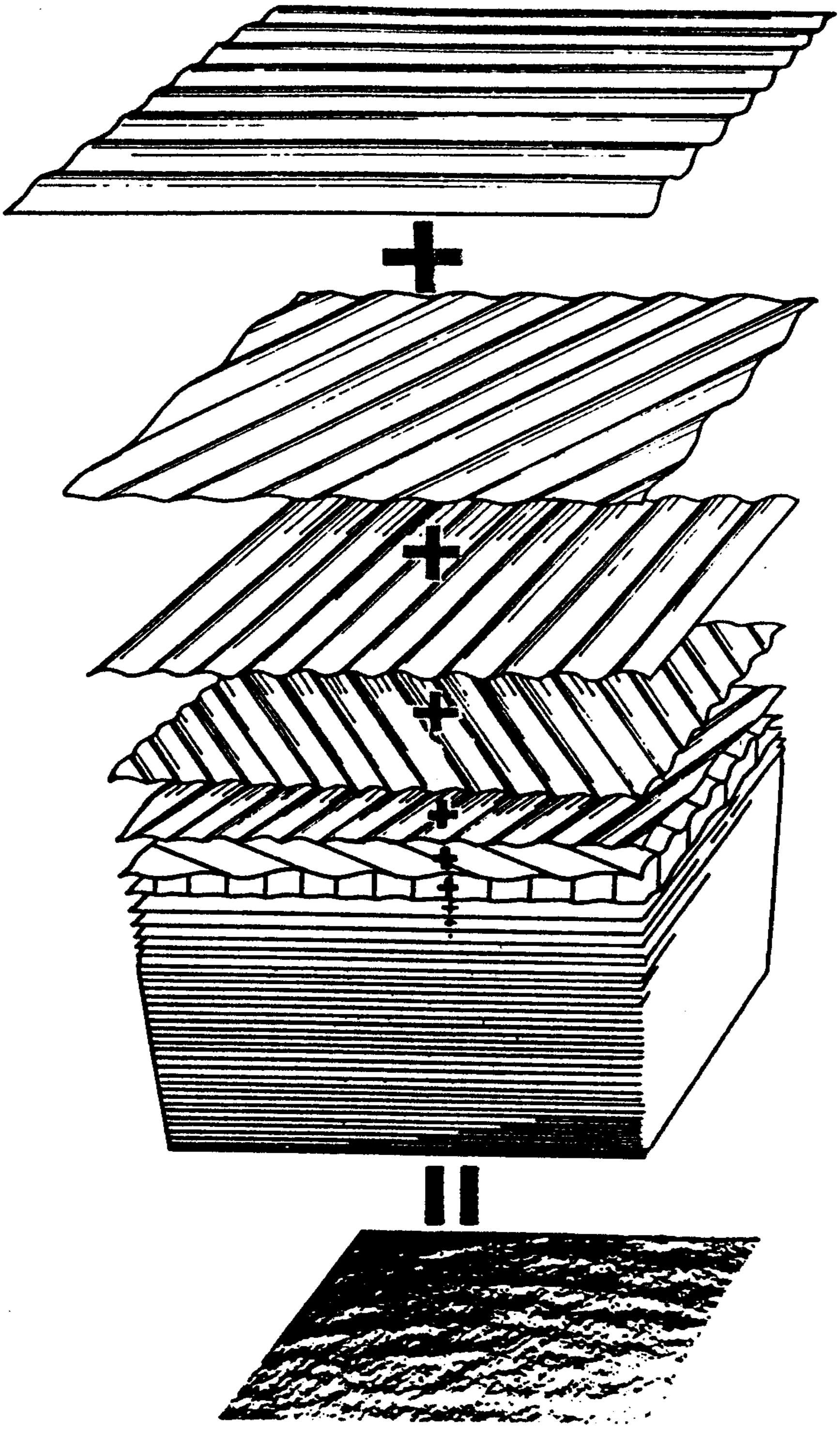

Figure 4.4-3. A sum of many simple sine waves makes a sea (from [4.4-8])

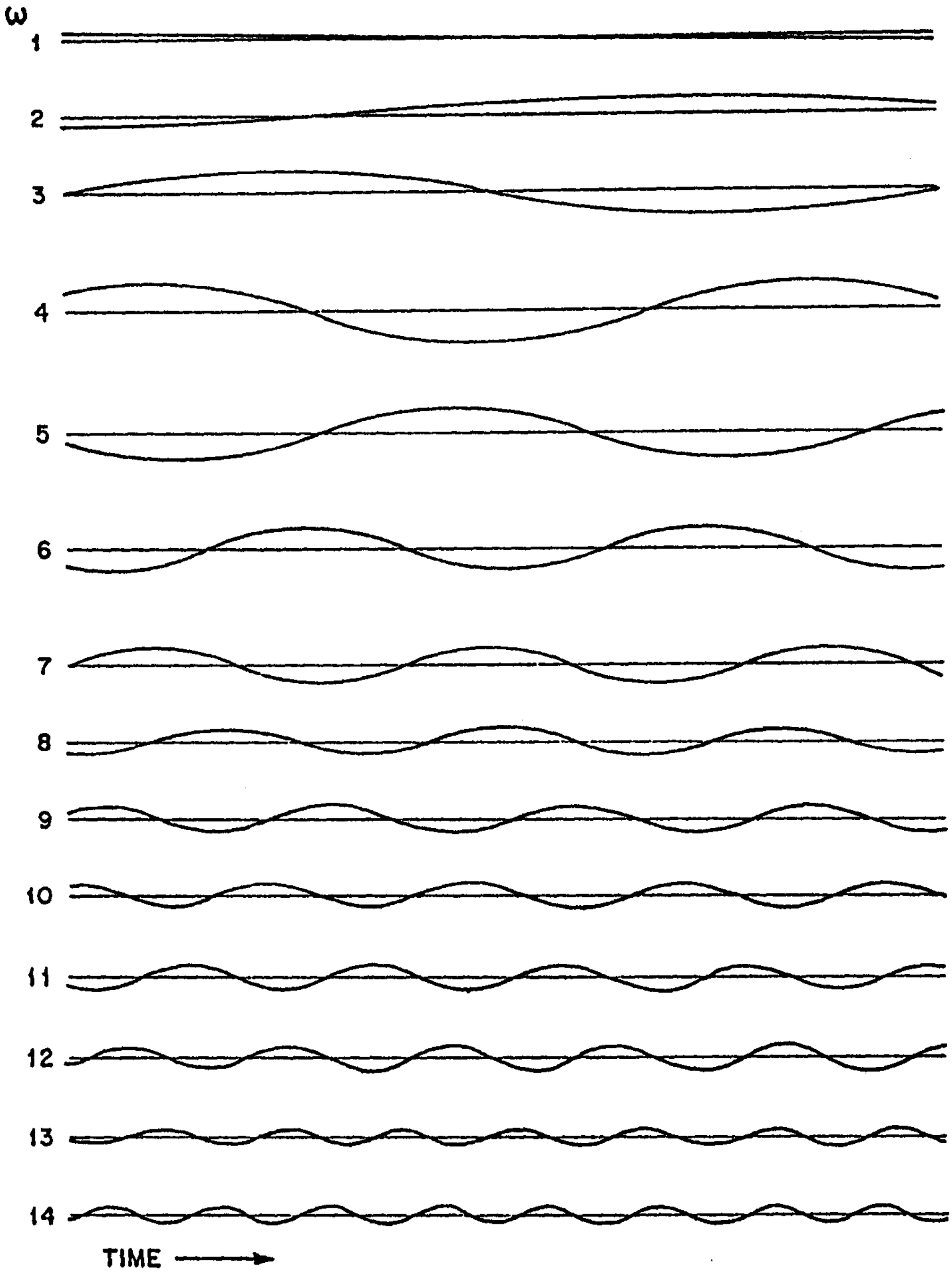

Figure 4.4-4. Summation of regular wave components

4.4.4 Comparison of the main features of both wave models

There is no question that the periodic wave model is a stringent idealisation and that the random wave model is a far more realistic representation of the ocean environment. The latter model is, for example, capable of reflecting the broad frequency content as well as the three-dimensional nature of real waves, thus avoiding the constraints of periodicity and longcrestedness. In contrast with this, it cannot include non-linearities associated with wave surface elevation.

Extensive and carefully controlled laboratory experiments have clearly shown that the random model is superior in many respects. An example of such experiments are those conducted in the early 1980s by the Delft Hydraulics Laboratory for the Netherlands Marine Technological Research programme MaTS [4.4-11]. Measurements at sea have also confirmed the basic correctness and usefulness of the random model, see e.g. [4.4-12]. In many circumstances the accuracy of the model is perhaps surprisingly good, even in severe seas. However, the experiments have naturally also demonstrated that there are limitations to what the linear random model can provide. As a matter of interest, a summary of the main conclusions quoted from [4.4-11] are attached in Annex C to this chapter.

For practical applications to offshore structures an engineer needs a suitable model that describes the water surface elevation together with the corresponding velocities and accelerations of the water particles as a function of time and space. Spacewise the model needs to be valid over a three-dimensional region of the size of the (largest) dimensions of the structure. Both the periodic and the random model are extensively used in design and engineering practice. In line with the discussion in chapter 3, the choice which model is best suited for a particular application is made by considering all circumstances that are relevant to the problem under consideration together with the purpose of the analysis.

4.4.5 Wave spectra

A real sea is best described as a random process. It may be viewed as the superimposition of many small individual frequency components, each of which is a periodic wave with its own amplitude, frequency and direction of propagation, which have random phase relationships with respect to each other. A unidirectional random sea is a special case of this, where all frequency components propagate in the same direction. The surface of a unidirectional sea is long-crested, whereas the surface of a real or directional sea is short-crested. In the linear random wave model, the sea state is completely described by the directional wave spectrum $S(\omega,\theta)$ of the water surface elevation, which specifies the distribution of wave energy over frequencies and directions. The directional characteristics are often assumed to be independent of frequency, allowing a separation of variables so that the directional wave spectrum can be expressed as the product of a directional spreading function $D(\theta)$, independent of frequency, and a wave frequency spectrum $S(\omega)$, which is independent of direction. The general relationship:

$$S(\omega,\theta) = D(\omega,\theta)\cdot S(\omega) \tag{4.4-4}$$

is then replaced by:

$$S(\omega,\theta) = D(\theta)\cdot S(\omega) \tag{4.4-5}$$

where the directional spreading function by definition satisfies the relationship:

$$\int_{-\pi}^{+\pi} D(\theta)d\theta = 1.0 \tag{4.4-6}$$

Based on a combination of measurements in the ocean and theoretical considerations oceanographers have proposed various standard formulations for the wave frequency spectrum as well as the directional spreading function. Each of these two topics will be briefly discussed in this section. For a more thorough discussion reference is made to the literature; the recent book by Ochi [4.4-10] presents an especially good and comprehensive treatment of the subject.

Definition of frequency

The wave frequency may either be expressed in terms of ω in radians per second (rad/s) or in terms of f in cycles per second or Hertz (Hz), where:

$$\omega = 2\pi f = \frac{2\pi}{T} \tag{4.4-7}$$

The energy of the sea per frequency and direction band is obviously independent of its mathematical formulation, so that we must have:

$$S(\omega,\theta)\, d\omega\, d\theta = S(f,\theta)\, df\, d\theta$$

or:

$$D(\theta)d\theta \cdot S(\omega)d\omega = D(\theta)d\theta \cdot S(f)df$$

With equation 4.4-7 the relationship between the two alternative expressions of the wave frequency spectrum is hence found to be:

$$S(f) = 2\pi \cdot S(\omega) \tag{4.4-8}$$

In the further discussion in this section we will need the moments of the wave frequency spectrum, which are defined as:

$$\begin{aligned} m_n(\omega) &= \int_0^\infty \omega^n S(\omega)d\omega \\ m_n(f) &= \int_0^\infty f^n S(f)df \end{aligned} \tag{4.4-9}$$

Once more using equation 4.4-7 it is easily derived that the relationship between these two moment expressions is:

$$m_n(\omega) = (2\pi)^n m_n(f) \tag{4.4-10}$$

In the present discussion all formulations will be presented in terms of ω.

The wave frequency spectrum

The shape of wave spectra varies widely with the wave conditions that are actually experienced. Two broad classes of wave conditions can be distinguished, wind seas and swells. Wind seas in an area are generated by local wind; the corresponding shape of the wave spectrum will thus clearly depend on the wind velocity, the fetch length of the wind over open water and the duration during which the wind has been blowing. Waves from a wind driven sea that travel out of the area may cause swell in another area, far away from where the waves were generated. For swells there is thus no direct connection with the local wind regime. Spectra for swells and wind seas should hence be clearly distinguished. Within the category of wind seas a further distinction needs to be made for wave conditions that are fully developed and wave conditions that are still developing. In the first case the sea is in a state of equilibrium; the energy input by the wind and the energy dissipation in the wave processes are in balance. In the second case there is net energy input and the waves are consequently still growing.

The standard parametric spectral forms developed by oceanographers all relate to wind seas, and most of them to fully developed seas. They express the wave spectrum in terms of the steady state local wind speed only. This implicitly involves a mechanism for wave generation and results in a one-parameter spectral formulation. For offshore engineering applications the use of such spectra is generally avoided in favour of a two-parameter spectral formulation. For offshore use the wave frequency spectrum is hence nearly always directly expressed in the sea state severity at the site, regardless of the wind. The parameters concerned are the significant wave height H_s (which is a measure of the total energy content in the sea) and a characteristic frequency, for which may be chosen:

(i) the peak or modal frequency ω_m of the wave frequency spectrum;
(ii) the average zero-crossing frequency ω_z of the water surface elevation;
(iii) an alternative mean frequency ω_1 of the wave spectrum.

Both the significant wave height and the characteristic frequency are usually obtained from site measurements. The two-parameter wave frequency spectrum then only uses the *shape* of the one-parameter wave frequency spectrum to distribute the total wave energy over frequency. This involves some reformulation of the standard spectra as originally proposed by the oceanographers. The two most frequently used standard formulations of the wave frequency spectrum $S(\omega)$ in marine applications are the Pierson Moskowitz (PM) spectrum for a fully developed sea and the Jonswap (JS) spectrum for a developing sea.

One of the oldest and most popular standard spectra dates from as early as 1959 and is due to Bretschneider. The original form of the Bretschneider spectrum represented fully as well as partially developed sea states and was expressed in terms of an average wave height, an average wave period and the wind speed. When reformulated as mentioned above and modified to allow for different definitions which are used in the formulations, the Bretschneider spectrum can be rewritten in the form of a two-parameter spectrum in terms of the significant wave height and a suitable period parameter. It is then fully analogous to the reformulated two-parameter Pierson-Moskowitz spectrum that will be discussed later.

The original one-parameter Pierson-Moskowitz spectrum

Pierson and Moskowitz developed their spectral formulation in 1964 from measured wave data in the North Atlantic [4.4-13]. It is a one-parameter spectrum with the wind speed U as the only variable. The original formulation was of the following form:

$$S_{PM}(\omega)=\frac{\alpha g^2}{\omega^5}\exp\left\{-\beta\left(\frac{g}{\omega U}\right)^4\right\} \tag{4.4-11}$$

with:
α = 0.0081 (a numerical constant)
β = 0.74 (another numerical constant)
g = acceleration of gravity
U = wind speed at 19.5 m above the sea surface in m/s

The factor ω^{-5} controls the high frequency flank of the spectrum, whereas the exponential function controls the low frequency flank.

The frequency at the peak of the spectrum, the modal frequency ω_m, is obtained by putting $dS(\omega)/d\omega=0$. Using equation 4.4-11 this results in:

$$\omega_m^4=\frac{4\beta}{5}\cdot\left(\frac{g}{U}\right)^4 \tag{4.4-12}$$

from which a non-dimensional modal frequency can be defined as:

$$\tilde{\omega}_m=\frac{\omega_m}{g/U}=\left(\frac{4\beta}{5}\right)^{1/4}=0.87 \tag{4.4-13}$$

Substitution of $(g/U)^4$ from equation 4.4-12:

$$\left(\frac{g}{U}\right)^4=\frac{5}{4}\cdot\frac{\omega_m^4}{\beta} \tag{4.4-14}$$

into equation 4.4-11 we obtain the PM spectrum as it is usually cited:

$$S_{PM}(\omega)=\frac{\alpha g^2}{\omega^5}\exp\left\{-\frac{5}{4}\left(\frac{\omega_m}{\omega}\right)^4\right\} \tag{4.4-15}$$

Integration of equation 4.4-11 over frequency gives the area under the spectrum, which is related to the total energy content of the sea and the significant wave height through the following relationship:

$$m_0(\omega)=\int_0^\infty S_{PM}(\omega)\,d\omega=\frac{\alpha}{4\beta}\cdot\frac{U^4}{g^2}=\left(\frac{H_s}{4}\right)^2 \tag{4.4-16}$$

from which it follows that:

$$H_s = 2\sqrt{\frac{\alpha}{\beta}} \cdot \frac{U^2}{g} = 0.21\frac{U^2}{g} \tag{4.4-17}$$

Using this equation in reverse the spectrum 4.4-11 can also be formulated in terms of the significant wave height instead of the wind speed. The modal frequency, expressed in *U*, is given in equation 4.4-12 or 4.4-13. Using equation 4.4-17 to eliminate U from equation 4.4-12 we obtain ω_m in terms of H_s:

$$\omega_m = 0.40\sqrt{\frac{g}{H_s}} \tag{4.4-18}$$

These equations completely specify sea states in terms of the one-parameter PM spectrum, either using the wind velocity U or the significant wave height H_s as the variable. However, in offshore applications a two-parameter spectrum is strongly preferred and this one-parameter spectrum is not normally used.

The two-parameter Pierson-Moskowitz spectrum

Equation 4.4-11 may be generalised by releasing the constraints associated with the numerical constants and the dependency on the wind velocity by writing it as:

$$S_{PM}(\omega) = \frac{A}{\omega^5}\exp\left\{-\frac{B}{\omega^4}\right\} \tag{4.4-19}$$

This is the two-parameter PM spectrum. Through the moments of the spectrum (see equations 4.4-20) and the relationships between spectral moments and the statistical parameters of the water surface elevation (see equations 4.4-21), the two-parameter spectrum can be rewritten in terms of the significant wave height and a characteristic frequency or period of the sea state. The moments of the PM spectrum are:

$$\begin{aligned}
m_n(\omega) &= \int_0^\infty \omega^n S(\omega)d\omega \\
m_0(\omega) &= \frac{A}{4B} \\
m_1(\omega) &= \frac{\Gamma(3/4)}{4} \cdot \frac{A}{B^{3/4}} \\
m_2(\omega) &= \frac{\sqrt{\pi}}{4} \cdot \frac{A}{\sqrt{B}} \\
m_4(\omega) &= \infty
\end{aligned} \tag{4.4-20}$$

In the linear random wave model the statistical distributions of the water surface elevation, as well as the water particle velocities and accelerations are all gaussian. The relationships between the moments of the spectrum and the statistical parameters of the water surface elevation are:

$$H_s = 4\sqrt{m_0(\omega)} = 2\sqrt{\frac{A}{B}}$$
$$\omega_1 = \frac{2\pi}{T_1} = \frac{m_1(\omega)}{m_0(\omega)} = B^{1/4}\Gamma(3/4)$$
$$\omega_z = \frac{2\pi}{T_2} = \frac{2\pi}{T_z} = \sqrt{\frac{m_2(\omega)}{m_0(\omega)}} = (\pi B)^{1/4}$$
$$\omega_m = \frac{2\pi}{T_p} = \left(\frac{4}{5}B\right)^{1/4}$$
$$\varepsilon = \sqrt{1 - \frac{m_2^2(\omega)}{m_0(\omega)m_4(\omega)}} \tag{4.4-21}$$

where: $\Gamma(3/4)$ = the gamma function $\Gamma(x)$ for $x = 3/4$; $\Gamma(3/4) = 1.2254$

T_1 = a mean period of the water surface elevation, defined by the zeroth and first order spectral moments

$T_2 = T_z$ = the average zero crossing period of the water surface elevation, defined by the zeroth and second order spectral moments

T_p = the modal or peak spectral period

(NB: to avoid erroneous interpretation of the subscript *m* as indicating the mean period, preferably the subscript *p* for peak period is used)

ε = the spectral width parameter with $0 \le \varepsilon \le 1.0$.

Note that the fourth spectral moment m_4 of the PM spectrum is infinite, when the spectrum is integrated from $\omega = 0$ to infinity. This means that $\varepsilon = 1.0$ and that the spectrum is broad banded. This does not correspond with the relationship 4.4-16 between m_0 and H_s , which is only valid for a narrow spectrum. This internal inconsistency is generally accepted, however. In numerical calculations the PM spectrum must always be truncated at a sufficiently high frequency, resulting in a finite m_4 and a (relatively high) value of the spectral width parameter $\varepsilon < 1.0$.

Using equations 4.4-21 we can express A and B by choice in H_s and $T_z = T_2$ (see equation 4.4-22), or in H_s and T_1 (see equation 4.4-24), or in H_s and T_p (see equation 4.26). The units of *A* and *B* are [$m^2(r/s)^4$] and [$(r/s)^4$], respectively. With the mean zero-crossing period $T_z = T_2$ and the second spectral moment we obtain:

$$B = \frac{1}{\pi}\cdot\left(\frac{2\pi}{T_z}\right)^4 = \frac{16\pi^3}{T_z^4} = \frac{496.1}{T_z^4}$$
$$A = 4B\cdot\left(\frac{H_s}{4}\right)^2 = \frac{BH_s^2}{4} = \frac{4\pi^3 H_s^2}{T_z^4} = 124.0\cdot\frac{H_s^2}{T_z^4} \tag{4.4-22}$$

and the spectral formulation:

$$S_{PM}(\omega) = 4\pi^3 \cdot \frac{H_s^2}{T_z^4} \cdot \frac{1}{\omega^5} \cdot \exp\left\{ -\frac{16\pi^3}{T_z^4} \cdot \frac{1}{\omega^4} \right\} \tag{4.4-23}$$

Using the average period T_1 based on the first spectral moment $m_1(\omega)$, instead of the mean zero-crossing period T_z based on $m_2(\omega)$, we obtain in a similar manner:

$$\begin{aligned} B &= \left(\frac{1}{\Gamma(3/4)} \right)^4 \cdot \left(\frac{2\pi}{T_1} \right)^4 = \left(\frac{7.096\,\pi^4}{T_1^4} \right) = \frac{691.2}{T_1^4} \\ A &= 4B \cdot \left(\frac{H_s}{4} \right)^2 = \frac{BH_s^2}{4} = \left(\frac{1}{4} \right) \cdot \left(\frac{2\pi}{\Gamma(3/4)} \right)^4 \cdot \left(\frac{H_s^2}{T_1^4} \right) = 1.774\pi^4 \left(\frac{H_S^2}{T_1^4} \right) = 172.8 \cdot \frac{H_s^2}{T_1^4} \end{aligned} \tag{4.4-24}$$

and the spectral formulation:

$$S_{PM}(\omega) = 1.774\,\pi^4 \cdot \frac{H_s^2}{T_1^4} \cdot \frac{1}{\omega^5} \cdot \exp\left\{ -\frac{7.096\,\pi^4}{T_1^4} \cdot \frac{1}{\omega^4} \right\} \tag{4.4-25}$$

Finally, using the modal frequency ω_m (or its inverse in the form of the peak spectral period T_p) of the spectrum results in:

$$\begin{aligned} \omega_m &= \left(\frac{4}{5} B \right)^{1/4} = 0.946(B)^{1/4} \\ B &= \frac{5}{4} \cdot \left(\frac{2\pi}{T_p} \right)^4 = \frac{20\pi^4}{T_p^4} = \frac{1948}{T_p^4} \\ A &= 4B \cdot \left(\frac{H_s}{4} \right)^2 = \frac{BH_s^2}{4} = 5\pi^4 \cdot \frac{H_s^2}{T_p^4} = 487.1 \cdot \frac{H_s^2}{T_p^4} \end{aligned} \tag{4.4-26}$$

while the spectrum becomes:

$$S_{PM}(\omega) = 5\pi^4 \cdot \frac{H_s^2}{T_p^4} \cdot \frac{1}{\omega^5} \cdot \exp\left\{ -\frac{20\pi^4}{T_p^4} \cdot \frac{1}{\omega^4} \right\} \tag{4.4-27}$$

Care should hence be taken to combine the correct formulation of the spectrum with the period chosen to represent the sea state. The choice is likely to depend on the type of data that is available as well as user preference. The ratios between the peak (the modal) period T_p, the average zero-crossing period $T_z = T_2$ and the mean period T_1 for a PM spectrum are further found to be:

$$\begin{array}{rcccc} T_1 & = & 1.086\,T_z & =0.772 & T_p \\ 0.920\ T_1 & = & T_z & =0.710 & T_p \\ 1.296\ T_1 & = & 1.408\,T_z & = & T_p \end{array} \tag{4.4-28}$$

The Jonswap spectrum

The Jonswap spectrum resulted from extensive measurements by Hasselman et al (1973) in the Joint North Sea Wave Project off the coast of the German island of Sylt [4.4-14]. It is formulated as a modification of the PM spectrum for a developing sea state in a fetch limited situation. The one-parameter JS spectrum is:

$$S_{JS}(\omega) = nf \cdot S_{PM}(\omega) \cdot \left\{ \gamma^{\exp\left\{-\frac{1}{2}\cdot\left(\frac{\omega-\omega_m}{\sigma\omega_m}\right)^2\right\}} \right\} = nf \cdot \frac{\alpha g^2}{\omega^5} \exp\left\{-\frac{5}{4}\left(\frac{\omega_m}{\omega}\right)^4\right\} \cdot \left\{ \gamma^{\exp\left\{-\frac{1}{2}\cdot\left(\frac{\omega-\omega_m}{\sigma\omega_m}\right)^2\right\}} \right\} \qquad (4.4\text{-}29)$$

where: γ = (non-dimensional) peak shape parameter

σ = a numerical parameter

= σ_a for $\omega < \omega_m$

= σ_b for $\omega \geq \omega_m$

nf = a normalising factor to ensure that both spectral forms have the same H_s

The factor in the large brackets in equation 4.4-29 is a peak enhancement factor. The JS spectrum is thus the product of the PM spectrum and the peak enhancement factor. For $\gamma = 1$ the JS spectrum reduces to the PM spectrum. For $\gamma > 1.0$ the peak enhancement factor is larger than 1.0 for all frequencies. Without the normalising factor nf the JS spectrum would hence have a larger energy content (a larger H_s) than the corresponding PM spectrum for the same sea state. Its modal frequency is also larger: $\omega_{m,JS} \geq \omega_{m,PM}$. The normalising factor is defined by:

$$nf = \frac{\int_0^\infty S_{PM}(\omega)\,d\omega}{\int_0^\infty S_{JS}(\omega)\,d\omega} = \frac{\int_0^\infty S_{PM}(\omega)\,d\omega}{\int_0^\infty S_{PM}(\omega)\left\{ \gamma^{\exp\left\{-\frac{1}{2}\cdot\left(\frac{\omega-\omega_m}{\sigma\omega_m}\right)^2\right\}} \right\} d\omega}$$

(4.4-30)

The peak enhancement factor is a function of 3 parameters (γ, σ_a and σ_b). The parameters γ, σ_a and σ_b were not constant in the North Sea data but showed appreciable scatter. Average values from the Jonswap data were:

$$\gamma = 3.3$$
$$\sigma_a = 0.07 \qquad (4.4\text{-}31)$$
$$\sigma_b = 0.09$$

The shape parameter γ varied between about 1 and 6 and was approximately normally distributed with mean 3.3 and standard deviation 0.79. In different geographical areas the JS spectral form also appears to be capable of representing the observations rather well, provided that the parameters γ, σ_a and σ_b are chosen in accordance with the local data [4.4-10]; their values are likely to be very different from the above Jonswap data.

As noted previously, one-parameter formulations are not normally used in offshore engineering applications. The two-parameter JS spectrum is defined in full analogy with equation 4.4-29 by:

$$S_{JS}(\omega) = nf \cdot S_{PM}(\omega) \cdot \left\{ \gamma^{\exp\left\{-\frac{1}{2}\cdot\left(\frac{\omega-\omega_m}{\sigma\omega_m}\right)^2\right\}} \right\} = nf \cdot \frac{A}{\omega^5}\exp\left\{-\frac{B}{\omega^4}\right\} \cdot \left\{ \gamma^{\exp\left\{-\frac{1}{2}\cdot\left(\frac{\omega-\omega_m}{\sigma\omega_m}\right)^2\right\}} \right\} \qquad (4.4\text{-}32)$$

The relationships between the spectral moments and the statistical parameters of the water surface elevation $(H_s, T_1 \text{ and } T_z = T_2)$ in the equations 4.4-21 remain entirely valid, also for the JS spectrum. However, the JS spectrum cannot be integrated analytically so that no closed form expressions for the spectral moments in terms of the coefficients *A* and *B* can be determined. Therefore, the normalising factor can only be calculated numerically. Based on curve fitting through the results of a number of numerical exercises for different peak shape parameter values, *but always using* $\sigma_a = 0.07$ *and* $\sigma_b = 0.09$, three expressions for the normalising factor were

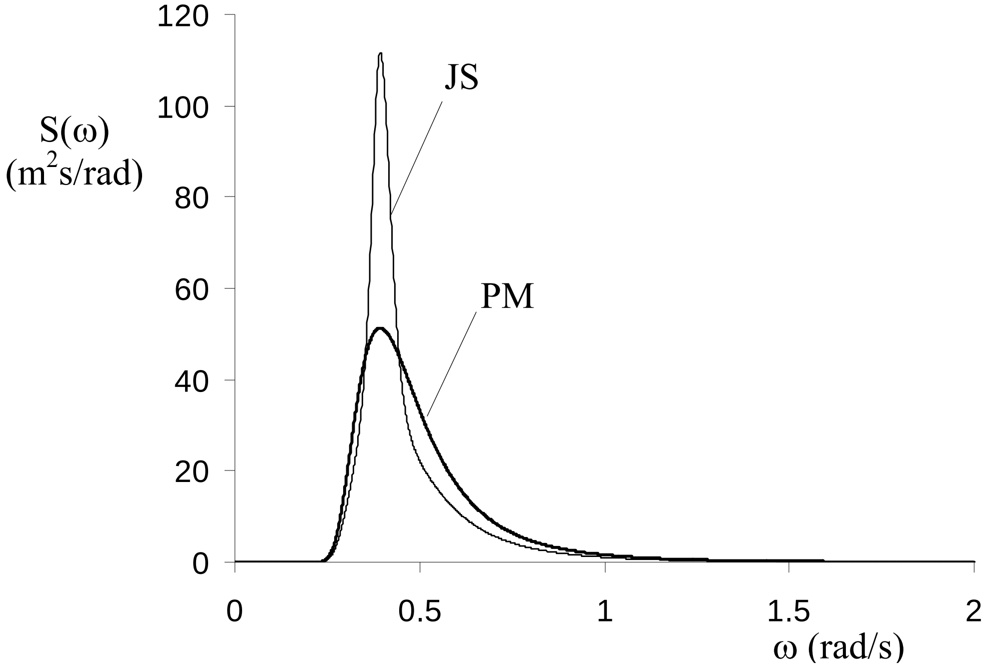

Figure 4.4-5a. Comparison of PM spectrum and JS spectrum for H_s = 15 m and T_p

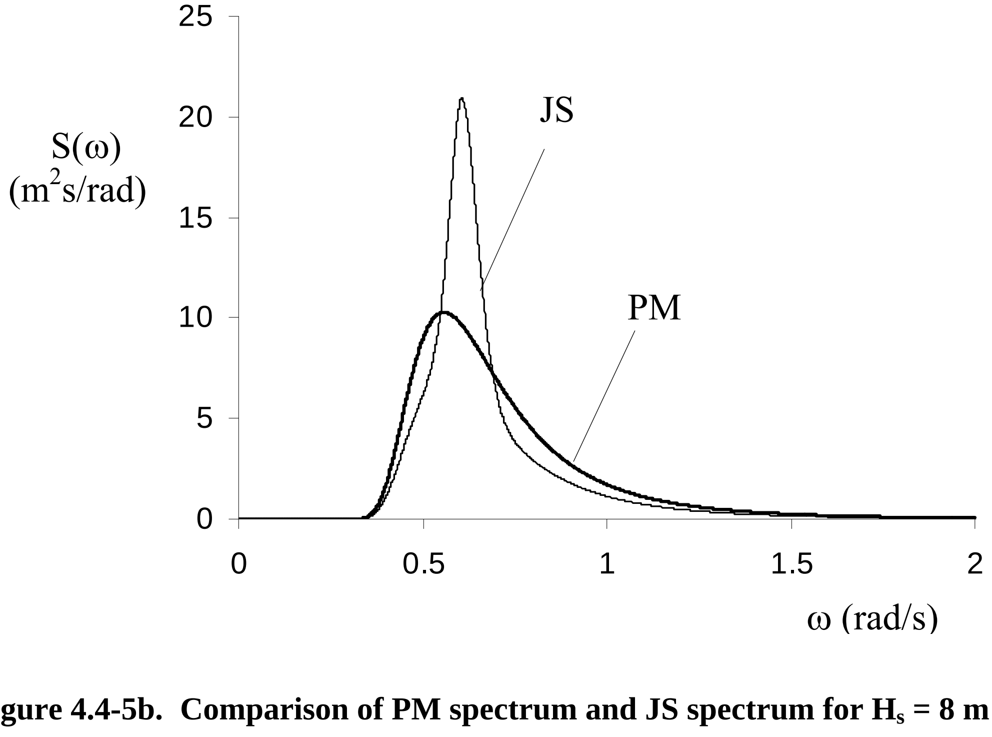

Figure 4.4-5b. Comparison of PM spectrum and JS spectrum for H_s = 8 m and T_z = 8 s

obtained as shown in equation 4.4-33. The validity range for γ in $nf\,(1)$, which was derived by Ewing, is not known. Yamaguchi derived expression $nf\,(2)$ for $1 \leq \gamma \leq 10$. Numerical integrations in the offshore group at the Delft University of Technology for $\gamma = 3.3$ and a wide range of spectral peak periods resulted in the factor $nf\,(3)$. In summary:

$$\begin{array}{lll} nf\,(1) = \left[0.78 + 0.22\gamma\right]^{-1} & & \\ nf\,(2) = \left[5\left(0.065\gamma^{0.803} + 0.135\right)\right]^{-1} & \text{for } 1 \leq \gamma \leq 10 & \qquad (4.4\text{-}33) \\ nf\,(3) = 0.652 & \text{for } \gamma = 3.3 & \end{array}$$

For γ = 3.3 the 3 expressions produce virtually identical results: 0.66, 0.66 and 0.65. For different values of γ the second expression results, by way of example, in:

$$\begin{array}{llll} \gamma & = 1 & nf\,(2) = & 1.00 \\ & = 2 & = & 0.81 \\ & = 3 & = & 0.68 \\ & = 5 & = & 0.54 \\ & = 10 & = & 0.36 \end{array}$$

Data on the parameters γ, σ_a and σ_b for a local area of interest are rarely known, so that by lack of better information the average values from the Jonswap project are nearly always used. Numerical integration of the JS spectrum *for the average values of* $\gamma = 3.3$, $\sigma_a = 0.07$ *and* $\sigma_b = 0.09$ results in the following ratios between $T_p, T_z = T_2$ and T_1:

$$\begin{array}{rcrcr} T_1 & = & 1.073\ T_z & = & 0.834\ T_p \\ 0.933\ T_1 & = & T_z & = & 0.777\ T_p \\ 1.199\ T_1 & = & 1.287\ T_z & = & T_p \end{array} \qquad (4.4\text{-}34)$$

These ratios should not be used for JS spectra with other values of the parameters γ, σ_a and σ_b, and are also clearly different from the ratios for the PM spectrum in equation 4.4-28.

Figure 4.4-5 shows two comparisons of a PM spectrum and a JS spectrum. In figure 4.4-5a the H_s and the peak period T_p are the same, while in figure 4.4-5b the H_s and the average zero-crossing period T_z are the same.

The high frequency branch of the spectrum

The high frequency branch of the PM and JS spectra decrease with frequency according to ω^{-5}. However, there is evidence that this is not entirely correct and that a power ω^{-4} is, at least partially, more appropriate. Broadly speaking there is wide support for ω^{-4} in the frequency range of approximately $1.5\omega_m < \omega < 3\omega_m$ and ω^{-5} for $\omega > 3\omega_m$ [4.4-10].

The directional spreading function

Standard formulations for the directional spreading function have also been proposed in the literature. However, directional wave information is difficult to measure and data to validate directional spreading functions are hence scarce. It is hence very difficult to judge the appropriateness of the proposed distributions. In practical applications unidirectional sea states are therefore often assumed. If the influence of directional wave spreading is expected to be significant, sensitivity analyses may be performed to investigate the effect. In such cases one of the distributions shown in equation 4.4-35 may be used.

The full two-parameter spreading function $D(\omega,\theta)$ is poorly known and hardly ever used. In general it may be said that directional spreading is smallest around the spectral peak and increases for frequencies further away from the peak, both below and above the peak.

The directional spreading functions $D(\theta)$ all assume a symmetric behaviour around the mean direction $\overline{\theta}$ over a sector of $\pi/2$ on either side; outside this sector $D(\theta)=0$. The mean wave direction is normally assumed to coincide with the mean wind direction. There are 3 expressions for $D(\theta)$ in common use:

$$\begin{aligned}
&D_1(\theta)=C_1(n)\cdot\left(\cos(\theta-\overline{\theta})\right)^n && -\tfrac{1}{2}\pi\le\theta-\overline{\theta}\le+\tfrac{1}{2}\pi \\
&D_2(\theta)=C_2(s)\cdot\left(\cos(\frac{\theta-\overline{\theta}}{2})\right)^{2s} && -\pi\le\theta-\overline{\theta}\le+\pi \\
&D_3(\theta)=C_3(\sigma)\cdot\frac{1}{\sigma\sqrt{2\pi}}\cdot\exp\left(-\frac{(\theta-\overline{\theta})^2}{2\sigma^2}\right) && -\tfrac{1}{2}\pi\le\theta-\overline{\theta}\le+\tfrac{1}{2}\pi \\
&D_1(\theta)=D_2(\theta)=D_3(\theta)=0 && \text{otherwise}
\end{aligned} \tag{4.4-35}$$

The functions all have a peak at $\theta=\overline{\theta}$, the sharpness of which depends on the power n and $2s$ in $D_1(\theta)$ and $D_2(\theta)$, or the standard deviation σ of the normal distribution $D_3(\theta)$. The constants C are normalising constants to ensure that the integral of $D(\theta)$ from $-\frac{1}{2}\pi$ to $+\frac{1}{2}\pi$ is equal to 1.0. For appropriately chosen values of the parameters the functions $D_1(\theta)$ and $D_2(\theta)$ are virtually indistinguishable. In engineering applications $D_1(\theta)$ is often used with $n=2$ for wind seas; the corresponding factor $C_1(2)=2/\pi$. For swells the value $n=6$ or higher is more appropriate. For $D_2(\theta)$ typical values of s are $s=6$ to 10 for wind seas and $s=5$ to 75 for swells.

4.4.6 Waves in the presence of a current or a ship at forward speed

Waves in the presence of a current

The discussion of the periodic and random wave models in the preceding sections relates to waves generated in water that is otherwise at rest. For waves in the presence of a current two different situations should be distinguished:

a) Waves, generated in an area where the water is at rest, but propagating into an area in which there is a current;
b) Waves, which are both generated and propagating on a flowing body of water as a result of a co-existing current.

Situation (a) involves physical interaction between waves and currents. For the most general case of a variable current velocity (horizontal, but variable over depth - in magnitude and/or direction, or varying as a function of time) the spatial and temporal interaction is very complex and to the knowledge of the present author not really well understood. Only simple cases with a uniform current velocity $U_c(x,y,z;t)=U_c$ have been adequately treated in the literature. The situation (a) can be relevant, for example, for swell running into an area with significant tidal currents or into an area around the mouth of a large river with significant outflow. We will not discuss case (a) in this handbook; the reader may be referred to the textbooks on waves. Let it suffice to say that the wave period is unaffected by the current and remains the same. If waves propagate into an area with an opposing current the waves get steeper, that is the wave height increases and the wave length decreases. Conversely, if the current velocity is in the direction of wave propagation, the wave height decreases and the wave length increases.

Situation (b) does not concern physical interaction between waves and current; it reflects a co-ordinate transformation depending on the viewpoint from which the situation is looked at. This case merits some further discussion. An example of such a situation is the case of a fixed structure in an environment of co-existing waves and current. With respect to a co-ordinate system that moves with constant forward velocity V in the direction of wave propagation, where V is equal to the velocity of the flowing body of water, the physical situation is identical to the situation described in the previous sections where the water was at rest: the relative movement between the water particles that take part in the wave action and the fluid environment is unchanged, regardless of the fact that the whole body of water moves with the velocity V. However, to a stationary observer in an earth fixed co-ordinate system attached to the structure the physical phenomena *appear* to be quite different. This can be explained as follows.

Adopt two parallel co-ordinate systems, both with their horizontal Oxy-planes in the still water surface and their z-axes positive upward. One system is fixed in space; this will be denoted by a subscript f for ‘fixed’. The other system moves with a constant velocity V; this system will be denoted by a subscript m for ‘moving’. At an (arbitrary) time $t=0$ the two systems coincide. Assume now that there is a periodic wave with amplitude $\hat{\zeta}=\frac{1}{2}H$ and period T. The wave propagates along the positive $Ox_f=Ox_m$-axis. Assume further that there is a uniform current velocity U_c, the vector of which makes an angle θ_c with the positive x-axis, and let the moving system move with the component of the current velocity that is in-line with the direction of wave propagation. The velocity of the moving system relative to the fixed system is then:

$$V=U_c\cos\theta_c \tag{4.4-36}$$

In the moving system all wave relationships from section 4.4.2 and Annex B remain entirely the same as when the water is at rest. These wave properties are called the *intrinsic properties* and are given a subscript ‘*i*’. In the fixed system some relationships remain the same and some change. The wave properties as they appear to a *stationary observer* in the fixed system are called the *apparent properties*. To distinguish them from the intrinsic properties they will be given a subscript ‘*app*’.

Dimensions and distances are not affected by the translation of the moving co-ordinate system. Hence the wave height (or amplitude) and the wave length in both systems are the same:

$$\hat{\zeta}_{app} = \hat{\zeta}_i = \zeta \qquad \lambda_{app} = \lambda_i = \lambda \tag{4.4-37}$$

However, the velocity at which a wave crest appears to propagate in the fixed system is the sum of the intrinsic wave celerity c_i and the uniform velocity V :

$$c_{app} = c_i + V = c_i + U_c \cos\theta_c \tag{4.4-38}$$

Thus, the apparent wave period is also different:

$$T_{app} = \frac{\lambda}{c_{app}} = \frac{\lambda}{c_i + V} \tag{4.4-39}$$

Writing this relationship in terms of the circular frequency we obtain:

$$\omega_{app} = \frac{2\pi}{T_{app}} = \frac{2\pi c_{app}}{\lambda} = \frac{2\pi c_i}{\lambda} + \frac{2\pi V}{\lambda} = \omega_i + kV = \omega_i + kU_c \cos\theta_c \tag{4.4-40}$$

where the intrinsic frequency and the wave number or wave length are further coupled through the dispersion equation:

$$\omega_i^2 = kg \tanh kd = \frac{2\pi g}{\lambda} \cdot \tanh \frac{2\pi d}{\lambda} \tag{4.4-41}$$

This means that there is a Doppler shift in frequency: the apparent wave frequency to a stationary observer or a stationary object is higher for positive V (i.e. a current in the same direction as the waves, $-90° < \theta_c, +90°$) and lower for negative V (i.e. a current in a direction opposite to the waves, $90° < \theta_c < 270°$). For currents at $\theta_c = \pm 90°$ the relative velocity $V = 0$ and the apparent and intrinsic frequencies are the same.

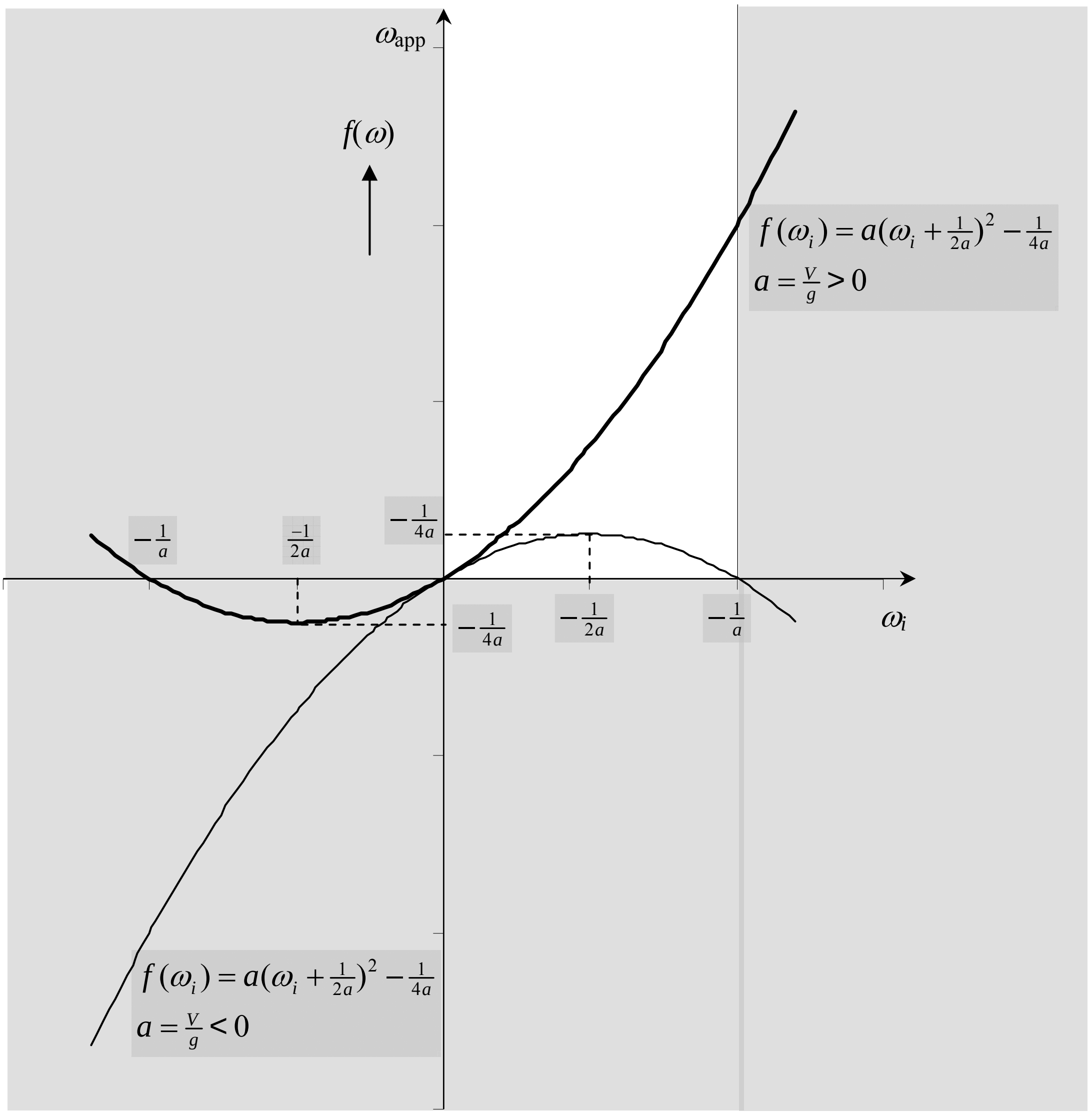

Figure 4.4-6. Behavior of the function $f(\omega) = \omega_i + \frac{V}{g}\omega_i^2$

There is obviously a limit to the negative values of V that are allowed. If waves are to pass the object at all, the apparent wave celerity c_{app} must be larger than 0 and the intrinsic wave celerity c_i must thus be larger than the opposing in-line current component (see equation 4.4-38); hence $c_i + V > 0$ or $V > -c_i$. For more negative values of V the waves are moved faster downstream by the current than they can propagate forward and no waves will reach the position of the observer at $x_f = 0$.

Note that the relationship between $k = k(\omega_i)$ and ω_i is an implicit function (see equation 4.4-41), so that for the general case of intermediate water depth the relationship between the apparent and the intrinsic frequency is quite complex, even though the mixed mode expression of equation 4.4-40 looks very simple.

However, for deep water waves the function $k(\omega_i)$ simplifies to $kg = \omega_i^2$ and equation 4.4-40 indeed becomes a relatively simple quadratic equation:

$$\omega_{app} = \omega_i + \frac{V}{g}\omega_i^2 \qquad (4.4\text{-}42)$$

Solutions are restricted to the domain $\omega_i > 0$ (for zero intrinsic frequency there are no waves and negative values are physically unrealistic), $\omega_{app} \geq 0$ and $V \geq -c_i$, which for deep water waves becomes $V \geq -g/\omega_i$. Every intrinsic wave frequency ω_i translates into a unique apparent wave frequency ω_{app} for all V. For $V > 0$ the result is $\omega_{app} > \omega_i$, while for $-c_i \leq V < 0$ it is $\omega_{app} < \omega_i$. Further, for negative values of V, ω_{app} reaches a maximum for $\omega_i = -g/2V > 0$ with the value of $\omega_{app} = -g/4V$; see also below. For $V = -c_i$ the apparent frequency is $\omega_{app} = 0$.

If, on the other hand, the apparent frequency is known from measurements in the fixed system, the intrinsic wave frequency for deep water waves must be obtained by solving the quadratic equation 4.4-42. Putting for convenience $a = V/g$ this can be rewritten in the form:

$$\omega_{app} = a\omega_i^2 + \omega_i = a\left\{\left(\omega_i + \frac{1}{2a}\right)^2 - \frac{1}{4a^2}\right\} = a\left(\omega_i + \frac{1}{2a}\right)^2 - \frac{1}{4a} \qquad (4.4\text{-}43)$$

Solutions can be found by considering the behaviour of the function:

$$f(\omega_i) = a\left(\omega_i + \frac{1}{2a}\right)^2 - \frac{1}{4a} \qquad (4.4\text{-}44)$$

which is shown in figure 4.4-6. The invalid regions are shaded, with the limit for negative values of V, i.e. $-c_i = -g/\omega_i \leq V < 0$, translating into $0 < \omega_i \leq -g/V = -1/a$. For $V > 0$ the function $f(\omega_i)$ represents a parabola with a *minimum* of $-1/4a = -g/4V < 0$ at $\omega_i = -1/2a = -g/2V < 0$. As figure 4.4-6 shows there is only one solution for $\omega_i > 0$ that is physically realistic. Similarly, for $-c_i < V < 0$ the parabola has a *maximum* $-1/4a = -g/4V > 0$

at $\omega_i = -1/2a = -g/2V > 0$. The value of ω_{app} is limited to the range $0 \le \omega_{app} \le -1/4a = -g/4V$ for which there may be two values of the intrinsic wave frequency $\omega_i > 0$, which are both larger than ω_{app} (see figure 4.4-6).

The change in spatial relationships can be obtained in a similar manner as the change in the temporal relationships above. A point $(x_m,0)$ in the moving system corresponds with the point $(x_f,0)$ in the fixed system, where:

$$x_f = x_m + Vt \tag{4.4-45}$$

The space and time dependent factor in the wave equations $(kx_m - \omega_i t)$ hence becomes:

$$kx_m - \omega_i t = k(x_f - Vt) - \omega_i t = kx_f - (\omega_i + kV)t = kx_f - \omega_{app} t \tag{4.4-46}$$

In other words, the time dependent factors for the water surface elevation, velocities and accelerations in the fixed system are of the same form as the intrinsic equations in the moving system, provided that x_m is replaced by x_f and the intrinsic frequency ω_i is replaced by the apparent frequency ω_{app}.

As a consequence of the co-ordinate transformation, in the fixed system the formulation of the wave spectrum of the random wave model also changes. The total energy in the sea is obviously invariant to the choice of co-ordinate system. Thus, the energy per frequency band must also remain the same:

$$S(\omega_{app})d\omega_{app} = S(\omega_i)d\omega_i$$

or:

$$S(\omega_{app}) = S(\omega_i) \cdot \frac{d\omega_i}{d\omega_{app}} \tag{4.4-47}$$

For the general case of an intermediate water depth the differentiation is a complex operation that will not be pursued here. However, for deep water waves the solution of equation 4.4-42 is:

$$(\omega_i)_{1,2} = \frac{-1 \pm \sqrt{1 + (4V/g)\omega_{app}}}{(2V/g)} \tag{4.4-48}$$

so that the derivative is:

$$\frac{d\omega_i}{d\omega_{app}} = \frac{1}{(2V/g)} \cdot \frac{1}{2} \cdot \frac{(4V/g)}{\sqrt{1 + (4V/g)\omega_{app}}} = \frac{1}{\sqrt{1 + (4V/g)\omega_{app}}} \tag{4.4-49}$$

and:

$$S(\omega_{app}) = \frac{1}{\sqrt{1 + (4V/g)\omega_{app}}} \cdot S(\omega_i) \tag{4.4-50}$$

For an anchored or dynamically positioned floating structure the situation is the same as for the fixed structure discussed above. Its average position relative to earth is fixed, so that a body fixed co-ordinate system is earth fixed as well and all the above equations remain valid.

Waves and a ship at forward speed

For a ship (vessel) that is not anchored but sails at forward speed in an existing wave system, the situation is analogous but not exactly the same. The co-ordinate system $(Oxyz)_s$ that is fixed to the ship now moves forward in the direction of the waves with a velocity $V_s \cos\theta_s$, where V_s is the forward speed of the ship and θ_s is the angle of her course with the positive x-axis; i.e. the angle between the ship's course and the direction of wave propagation, measured from the wave direction. In order not to complicate things unnecessarily we will further assume that there is no current in combination with a ship at forward speed. The wave properties in the ship fixed system are now called the *encounter properties* and will be given a subscript '*enc*'. The velocity V of the co-ordinate system that is fixed to the ship, relative to the earth fixed system in which the wave equations in the absence of a current are defined, is:

$$V = -V_s \cos\theta_s \qquad (4.4\text{-}51)$$

This is the equivalent of equation 4.4-36 for the current case, while the equation corresponding with 4.4-38 becomes:

$$c_{enc} = c_i + V = c_i - V_s \cos\theta_s \qquad (4.4\text{-}52)$$

The problem for a sailing ship is hence the opposite of the problem for a co-existing current. The frequency of (wave) encounter for the ship at forward speed but zero current is thus (compare with equation 4.4-40):

$$\omega_{enc} = \omega_i + kV = \omega_i - k \cdot V_s \cos\theta_s \qquad (4.4\text{-}53)$$

For deep water waves this results in, by analogy with equation 4.4-42:

$$\omega_{enc} = \omega_i + \frac{V}{g}\omega_i^2 = \omega_i - \frac{V_s \cos\theta_s}{g}\omega_i^2 \qquad (4.4\text{-}54)$$

If the ship heads into the waves (i.e. $90° < \theta_s < 270°$), $\cos\theta_s < 0$ and the relative velocity $V > 0$. The waves are called head waves, and because of the Doppler shift the frequency of encounter is higher than the intrinsic wave frequency. By analogy with the case of waves in the presence of a current, every ω_i provides one value of ω_{enc}, and conversely every known value of ω_{enc} gives one value of the intrinsic wave frequency.

If the ship moves in the same direction as the waves (i.e. $-90° < \theta_s < +90°$), $\cos\theta_s > 0$ and the relative velocity $V < 0$. These waves are called following waves and the frequency of encounter is lower than the wave frequency. The solution is obtained in a similar manner as for opposing current velocities, see figure 4.4-6. There are now certain conditions to be satisfied to achieve realistic solutions. Every given ω_i still provides one ω_{enc}, but one particular ω_{enc} may correspond to more than one value of the intrinsic wave frequency. For the choice of the correct frequency more information is needed. A special case to be considered is that at high forward speeds the ship may outrun the waves: the waves then *appear* to approach the ship from the bow as if they are head waves, while in reality they are still stern waves running in the same direction as the ship. The case of $V < 0$ is rather involved and will not be elaborated here any further. It should finally be noted that as the course of the ship is in the direction θ_s with respect to the waves, the waves in the ship based system $(Oxyz)_s$ are propagating in the direction $-\theta_s$ with respect to the ship's longitudinal axis Ox_s.

Final observation

The physical interaction between a wave field and a current field (condition (a) at the beginning of this section) is rarely if ever considered in offshore engineering. The kinematics of waves and a co-existing current are simply determined by vectorial addition of the current velocity and the wave orbital velocity. This simplification is almost universally adopted. In the case of a ship sailing in a wave field there clearly is no physical interaction between flow fields, and the vectorial addition of the forward speed vector and the wave orbital velocity vector is a correct representation of the occurrences. However, in both cases the Doppler shift in frequency and the associated modifications to all relevant equations (such as the time dependent factor and the formulation of the wave spectrum) in the co-ordinate system in which one works must be included.

4.5 Aero- and hydrodynamic load models

4.5.1 General

The discussions in the following sections aim at basic principles to enhance understanding of the phenomena and will not go into physical or mathematical detail. For these purposes reference is made to textbooks on fluid mechanics. An object placed in a flow will experience certain loads. These loads naturally depend on both the characteristics of the object and the characteristics of the flow. It will be assumed that the object is placed in an unbounded fluid domain, 'fluid' being a general term including both air and water. Free surfaces are thus not present. For the purpose of these discussions two-dimensional considerations suffice, but the principles remain entirely valid and can easily be extended to three-dimensional cases.

An arbitrary object is fully characterised by its *shape*, its *dimensions*, its *orientation* with respect to the flow and the *roughness* of its surface. Objects that are of interest in relation to offshore structures are almost without exception bluff bodies rather than streamlined shapes. They may have flat surfaces with sharp corners (e.g. rectangular boxes in the superstructure) or smooth shapes (e.g. circular cylinders in the substructure) and they usually have at least one plane of symmetry.

The flow is fully characterised by the *properties of the fluid* (i.e. its *density*, *compressibility* and *viscosity*) and its *state of motion*. The two 'fluids' that are particularly relevant to offshore engineering are water and air. Water is virtually incompressible, while for the flows and velocities that are of interest here air also behaves as being incompressible, i.e. its density does not depend on the state of motion. This means that the densities of both water and air are constant in the entire flow field. In flowing conditions pressure differences in place or time therefore result in velocity variations and not in density variations. Under static conditions air is of course not incompressible and its density then depends on the absolute value of the pressure. Viscosity as the third fluid property leads to an important distinction between *ideal fluids* having no viscosity and *real fluids* where viscosity cannot be neglected. Finally, with regard to its state of motion, a flow may be *steady*, i.e. independent of time, or *unsteady*, i.e. dependent of time.

4.5.2 Steady flow conditions

It may appear paradoxical, but a body of any shape or size placed in a *steady* flow of an *ideal* fluid will not experience any load. This can be shown theoretically and is known as d'Alembert's paradox. In an ideal fluid no boundary layers develop and there will consequently be no flow separation from the surface of the body. The streamlines follow the body contours irrespective of shape and the integration of fluid pressures over the body surface always yields a result that is identically equal to zero in any direction.

However, a bluff body in a *steady* flow of a *real* fluid does experience a load that is proportional to the area of the body exposed to the flow, the density of the fluid and the square of the velocity. This is an empirical relationship, established by observations from experiments. The component of the load in the direction of the flow is called drag, while the component of the load perpendicular to the direction of the flow is called lift. In a two-dimensional situation both components can be expressed mathematically as:

$$F_1 = C_1 \cdot \tfrac{1}{2}\rho v^2 \cdot b \tag{4.5-1}$$

where: F_1 = load per unit length (either drag or lift) [N/m]

C_1 = an empirical coefficient (of either drag or lift) [-]

ρ = density of the fluid [kg/m^3]

v = free field velocity of the fluid [m/s]

(the factor $\frac{1}{2}$ is introduced for convenience as $\frac{1}{2}\rho v^2$ is the stagnation pressure, a well known quantity in fluid mechanics)

b = the cross-sectional dimension perpendicular to the flow [m]

(b represents the area per unit length exposed to the flow)

This is the basic expression for wind loads per unit length on (elements of) the superstructure, as well as for current loads per unit length on members of the substructure. It is also the basic expression for one component of the wave load in unsteady flows, as we will see in the next section.

4.5.3 Unsteady flow conditions

The load experienced by a bluff body in an *unsteady* flow is somewhat more complicated. In an *ideal* fluid (i.e. a fluid having no viscosity) the load is found to be proportional to the displaced volume of the body, the density of the fluid and the acceleration of the fluid at the location of the body. This can be established theoretically by potential flow calculations and has been confirmed by experiments. The direction of the load coincides with the direction of the acceleration. As a reference value for the acceleration it is common to use the acceleration in the undisturbed flow field at the centre of the body, i.e. without the body being present. Again using a two-dimensional representation the load can hence be expressed mathematically as:

$$F_2(t) = C_2 \cdot \rho A \cdot \dot{v}(t) \tag{4.5-2}$$

where: F_2 = load per unit length [N/m]

t = time [s]

C_2 = a coefficient [-]

ρ = density of the fluid [kg/m^3]

A = the cross-sectional area of the body [m^2]

(which represents the displaced volume per unit length and is of the order b^2, if b is a typical cross-sectional dimension similar to that used in F_1)

$\dot{v}(t) =$ dv/dt = the acceleration of the fluid [m/s^2]

(taken at the centre of the body and undisturbed by its presence, i.e. as if the body is not present)

This is the basic expression for the inertial load in an unsteady flow, both in air and in water.

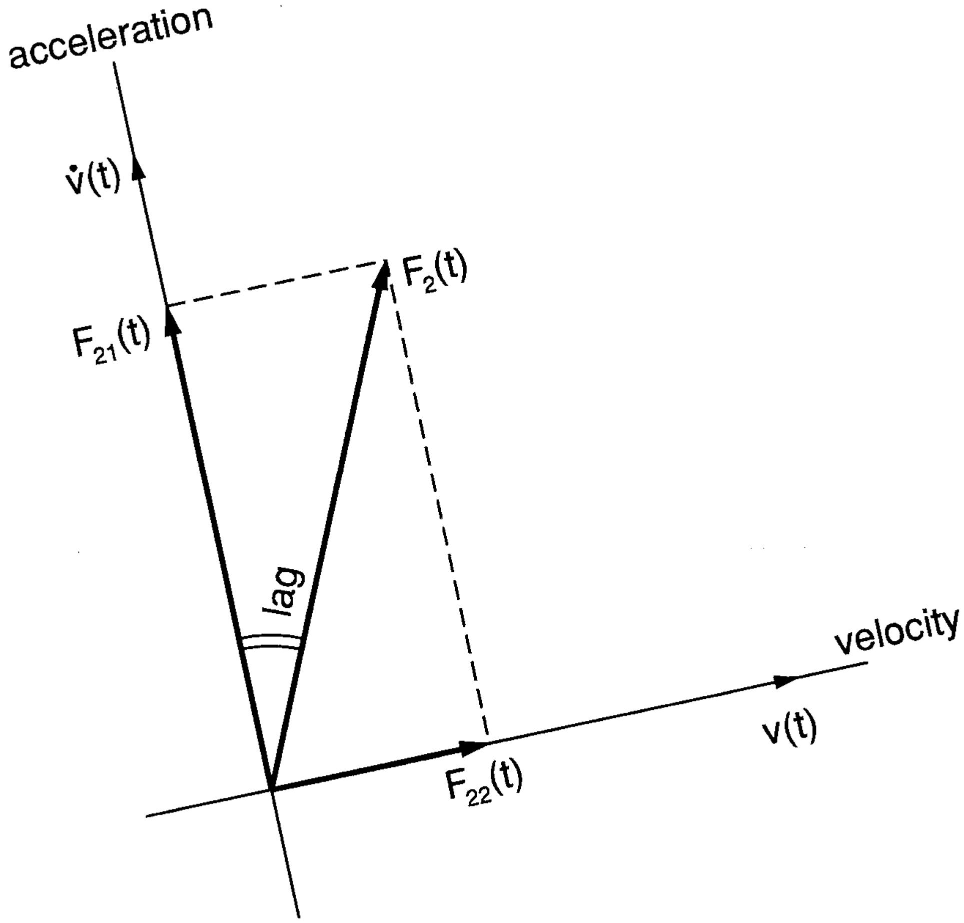

Figure 4.5-1. Vector diagram showing resolution of the unsteady hydrodynamic force $F_2(t)$ in a real fluid into components in phase with acceleration and velocity

In an *unsteady* flow of a *real* fluid the above remains essentially valid, but due to the influence of viscosity two things will happen: firstly, the coefficient C_2 will become different and, secondly, the load will no longer be synchronous with the acceleration, i.e. it will lag or lead (generally lag) the acceleration. For flows where the time variation is harmonic, a time lag can be expressed as a phase difference between the load and the acceleration; the load will thus have a phase lag with respect to the acceleration. When load and acceleration are not in phase, the load can always be resolved into a component in phase with the acceleration and a component in phase with the velocity; see the illustration in vector diagram form in figure 4.5-1. Mathematically this can be formulated as follows. Let the velocity be $v(t) = \hat{v}\sin\omega t$ and the acceleration $\dot{v}(t) = \hat{\dot{v}}\cos\omega t = \hat{v}\omega\cos\omega t$. According to equation 4.5-2 and the above modifications the load F_2 in a real as opposed to an ideal fluid then becomes:

$$F_2(t) = C_3 \cdot \rho A \cdot \hat{\dot{v}}\cos(\omega t - \theta) \qquad (4.5\text{-}3)$$

Resolving this into two components we obtain:

$$\begin{aligned} F_2(t) &= C_3\cos\theta\cdot\rho A\cdot\hat{v}\cos\omega t + C_3\sin\theta\cdot\rho A\cdot\hat{v}\sin\omega t \\ &= C_3\cos\theta\cdot\rho A\cdot\dot{v}(t) + C_3\omega\sin\theta\cdot\rho A\cdot v(t) \\ &= F_{21}(t) + F_{22}(t) \end{aligned} \tag{4.5-4}$$

with the two components of the load being:

$$\begin{aligned} F_{21}(t) &= C_3\cos\theta\cdot\rho A\cdot\dot{v}(t) = C_{21}\cdot\rho A\cdot\dot{v}(t) \\ F_{22}(t) &= C_3\omega\sin\theta\cdot\rho A\cdot v(t) = C_{22}\cdot\rho A\cdot v(t) \end{aligned} \tag{4.5-5}$$

By this formulation the coefficients C_{21} and C_{22} are defined in a similar manner and analogous to the definition of C_2. This underlines that in a real fluid the two terms are components of the same load $F_2(t)$, modelled on the load in an ideal fluid in equation 4.5-2. By implication this formulation results in a coefficient C_{22} which has the dimension of [s^{-1}], which is generally undesirable. However, the component in phase with the velocity could also have been formulated by analogy with equation 4.5-1 as:

$$F_{22}(t) = C_{22}^{*}\cdot\tfrac{1}{2}\rho\{v(t)\}^2\cdot b \tag{4.5-6}$$

Whereas the coefficient C_{22} is by definition:

$$C_{22} = \frac{\hat{F}_{22}}{\rho A\hat{v}} \tag{4.5-7}$$

the coefficient C_{22}^{*} is now defined by:

$$C_{22}^{*} = \frac{2\hat{F}_{22}}{\rho b\hat{v}^2} \tag{4.5-8}$$

The relationship between the dimensional coefficient C_{22} and the non-dimensional coefficient C_{22}^{*} is hence:

$$C_{22}^{*} = \frac{2\rho A\hat{v}}{\rho b\hat{v}^2}\cdot C_{22} = \frac{2A}{b\hat{v}}\cdot C_{22} \tag{4.5-9}$$

Accordingly, we can write for the load on a body in an *unsteady* flow of a *real* fluid:

$$F_2(t) = C_{21}\cdot\rho A\cdot\dot{v}(t) + C_{22}\cdot\rho A\cdot v(t) \tag{4.5-10}$$

or alternatively:

$$F_2(t) = C_{21}\cdot\rho A\cdot\dot{v}(t) + C_{22}^{*}\cdot\tfrac{1}{2}\rho b\cdot\{v(t)\}^2 \tag{4.5-11}$$

where in addition to the parameters in equation 4.5-2:

$v(t)$ = the velocity of the undisturbed fluid at the centre of the body, i.e. as if the body is not present [m/s]

C_{21} = an empirical coefficient for the component of the load that is in phase with the acceleration [-]

C_{22} = an empirical coefficient for the component of the load that is in phase with the velocity, defined by equation 4.5-7 [s^{-1}] (note that the coefficient C_{22} has the dimension of s^{-1})

C_{22}^* = an empirical coefficient for the component of the load that is in phase with the velocity, defined by equation 4.5-8 (the coefficient C_{22}^* is non-dimensional)

b = the cross-sectional dimension perpendicular to the flow [m]

Any flow that is dependent on time is by definition unsteady, but the characteristics of different flows may vary widely. The general situation is described by equations 4.5-3 to 4.5-11. If the flow is subject to large and rapid fluctuations, acceleration dependent effects will tend to dominate over velocity dependent effects. Alternatively, the flow velocity may vary only slowly so that accelerations are negligibly small, thus approaching the steady flow situation described by equation 4.5-1. By analogy with equation 4.5-1 the velocity v will then no longer be constant but be a slowly varying function of time $v(t)$. The load F_1 will now similarly be a slowly varying function of time $F_1(t)$. To make it possible to express that the magnitude of F_1 is quadratically dependent on $v(t)$, but that the load naturally has the same direction as the velocity, equation 4.5-1 is conveniently modified to maintain the sign of the velocity:

$$F_1(t) = C_1 \cdot \tfrac{1}{2}\rho |v(t)| \cdot v(t) \cdot b \tag{4.5-12}$$

This completes the description of the four basic cases of aero- and hydrodynamic loads on a body placed in a flow. Any further discussion is concerned with the specification of the velocity $v(t)$ and acceleration $\dot{v}(t)$ of the flow, and the magnitude of the empirical coefficients C_1, C_{21} and C_{22} or C_{22}^* for all possible situations of practical interest. An enormous number of investigations have been performed and numerous reports and books have been written on these "details". A large body of data exists, but a lot of uncertainty still remains. However, further treatment of the subject belongs to a much more specialised area of hydromechanics that will not be elaborated on in this handbook.

4.5.4 Arbitrary flow conditions

For a general flow of a real fluid, where both velocity dependent influences (as in steady flow) and acceleration dependent influences (as in unsteady flow) are present, the total load F may be postulated to be the sum of F_1 and F_2. With this assumption, the aero- and hydrodynamic loads on an object can be described by (a combination of) the loads F_1 and F_2 as required.

In summary, the above together with the two preceding sections and distinguishing between ideal and real fluids as well as between steady and unsteady flows, we obtain the following overview:

	total load $F(t)$ on an object	
	steady flow	unsteady flow
ideal fluid	$F=0$	$F(t)=F_2(t)$ (eqn. 4.5-2)
real fluid	$F=F_1$ (eqn. 4.5-1)	$F(t)=F_2(t)$ (eqn. 4.5-10 or 11) or: $F(t)=F_1(t)+F_2(t)$

All three non-zero situations are relevant for offshore structures. The steady flow case of a real fluid is the common model for wind loads and current loads, as already mentioned. The unsteady flow case of an ideal fluid is nearly always an adequate approximation for structures consisting of large size elements (e.g. shafts and caisson of a concrete gravity base structure, columns and pontoons of a semi-submersible platform). In these cases the influence of fluid viscosity is negligibly small and inertial effects dominate the loads. In other words, $F_2(t)$ is much larger than $F_1(t)$. This can further be illustrated by considering that F_2 is proportional to $A \sim b^2$ as opposed to F_1 which is proportional to b.

The most general case of an unsteady flow of a real fluid is of greatest relevance for structures with long and slender members (such as steel space frame structures) in a combined wave and current environment. As noted, the load may be assumed to be the sum of F_1 and F_2.

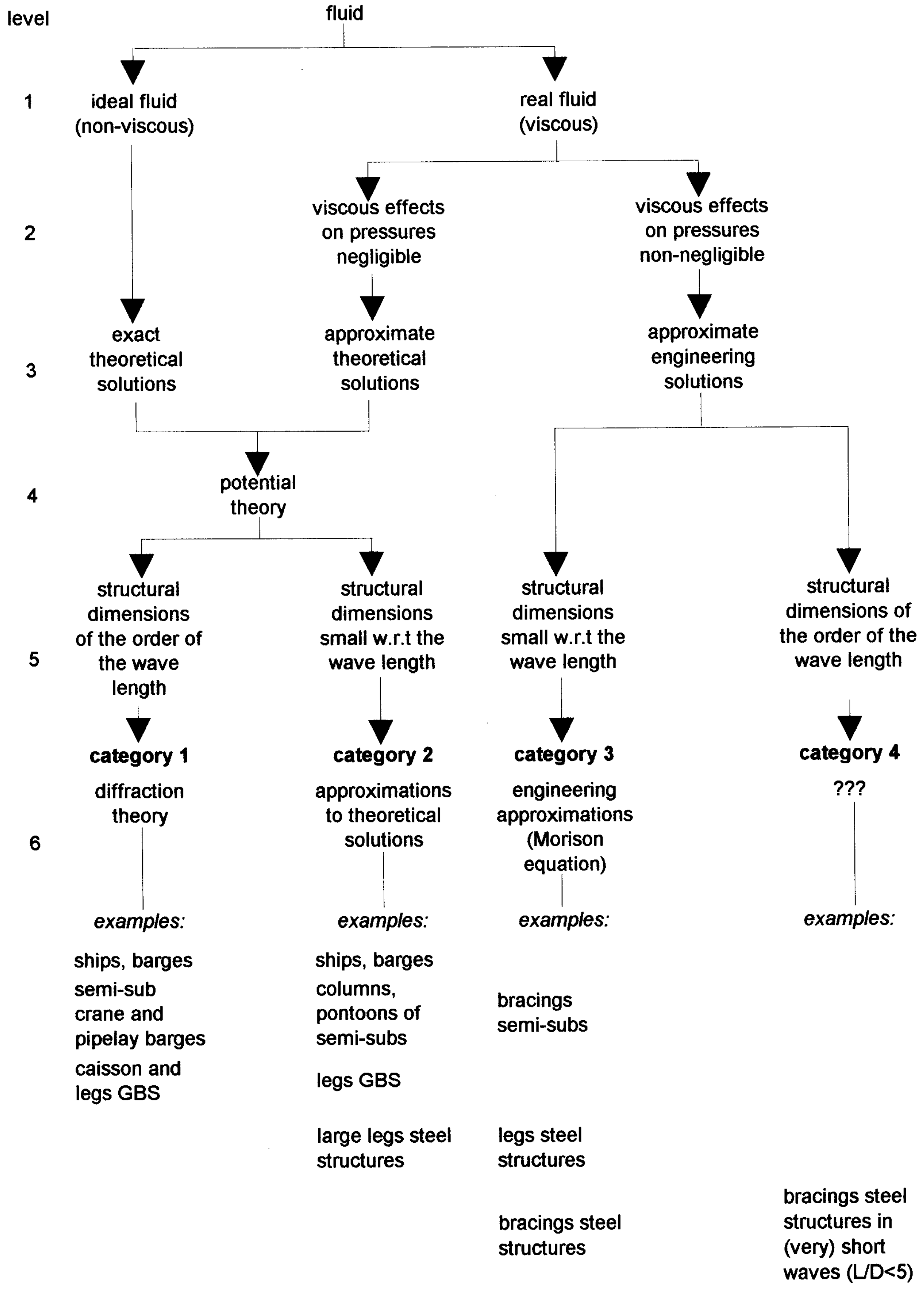
level
fluid
1
ideal fluid (non-viscous)
real fluid (viscous)
2
viscous effects on pressures negligible
viscous effects on pressures non-negligible
3
exact theoretical solutions
approximate theoretical solutions
approximate engineering solutions
4
potential theory
5
structural dimensions of the order of the wave length
structural dimensions small w.r.t the wave length
structural dimensions small w.r.t the wave length
structural dimensions of the order of the wave length
6
category 1
diffraction theory
category 2
approximations to theoretical solutions
category 3
engineering approximations (Morison equation)
category 4
???
examples:
ships, barges
semi-sub
crane and pipelay barges
caisson and legs GBS
examples:
ships, barges
columns, pontoons of semi-subs
legs GBS
large legs steel structures
examples:
bracings semi-subs
legs steel structures
bracings steel structures
examples:
bracings steel structures in (very) short waves (L/D<5)

Figure 4.5-2. Classification of wave force calculation methods

Considering this case a bit further, using equation 4.5-12 as a formulation of F_1 and equation 4.5-10 as a formulation of F_2, the total load $F(t)$ may be rewritten as:

$$\begin{aligned} F(t) &= F_1(t) + F_2(t) \\ &= C_1 \cdot \tfrac{1}{2}\rho|v(t)| \cdot v(t) \cdot b + C_{21} \cdot \rho A \cdot \dot{v}(t) + C_{22} \cdot \rho A \cdot v(t) \\ &= C_{21} \cdot \rho A \cdot \dot{v}(t) + \left(C_1 + C_{22} \cdot \frac{2A}{b|v(t)|} \right) \cdot \tfrac{1}{2}\rho|v(t)| \cdot v(t) \cdot b \end{aligned} \qquad (4.5\text{-}13)$$

Using equation 4.5-11 instead of 4.5-10 as a formulation of F_2 the result is more simple:

$$\begin{aligned} F(t) &= F_1(t) + F_2(t) \\ &= C_1 \cdot \tfrac{1}{2}\rho|v(t)| \cdot v(t) \cdot b + C_{21} \cdot \rho A \cdot \dot{v}(t) + C_{22}^* \cdot \tfrac{1}{2}\rho b \cdot \{v(t)\}^2 \\ &= C_{21} \cdot \rho A \cdot \dot{v}(t) + (C_1 \pm C_{22}^*) \cdot \tfrac{1}{2}\rho|v(t)| \cdot v(t) \cdot b \end{aligned} \qquad (4.5\text{-}14)$$

Both these results have the form of the Morison Equation, which is the universal model to calculate the in-line hydrodynamic load per unit length on slender members in waves and waves plus current (see also section 4.6):

$$F(t) = C_m \cdot \rho A \cdot \dot{v}(t) + C_d \cdot \tfrac{1}{2}\rho b|v(t)| \cdot v(t) \qquad (4.5\text{-}15)$$

where the coefficient C_m is the inertia coefficient and C_d is the drag coefficient. When these are equated to the coefficients in 4.5-13 or 4.5-14 we find:

$$\begin{aligned} C_m &= C_{21} \\ C_d &= C_1 + C_{22} \cdot \frac{2A}{b|v(t)|} = C_1 \pm C_{22}^* \end{aligned} \qquad (4.4\text{-}16)$$

The velocity and the acceleration to be used in the equations are the components normal to the axis of the member; furthermore, the velocity is the vectorsum of the wave orbital and current velocity vectors. The coefficients in all these equations are empirical, although C_m has a theoretical basis in an ideal fluid.

The same expressions are in principle valid for the aerodynamic load on an object in an unsteady wind field; however, the inertia load in an air environment is so small that it can normally be neglected, leaving only the time varying drag load, which is analogous to the generalisation of the steady flow situation by equation 4.5-12.

4.5.5 Classification of wave load calculation methods

Figure 4.5-2 shows in a schematic form an overview and selection procedure of the methods to calculate wave loads on offshore structures that was first presented in [4.4-15]. The selection depends on a balanced consideration of three major aspects, i.e. the importance of the fluid properties, notably with regard to its viscosity (levels 1 and 2 in the figure); the approach to the hydrodynamics in relation to the fluid properties adopted for the formation of a load model (levels 3 and 4); and the dimensions of the structure or structural element relative to the dimensions of the wave field, typified by the wave lengths involved (level 5). The corresponding type of solution is finally shown in level 6.

These distinctions lead to 4 different categories; of each category a few typical examples are presented. Categories 1 and 2 are firmly based on classical hydrodynamic theory, while categories 3 and 4 are the domain of (semi-)empirical engineering solutions. Category 4 finds a logical place in the schematic, but its relevance and solution are uncertain. The loads on a structural member in waves with wave lengths that are of the same order as the cross sectional dimensions of the member will rapidly become very small and may well be negligible. This can easily be demonstrated for the theoretical solutions in category 1. Whether viscous effects will change this result to any significant degree is not immediately clear. However, if under these conditions appreciable loads do exist these could become important for the dynamic response of individual structural members at natural frequencies of some 0.4 to 1 Hz associated with waves of about 10 m to 1.5 m in length.

4.6 Hydrodynamic loads on slender members

4.6.1 General discussion

The basic model for hydrodynamic loads on slender members is the Morison equation, named after J.R. Morison who derived it in 1950 (together with 3 colleagues) to describe the results of laboratory tests with a vertical cylinder of circular cross section in regular waves [4.6-1]. It was during the early days of offshore experience, and despite its weaknesses and an enormous amount of research on hydrodynamic loading since then a better formulation has still not been found. The equation reads:

$$f = f_i + f_d = C_m \cdot \frac{\rho \pi D^2}{4} \cdot \dot{u} + C_d \cdot \tfrac{1}{2} \rho D \cdot |u| u \qquad (4.6\text{-}1)$$

where: f = dF / dz = total hydrodynamic load per unit length [N/m]
f_i = dF_i / dz = hydrodynamic inertia load per unit length [N/m]
f_d = dF_d / dz = hydrodynamic drag load per unit length [N/m]
dz = length of an element of the cylinder [m]
C_m = inertia coefficient [-]
C_d = drag coefficient [-]
D = cylinder diameter [m]
ρ = density of water [kg/m^3]
$\dot{u}$ = horizontal water particle acceleration [m/s^2]
u = horizontal water particle velocity [m/s]

It should be noted that the water particle velocity and acceleration, as well as the loads are all functions of place (x, y, z) and time t.

A phenomenological explanation of the form of the Morison equation has been given in section 4.5.4, but it remains an essentially empirical equation. Since its introduction in 1950 the original formulation has undergone a number of plausible generalisations, such as:

- replacing the cylinder diameter D by a characteristic cross sectional dimension, and the cylinder cross sectional area $\pi D^2 / 4$ by volume per unit length, for members with other than circular shapes;
- replacing the horizontal water particle velocity u and acceleration $\dot{u}$ by the components of velocity and acceleration that are perpendicular to the member, for members that are inclined instead of vertical;
- replacing u alone by the vectorsum (normal to the member) of the water particle velocity (u, v, w) and the current velocity U_c, for situations where waves and currents co-exist;
- extending the concept even further, replacing u by the vectorsum of the wave orbital velocity (u, v, w), the current velocity U_c and the local velocity $(\dot{x}, \dot{y}, \dot{z})$ of the member, if the member itself is not stationary but oscillates.

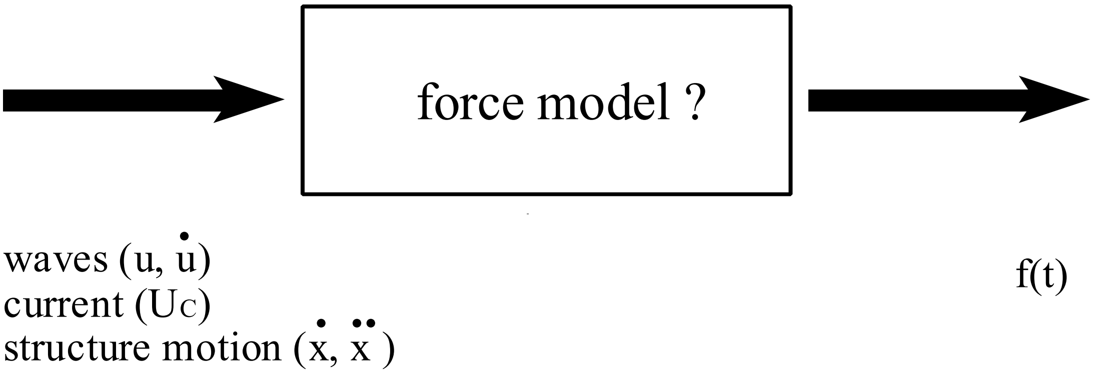

Figure 4.6-1. Schematic representation of the hydrodynamic force problem

When one accepts the form of the equation as a correct representation of the physical occurrences, these are indeed plausible generalisations. However, it is stressed that they are in fact nothing else than engineering postulates, the validity of which needs to be demonstrated by suitable experiments under a variety of relevant environmental conditions. Against this background it should further be noted that empirical adjustment of the drag and inertia coefficients in periodic waves, with or without current, provides ample scope to match the outcome of the equation to measured values of the hydrodynamic load for a given set of circumstances. The fact that it is consistently found that the coefficients do indeed need to be tailored to every set of conditions clearly indicates that the equation is an engineering model rather than a reflection of an inherent physical process.

Let us now take a step back and consider the problem somewhat more fundamentally as a modelling task according to the discussion in chapter 3. For the purpose of illustration we will consider the base case of an element of a vertical circular cylinder and will adopt the original form of the Morison equation as a basic load model. We know from observations that the component of the load that is dependent on velocity is non-linear and involves the velocity squared, while the component that is dependent on acceleration is linear. The question is how we can extend the Morison equation to apply to other situations than the load in a periodic wave on a fixed cylinder; the problem is schematically shown as an input-output problem in figure 4.6-1. As discussed in section 3.2, for relationships involving non-linear terms the sequence of events is important, so that we must specify how we assume that the various inputs in figure 4.6-1 operate on the structural element. The incident flow condition consists of a steady part due to current and an unsteady part due to waves, while additionally the structural element (the body) may itself move in an absolute sense. Thus there are 3 velocity and 2 acceleration components involved. We may now make different assumptions, as e.g. described in [4.6-2]. Four plausible modelling assumptions are:

a) The 3 flow fields may all be assumed to be independent, each of them resulting in a separate load on the element. The total load is thus the sum of 3 loads due to 3 unrelated flow fields. This independent flow field or absolute velocity model is shown in figure 4.6-2a. It leads to the following extended form of the Morison equation:

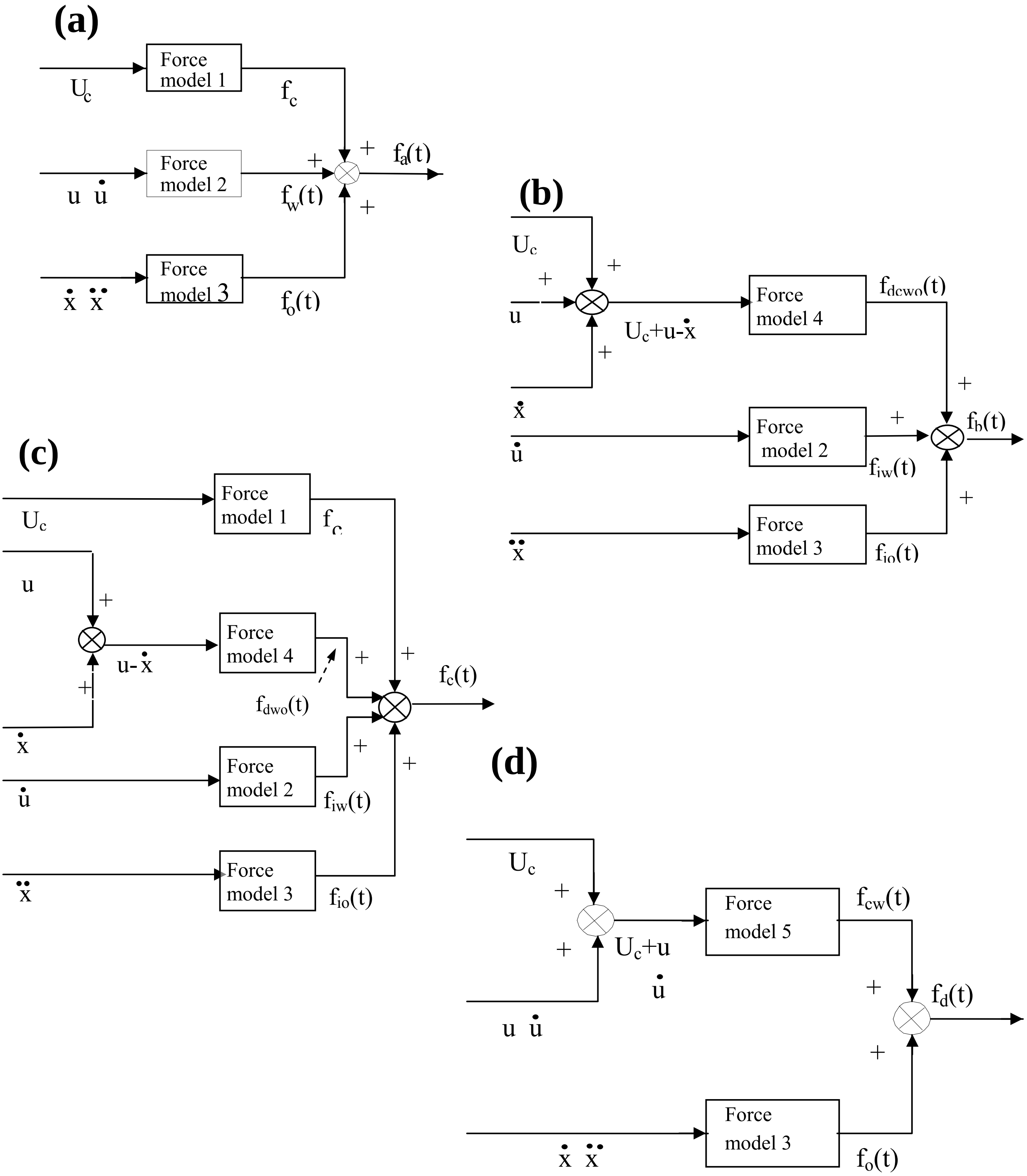

Figure 4.6-2 Block diagrams illustrating four different concepts to model the hydrodynamic load on an element of an oscillating cylinder in current and waves

$$f_a(t) = f_c + f_w(t) + f_o(t)$$

$$f_a = \left[C_{dc} \cdot \frac{1}{2}\rho D \cdot U_c^2\right] + \left[C_{daw} \cdot \frac{1}{2}\rho D \cdot |u| u + C_{maw} \cdot \frac{\rho\pi D^2}{4} \cdot \dot{u}\right] + \left[-C_{dao} \cdot \frac{1}{2}\rho D \cdot |\dot{x}| \dot{x} - C_{Aao} \cdot \frac{\rho\pi D^2}{4} \cdot \ddot{x}\right] \tag{4.6-2}$$

where the drag coefficient C_d , the inertia coefficient C_m and the added mass coefficient C_A carry additional subscripts to link them to the specific case described here; the additional subscripts refer to current (c), absolute wave velocity / acceleration (aw) and absolute velocity / acceleration of the body oscillation (ao).

b) As a second case it may be assumed that the drag load on the element is due to the relative velocity between the fluid and the element. The acceleration dependent load components are linearly dependent on the two accelerations and must therefore remain of the same form as in case (a); see section 3.2. This relative velocity model is depicted in figure 4.6-2b and results in the following equation:

$$f_b(t) = f_{dcwo}(t) + f_{iw}(t) + f_{io}(t)$$

$$f_b = \left[C_{dr} \cdot \frac{1}{2}\rho D \cdot \left|U_c + u - \dot{x}\right| (U_c + u - \dot{x})\right] + \left[C_{maw} \cdot \frac{\rho\pi D^2}{4} \cdot \dot{u}\right] + \left[-C_{Aao} \cdot \frac{\rho\pi D^2}{4} \cdot \ddot{x}\right] \tag{4.6-3}$$

where the additional subscript ‘ r ’ in the first term refers to ‘relative’, i.e. the relative velocity between the flow and the cylinder.

c) A third option is to assume that the loads due to the steady flow of the current and due to the unsteady flow of wave and body oscillation produce separate load components. As the current does not affect the inertia load terms these remain again the same as in the two previous cases. This hybrid load model is a model in between the models (a) and (b) and is shown in figure 4.6-2c: It results in:

$$f_c(t) = f_c + f_{dwo}(t) + f_{iw}(t) + f_{io}(t)$$

$$f_c = \left[C_{dc} \cdot \frac{1}{2}\rho D \cdot U_c^2\right] + \left[C_{drwo} \cdot \frac{1}{2}\rho D \cdot |u - \dot{x}| (u - \dot{x})\right] + \left[C_{maw} \cdot \frac{\rho\pi D^2}{4} \cdot \dot{u}\right] + \left[-C_{Aao} \cdot \frac{\rho\pi D^2}{4} \cdot \ddot{x}\right] \tag{4.6-4}$$

where the additional subscript ‘ rwo ’ in the second term now refers to the relative velocity between the wave and body oscillation only.

d) A fourth option is to distinguish between the incident flow field of current and waves (the far field flow condition) and the flow resulting from the body oscillation, which is only noticeable close to the body (the near field flow). We may accordingly assume that these two flow fields result in separate loads. This far field / near field model is depicted in figure 4.6-2d and leads to the following equation form:

$$f_d(t) = f_{cw}(t) + f_o(t)$$

$$f_d = \left[C_{drcw} \cdot \frac{1}{2} \rho D \cdot \left| U_c + u \right| (U_c + u) + C_{maw} \cdot \frac{\rho \pi D^2}{4} \cdot \dot{u} \right] + \left[-C_{dao} \cdot \frac{1}{2} \rho D \cdot \left| \dot{x} \right| \dot{x} - C_{Aao} \cdot \frac{\rho \pi D^2}{4} \cdot \ddot{x} \right] \tag{4.6-5}$$

where the additional subscript 'rcw' refers to the relative velocity between current and waves only; other subscripts are as explained before.

The 4 equations (4.6-2) to (4.6-5) are all extensions of the original Morison equation; each relates to a different view of the same set of circumstances on the basis of certain reasonable postulates. Note that the inertia coefficient C_{maw} for the inertial wave load component, and the added mass coefficient C_{Aao} for the component of the fluid reaction force that is due to the body acceleration are the same in all models (under the assumptions made), but that the drag coefficients in the respective formulations are all different. The 4 options described above may not be exhaustive; it is quite possible that other assumptions can be postulated leading to yet different forms of Morison extensions; not even mentioning that an investigator may decide that the Morison equation is not a suitable basic load model to start from.

To investigate the 4 above models (and others) Shafiee-far performed an extensive series of well-controlled laboratory experiments at Delft University of Technology [4.6-3]. These resulted in a large database of experimental data to which the models could be fitted. He concluded that none of the models was appropriate in all circumstances, but that the relative velocity model (b) and equation 4.6-3 performed best under most conditions, *provided that* the empirical set of coefficients C_{dr}, C_{maw} and C_{Aao} was used, reflecting the combined flow situation of current, waves and oscillations during the tests. These coefficients are likely to differ from the values found in the literature for situations with e.g. current alone or waves alone. The overall conclusion is that the relative velocity model (b) and the corresponding extended Morison equation 4.6-3 is generally the best available description for the hydrodynamic load on a structural element. However, it is not justified to adopt it uncritically in all circumstances. One needs to remain alert and careful, especially in cases involving structural vibrations. In those cases the hydrodynamic damping of the vibration, associated with the body velocity $\dot{x}$, is implicit and through equation 4.6-3 inherently coupled with the applied loading. Experience shows that the hydrodynamic damping may then be appreciably overestimated if the displacements of the element are smaller than approximately one diameter.

Another attempt at better understanding of the hydrodynamic loading problem through extremely well controlled laboratory experiments in random waves and higher order spectral analysis is reported in reference [4.6-4]. The discussion of the hydrodynamic loads on slender members in this section is of a rather advanced nature. It illustrates the complexity of the problem and puts Morison's equation with its extensions in proper perspective. An important further objective of the discussion is to serve as an exercise in modelling, which is so fundamentally important to all engineering effort, as discussed in chapter 3. For the remainder of section 4.6 we will more pragmatically adopt the Morison equation, including its plausible generalisations, as the best available method for practical applications. The choice of appropriate coefficients remains a difficult issue, however. In practice the choice is largely based on experience and the resulting load calculation is accompanied by an appreciable level of uncertainty. As a result of this it should further expressly be noted that coefficients, kinematics of the flow field and modelling assumptions form an inseparable whole in the calculation process of hydrodynamic loading.

4.6.2 Hydrodynamic loads at a particular point

It is important to have a good grasp of the hydrodynamic loading on offshore structures. Therefore we will elaborate a bit further on the loads due to the Morison equation; these loads are especially important for space frame type structures. In this section we will discuss the loads at a particular point in the fluid domain and in the next section the correlation between loads at two different points in space. For the purpose of illustration we will again consider the base case of a vertical circular cylinder in periodic Airy waves; the cylinder is positioned at point s in the direction of wave travel.

The two components of the load are the inertia load per unit length:

$$f_i(s,z,t) = C_m \cdot \frac{\rho\pi D^2}{4} \cdot \dot{u}(s,z,t) = A \cdot \dot{u}(s,z,t) \tag{4.6-6}$$

and the drag load per unit length:

$$f_d(s,z,t) = C_d \cdot \tfrac{1}{2}\rho D \cdot \left| u(s,z,t) \right| u(s,z,t) = B \cdot \left| u(s,z,t) \right| u(s,z,t) \tag{4.6-7}$$

where A and B are constants with dimensions [kg/m] and [kg/m^2], respectively.

Both components are controlled by the kinematics of the flow field (see Annex B), from which we see that the kinematics for linear waves on intermediate water depth are:

$$\begin{aligned} u(s,z,t) &= \hat{\zeta}\omega \cdot D(z) \cdot \cos(ks - \omega t) = \hat{u}_0 \cdot D(z) \cdot \cos(ks - \omega t) \\ \dot{u}(s,z,t) &= \hat{\zeta}\omega^2 \cdot D(z) \cdot \sin(ks - \omega t) = \omega\, \hat{u}_0 \cdot D(z) \cdot \cos(ks - \omega t - \frac{\pi}{2}) \end{aligned} \tag{4.6-8}$$

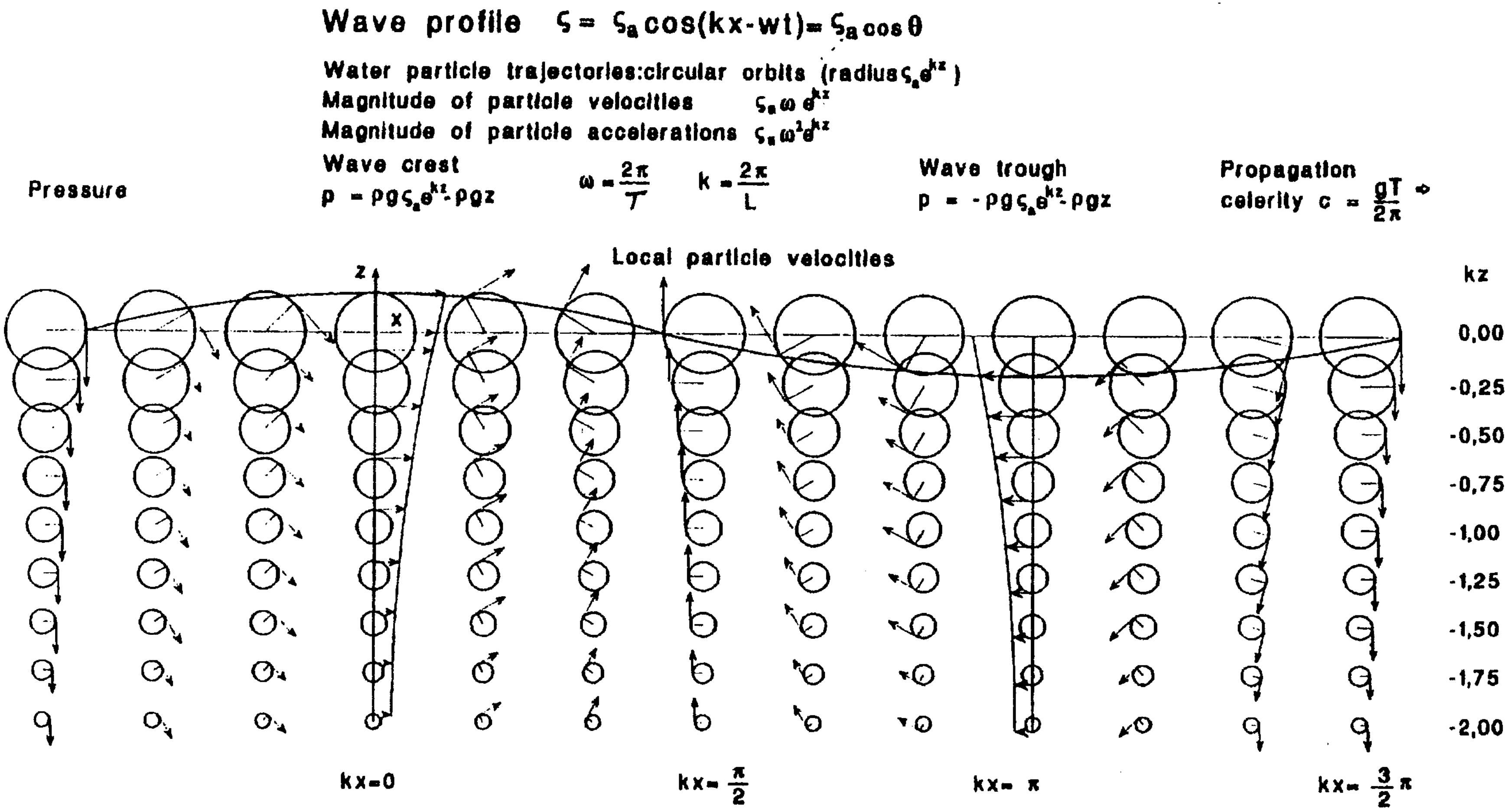
Wave profile $\varsigma = \varsigma_a \cos(kx - \omega t) = \varsigma_a \cos\theta$
Water particle trajectories:circular orbits (radius $\varsigma_a e^{kz}$)
Magnitude of particle velocities $\varsigma_a \omega e^{kz}$
Magnitude of particle accelerations $\varsigma_a \omega^2 e^{kz}$
Pressure
Wave crest
$p = \rho g \varsigma_a e^{kz} - \rho g z$
$\omega = \frac{2\pi}{T}$
$k = \frac{2\pi}{L}$
Wave trough
$p = -\rho g \varsigma_a e^{kz} - \rho g z$
Propagation celerity $c = \frac{gT}{2\pi}$
Local particle velocities
z
x
kz
0,00
-0,25
-0,50
-0,75
-1,00
-1,25
-1,50
-1,75
-2,00
kx=0
$kx = \frac{\pi}{2}$
$kx = \pi$
$kx = \frac{3}{2}\pi$

Figure 4.6-3. Particle orbits and dynamics of a deepwater wave by linear theory (from [4.6-5])

where:

$\hat{u}_0 = \hat{\zeta}\omega$

$D(z)$ = depth decay function

k = wave number

Note that in equation 4.6-8 the influences of the variables s, z and t are separated into different factors. $\hat{u}_0$ is the velocity amplitude at the free surface and hence an independent parameter; the variables s and t only appear in the argument of the cosine function, while the variable z only manifests itself in the depth decay function $D(z)$:

$$D(z) = \frac{\cosh k(z+d)}{\sinh kd} \qquad (4.6\text{-}9)$$

$$-d \le z \le 0 \quad \text{(for Airy waves)}$$

For deep water waves $kd \to \infty$ and the depth decay function reduces to:

$$D(d \to \infty) = e^{kz} \qquad (4.6\text{-}10)$$

For $z = -\frac{1}{2}\lambda$ the exponent assumes the value $kz = -\pi$ and $e^{-\pi} \approx 0.04$, which is usually considered negligibly small. Therefore, wave loads practically vanish for depths greater than half the wavelength.

In addition to the above we can draw the following conclusions from these equations:

- The time dependent factors in $\dot{u}$ and u depend on the horizontal position s and not on the vertical position z. For a vertical element the inertia loads are therefore mutually in phase over the entire length of the cylinder. Similarly, the drag loads are mutually in phase over the entire length of the cylinder. However, for an inclined member s varies over the length of the member, so that the contributions per unit length for each component of the load differ in phase from point to point along the member.
- The inertia load leads the drag load by 90 degrees, i.e. a quarter of a period; see equation 4.6-8. Note that a phase angle of $-\pi/2$ means a phase *lead* as the time dependency $-\omega t$ is also negative. This can perhaps more easily be appreciated by choosing the cylinder to be located at $s = 0$ and reversing the sign of the argument, which is allowable for a cosine function. The time dependent factor for $\dot{u}$ then becomes $\cos(\omega t + \pi/2)$ which is indeed a 90 degrees phase lead over $\cos(\omega t)$.
- The inertia load decreases with depth according to the factor $D(z)$.
- The drag load decreases with depth according to the factor $\left(D(z)\right)^2$.
- As the magnitudes of the inertia and the drag loads per unit length do not decrease with depth *at the same rate*, the phase of the total load $f(t) = f_i(t) + f_d(t)$ is *not* constant over the length of the member, not even for a vertical member!

The water particle velocities under a deep water wave are shown in figure 4.6-3 from reference [4.6-5]. The velocities are a function of both time and location. The figure shows the particle orbits and velocities as a function of location $s = x$ for time $t = 0$, which means a wave crest at $s = x = 0$; for increasing time the wave progresses from left to right. Since for circular orbits the acceleration is directed towards the centre of the circle (the centripetal acceleration), the inertia load is a maximum and directed to the right at the zero crossing in the centre of the figure at $ks = kx = \pi/2$. Focusing on this location and now letting the time increase (the wave progresses from left to right) the inertia load is hence largest at the time when the water surface crosses through zero in an upward direction, i.e. at the zero crossing prior to a wave crest passing the location. The drag load is obviously a maximum when a wave crest passes the location. For linear Airy waves the drag load under a wave trough is equal and opposite to the drag load under a wave crest. For non-linear periodic waves, and more generally when there is also a current present, this is no longer true, however.

4.6.3 Correlation between loads at spatially separated points

Now consider two identical vertical cylinders, one located at $s = s_1$ and one at $s = s_2$. The horizontal distance between the two cylinders is $\Delta s = |s_2 - s_1| = \ell$; without loss of generality we may take $s_1 = -\frac{1}{2}\ell$ and $s_2 = +\frac{1}{2}\ell$.

The inertia load

Using equations 4.6-6 to 4.6-8 we can write for the inertia load per unit length at any elevation z:

$$\begin{aligned} f_{i,2cyl}(z,t) &= A\cdot\{\,\dot{u}(s_1,z,t)+\dot{u}(s_2,z,t)\} = \\ &= A\cdot\omega\hat{u}_0\,D(z)\cdot\left\{\cos(ks_1-\omega t-\frac{\pi}{2})+\cos(ks_2-\omega t-\frac{\pi}{2})\right\} \\ &= A\cdot\omega\hat{u}_0\,D(z)\cdot\left\{2\cos\left(\frac{k(s_1+s_2)-2\omega t-\pi}{2}\right)\cdot\cos\left(\frac{k(s_1-s_2)}{2}\right)\right\} \\ &= A\cdot\omega\hat{u}_0\,D(z)\cdot\left\{2\cos\left(-\omega t-\frac{\pi}{2}\right)\cdot\cos(\tfrac{1}{2}kl)\right\} \\ &= \hat{f}_i(z)\cdot\left\{2\cos\left(-\omega t-\frac{\pi}{2}\right)\cdot\cos(\tfrac{1}{2}kl)\right\} \end{aligned} \tag{4.6-11}$$

where:

$$\hat{f}_i(z) = A\cdot\omega\hat{u}_0 D(z) = C_m\cdot\frac{\rho\pi D^2}{4}\cdot\omega^2\hat{\zeta}\cdot\frac{\cosh k(z+d)}{\sinh kd} \tag{4.6-12}$$

Hence:

$$f_{i,2cyl}(z,t) = 2\cos(\tfrac{1}{2}kl)\cdot\hat{f}_i(z)\cdot\cos\left(-\omega t-\frac{\pi}{2}\right) = 2\cos(\tfrac{1}{2}kl)\cdot f_i(z,t) \tag{4.6-13}$$

where $f_i(z,t)$ is the wave load on an element of a single cylinder at the centre $(s=0)$ of the two-cylinder configuration.

The factor $\cos(\frac{1}{2}kl)$ may either be considered as a function of the distance ℓ for a fixed wavelength λ or as a function of the wave length λ for a fixed distance ℓ. Looking at equation 4.6-13 now as a function of the distance ℓ, the total inertia load per unit length on the 2 cylinders has maxima (positive or negative) equal to twice the amplitude of the load on a single cylinder if:

$$\cos(\tfrac{1}{2}kl) = \pm 1$$
$$\tfrac{1}{2}kl = 0 \pm n\cdot\pi, \quad \text{for } n = 1,\ 2,\ 3,\ ....$$

that is for distances ℓ:

$$\ell = \frac{n\cdot 2\pi}{k} = n\cdot\lambda \quad \text{for } n = 1,\ 2,\ 3,\ ...... \tag{4.6-14}$$

Entirely similar, the total inertia load per unit length on the 2 cylinders is identically equal to zero for all time t if:

$$\cos(\tfrac{1}{2}kl) = 0$$
$$\tfrac{1}{2}kl = \pm(\tfrac{1}{2}+n)\cdot\pi, \quad \text{for } n = 0,\ 1,\ 2,\ 3,\ ......$$

that is for distances ℓ:

$$\ell = \frac{(\frac{1}{2}+n)\cdot 2\pi}{k} = (\tfrac{1}{2}+n)\cdot\lambda \quad \text{for } n = 0,\ 1,\ 2,\ 3,\ ...... \tag{4.6-15}$$

The drag load

For the drag load per unit length on two cylinders a similar treatment is somewhat more complicated due to the non-linear form of equation 4.6-7, but otherwise fully analogous. To show this we develop $|\cos(ks-\omega t)|\cos(ks-\omega t)$ first in a series expansion:

$$\begin{aligned}&|\cos(ks-\omega t)|\cdot\cos(ks-\omega t) = \\ &\quad \frac{8}{3\pi}\cos(ks-\omega t) + \frac{8}{15\pi}\cos\big(3(ks-\omega t)\big) + \frac{8}{105\pi}\cos\big(5(ks-\omega t)\big) + ...\end{aligned} \tag{4.6-16}$$

When applied to the locations $s = s_1$ and $s = s_2$ each couple of terms in the series expansion may be transformed as follows:

$$\cos\big(m(ks_1-\omega t)\big) + \cos\big(m(ks_2-\omega t)\big) = 2\cos\big(-m\omega t\big)\cdot\cos\big(\tfrac{1}{2}mk\ell\big) \qquad m = 1,3,5,.... \tag{4.6-17}$$

Therefore, the drag load per unit length on 2 cylinders may be written in a fully analogous form to equation 4.6-13 as:

$$f_{d,2cyl}(z,t) = 2\sum_m\Big\{\cos\big(\tfrac{1}{2}mk\ell\big)\cdot\hat{f}_d(z)\cdot\cos(-m\omega t)\Big\} = 2\sum_m\Big\{\cos\big(\tfrac{1}{2}mk\ell\big)\cdot f_d(z,t)\Big\} \tag{4.6-18}$$

The factor $\cos(\frac{1}{2}kl) = \pm 1$ for $\frac{1}{2}kl = n\pi$. For all integer values of m the factor $\cos(\frac{1}{2}mkl)$ is then also equal to ± 1. Similarly, the factor $\cos(\frac{1}{2}kl) = 0$ for $\frac{1}{2}kl = (\frac{1}{2}+n)\cdot\pi$. As m is an odd integer, the factor $\cos(\frac{1}{2}mkl)$ remains zero for all m. Therefore, all terms in the series expansion for the drag load are maximum / minimum and zero for the same distances as the inertia load; see equations 4.6-14 and 4.6-15.

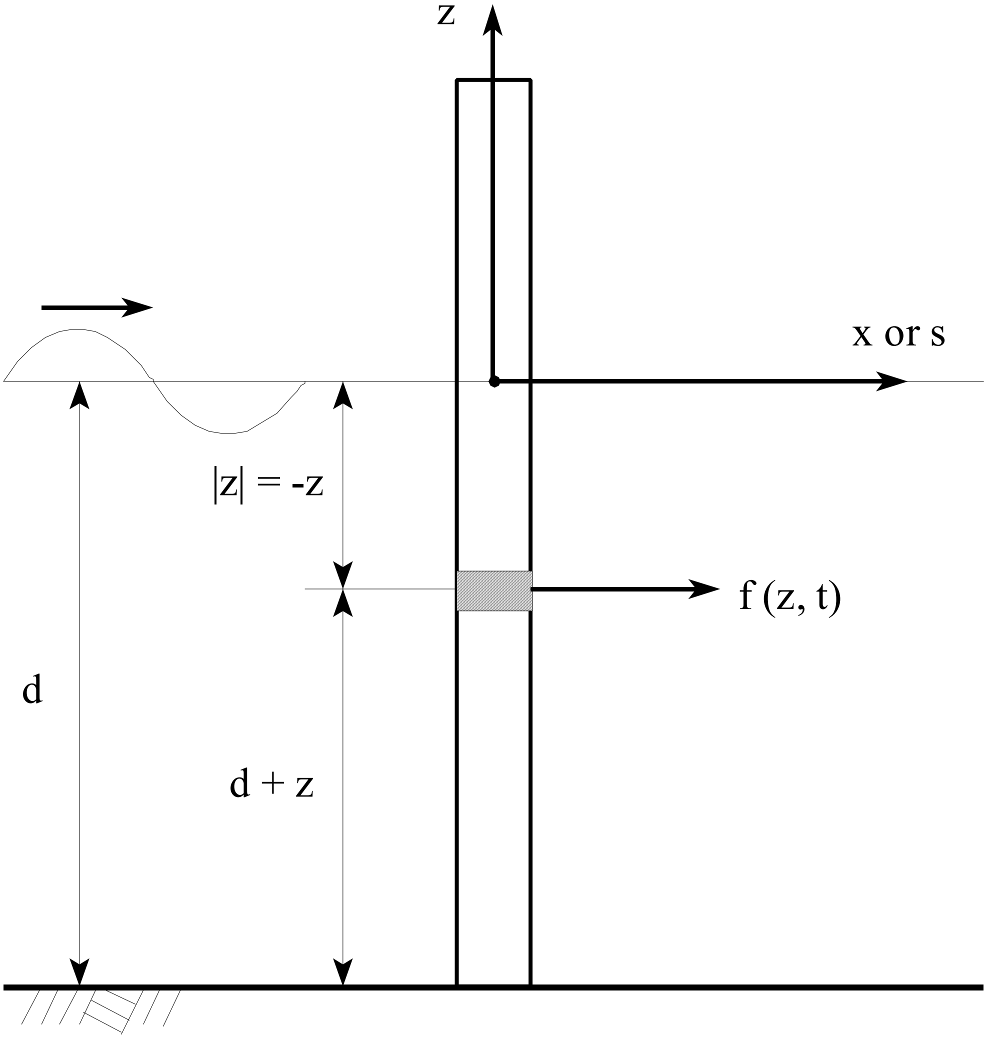

Figure 4.6-4. Wave force on an element of a vertical cylinder and moment arm about the sea floor

The total wave load

The total wave load per unit length on the 2 cylinders at elevation z is the sum of the inertia load in equation 4.6-13 and the drag load in equation 4.6-18:

$$f_{2cyl}(z,t) = 2 \cdot \left\{ \cos(\tfrac{1}{2}k\ell) \cdot f_i(z,t) + \sum_m \left\{ \cos(\tfrac{1}{2}mk\ell) \cdot f_d(z,t) \right\} \right\} \tag{4.6-19}$$

As was shown above, the terms in the drag load are maximum / minimum or zero for the same distances as the inertia load. This means that at each elevation z the wave loads on 2 vertical cylinders reinforce each other when the cylinders are placed at distances of $n\lambda \, (n = 1, 2, 3, ...)$ and cancel each other for distances of $(\tfrac{1}{2} + n)\lambda \, (n = 0, 1, 2, 3, ...)$. This applies equally to the linearised drag load ($m = 1$ only) and to the full non-linear drag load.

4.6.4 Global loads on a structure

It is clear from the preceding sections that the calculation of hydrodynamic loads on a space frame structure is a difficult and laborious process. The large number of members involved, their different positions and orientations in the structure, the influence of horizontal spatial separation and vertical depth decay, as well as the time dependency of all contributions to the applied loading make the calculation very complicated and full of possibility for errors. Therefore, the calculation of hydrodynamic loads for real structures is invariably made using a thoroughly verified computer program. The global hydrodynamic loads on the structure are the total applied horizontal load at the sea floor, which is often called the base shear, and the total moment about the sea floor, which is called the overturning moment. However, for structural design we will generally not only need these global loads, but also the three dimensional load distribution over the structure, as well as its time dependency. This is a formidable problem that, other than for the simplest geometries, can only be solved adequately by computer calculations.

In some preliminary design situations highly simplified manual or spreadsheet type calculations of extreme design loads are nonetheless very useful. The structure is then normally represented by a single vertical member, or a collection of vertical members, where phase differences due to spatial separation in the horizontal plane are neglected. Guidelines for modelling a structure as an equivalent vertical stick are given in Annex D.

As a further illustration of some important aspects of hydrodynamic loading we will continue with the analytical treatment and discussion of the loads on two vertical cylinders positioned in the wave direction at a distance ℓ. This is the simplest representation of a two-dimensional frame of an offshore structure parallel to the wave direction.

The total applied wave load is obtained by integrating the loads per unit length over the full water column. Similarly, the total applied moment about the sea floor is obtained by integrating the product of the wave load per unit length and the arm $(d+z)$ about the sea floor, again over the full water column; see figure 4.6-4. For two vertical cylinders both the inertia and the drag loads are in phase over the full length of the cylinders, but the phases for the inertia and drag loads are not the same. Therefore they are best integrated separately before they are combined. The only factor that is dependent on z is the depth decay function $D(z)$; integration over z thus means integration of $D(z)$ and $(d+z)D(z)$ over the water column. To show what we want to show and avoid unnecessary complications with the hyperbolic functions we shall further assume deep water linear waves. It should be noted that deep water also means that $d > \frac{1}{2}\lambda$ and $e^{-kd} < 0.04$; therefore, in the analytical evaluations the factor $e^{-kd} < 0.04$ will be put equal to zero. Then:

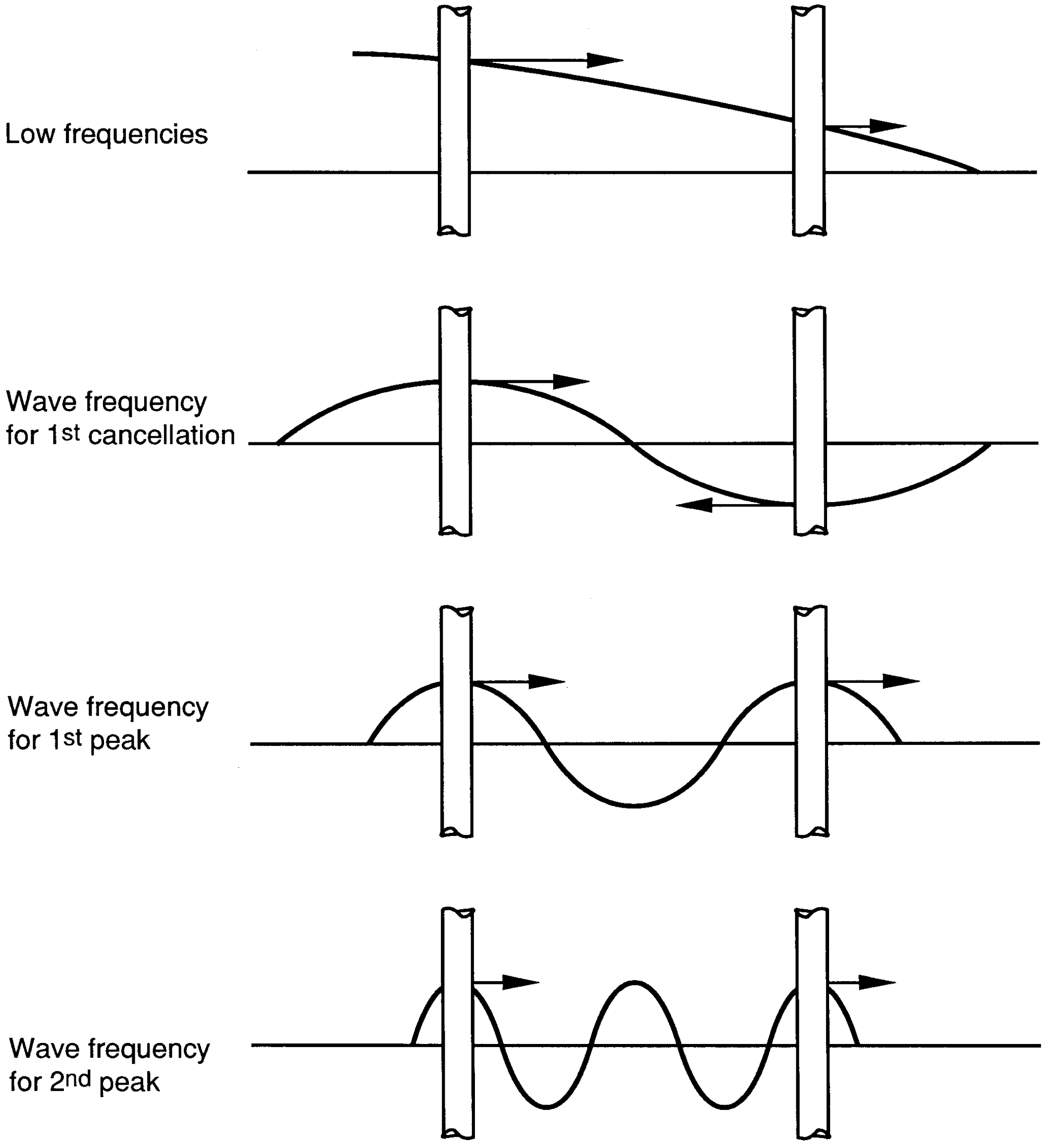
Low frequencies
Wave frequency for 1st cancellation
Wave frequency for 1st peak
Wave frequency for 2nd peak

Figure 4.6-5. Reinforcement and cancellation effects for wave drag loading due to horizontal separation of cylinders

$$\begin{aligned}
&\int_{-d}^{0} D(z)dz = \int_{-d}^{0} e^{kz}dz = \frac{1}{k}\left[e^{kz}\right]_{-d}^{0} = \frac{1}{k} = \frac{g}{\omega^2}\\
&\int_{-d}^{0} D^2(z)dz = \int_{-d}^{0} e^{2kz}dz = \frac{1}{2k}\left[e^{2kz}\right]_{-d}^{0} = \frac{1}{2k} = \frac{g}{2\omega^2}\\
&\int_{-d}^{0} (d+z)D(z)dz = \int_{-d}^{0} (d+z)e^{kz}\,dz = \frac{d}{k}\left[e^{kz}\right]_{-d}^{0} + \frac{1}{k}\left[\frac{kz-1}{k}\cdot e^{kz}\right]_{-d}^{0} = \frac{d}{k} - \frac{1}{k^2} = \frac{1}{k}\left(d - \frac{1}{k}\right)\\
&\int_{-d}^{0} (d+z)D^2(z)dz = \int_{-d}^{0} (d+z)e^{2kz}\,dz = \frac{d}{2k}\left[e^{2kz}\right]_{-d}^{0} + \frac{1}{2k}\left[\frac{2kz-1}{2k}\cdot e^{2kz}\right]_{-d}^{0} = \frac{1}{2k}\left(d - \frac{1}{2k}\right)
\end{aligned} \tag{4.6-20}$$

The integration limits applied here are in line with the assumption of linear waves. For the full non-linear case the integration should extend from $(-d)$ to $\zeta(t)$. As the inertia load is largest at wave zero-crossings, the linearisation of the upper integration limit from $z = \zeta(t)$ to $z = 0$ does not affect the magnitude of the inertia load at all. However, the drag load is largest under wave crests / troughs and therefore linearisation of the integration limit clearly does have an important effect. As Airy theory is only valid up to the still water level this begs the question how to extrapolate the wave orbital velocities for $\zeta(t) > 0$. Some options for this will be presented at the end of this section.

For $-d \le z \le 0$ the total inertia and drag loads and the associated overturning moments on the two cylinders become:

$$\begin{aligned}
&F_i(t) = \left\{2C_m \frac{\rho\pi D^2}{4}\cdot g\hat{\zeta}\cdot\cos(\tfrac{1}{2}kl)\right\}\cdot\cos(-\omega t - \tfrac{1}{2}\pi)\\
&F_d(t) = \left\{2C_d\cdot\tfrac{1}{2}\rho D\cdot\tfrac{1}{2}g\hat{\zeta}^2\right\}\cdot\sum_m \cos(\tfrac{1}{2}mkl)\cdot\cos(-m\omega t)\\
&M_i(t) = \left\{2C_m \frac{\rho\pi D^2}{4}\cdot g\hat{\zeta}\cdot\cos(\tfrac{1}{2}kl)\right\}\cdot(d - \frac{\lambda}{2\pi})\cdot\cos(-\omega t - \tfrac{1}{2}\pi)\\
&M_d(t) = \left\{2C_d\cdot\tfrac{1}{2}\rho D\cdot\tfrac{1}{2}g\hat{\zeta}^2\right\}\cdot(d - \frac{\lambda}{4\pi})\cdot\sum_m \cos(\tfrac{1}{2}mkl)\cdot\cos(-m\omega t)
\end{aligned} \tag{4.6-21}$$

From equation 4.6-21 we can draw the following conclusions for the global load on 2 vertical cylinders that are a distance ℓ apart; note that the results assume linear waves and deep water:

- The inertia load is linearly proportional to the wave amplitude, as expected. Its magnitude varies with wave length according to the factor $\cos(\frac{1}{2}kl)$. The loads on the two individual cylinders thus add and reinforce each other for $\ell = n\lambda \quad (n = 1, 2, 3, ...)$, while they subtract and cancel out for $\ell = (\frac{1}{2} + n)\lambda \quad (n = 0, 1, 2, 3, ...)$, as was already seen for the loads per unit length.

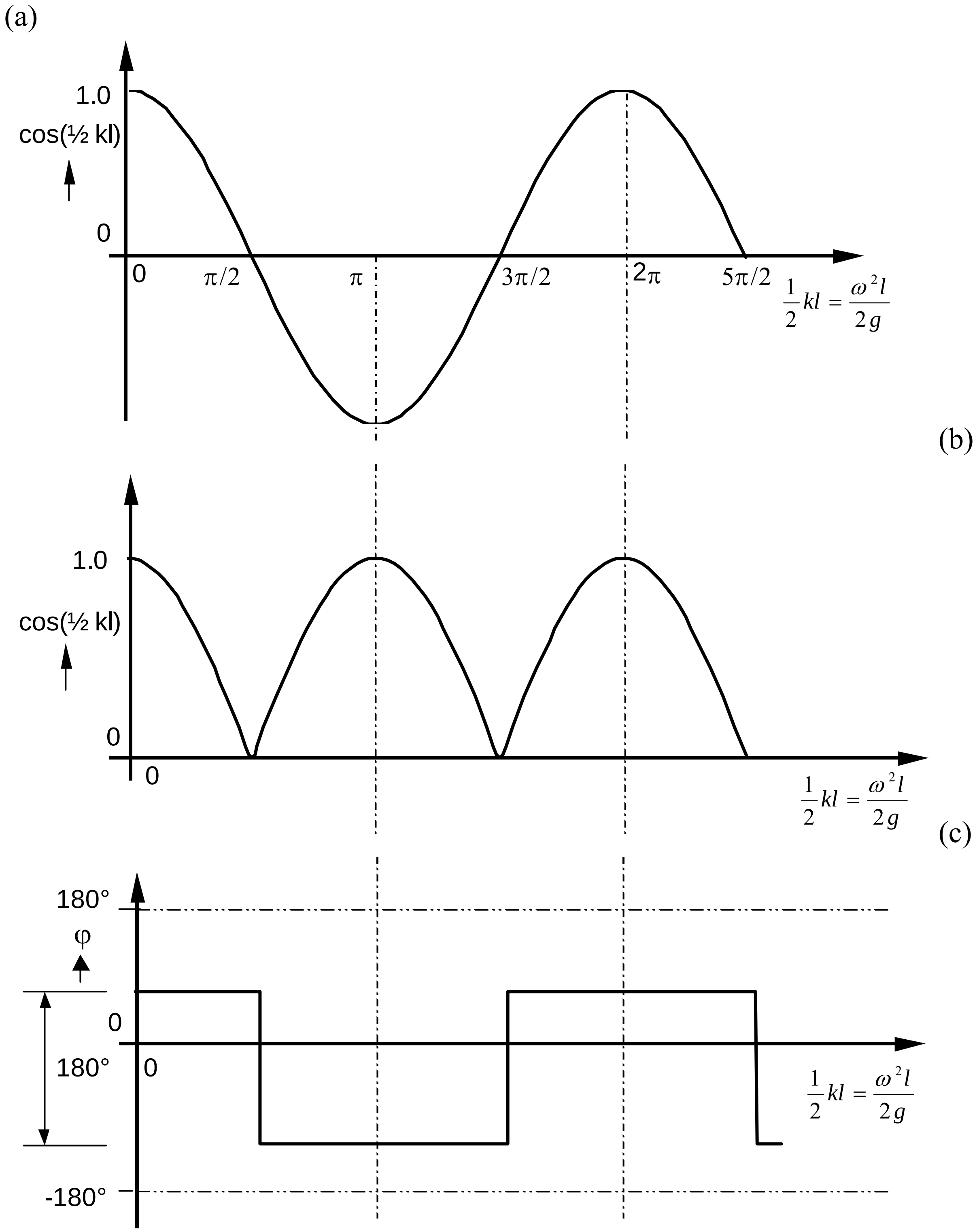

Figure 4.6-6. Amplitude and phase of the global applied wave load on two vertical cylinders (linear waves, deep water)

- The drag load is quadratically proportional to the wave amplitude, as it should. Its magnitude varies with wave length according to the factor $\sum_{m} \cos(\frac{1}{2}mkl)$. This results in reinforcement and cancellation for the same wave lengths as for the inertia load, as was demonstrated in section 4.6.3. For the drag loads this phenomenon is pictorially shown in figure 4.6-5. The same picture applies to the inertia loads, provided that the wave is moved over a quarter of the wave period.
- Both the inertia and the drag load is independent of the water depth. This is not a general characteristic of wave loading, but a direct consequence of the deep water assumption: the lower parts of the cylinders between $z = -\frac{1}{2}\lambda$ and $z = -d$ are not loaded at all. Therefore, as long as $d > \frac{1}{2}\lambda$ the loads are the same for all water depths.
- The overturning moment due to the inertia load naturally follows the same pattern as the inertia load itself, except that the water depth now clearly is an important factor. The application point of the inertia load lies at a distance of $1/k = \lambda/2\pi$ below the still water surface.
- Similarly, the overturning moment due to the drag load follows the same pattern as the drag load itself. The application point of the drag load lies at a distance of $1/2k = \lambda/4\pi$ below the still water surface, that is half the distance of the inertia load.

To investigate the shape of the total applied wave loading function as a function of wave length (or wave frequency), but for a fixed distance ℓ of the two cylinders, it suffices to take the linearised drag load for $m = 1$. This has no influence on the *position* of the maxima / minima and the zero points of the applied loading as a function of wave length, as was demonstrated in section 4.6.3. The *magnitude* of the maxima / minima and the value of the load as a function of time during a full cycle are, of course, influenced by the non-linear terms. We can write the linearised total load as:

$$\begin{aligned} F(t) &= F_i(t) + F_d(t) \\ &= A^* \cdot \cos(\tfrac{1}{2}kl) \cdot \left[\cos(-\omega t - \tfrac{1}{2}\pi)\right] + B^* \cdot \cos(\tfrac{1}{2}kl) \cdot \cos(-\omega t) \\ &= \sqrt{(A^*)^2 + (B^*)^2} \cdot \cos(\tfrac{1}{2}kl) \cdot \cos(-\omega t - \varphi) \\ &= \hat{F}\cos(-\omega t - \varphi) \end{aligned} \tag{4.6-22}$$

where:

$$\begin{aligned} A^* &= 2C_m \cdot \frac{\rho\pi D^2}{4} \cdot g\hat{\zeta} \\ B^* &= 2C_d \cdot \tfrac{1}{2}\rho D \cdot \tfrac{1}{2} g\hat{\zeta}^2 \\ \hat{F} &= \sqrt{(A^*)^2 + (B^*)^2} \cdot \cos(\tfrac{1}{2}kl) \\ \tan\varphi &= \frac{A^*}{B^*} = \pi \cdot \frac{C_m}{C_d} \cdot \frac{D}{\hat{\zeta}} \end{aligned} \tag{4.6-23}$$

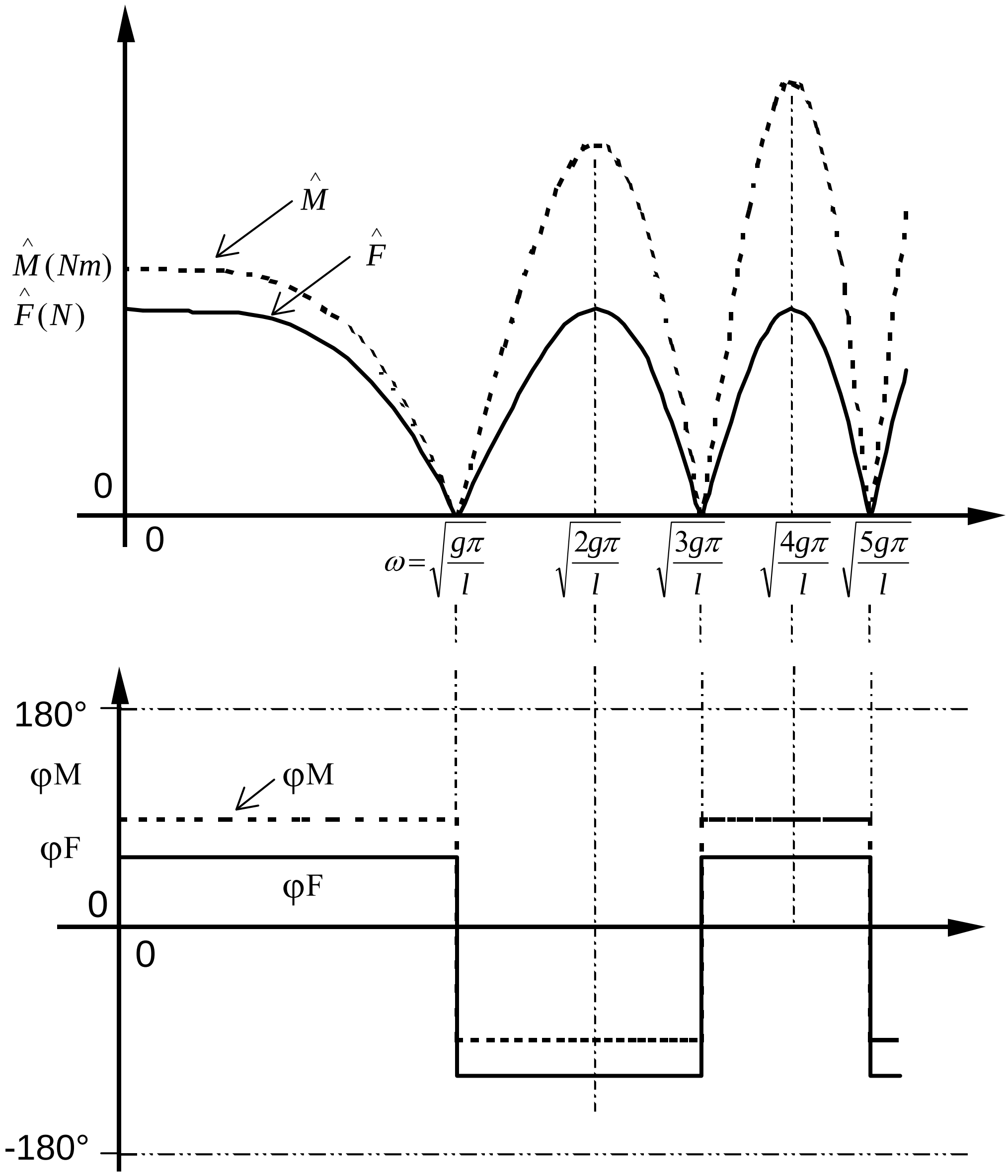

Figure 4.6-7. Applied wave load and overturning moment on two vertical cylinders (linear waves, deep water)

The amplitude $\hat{F}$ of the global applied load is the product of two factors. For given conditions the first of these (the square root) is a constant, but the second depends on the wave length or (as wave length is interchangeable with frequency) on wave frequency. The factor $\cos(\frac{1}{2}kl)$ is sketched in figure 4.6-6a on the basis of $\frac{1}{2}kl$; for deep water waves as assumed here $\frac{1}{2}kl = \omega^2 \ell / 2g$. For low frequencies (long wave lengths) the factor decreases gradually from its initial value of 1.0. At $\frac{1}{2}kl = \pi/2$, i.e. $\omega^2 = \pi g / \ell$, the factor becomes zero for the first time so that $\hat{F}$ is also zero. It further passes from positive to negative at this point. This means that the load changes direction: instead of acting in the direction in which the wave progresses under a wave crest, it now acts in the opposite direction under a wave trough, i.e. against the wave. This change of direction is equivalent with a shift of 180° in the phase angle φ, so that the factor $\cos(\frac{1}{2}kl)$ can also be expressed as $\left|\cos(\frac{1}{2}kl)\right|$ in combination with a jump of 180° in phase, as shown in figure 4.6-6b. For increasing values of $\frac{1}{2}kl$, i.e. reducing wave lengths and increasing frequencies, the process of wave load reinforcement and cancellation, together with 180° phase jumps, repeats itself many times. When the wave load magnitude $\hat{F}$ is plotted on a linear instead of a quadratic frequency scale we obtain figure 4.6-7.

The magnitude $\hat{M}$ of the overturning moment is also plotted in figure 4.6-7. It follows the same pattern as $\hat{F}$, except that $\hat{M}$ increases for increasing ω (shorter waves) because the application point of the total horizontal load moves upwards.

This behaviour of the applied wave loading and the associated overturning moment is due to the spatial separation of (near) vertical elements and is typical for steel space frame structures, concrete gravity base structures with two or more vertical columns and jack-ups. The phenomenon is very important and must always be accounted for. In some cases it is even consciously applied in design to position legs, conductors or other members such that the applied loading is minimised at frequencies where the structural response is particularly sensitive (e.g. resonance frequencies) or over a range of frequencies where significant applied loading is experienced in respect of fatigue considerations. The relatively low, high frequency waves occur so often during the structure's lifetime that they are responsible for much of the fatigue damage. Therefore, minimising wave loading in short waves by using the spatial separation effect to advantage can pay off nicely. However, in extreme storm conditions waves are invariably long compared to the dimensions of a structure and phase differences from one end to the other will remain limited. For example, for design waves with a length of 10 times the width or length of the structure the maximum phase difference is $(\ell_{\max} / \lambda) \cdot 2\pi$ or (0.1)x(360) degrees = 36 degrees. Notwithstanding this, phase differences over the structure due to spatial separation of components must always be taken into account; an algebraic addition of individual maximum loads is unduly conservative. The only exception is early estimates of extreme hydrodynamic loading during preliminary design efforts, for which these phase differences are often neglected; see Annex D.

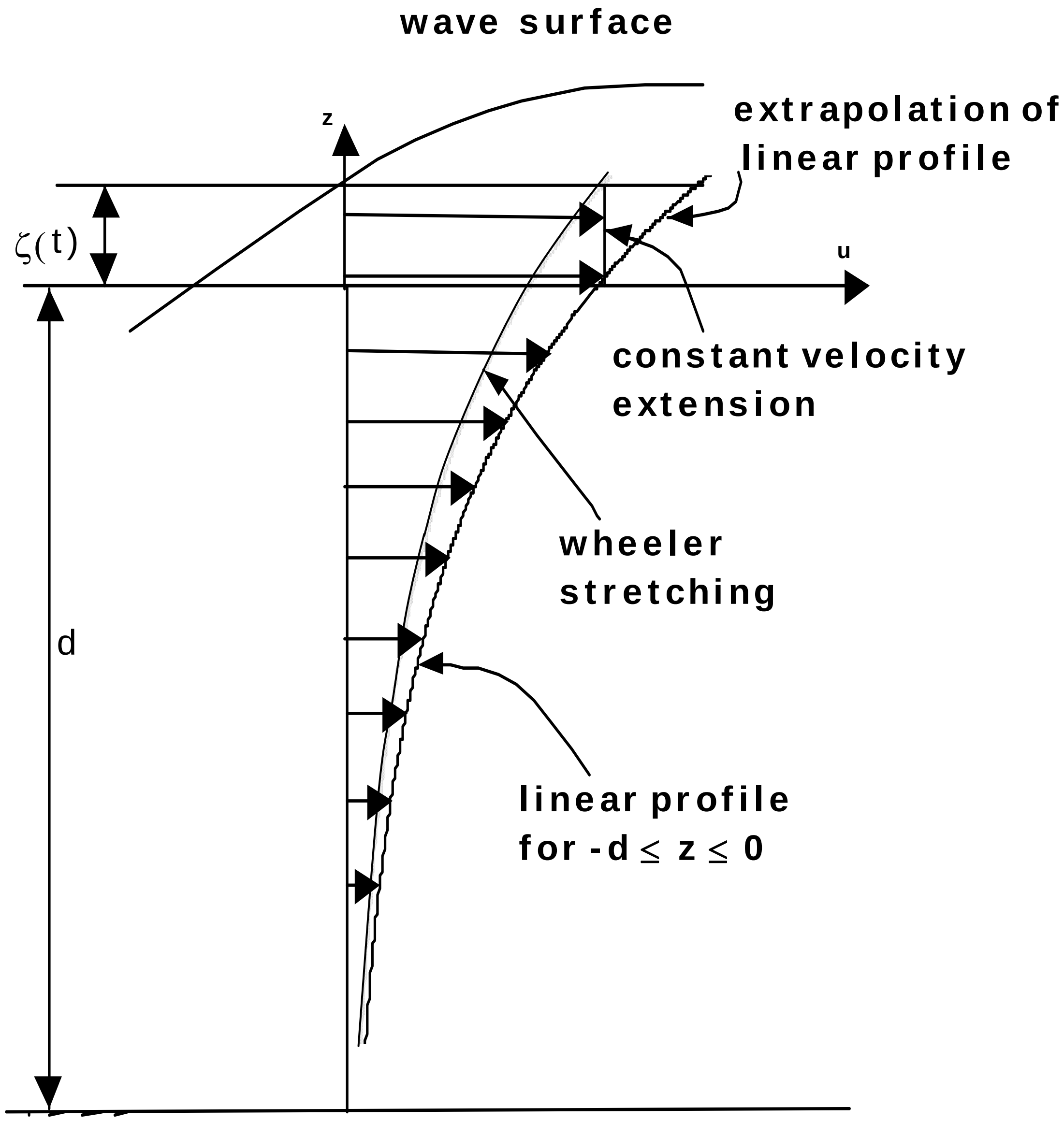
wave surface
z
extrapolation of linear profile
ζ(t)
u
constant velocity extension
wheeler stretching
d
linear profile for -d ≤ z ≤ 0

Figure 4.6-8. Three engineering assumptions for the extension of the horizontal velocity for $z > 0$ in linear waves

For real structures the effects of spatial separation may not always show up so clearly as in the simple case of two vertical cylinders. The fact that many members contribute to the global loading, that several members are sloping instead of vertical, and the influence of current will all tend to spread reinforcement and cancellation effects more widely than to focus them at one single frequency. However, peaks and valleys, as well as zero points with 180° phase jumps, will nearly always be present in the applied wave loading and overturning moment functions on structures.

To conclude this section on the global hydrodynamic loading of structures a few observations are made that engineers need to be aware of:

- Figure 4.6-7 applies to deep water waves. However, for (very) low frequencies the wave lengths are so long that the assumption of deep water invariably breaks down. The limiting case is approximately $\lambda = 2d$ or $\omega = \sqrt{\pi g/d}$. Below this frequency the figure therefore does not show the correct trend.
- It may further seem strange that the peaks of $\hat{F}$ in figure 4.6-7 have the same magnitude for all ω, while the peaks of $\hat{M}$ even increase with frequency. However, it should be remembered that $\hat{\zeta}$ was assumed to be constant, i.e. independent of ω. Therefore, figure 4.6-7 may be interpreted as transfer functions of $\hat{F}/\hat{\zeta}$ and $\hat{M}/\hat{\zeta}$, although the full $\hat{F}$ and $\hat{M}$ values are actually plotted. In real wave conditions the wave amplitude $\hat{\zeta}$ is of course also dependent on ω, so that the absolute magnitudes of $\hat{F}$ and $\hat{M}$ decrease for increasing ω.
- For the same reason the phase angle φ is in reality neither constant between jumps (as in figure 4.6-7) but changes with frequency.
- The gradient of the hydrodynamic load over water depth is very steep and strongly curved, especially close to the still water surface. For the drag load it is even steeper than for the inertia load. Therefore, when the integration over depth is performed numerically instead of analytically, whether by means of an existing computer program or a specially made spreadsheet, then the discretisation near the water surface must be very fine to achieve sufficient accuracy.
- As mentioned earlier, in high waves and small to moderate waterdepths the influence of the wave crest above the still water surface on the drag load can be significant and should not be ignored. Non-linear wave theories do not suffer from this problem as these theories calculate the velocities up to the actual wave surface. For Airy waves this effect can be taken into account by making an engineering assumption for the horizontal velocity above still water. There are various options for doing this; see figure 4.6-8. A rather common assumption is to assume that the horizontal velocity above still water remains constant. This is a typical engineering simplification that is highly questionable from a physical point of view; a velocity profile over depth should not only be continuous but also differentiable. Other options are to extend the linear profile beyond its range of validity for $0 < z \le \zeta(t)$ (which is often called extrapolation), or to “stretch” the linear profile by mapping the vertical co-ordinate for the still water depth onto the full water column $d + \zeta(t) \ge d$. This is called Wheeler stretching [4.6-6]. Both these options are also sketched in figure 4.6-8. It is immediately clear from the velocity profiles in this figure that extrapolation provides an unrealistically large upper bound for the drag force, while Wheeler stretching returns a low estimate. The constant velocity above still water is a simple and in-between approach that gives reasonably accurate answers.

4.7 Special loads

In addition to the aero- and hydrodynamic loads discussed in sections 4.5 and 4.6 there are still other loads that may act on members of the structure around the interface of air and water. These fall into two categories, i.e. special hydrodynamic loads due to:

- intermittent inundation of members
- wave breaking
- wave slam
- wave slap

and loads due to ice, which may be distinguished into loads due to:

- sheet ice
- ice floes
- icebergs.

All these loads require detailed specialist treatment. Discussion of these loads is beyond the scope of this handbook; for more information the reader is referred to the literature. It should be noted though that, generally speaking, most of these topics are far from conclusively resolved. Let it suffice here to say a few words about each of them.

Horizontal members located around the still water line at an elevation between the maximum wave crest and the minimum wave trough of the design storm may intermittently be in air and submerged. Consequently they will only experience hydrodynamic loading during a part of the wave cycle. When they are in air these members are only subjected to their own weight; when they are submerged they are loaded by the net effect of their own weight, upward buoyancy loads and both horizontal and vertical wave loading due to the varying wave kinematics during the passage of a wave. This is a discontinuous and non-linear loading situation. Especially the repeated stress variations that are experienced at the top and the bottom of the member (the 12 and 6 o'clock positions in the member's cross section) as a result of self-weight, buoyancy and vertical water particle velocities may cause fatigue damage. This is the reason why horizontal framing levels should be located high enough above and low enough below the mean still water level to cause only occasional submergence or emergence, respectively, thus limiting both the number and the magnitude of such stress cycles.

The kinematics in breaking waves are poorly understood, and as the kinematics are the prime factors that control wave loads the loads due to breaking waves are also quite uncertain. Additionally, there are different types of breaking waves, while furthermore the air entrained in spilling or plunging breakers may greatly affect the loads experienced.

Loads due to wave slam and wave slap are impulsive (impact) type loads when an object is suddenly immersed in water. Wave slamming is generally associated with the vertical immersion at some velocity. The classical example is when the bow of a ship re-enters the water after having emerged from it due to excessive relative vertical motion. The bottom of the bow section may then be subjected to significant impact loads. Analogously, in case of a space frame structure wave slamming is associated with fixed horizontal members in a frame that is more or less perpendicular to the wave direction and a water surface that is rapidly rising from below over the full length of the member during the passage of a wave.

Slamming loads are thus (near to) vertical. Wave slap, on the other hand, is generally associated with loading that may occur during the breaking of waves on members or (flat) surfaces that also lie in a plane perpendicular to the wave direction. Wave slap is likely to be most severe when the objects are (near to) vertical, but it may also happen on members and surfaces with other orientations. The direction of loading due to wave slap is thus often approximately horizontal, but may vary with the orientation of the object. The hydrodynamics of wave slam and wave slap are very complex and again not well understood. Furthermore, as the loading is impulsive in nature with very short rise times of milliseconds and overall short durations, the phenomena involved are affected by the interaction between the loading and the dynamic response of the structure. Therefore loading and structural behaviour are interlinked, and the problem is actually more a dynamic response problem than a pure loading problem.

Ice forces are similarly very difficult to predict. They depend on the mechanical properties of the ice (which may vary widely with conditions and the type of ice), on the configuration of the ice cover on the water (sheet ice, ice floes), on the current condition and on the failure mechanism of the ice as it is broken by the structure (compression, shear or bending failures). Furthermore, there is firm evidence that the build-up of ice loads due to the moving ice or their release when the ice breaks may be accompanied by significant dynamic response. Icebergs are massive floating bodies of irregular shape, with more than 90% of their volume under water. Any structure is highly unlikely to survive a collision with an iceberg. The usual strategy in offshore areas where icebergs are a hazard is therefore to try and avoid this from happening rather than to try and resist icebergs. For fixed structures this may be achieved by warning systems and altering the course of the iceberg by towing it out of the structure’s path, while floating structures may have quick release mechanisms to allow them to move rapidly off location.

4.8 References

4.1-1 Lamb, T.W. and Whitman, R.V., ***Soil Mechanics***; Series in Soil Engineering, John Wiley & Sons, New York, 1969.

4.1-2 Verruijt, A., ***Grondmechanica***; Delftse Uitgevers Maatschappij b.v., 3e druk, 1990; ISBN 90 6562 045 1.

4.1-3 Verruijt, A., ***Offshore Soil Mechanics***; lecture notes, Delft University of Technology, Faculty of Civil Engineering, 1992.

4.2-1 Hoven, I. van der, ***Power spectrum of horizontal wind speed in the frequency range from 0.0007 to 900 cycles per hour***; Journal of Meteorology, 14, 1957; pp. 160-164.

4.2-2 International Standard ISO 19901-1, ***Petroleum and natural gas industries-Offshore structures- Part 1-1: Metocean design and operating conditions***; in preparation.

4.2-3 Barltrop, N.D.P. and Adams, A.J., ***The dynamics of fixed marine structures***; Butterworth Heinemann Ltd., London, 3rd edition 1991; sections 8.1, 8.2 and 8.3.1; ISBN 0 7506 1046 8.

4.2-4 Engineering Sciences Data Unit; ESDU International, London. ESDU has published several data items on the characteristics of wind and atmospheric turbulence, as well as the response of flexible structures to wind loading, and continues to do so.

4.4-1 Kinsman, B., ***Wind Waves, their generation and propagation on the ocean surface***; Prentice Hall Inc., NJ, 1965.

4.4-2 Rice, S.O., ***Mathematical analysis of random noise***; Bell System Tech. Journal 23, 1944, p.282-332 and 24, 1945, p.46-156.

4.4-3 Journée, J.M.J. and Massie, W.W., ***Offshore Hydromechanics***; Delft University of Technology, August 1998.

4.4-4 Battjes, J.A., ***Korte Golven***; lecture notes CTwa 9320, subfaculty Civil Engineering, Delft University of Technology, March 1998.

4.4-5 Sarpkaya,T. and Isaacson, M., ***Mechanics of wave forces on offshore structures***; Van Nostrand Reinhold Company, 1981; ISBN 0-442-25402-4.

4.4-6 Clauss, G.; Lehmann, E. and Östergaard, C., ***Offshore Structures***; Volume 1: Conceptual design and hydrodynamics, Springer Verlag, Berlin, 1992.

4.4-7 American Petroleum Institute, ***Recommended Practice for Planning, Designing and Constructing Fixed Offshore Platforms - Load and Resistance Factor Design***; API Recommended Practice RP 2A-LRFD, first edition, July 1, 1993.

4.4-8 Pierson, W.J.; Neumann, G. and James, R.W., ***Practical methods for observing and forecasting ocean waves by means of wave spectra and statistics***; published by the Hydrographic Office in the USA, H.O. Publication No. 603, 1955 (reprinted 1958).

4.4-9 Holthuijsen, L.H., ***Windgolven***; lecture notes CTwa 5316, subfaculty Civil Engineering, Delft University of Technology, March 1998.

4.4-10 Ochi, M.K., ***Ocean Waves, the stochastic approach***; Cambridge Ocean Technology Series no. 6, Cambridge University Press, Cambridge, 1998; ISBN 0 521 56378.

4.4-11 MaTS (Netherlands Marine Technological Research programme), ***Wave kinematics in irregular waves;*** Report VM-I-4, parts I to III, Prepared by Delft Hydraulics Laboratory as report on investigation M1628, April 1983.

4.4-12 Battjes, J.A. and Van Heteren, J., ***Measurements of wind wave kinematics***; Report WWKZ-G007, Rijkswaterstaat, The Netherlands, 1983.

4.4-13 Pierson, W.J. and Moskowitz, L***., A proposed spectral formulation for fully developed wind seas based on the similarity theory of S.A. Kitaigorodskii;*** Journal of Geophysical Research, vol. 69, no. 24, 1964; p.5181-90.

4.4-14 Hasselman, K. et al, ***Measurements of wind-wave growth and swell decay during the Joint North Sea Wave Project (JONSWAP);*** Deutsche Hydrografische Institut, Hamburg, 1973.

4.4-15 Vugts, J.H., ***A review of hydrodynamic loads on offshore structures and their formulation***; Proceedings of the 2nd international conference on the Behaviour of Off-Shore Structures (BOSS '79), London, 1979; volume 3, paper 54; ISBN 0 906085 34 9.

4.6-1 Morison, J.R.; O'Brien, M.P.; Johnson, J.W. and Schaaf, S.A., ***The forces exerted by surface waves on piles***; Journal of Petroleum Technology, American Institute of Mining Engineers, vol. 189, 1950; p. 149-154.

4.6-2 Shafiee-far, M.; Massie, W.W. and Vugts, J.H., ***A generalised approach to hydrodynamic interaction of slender oscillating cylinders in waves and currents***; Proceedings of the 8th international conference on the Behaviour of Off-Shore Structures (BOSS '97), Delft, 1997; volume 2, p. 65-78; ISBN 0-08-042834-70.

4.6-3 Shafiee-far, M., ***Hydrodynamic interaction between fluid flow and oscillating slender cylinders***; dissertation, Delft University of Technology, 1997; ISBN 90-803604-1-4.

4.6-4 Vugts, J.H. and Bouquet, A.G., ***A non-linear, frequency domain description of wave forces on an element of a vertical pile in random seas;*** Proceedings of the 4th international conference on the Behaviour of Off-Shore Structures (BOSS '85), Delft, 1985; paper A13, p. 239-253; ISBN 0-444-42513-6 (vol. 2).

4.6-5 European Steel Design Education Programme (ESDEP), Working Group 15A "Structural Systems: Offshore", lecture 15A.2, Loads; 1993.

4.6-6 Wheeler, J.D., ***Method for calculating forces produced by irregular waves***; Offshore Technology Conference, Houston, 1969, paper OTC 1006.

Annex A – An alternative wind model [14]

The wind field may generally be formulated in the form of the vector equation 4.2-1 (see section 4.2):

$$\underline{U_{wi}}(x,y,z;t)=\underline{U_w}(x,y,z)+\underline{u_w}(x,y,z;t) \tag{4.2-1}$$

where: $\underline{U_{wi}}$ = local and instantaneous wind velocity vector

$\underline{U_w}$ = mean wind velocity vector at point *(x,y,z),* which is constant in magnitude and direction over a period of time that is long compared to the time *t*

$\underline{u_w}$ = turbulent wind velocity vector around the mean at point *(x,y,z);* $\underline{u_w}$ varies in magnitude and direction as a function of time, the time average of $\underline{u_w}$ is by definition zero.

In section 4.2 it was subsequently argued that for most purposes this model could be simplified to the following scalar equation in the mean wind direction θ_w:

$$U_{wi}(z;t)=U_w(z)+u_w(z;t) \tag{A.1}$$

where: $U_w(z)$ = mean wind velocity at elevation *z* above sea level, averaged over a particular time interval

$u_w(z;t)$ = wind gust velocity at elevation *z* around and in the same direction as $U_w(z)$

Norwegian investigations using measurements for representative offshore conditions found that the mean velocity $U_w(z)$ in storm conditions can be more accurately described by a logarithmic instead of a power law profile:

$$\begin{aligned} U_{w,1hr}(z) &= U_{w0}\cdot\left[1+C.\ln\left(\frac{z}{10}\right)\right] \\ C &= (5.73)\cdot(10^{-2})\cdot(1+0.15\,U_{w0})^{1/2} \end{aligned} \tag{A.2}$$

where: $U_{w,1hr}(z)$	=	the 1 hour mean wind velocity at *z* m above MSL	[m/s]
U_{w0}	=	the sustained wind velocity	
	=	the 1 hour mean wind velocity at 10 m above MSL	[m/s]
C	=	a coefficient	[-]
z	=	height above MSL	[m]

In *storm conditions*, the mean wind velocity for averaging times shorter than 1 hour may further be expressed in the 1 hr mean wind velocity $U_{w,1hr}(z)$ of eq. (A.2) through the following relationship [4.5]:

---

[14] This annex on the wind model is an earlier version, which is still to be updated.

$$
\begin{aligned}
U_{w,t}(z) &= U_{w,1hr}(z)\cdot\left[1-0.41\cdot I_u(z)\cdot\ln(t/t_0)\right]\\
I_u(z) &= (0.06)\cdot\left[1+0.043\,U_{w0}\right]\cdot\left(\frac{z}{10}\right)^{-0.22}
\end{aligned}
\qquad \text{(A.3)}
$$

where additionally:

$U_{w,t}(z)$ = the mean wind velocity at z m above MSL, averaged over a time interval $t \leq 1\ hr$ [m/s]

$U_{w,1hr}(z)$ = the 1 hour mean wind velocity at z m above MSL from eq. A.2 [m/s]

$I_u(z)$ = the turbulence intensity given in eq. A.3 [-]

t = time averaging interval with $t \leq t_0$ [s]

t_0 = time averaging interval of 1 hr = 3600 s [s]

Note that the equations A.2 and A.3 are only valid in SI units, as indicated. The equations are typical engineering equations derived from curve fitting through large numbers of data and are internally not consistent.

The fluctuating or gust velocity $u_w(z;t)$ can be described in the frequency domain by a wind gust spectrum, analogous to the way in which the wave spectrum describes the water surface elevation (see section 4.4.5). The energy density spectrum of the longitudinal velocity fluctuations at a particular point may be described by [4.5]:

$$
\begin{aligned}
S(f) &= \frac{(320)\cdot\left(\frac{U_{w0}}{10}\right)^{2}\cdot\left(\frac{z}{10}\right)^{0.45}}{\left[1+\tilde{f}^{\,n}\right]^{5/3n}}\\
\tilde{f} &= (172)\cdot f\cdot\left(\frac{z}{10}\right)^{2/3}\cdot\left(\frac{U_{w0}}{10}\right)^{-0.75}
\end{aligned}
\qquad \text{(A.4)}
$$

where further to earlier definitions:

$S(f)$ = spectral energy density at frequency f [m^2s^{-2}/Hz]

f = frequency in Hz [Hz]

$\tilde{f}$ = a function specified above [Hz]

n = 0.468 [-]

For practical applications the wind gust spectrum needs to be supplemented by a description of the spatial coherence of the gust velocities over the exposed surface of the structure or the structural element. Suitable coherence functions may be found in the literature, e.g. in references [4.5] to [4.7].

Annex B – Airy water wave formulae

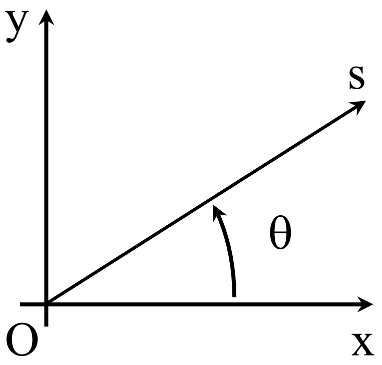

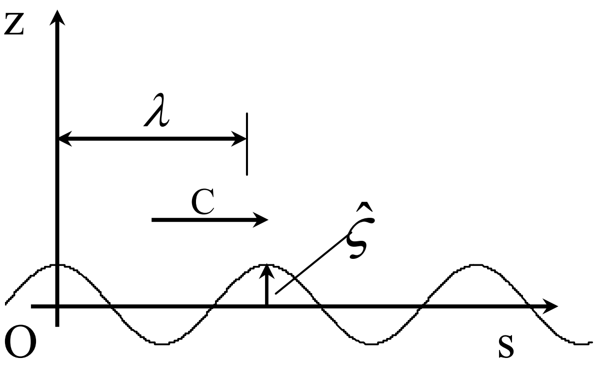

B.1 General observations

In linear water wave theory all variables in the wave field can be derived form a velocity potential, which is a function of location (x,y,z) and time (t). For the co-ordinate system $(Oxyz)_H$ used in this handbook and illustrated in the above figure the velocity potential in real number notation is:

$$\begin{aligned} \Phi(x,y,z;t) &= \frac{\hat{\zeta} g}{\omega} \cdot D(z) \cdot \sin(kx\cos\theta + ky\sin\theta - \omega t) \\ D(z) &= \frac{\cosh k(z+d)}{\cosh kd} \end{aligned} \tag{B.1-1}$$

where:

$\hat{\zeta}$ = wave amplitude [m]
ω = (circular) wave frequency [rad/s]
g = acceleration due to gravity [m/s^2]
$D(z)$ = depth decay function [-]
$k = \frac{2\pi}{\lambda}$ = wave number [m^{-1}]
λ = wave length [m]
d = waterdepth [m]
θ = direction of wave travel with respect to the positive Ox-axis [deg or rad]

The co-ordinate system adopted here is the most common co-ordinate system, but readers should be aware that in some textbooks other systems are used. For example, a system with the horizontal Oxy-plane in the still water surface as above but the z-axis vertically downwards instead of upwards, to enable working in the positive half-plane with $z \geq 0$ as opposed to the negative half-plane in which $z \leq 0$. Another example is a system with the Oxy-plane at the sea floor. A disadvantage of this latter system is that in the upper part of the water column (which is the most important region) the vertical co-ordinate and hence the arguments of the hyperbolic functions become very large, which makes the hyperbolic functions rather awkward to evaluate. When the Oxy-plane is in the free surface the hyperbolic functions can easily be simplified for large arguments by using their asymptotic forms for $z \to -\infty$.

Reformulation of the velocity potential to or from another co-ordinate system can most readily be achieved through a formal co-ordinate transformation.

The velocity in a particular direction anywhere in the wave field is by definition equal to the derivative of the velocity potential in that direction [15]. For the three principal co-ordinate directions we thus have:

$$\begin{aligned} u(x,y,z;t) &= \frac{\partial \Phi(x,y,z;t)}{\partial x} = \frac{\hat{\zeta} kg \cos\theta}{\omega} \cdot D(z).\cos(kx\cos\theta + ky\sin\theta - \omega t) \\ v(x,y,z;t) &= \frac{\partial \Phi(x,y,z;t)}{\partial y} = \frac{\hat{\zeta} kg \sin\theta}{\omega} \cdot D(z).\cos(kx\cos\theta + ky\sin\theta - \omega t) \\ w(x,y,z;t) &= \frac{\partial \Phi(x,y,z;t)}{\partial z} = \frac{\hat{\zeta} g}{\omega} \cdot \frac{\partial D(z)}{\partial z} \cdot \sin(kx\cos\theta + ky\sin\theta - \omega t) \\ &= \frac{\hat{\zeta} kg}{\omega} \cdot \frac{\sinh k(z+d)}{\sinh kd} \cdot \sin(kx\cos\theta + ky\sin\theta - \omega t) \end{aligned} \tag{B.1-2}$$

The wave surface is related to the velocity potential by:

$$\zeta(x,y,z;t) = -\frac{1}{g}\frac{\partial \Phi(x,y,z;t)}{\partial t} \quad \text{for } z = 0 \tag{B.1-3}$$

which results in:

$$\zeta(x,y,z;t) = \hat{\zeta}\cos(kx\cos\theta + ky\sin\theta - \omega t) \tag{B.1-4}$$

while the (absolute) pressure at any point in the wave field is given by:

$$\begin{aligned} p(x,y,z;t) &= -\rho\frac{\partial \Phi(x,y,z;t)}{\partial t} - \rho g z + p_{atm} \\ &= \rho g \hat{\zeta} \cdot D(z) \cdot \cos(kx\cos\theta + ky\sin\theta - \omega t) - \rho g z + p_{atm} \end{aligned} \tag{B.1-5}$$

with:

p_{atm} = the atmospheric pressure at the free water surface

The wave length and wave period (wave frequency) are related through the dispersion equation:

$$\omega^2 = kg \cdot \tanh kd \tag{B.1-6}$$

---

[15] Note that definitions of the velocity potential based on $u = -\frac{\partial \Phi}{\partial x}$, etc. do also occur in the literature.

while the phase speed with which the wave propagates (the wave celerity) is:

$$c = \frac{\lambda}{T} = \frac{g}{\omega} \cdot \tanh kd = \frac{gT}{2\pi} \cdot \tanh kd \qquad \text{(B.1-7)}$$

In concluding this general section the following observations are made of which users should be very much aware:

- The place and time dependent terms in the argument of the harmonic function are of opposite sign: $(kx\cos\theta + ky\sin\theta - \omega t)$, which ensures that the wave progresses spatially as well as temporally in the positive directions. This means that:
  - when the wave elevation is plotted as a function of place $s = kx\cos\theta + ky\sin\theta$, the wave crest shifts in the positive s-direction when time increases;
  - when the wave elevation is plotted as a function of time t, the wave crest similarly shifts in the positive t-direction when s increases.
- For equal signs in the argument, i.e. for $(kx\cos\theta + ky\sin\theta + \omega t)$ or $(-kx\cos\theta - ky\sin\theta - \omega t)$, the wave progresses in the opposite direction. That is, when the wave elevation is plotted as a function of place, the wave crest now shifts in the negative s-direction for increasing values of t. And similarly, when the wave elevation is plotted as a function of time, the wave crest shifts in the negative t-direction for increasing values of s.
- Whether the harmonic function is a sine-or a cosine-function is of no particular significance; it merely means a phase shift of 90 degrees with respect to the spatial and temporal origins of $s = 0$ and $t = 0$.
- All quantities in the wave field are derived from the velocity potential, often by differentiating the potential with respect to s or t. During these derivations the sine- or cosine-function and the argument in the velocity potential must be fully maintained in order to obtain a consistent set of formulae, with correct signs and phases relative to one another. Simplifications of the argument may only be introduced *after the derivation is complete*. In applications of a correct and mutually consistent set of derived formulae simplification can no longer harm; e.g. for $x = y = 0$ we may then simplify $\cos(kx\cos\theta + ky\cos\theta - \omega t)$ to $\cos(-\omega t) = \cos\omega t$. Making such simplifications prior to taking the derivatives can introduce serious errors.
- A phase angle $\pm\varphi$ with the same sign as the time dependent factor $\pm\omega t$ means a phase lead; different signs mean a phase lag.

B.2 Complex number notation

A harmonic time dependent factor is often expressed in the form of a complex number:

$$\begin{aligned} \cos\omega t &\Rightarrow e^{i\omega t} = \cos\omega t + i\sin\omega t \\ \sin\omega t &\Rightarrow -ie^{i\omega t} = -i(\cos\omega t + i\sin\omega t) = -i\cos\omega t + \sin\omega t \end{aligned} \tag{B.2-1}$$

where by convention it is understood that only the real part should be taken.

The velocity potential in equation B.1-1 would then be written as:

$$\Phi(x,y,z;t) = -\frac{\hat{\zeta}\, g}{\omega}\cdot D(z)\cdot ie^{i\{kx\cos\theta + ky\sin\theta - \omega t\}} \tag{B.2-2}$$

Using equations B.1-2 to B.1-7, performing the differentiations and thereafter taking the real part produces the same results as given in the real notation. When for the time dependent function a cosine-function would have been chosen the velocity potential would be:

$$\Phi(x,y,z;t) = \frac{\hat{\zeta}\, g}{\omega}\cdot D(z)\cdot e^{i\{kx\cos\theta + ky\sin\theta - \omega t\}} \tag{B.2-3}$$

The appropriate relationships for other variables in the wave field are again obtained by applying the equations B.1-2 to B.1-7, performing the differentiations and thereafter taking the real part.

B.3 Summary of a consistent set of equations in the direction of wave propagation for all waterdepths

Using the equations in section B.1 and simplifying the general three-dimensional case to a two-dimensional description along the direction of wave propagation we obtain the following results:

Position along the oblique axis: $$s = x\cos\theta + y\sin\theta \tag{B.3-1}$$

wave elevation: $$\zeta = \hat{\zeta}\cos(ks-\omega t) \tag{B.3-2}$$

---

velocity potential: $$\Phi(s,z;t) = \frac{\hat{\zeta}g}{\omega}\,\frac{\cosh k(z+d)}{\cosh kd}\sin(ks-\omega t) \tag{B.3-3}$$

---

kinematic relationships:

$$\begin{aligned} u(s,z;t) &= \hat{\zeta}\omega\frac{\cosh k(z+d)}{\sinh kd}\cos(ks-\omega t)\\ w(s,z;t) &= \hat{\zeta}\omega\frac{\sinh k(z+d)}{\sinh kd}\sin(ks-\omega t)\\ \dot{u}(s,z;t) &= \hat{\zeta}\omega^2\frac{\cosh k(z+d)}{\sinh kd}\sin(ks-\omega t)\\ \dot{w}(s,z;t) &= -\hat{\zeta}\omega^2\frac{\sinh k(z+d)}{\sinh kd}\cos(ks-\omega t) \end{aligned} \tag{B.3-4}$$

orbital motion:

half long axis: $$a = \hat{\zeta}\frac{\cosh k(z+d)}{\sinh kd} \tag{B.3-5}$$

half short axis $$b = \hat{\zeta}\frac{\sinh k(z+d)}{\sinh kd} \tag{B.3-6}$$

---

dispersion relation and wave length:

$$\omega^2 = kg\cdot\tanh kd \tag{B.3-7}$$

$$\lambda = \frac{2\pi g}{\omega^2}\cdot\tanh\left(\frac{2\pi d}{\lambda}\right) = \frac{gT^2}{2\pi}\cdot\tanh\left(\frac{2\pi d}{\lambda}\right) \tag{B.3-8}$$

---

pressure: $$p(s,z;t) = \rho g\hat{\zeta}\cdot\frac{\cosh k(z+d)}{\cosh kd}\cdot\cos(ks-\omega t) - \rho gz \tag{B.3-9}$$

---

wave celerity: $$c = \frac{g}{\omega} \cdot \tanh\left(\frac{2\pi d}{\lambda}\right) = \frac{gT}{2\pi} \cdot \tanh\left(\frac{2\pi d}{\lambda}\right) \qquad \text{(B.3-10)}$$

B.4 Summary of a consistent set of equations in the direction of wave propagation for deep water

---

Position along the oblique axis: $s = x\cos\theta + y\sin\theta$ (B.4-1)

wave elevation: $\zeta = \hat{\zeta}\cos(ks - \omega t)$ (B.4-2)

---

velocity potential: $\Phi(s,z;t) = \dfrac{\hat{\zeta} g}{\omega}\, e^{kz} \sin(ks - \omega t)$ (B.4-3)

---

kinematic relationships:

$$\begin{aligned} u(s,z;t) &= \hat{\zeta}\,\omega\, e^{kz} \cos(ks - \omega t) \\ w(s,z;t) &= \hat{\zeta}\,\omega\, e^{kz} \sin(ks - \omega t) \\ \dot{u}(s,z;t) &= \hat{\zeta}\,\omega^2 e^{kz} \sin(ks - \omega t) \\ \dot{w}(s,z;t) &= -\hat{\zeta}\,\omega^2 e^{kz} \cos(ks - \omega t) \end{aligned} \qquad \text{(B.4-4)}$$

radius of orbital motion: $a = b = \hat{\zeta}\, e^{kz}$ (B.4-5=B.4-6)

---

dispersion relation and wave length:

$$\omega^2 = kg \qquad \text{(B.4-7)}$$

$$\lambda = \frac{2\pi g}{\omega^2} = \frac{gT^2}{2\pi} \approx 1.56\, T^2 \quad \text{(in units of m and s)} \qquad \text{(B.4-8)}$$

---

pressure: $p(s,z;t) = \rho g \hat{\zeta} \cdot e^{kz} \cos(ks - \omega t) - \rho g z$ (B.4-9)

---

wave celerity: $c = \dfrac{g}{\omega} = \dfrac{gT}{2\pi}$ (B.4-10)

Annex C – Summary of main conclusions from the laboratory measurements performed for the Netherlands Marine Technical Research programme (MaTS, [4.4-11])

1) The results show conclusively that the linear random wave model provides a valid theoretical description of the wave kinematics in an irregular sea, the accuracy of which is adequate for the great majority of engineering applications over the full range of sea states covered by the investigation. With few exceptions (described in 2) below) the linear random wave model is superior to periodic wave theories, both linear and non-linear.

2) The comparison of calculations according to linear random wave theory with measurements indicate that this theory has limitations in providing a very good fit in three respects:
   a) The measurements show a crest/trough distortion of the surface elevation for the highest waves. That is, the crests are at a greater distance from the still water level than the troughs. This is not represented in any linear theory. The higher order periodic wave theories do correctly predict the occurrence of this distortion although not necessarily in quantitative terms.
   The measured horizontal velocities under crests and troughs also show a distortion in that the absolute magnitude of the horizontal velocities is greater under deep wave troughs than under high wave crests. That is, the distortion of the horizontal velocities is opposite to that of the surface elevations. This is associated with a set-down of the mean water level under groups of high waves caused by a second order physical phenomenon. This effect again cannot be represented by a linear theory, whereas the higher order periodic wave theories predict a distortion of the velocities in the same rather than the opposite sense to that of the surface elevation and hence also opposite to that found in the measurements.

   b) The linear random wave theory fails to predict the most extreme events to a high degree of accuracy as the influence of higher order effects in the measurements become apparent.

   c) Linear theory is in principle incapable of predicting fluid velocities above the mean still water level and also fails to predict the intermittent nature of the velocities in the region between the still water level and the deepest wave trough. A description of wave kinematics above, and more generally around the mean still water level, requires a theoretical or an empirical modification to the strictly linear random wave model.

3) Comparisons between measurements and the periodic wave theories show very little consistency. They show substantial differences between the theoretical and measured results for the horizontal and vertical velocities in the fluid domain below the wave trough; no comparisons were made in the region around the still water level. In many cases the periodic theories overpredict measured velocities, but underpredictions also occur frequently. The comparisons with the measurements show that no advantage is gained by choosing a higher order theory over a linear one.

Annex D – Guidance for modelling a structure as an equivalent vertical stick

D.1 Introduction

For approximate manual calculations of wave loading on an offshore structure the structure may be represented by an assembly of vertical sticks, or even a single vertical stick. In all such cases the only objective of the calculations is to estimate the distribution of *horizontal* wave (and current) loads over the height of the structure in a periodic design wave (and current), thus providing estimates of the total applied horizontal loading and the associated overturning moment about the sea floor for preliminary design exercises with a view to structural strength in extreme environmental conditions.

If an assembly of vertical sticks in a horizontally spread arrangement is used the phase relationships due to spatial separation between members can be accounted for in an approximate manner. The (near) vertical legs are then modelled as equivalent and truly vertical sticks of the same diameter as the legs. For each leg the stick is best placed at the position of the leg at mean sea level since wave loads are largest around the still water surface, rather than at the position of the leg at the sea floor. Alternatively, the stick may be placed at a (weighted) average position along the sloping leg. Frame members in a plane between the legs contribute to the horizontal loads on the structure as well and may be modelled by one or more additional vertical sticks with an equivalent diameter, positioned at the centre of the frame.

Instead of modelling the individual legs and frame members by corresponding sticks, an entire (near vertical) frame may be modelled by one stick of an equivalent diameter at the centre of the frame. The phase relationships between wave load contributions on different sticks are then more crudely approximated, but for the purposes for which such manual calculations are used this is usually of no great concern. The most important thing is that the vertical distribution of the loads is fairly accurately represented, because otherwise the overturning moment can be significantly in error.

The ultimate simplification is, of course, to place all the sticks at the geometrical centre of the structure. In this case phase relationships due to spatial separation are completely neglected and the result is a conservative estimate. Rather than having several sticks at the geometrical centre of the structure, they may now also be combined into one vertical stick of an equivalent diameter. However, as drag loads are proportional to the diameter and inertia loads are proportional to the diameter squared, the equivalent diameters of the ‘drag stick’ and of the ‘inertia stick’ will be different, so that there are in fact always two sticks needed at the geometrical centre of the structure. In this Annex the single ‘drag stick’ and the single ‘inertia stick’ model will be described.

To do the modelling correctly it is important to start from the fundamental assumption underlying the wave load model. This is that hydrodynamic loads are due to velocities and accelerations normal to the member; any tangential components of the fluid particle kinematics can only produce frictional forces and are neglected. For steel space frame structures the wave load model is the (extended) Morison equation. For the hydrodynamic

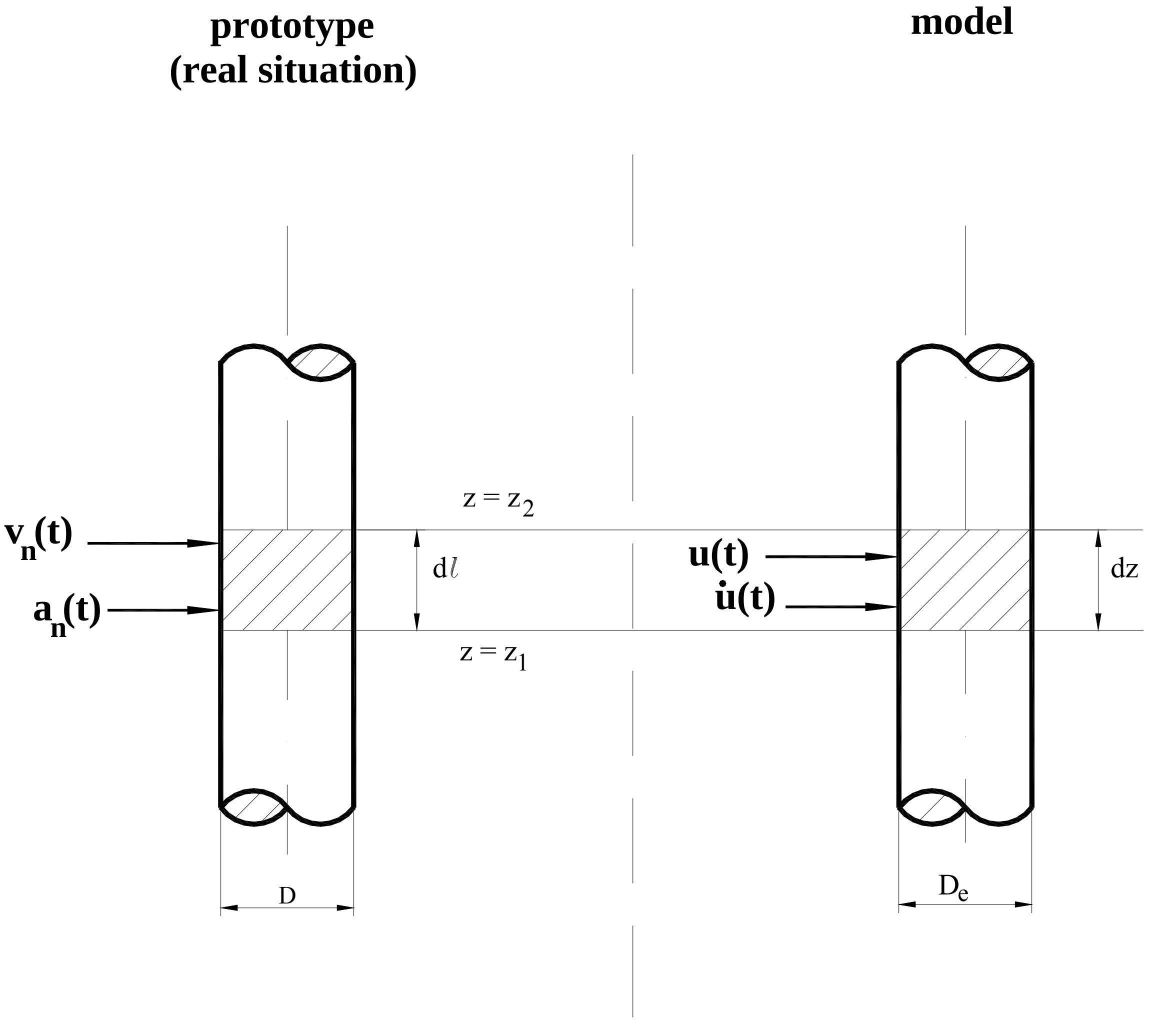

Figure D.4.1. Mapping of a vertical member onto a stick

loads on the legs of a concrete gravity structure the same modelling principles apply. Drag loads on such large diameter legs can normally be neglected so that only the inertia term of the Morison equation needs to be included. However, the inertia coefficient may need to be adjusted for certain frequencies to account for the effect of diffraction according to the ratio D/λ.

As the position of the sticks is given, the problem is reduced to the determination of the equivalent diameter of each stick. To do this a segment of a real member must be mapped onto the corresponding segment of the equivalent stick, in such a manner that the same magnitude of the horizontal load is obtained. In the following sections we will describe how this is done for members that are, respectively:

- (near to) vertical
- lie in a (near to) vertical plane perpendicular to the wave direction
- lie in a (near to) vertical plane parallel to the wave direction
- lie in a horizontal plane
- are arbitrarily inclined.

D.2 Vertical members

Vertical or near vertical members subject to hydrodynamic loading are legs, conductors, risers, caissons and sump pipes. Figure D.1 depicts the real situation for a segment of such a member on the left and its corresponding stick model on the right, both between the elevations $z = z_1$ and $z = z_2$. The wave is a periodic wave running from left to right. The plane of the drawing is parallel to the plane of wave propagation. The wave kinematics thus lie in the plane of the drawing; velocities and accelerations perpendicular to the plane of the drawing are zero.

For a vertical member the velocity and acceleration normal to the segment of the member in the real situation (the prototype) are horizontal and in line with the wave direction. Using linear wave kinematics (Airy waves) they are given by (see Annex B):

$$\begin{aligned} v_n(t) &= \hat{v}_n \cos(ks_p - \omega t) \\ a_n(t) &= \hat{a}_n \sin(ks_p - \omega t) \end{aligned} \tag{D.1}$$

In the model the horizontal in-line velocity and acceleration normal to the stick are:

$$\begin{aligned} u(t) &= \hat{u} \cos(ks_m - \omega t) \\ \dot{u}(t) &= \hat{\dot{u}} \sin(ks_m - \omega t) \end{aligned} \tag{D.2}$$

In these equations the subscript 'p' refers to the prototype (= real situation) and the subscript 'm' to the model. When we choose the origin of the co-ordinate system at the geometrical centre of the structure, i.e. at the location of the stick, the distance to the stick in the stick model is $s_m = 0$. The distance to the real member is in general not equal to zero and may be positive or negative. For a vertical orientation of the real member the following relationships are obviously valid:

$$\begin{aligned} \hat{v}_n &= \hat{u} \\ \hat{a}_n &= \hat{\dot{u}} \\ d\ell &= dz \end{aligned} \tag{D.3}$$

The velocity at the drag stick is maximum for $t=0$ with $u(t=0)=\hat{u}$, while at that instant the velocity at the real member is $v_n(t=0)=\hat{v}_n\cos(ks_p)\le\hat{u}$. Similarly, the acceleration at the inertia stick is maximum for $\omega t=-\frac{1}{2}\pi$ or $t=-\frac{1}{4}T$; the magnitude of the acceleration is then $\dot{u}(t=0)=\hat{\dot{u}}$. At this moment the acceleration at the real member is $a_n(t=0)=\hat{a}_n\sin(ks_p)\le\hat{\dot{u}}$. Hence, ignoring the phase difference ks_p for the spatial separation between the real member and the model stick is indeed always somewhat conservative.

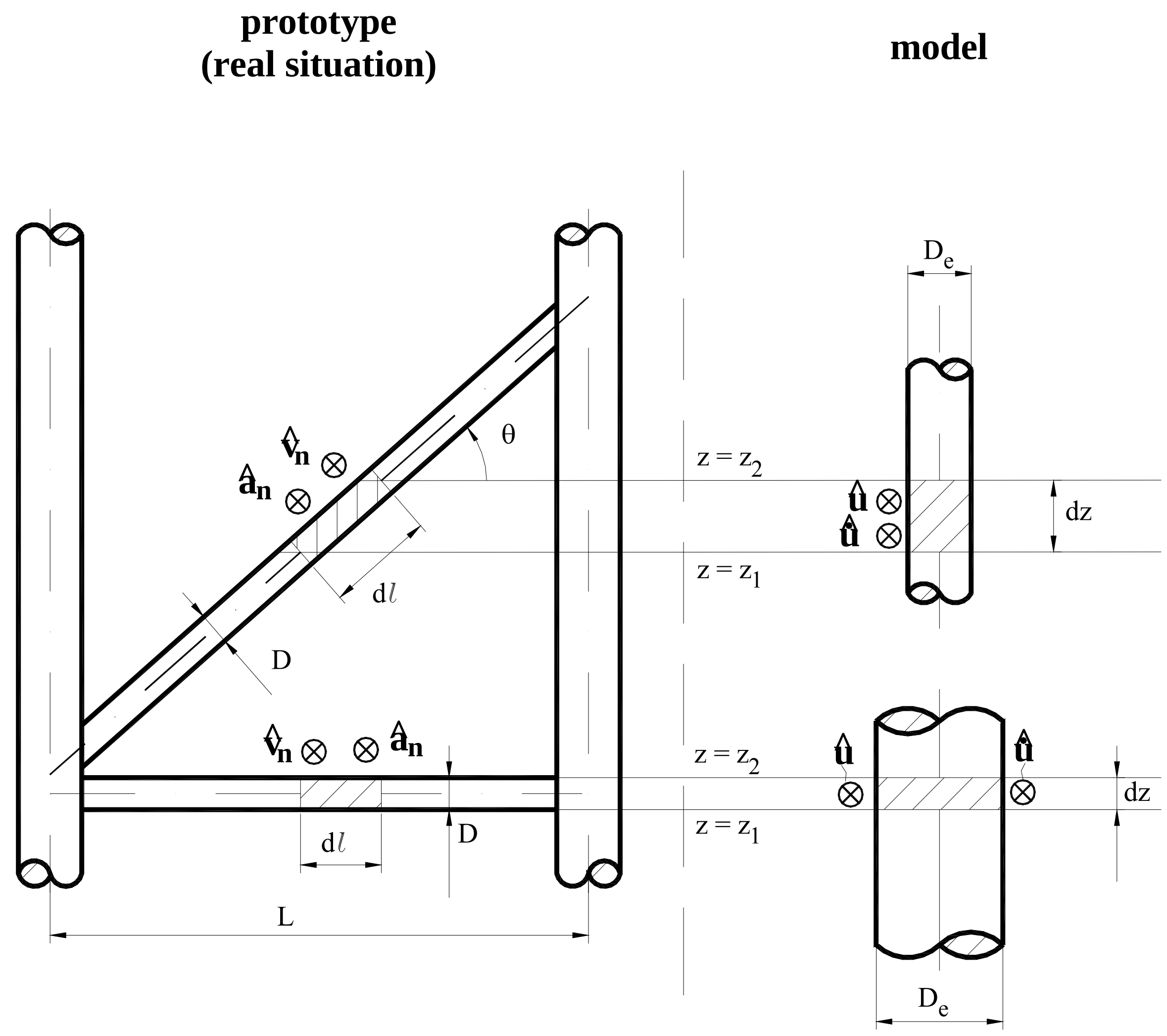

Figure D.4.2. Mapping of members in a vertical plane perpendicular to the wave direction onto a stick

The magnitudes of the drag load on the segment of the real member and on the drag stick are, respectively:

$$\begin{aligned} \hat{F}_{dp} &= C_d \cdot \tfrac{1}{2}\rho\, \hat{v}_n^2 \cdot D\, d\ell \\ \hat{F}_{dm} &= C_d \cdot \tfrac{1}{2}\rho\, \hat{u}^2 \cdot D_{de}\, dz \end{aligned} \tag{D.4}$$

The objective of the modelling is to make $\hat{F}_{dm} = \hat{F}_{dp}$. Using equations D.3 it then follows directly from equation D.4 that:

$$D_{de} = D \tag{D.5}$$

In an entirely analogous manner equality of the inertia loads $\hat{F}_{im} = \hat{F}_{ip}$ on corresponding segments:

$$\begin{aligned} \hat{F}_{ip} &= C_m \cdot \rho \frac{\pi D^2}{4} \cdot \hat{a}_n \cdot d\ell \\ \hat{F}_{im} &= C_m \cdot \rho \frac{\pi D_{ie}^2}{4} \cdot \hat{\dot{u}} \cdot dz \end{aligned} \tag{D.6}$$

results in:

$$D_{ie}^2 = D^2 \qquad \text{or} \qquad D_{ie} = D \tag{D.7}$$

The equivalent diameters of the drag stick and of the inertia stick are thus both equal to the real diameter of the member at the elevation concerned. This is, of course, no surprise. After all we are dealing with the utterly simple case of a segment of a vertical member in the real situation that is mapped onto a segment of a vertical stick in the model situation, with the simplification that the phase difference due to spatial separation is neglected. However, this rather formal derivation shows the procedure to be followed for the other cases, in which the results will be different. From now on we will neglect phase differences right from the beginning. Time dependencies have therefore become irrelevant and it suffices to consider only the magnitudes of velocities, accelerations and loads.

D.3 Members in a vertical plane perpendicular to the wave direction

The real and model situations are depicted side by side in figure D.2. The planes of the two drawings are both perpendicular to the wave direction; they are hence parallel, but a distance of ks_p apart. In view of the orientation of the plane in which the members lie, the velocity and acceleration for maximum horizontal hydrodynamic loading of the real member are horizontal and in line with the wave direction. They are thus parallel with the horizontal in-line velocity and the horizontal in-line acceleration at the vertical stick. Neglecting phase differences due to spatial separation we have once more:

$$\begin{aligned} \hat{v}_n &= \hat{u} \\ \hat{a}_n &= \hat{\dot{u}} \end{aligned} \tag{D.8}$$

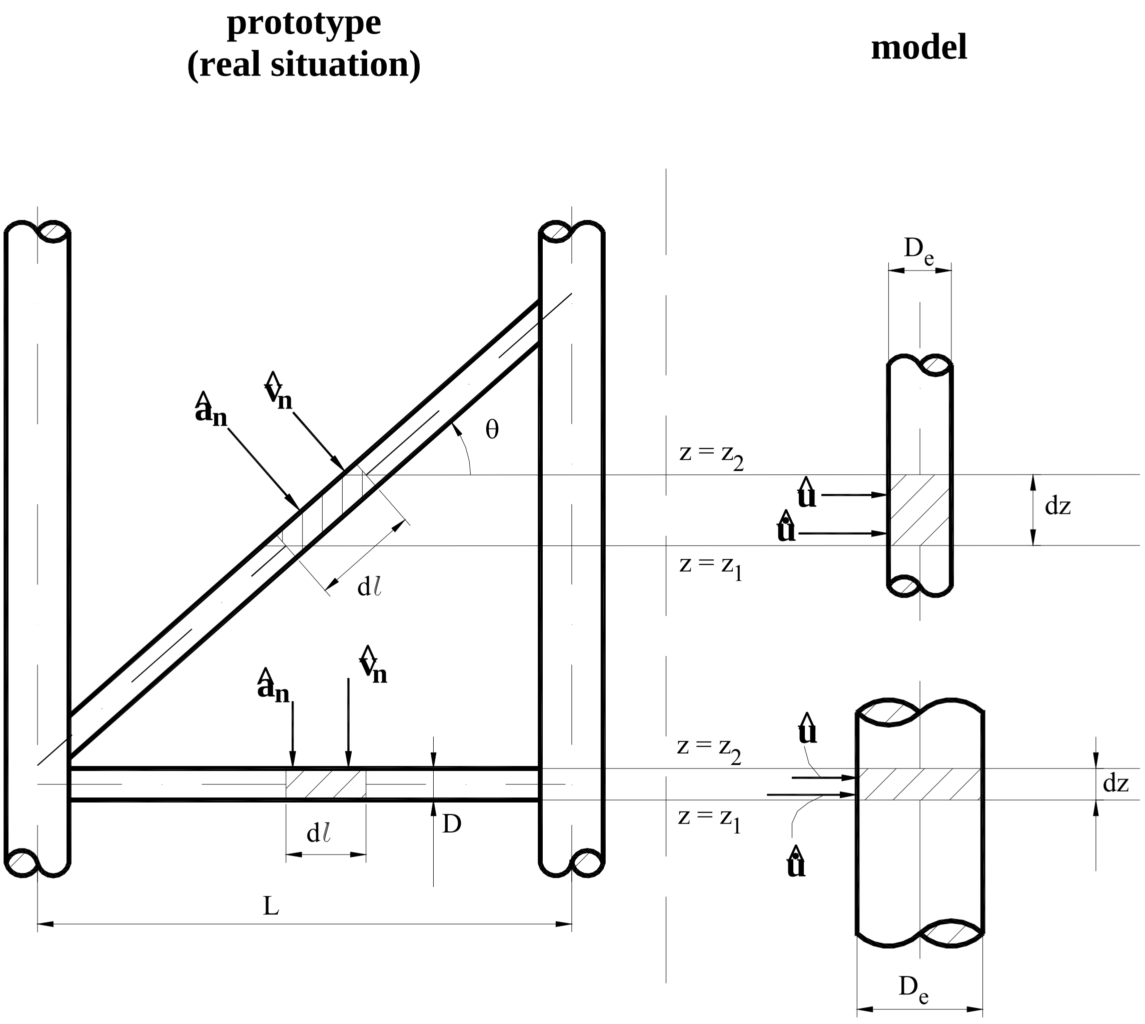

Figure D.4.3. Mapping of members in a vertical plane parallel to the wave direction onto a stick

The horizontal velocities and accelerations are shown in figure D.2 as the tails of arrows normal to the paper.

Inclined member

The segment lengths between the elevations z_1 and z_2 are now no longer equal:

$$dz = d\ell \cdot \sin\theta \tag{D.9}$$

Equality of hydrodynamic drag loads $\hat{F}_{dm} = \hat{F}_{dp}$ on the two segments gives, with the aid of equations D.8, D.9 and D.4:

$$D_{de} = \frac{D \cdot d\ell}{dz} = \frac{D \cdot d\ell}{d\ell \cdot \sin\theta} = \frac{D}{\sin\theta} \tag{D.10}$$

Equality of hydrodynamic inertia loads $\hat{F}_{im} = \hat{F}_{ip}$ gives with the aid of equations D.8, D.9 and D.6:

$$D_{ie}^2 = \frac{D^2 \cdot d\ell}{dz} = \frac{D^2 \cdot d\ell}{d\ell \cdot \sin\theta} = \frac{D^2}{\sin\theta} \quad \text{or} \qquad D_{ie} = \frac{D}{\sqrt{\sin\theta}} \tag{D.11}$$

Horizontal member

The segment length $d\ell$ along the member's axis is now orientated horizontally, while the segment length dz of the stick is as always orientated vertically. To enclose the full diameter of the member between the two elevations z_1 and z_2 we must choose z_1 at the lower and z_2 at the upper point of the horizontal member, making $dz = D$. To make the drag load on the full length of the horizontal member equal to the drag load on the stick segment we must meet the condition (see equation D.4):

$$D_{de} = \frac{D.L}{dz} = \frac{D.L}{D} = L \tag{D.12}$$

For the inertia load we obtain similarly, using equation D.6:

$$D_{ie}^2 = \frac{D^2 \cdot L}{dz} = \frac{D^2 \cdot L}{D} = D \cdot L \quad \text{or} \qquad D_{ie} = \sqrt{D \cdot L} \tag{D.13}$$

The equivalent diameters of the drag and the inertia sticks are thus mutually different, and they vary with the orientation of the member. The length L is usually taken to be the length between the intersection points of the centrelines of the members involved.

D.4 Members in a vertical plane parallel to the wave direction

The situation is depicted in figure D.3. The plane of the drawing is parallel to the plane of wave propagation.

Inclined member
The drag and inertia loads normal to the member and the stick segments are again given by equations D.4 and D.6. However, only the horizontal components of the loads on the member are to be matched by the loads on the stick. Hence:

$$\begin{aligned}\hat{F}_{hd} &= \hat{F}_d \sin\theta \\ \hat{F}_{hi} &= \hat{F}_i \sin\theta\end{aligned} \qquad \text{(D.14)}$$

where the subscript '*h*' indicates the horizontal load.

For waves in deep water the water particles describe circular orbits and the magnitudes of the velocity and the acceleration vectors are constant along the entire orbit. This means that for the largest normal velocity and acceleration in deep water waves and for all member orientations $\hat{v}_n = \hat{u}$ and $\hat{a}_n = \hat{\dot{u}}$, but the maxima occur at different times due to the phase differences resulting from the spatial separation. However, for waves in intermediate water depths the water particles describe elliptical orbits, in which the horizontal axis is the long axis and the vertical axis is the short axis. Consequently, the magnitudes of the velocity and acceleration vectors change with their orientation in space; the only thing we can confidently say is that $\hat{v}_n \le \hat{u}$ and $\hat{a}_n \le \hat{\dot{u}}$. Considering the largest local normal load on the real member, irrespective of the moment at which this occurs, we may now adopt a further conservative approximation by always putting $\hat{v}_n = \hat{u}$ and $\hat{a}_n = \hat{\dot{u}}$, regardless of water depth. We can then determine equivalent diameters in the same manner as before.

The segment lengths between the elevations z_1 and z_2 are once more given by equation D.9. From the requirement that $\hat{F}_{dm} = \hat{F}_{hdp}$ we obtain for the equivalent diameter of the drag stick:

$$D_{de} = \frac{D \cdot d\ell \cdot \sin\theta}{dz} = \frac{D \cdot d\ell \cdot \sin\theta}{d\ell \cdot \sin\theta} = D \qquad \text{(D.15)}$$

and for the equivalent diameter of the inertia stick:

$$D_{ie}^2 = \frac{D^2 \cdot dl \cdot \sin\theta}{dz} = \frac{D^2 \cdot dl \cdot \sin\theta}{dl \cdot \sin\theta} = D^2 \quad \text{or} \qquad D_{ie} = D \qquad \text{(D.16)}$$

Horizontal members
Horizontal members in a plane parallel to the wave direction experience only vertical hydrodynamic loading. Consequently the horizontal component of the loading on the real member is zero and there is no contribution to be included in the stick model:

$$D_{de} = D_{ie} = 0 \qquad \text{(D.17)}$$

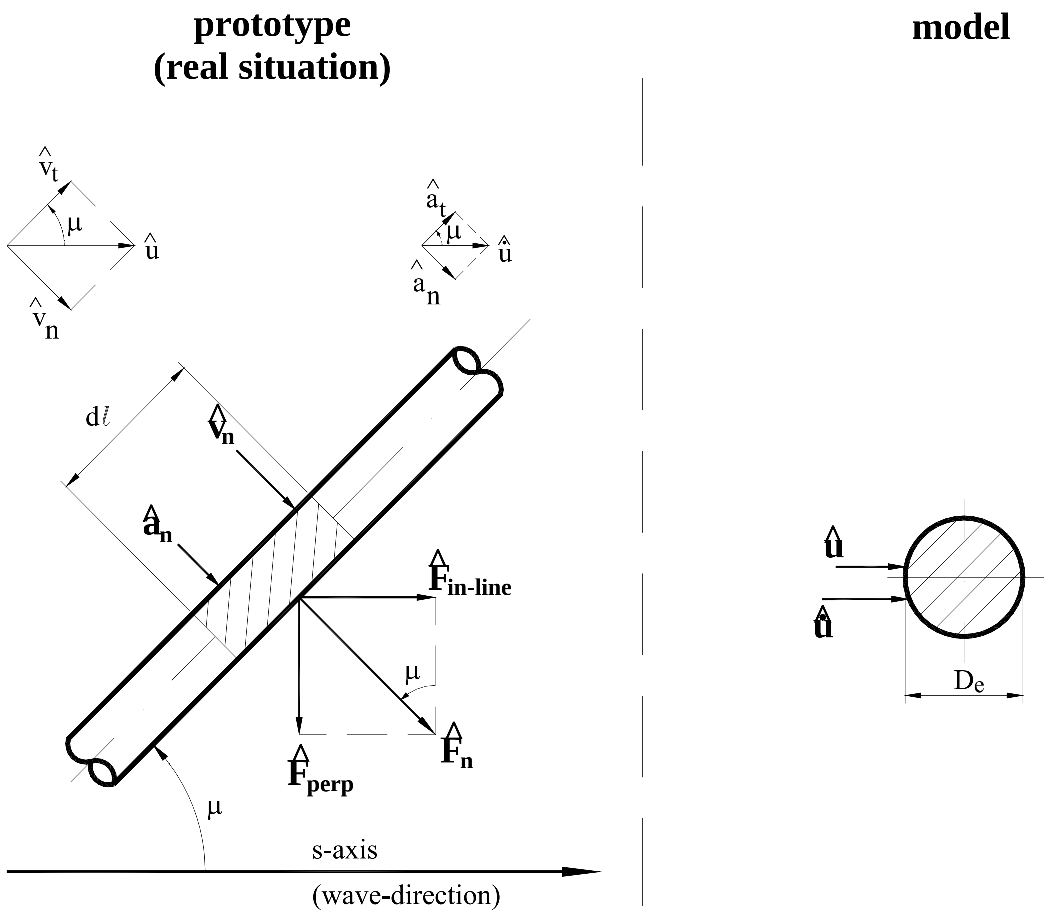

prototype (real situation)

model

Figure D.4. Mapping of members in a horizontal plane onto a stick

D.5 Members in a horizontal plane

Horizontal members perpendicular and parallel to the wave direction have already been discussed in section D.3 and D.4, respectively. Therefore it remains to consider members under an angle μ with the plane of wave propagation; see figure D.4. The plane of the drawing is now a horizontal plane in which the wave travels in the direction of the positive s-axis. The wave kinematics are accordingly parallel to the s-axis. The elevations z_1 and z_2 are at the lower and upper point of the member as before, so that again $dz = D$. The components of the horizontal wave kinematics normal to the member are then:

$$\begin{aligned} \hat{v}_n &= \hat{u}\sin\mu \\ \hat{a}_n &= \hat{\dot{u}}\sin\mu \end{aligned} \tag{D.18}$$

and the components of the loading in the direction of the wave are similarly (see figure D.4):

$$\hat{F}_{in-line} = \hat{F}_n \sin\mu \tag{D.19}$$

The drag load on the full length of the horizontal member must be represented by the drag load on the corresponding segment of the vertical stick. Combining equations D.18 and D.19 with equation D.4 for the load in the wave direction gives for the diameter of the drag stick:

$$D_{de} = \frac{(\sin\mu)^2 \cdot D \cdot L \cdot \sin\mu}{dz} = \frac{(\sin\mu)^3 \cdot D \cdot L}{D} == (\sin\mu)^3 \cdot L \tag{D.20}$$

Analogously, combining equations D.18 and D.19 with equation D.6 for the load in the wave direction gives for the diameter of the inertia stick:

$$D_{ie}^2 = \frac{\sin\mu \cdot D^2 \cdot L \cdot \sin\mu}{dz} = \frac{(\sin\mu)^2 \cdot D^2 \cdot L}{D} = (\sin\mu)^2 \cdot DL \quad \text{or} \quad D_{ie} = \sin\mu \cdot \sqrt{D \cdot L} \tag{D.21}$$

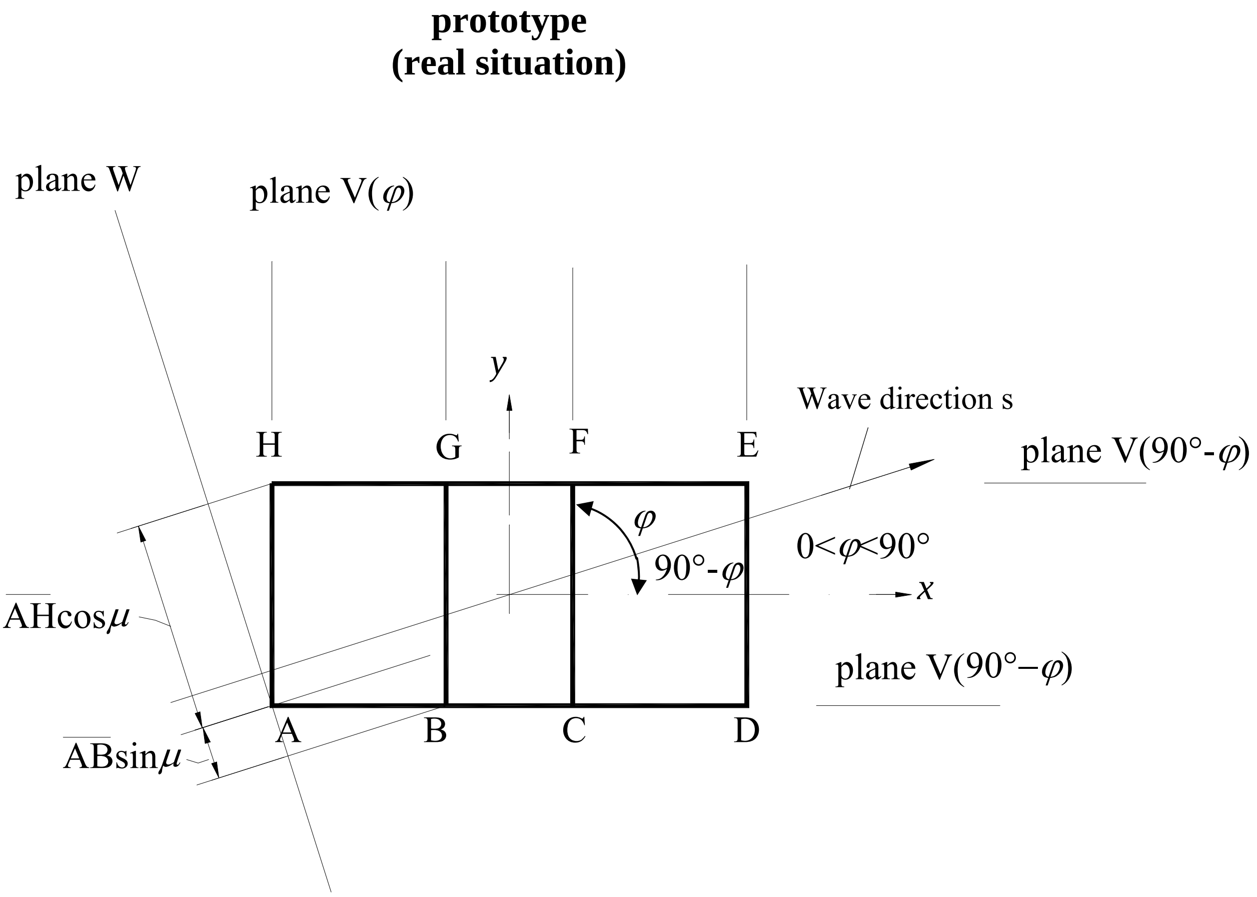

Figure D.5. Plan view of an eight-leg structure (illustration of procedure for oblique wave direction)

For $\mu = 90°$ the equations D.20 and D.21 reduce to equations D.12 and D.13, respectively. Similarly, for $\mu = 0$ they both reduce to equation D.17. In both these cases this is exactly what they should do.

D.6 Arbitrarily inclined members

The complex problem of wave loading on cylinders that are arbitrarily inclined in two directions has not yet been satisfactorily resolved. In principle, and quite pragmatically, we can again adopt an extended form of the Morison equation. By determining the velocity and acceleration normal to the member, the normal drag and inertia loads on a segment of the member can be calculated. Decomposing these normal loads, their horizontal components in the wave direction can subsequently be modelled by a load on a corresponding segment of a vertical stick as before. However, whether the hydrodynamic coefficients for the flow situation around the arbitrarily inclined member and the vertical stick may be assumed to be the same is questionable.

Considering this uncertainty as well as the fact that there will only be few members that fall into this category, it would appear rather overdone to derive the complex geometrical relationships for normal kinematics and loads in three dimensions. The problem of members inclined in two directions will mainly arise for members in the (near) vertical longitudinal and transverse frames of a structure in oblique wave directions. Two practical options then present themselves, as described below.

Let PQ be such an arbitrarily inclined member and let a vertical plane through PQ be plane V. As before (cf. figure D.4), the orientation of the plane V is defined by an angle φ with respect to and measured from the wave direction. Figure D.5 shows a plan view of an eight-leg example structure. The transverse frames AH to DE correspond with planes V under an angle φ with the wave direction, while the longitudinal frames ABCD and EFGH correspond with planes V under an angle $-90° < \varphi < 0$, or in an absolute sense $(90° - \varphi)$, with the wave direction. Any member not in the transverse or longitudinal frames will lie in another plane V with a different angle φ. However, always choose the angle φ such that $-90° < \varphi < 90°$ to ensure that sine- and cosine-functions in equations D.22a and b below are positive.

Within the plane V the member PQ makes an angle θ with the horizontal, again as before. The member PQ in V will experience loads that are in between those for an equivalent diameter in accordance with equation D.15 or D.16 for $\varphi = 0$, and an equivalent diameter in accordance with D.10 or D.11 for $\varphi = 90°$. The first option that suggests itself is therefore interpolation; linear interpolation will be adequate for the purpose. The second option is to project member PQ onto a vertical plane W perpendicular to the wave direction and to calculate the wave loads on the projected member in W using equations D.10 and D.11.

Using first interpolation, the results for an example member with an angle $\theta = 45°$ are shown in the table below in the form of the ratios D_{de} / D and D_{ie} / D.

	Member PQ in frame AH (angle φ) using interpolation of D.10 and D.15, or D.11 and D.16, respectively		Member PQ in frame AB (angle $90°-\varphi$) using interpolation of D.10 and D.15, or D.11 and D.16, respectively	
φ (deg)	D_{de} / D	D_{ie} / D	D_{de} / D	D_{ie} / D
0	1.00	1.00	1.41	1.19
30	1.14	1.06	1.28	1.13
45	1.21	1.09	1.21	1.09
60	1.28	1.13	1.14	1.06
90	1.41	1.19	1.00	1.00

Due to the complementarity of the angles of the longitudinal and the transverse frames, the results on the right are the same as those on the left, but in reverse order (at least for $\theta = 45°$).

The second option is projection. Let the angle of the projected member with the horizontal in plane W be denoted by ψ. When PQ lies in the transverse frames that are under an angle φ with the wave direction:

$$\tan\psi = \frac{\sin\theta}{\cos\theta\sin\varphi} \qquad (0 < \varphi < 90°) \tag{D.22a}$$

and when PQ lies in the longitudinal frames under an angle $(90°-\varphi)$ with the wave direction, for which in accordance with the definition of φ is $-90° < \varphi < 0$:

$$\tan\psi = \frac{\sin\theta}{\cos\theta\cos\varphi} \qquad (-90° < \varphi < 0) \tag{D.22b}$$

To calculate the contribution of PQ to the horizontal load in the wave direction we can use the equations D.10 and D.11, if we replace the angle θ by the angle ψ in these equations.

The results for the same example member with an angle $\theta = 45°$ are shown in the next table.

	Member PQ in frame AH (angle φ) using ψ from D.22a in D.10/D.11		Member PQ in frame AB (angle $90°-\varphi$) using ψ from D.22b in D.10/D.11	
φ (deg)	D_{de} / D	D_{ie} / D	D_{de} / D	D_{ie} / D
0	1.00	1.00	1.41	1.19
30	1.12	1.06	1.32	1.15
45	1.22	1.11	1.22	1.11
60	1.32	1.15	1.12	1.06
90	1.41	1.19	1.00	1.00

Comparing the two tables it can be seen that the results from the two procedures do not differ much.
Vertical and horizontal members in the frames are treated as described in sections D.2 and D.5, respectively, also for oblique wave directions.

D.7 Waves and current

The addition of a current velocity has no effect on the accelerations of the water particles so that the equivalent diameters of the inertia stick are unaltered. However, a co-existing current does affect the drag loads in the (extended) Morison equation. As the modelling process maps a segment of a real member onto a segment of a vertical stick at the same elevation the current profile over depth plays no role in the procedure; it is the same in the prototype and in the model.

It is easily verified that the discussion in sections D.2 and D.3 for members that are vertical and members that lie in a vertical plane perpendicular to the wave direction remain completely valid for hydrodynamic loading due to waves combined with a current, provided that the waves and the current are collinear. The relevant velocities v_n and u are then both horizontal and parallel, so that nothing changes when both are increased with an equally horizontal current velocity U_c. The equivalent diameters of the drag sticks thus remain the same.

For members in a horizontal plane the addition of a current does not change anything either. The normal velocity $\hat{v}_n$ in equation D.18 now becomes $\hat{v}_n = (\hat{u} + U_C)\sin\mu$ while the velocity for the stick model becomes $(\hat{u} + U_C)$. This factor hence appears in both loads and equation D.20 remains valid as well.

However, for inclined members in a plane parallel to the wave direction this is no longer true. The normal velocity in the prototype is now increased with $U_C \sin\theta$, while for the vertical stick it is increased with the full current velocity U_c. Hence the ratio $\left[(\hat{u} + U_C \sin\theta) / (\hat{u} + U_C)\right]^2$ should now in fact be included in equation D.15. However, this is not normally done. Ignoring this ratio and including the current velocity with the horizontal wave orbital velocity in the hydrodynamic calculations for the stick model is again somewhat conservative for these members.

D.8 Variable submergence of members around the still water line

Horizontal drag loads and the associated overturning moment are largest when a wave crest passes the structure. Therefore, members are loaded over a length between $z = -d$ (the bottom) and $z = +\hat{\zeta}$ (the wave crest). For high waves and small to moderate waterdepths this effect can be significant and should be accounted for in the calculations; see also section 4.6.4 and figure 4.6-8. As the horizontal inertia loads are largest when a wave zero-crossing passes the structure, members are only loaded by inertia loads up to $z = 0$ and no special measures need to be taken to account for variable submergence.

D.9 The influence of marine growth

Members are subject to biofouling by marine organisms, especially in the upper layers near the still water line where light penetrates most easily and the oxygen content of the water is highest. The resulting marine growth attached to the members increases the diameter for

		Equivalent drag diameter D_{de}	Equivalent inertia diameter squared D_{ie}^2	Equivalent inertia diameter D_{ie}
1	*(near) vertical members*	D	D^2	D
2	*members in a (near) vertical plane perpendicular to the wave direction*			
	inclined members	$D/\sin\theta$	$D^2/\sin\theta$	$D/\sqrt{\sin\theta}$
	horizontal members	L	$D\cdot L$	$\sqrt{D\cdot L}$
3	*members in a (near) vertical plane parallel to the wave direction*			
	inclined members	D	D^2	D
	horizontal members	0	0	0
4	*members in a horizontal plane*			
	oblique members	$L\cdot(\sin\mu)^3$	$D\cdot L\cdot(\sin\mu)^2$	$\sqrt{D\cdot L}\cdot(\sin\mu)$
5	*arbitrarily inclined members in a (near) vertical plane V under an angle $-90<\varphi<90$ with the wave direction*			
	use projection onto a plane W perpendicular to the wave direction and replace θ in group 2 by ψ with: $0<\phi<90°$ $\tan\psi=\dfrac{\tan\theta}{\sin\phi}$ $-90°<\phi<0$ $\tan\psi=\dfrac{\tan\theta}{\cos\phi}$	$D/\sin\psi$	$D^2/\sin\psi$	$D/\sqrt{\sin\psi}$

Table D.4.1. Overview of equivalent diameters from sections D.2 to D.6

hydrodynamic loading due to both drag and inertia loads, while the increased roughness of the member also increases the drag coefficient compared to a smooth member.

The effect of marine growth is usually accounted for by the introduction of a hydrodynamic diameter that is larger than the actual structural diameter. When the thickness of the marine growth layer at a particular elevation is t, the effective hydrodynamic diameter at that elevation is $(D+2t)$. Drag loads are correspondingly increased by the ratio $(D+2t)/D$, while the inertia loads are increased by the ratio $\left[(D+2t)/D\right]^2$. Additionally, the drag loads may be further increased by the ratio $C_{d,rough}/C_{d,smooth}$. For extreme storm loading on steel space frame structures, where the influence of inertia loads is often small, adjusting the diameter for the inertia load calculations is in most cases neglected.

These effects are to be included in the calculations of the total applied hydrodynamic loading and the overturning moment. However, these are separate issues that are unrelated to the modelling process of representing a structure by a stick model.

D.10 Complete stick model

When the procedure in the previous sections has been completed for all (groups of) members the equivalent drag diameters at each elevation may be added up to form one equivalent drag stick, and the equivalent inertia diameters squared may be added up to determine the diameter of one equivalent inertia stick. These diameters are not the same and they vary with elevation. Table D.1 gives an overview of all the results from the sections D.2 to D.6.

As the drag loads on the drag stick are in phase at all elevations they can simply be summed to obtain the total drag load $\hat{F}_{d,\,total}$ on the structure. The inertia loads on the inertia stick are also in phase at all elevations and these can similarly be summed to obtain the total inertia load $\hat{F}_{i,\,total}$ on the structure. The total horizontally applied hydrodynamic load on the structure $F_{str}(t)$, as determined by the stick model, and including the time dependent factors (see equation D.2), is hence:

$$\begin{aligned} F_{str}(t) &= F_{i,total}(t) + F_{d,total}(t) \\ &= \hat{F}_{i,total}\sin(-\omega t) + \hat{F}_{d,total}\cos(-\omega t)\left|\cos(-\omega t)\right| \end{aligned} \tag{D.23}$$

In view of the $\cos(-\omega t)\left|\cos(-\omega t)\right|$ -factor the total load splits into two different cases:

$$\begin{aligned} &\text{for } 0 \le \omega t \le \pi/2 \text{ and } 3\pi/2 \le \omega t \le 2\pi \\ &F_{str}(t) = -\hat{F}_{i,total}\sin\omega t + \hat{F}_{d,total}(\cos\omega t)^2 \end{aligned} \tag{D.24}$$

and:

$$\begin{aligned} &\text{for } \pi/2 < \omega t < 3\pi/2 \\ &F_{str}(t) = -\hat{F}_{i,total}\sin\omega t - \hat{F}_{d,total}(\cos\omega t)^2 \end{aligned} \tag{D.25}$$

$F_{str}(t)$ has a maximum for $dF_{str}(t)/dt = 0$. For equation D.24 this results in:

$$\begin{aligned}&\text{for } 0 \le \omega t \le \pi/2 \text{ and } 3\pi/2 \le \omega t \le 2\pi \\ &-\omega \hat{F}_{i,total} \cos\omega t - 2\omega \hat{F}_{d,total} \cos\omega t \cdot \sin\omega t = 0\end{aligned} \qquad \text{(D.26)}$$

and for equation D.25 in:

$$\begin{aligned}&\text{for } \pi/2 < \omega t < 3\pi/2 \\ &-\omega \hat{F}_{i,total} \cos\omega t + 2\omega \hat{F}_{d,total} \cos\omega t \cdot \sin\omega t = 0\end{aligned} \qquad \text{(D.27)}$$

The first solution of D.26 as well as D.27 is:

$$\begin{aligned}&\cos\omega t_1 = 0 \\ &\omega t_1 = \frac{\pi}{2} \qquad \rightarrow t_1 = \tfrac{1}{4}T \\ &\omega t_1 = \frac{3\pi}{2} \qquad \rightarrow t_1 = \tfrac{3}{4}T\end{aligned} \qquad \text{(D.28)}$$

Both values of t_1 satisfy the requirements associated with equation D.24. In the limit D.25 is also satisfied, although strictly speaking the solutions are not within the conditional range for ωt. Both values of t_1 are thus valid solutions. At t_1 the drag load is zero. For $t_1 = \tfrac{1}{4}T$ the total load is hence $F_{str}(t) = -\hat{F}_{i,total}$ (a minimum), while for $t_1 = \tfrac{3}{4}T$ (or $t_1 = -\tfrac{1}{4}T$) it is $F_{str}(t) = +\hat{F}_{i,total}$ (a maximum). At both times t_1 the total load has a horizontal tangent, but whether this is a local maximum / minimum or an absolute maximum / minimum can only be established by investigating the behaviour of $F_{str}(t)$ in the neighbourhood of t_1. We will consider the maximum and determine $F_{str}(t)$ for $\omega t = 3\pi/2 \pm \varepsilon$ $(\varepsilon > 0)$. Substitution into equation D.23 gives:

$$\begin{aligned}F_{str}(t) &= \hat{F}_{i,total} \sin\left\{-(\frac{3\pi}{2} \pm \varepsilon)\right\} + \hat{F}_{d,total} \cos\left\{-(\frac{3\pi}{2} \pm \varepsilon)\right\} \cdot \left|\cos\left\{-(\frac{3\pi}{2} \pm \varepsilon)\right\}\right| \\ &= \hat{F}_{i,total} \cos(\mp\varepsilon) + \hat{F}_{d,total} \{-\sin(\mp\varepsilon)\} \left|-\sin(\mp\varepsilon)\right|\end{aligned}$$

For the two different signs this results in:

$$F_{str}(t) = \hat{F}_{i,total} \cos\varepsilon - \hat{F}_{d,total} (\sin\varepsilon)^2 \qquad \text{for the} + \text{ sign } (\varepsilon > 0)$$

$$F_{str}(t) = \hat{F}_{i,total} \cos\varepsilon + \hat{F}_{d,total} (\sin\varepsilon)^2 \qquad \text{for the } - \text{ sign } (\varepsilon > 0)$$

Introducing:

$$\hat{F}_{d,total} = a \cdot \hat{F}_{i,total}$$

we can write these two expressions together as:

$$F_{str}(t) = \hat{F}_{i,total} \left(\cos\varepsilon \mp a \cdot (\sin\varepsilon)^2\right) \qquad (\varepsilon > 0)$$

The function $f(\varepsilon) = \cos\varepsilon \mp a \cdot (\sin\varepsilon)^2$ has a maximum for:

$$\frac{df(\varepsilon)}{d\varepsilon} = -\sin\varepsilon \mp 2a \cdot \sin\varepsilon \cdot \cos\varepsilon = -\sin\varepsilon(1 \pm 2a\cos\varepsilon) = 0$$

For $a < \frac{1}{2}$ the factor in brackets cannot be zero, so that $\varepsilon = 0$ is the only solution. However, for $a \geq \frac{1}{2}$ there is another solution, namely $\cos\varepsilon = \mp 1/2a$. This means that in the first case we have an *absolute* maximum, while in the second case there is only a *relative* maximum in which we are not really interested. Consequently, the maximum of the total load on the structure is:

$$F_{str}(t_1) = \hat{F}_{i,total} \qquad \text{for} \quad \omega t_1 = 3\pi/2 \quad \rightarrow t_1 = \tfrac{3}{4}T \text{ (or -} \tfrac{1}{4}T) \tag{D.29a}$$

provided that:

$$\hat{F}_{i,total} > 2\hat{F}_{d,total} \tag{D.29b}$$

The second solution of D.26 is:

$$\sin\omega t_2 = -\frac{\hat{F}_{i,total}}{2\hat{F}_{d,total}} < 0 \;\rightarrow \qquad \frac{3\pi}{2} < \omega t_2 < 2\pi \tag{D.30}$$

A negative value of $\sin\omega t_2$ excludes the range $0 \leq \omega t \leq \pi/2$ associated with equation D.26 and only the second range minus its end points remains. As furthermore $|\sin\omega t| \leq 1.0$ it follows that at this time t_2:

$$\hat{F}_{i,total} \leq 2\hat{F}_{d,total} \tag{D.31}$$

The value of the cosine-function at t_2 becomes:

$$\cos\omega t_2 = 1 - (\sin\omega t_2)^2 = 1 - \frac{\hat{F}^2_{i,total}}{4\hat{F}^2_{d,total}} \tag{D.32}$$

Then, substituting equations D.30 and D.32 into D.24 we obtain for the maximum load on the structure at t_2:

$$F_{str}(t_2) = +\frac{\hat{F}^2_{i,total}}{2\hat{F}_{d,total}} + \hat{F}_{d,total}\left(1 - \frac{\hat{F}^2_{i,total}}{4\hat{F}^2_{d,total}}\right) = \hat{F}_{d,total} + \frac{\hat{F}^2_{i,total}}{4\hat{F}_{d,total}} \tag{D.33a}$$

provided that:

$$3\pi/2 < \omega t_2 < 2\pi \qquad \rightarrow \tfrac{3}{4}T < t_2 < T$$

and (D.33b)

$$\hat{F}_{i,total} \leq 2\hat{F}_{d,total}$$

The second solution of equation D.27 as opposed to D.26 is analogously:

$$\sin\omega t_3 = +\frac{\hat{F}_{i,\,total}}{2\hat{F}_{d,\,total}} > 0 \;\rightarrow \qquad \frac{\pi}{2} < \omega t_3 < \pi \tag{D.34}$$

The ranges $0 < \omega t \leq \pi/2$ and $\pi \leq \omega t < 3\pi/2$ in which the sine-function is also positive are excluded from the solution by the general requirement associated with equation D.27. As again $|\sin\omega t| \leq 1.0$ we also have at time t_3:

$$\hat{F}_{i,total} \leq 2\hat{F}_{d,total} \tag{D.35}$$

and:

$$\cos\omega t_3 = 1 - (\sin\omega t_3)^2 = 1 - \frac{\hat{F}^2_{i,total}}{4\hat{F}^2_{d,total}} \tag{D.36}$$

Substituting equations D.34 and D.36 into D.25 we obtain for the load on the structure at t_3:

$$F_{str}(t_3) = -\frac{\hat{F}^2_{i,\,total}}{2\hat{F}_{d,\,total}} - \hat{F}_{d,\,total}\left(1 - \frac{\hat{F}^2_{i,\,total}}{4\hat{F}^2_{d,\,total}}\right) = -\hat{F}_{d,\,total} - \frac{\hat{F}^2_{i,\,total}}{4\hat{F}_{d,\,total}} \tag{D.37a}$$

provided that:

$$\pi/2 < \omega t_3 < \pi \;\rightarrow \tfrac{1}{4}T < t_3 < \tfrac{1}{2}T$$

and (D.37b)

$$\hat{F}_{i,total} \leq 2\hat{F}_{d,total}$$

This is the negative value of the magnitude of equation D.33a at a time instant t_2 and half a period different from t_2 in D.33b. In other words, it represents an equally valid *minimum* instead of a *maximum* load on the structure.

Summarising these results we conclude that the maximum total load on the structure is as follows:

if: $\hat{F}_{i,total} > 2\hat{F}_{d,total}$ (D.38a)

the maximum of the total load is:

$$F_{str}(t_1) = \hat{F}_{i,total} \qquad \text{for} \;\; \omega t_1 = 3\pi/2 \;\; \rightarrow t_1 = \tfrac{3}{4}T \;\; (\text{or } t_1 = -\tfrac{1}{4}T) \tag{D.38b}$$

if: $\hat{F}_{i,total} \leq 2\hat{F}_{d,total}$ (D.39a) the maximum of the total load is:

$$F_{str}(t_2) = \hat{F}_{d,total} + \frac{\hat{F}_{i,total}^2}{4\hat{F}_{d,total}} \quad \text{for} \quad \frac{3\pi}{2} < \omega t_2 < 2\pi \ \rightarrow \frac{3}{4}T < t_2 < T \ \text{(or} \ -\frac{1}{4}T < t_2 < 0) \qquad \text{(D.39b)}$$

One further note should be made. The above equations are valid for the total load on the whole structure, as well as for the load per unit length at an elevation z. As the relative proportion of the drag and the inertia loads varies with elevation, we will find that, when the equations are applied to the load per unit length at elevation z, the phase (the time) at which the maximum is reached will vary with elevation. Because of this the maximum total loads per elevation cannot simply be summed to determine the total load on the whole structure. For this latter purpose we have to first separately sum the inertia loads and the drag loads, and then apply equation D.38 or D.39 to the total drag and inertia loads on the whole structure.

This analytical solution is perhaps of somewhat academic interest, as the calculations will normally be performed numerically, resulting in a numerical solution for the maximum load on the structure and for the time at which it is achieved. However, equations D.38 and D.39 can be used as a useful check that the maximum is not missed. For the overturning moment entirely the same results are obtained with M replacing F.

Another, approximate solution is to write the total applied load on the structure $F_{str}(t)$ as a linear combination of the time dependent total drag load $\hat{F}_{d,\,total}$ and total inertia load $\hat{F}_{i,\,total}$, instead of the non-linear equation D.23:

$$F_{str}(t) \approx -\hat{F}_{i,total}\sin\omega t + \hat{F}_{d,total}\cos\omega t = \hat{F}_{str}\cos(\omega t + \varphi_F) \qquad \text{(D.40)}$$

This is not a formal and correct way of linearising the hydrodynamic load on the structure because the magnitude of the drag load remains non-linear; only the non-linearity in the time dependent factor is ignored. The drag and inertia loads are now 90 degrees out of phase; i.e. the inertia load leads the drag load by a quarter of the wave period. The grand total applied horizontal hydrodynamic load on the structure and its associated phase relative to the wave are now:

$$\begin{aligned} \hat{F}_{str} &= \left[\hat{F}_{i,total}^2 + \hat{F}_{d,total}^2\right]^{1/2} \\ \tan\varphi_F &= -\frac{\hat{F}_{i,total}}{\hat{F}_{d,total}} \end{aligned} \qquad \text{(D.41)}$$

For the overturning moment the procedure is similar. The contributions for all elevations can again be summed, for the drag and the inertia loads separately, and the result is:

$$\begin{aligned} \hat{M}_{str} &= \left[\hat{M}_{i,total}^2 + \hat{M}_{d,total}^2\right]^{1/2} \\ \tan\varphi_M &= -\frac{\hat{M}_{i,total}}{\hat{M}_{d,total}} \end{aligned} \qquad \text{(D.42)}$$

These approximations may be compared with the correct non-linear result for the maximum load and the associated phase angles ωt_1 or ωt_2 from equations D.38 or D.39. The results are unlikely to be very different.

For design loading estimates on steel space frame structures in extreme storm conditions the influence of the inertia load will often be relatively small. Therefore the calculation of the inertial loads is often omitted and no inertia stick is included in the stick model. This may indeed be justifiable in view of its small contribution and the approximate nature of the calculations. However, it should be recognised that deleting the inertia loads is a non-conservative approximation, which is somewhat in conflict with the overall objective of the estimating procedure. Furthermore, for steel structures with substantial leg diameters the contribution of the inertia loads may not always be so small as is usually assumed. It is therefore safer to follow the procedure described in this Annex in full.

For the large diameter legs of concrete structures the reverse of the above observation may be the case: now the drag loads are relatively small and can often be neglected, so that a drag stick can be omitted. However, the same argument that it is better to follow the full procedure applies to this case as well.

5 DESIGN

5.1 A few words on design in general

Still to be written.

5.2 Differences between structures on land and at sea

5.2.1 General aspects

All offshore structures consist generically of three parts, i.e. a superstructure above water, a support- or substructure in the water and a foundation under the water, on or in the sea floor. The superstructure generally contains all the facilities and has some similarity, but also many differences, with a building on land; these aspects will be discussed in the next section. The substructure serves as a support for the superstructure by creating an "artificial island". This island may sit on the sea floor or float. For bottom supported structures the distinction in support structure and superstructure is usually rather pure, e.g. for a fixed steel space frame or concrete gravity structure supporting drilling and/or production facilities. For floating structures the substructure and the superstructure are often more integrated, both from a functional and from a structural point of view. In addition to its structural role the substructure may of course cater for some functional requirements (e.g. storage of oil in the caisson of a concrete gravity structure or in a ship's hull) or contain a part of the equipment (such as in the shafts of a concrete gravity structure or in the columns and pontoons of a semi-submersible). The foundation finally supports the substructure and transfers the loads to the earth. In the case of bottom founded structures load transfer to the earth is direct through a deep pile or a shallow bearing foundation. In the case of floating structures load transfer is indirect via the water column, which supports the floating structure through buoyancy; generically the water and the sea floor underneath may be seen as the 'foundation' for a floater.

Structures on land (i.e. buildings) and (bottom-founded) structures at sea are different in almost every respect, with regard to the structure as such as well as the manner in which they are constructed. The first major difference clearly is that buildings on land do not require a substructure that lifts them out of the water. Therefore the superstructure is essentially the only part that can meaningfully be compared to a building on land. The main technical differences are given below under a number of different headings.

5.2.2 Main technical differences

Design requirements

The specific functional demands will vary from case to case, both onshore and offshore, and will generally be radically different for each case. However, there are a number of more generic requirements that can usefully be compared:

- For a building onshore, concern is in particular with the enclosed spaces. These are the useful parts of a building. The spaces on or in the superstructure offshore, which are used for the installation's ultimate purpose, may or may not be enclosed. Where possible, open spaces are normally preferred to avoid the potential accumulation of flammable and explosive gases. For the substructure, concern is first and foremost with a strong and stable support structure. It is designed to be as small, slender and transparent as possible to reduce hydrodynamic loading by waves and currents.

- Onshore there is normally no need to provide accommodation for people who work in the building to also live in it. In view of the remoteness of offshore platforms the daily shuttling of people to and from the platform is usually not a realistic option. Therefore living quarters with everything that comes with it (e.g. catering and laundry facilities as for a hotel) must normally be provided.
- General facilities and services such as electricity, communication facilities (e.g. telephone), drinking water, sewerage are routinely available onshore but not offshore. Everything must be specially provided.
- Maintenance requirements during the service life should be kept as low as possible in view of the very high cost of offshore work.
- On the other hand, unlike on land, aesthetic considerations hardly play a role offshore.

Site specific structural design data
Design data are usually amply available or easily obtained on land, but for offshore applications the site-specific data are scarce and difficult to get. The data required include e.g. water depth and tidal information; wind, wave and current data; data on the seabed and soil conditions. The costs associated with collecting such data offshore are often very high.

Design regulations
The regulatory framework, the authorities involved and the applicable design and construction rules for offshore platforms are all completely different from those for an onshore building.

Design loadings
Design loadings derive from two generic types of condition, i.e. the in-place condition and the various stages during construction:

- The self-weight of the structure and the functional loads (weight of facilities, supplies, people, operation of equipment, etc.) are components of the in-place loadings that are common to both onshore and offshore cases, although the ratio of the functional loads to the selfweight is generally much greater for offshore structures than for buildings on land. However, the major difference is in the environmental loading, where offshore structures are exposed to enormous loads due to waves and currents. This leads to three very important differences:
  (i) Offshore structures have to accommodate much larger *horizontal* loads than onshore buildings; the ratio of horizontal to vertical loads is a very significant factor for offshore design.
  (ii) The hydrodynamic loads vary continuously with time. As a result, the ratio of time varying (dynamic) to constant (static) loads is usually also very much greater offshore than onshore. This is again a significant factor for offshore design and brings with it a need to check for the potential of fatigue damage that may be done to the material as a result of the accumulated effect of stress variations over the entire service life.
  (iii) The hydrodynamic load variations offshore are of a stochastic nature and are not so simple to describe, quantify and incorporate into design procedures. While this type of loading is not unique to offshore structures, its magnitude and the number of cycles involved are indeed unusual. The need for realistic models to include stochastic loadings for design situations is more of an exception onshore, but is virtually the rule offshore.
- The loadings during construction will tend to be case specific, but are generally less important for buildings on land than for offshore structures. This is due to the radically different way of onshore fabrication and offshore construction; see further below under

'Method of construction'. For offshore structures the designer should try and apply his skills in such a manner that the temporary construction stages do not control dimensioning of the structure over the in-place loading condition. This would be a waste of material and money that the structure would have to carry along during its entire service life.

Foundation

There are several differences between foundations on land and those of bottom supported offshore structures. The differences start already with the soil investigation to obtain the necessary soil data to enable foundation design to proceed:

- Soil investigations offshore must be performed under water, often from a floating vessel which moves considerably in the waves, making the deployment of equipment, taking cores and in-situ measurements much more difficult.
- Preparation of the ground and soil improvement measures can have a very beneficial effect on foundations and are rather common on land. None of these can normally be applied offshore.
- An offshore pile foundation must be installed "from a distance". Traditionally piles have been driven by steam hammers from above water using loose extensions, the so-called followers, to extend the pile when it disappeared under water. The modern hydraulic underwater hammers can follow the pile on their way down through the water and have obviated the need for followers. However, the whole operation remains to be performed and controlled from above water with the aid of remotely controlled vehicles (ROV's) or divers to monitor the process.
- In view of the differences in structural configuration and the high cost of offshore installation, pile foundations offshore use fewer but larger diameter piles than onshore. Furthermore, offshore piles are as a rule open ended hollow steel piles. Onshore there is usually a range of pile options, with in many cases solid concrete piles being the preferred and most economical choice.
- Due to the large overturning moments resulting from the lateral loads on the structure, foundation piles offshore are often also subjected to substantial tension forces. In several cases these tension forces are of a similar order of magnitude as the compression forces. For buildings on land tension piles are uncommon, although they do occur for other civil engineering structures such as retaining walls, harbour quays or tunnels.
- Applying test loads to piles to investigate or demonstrate their bearing capacity is standard practice on land. This cannot be done offshore for a variety of reasons; these reasons include the usually much larger offshore pile capacities than those for piles on land, and that offshore piles are in most cases installed under an angle rather than vertical.
- On good sandy soils onshore, a building may be founded on a base slab directly on the ground without piles. This is a shallow bearing foundation along the same principle as for an offshore gravity structure. However, the size and weight of an offshore gravity structure and its associated foundation are unparalleled onshore.
- Offshore foundation loads vary continuously with time making foundation behaviour under cyclic loading a subject of prime consideration. Onshore this hardly plays a role.
- The seabed under and around an offshore structure is subject to morphologic phenomena due to flowing water, such as scour, erosion and moving sand ripples. Similar phenomena do occur in hydraulic structures such as sluices and locks, but not in association with buildings on land.
- Due to the extraction of oil or gas from the reservoir the pressure distribution may change and the reservoir rock may compact. As a result of this the sea floor together with the entire structure and its foundation may sink relative to the water surface, thus increasing

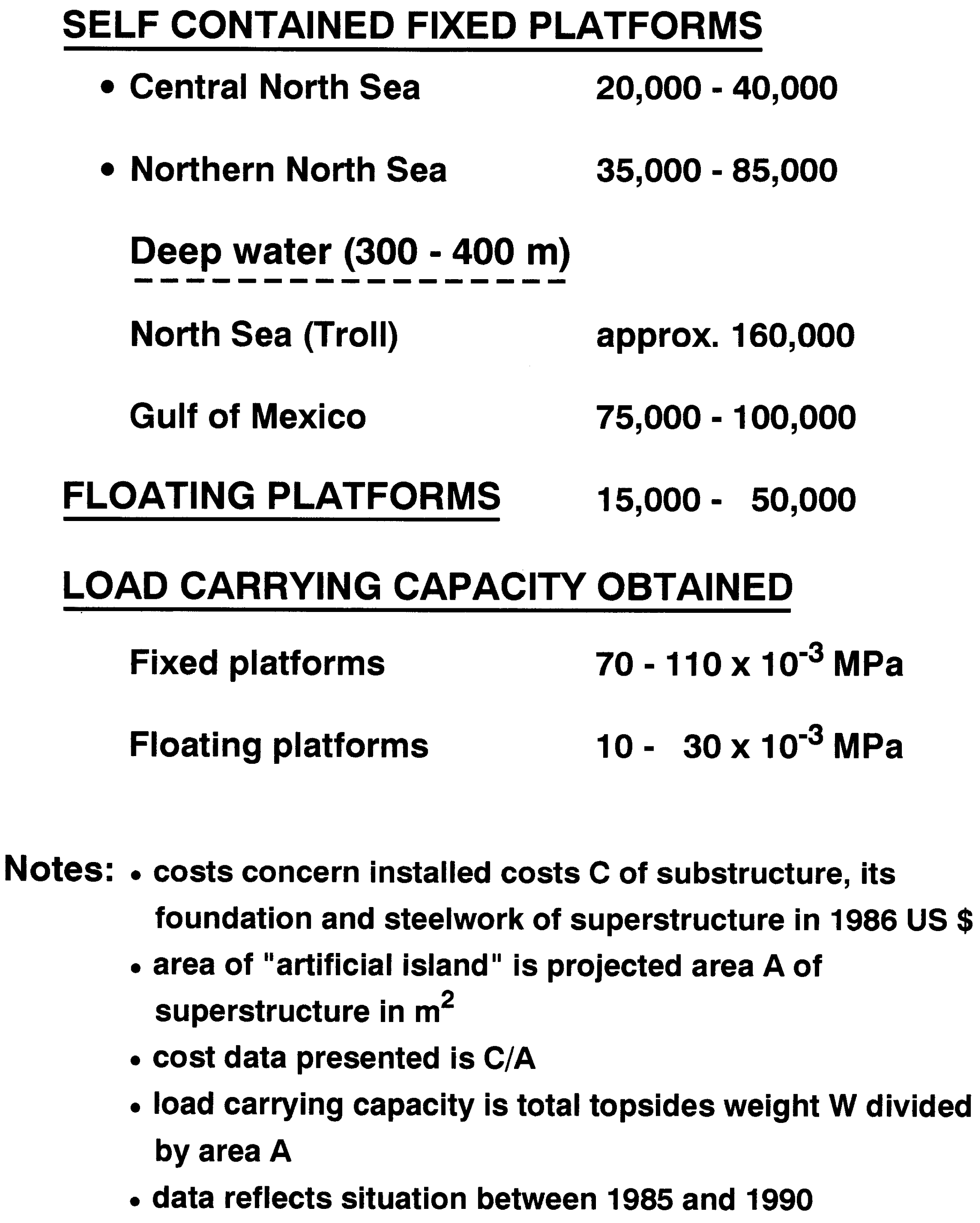

SELF CONTAINED FIXED PLATFORMS

• Central North Sea	20,000 - 40,000
• Northern North Sea	35,000 - 85,000
Deep water (300 - 400 m)	
North Sea (Troll)	approx. 160,000
Gulf of Mexico	75,000 - 100,000
FLOATING PLATFORMS	15,000 - 50,000

LOAD CARRYING CAPACITY OBTAINED

Fixed platforms	70 - 110 x 10^{-3} MPa
Floating platforms	10 - 30 x 10^{-3} MPa

Notes:
- costs concern installed costs C of substructure, its foundation and steelwork of superstructure in 1986 US $
- area of "artificial island" is projected area A of superstructure in m^2
- cost data presented is C/A
- load carrying capacity is total topsides weight W divided by area A
- data reflects situation between 1985 and 1990

Figure 5.2-1. Offshore developments – approximate costs in US dollars per m2 of 'artificial' island

the local water depth. This is a phenomenon that needs to be accounted for in design; the amount of sea floor lowering depends on the reservoir rock.

- Foundation conditions often have a decisive influence on the structural concept selected and the subsequent design of an offshore structure.
- Last but certainly not least, the sequence of installation is radically different. For buildings on land, the foundation is invariably installed first after which the building is built on top of it. For bottom founded offshore structures this is always the other way round: the structure is positioned at its definitive location and only thereafter the foundation piles are installed!

Method of construction

As for the foundation, there are several important and characteristic differences between the method of construction of a building on land and an offshore structure:

- A building is constructed on site, whereas an offshore structure is wholly or largely prefabricated on land in a fabrication yard.
- During prefabrication on land an offshore structure is usually on its side, i.e. in a different orientation than it is during its service life. Hence, in this situation it is subject to a completely different load condition that needs to be assessed carefully.
- Load out from the fabrication yard onto a transportation barge provides another special loading condition for an offshore structure, with no comparable case for a building on land.
- Transportation of the structure in its entirety or in a small number of large parts to the offshore location, across open seas and often over large distances, is unique with no parallel on land. During the tow the structure may be subjected to substantial barge movements with the associated mass inertial forces, which may well provide a governing load condition for certain parts of the structure.
- Installation of the structure at the offshore location requires heavy and expensive marine equipment (e.g. crane capacity, powerful pile driving hammers, etc.). This equipment as well as its associated auxiliary craft is usually floating, which means that they do not always provide a firm platform to work from. Consequently, the ability to operate this equipment and the efficiency of its operation is weather dependent. In the interest of both costs and safety, all offshore construction work should therefore be designed to be as simple and to take as little time as possible.

Construction environment

All construction activities at a construction site present potential safety hazards. However, the offshore environment is openly hostile and dangerous to humans. Extensive precautions are therefore absolutely necessary. Furthermore, offshore logistics are difficult, time consuming and costly.

Offshore operations and management

Finally, effective inspection and monitoring of the condition of an offshore structure during its service life, as well as its maintenance and repair when required, are very difficult and expensive. This is yet another important difference with buildings on land. Minimum maintenance is therefore an important design factor for an offshore structure.

Summary of structural differences

From a purely structural point of view, the three major differences between the design and construction of an offshore structure and a building on land are the design loadings, the foundation, and the method and sequence of construction.

5.2.3 Cost differences

As a final illustration of the consequences of working offshore, figure 5.2-1 (initially compiled for reference [5.2-1]) presents some typical costs for a substructure supporting production facilities per square metre of “artificial island” created by the structure, together with some indications of their load carrying capacity. The data reflect the situation during the mid to late1980s and may not be entirely accurate any more, but figure 5.2-1 does serve to highlight the very high cost of real estate offshore. Comparable onshore costs would be the cost of land plus the cost of the foundation of a building and would generally be significantly lower, even in the downtown areas of most large cities.

Another indicative cost figure is the dayrate of large semi-submersible crane vessels, such as Heerema's large Thialf or the somewhat smaller Balder and Hermod, together with their associated equipment (such as pile driving hammers) and support craft (e.g. tugs and anchor handling vessels). The actual day rate of the total crane vessel spread depends on many factors, such as the size of the capital investment, the operational costs (crew, subsistence, fuel, onshore base and support staff, etc.) as well as the market forces at the time a contract is let. However, it will in any event be in the range of several hundred thousands US dollars per day. Generally speaking, the costs of working offshore may be some 5 to 10 times as high as working onshore.

5.3 Conceptual design

5.3.1 Historical overview

The jubilee book '50 Years Offshore' [5.3-1] includes brief descriptions and historical overviews of steel space frame structures and foundations. These overviews are good general introductions to the subject. Therefore the text is attached to this chapter as Annex A (for space frame structures) and as Annex B (for foundations).

5.3.2 General design considerations for bottom founded structures

The design of an offshore platform is governed by:
- the user or functional requirements
- the operating requirements
- the environmental conditions
- the method of construction (including onshore fabrication, transportation to site, and offshore installation)
- the management of the platform during its service life (inspection, maintenance and repair)

General consideration will further need to be given to *platform decommissioning* at the end of its useful life, but this will rarely translate into specific design requirements. Considerations of abandonment will generally more relate to factors that should be kept in mind and factors that may lead to a preference for choosing between different concepts or options, rather than that they directly impact on the design of the platform as such.

Safety
Section 1.5.3 includes a general discussion on safety issues. These are of paramount importance. Considerations on safety offshore need to be incorporated into every aspect of the design from the very first moment. They need to encompass the entire system from the reservoir, via the drilling and production facilities and any oil or gas that may be imported to the platform, to the export by pipeline or through offshore loading. Supply of goods and transportation of personnel must also be included. It is often necessary that parts of the platform, or even the entire platform, can be isolated by valves in pipework, risers or (subsea) pipelines. Safety hazards should be systematically assessed and reduced, or even better eliminated, by such techniques as hazard and operability studies (HAZOPS). A modern development is that for each installation a so-called safety case is prepared, which carefully reviews all safety aspects, documents the safety precautions and the measures to be taken in case of an incident.

The superstructure is usually the most vulnerable part of a platform with respect to safety. It contains a chemical plant where several potentially dangerous activities may go on at the same time. The very beginning of safety is therefore a simple and logical layout of the various processes and the associated equipment. In shallow waterdepths safety is often pursued using separate platforms for different functions, together forming a platform complex where the platforms are often interconnected by bridges. Otherwise physical separation between areas where the various processes take place is desirable and an effective contributor to improving safety. For example, where possible we should arrange for a separate drilling area; production area (separators, pumps, treatment facilities); gas compression area; utilities area (power

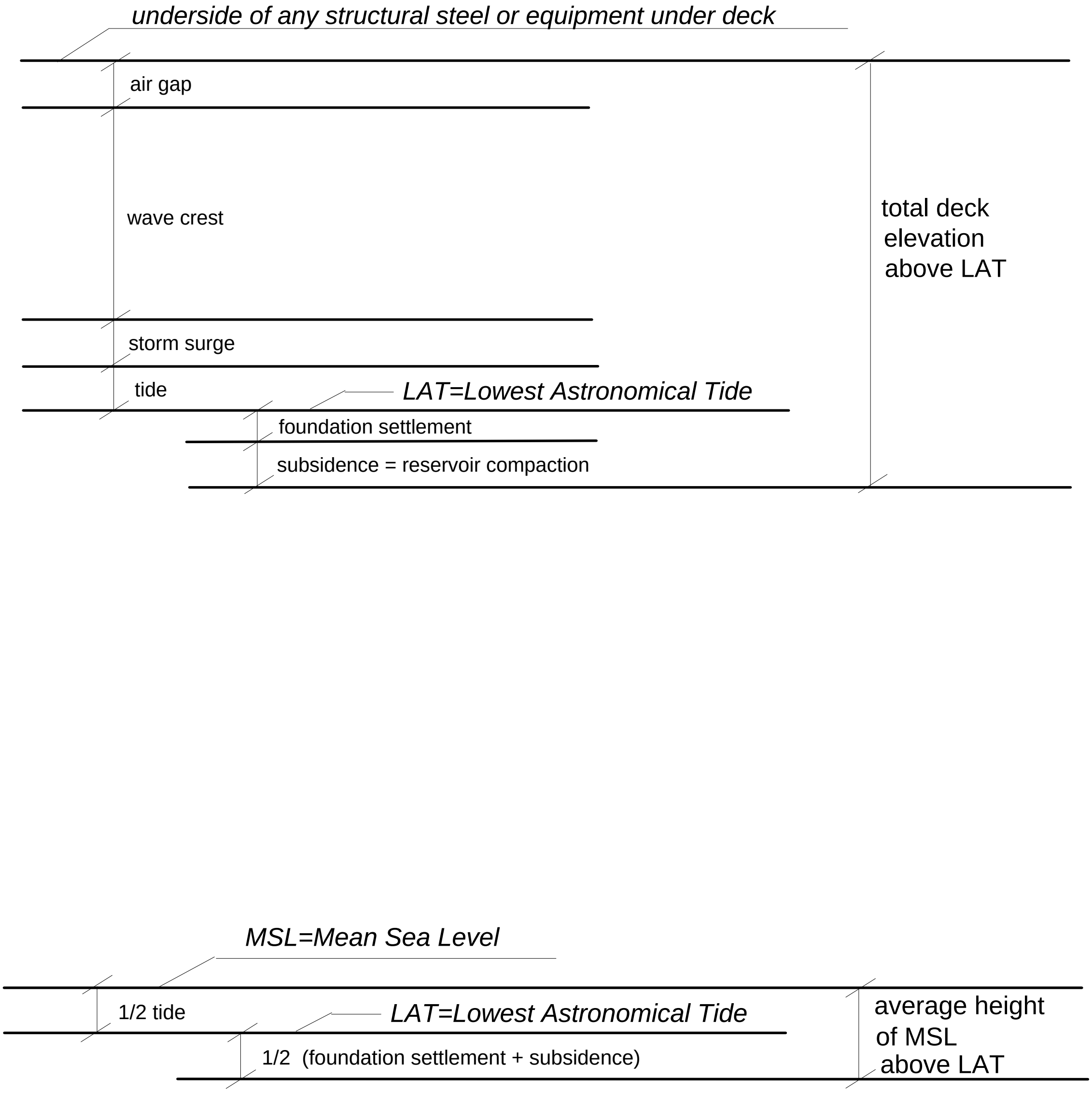
underside of any structural steel or equipment under deck
air gap
wave crest
total deck
elevation
above LAT
storm surge
tide
LAT=Lowest Astronomical Tide
foundation settlement
subsidence = reservoir compaction
MSL=Mean Sea Level
1/2 tide
LAT=Lowest Astronomical Tide
average height
of MSL
above LAT
1/2 (foundation settlement + subsidence)

Figure 5.3-5.1. Deck elevation and mean sea level above Lowest Astronomical Tide

generation, drinking water) and accommodation. This allows the separation of hazardous from non-hazardous areas. Fire resistant walls and blast walls may provide protection against fire and explosions where necessary, but prevention will always be more effective and should be the first aim. If notwithstanding all precautions an accident occurs, containment and control is the first priority. If this is unsuccessful and an accident escalates after all, evacuation may become necessary. Escape routes should be straight, sufficiently wide, unobstructed, clearly lit by emergency lighting, clearly marked and must lead to (a) muster station(s) from where the platform may be abandoned by (free fall) life boats, helicopter or other means.

Deck elevation

The superstructure needs to be above the water at all times. Therefore, *the elevation of the superstructure* should be determined in such a way that it is above the highest crest of the waves expected to occur in the most severe sea state at the location for which the installation is designed. This should take into account water level increases due to tide, storm surge and wave crests, as well as a possible lowering of the sea floor due to settlement of the foundation and/or subsidence of the entire sea floor resulting from compaction of the reservoir deep down in the earth. In addition to these factors one usually includes an air gap of 1.5 m as a safety margin between the underside of any structural element under the deck and the top of any green water. The procedure is illustrated in figure 5.3-1. The 1.5 m is a general allowance for uncertainties in the various contributions for setting the elevation of the deck and rather common practice. However, this practice is not really rationally based. Instead of a fixed value the magnitude of the air gap should be related to the magnitude and degree of uncertainty of the individual contributions and be determined in a probabilistic manner. The consequences of elements of the deck becoming inadvertently inundated can be very serious, both with regard to damage done to the deck structure or the equipment it carries and with regard to overloading of the substructure and/or its foundation. The deck is usually made up of many flat surfaces (e.g. beams, walls of modules), as opposed to the circular members used in substructures. Therefore, horizontal wave loads on the deck quickly become very large, while these loads also act at a very high point resulting in huge additional overturning moments.

Well drilling

Many platforms have wells. These wells may have been drilled from the platform itself or by means of a mobile drilling unit that is positioned adjacent to the platform. In the first case the platform needs to be designed to carry the full weight of the drilling installation together with any additional loads associated with the drilling operation. If a mobile drilling unit is used adjacent to the platform and this unit is a jack-up, the substructure will often need to have one vertical side to enable the jack-up to come close enough to reach the drilling slots on the platform. For the same reason, the deck can normally not be cantilevered over the side of the substructure. Another point to pay attention to is the possible interaction of soil forces in the soil layers underneath the spud cans carrying the jack-up legs (which are usually very large) with the relatively small piles supporting the fixed structure. If the mobile drilling unit is a floating unit, e.g. a semi-submersible, we will need to arrange for an adequate anchoring system that will not interfere with the platform nor with any equipment on the sea floor (such as pipelines, manifolds, subsea wells). Furthermore, a floating unit will move due to wave action and we will thus need to take care that it will never be in contact with the platform.

Conductors

Wells are drilled through a protective conduit between the drill floor and a certain depth below the seabed; this conduit is usually called the conductor or also the stove pipe. Through the water column the conductors are laterally supported by the substructure to prevent buckling under their own weight, the weight of fluids inside and any possible weight on top. Another reason for providing lateral supports is to avoid vortex induced vibrations. By reducing the length of free spans the natural frequencies of conductor vibration are increased and better separated from the vortex shedding frequencies that are the source of excitation. Conductors are laterally supported by guides, but axially free to move up and down (e.g. due to differential deformations or temperature effects).

Interfaces with petroleum engineering
- platform location
- number and type of wells
- requirement for curved conductors
- number of risers and J-tubes, including their orientation
- reservoir compaction and seabed subsidence

Interfaces with metocean engineers
- water depth
- environmental conditions
- platform orientation

Interface with geotechnical engineers
- seabed topography
- soil conditions
- foundation design

Interfaces with drilling (equipment) engineers
- spacing between wells
- accessibility of wells by a platform mounted or a mobile drilling rig
- space and weight for drilling rig and associated equipment
- design and setting depth of well conductors
- allowing relative movements between wells and structure

Interfaces with process -, facilities -, mechanical equipment - and piping engineers
- lay-out of deck(s), horizontal as well as vertical
- routing of pipework, pipe supports
- expansion loops in pipework to allow relative movements or extensions e.g. due to temperature
- foundations for vessels, storage tanks, other heavy equipment
- access for inspection and maintenance
- level adjustment for sensitive equipment
- avoiding or coping with machinery vibrations, isolating vibrating machinery from the structure
- support for deck cranes
- support for and design/construction of a flare boom or flare stack.

Interfaces with electrical and instrumentation engineers
- foundations for generators
- access for maintenance and repair
- routing of electrical cabling and support of cable trays
- positioning and fixing of light fixtures
- positioning and fixing of instrument panels, together with accessibility in case of breakdown

Interfaces with pipeline engineers
- riser supports to substructure and deck(s) (N.B. the riser itself is a pressure conduit and its design belongs to the pipeline discipline)
- J-tubes for riser pull-in
- expansion loops on deck and/or at the base of the structure
- pigging facilities on board

Interfaces with safety engineers
- fire, smoke and gas detection
- fire fighting systems (pumps, ring main, deluge, sprinklers)
- explosion protection (pressure relief, blast walls)
- escape routes
- life saving equipment (rafts, life boats, etc.)
- safety during (onshore) fabrication and (offshore) installation

Interfaces with materials and corrosion engineers
- determining type and quality of materials for structural design
- welding procedures and weld testing
- (cathodic) corrosion protection below water
- corrosion protection by painting above water

Interfaces with drilling/production operations
- boat bumpers, boat landings, supply boat moorings
- loading and unloading facilities (platform cranes, etc.)
- helicopter landing areas
- access platforms, stairs, ladders
- structural inspection and maintenance above and below water

Figure 5.3-2. Typical interfaces between a structural designer and other disciplines

Curved conductors
In many cases wells are drilled from one central location above water, but radiating out to a much wider circle at reservoir depth in order to drain a much larger area. This is called deviated drilling. The rate of deviation is typically some 4 degrees per 100 feet (30 m). More recently wells have become ever more deviated, up to being horizontal in the reservoir region. In these cases the rate of deviation may be greater. The deviation will often start in the ground, below the depth at which the straight conductors have been set. However, sometimes the deviation needs to start already above water. In this case the conductors must be curved and the framing pattern is consequently different at each plan level at which the conductors are supported, considerably complicating design. The complications do not only arise from geometrical factors, but are also due to vertical loads on the frames during conductor driving arising from friction between the conductor and the conductor guides in the frames.

Interfaces
Design of an offshore installation is a *multi-functional activity*, with structural design being only one of the many aspects involved. It should be recognised that satisfying functional and operating requirements can be more important than optimal structural design. There are numerous *interfaces* between structural design and the design activities of other disciplines. All parties must be aware of these interfaces and co-operate in a constructive manner to resolve any problems that may arise; however, there are no simple or firm rules to guide the process or the resolution of conflicts. Typical interfaces are listed in figure 5.3-2.

5.3.3 Design of the superstructure

The functional and operating requirements are mostly embodied in the superstructure, which contains one or more decks. The superstructure can be *an integrated deck*, which means that all functions and associated equipment are integrated with the structural framework into one large unit. An integrated deck is fabricated, transported to location and installed offshore in one piece. The superstructure can also consist of several so-called *modules*, each module being a separate unit with a particular function; for example a drilling module, a production module, a compression module, the living quarters module. These modules are normally fabricated in different yards, individually transported to the field, offshore lifted onto the already installed substructure and subsequently interconnected (hooked-up) with regard to piping, electrical cabling, etc. The modules are supported by a module support frame or MSF. A third possibility is that the superstructure consists of one or more decks with equipment arranged in the form of *packages* or simply installed as individual equipment items in the open air. Deck legs from the top of the substructure support the module support frame or the deck(s); the deck legs are nearly always vertical and may or may not be braced to provide lateral stiffness.

The choice of an enclosed or an open deck configuration is made with a view to the prevailing weather and its impact on working conditions on board, and the potential risks associated with the accumulation of gas mixtures. Open decks provide adequate natural ventilation to avoid the formation of an explosive atmosphere in case of any leaks. In enclosed spaces forced ventilation will need to be provided.

The selection of the type of superstructure depends on many circumstances such as the time available for design and construction, lead times and scheduling of equipment deliveries, onshore fabrication facilities and offshore lifting equipment in the area, and the like. However, generally speaking experience has clearly shown that minimising offshore work (e.g. reducing the number of lifts to be made, reducing hook-up and commissioning offshore) is advantageous from both cost and safety points of view. Therefore, modern platforms often have either integrated decks or modules.

The detailed functional requirements for an offshore installation may differ from case to case but can be summarised in the following two basic requirements that must be satisfied during the entire service life of, typically, some 20 to 30 years:
- to provide space and load carrying capacity above water for all functions and services that are needed to let the installation perform its function;
- to provide structural support for wells, risers, caissons, sumps and other pipework between the sea floor and the superstructure.

The structural support is provided by the substructure, but the requirement has an important impact on the design of the superstructure (also called topside design) due to its influence on the topside layout. This is an area where the design of the two parts of the structure clearly interact. Important pipework should be positioned such that it can be easily connected to the framework lower down and can be adequately protected, especially in the vulnerable area around the still waterline. An attractive location for such pipework is, for example, close to and on the innerside of the legs. On deck, pipe runs should be as straight and short as possible.

The superstructure is in fact a factory in a remote and inhospitable location; it needs to be as self-contained as practically possible. The size of the factory may range from small to very large. The nature and amount of space, as well as the load carrying capacity required depend entirely on the function of the platform. For example, provisions may need to be made for the installation of drilling equipment; mud tanks, pipe storage, etc.; gas-lift of wells that do not sufficiently flow under the natural reservoir pressure; oil and gas treatment facilities; water or gas (re-)injection equipment to maintain reservoir pressure; gas compressors for pipeline export; a boom for emergency gas flaring. These are only examples - the specifics need to be determined on a case by case basis. In addition to these function dependent provisions there are a number of ancillary requirements and general services that are usually needed, such as:
- Power generation with its associated equipment (e.g. engines, turbines, generators) and storage for the fuel they consume.
- General facilities to load, unload and store supplies on board (e.g. deck cranes, tanks, store rooms).
- Maintenance facilities for the equipment on board (e.g. access ways, spare parts storage, workshop) and for the structure itself above and below water (e.g. a remotely operated vehicle or ROV, sometimes a diving bell).
- Living quarters, including cabins, washrooms, kitchen, mess room, laundry, recreation facilities, sick bay, etc.
- Personnel access by boat (boat landing) or helicopter (helicopter deck), with the associated platforms, stairs and other facilities.
- Communications (radio, telephone) with shore base, ships, helicopters and other platforms, as well as an on board communication system; in some cases communications need to include remote control of the whole process from some other point.
- Heating and ventilation for living quarters and working areas.
- Safety systems, such as fire detection and fire fighting, smoke and gas detection, life saving appliances, evacuation systems.

5.3.4 Design of the foundation

Types of foundation

Two types of foundation may be distinguished, i.e. deep piled foundations and shallow bearing foundations. The latter type is also called gravity foundations, because the stability of the platform is derived from the weight of the structure. Steel structures are almost without exception piled while concrete structures have a bearing foundation; see also Annex B.

In the mid 1980s an intermediate form of foundation has been developed for concrete gravity structures. The base of these structures is usually provided with skirts of a certain height that penetrate the seabed to mobilise lower and more competent soil layers, thus contributing to both sliding and bearing resistance. Norwegian concrete structures of the Condeep type have a caisson that consists of circular cells and the skirts underneath the base are thus also circular. By extending these skirts in height large diameter compartments with concrete walls, open at the bottom, are formed underneath the platform; these compartments have H/D ratios typically ranging from about 0.5 to 3. The behaviour of these so-called skirt pile foundations (designated SP) is a bit of an intermediate between shallow bearing and ‘deep’ pile foundations. They have been successfully applied to several concrete structures, especially on softer soils.

For steel structures the principle of the suction anchor has recently been suggested as an alternative to piles. The corners of a space frame structure are then equipped with large diameter cans or ‘buckets’ that are open at the bottom and are forced into the seabed by a combination of the weight of the structure and differential hydrostatic pressure on the top of the cans. These ‘suction cans’ are a similar intermediate form of bearing and pile foundation, like the skirt pile foundation referred to above. Statoil has installed the first steel structure using this foundation concept in the Norwegian sector of the North Sea in the summer of 1994.

General foundation considerations

Wells penetrate the earth underneath a structure to depths of several thousand metres below the seabed. Hence they pass through the same soils on which the structure is founded. Drilling in an open hole may easily cause failure (fracturing) of the formation (due to hydraulic pressure differences arising from the weight of the mud column inside and the hydrostatic pressure outside the hole) or a wash-out of granular material. This is one reason why the drilling through the upper soil layers takes place through a protective conduit, the conductor. In case of any uncertainty the conductor is driven to a depth well below the penetration of the foundation piles, so that a drilling mishap will not affect the foundation layers. Only when one is confident that the soil conditions and the drilling process will not present any hazard to the foundation will it be considered to set the conductors at a reduced depth above the tips of the piles. This obviously provides a cost reduction due to savings in material and installation time. In case of a gravity foundation the conductors are similarly driven to a depth which is beyond the depth where soil layers are still important with regard to foundation behaviour.

Pile foundations

For the present discussion we will assume that the steel structure has a conventional pile foundation. Nearly without exception offshore piles are open ended, steel tubular piles that are driven into the ground by a hammer. However, despite this observation there are different kinds of piles, see figure 5.3-3 from reference [5.3-2]. In some cases driving may be facilitated by first drilling an undersized hole. In very hard or difficult soils (e.g. calcareous

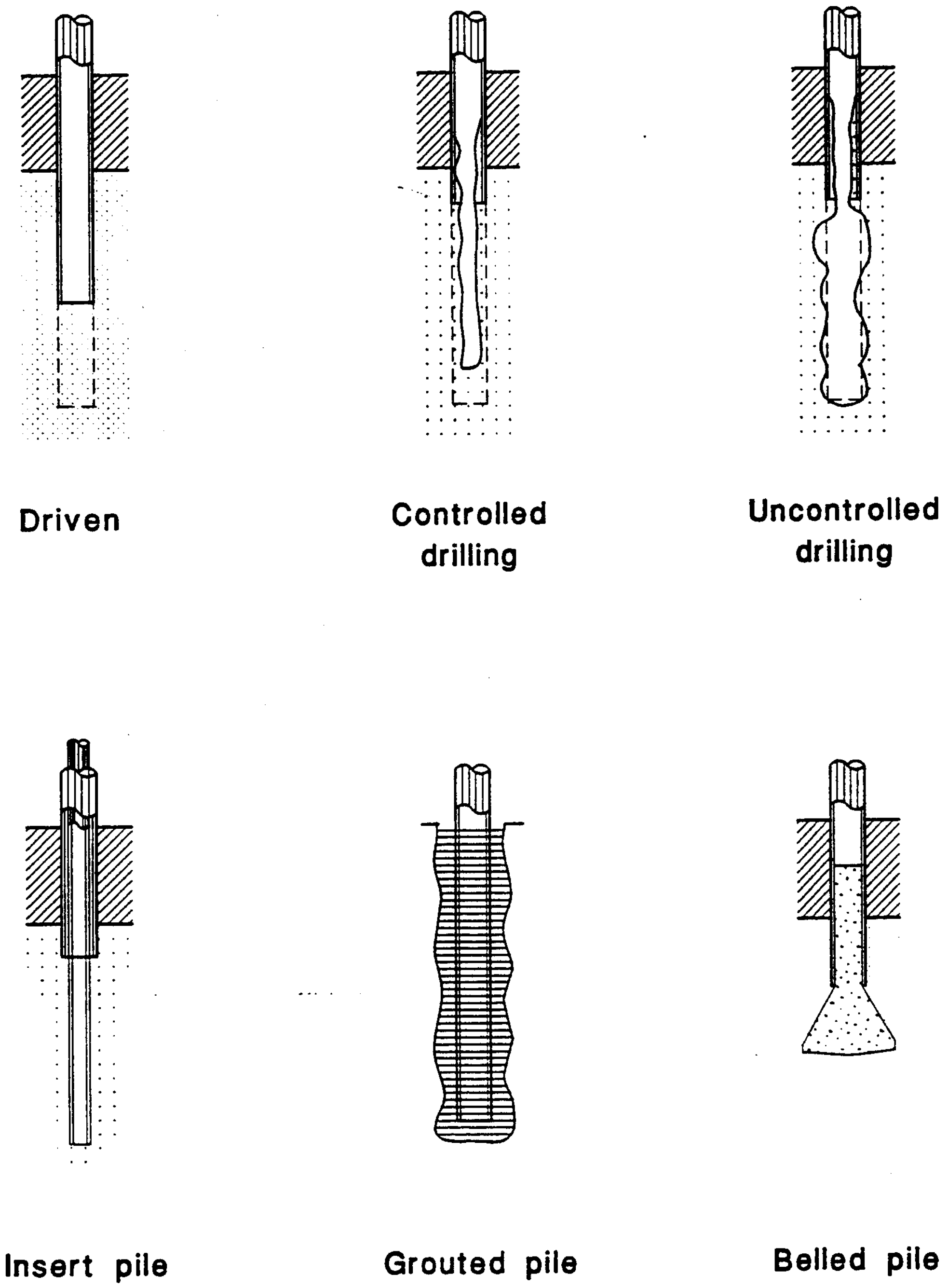

Figure 5.3-3. Different kinds of piles (from [5.3-2])

material) the piles may be installed in a pre-drilled oversized hole and grouted into place; such piles are called drilled and grouted piles. Piles may also be built up in stages: a first stage pile extended by a second stage pile of smaller diameter. These so-called insert piles may be driven or drilled and grouted. A special type of pile is the belled pile (figure 5.3-3), which provides axial support by large-scale end bearing. In this handbook only some elementary observations on pile foundations will be made. For more detailed discussions of soil mechanics and foundation design issues reference is made to various textbooks, such as [5.3-3] to [5.3-6], and an extensive body of special literature on those subjects.

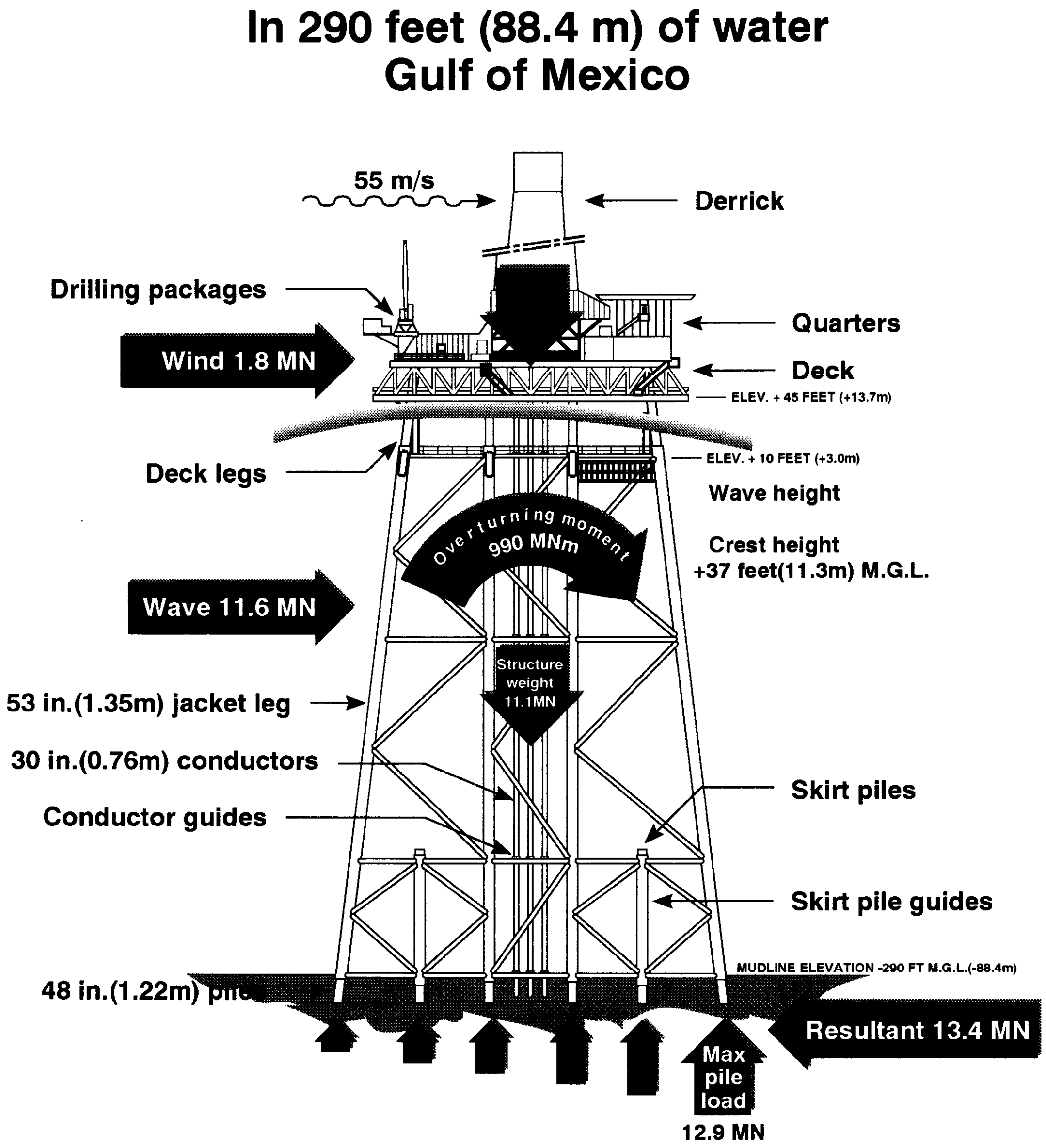

Figure 5.3-4. Example of a jacket structure with leg piles and skirt piles

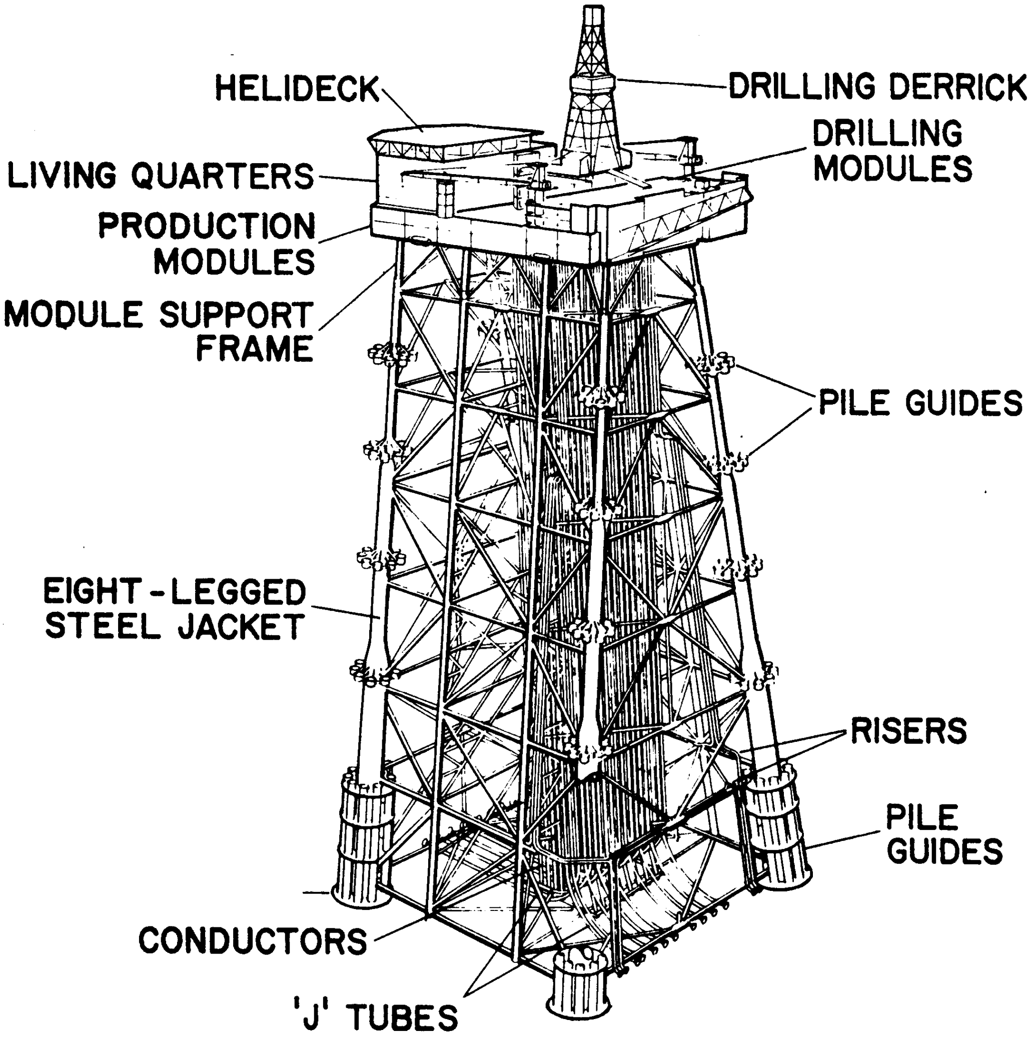

Figure 5.3-5. Example of a tower structure with cluster piles

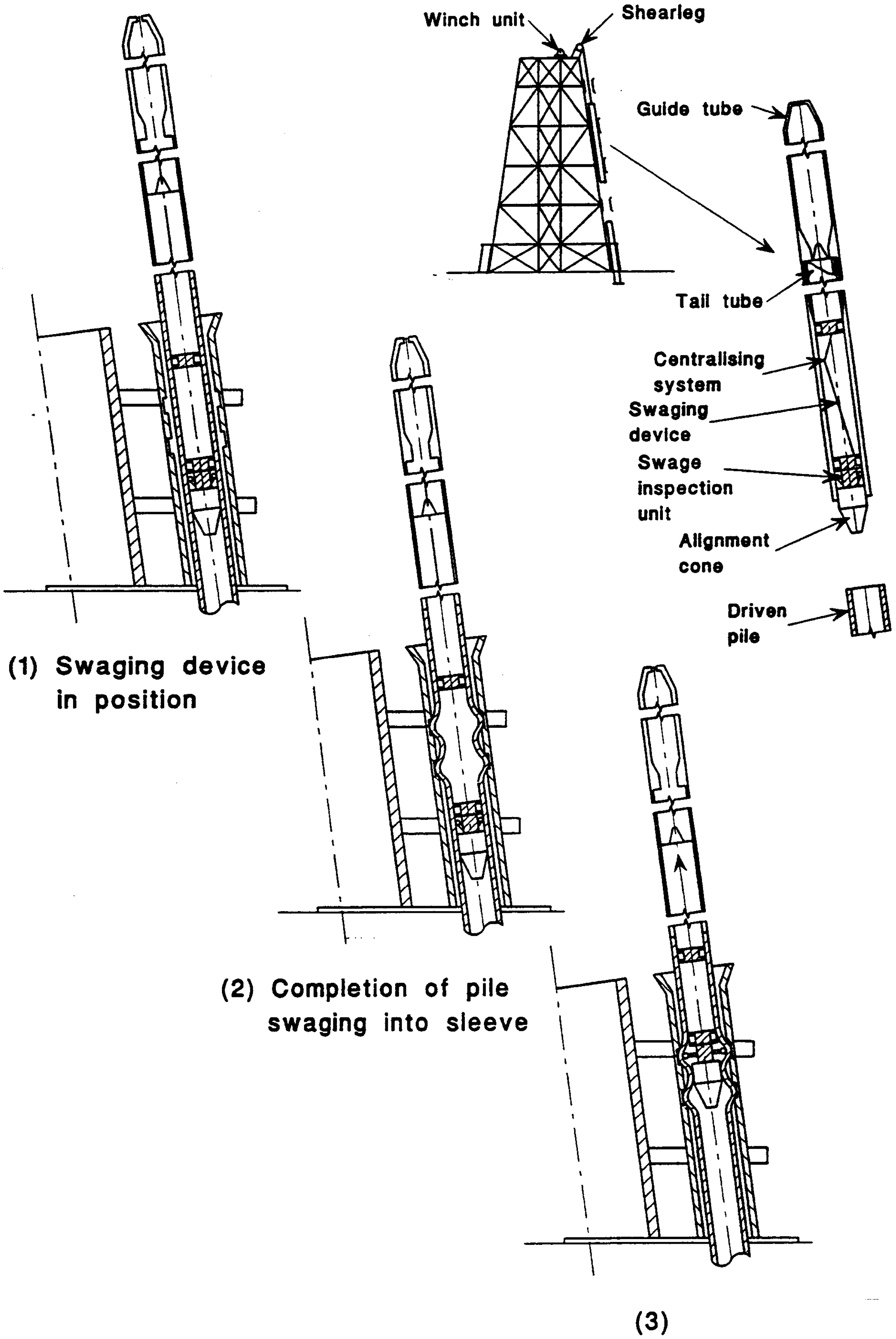

(1) Swaging device in position

(2) Completion of pile swaging into sleeve

(3)

Figure 5.3-6. Hydralock system (from [5.3-2])

The advantages of piles are rather obvious:
- their number, diameter, wall thickness, penetration depth and disposition can be varied within wide ranges to suit circumstances; therefore they have an inherent flexibility for adjustment to the specific requirements of each particular case;
- they can take up compressive as well as tensile loads.

The configuration of a space frame lends itself particularly well to being supported in a limited number of discrete points. The foundation and the substructure strongly interact with one another. It is therefore very important to make a realistic first estimate of the required foundation configuration, so that the design of the structure can (literally) proceed from a sound base. Failing to do so may result in several laborious and time-consuming iterations or end up in a far from optimal design.

Piles can be installed through the legs of the structure. In this pile-through-leg type the connection between the piles and the structure is usually made at the top of the legs by inserting steel wedges in the annulus between pile and leg and welding the assembly of pile-wedges-leg solidly together. This is the traditional method. Instead of using wedges at the top, some companies prefer to grout the annulus between pile and leg over the full length of the leg, thus creating a composite member. In any event, in these cases the structure's legs serve to guide the piles down through the water to the sea floor during installation, after which they are driven into the ground using an above water hammer. The piles pass as it were through the legs as arms through the sleeves of a jacket, from which the name *jacket* for this type of steel structure has been derived. An alternative name is a *template* structure, because the structure serves as a template for pile installation.

If more piles are required than the number of legs, these may be added as skirt piles around the perimeter of the structure in between the legs. They are inserted through partial sleeves extending over the bottom bay of the structure only; see figure 5.3-4. Alternatively, in case of more piles than legs these may be clustered around the legs as shown in figure 5.3-5. The piles are then guided down during their installation by pile guides at regular intervals along the leg as also shown in figure 5.3-5. These pile guides are purely an installation aid but they do attract additional wave loads and are therefore sometimes cut off after installation. At the base of the structure there are partial sleeves around the legs, similar to the case of skirt piles. The connection between the skirt piles or cluster piles and the structure is now made under water, usually by grouting the annulus between the piles and the partial sleeves. An alternative to grouting is a metal-to-metal connection by a mechanical locking system; see figure 5.3-6 from [5.3-2]. This connection is made by expanding the pile wall by hydraulic pressure into machined grooves in the sleeves at two or three elevations. These mechanical connections are known under the trade name Hydra-Lok® and are increasingly used. The connection is quick and relatively cheap. Furthermore, and in contrast with grouted connections that take time for the grout to set and the bond between pile and sleeve to develop, the Hydra-Lok® connection provides immediate strength. The type of steel structure supported by cluster piles is called a *tower* structure. As a result of the different support points for the space frame, i.e. at the top for a jacket and at the base for a tower, the structural behaviour of a jacket and a tower is markedly different, as will be discussed in chapter 6. The definitions of a jacket structure and a tower structure that are proposed for the new ISO design standard [5.3-7] under development are given in Annex C to this chapter.

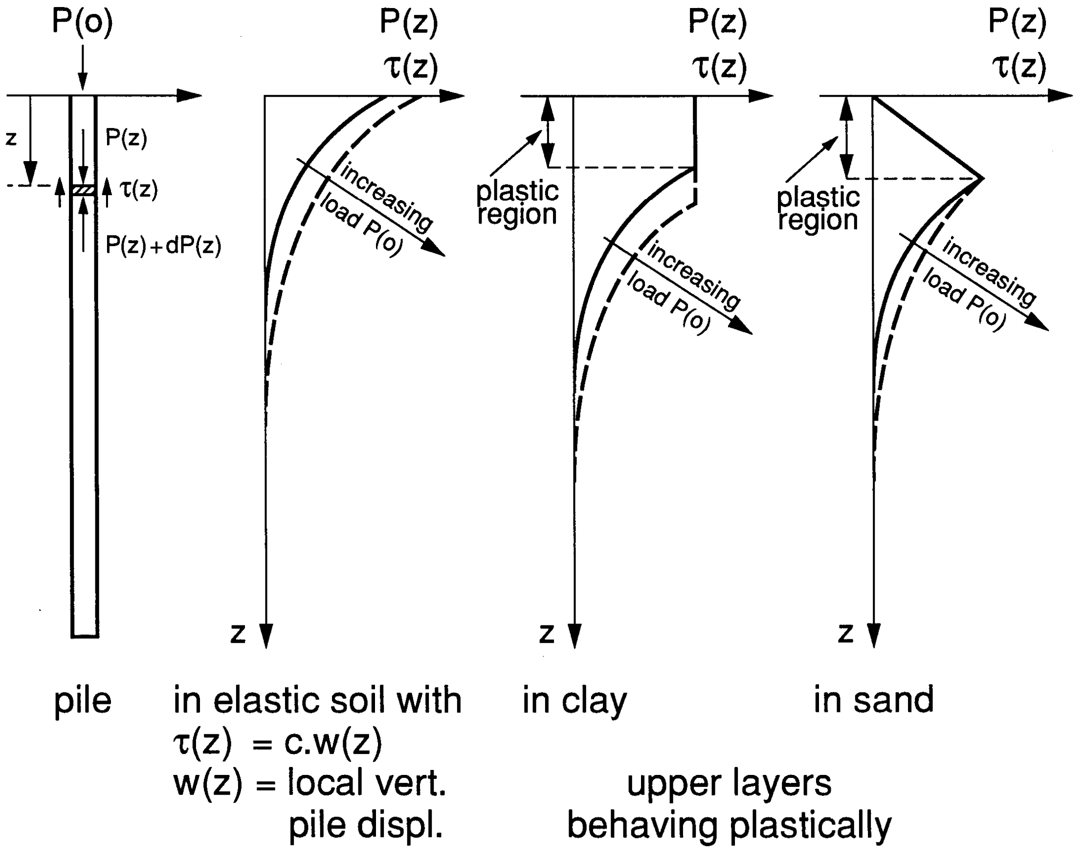

Figure 5.3-7. Pile behaviour under axial loading

A small angle with the vertical of legs and piles of a space frame structure has a very favourable effect, both on the transmission of horizontal loading on the structure through the bracing members of the frame and on the lateral pile forces; this will also be discussed further in chapter 6. Therefore, in most cases the piles and the legs are inclined; this is called “battered” (US terminology) or also “raked” (UK terminology). Typical batter angles within the plane of the (inclined) frame are $1{:}10$. Corner legs and piles are mostly battered in two directions, making the real batter $\sqrt{2}{:}10$ or $1{:}7.07$. A slope of $1{:}6$ is generally considered a practical limit for pile installation. This is due to the bending stresses in the pile during installation that are caused by the eccentric weight of the hammer on top of the free-standing upper part of the pile or add-on, as well as to the lack of effectiveness of the hammer blows.

Vertical piles are certainly possible and are indeed regularly used. For tower structures their main advantage is easier installation and hence reduced pile installation costs. Furthermore, when using a hydraulic under water hammer in combination with vertical piles the pile guides can be eliminated with an associated weight and even more cost reduction. Due to the absence of batter the lateral loading per pile will, however, be greater. This will tend to result in greater wall thicknesses in the upper part of the piles, and possibly in greater pile diameters and/or a larger number of piles. This, of course, increases costs. The most effective and cheapest alternative depends on many factors and needs to be decided on a case by case basis.

Another advantage of leg batter (which as discussed above is not necessarily accompanied by pile batter) is that the *base* dimensions of the structure are appreciably larger than at the top. This is beneficial in two respects. Firstly, it enhances the stability of the structure on bottom against wave attack in the unpiled condition during the early installation phase. During this stage stability is purely derived from the submerged weight of the structure and severe wave action under a summer storm could topple the structure before the piles are installed. Secondly, it enlarges the moment arm of the vertical reaction forces and consequently reduces the axial forces in the piles, which will reduce the required pile penetration. The *top* dimensions of the structure are generally kept as small as practically possible with a view to hydrodynamic loading considerations. Hydrodynamic loads are largest near the free water surface and the smallest possible exposed area and volume (but especially area) will result in the smallest lateral loading and overturning moment.

We will further refer to a pile as that portion that is surrounded by soil below the sea floor. Regardless of the difference between a jacket and a tower, a pile is then subjected at its top to the same axial and lateral loads by the structure that it supports. The axial load is due to the structure's functional loading, its (submerged) self weight and the overturning moment due to environmental loads. It has a constant compressive and a time varying component, which alternates between compression and tension. The lateral load is due to the environmental loading and may also have a small constant part due to current and wind, but is in the main always time varying. Load transfer from the pile to the soil is a complex process that will not be dealt with in any detail in this handbook.

Another important aspect of foundation design is to ensure that the piles can actually be driven down to the design penetration by the pile driving hammers available. During driving the piles can be "plugged" or "unplugged", i.e. the soil plug within the pile can move down with the pile or the plug can stay behind when the hollow steel pile advances. At final penetration this manifests itself in a possible difference between the soil level within the pile and the surrounding sea floor. Furthermore, during pile driving the stresses in the piles as well as the loads on or vibrations of the substructure should remain within acceptable limits to avoid damage during driving. To verify these aspects pile driveability analyses are normally performed as well.

Axial pile behaviour

An axially loaded pile gradually transfers its load along its length to the ground by *friction* between the outer surface of the pile and the soil. Any remaining load at the pile tip will be transferred by end bearing. The steel pile itself will deform elastically, while the soil deformation will depend on the type of soil (e.g. clay or sand) and the properties of the soil layers through which the pile passes. In virtually all cases the soil layers will deform partially elastically and partially plastically. The axial force in the pile $P(z)$ as well as the shear force transfer to the soil $\pi D \cdot \tau(z) \cdot dz$ will tend to decrease with depth z; see figure 5.3-7. With increasing load at the top an increasing part of the pile length will be mobilised. Below the depth at which the whole force has been transferred the pile and the soil layers will remain unloaded.

The process of axial load transfer is essentially that of an elastic spring (the steel pile), supported axially by a number of soil springs along its length. The process can be illustrated as follows (see figure 5.3-8). Imagine that the pile is discretised into a number of small elements, each of length ℓ. The elements themselves are considered to be undeformable while they are connected by discrete axial springs, the stiffness of which reflects the elastic axial stiffness of the steel pile elements, i.e. $k_t = EA/\ell$. Each element is further supported by an axial soil spring. The soil springs have different stiffnesses with depth below the sea floor. The steel springs act in series (the pile is one continuous beam), while the soil springs are assumed to act all individually. At each element, the combination of a steel and a soil spring forms a set of springs in parallel.

Load transfer from the pile to the soil will occur in relation to the various stiffnesses. The elastic stiffness of the steel pile is usually much greater than the elastic stiffness of the soil layers, but it is not infinitely large. Infinite stiffness would imply that the pile would displace as a rigid body and that all soil layers would experience the same pile displacement w. As this is not the case there is a clear interaction between pile and soil behaviour, with the local pile displacement $w(z)$ being dependent on depth; load transfer thus takes place gradually. Furthermore, the upper soil layers will often be strained beyond their elastic range in which case the soil springs have distinctly non-linear $t-z$ characteristics; this is also illustrated in figure 5.3-8. Typical behaviour of a pile under axial loading is illustrated in figure 5.3-7. The local vertical displacement of the pile and the shear stress along the pile wall both decrease exponentially with depth, but the shear stress near the top of the pile is modified in accordance with the plastic behaviour of the soil in that region.

The maximum bearing capacity of a pile will be the integral of the friction forces along its outer surface over the full pile length, plus any end bearing force at the pile tip. The end bearing acting on the steel rim can in principle be relied upon. However, the end bearing on the core within the pile will only be effective if the soil plug inside the pile can sustain the point force on its end. Otherwise the soil plug will slip along the inside of the pile wall and the point force cannot be fully mobilised. To ensure that end bearing can be counted on over the entire end surface of the pile, characterised by the outside pile diameter, the soil plug inside the pile may be wholly or partially removed after driving and replaced by a grout plug of sufficient strength.

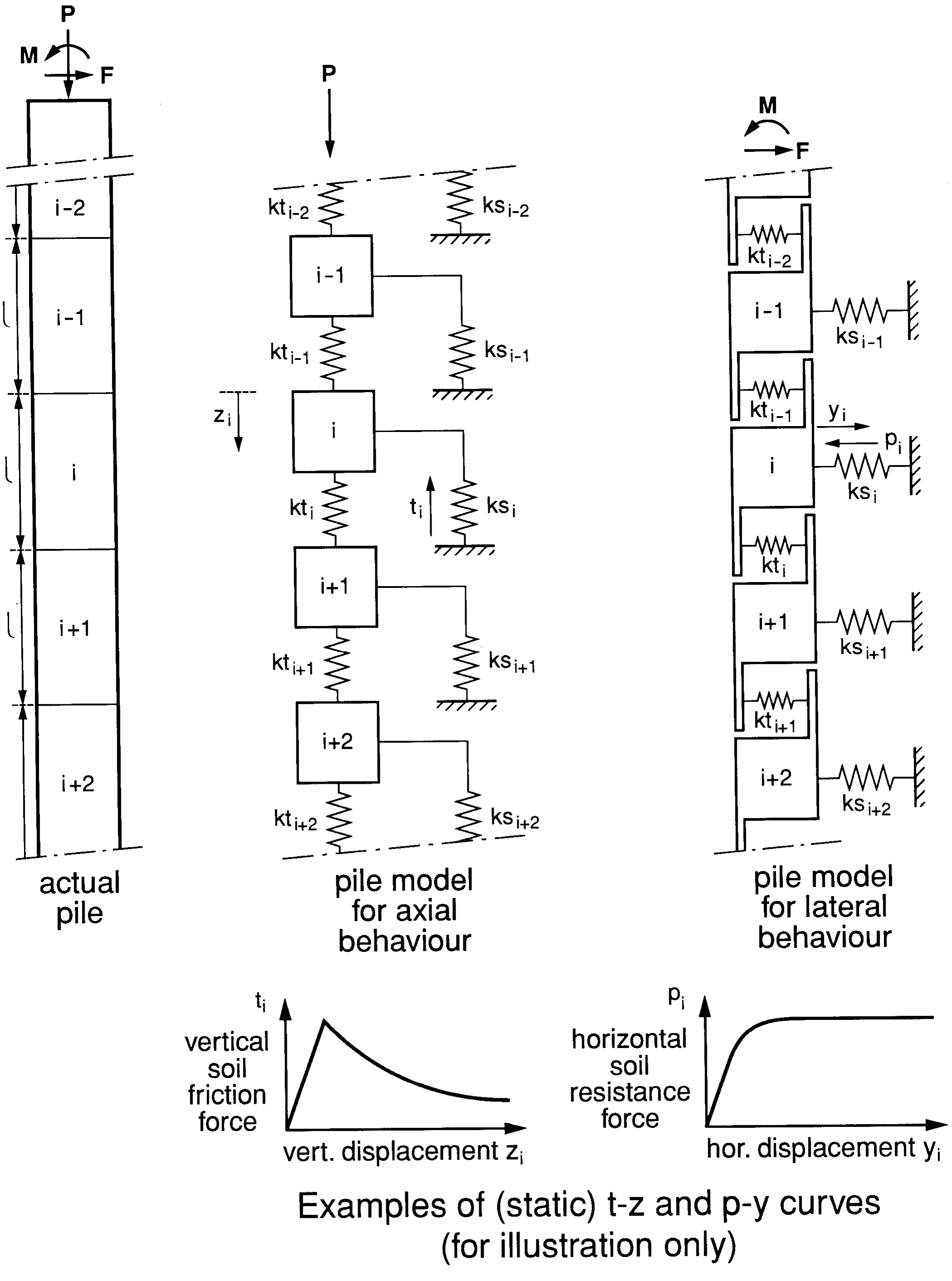

Figure 5.3-8. Conceptual models of axial and lateral pile behaviour

The contribution of *end bearing* to the total pile capacity will obviously depend on the relative characteristics of the frictional springs along the pile length and the end bearing spring at the pile tip, in combination with the local pile displacements experienced. The stiffness of the end bearing spring is often (considerably) less than those of the frictional springs, while furthermore the local pile displacement is smallest at the pile tip. Therefore, end bearing will only be generated after all available friction capacity has been mobilised and the pile has undergone some appreciable displacement. This does, incidentally, not necessarily mean that the overall contribution of end bearing to the total pile bearing capacity is always small.

Apart form the weight of the (submerged) pile itself and, possibly, the weight of the soil column within the pile, the *tension capacity* of a pile is determined by friction along the outer surface of the pile wall only. As friction coefficients for tension are often conservatively assumed to be smaller than friction coefficients for compression, a pile's tension capacity is invariably smaller than its bearing capacity.

Lateral pile behaviour
A laterally loaded pile is similarly an elastic steel beam supported by a number of lateral soil springs along its length. To illustrate the lateral force transfer an analogous discretisation as for axial pile behaviour is used; see figure 5.3-8. The pile is again divided into a number of small and undeformable elements. The elements are now connected by discrete lateral springs reflecting the bending and shear stiffness of the pile. Each element is further supported by a lateral soil spring. These soil springs will generally have non-linear $p-y$ characteristics that will as a rule be strongly influenced by cyclic loading of the soil, laterally much more so than axially. As for axial behaviour, the pile is one continuous beam and therefore the steel springs all act in series while the soil springs act individually. For each element, the combination of a steel and a soil spring again forms a set of parallel springs.

As for axial behaviour, the elastic stiffness of the steel pile is normally (much) greater than the stiffness of the lateral soil springs, but it is not infinitely large and the pile will thus deform. In case of an infinitely stiff pile it would translate and/or rotate in the soil while remaining straight, which is not the case. Hence, laterally there is also a clear interaction between pile and soil behaviour.

The pile is loaded by a horizontal (point) load at its top, while top rotation is prevented by the pile being grouted in the pile sleeve (or top rotation is at least limited by the pile being enclosed by the leg through which it passes). This boundary condition clearly necessitates a moment at the top of the pile and the pile thus deforms in an S-shaped pattern. The pile displacement, soil reaction and internal pile moment along the length of the pile are illustrated in figure 5.3-9 taken from [5.3-8]. As can be seen, the pile has a few points of inflection where the internal moment is zero. In between the first and the second points of inflection there is a point where the pile displacement remains zero. Over some distance below this point the pile displaces against the direction of the external load. However, displacements and rotations have become very small here and it could be assumed that the pile is basically clamped somewhere between the first and the second point of zero displacement. In figure 5.3-9 this is at a depth of approximately 15 m or $10D$ below mudline. Alternatively, we may only be interested in representing the behaviour of the pile head, which forms the boundary condition for the structure. We may then also model the pile by an equivalent member that is hinged at a depth somewhere between the first points of inflection and zero displacement. In

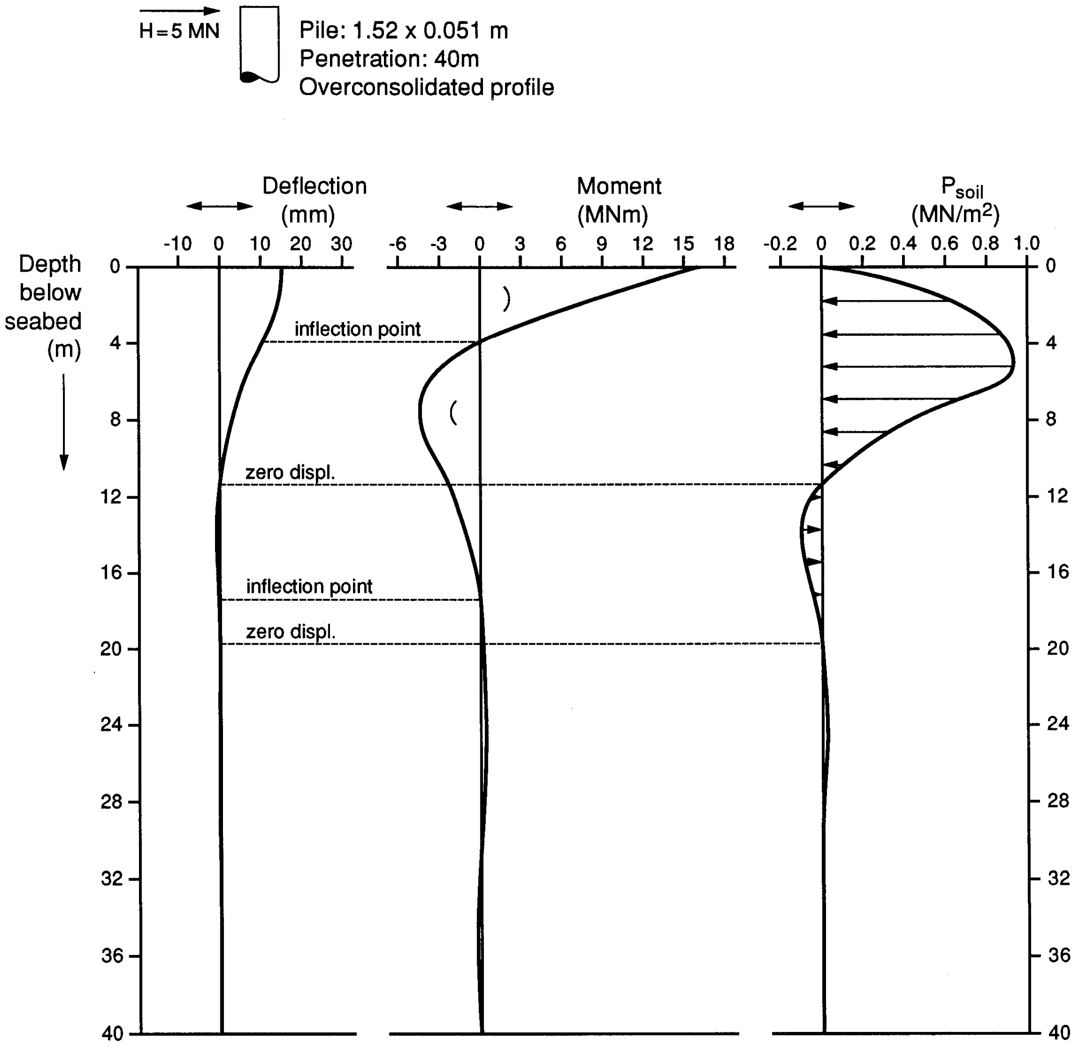

Figure 5.3-9. Pile behaviour under lateral loading (deflections, pile moments and soil resistances), (from [5.3-8])

figure 5.3-9 this would be at depth of approximately 8 m or some $5D$ below mudline. Refer also to the section *on structure-foundation interaction* below.

As the pile is simultaneously loaded axially by a (very) large load there are additional, secondary bending moments generated in the cross sections of the pile, which are equal to the axial force times the differential displacement between the cross section considered and the top of the pile. The pile therefore behaves as a beam column rather than as a pure beam.

Another factor to be taken into account is the possibility of sea floor erosion or *scour* around the piles, in particular in granular soils such as sand. This causes a local depression of the sea floor and hence a certain distance over which the pile is laterally unsupported. This obviously has an influence on the stresses in the pile. During pile design a scour depth of one to two pile diameters is usually assumed, where appropriate.

Structure-foundation interaction

Deck, substructure and foundation piles form in fact one integral structural system. However, to facilitate design and analysis it is often desirable to divide the overall system into three separate sub-systems. One reason for this is that finite element programs for structural analysis are normally linear, while the pile-soil interaction problem definitely requires a non-linear program. To enable the structure to be analysed by means of a linear program, the structure must be supported in a linearised manner that reflects the real non-linear interaction between the structure and the foundation in the equilibrium condition as well as possible. There are several ways in which a linear structural support can be modelled. Conceptually the simplest is probably to replace the actual pile by a hypothetical member with equivalent properties. This member may be clamped or hinged at some depth below the sea floor, as noted above. The structural properties of such a member will obviously vary with the end condition assumed. In its most general form the support of the structure can be represented by a set of springs: a vertical (axial) spring, two horizontal (lateral) springs and two rotational springs about horizontal axes (axes perpendicular to the pile); the torsional spring about the member's own axis is normally neglected. The separate structural and foundation analyses must then produce the same loads and deformations at the intersection between the structure and the piles, which usually requires a few iterations by adjusting the spring coefficients. Modern computer software for offshore applications often incorporates both a linear structural analysis module and a non-linear pile analysis module, and performs the solution iteratively within the program without any user intervention. This is, of course, very efficient but removes the critical steps in the process from user observation and intervention, which unfortunately does not enhance understanding and learning.

The loads on and the associated deformation pattern of the pile in the ground may be described by considering pile behaviour as a summation of two separate cases in which only one of the two deformations at the top is permitted in each case. Firstly, the pile is allowed to displace freely, while being restrained from rotation at the top, when subjected to a horizontal load. This is referred to as the fixed head problem. The non-linear relationship between the imposed horizontal load, the resulting displacement and the moment required at the top of the pile to prevent it from rotating is shown in the left hand part of figure 5.3-10. Secondly, the pile is allowed to rotate freely, while being restrained from any displacement at the top, when subjected to a moment. This is referred to as the relaxation problem; in this case relaxation around a zero displacement of the pile head. Under these conditions there will analogously be a horizontal force required at the top of the pile to keep it from also displacing horizontally.

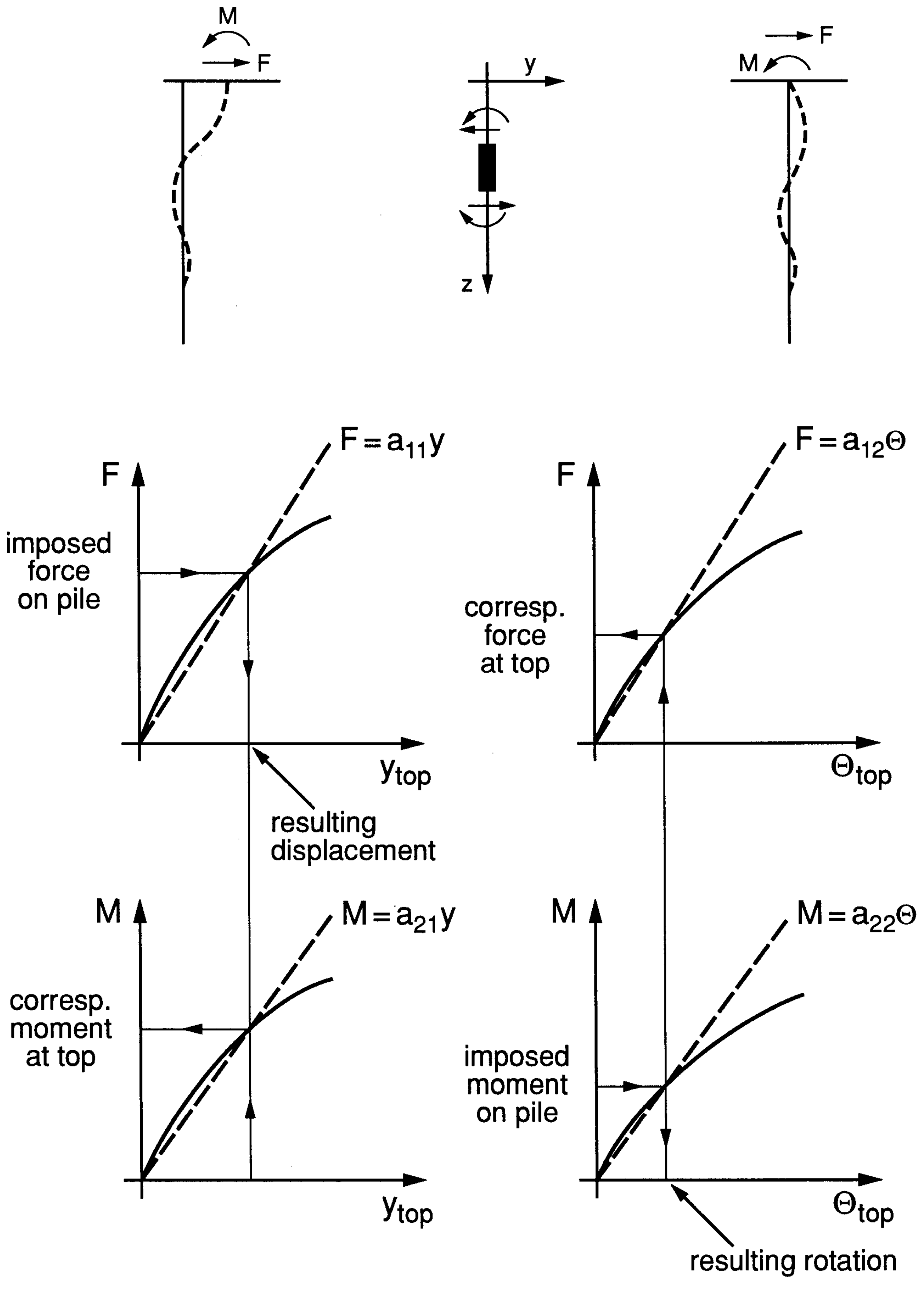

Figure 5.3-10. Non-linear foundation springs

For this second loading condition the relationship between the imposed moment, the resulting rotation and the force required at the top of the pile is similarly shown in the right hand part of figure 5.3-10.

When the pile head under externally applied loading is displaced over a distance y and experiences a rotation θ, the total force and total moment at the top of the pile, which are the resultant of the soil reactions on the pile, are as depicted in figure 5.3-10 for a two-dimensional case:

$$\begin{aligned} F(y,\theta) &= F_1(y,0) + F_2(y,\theta) \\ M(y,\theta) &= M_1(y,0) + M_2(y,\theta) \end{aligned} \tag{5.3-1}$$

In an index notation for the general three-dimensional case, with $i = 1,2$ indicating horizontal directions and $i = 3$ the vertical direction, this may be written as:

$$R_i = \sum_j k_{ij} \cdot x_j \tag{5.3-2}$$

where for the pile top at the sea floor:

$R_{1,2}$ = horizontal force
R_3 = vertical force
$R_{4,5}$ = moment about a horizontal axis
R_6 = torsional moment
k_{ij} = spring constants
$x_{1,2}$ = horizontal displacement
x_3 = vertical displacement
$x_{4,5}$ = top rotation
x_6 = torsion

The linear spring matrix k_{ij} is of the form:

$$k_{ij} = \begin{bmatrix} k_{11} & 0 & 0 & 0 & k_{15} & 0 \\ 0 & k_{22} & 0 & k_{24} & 0 & 0 \\ 0 & 0 & k_{33} & 0 & 0 & 0 \\ 0 & k_{42} & 0 & k_{44} & 0 & 0 \\ k_{51} & 0 & 0 & 0 & k_{55} & 0 \\ 0 & 0 & 0 & 0 & 0 & 0 \end{bmatrix} \tag{5.3-3}$$

For reasons of linearity the coefficients $k_{15} = k_{51}$ and $k_{24} = k_{42}$ must be mutually equal, while due to sign conventions these two pairs have opposite signs. As the loading of the pile in the two orthogonal directions is usually not the same, the corresponding linearised spring constants will in general not be equal either: $k_{11} \neq k_{22}$ and $k_{44} \neq k_{55}$.

5.3.5 Design of the substructure

General considerations

The main dimensions of the substructure are determined by:
- the plan dimensions at the top of the structure in view of deck size and deck support requirements
- the plan dimensions at the base of the structure in view of foundation requirements
- the waterdepth (a site dependent parameter)
- the elevation of the top horizontal framing level above the still waterline.

Important additional aspects for global structural design are:
- the number and position of the legs
- the number and disposition of the foundation piles
- the number and disposition of well conductors
- the number and disposition of other pipework in the water (risers, caissons, sumps)

A fixed steel structure is a *three-dimensional space frame*; the historical development of this now common concept is briefly described in Annex A. The (near) vertical frames are divided into a number of panels by bracings. The braces provide in-plane stiffness to the panel and transfer in-plane lateral forces (shears) from one leg to the other. There are a number of common brace patterns, notably diagonal braces, X-braces and K-braces (see figure 5.3-11). As for all plane frames, the basic idea is to divide the frame into triangles. A triangle is a fixed form and carries in-plane loads predominantly through axial loads in the 3 braces. This is contrary to e.g. a portal or a rectangular frame, which carries loads through significant internal shears and moments in the members (see figure 5.3-12).

Steel must be protected against *corrosion*. Under water this is mostly done through cathodic protection by distributing a large number of sacrificial anodes over the steel surface area. The alternative to provide cathodic protection by an impressed current system is not frequently used. The area around the still waterline is an area that requires special attention. It is particularly sensitive to corrosion attack as the upper water layers are relatively oxygen rich, while corrosion protection is difficult in view of the intermittent wetting of the steel. This area is also most vulnerable to mechanical damage by floating objects or collision with e.g. a supply boat. The parts of the substructure which are in the splash zone as well as the above water parts are normally protected by painting or some other coating. Structural members in this region may also be given a corrosion allowance in the form of several millimetres extra wall thickness, which may be consumed by corrosion during the service life.

Steel surfaces under water may further be subject to *biofouling* from a variety of marine organisms, especially in warm climates. As for corrosion, this is most pronounced in the upper water layers due to temperature, oxygen content and light penetration into the water. Marine growth can be distinguished into hard growth and soft growth. Hard growth may easily reach thicknesses of some 0.05 m, while soft growth may be several metres long. Marine growth adds to the fluid loading due to an increase in the drag loads by enlarging the diameter of the members and by making their surface (very) rough; the drag coefficient for a rough member is appreciably larger than for a smooth member. The increased dimensions naturally also increase the inertial part of the wave loads, but this is usually of less significance. Furthermore, marine growth is an obstacle to inspection of the underwater structure for general deterioration due to corrosion and for cracks that may have formed, for

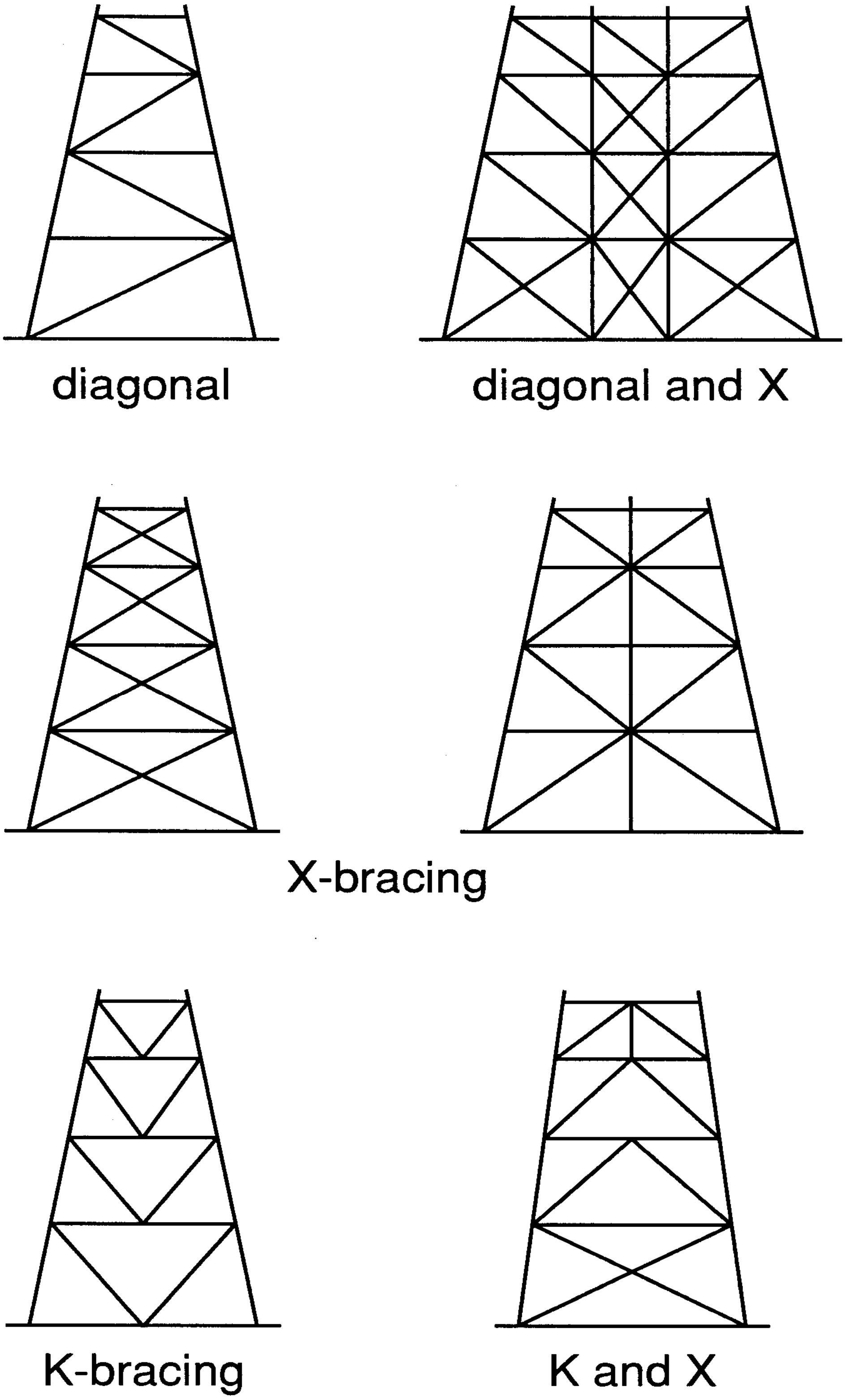

Figure 5.3-11. Some example brace patterns

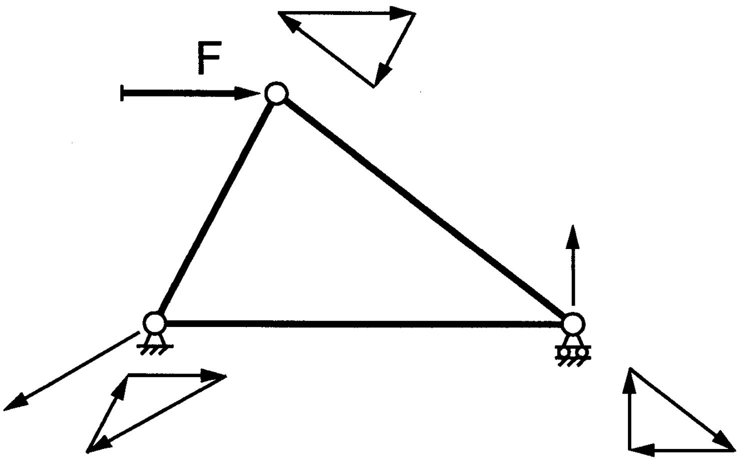

Statically determinate triangular frame
with axial member forces only.

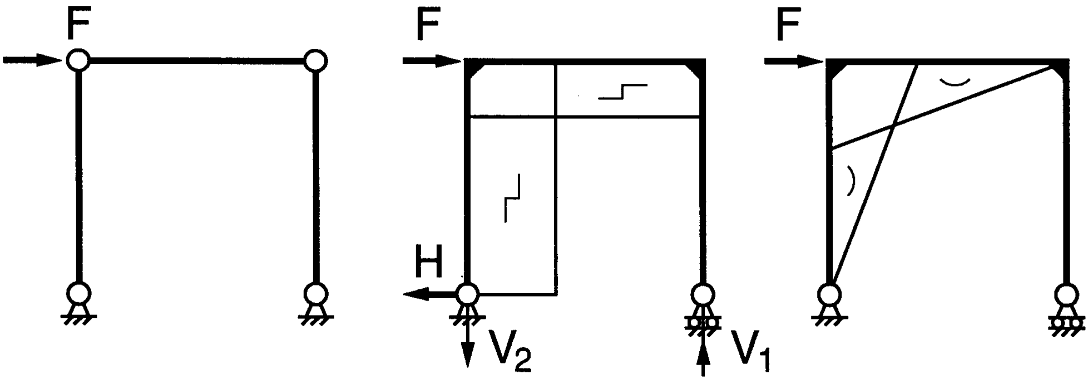

a mechanism!

reactions and
shear forces

moments

Portal frame with members having axial forces,
shear forces and moments.
(N.B. a 4th member to close the frame is unloaded and
does not change the picture)

Figure 5.3-12. Illustration of forces in a triangular, a portal and a rectangular frame

example as a result of fatigue. The welds at the tubular joints are highly stressed and most susceptible to potential fatigue cracking, and hence prime objects for under water inspection. For both these reasons marine growth may be required to be regularly removed.

Wave and current loads were discussed in chapter 4. These loads are large and to minimise them as much as one can the structural configuration is made as transparent as possible, while individual framing members are chosen to have a circular cross section. An additional advantage of tubulars is that they are axisymmetric so that elementary forces and resistances are the same in all directions. Wave loads are largest near the water surface and decrease exponentially with depth. Furthermore, the waves act directly on the structural members in the form of distributed loads, introducing potentially significant bending moments on top of the axial forces from main frame action. Members around the still waterline may also be subject to wave slamming onto both horizontal and vertical members. Additionally, horizontal members above and below the waterline may be intermittently in and out of the water in (high) wave crests or (deep) wave troughs, thereby experiencing variable buoyancy forces that could lead to fatigue. In cold climates members in this area can further be exposed to the forces of floating ice. Below approximately $z = -\frac{1}{2}\lambda$ external loads are only due to currents, which are much smaller than loads due to waves. Therefore, internal forces in the frame below this elevation are basically axial as a result of main frame action. Moment transfer from member to member takes place through the stiff connection of members at the joints.

Waves may approach a structure from any direction, including diametrically opposite directions. The direction of global horizontal loading will change accordingly. However, even for one particular wave direction the load reverses between the passage of the wave crest and the wave trough, albeit that the magnitude of the wave load at these two instances is generally not exactly the same. Therefore, members will always experience both tension and compression loading and cannot be dimensioned on tension only.

Structural responses

Wave loads always vary with time. The loads are not necessarily symmetric with respect to zero due to wave asymmetry and the possible presence of a current. In regular waves, the loads change periodically with the same period as the waves. A natural sea is, however, random and in reality loads therefore also change randomly in time. Wave loads act both horizontally and vertically. For bottom founded structures the horizontal loads are by far the most important, but for example for floating structures the vertical loads are also very significant. The horizontal and vertical loads will broadly be 90 degrees out of phase and are therefore not a maximum at the same time. Horizontal and vertical loads are jointly responsible for the generation of (overturning) moments. For a fixed steel structure the overturning moments are mainly due to the horizontal loads. However, for a fixed concrete structure the vertical loads on the top of the caisson also provide a significant contribution to the overturning moments.

As wave loads vary with time, two special features arise with respect to the design and the behaviour of a structure. The first is the possibility of *material fatigue*, the second is the possibility of *dynamic structural response*. Fatigue is a phenomenon where due to repeated straining of the material small, microscopic cracks may be formed that will grow under continued variable loading and may eventually lead to complete fracture. It is a cumulative effect and hence the potential damage done by stress or strain reversals of all magnitudes and during the entire service life of the structure must be accounted for. Both steel and concrete

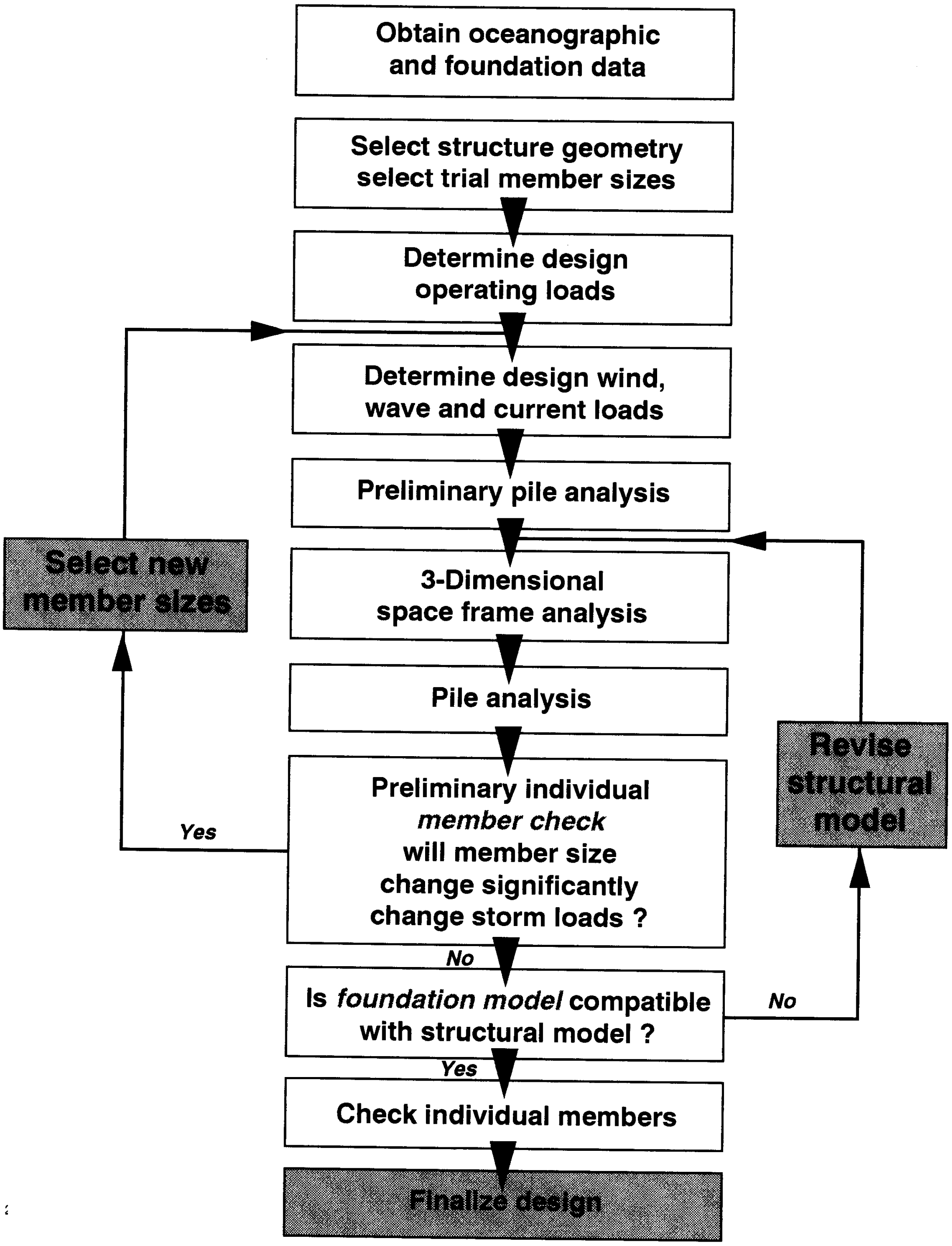
Obtain oceanographic and foundation data
Select structure geometry select trial member sizes
Determine design operating loads
Determine design wind, wave and current loads
Preliminary pile analysis
3-Dimensional space frame analysis
Pile analysis
Preliminary individual member check will member size change significantly change storm loads ?
Yes
Select new member sizes
No
Is foundation model compatible with structural model ?
No
Revise structural model
Yes
Check individual members
Finalize design

Figure 5.3-13. Design procedure for steel structures

are sensitive to fatigue and both types of structure should therefore be designed to be adequately resistant to fatigue. However, as steel is significantly more vulnerable to this phenomenon, fatigue design assumes a more prominent place in the design of steel structures than in the design of concrete structures.

Fixed structures that are dynamically loaded will experience time varying elastic deformations, which will generate mass inertial forces. As long as the mass inertial forces are negligibly small compared to the elastic forces, the deformation of a fixed structure will follow the time varying load in an essentially unmodified manner. That is, at each instant in time the deformation is the same as if the load at that instant was applied statically. The structural deformation will therefore vary with time in the same manner as the load, and the response is a quasi-static structural response. However, when the mass inertial forces increase and become an appreciable fraction of the elastic restoring forces, the deformation of the structure at each point in time will increasingly deviate from the deformation imposed by the loading if it were applied statically. The mass inertial forces must now be included in the analysis and the response of the structure is a truly dynamic structural response. This complicates design by no small amount; it usually significantly increases the required structural strength and aggravates the potential damage done by fatigue. In general, space frame structures with a highest natural period that does not exceed 2.5 to 3.0 s may be assumed to have quasi-static structural response. However, the assessment whether dynamic effects are negligible or must be expressly accounted for should always be made with great care and should be based on sound knowledge and experience. For example, monopod structures do not benefit from load reduction due to spatial separation effects in short waves and dynamic amplification may well be significant for natural periods as low as 1 s.

Member sizing and structural design

Once the main dimensions of the structure have been determined and a basic structural configuration has been selected, the diameters of the bracing members can initially be estimated based on slenderness considerations to avoid member buckling. The hydrodynamic loading on the structure depends on the member diameters and member sizing is therefore an iterative process. This is illustrated in the schematic design procedure shown in figure 5.3-13; member sizing will be further discussed in section 5.4. A similar iteration is required to achieve compatibility between the structural reactions of the foundation and the substructure where these two parts are connected; see section 5.3.4.

Structural calculations of a multi-member three-dimensional space frame subject to spatially distributed hydrodynamic loading and other loads are complicated and are invariably performed by computer using a finite element program. This is a powerful tool, but usually not very helpful in promoting understanding of basic structural behaviour. To that end simple hand calculations are often much more instructive. It goes without saying that such good understanding is essential for proper design. In addition to the design for strength under extreme storm loading in the in-place condition, the structure will need to be checked for fatigue as well as for completely different load conditions during the various construction stages.

As already mentioned, the basic structural pattern of a plane frame is the triangle, with 3 members and 3 joints or nodes. For each additional node there are 2 additional members needed to connect it rigidly to the basic triangle; see figure 5.3-14. Therefore, for a plane frame the minimum number of members is:

$$M_{\min} = 2(N-3)+3 = 2N-3 \tag{5.3-4}$$

where N is the number of nodes. If the nodes are considered to be hinges, the frame is fully statically determinate. For $M > M_{\min}$ there are $R = M - M_{\min}$ extra or redundant members, as a result of which the plane frame becomes statically indeterminate.

For a three-dimensional space frame the basic structural pattern is the tetrahedron with 6 members and 4 nodes. Each additional node now requires 3 additional members to connect it rigidly to the basic tetrahedron; see figure 5.3-14. For a space frame the minimum number of members is therefore

$$M_{\min} = 3(N-4)+6 = 3N-6 \tag{5.3-5}$$

with N again the number of nodes. Any additional members are once more redundant and make the space frame statically indeterminate.

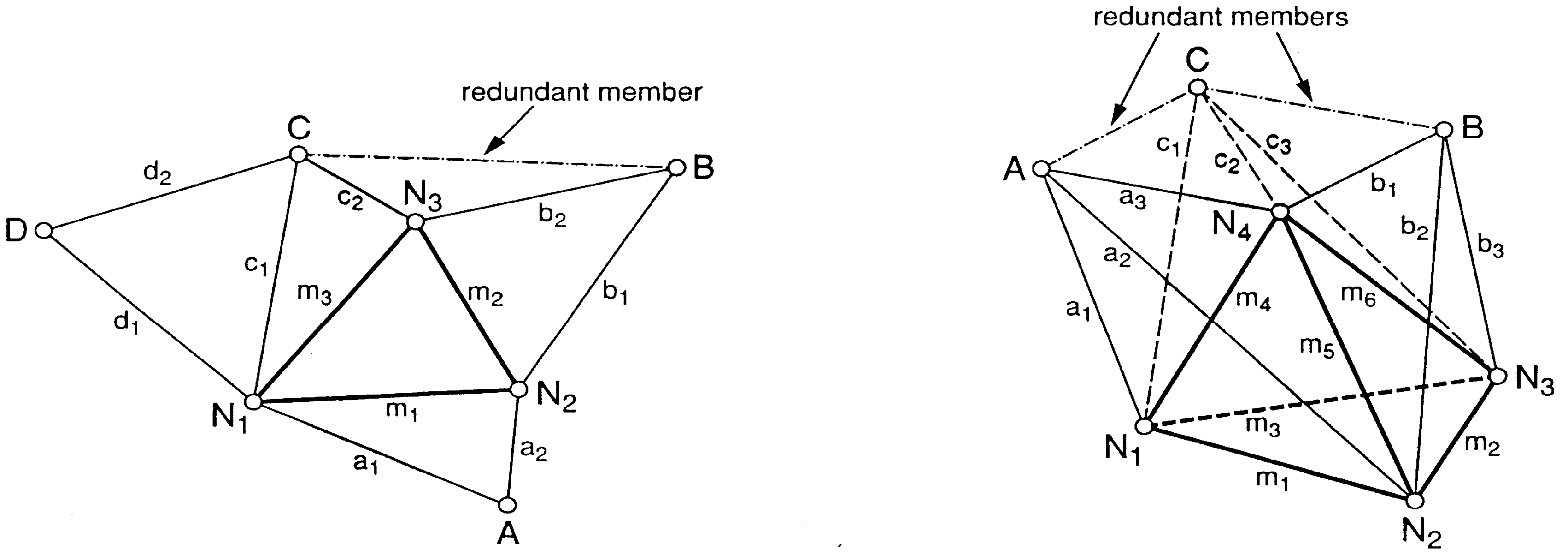

- Original triangle $N_1N_2N_3$ and $m_1m_2m_3$
- Additional nodes A, B, C, D with 2 additional members each

Figure A. Nodes and members for a plane frame built up of elementary triangles

- Basic tetrahedron $N_1 \rightarrow N_4$ and $m_1 \rightarrow m_6$
- Additional nodes A, B, C with 3 additional members each

Figure B. Nodes and members for a space frame built up of elementary tetrahedrons

Figure 5.3-14. Minimum number of members for plane frames and space frames

5.3.6 Design for fabrication, transportation and installation

Offshore structures are pre-fabricated on land, after which they are transported to the offshore site in one piece and installed on location. The overall process may be divided into 8 steps:

- Fabrication onshore (usually lying on its side)
- Load out from the yard onto a barge (occasionally float out from a dock)
- Transportation to the site on a barge (occasionally self-floating)
- Launching or lifting from the barge into the water
- Upending and setting on bottom
- Driving the foundation piles into the sea floor
- Driving the well conductors (if any)
- Installing the deck(s), MSF and modules, or integrated deck

Transportation and installation are in most cases very demanding and very costly operations. Therefore these need to be considered in detail and very carefully, from an early stage in the design. The above pattern of 8 steps is common, but for each individual step there are many variations depending on circumstances, local practices and available equipment. When the platform has been installed, hook-up and commissioning are initiated and only when these are completed the platform is ready for operation.

5.4 Preliminary design of the support structure

Overall configuration and main dimensions
Based on all of the considerations in section 5.3 we may select the support structure to be a jacket or a tower type and determine first estimates of:

- the plan dimensions at the top of the structure, together with the support points for the superstructure;
- the total height of the structure from the sea floor to the top horizontal framing level, and the elevation of the workpoints at the top of the legs (for a tower) or at the top of the piles (for a jacket) on which the deck legs are supported;
- the plan dimensions at the base of the structure, together with the associated configuration of the foundation including the number, size and disposition of the piles.

Leg distances at the top of the structure vary from design to design; typical leg spacings are from 10 to 25 m, but larger distances are by no means excluded. Due to leg batter the distances between the legs increase towards the base of the structure. The diameters of the deck legs are normally chosen to match the diameter of the tower legs or the jacket piles that support them. If the deck legs are smaller in diameter than the tower legs or the jacket piles, conical transition pieces may be used.

The position of the top horizontal framing level of the substructure is chosen such that it will remain above the top of the waves in normal operational weather conditions. This is with a view to fatigue considerations. When the horizontal members are inundated they develop buoyancy forces during the passage of a wave crest that load the frame vertically. During the passage of a wave trough the frame is loaded by its own weight. The fluctuating vertical bending moment resulting therefrom may cause fatigue problems in the frame if this happens too often. Therefore the elevation of the top horizontal framing level is chosen in relation to the severity of the wave environment. In mild areas it may be 3 m above the mean still water level (MSL), in very severe areas it may be as high as 10 m above MSL. For the North Sea common elevations are e.g. 6 m above MSL in the southern North Sea and 8 m above MSL in the northern North Sea. The legs (and the piles, in case of a jacket) extend some 2 to 3 m above the top framing level to allow for the physical length of the top joint can and the shimmed pile-to-leg connection, if the structure is a jacket. This leg/pile cut-off is the elevation that forms the separation between the substructure and the superstructure; it is the workpoint where the vertical deck legs are connected to the inclined legs of the space frame.

First estimates of the foundation requirements are usually based on previous experience. If such experience is not available it becomes a matter of trial and error and iteration until an acceptable foundation has been achieved. For pile-through-leg type structures (jackets) the leg diameter is dictated by the pile size. The internal diameter of the leg should be some 0.06 to 0.08 m larger than the external diameter of the pile to allow for spacer plates in the annulus at the horizontal plan framing levels and clearance between the external pile wall and the inside of the spacer plates. Spacer plates are e.g. 0.025 m (1 inch) in thickness and the required clearance is of the order of 0.010 m to 0.015 m (1/2 inch) on radius. In some cases this leads to leg sizes that are larger than necessary for the space frame to support the topside and to carry the environmental loads. As the legs attract considerable wave loading this is undesirable and selecting a tower structure configuration may then be beneficial.

Panel height and panel framing

The structural functions of the space frame may be summarised as follows:

- transmitting vertical and horizontal loads to the sea floor
- providing stiffness against lateral vibrations
- restricting the buckling length of legs and piles
- providing a template for pile driving.

The three dimensional configuration of the space frame comprises a number of (near) vertical plane frames. The height of the structure is divided into a chosen number of horizontal plan framing levels, a number that is yet to be determined. The panels in a vertical frame are basically of triangular form with bracings approximately under 45° with the horizontal; see section 5.3.5. The choice of a bracing pattern depends on a combination of rational considerations, industry or company tradition and individual designer preferences, the latter often being (consciously or unconsciously) rather influential. The rational considerations include weight and/or cost, redundancy and reserve strength aspects.

Redundancy is a difficult and ill-defined concept, but is basically concerned with the degree of indeterminacy. Thereby it refers to the ability of a frame to continue to carry loads when one or more structural members fail, as a result of the presence of alternate load paths. A statically determinate triangle collapses when one of the three members fails: it is unredundant. Therefore, the number of members in excess of the minimum number needed to form triangles could be used as a measure of redundancy. Using this yardstick, diagonal and K-brace patterns are unredundant while an X-brace pattern is redundant. The presence of such extra members generally requires more steel and hence increases costs. They will also tend to increase the hydrodynamic loads, with an associated tendency for further cost increases. Another factor to consider is the extra joint of the cross or K-braces, which needs a joint can and careful design.

However, the number of members is not a very satisfactory yardstick of redundancy. When unloaded (or only lightly loaded) it is true that a panel in a frame, which has ‘redundant’ members, will retain its shape if a member fails (e.g. due to collision or dropping a heavy weight on it). However, when failure of a member is due to overload it is far from certain that the failure will not initiate other failures with collapse as the overall result, despite the existence of 'redundant' members. On the other hand, a non-redundant frame in reality does not consist of statically determinate panels with hinged members that are only axially loaded. The joints between the members are fixed connections and loads can therefore also be transferred through shear and moment action (e.g. as in a portal), if the main force transfer through axial member forces becomes inactive. This capacity cannot simply be expressed by a member and joint count because it depends on the strength and stiffness properties of the members around the failure location. Therefore, the *reserve strength* of a panel (or better still of the frame as a whole) is a much better indicator of structural safety. The reserve strength is the ratio of the load at which the panel (or the frame) collapses to the load at which the first member fails. Sometimes a different and alternative definition of reserve strength is used in the form of the ratio of the load at which the panel/frame collapses to the maximum *design load*. The collapse load represents the ultimate capacity (ultimate strength) of the panel or the frame under static loading.

The reserve strength is not a straightforward quality of a particular bracing pattern as it depends as much on configuration as on strength and stiffness of the members involved; it can only be determined by a proper non-linear structural analysis. In very broad terms, single diagonals are a good and effective choice. A degree of reserve strength is provided by the portal action of the strong legs and the horizontal braces connecting them. K-braces tend to exhibit a rather brittle failure behaviour and require usually careful consideration and design. X-braces tend to show the most ductile failure behaviour with often significant reserve strength. For this reason they are frequently used in modern designs of offshore structures. Structures subjected to earthquake conditions are often even required to have X-braced panels by design codes. However, it is stressed once more that one should be careful with a generalisation of these observations; it is normally necessary to assess structural behaviour and ultimate strength on a case by case basis.

It can be advantageous to select the height of the panels (the *bay height*) such that the panels are geometrically similar. In this way the brace angles are the same for the whole frame and can be chosen optimally, while all leg joints are of similar geometry which facilitates their detailed design and their fabrication. To achieve geometrically similar bays we should divide the height of a frame with a given outline (height, top width, batter angles) into a chosen number of geometrically similar panels. The solution is given in Annex D.

Preliminary member sizing
When the configuration of the frame has been determined and the centre-to-centre member lengths are thus known, it remains to estimate initial diameters and wall thicknesses. As individual members generally experience both tension and compression loading, and as stability requirements limit the allowable loading of slender members more stringently than strength criteria, member *diameters* are primarily determined by stiffness rather than by strength considerations. Initial member sizes are therefore usually selected on the basis of slenderness. The slenderness parameter λ is defined as $\lambda = KL/r$. The length L is normally taken as the nominal length between nodal points in a line diagram of the structure; in some special cases it is refined to be the actual length between the tubular faces. The coefficient K expresses the effective buckling length of the member and depends on the boundary conditions at its ends. Base values are:

- simply supported (hinges) at both ends $K = 1.0$
- clamped at both ends $K = 0.5$
- clamped at one end and free at the other $K = 2.0$

The true value of K can only be determined by a detailed finite element analysis taking into account the local and global stiffnesses of the members involved. A value of $K = 0.8$ is rather commonly used for diagonal and K-braces; it is probably slightly conservative with a value of $K = 0.7$ being more realistic in most cases. For X-braces a value of $K = 0.5$ may be used in combination with the total length of the member, provided that one brace of the X is indeed in tension while the other is in compression. For the legs, which are much stiffer and do not derive much restraint from braces as far as joint rotation is concerned, $K = 1.0$ is used, while deck legs and similar columns are normally designed with $K = 2.0$.

The radius of gyration r is defined by:

$$r = \sqrt{\frac{I}{A}} \tag{5.4-1}$$

where I is the line moment of inertia and A the area of the cross section. For a tubular member with outside diameter D_o, inside diameter D_i and wall thickness t we have:

$$I = \frac{\pi}{64}\left(D_o^4 - D_i^4\right) \cong \tfrac{1}{8}\pi D^3 t \quad \text{and} \quad A = \frac{\pi}{4}\left(D_o^2 - D_i^2\right) \cong \pi D t \tag{5.4-2}$$

where D is best taken as the average diameter [1] $D = D_{av} = D_o - t = D_i + t$. Consequently, r becomes independent of the wall thickness and reduces to:

$$r \cong \sqrt{\tfrac{1}{8} D^2} = D / 2\sqrt{2} \cong 0.35 D. \tag{5.4-3}$$

This allows very quick estimates of the diameter as a function of member length, K factor and slenderness value λ; such estimates are entirely adequate in the early design stages:

$$\frac{D}{L} = \frac{K}{0.35} \cdot \frac{1}{\lambda} = \begin{cases} 2.28/\lambda & \text{for K} = 0.8 \\ 2.00/\lambda & \text{for K} = 0.7 \end{cases} \tag{5.4-4}$$

For main bracing members the slenderness parameter KL/r is usually taken between 60 and 80; for less important members it varies from 70 to 90, while 100 to 120 is a practical upper limit. This means that the diameter of main bracing members ranges between 2.5 and 3.8 % of their length. A practical size of around 3 % of the length is usually chosen as an initial estimate. Member buckling behaviour is further discussed in chapter 7. When the diameters have been chosen, the hydrodynamic loading can be determined; wall thicknesses are not needed for this.

At this stage of the design wall thicknesses do not yet need to be chosen. However, since we are discussing the sizing of members we will make some observations with regard to wall thicknesses as well. The wall thickness of a member is governed by the loading that the member is to carry; in general this loading is a combination of axial loading from its function in the space frame and bending moment due to direct loading normal to the member. Both these loadings are at this stage still completely unknown. An *initial wall thickness* may be chosen from a set of standard tubular sizes in accordance with certain practical considerations on D/t ranges. D/t should not be smaller than approximately 24 to ensure that steel plates can still be cold-rolled into tubulars; for smaller D/t values the member would need to be heat treated after rolling. This governs the maximum wall thickness for a given diameter. On the other hand, D/t should not be too large to prevent local shell buckling becoming more restrictive than global member buckling. An upper limit is in the range of $D/t = 60$. In practice, members in the top part of the structure are often relatively thick with D/t values of around 25. This is due to a number of reasons, including that they are subject to significant direct wave loading, that they may be exposed to loading by a collision, and that they are more vulnerable to corrosion. Main members much lower down in the structure are primarily subjected to frame action and external hydrostatic pressure; these members often have D/t values of around 40. However, it is once more stressed that wall thicknesses are to be based on the loading of members. The D/t values only serve as a check on reasonableness and practicality.

---

[1] These approximate expressions are remarkably accurate, provided that indeed the average diameter is used. When used in combination with the outside diameter they tend to become rather quickly fairly inaccurate.

The preliminary diameters of members are, in according with the above guidelines, based on slenderness in relation to their principal role of carrying axial forces by transferring environmental loads to the foundation; this is a result of their function in a frame. However, members are of course also subject to other loads, such as:

- loads due to selfweight and buoyancy;
- direct hydrodynamic loads due to wave and current action.;
- hydrostatic pressure on internally dry members;
- shear forces and bending moments at their joints, transmitted by other members to which they are connected.

The shear forces and bending moments at the joints can only be properly determined by a three-dimensional stiffness analysis and hence by computer analysis. Hydrostatic pressures only become significant in deeper water, say for waterdepths in excess of some 200 m. There is no simple way of incorporating the effects of hydrostatic pressure and its interaction with other load cases. However, the effects of the other two loadings can reasonably well be determined by manual calculations.

All internally dry and submerged members are subject to gravity loads from their own weight and buoyancy loads due to the displaced water. The resultant of these forces may act downwards or upwards depending on the diameter and wall thickness of the member. For a neutrally buoyant member we have the following condition:

$$\rho_w g \cdot \frac{\pi}{4} D_o^2 = \rho_s g \cdot \frac{\pi}{4}(D_o^2 - D_i^2) \tag{5.4-5}$$

or:

$$\frac{D_o}{t - \frac{t^2}{D_o}} = \frac{1}{\left(\frac{t}{D_o}\right) - \left(\frac{t}{D_o}\right)^2} = 4 \cdot \frac{\rho_s}{\rho_w} \tag{5.4-6}$$

Neglecting the quadratic term on the left we obtain approximately:

$$\frac{D_o}{t} \approx 4 \cdot \frac{\rho_s}{\rho_w} = 4 \cdot \frac{7850}{1025} = 30.6 \tag{5.4-7}$$

so that dry members with a D/t ratio of about 30 are neutrally buoyant, i.e. they are unloaded by selfweight and buoyancy. For smaller D/t ratios selfweight is more important and members are loaded by a uniformly distributed vertical load downwards. For larger D/t ratios buoyancy is more important and members are loaded by a uniformly distributed vertical load upwards.

Direct hydrodynamic loading due to wave and current action can be estimated rather easily by considering that for steel space frame structures in extreme storm conditions drag loading on members will usually dominate over inertia loading. Therefore, a good approximation is obtained by taking the component of the resultant water particle velocity due to waves and current perpendicular to the member at mid-length (v_n). This velocity induces a distributed load normal to the member of:

$$q_{n,wc} = C_d \cdot \frac{1}{2} \cdot \rho v_n^2 \cdot D \qquad \text{(N/m)} \qquad (5.4\text{-}8)$$

which may be taken constant over the entire length of the member. The inertia load term in Morison's equation can of course be included in this estimate, if desired or necessary. The total distributed load on the member is:

$$q = (q_{wt} - q_{bu}) \cdot \cos\theta + q_{n.wc} \qquad \text{(N/m)} \qquad (5.4\text{-}9)$$

where:

q	=	total and approx. uniformly distributed load normal to the member axis	[N/m]
q_{wt}	=	uniformly distributed load from selfweight of the member	[N/m]
q_{bu}	=	uniformly distributed buoyancy load on the member	[N/m]
$q_{n,wc}$	=	approximately uniformly distributed hydrodynamic load on the member due to waves and current	[N/m]
θ	=	angle between brace and horizontal	

To obtain the maximum value of q the terms in equation 5.4-9 must be summed in an absolute sense.

For a beam (nearly) fixed at both ends, the end moments in the member are smaller than $\frac{1}{12}qL^2$, while the moment at mid-length is larger than $\frac{1}{24}qL^2$ (but smaller than $\frac{1}{8}qL^2 = \frac{3}{24}qL^2$ for a pinned member). A maximum moment value of $\frac{1}{12}qL^2$ is therefore a good indication of the bending moments in the member. This moment occurs both at midspan and at the member ends. In this manner approximate member bending moments can be determined manually. In addition to the primary axial load in the member this serves as input to the member checks that will be discussed in chapter 7.

5.5 Design loads and design situations

Structural design encompasses the entire structural system consisting of superstructure, support structure and foundation. Structural design of the superstructure can usually be considered reasonably independently from the support structure and the foundation; it is an entirely separate subject that is usually dealt with separately as well. Support structure and foundation interact in many ways with each other; see also chapter 6. In this section we will describe design loads and design situations in a general manner, but with special focus on the support structure.

Design loads comprise:

a) *permanent loads*, that are likely to act throughout a particular design situation and for which variations in magnitude with time are negligible in relation to their mean or maximum value; examples of permanent loads are:
    - self weight in air
    - weight of topsides and functional equipment
    - loads due to water pressure (buoyancy and hydrostatic pressure)
b) *variable loads*, that are unlikely to act throughout a particular design situation or to act simultaneously with other loads; examples of variable loads are:
    - self weight of temporary structures
    - weight of non-permanent equipment and facilities
    - weight associated with occupancy, personal effects and supplies
    - loads associated with operations, such as crane loads, drilling loads, variable ballast loads, helicopter loads
c) *environmental loads*, due to wind, waves and current; however, environmental loads may also be due to such circumstances as marine growth, snow, ice accumulation above water or ice in the water; loads caused by earthquakes are sometimes also considered to be environmental loads;
d) *repetitive loads,* that occur repeatedly while their variation with time is significant, possibly leading to fatigue damage;
e) *accidental loads,* examples of which are collisions, dropped objects, fire, explosion and unintentional flooding of buoyant compartments.

For all structures it is necessary to consider a number of distinctly different design situations. For each of these design situations we will generally need to consider corresponding but different structural models, design loads, environmental conditions, design resistances and design criteria. Design situations may be classified into three groups:

i. *persistent situations*, with a duration that is of the same order as the life of the structure;
ii. *transient situations*, with a shorter duration and varying levels of intensity;
iii. *abnormal or accidental situations* (during as well as after an incident), normally of short duration and with a low probability of occurrence.

Structural design of the support structure must ensure that the structure can sustain all loadings to which it may be subjected in-situ during its entire service life. While the design of onshore buildings is primarily governed by permanent and variable loads, offshore structures are generally dominated by environmental loads, especially those due to waves. The structure should further be able to sustain any loadings that it may experience during the various transitional stages of fabrication, transportation and installation. The broad distinction between in-place design conditions, a persistent situation with a permanent exposure to severe design loads that may actually never happen, and temporary construction situations is important. Construction situations are transient situations in which the structure experiences greatly different loadings in greatly different circumstances. However, for a truly efficient structure its structural design should as much as possible be controlled by the in-place conditions. If large parts of the design would be governed by one or more temporary situations this would mean that a significant amount of additional steel has to be provided for only a brief period of time during the full structure life cycle. This additional steel is literally carried as unnecessary ballast during its useful lifetime on location and will only require additional capital investment that does not provide a return.

Both the in-place condition and the construction condition present a number of different design situations. The following may be distinguished:

in-place:

- one or more operating conditions
- an extreme storm condition
- a fatigue condition
- one or more accidental load conditions
- one or more earthquake conditions, where relevant

construction:

- various stages of fabrication on land (e.g. frame roll-up)
- load-out from the fabrication yard onto the transportation barge
- transportation to site
- launch or lift-off from the transportation barge into the water
- upending on location
- on bottom stability before piling
- pile driving.

All these situations will have to be duly considered, but discussion in this handbook will be restricted to the in-place conditions, and even more particularly to the extreme storm condition. By their very nature, all offshore structures need to be designed for an extreme storm condition; in many cases this will also be the governing case for *global* structural design. Accidental load conditions may represent more severe *local* conditions, especially around the still waterline. Furthermore, for some wave climates fatigue requirements may control member sizing and joint detailing in parts of the structure, while earthquakes often are the controlling condition for (parts of) the substructure when the structure is situated in earthquake prone geographical areas.

During detailed design an extensive number of finite element calculations are performed for a substantial number of different load cases. These determine the final foundation and member forces that the structure needs to accommodate. These forces are then the input to detailed separate design and analysis exercises for foundation piles, individual members, tubular joints and other relevant components.

Condition	**Normal**	**Extreme**
Allowable stress		
Axial stress	0.60	0.80
Bending stress	0.66	0.88

Table 5.6-5.1. Typical safety factors (allowable stress divided by the yield stress) for strength checks in API RP2A (WSD)

5.6 Allowable stress and partial factor design methods

Structural design
The structural design process generally consists of several stages:

a) an analysis of the global behaviour of the structure that provides the global structural responses (forces, moments, displacements, accelerations) for the whole structure and its foundation;
b) a structural analysis that provides structural responses (forces and moments) in cross-sections at various elevations;
c) an analysis of members, joints, etc. to investigate their behaviour in greater detail and to compare their internal forces to their resistances;
d) an analysis of localised features and local details, e.g. at discontinuities and at connections of different structural components.

The results of structural calculations are eventually to be assessed against certain criteria, see figure 3.4. Structural design is traditionally based on the design of individual components, in accordance with a given method and a particular set of rules. When all components satisfy the specified criteria, the whole structure satisfies these criteria as well. Primary components in steel offshore structures of the space frame type are line elements (legs and braces) and their connections (tubular joints). The design or verification of a line element consists of comparing a representative force or stress in the element to its representative resistance. This includes:

- a strength check, where the representative resistance is related to the yield strength of the element;
- a stability check for elements that are in compression, where the representative resistance is related to the buckling limit of the element.

For connections (tubular joints) between structural members in framed offshore structures the representative resistance to static loads is similarly checked. These checks will be discussed in chapter 7. All components are further to be checked for the possibility of cumulative damage due to fatigue by repeated load variations, as will be discussed in chapter 8.

The allowable stress design method
There are two methods for such design checks in common use, the allowable stress method (also called Working Stress Design or WSD) and the partial factor design method (also called Load and Resistance Factor Design or LRFD). WSD is the oldest method; it was used when the American Petroleum Institute issued its first ever Recommended Practice 2A for the Planning, Designing and Constructing Fixed Offshore Platforms (API RP2A) in 1969. This Recommended Practice has gradually become a basis for the design of steel offshore structures in the whole world. The 21st edition of RP2A is the currently latest version. WSD is still regularly used in the USA and many other countries outside Europe. In WSD the loads remain unfactored, while a single coefficient (safety factor) is applied to the resistance side (normally expressed in terms of the yield stress) to derive representative resistances in the form of allowable stresses. The coefficients (safety factors) that are applied are different for so-called ‘normal’ and ‘extreme’ conditions. Extreme conditions refer to the most severe environmental loading in a storm. API RP2A states that under extreme conditions the allowable stresses may be increased by one-third. Typical safety factors for strength checks in

API RP2A (WSD) are given in table 5.6-1; they are expressed as the allowable stress divided by the yield stress.

Limit states and the partial factor design method

The more modern method for checking the structural performance of a whole structure or part of it makes use of limit states. In this method the state of a structure is described with reference to a specified set of limit states. A limit state is defined as *a state beyond which the structure no longer satisfies the design (performance) requirements*. Limit states separate desired states (no failure) from undesired states (failure), where 'failure' should be understood to mean 'not meeting the design requirements'; it usually does not directly imply real structural failure. The design format that is compatible with limit states is the partial factor or LRFD method. This is presently the accepted standard procedure in Europe, because it can provide more uniform reliability between different components of the same structure, as well as between structures subject to different loading regimes. It has recently also been adopted by API who published its first issue of RP2A in LRFD format in 1993 [5.6-1]. However, the LRFD method is still not commonly applied in the USA. In this method partial factors are applied to representative values of the loads as well as to representative values of the resistances for the structural components. An offshore structure is designed to satisfy four categories of limit states, each of which may be subdivided further. These are:

ultimate limit states (ULS):

limit states that correspond to the maximum resistance (load-carrying capacity) of (a part of) the structure.

Ultimate limit states are safety related. Examples of ULS for bottom founded structures are:

- loss of static equilibrium of the structure, or a part of the structure, considered as a rigid body (e.g. overturning);
- failure of (a) critical component(s) caused by exceeding the ultimate strength (that has possibly been reduced by repeated loading) or the ultimate deformation capacity of the component(s);
- transformation of the structure or a part of it into a mechanism;
- instability of the structure or part of it (buckling).

serviceability limit states (SLS):

limit states that correspond to the ability of the structure and its structural components to perform adequately in normal use.

Serviceability limit states are thus function related. Examples of SLS for bottom founded structures are:

- deformations or movements that affect the efficient use of structural or non-structural components, or exceed the limitations of equipment;
- excessive vibrations that produce discomfort to people, or affect non-structural components or equipment (especially if resonance occurs);
- local damage, including cracking, that reduces the durability of a structure, or affects the use of structural or non-structural components;
- corrosion that reduces the durability of the structure and affects the properties and geometrical parameters of structural and non-structural components.

Condition	**ULS normal**	**ULS extreme**	**FLS**
Partial load factors for:			
(adding to environmental loads)			
Permanent loads	1.3	1.1	0.0
Variable loads	1.5	1.1	0.0
(subtracting from environmental loads)		0.9	0.0
Permanent loads		0.8	0.0
Variable loads			
Environmental loads	1.2	1.35	1.0
Resistance factors(1) for:			
Yielding due to axial tension	0.95	0.95	
Yielding due to axial compression	0.85	0.85	
Bending	0.95	0.95	
Shear	0.95	0.95	

Table 5.6-2. Typical partial load and resistance factors for strength checks in API RP2A (LRFD)

---

(1) Resistance factors may be expressed in one of two ways, i.e. as a factor by which the characteristic resistance is multiplied or as a factor by which the characteristic resistance is divided. In the first case the factors are ≤ 1.0 (as in the above table), in the second case their numerical value is the reverse of the first case and they are ≥ 1.0.

fatigue limit states (FLS):

limit states that correspond to cumulative damage resulting from the accumulated effect of repeated loading.

Fatigue limit states can be both safety (ULS) and function (SLS) related.

accidental damage limit states (ALS):

limit states that correspond to a situation where damage has occurred as a result of an accidental event.

The accidental damage limit state check ensures that local damage or flooding does not lead to complete loss of performance or integrity of the structure. The intention of this limit state is to ensure that damage is not disproportionate to the event. A structure should be able to tolerate damage due to specified accidental events, and subsequently maintain its structural integrity in the damaged state under specified environmental conditions for a sufficient period of time to enable a safe close down and/or evacuation.

Sometimes there is still another limit state specified, the so-called *progressive collapse limit state* or *PLS*. This is partly related to accidental events with the associated damage; it is then essentially covered by the accidental damage limit states. However, for another part the PLS is intended to cater for the possibility of failures by a sort of chain reaction. In this case it is not necessarily related to accidental events only. It may, for example, also serve to check that overload from unusually severe environmental loading due to wave conditions, which are e.g. expected to occur on average only once every 10,000 years, does not lead to failure of (a) critical component(s) followed by collapse of the entire structure. To reduce the risk that progressive collapse may occur there are three general sorts of measures one can take:

a) *avoidance or protection*;
   this involves controlling the possibility of harmful events by taking measures that are aimed at avoiding incidents (such as falling objects, ship collisions, fires, explosions, etc.) to occur, which could potentially lead to such catastrophic failures; alternatively, one may take measures that do not avoid incidents to occur, but protect components or equipment against the consequences such incidents may have (an example is a protective housing around a valve);
b) *component design*;
   critical components may be designed to be so strong, that they cannot be made ineffective in case of incidents or overload due to certain types of foreseen damage;
c) *system design*;
   a structure may be designed to be damage tolerant by invoking its capability to act as a structural system, rather than acting only as an assembly of individual components. This relates to concepts such as robustness, redundancy and ductility (as a property of the structural system, not as a material property). One way to create this capability is by providing alternative load paths to enable redistribution of the forces within the structure, if damage of whatever form may occur.

As already said, structural design is normally component rather than system based. Consequently, the four limit states ULS, SLS, FLS and ALS refer essentially to structural components. System behaviour associated with the fact that the structure consists of a (large) assembly of co-operating components is very difficult to handle and not normally considered in design to any great extent. However, there is an increasing trend to do so, and the tools to

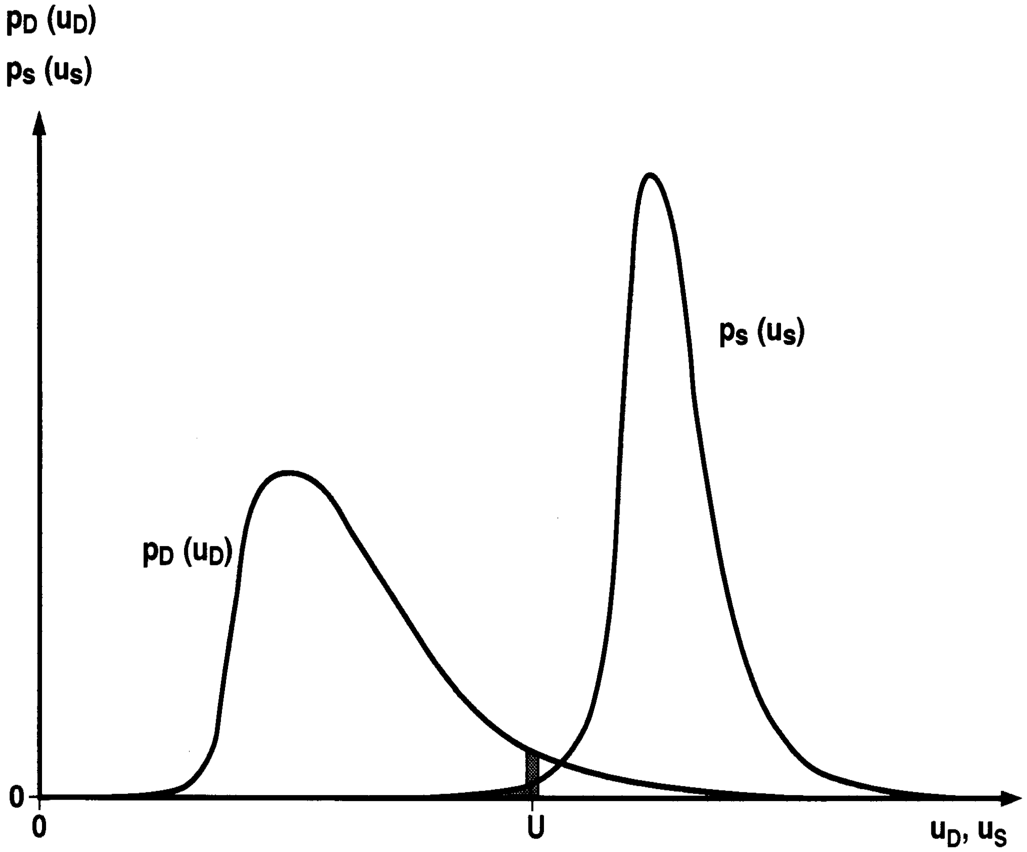

Figure 5.6-1. Illustration of the concept of structural reliability assessment

make this possible are gradually becoming available. The PLS is the only limit state that, at least in principle, addresses system requirements.

The loads used for structural design are always uncertain, but some loads are more uncertain than others. For example, self weight and other permanent loads are known with much greater confidence than the environmental loads. In a very similar manner the resistances of the material or of the structural component against failure are uncertain to different degrees. Partial factor methods make it possible to account for such differences in uncertainties in a rational manner. Typical values of the partial load and resistance factors for strength checks in API RP2A (LRFD) for ULS are summarised in table 5.6-2. The resistance factors for stability checks cannot so easily be expressed in a simple number; see chapter 7. For other limit states than the ULS the procedures are usually more involved. However, to give an indication the partial load factors that apply to the FLS are also shown in table 5.6-2.

Structural reliability assessment

The ultimate approach to structural design would be a full probabilistic treatment of loads and resistances in a structural reliability analysis of the entire structural system. However, this is as yet generally beyond the state-of-the-art, despite great advances that have been made; see e.g. references [5.6-2] and [5.6-3]. But structural reliability analyses are increasingly used at the level of structural components for the calibration of codes; this makes it possible to determine consistent sets of values for the partial factors. The differences between WSD and LRFD methods can further nicely be illustrated using reliability analysis principles.

The basic principle of a structural reliability assessment (further abbreviated to SRA) is extremely simple. Reliability is defined as the ability of a component or a system to perform its required function without failure during a specified time interval. To determine the reliability we need to calculate the probability that the demand D does not exceed the capacity or supply S, where D and S are both probabilistic quantities with given probability density functions (further abbreviated to pdf and indicated by the symbol p). The reliability $prob_R$ is the chance that S exceeds D and, conversely, the probability of failure $prob_F$ is the complementary probability that D exceeds S. Both are numbers between 0 and 1.0 and the following relationship always holds:

$$prob_R + prob_F = 1.0 \tag{5.6-1}$$

Figure 5.6-1 illustrates the two $pdfs$ of demand and supply $p_D(u_D)$ and $p_S(u_S)$, where u_D and u_S are separate and independent variables that are expressed in a common unit u. For example, u may be a stress with u_D the stress experienced by a structural component under extreme environmental loading conditions and u_S some critical limiting stress, e.g. the yield stress or the ultimate tensile stress, as appropriate. In many cases the ranges of u_D and u_S will be bounded on the lower and possibly also on the upper side, but it is most convenient to assume that they both vary from minus infinity to plus infinity.

The probability that the demand assumes a particular value $u_D = U$ is by definition:

$$p_D(U)du \tag{5.6-2}$$

while the probability that the supply is smaller than U is:

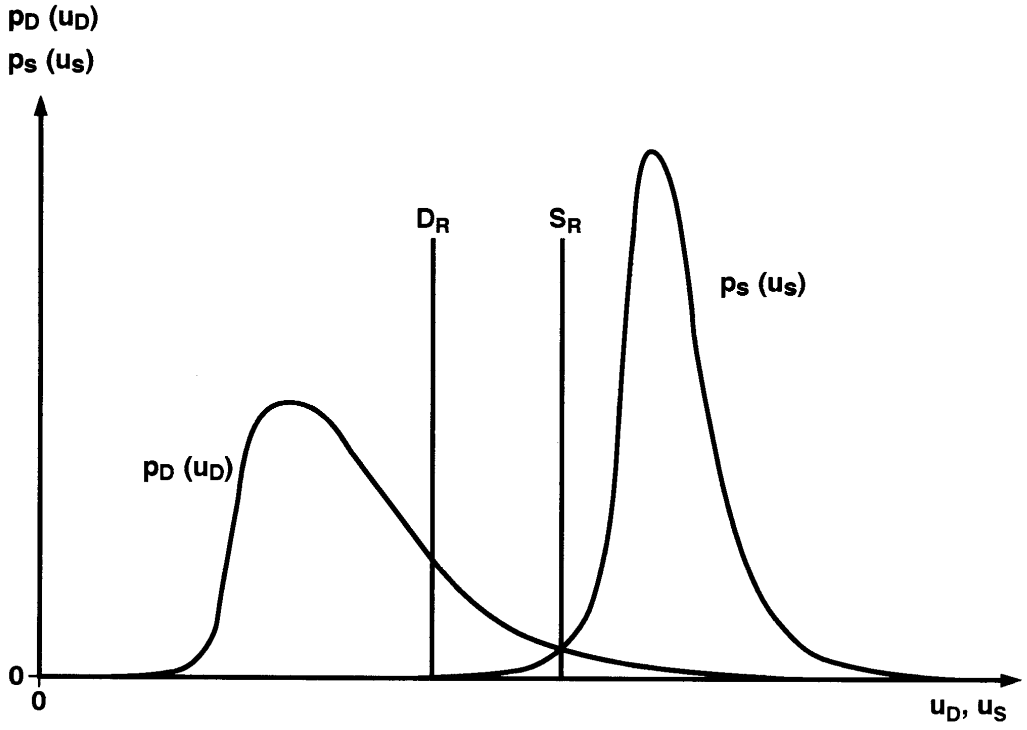

Figure 5.6-2. Design practice according to the WSD method against the background of probabilistic demand and supply distributions

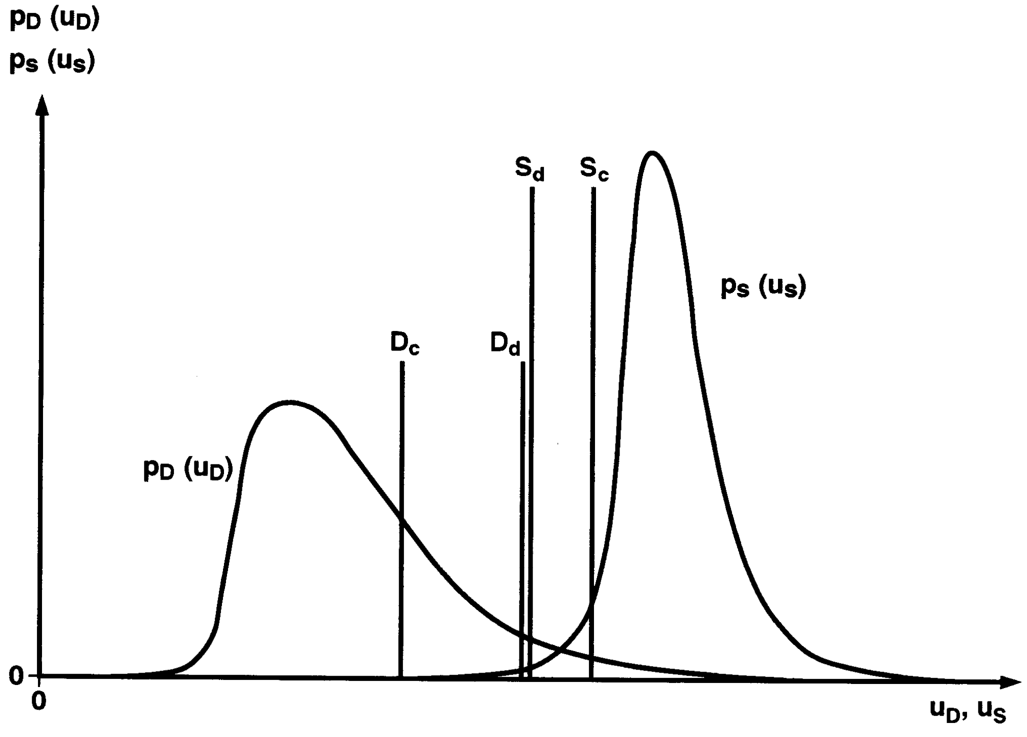

Figure 5.6-3. Design practice according to the LRFD method against the background of probabilistic demand and supply distributions

$$P_S(U) = \int_{-\infty}^{U} p_S(u)du \qquad (5.6\text{-}3)$$

Therefore, the joint probability of the demand being U and the supply being smaller than U (i.e. the contribution to the probability of failure for this particular combination of demand and supply) is the product of these two:

$$prob_F(u_D = U, u_S < U) = p_D(U)du.P_S(U) = p_D(U)du.\int_{-\infty}^{U} p_S(u)du \qquad (5.6\text{-}4)$$

The total probability of failure is thus obtained by summing the contributions for all possible values of U, i.e. integrating equation 5.6-4. Analogously, one may start by assuming that the supply has a particular value $u_S = U$ and that the demand exceeds U. This results in the following two alternative expressions for the probability of failure:

$$prob_F = \int_{-\infty}^{+\infty} [P_S(u) \cdot p_D(u)]du = \int_{-\infty}^{+\infty} [\{1 - P_D(u)\} \cdot p_S(u)]du \qquad (5.6\text{-}5)$$

each of which contains an integral within the integral.

The central issue of SRA is therefore to numerically determine either one of these integrals. The key problem is clearly to determine the two *pdfs* with sufficient accuracy, including their tails for (very) low and (very) high values of u_D and u_S. As the probability of failure must clearly be low, the outcome of the numerical integration will be decisively influenced by the robustness of the upper tail of the demand function and the lower tail of the supply function.

The SRA methodology described here and illustrated in figure 5.6-1 is very simple in concept, but reality is immensely more complex and realistic applications remain therefore difficult and usually restricted to (severely) simplified cases. However, to illustrate regular design practice by the WSD and LRFD methods this discussion of the concept suffices.

Let the variable u_D represent a suitable response variable, such as an internal force, a stress or a displacement. The variable u_S is a corresponding limiting criterion. In the WSD methods both *pdfs* are replaced by a single representative value D_R and S_R, which are determined in accordance with a particular set of rules; see figure 5.6-2. The safety factor is the ratio of these two values, i.e.

$$SF = S_R / D_R \qquad (5.6\text{-}6)$$

In the LRFD method the procedure is broadly similar, but more refined and much more rational. The somewhat arbitrary representative values D_R and S_R are now replaced by more rigorously determined characteristic values D_C and S_C; see figure 5.6-3. These may be defined as values that have a prescribed probability of e.g. 5% of not being exceeded during a specified time interval, chosen in relation to the intended service life or the duration of the design situation. The values used in design, D_d and S_d are now derived from the characteristic values by multiplication or division by partial factors. These factors take account of natural and unfavourable deviations of the actual values from the characteristic values, as well as uncertainties in the determination of the characteristic values themselves. They thus reflect the individual variabilities of the different parameters involved. Furthermore, the demand side may be built up by distinguishing different contributions, each of which may exhibit a different degree of variability and/or uncertainty. Each of these contributions can then be represented by an associated and different magnitude of the partial coefficient. Hence:

$$\begin{aligned} D_d &= \gamma_{D1} \cdot D_{C1} + \gamma_{D2} \cdot D_{C2} + \cdots \\ S_d &= S_C / \gamma_S \\ S_d - D_d &\geq 0 \end{aligned} \tag{5.6-7}$$

For a single demand the procedure is illustrated in figure 5.6-3. The values of D_C and S_C and their associated γ-values may be obtained from available databases, they may be determined on the basis of experience or by more or less rigorous mathematical models in combination with postulated distribution types for u_D and u_S.

Based on the above descriptions and figures 5.6-1 to 5.6-3 the following observations should be made:

- the *pdfs* in figures 5.6-1 to 5.6-3 are purely hypothetical and are shown for the purpose of illustration only; however, they show the following typical and realistic trends:
  - since the *pdf* of demand (the load) is normally dominated by the highly variable environmental loading (especially wave loading) it is usually low and wide, and skewed with a significant tail on the right;
  - by contrast, the *pdf* of supply (the resistance) is normally fairly narrow and much more symmetric;
- the safety factor in WSD and the applicable set of rules by which the representative values D_R and S_R are determined are strongly interlinked;
- D_R in WSD is the total response (demand) due to all unfactored loads acting together; there is consequently no possibility to treat different sources of uncertainty in the loads and their magnitudes individually;
- D_d in LRFD consists of a summation of separate characteristic components, which enables different contributions to be factored by different partial factors;
- in WSD all influences must by necessity be grouped into one factor; therefore this procedure is essentially empirically based; as a consequence the resulting reliabilities for different components in the same structure, and for structures subject to different loading regimes, will be highly variable;
- LRFD allows differentiation to be introduced, enabling a much more uniform reliability of components experiencing different loads within the same structure, as well as from one structure to another structure;
- the single representative value for demand and supply in WSD does not contain any obvious statistical information; therefore, there is no basis for estimating the corresponding *pdfs* and hence no way to estimate a probability of failure;
- by contrast, the characteristic values in LRFD do contain certain probabilistic information (e.g. 5% exceedence) and are often associated with (assumed) types of distributions; it is consequently possible to estimate the underlying *pdfs* and to quantify the probability of failure to some degree. As the distributions are assumed rather than actual distributions,

these quantifications cannot be very precise, reason why the calculated probability of failure is normally referred to as a notional probability. For the calibration of codes this is often sufficient.

A final word of caution

One final comment should expressly be made. There is a proviso to the statement that partial factor methods are rational and transparent in their application. The statement is indisputably true when applied to (quasi-)static design problems. However, caution is urged for problems where the time variation of the loads needs to be included in a realistic manner. Different time varying loads usually do not vary synchronically; different contributions to the overall loading have time lags (phase differences) between them. This is e.g. very obvious for offshore structures, which are subjected to large random loads due to waves and wind. The governing maximum of the combined loads is then usually not given by a simple algebraic addition of individual load contributions; certain loads may never peak at the same time, while other loads may more or less oppose primary contributions. Consequently, it is not at all so straightforward to determine how a partial factor method should be used under these circumstances. As all structural dynamic problems suffer from this difficulty, the application of partial factor methods to truly dynamic problems is therefore the subject of continuing investigation; examples are joint industry projects that attempt to develop partial factor design codes for the global behaviour of TLP's and for anchored floating structures. In such cases a workable design procedure, as an alternative to a partial factor method, is to use best estimates rather than factored loads for design and to supplement the design calculations with sensitivity analyses using different values (within realistic ranges) of the various parameters involved. Resistance variables are not usually subject to such influences from time variations and can therefore normally be used unchanged in both static and dynamic problems.

5.7 Materials

Still to be written.

5.8 Offshore structures standards

Still to be written.

5.9 References

5.2-1 Dam, J. van; Vugts, J.H. and Opstal, G.H.C. van, ***Position and future of R&D in offshore technology***; Shell Internationale Petroleum Maatschappij B.V., Exploration and Production, 1986.

5.3-1 Veldman, H.E. and Lagers, G.H.G., ***50 Years Offshore***; Foundation for Offshore Studies, Delft, 1997; distributed by Veldman Bureau voor Bedrijfsontwikkeling, Sittard; ISBN 90-803677-1-0.

5.3-2 European Steel Design Education Programme (ESDEP), Working Group 15A "Structural Systems: Offshore", lecture 15A.6, ***Foundations***; 1993.

5.3-3 Lamb, T.W. and Whitman, R.V., ***Soil Mechanics***; Series in Soil Engineering, John Wiley & Sons, New York, 1969.

5.3-4 Verruijt, A., ***Grondmechanica***; Delftse Uitgevers Maatschappij b.v., 3e druk, 1990; ISBN 90 6562 045 1.

5.3-5 Verruijt, A., ***Offshore Soil Mechanics***; lecture notes, Delft University of Technology, Faculty of Civil Engineering, 1992.

5.3-6 Barltrop, N.D.P. and Adams, A.J., ***The dynamics of fixed marine structures***; Butterworth Heinemann Ltd., London, 3rd edition 1991; Chapter 5; ISBN 0 7506 1046 8.

5.3-7 International Standard ISO 19902-2, ***Petroleum and natural gas industries-Offshore structures- Part 2: Fixed steel structures***; in preparation.

5.3-8 Beringen, F.L., ***Geotechniek als basis van het stalen offshore platform***; PATO cursus, Delft, 1978-79.

5.6-1 American Petroleum Institute, ***Recommended Practice for Planning, Designing and Constructing Fixed Offshore Platforms - Load and Resistance Factor Design***; API Recommended Practice RP 2A-LRFD, first edition, July 1, 1993.

5.6-2 Vugts, J.H. and Edwards, G., ***Offshore structural reliability assessment- from research to reality?***; Proceedings of the 6th international conference on the Behaviour of Offshore Structures (BOSS '92), London, 1992, volume 3 (Supplement).

5.6-3 Shell Research, Rijswijk, ***The reliability of offshore structures***; Advances in EP Research, 1993 Special Issue, Shell Internationale Petroleum Maatschappij B.V.

Annex A – Jacket ^{2} platforms [5.3-1]

The most common support structure of the offshore industry is a steel space frame, most often called jacket. Above water, it carries a superstructure consisting of one or several decks for equipment used in production of oil and gas and all facilities which are needed to support and maintain the basic functions (power plant, accommodation for personnel, compressors, export pumps etc.). Often a drilling rig forms part of the equipment and then serves for first drilling and later maintaining the production wells. The production equipment and facilities are often called the topsides. The jacket is piled into the seabed, to avoid settlement, lateral displacements and overturning. Another name for a jacket is template. This name derives from its function to lower the foundation piles through its hollow legs to guide them from the water surface to the seabed.

The idea of using a prefabricated template to provide a basis for a platform deck has since long been taken for granted. In 1947, however, it was a novelty, introduced by M. Willey of J. Ray McDermott and embraced by Superior Oil Company. The basic motive to adopt this design was to save costly offshore time. An additional advantage that came up later was possible re-use. In 1955, for instance, Humble used salvaged template structures to economise on time and cost needed for a platform on a new site in the Gulf of Mexico. In any case, steel templates have quickly replaced wooden structures and installations of single, unguided piles for all but the smallest platforms.

The 1947 novelty used 6 templates to support a deck measuring 33 x 53 m in 6 m water depth. In 1955 the 100 feet (30 m) water depth mark was passed. By this time, jackets were much more 'transparent' than their early predecessors, thanks to the use of better materials and larger diameter members. Slowly water depth capacity increased, reaching 150 m in 1975. Jackets were now single template structures, built onshore, usually on their side, transported horizontally to the offshore location on a barge, launched on site and finally upended. The number of installed jacket platforms in the Gulf of Mexico increased steadily and reached some 1000 in 1963, 2000 in 1968 and over 4000 in 1996. In other shallow water offshore provinces of the world, the trend was the same. Worldwide, over 6000 platforms of this type have been placed.

Design of a jacket structure is a matter of determining overall dimensions based on water depth and functional requirements, evaluating hydrodynamic loads caused by currents and waves, determining scantlings of the space frame members, analysing stress concentrations in nodes and the associated risks for metal fatigue by unsteady loads, checking the risk of vibration of single braces or the complete structure, protecting against corrosion attack etc. Appropriate data to define extreme cur-rent and wave conditions are sometimes difficult to obtain. Statistical information has helped to define the 50 or 100 years wave height, but more often than not statistics are based on observations during a relatively short period, and not quite reliable. Wind loads, and sometimes ice or earthquake risks also play a role.

---

[2] Please note that the word ‘jacket’ is used here as a general name for a steel space frame structure. This is often done in daily practice. However, in a more distinctive use of terms the term ‘jacket’ is reserved for a specific type of steel structure that is supported by piles at the top of the structure, while the term ‘tower’ refers to a steel structure supported by piles at the base of the structure; see further Annex C.

Most horizontal loads are directly related to the diameters of legs and bracings, and therefore the design is a highly cyclical process. The design of the foundation piles is equally critical. The piles interact with the soil and its mechanical properties, and are required to transmit both vertical and lateral loads to the subsoil.
Two different ways of interaction between jacket or template and piles have been devised. One method was to drive piles through the template legs. The template itself served for lateral strength and stability. The decks were placed after pile driving and stood on top of the piles with short deck legs mated and welded to the piles. The other method was to equip the jacket base with short pile guides. Piles were driven through these guides by means of either pile followers or underwater hammers and were grouted to the guides. These jackets are often referred to as towers and their piles as skirt piles.

In 1969, the American Petroleum Institute published the first edition of Recommended Practice 2A, which has become the basic design guideline and standard for all steel offshore platforms.

The advent of fast computers and appropriate stress analysis programs bas helped enormously to fine-tune the design and thereby increase the waterdepth capability of the concept. A proper description of wave kinematics is essential for the calculation of wave induced forces. Several models have been worked out, such as Stokes 5th order wave theory and Dean's stream function theory. Loads are derived from the kinematics with the Morison equation, which according to cynics is only the least inaccurate description of reality. Again, applying these tools became only practical with the introduction of the computer. The cumbersomeness of calculations and lack of computers in the early days has sometimes led to high factors of safety - or ignorance - and by consequence old structures often show an incredible longevity due to overdesign.

The technology of building jackets had to follow the trend towards increasing water depths. Quality of welding and handling of the large space frames required highly skilled and specialised fabricators. In 1978 the ultimate seemed to have been reached by Shell’s Cognac platform in 312 m water depth in the Gulf of Mexico, which was built and installed in three sections stacked vertically, one upon the other. However, ten years later Shell improved its own record with the Bullwinkle platform, standing in 412 m waterdepth also in the Gulf of Mexico. In the North Sea with its high productivity wells, waterdepth was smaller, but the topsides volume and weight was larger, leading to heavy support structures. Primarily in the Norwegian sector of the North Sea, concrete gravity platforms have taken the lead over jacket platforms.

The steel weight of a jacket or template is a function of waterdepth, environmental conditions and topsides load. The continually increasing size and weight tended to exceed the capacity of existing transportation and launch barges**.** Larger structures in the North Sea and some other areas were then only possible by adding special floatation tanks (e.g. BP's Forties jacket) or making the structure self-floating by increasing the diameter of the jacket legs (e.g. Shell’s Brent A, BP's Magnus, Shell's Maui A off New Zealand). At a later stage, large size transportation and launch barges became available, with Heerema’s barge H851 as the ultimate. The H851 was specially designed and built to enable the Bullwinkle jacket to be transported and installed in one single piece in 1988**.** The increased capacity of the offshore cranes brought back the lift jackets where possible, which may be built lighter than an equivalent launch or float jacket.

A side step towards use of aluminium as the structural material (weight, and most importantly insensitivity to corrosion) remained restricted to application in Lake Maracaibo. In the 1980s the concept of 'slim jackets' for medium waterdepth was promoted. These were light enough to be lifted by a large crane, and could therefore avoid special structural provisions for launching and upending, making them light indeed. In the 30-50 m water depth range of the North Sea, some monopod platforms were placed, resembling the big 'Trading Bay' installed in Alaskan waters. The jacket platform with 3 to 8 main legs, however, remains the most common offshore platform to this day.

Annex B – Foundations [5.3-1]

All permanent structures in the offshore industry have the need for a proper foundation on and in the seabed as a common feature. As with many other aspects, the earliest foundations were extrapolations of land-based methods and experience with piers and jetties. Until the gluttonous Teredo [3] in Lake Maracaibo necessitated a different approach, the platform builders relied on wooden piles to be driven into the seabed. In Maracaibo, concrete (1927) and steel (1934) were introduced and in the course of time steel piling has become the standard method. In the shallow waters of the pre-war years the common concept for building a platform was to drive a certain number of piles into the seabed in a certain pattern, and then build a platform on top.

Superior in the Gulf of Mexico was the first to depart from the in-situ pile-by-pile construction of a platform, by introducing the jacket [4] or template structure. This structure provided the support between seabed and platform decks and could be prefabricated on land, thereby saving costly offshore time. Still, piling was required to provide vertical bearing capacity and to ensure that the template platforms would be capable of resisting horizontal and overturning loads. For this purpose, the hollow legs of the framed structure served as guides for lowering the piles to the seabed and for supporting them laterally during driving.
The piles have grown in size (number, diameter-and length) in line with the jacket platforms. Their weight became an important part of the total structural weight. For example, jacket and pile weights of the largest platforms in the Gulf of Mexico are 30400 and 14500 metric tons respectively for Cognac and 44800 and 9500 for Bullwinkle. For small structures in shallow water, the weight of the foundation piles may actually equal or even exceed the steel weight of the template. Almost exclusively hollow, open-ended tubular piles are used ever since steel became the principal pile material.

After the piles have been driven, they must be connected to the space frame structure of the template. For piles passing through the jacket legs, this is usually achieved by inserting steel wedges or shims in the annulus between the leg and the pile at the top of the leg, and welding these to both sides. For piles not extending above the pile sleeves at the base of the jacket, it is normally done by grouting the annulus by pumping a special cement into it and letting this harden.

The design of the piles is a function of soil conditions and loads. Soil information and empirical data are indispensable, but sometimes not enough, as in the case of the North Rankin (1982) and Goodwyn (1992) jackets offshore Australia. Both platforms are installed on a seabed consisting of notoriously difficult calcareous material. In the first case, the calcareous soil provided too little friction to achieve the required bearing capacity. The second foundation was designed with the first experience in mind. A two stage piling concept was chosen, with the first stage being a driven pile through the rather weak upper layers of the seabed. The second stage was to be a drilled and grouted pile in deeper and more competent

---

[3] A worm that works its way into wooden piles and starts to eat them from the inside. Through inspection there is hardly any damage noticeable, until after some 6 to 8 months the piles collapse.

[4] As in Annex A, the word 'jacket' is used as a general name for a steel space frame structure; see Annex C for a more distinctive use of the term.

layers. However, some of the first stage piles got squeezed during the installation such that the planned drilling through for the second stage became impossible.
Both the Rankin and the Goodwyn problem required costly corrective action. Most of the 6000 fixed platforms worldwide have been piled without particular difficulties, however. The need for heavy hammers to drive the large jacket piles has contributed to the development of the semi-submersible heavy lift crane barges, which logged much less downtime in piling than the conventional crane barges and ships. Steam driven hammers were followed by hydraulic hammers, operable under water. A modern, high-energy hammer for 8 ft diameter piles typically weighs some 160 tons.

The cost of piling is substantial. Starting in the North Sea with Ekofisk, a different foundation design has been introduced, called gravity platform**.** Here piles are not needed, since a gravity platform has a large footprint on the sea floor**,** keeping soil pressures acceptably low and providing sufficient stability against overturning without the need to be ‘nailed down’. By its sheer weight it provides for a low ratio of horizontal to vertical loads on the soil, which avoids the need for piles to resist transverse displacement. Most gravity platforms are built in concrete, which automatically brings the heavy weight, but also some steel gravity platforms exist, like Loango, offshore Congo, and Maureen A in the British sector of the North Sea.

The first gravity platforms were designed for hard seabeds and the concept was not considered suitable for soft bottoms. However, the later designs such as the Troll gas platform were provided with long skirts, which penetrated the soft seabed under the influence of the weight of the platform itself plus ballast. In this way, sufficient soil resistance was mobilised.

A third foundation type is the caisson, bucket or suction anchor foundation. It may be thought of as an inverted bucket, hence the name. It is pushed into the soil by the pressure difference over the 'bottom of the bucket' when water is pumped out from within the bucket. Suction anchors have in the first place been developed to provide anchoring points for Single Point Moorings (SPMs). With the installation of the large diameter bucket foundations under the Europipe riser platform 16/11E (1994) and the Sleipner Vest T platform (1996) this foundation type has won broader acceptance. The 'bucket' consists of a plate, usually circular, surrounded by a skirt. In the case of Sleipner Vest, the skirts are 5 m high and the plate bas a diameter of 14 m. This foundation type has a certain capacity for tension loading and thus combines features of pile and gravity foundations, however without the costly time needed for piling.

With the advent of floating production units, different foundation problems were introduced. A tension leg platform requires an anchoring point with a high-tension capacity. A traditional pile may provide this, but combinations of piles and dead weights are also applied to reduce the required length of the pile to be driven. A 'Floating Production, Storage and Offloading' vessel (FPSO) requires the same type of anchors, which are used for floating drilling rigs. These may be driven or bored piles, or drag anchors. The latter are designed for horizontal loads and can only hold minimal vertical pull. With the move to deeper water and the introduction of synthetic materials for mooring lines, the need for high slanted pulling on the anchor under an angle to the horizontal plane is now directing the attention to design of appropriate foundations for this purpose.

An obvious, but not too visible factor in all foundation considerations, is the condition of the seabed. Experience has taught that the variability of soil properties from site to site in the same general area may be high. It is therefore important that sufficient data sampling and proper analysis is done. Specialised companies provide such services with sophisticated apparatus, which usually have been developed specifically for offshore applications.

Annex C – Definitions of Fixed structure, Jacket and Tower structures [5.3-7]

Fixed structure
A structure that is bottom founded and transfers all actions that act upon it to the sea floor.

Jacket type
A jacket type structure is a fixed structure that consists of:
a) A substructure, called the jacket, made of a welded tubular space frame with three or more vertical (or near vertical) tubular chords, called legs, and a bracing system between the legs. The jacket provides support for the superstructure, conductors, risers, and other appurtenances.
b) Foundation piles that permanently anchor the structure and transfer both lateral and vertical actions to the sea floor. All or a number of the piles, called the leg piles, are inserted through the legs and connected to the legs at the top. Additional piles, called the skirt piles, may be inserted through and connected to sleeves at the base of the structure between the legs.
c) A superstructure consisting of the necessary trusses and decks to support permanent, variable and environmental actions from the facilities as well as related operational and other actions. The superstructure is supported on top of the piles.

Tower type
A tower-type structure is a fixed structure that consists of:
a) A substructure, called the tower, made of a welded tubular space frame with three or more vertical (or near vertical) tubular chords, called legs, and a bracing system between the legs. The tower provides support for the superstructure, conductors, risers and other appurtenances.
b) Foundation piles that permanently anchor the structure and transfer both lateral and vertical actions to the sea floor. All or a number of the piles, called the cluster piles, are inserted through and connected to sleeves around the (corner) legs at the base of the structure. Additional piles, called the skirt piles, may be inserted through and connected to sleeves at the base of the structure between the legs. Alternatively, a tower may be supported by another nonsuperficial foundation system that supports it at its base, such as bucket foundations.
c) A superstructure consisting of the necessary trusses and decks to support permanent, variable and environmental actions from the facilities as well as related operational and other actions. The superstructure is supported on top of the tower legs.

Annex D – Selection of bay heights

It can be advantageous to select the height of the panels (the *bay height*) such that the panels are geometrically similar. Brace angles are then the same for the whole frame so that all leg joints are of similar geometry, which facilitates their detailed design and fabrication. To achieve geometrically similar bays the height of a frame with a given outline (height, top width, batter angles) must be divided into a number of geometrically similar panels. The solution to this problem is described in this Annex.

In figure D an example frame with 4 bays is shown; for generality the batter angles are assumed to be unequal. The dimensions that are known are the top width $b_t = b_0$; the bottom width $b_s = b_4$ (in figure D) and $b_s = b_N$ for N panels (bays); the height of the frame between the lowest and the highest plan framing levels $h_t = h$; and the batter angles α_1 and α_2.

Each panel must be geometrically similar, i.e. from the top down each panel is a multiplication factor *m* times larger than the panel above it:

$$\begin{aligned} b_i &= m \cdot b_{i-1} = m^i \cdot b_0 \\ h_{i+1} &= m \cdot h_i = m^i \cdot h_1 \end{aligned} \qquad \text{for } i = 1,2,\cdots,N \tag{D.1}$$

For the dimensions that are given this means:

$$\begin{aligned} b_s &= b_N = b_t + \alpha_1 h + \alpha_2 h = m^N b_t \\ h &= \sum_{i=1}^{N} h_i = \sum_{i=1}^{N} \left(m^{i-1} h_1 \right) = h_1 \cdot \frac{m^N - 1}{m - 1} \end{aligned} \tag{D.2}$$

Hence: $$m = \left[\frac{b_s}{b_t} \right]^{\frac{1}{N}} = \left[1 + (\alpha_1 + \alpha_2) \frac{h}{b_t} \right]^{\frac{1}{N}} \tag{D.3}$$

For different batter angles the brace angles for the diagonals are also different in alternate panels; see figure D. For odd numbered panels form the top the angle is:

$$\tan \theta_{odd} = \frac{h_i}{b_i - \alpha_1 h_i} = \frac{h_i}{b_{i-1} + \alpha_2 h_i} \tag{D.4}$$

and for even numbered panels:

$$\tan \theta_{even} = \frac{h_i}{b_i - \alpha_2 h_i} = \frac{h_i}{b_{i-1} + \alpha_1 h_i} \tag{D.5}$$

Using the geometrical and scaling properties of each panel, the widths of the upper and the lower horizontal brace and the ratio of width to height are:

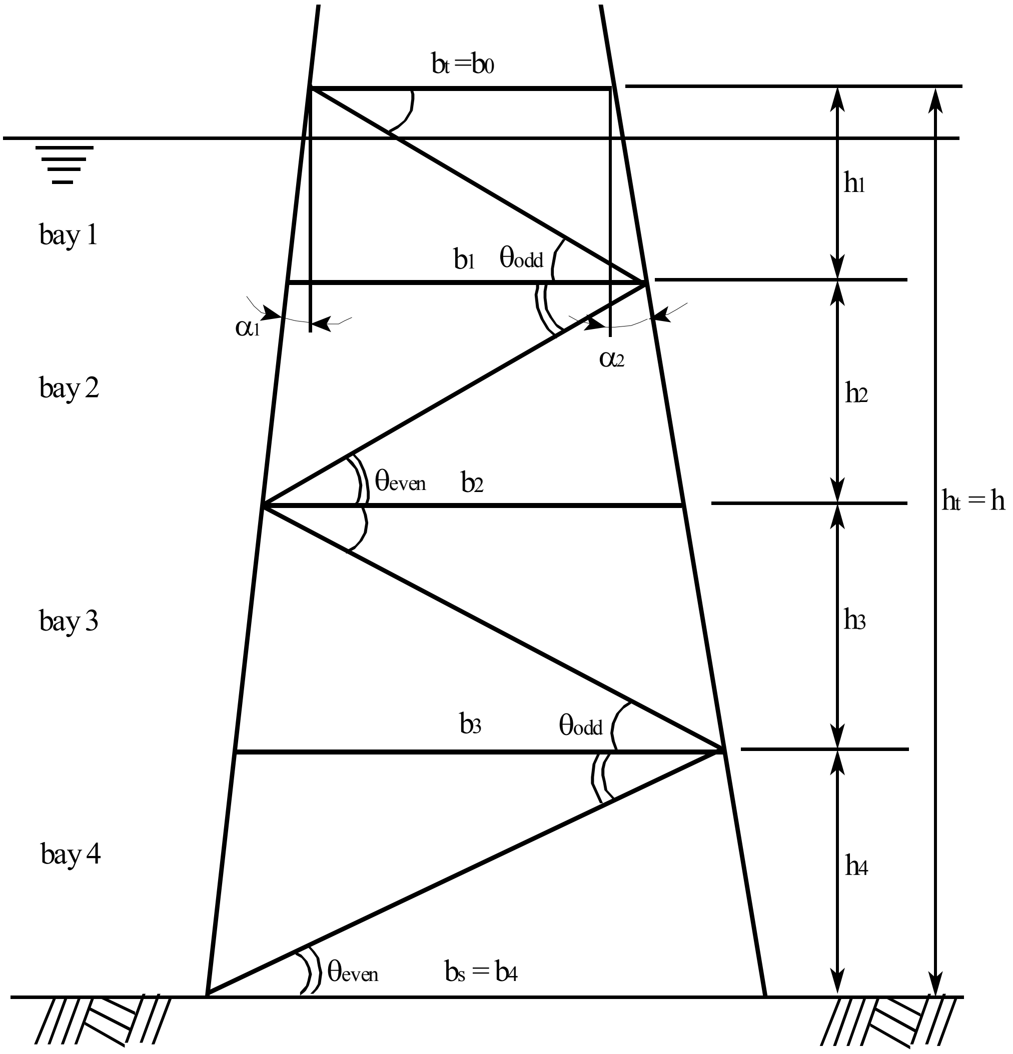

Figure D. A frame with 4 bays

$$b_i = m \cdot b_{i-1} = b_{i-1} + (\alpha_1 + \alpha_2)h_i$$

$$b_i = \frac{b_i}{m} + (\alpha_1 + \alpha_2)h_i$$

$$\frac{b_{i-1}}{h_i} = \frac{\alpha_1 + \alpha_2}{m-1} \tag{D.6}$$

$$\frac{b_i}{h_i} = \frac{m(\alpha_1 + \alpha_2)}{m-1}$$

Using either of the expressions in equation D.4 together with the ratio in equation D.6 we obtain:

$$\tan\theta_{odd} = \frac{m-1}{\alpha_1 + m\alpha_2} \tag{D.7}$$

and for either of the expressions in equation D.5:

$$\tan\theta_{even} = \frac{m-1}{m\alpha_1 + \alpha_2} \tag{D.8}$$

For equal batter angles the result is:

$$\tan\theta = \frac{m-1}{(m+1)\,\alpha} \tag{D.9}$$

Example:

h = 50 m

b_t = 10 m

b_s = 20 m

$\alpha_1 = \alpha_2 = 0.10$

Choose 3 bays ($N = 3$):

D.3: $m = \left(\frac{20}{10}\right)^{1/3} = 1.2599$

D.2: $h_1 = \frac{1.2599 - 1}{1.2599^3 - 1} \cdot 50 = 12.996\ \text{m}$

$h_2 = (1.2599)\cdot(12.996) = 16.374\ \text{m}$

$h_3 = (1.2599)\cdot(16.374) = 20.638\ \text{m}$

D.1: $b_2 = (1.2599)\cdot(10) = 12.599\ \text{m}$

$b_3 = (1.2599)\cdot(12.599) = 15.874\ \text{m}$

$b_4 = (1.2599)\cdot(15.874) = 20.00\ \text{m}$

D.9: $\tan\theta = \dfrac{1.2599-1}{(1.2599+1)\cdot(0.10)} = 1.1501$

$\theta = 48.99^\circ \approx 49^\circ$

Alternatively, choose 4 bays ($N = 4$):

D.3: $m = \left(\dfrac{20}{10}\right)^{1/4} = 1.1892$

D.2: $h_1 = \dfrac{1.1892-1}{1.1892^4-1}\cdot 50 = 9.460 \text{ m}$

$h_2 = (1.1892)\cdot(9.460) = 11.250 \text{ m}$

$h_3 = (1.1892)\cdot(11.250) = 13.378 \text{ m}$

$h_4 = (1.1892)\cdot(13.378) = 15.910 \text{ m}$

D.1: $b_2 = (1.1892)\cdot(10) = 11.892 \text{ m}$

$b_3 = (1.1892)\cdot(11.892) = 14.142 \text{ m}$

$b_4 = (1.1892)\cdot(14.142) = 16.818 \text{ m}$

$b_5 = (1.1892)\cdot(16.818) = 20.00 \text{ m}$

D.9: $\tan\theta = \dfrac{1.1892-1}{(1.1892+1)\cdot(0.10)} = 0.8643$

$\theta = 40.84^\circ$

6 FIXED STEEL SPACE FRAME STRUCTURES – QUASI-STATIC BEHAVIOUR

6.1 Introduction

In this chapter we are specifically concerned with the quasi-static in-place behaviour of fixed steel structures of tubular space frame configuration. Dynamic structural behaviour will be the subject of chapter 9. Quasi-static behaviour automatically excludes discussion of structural response to earthquakes. The structure is hence subject to permanent loads, variable loads and environmental loads due to wind, waves and current. As discussed before, the great majority of offshore structures is of the steel space frame type. It is an effective geometry for providing three-dimensional strength and stiffness, while minimising hydrodynamic loading from waves and currents as a result of its transparency. Experience has shown that the space frame is a very versatile type that is easily adaptable to different requirements. Two typical examples, one for the Gulf of Mexico and one for the northern North Sea, are shown in figures 5.3-4 and 5.3-5.

The three parts of an offshore structure, i.e. the superstructure, the substructure and the foundation piles, form an integral structural system. The interaction between the three parts in respect of the various design aspects was discussed in chapter 5. For the analysis of the structural system it would be most convenient when the three parts could be analysed independently. Generally speaking, this is not difficult to justify for the superstructure. However, the foundation piles and the substructure interact strongly. The discussion in this chapter focuses on the substructure; the superstructure and the foundation piles will only be considered to the extent necessary in connection with the substructure.

The mechanical behaviour of the substructure concerns the strength, stability and deformations of the components of the space frame. These are determined through structural analyses, which are nowadays always performed by computer, using programs that are invariably based on the finite element method. In the course of time several computer program packages for a wide variety of structural problems in the offshore environment have become available; they range from relatively simple to very complicated and sophisticated approaches. With the computing power that is presently available the execution of complicated structural analyses is generally quick and cheap, and it allows accurate determination of the deformations and stresses in the individual members. The point of greatest concern is usually not the computer program itself, but the familiarity of the analyst with the program, and even more specifically his underlying knowledge and understanding of what the program does. One of the gravest disadvantages of the sophisticated computerisation of the calculations is that insight gets increasingly lost. A good and effective offshore engineer needs such insight; he needs fundamental understanding of the environmental loading on offshore structures, of their mechanical behaviour and of the interaction between those parts of the problem. It would seem that only very experienced design engineers with many years of service, who often began their careers at a time that the computing and software infrastructure was not yet so well developed, have retained this skill.

Most structural analysis programs are linear, but some packages include certain non-linear features. Non-linearities in problem formulation can arise from physical aspects in the loading (e.g. wave loading), from physical aspects of the material (e.g. plastic behaviour of steel, concrete or soils), or from large deformations of the structure (resulting in geometric non-linearities). Hydrodynamic loads on steel space frame structures are non-linear with wave height; this is always included in design analyses; all computer programs allow for this. However, for some types of analysis the hydrodynamic loads may need to be linearised. In such cases special attention needs to be paid to the intended use, the manner of linearisation, and the possible application of a correction to the results for potential underestimation of the loading. The substructure is normally treated as a linear structural system, which means that all elements stay nominally within their elastic range. Non-linear behaviour of the substructure is only considered in special cases. However, soil and pile behaviour, together with the interaction between foundation piles and substructure, is distinctly non-linear and must be treated as such.

Large and well known computer program packages for a wide variety of offshore applications are SESAM (developed and supported by DNV, Norway) and ASAS (developed and supported by W.S. Atkins, UK). A smaller package more specifically dedicated to steel space frame structures is SACS (Structural Analysis Computer System, marketed by Engineering Dynamics Inc., USA).

It cannot be emphasised enough that the computer can only assist and not replace the designer or the analyst. There are at least two very good reasons why an engineer must have comprehensive knowledge and understanding of the hydrodynamic, structural and geotechnical aspects that govern the behaviour of an offshore structure. Firstly, before any computer analysis can be performed a preliminary design establishing overall dimensions and initial member sizes must be available. To produce this an engineer should have the ability to make estimates and perform some simple manual calculations at an early design stage. He can only do this if he understands the problem, knows what he is trying to achieve and how he can get there. Experience will, of course, greatly help him with this. Secondly, the results of computer calculations should be checked for correctness. There is always a possibility of undetected error, e.g. due to an unintended but incorrect application of a program or to a simple error in input data. An engineer will therefore have to verify that the results of computer calculations are reasonable and consistent with what he would expect and can rationally explain. He can only make this assessment by his understanding of the main characteristics of loading and structural behaviour in connection with the particular problem under investigation, by recognising and being able to interpret patterns of performance, and by an ability to explain in broad terms the nature and order of magnitude of the results obtained.

The emphasis in these notes is therefore placed on gross simplifications that allow manual or spreadsheet type calculations to be performed. The aim being to make the main features 'visible', thus promoting fundamental understanding. Through suitable modelling and formulation we will attempt to reduce problems to representative and manageable cases that can be solved by application of simple and fundamental principles of applied mechanics. These simplified methods should of course *not* be used for final dimensioning and final design calculations. A more definitive and accurate computer analysis remains necessary. However, the methods described in this chapter enable an engineer to prepare a sound preliminary design as a starting point for a converging design spiral and to perform reasonable checks on his ultimate computer calculations.

Most offshore structures are comparatively stiff in relation to the range of wave frequencies present in natural seas, which is the most relevant and most important source of environmental excitation. Structural response to environmental loading is therefore in most cases static, i.e. at any point in time the response is simply proportional to the load acting at that time. Quasi-static structural behaviour is governed by the equation:

$$\boldsymbol{K}\underline{x}(t) = \underline{F}(t) \tag{6.1-1}$$

where: $\boldsymbol{K}$ = stiffness matrix
$\underline{x}(t)$ = vector of structural deformations
$\underline{F}(t)$ = vector of applied loads.

As the environmental loads included in $\underline{F}(t)$ vary in time, the responses $\underline{x}(t)$ also vary in time. The response is therefore said to be quasi-static, or pseudo-static, rather than just static.

6.2 A two-dimensional idealisation of in-place structural behaviour under extreme storm loading

We are concerned with the quasi-static mechanical behaviour of the structure under the influence of permanent, variable and environmental loads. This problem includes the possible influence of the behaviour of the structure on these loads, as well as structural interactions between the 3 parts of the structural system. For quasi-statically responding structures the environmental loads are in principle equal to the loads that are experienced by a rigid object placed in a flow of air and water. A structural analysis then produces the internal forces in the members of the space frame and the foundation piles under the action of the applied loads. These internal forces (or stresses) must satisfy certain criteria to ensure that there is no foundation failure, and that no element of the structure is overstressed or suffers from instability in the form of member buckling.

In schematic form the overall problem to be investigated is illustrated in figure 6.2-1a. The figure shows 3 blocks on the left that represent the 3 parts of the environment and 3 blocks on the right that represent the 3 parts of the structure. The individual behaviour of each part (i.e. each block in the figure) can, at least in principle, be described by a set of mathematical equations representing its physical and/or mechanical behaviour. Additionally, each part is subject to certain boundary conditions and to influences from the other parts. Looking at the overall problem in a very general manner there may be mutual interactions between all 6 parts. Hence the full formulation of the overall problem constitutes a formidable challenge. However, a full formulation is not necessary for our far more limited purposes. The first question is therefore how we can complete the block diagram of figure 6.2-1a such that we obtain a simplified but adequate model for what we want to know. To answer this question we must look at simplified models to describe the behaviour of each block, as well as at the interactions of a block with other blocks.

Let us first consider the 3 blocks on the left. The air (wind) influences the sea (waves) and in all likelihood there will be interactions between these two blocks. The soil (sea floor) also influences the sea (waves) through the kinematic boundary condition at the sea floor, an effect that is always incorporated in the equations of an appropriate wave model. Conversely, the waves may also have an effect on the morphology of the sea floor: hydrodynamics and morphodynamics interact with each other. However, it is not our intention to investigate the physical environment of the structure. Our interest is purely in the structure's mechanical behaviour. For such offshore engineering applications we only need to specify the environment to the extent that this affects the behaviour of the structure. To achieve this purpose it suffices to specify the 3 parts of the environment as separate inputs; a separate model hence describes each of the inputs. Rather than incorporating complex models that e.g. describe how wave fields are generated and grow under the influence of wind fields, the waves in offshore engineering applications are specified independently and not as a function of wind velocity, fetch length and duration; see section 4.4. Similarly simplified, but fully appropriate models for wind only are presented in section 4.2. For waves only this is done in section 4.4, while the environmental loads are described in sections 4.5 and 4.6. Therefore, all interactions between the blocks on the left-hand side of the completed figure 6.2-1a can be omitted, as shown in figure 6.2-1b.

Let us next consider the three blocks on the right. There will be load transfer and structural interaction between the 3 parts. The substructure supports the superstructure and all

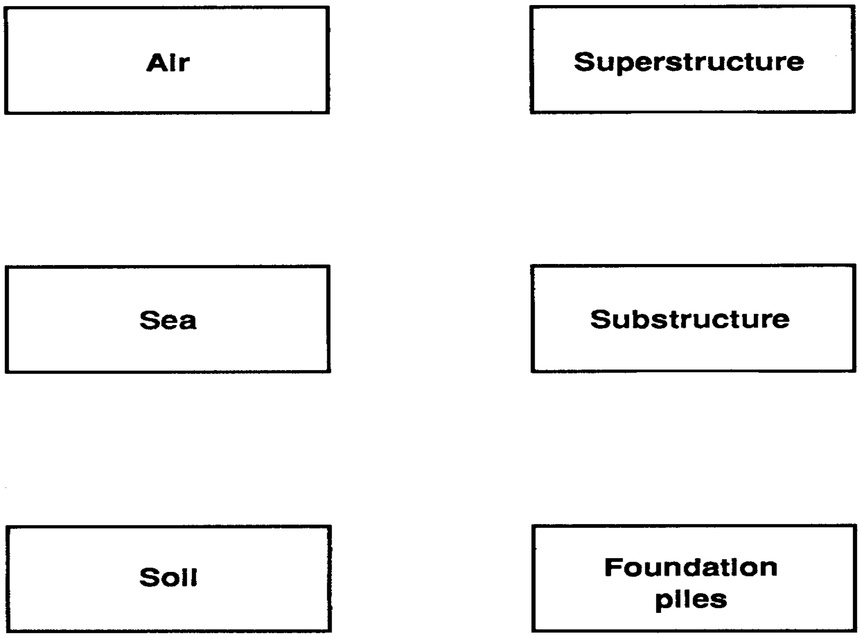

Figure 6.2-1a. Building blocks

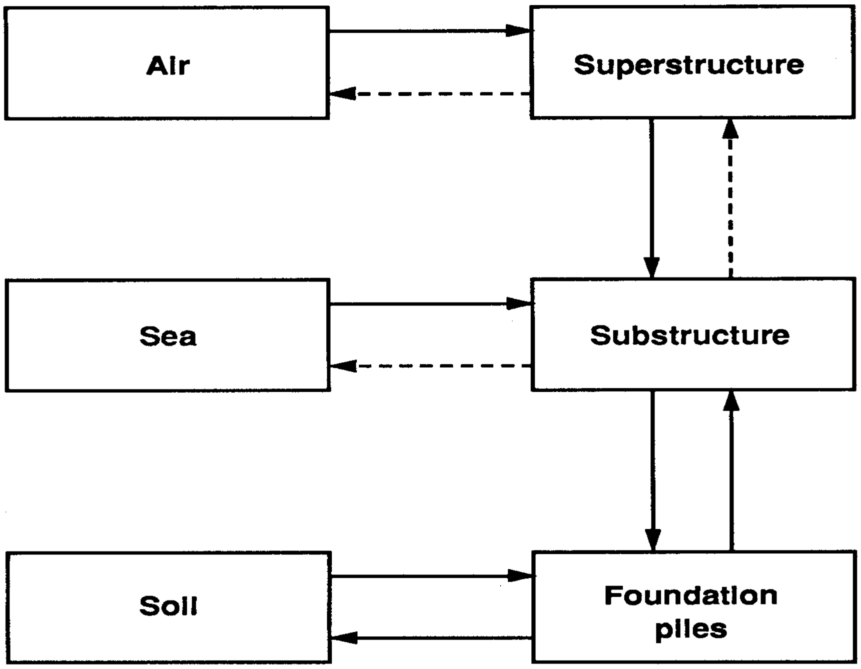

Figure 6.2-1b. Completed model

Figure 6.2-1. Diagrammatic model for the analysis of the in-place structural behaviour of quasi-statically responding steel structures

superstructure loads must thus be transferred to the substructure. For space frame structures, where the deck legs are supported in a number of separate points at the top of a stiff and framed substructure, the structural interaction is usually minimal. Hence, as long as load transfer is correctly modelled the two parts can be analysed independently without making an error of any significance. The fully drawn downward arrow and the dashed upward arrow in figure 6.2-1b reflect this situation. Readers should be reminded, however, that this is not necessarily always the case. They should, for example, think of the structural configuration of a typical concrete gravity structure where the superstructure is supported by 2 or more unbraced columns. In these cases the deck structure forms the upper beam of a portal frame and there is therefore a very strong structural interaction between the sub- and the superstructure. For such structures separate analyses will generally be unacceptable and an integral structural model of substructure and deck(s) is normally necessary to obtain correct predictions of the structure’s global behaviour.

As already mentioned, the structural interaction between the substructure and the foundation piles is strong and should be accounted for. This is reflected by the arrows between them in figure 6.2-1b, which are fully drawn in both directions. To determine the overall (global) behaviour of the substructure a well chosen, but simple structural model may still be sufficient. However, for the internal forces in the piles and in the local substructure elements around the connection with the piles much more detailed structural models with appropriately selected boundary conditions are necessary.

It remains to discuss the interactions between the 3 blocks on the left and the 3 blocks on the right. These interactions concern load transfer only; there are no structural interactions. The air environment may be considered to only act upon the superstructure, the sea environment to only act on the substructure and the soil environment to only act on the foundation piles. For quasi-static structural response the influence of platform deformations on the environmental loads from the air and the sea are negligibly small. Therefore the corresponding arrows from right to left in figure 6.2-1b are dashed rather than drawn; they could have been omitted to further simplify the diagram. This is contrasted by interactions between the pile deformations and the soil. As discussed in section 5.3.4 these interactions are essential and must be modelled correctly. Therefore the arrows between soils and piles are drawn in both directions.

The situation depicted in figure 6.2-1b satisfies our present requirements, but may not adequately represent all conceivable situations; it should therefore not be uncritically generalised. For example, dynamic structural response (that is not considered in this chapter) may be influenced by interactions between the superstructure and the substructure, as well as by interactions between blocks on the left and blocks on the right (e.g. using relative instead of absolute velocities in Morison’s drag load term). Dynamic response thus requires a re-evaluation of the diagram. However, even for quasi-static response there may be special circumstances that require modifications of the above result. For example, if the elevation of the superstructure above still water is not high enough to clear the crest of the highest wave for which the structure is designed, there should also be an arrow between the sea and the superstructure to indicate the loading on the superstructure due to waves.

The general conditions that normally apply to a steel offshore structure have been adequately discussed above; figure 6.2-1b thus forms a suitable basis for a computer analysis of the substructure and its foundation as a statically indeterminate and non-linear system. However, to achieve the learning goals of section 6.1 significant further simplifications to the modelling will be introduced. These simplifications relate to the environmental loading model, the foundation model, as well as the structural model. When the external loads on the structure are known, our approach may be divided into three stages:

a) first, determine the *support reactions* at the sea floor that satisfy the global (static) equilibrium of the structure; these form the interface between the space frame above and the foundation piles below the sea floor;
b) next, while considering the structure initially without any detail as an equivalent and continuous beam rather than as a space frame, determine the distribution of the *shear forces and moments in cross sections* over the height of the structure;
c) finally, determine the *internal forces in the discrete elements* of the actual space frame as well as in the piles.

From now on we will restrict ourselves to the treatment of a two-dimensional plane frame, representing a near vertical frame from the actual three-dimensional space frame. Accordingly, all loads are assumed to act in the plane of the frame. The frame is modelled by its well-known and effective idealisation of line elements along the centrelines of legs and braces. The joints, i.e. the points where the centrelines of the elements intersect, are assumed to be hinges where no moments are transferred. Further, the frame will be loaded exclusively by external point loads on the joints. Under these conditions all elements in the frame experience only axial forces.

The treatment in later sections follows a step by step procedure, with each step only being dealt with to the level of detail required for our purpose. This purpose is an intelligent estimate of the internal forces in the individual elements of the frame (legs and braces) and in the foundation piles.

The 3 stages referred to above may be detailed into 6 distinct steps. These are:
1) determine the applied (external) loads; see section 6.3
2) determine the support reactions at the sea floor; see sections 6.4, 6.5 and 6.6
3) determine the interaction and force transfer between frame and piles; see section 6.7
4) determine the internal forces in the piles; see section 6.7.5
5) determine models for frame behaviour, together with the section forces over the height of the frame when this is considered as a continuous beam; see sections 6.8, 6.9 and 6.10
6) determine the internal forces in the members of the frame when this is considered as an assembly of discrete members; see section 6.11.

Step 1 must obviously precede all structural mechanics considerations, while step 2 corresponds with stage (a) above. Step 3 serves to resolve the interaction between piles and frame, which was identified as an important aspect. After this, step 4 deals with the piles only while steps 5 and 6 subsequently deal with the frame only. If we do not want to investigate the separate behaviour of the foundation piles and the frame we do not need to execute step 3. In that case the piles must be considered as additional members of the ‘expanded’ frame. Steps 3 and 4 can then simply be bypassed. However, for a jacket the distinction in piles and frame is important and the only way to obtain separate pile and leg forces. If this distinction is not made all results will refer to an equivalent member consisting of the leg plus the pile inside. In either case, step 5 covers the above stage (b) while step 6 covers stage (c).

6.3 Modelling of the applied loads.

6.3.1 General

The external loads for the in-place analysis of a quasi-statically responding structure are permanent loads, variable loads and environmental loads; see section 5.5. The permanent and variable loads are almost without exception constant and act vertically. Several different combinations will have to be considered, but these are simply modelled and easily applied in a structural analysis as separate load cases. Permanent and variable loads are represented here in the most rudimentary form as two resultant loads, one for the superstructure and one for the substructure. The environmental loads act both horizontally (wind, current and wave loads) and vertically (wave and current loads on horizontal and inclined members). Wind loads and loads due to current without waves are also considered to be constant with time, but wave loads are definitely time varying. Currents in the presence of waves will not only produce a non-zero mean load but will also affect the magnitude of the time varying part of the hydrodynamic drag loads.

Design environmental conditions are usually selected to be those that occur on average only once in 100 years. This is expressed by saying that the return period of wind, wave and current conditions is 100 years. The concept is in fact somewhat loose, because the 100 year return period may refer to the total *applied loading* experienced as a result of the joint occurrence of certain wind, wave and current conditions, or alternatively *to the wind, wave and current conditions themselves*. As information on environmental data is usually limited, and information that includes the joint occurrence of wind, waves and current is only becoming available during the last several years (say in the 1990s), design will often be based on separate extremes of the 100 year wind, the 100 year wave and the 100 year current. It will be clear that this is always a conservative estimate of the loading with a 100 year return period, resulting from actual combinations of the environmental conditions.

The horizontal wind loads on the deck and all equipment on top often act at a considerable height above water, which contributes to the overturning moment on the structure. These wind loads are transferred to the top of the substructure frames through the deck legs that support the deck. The deck legs are mostly vertical, but occasionally they are a continuation of the inclined legs of the substructure; they may or may not be braced to provide lateral stiffness. Whatever the exact configuration, wind loading on the superstructure manifests itself as horizontal and vertical loads at the top of the substructure. The vertical load at the downwind side is downwards (compressive), while at the upwind side it is upwards (tension). Additionally, as the deck legs and the top of the frame are rigidly connected, there is generally some moment transfer at the support points as well. Wind loads are always included in the structural analysis, which can again be done in the form of one or several separate load cases. Wind loads are nearly always small compared to the hydrodynamic loads; they are typically 10 to 15 % of the total applied horizontal load on the structure.

6.3.2 Permanent and variable superstructure loads

Let the resultant of the permanent and variable loads of the superstructure (the topsides) be denoted by G_T; G_T acts vertically downwards. This is illustrated in figure 6.3-1, where in the interest of generality the angles of the (near) vertical chord members are assumed to be different. The load G_T is carried by the frame at the workpoints A and B of the deck legs. As

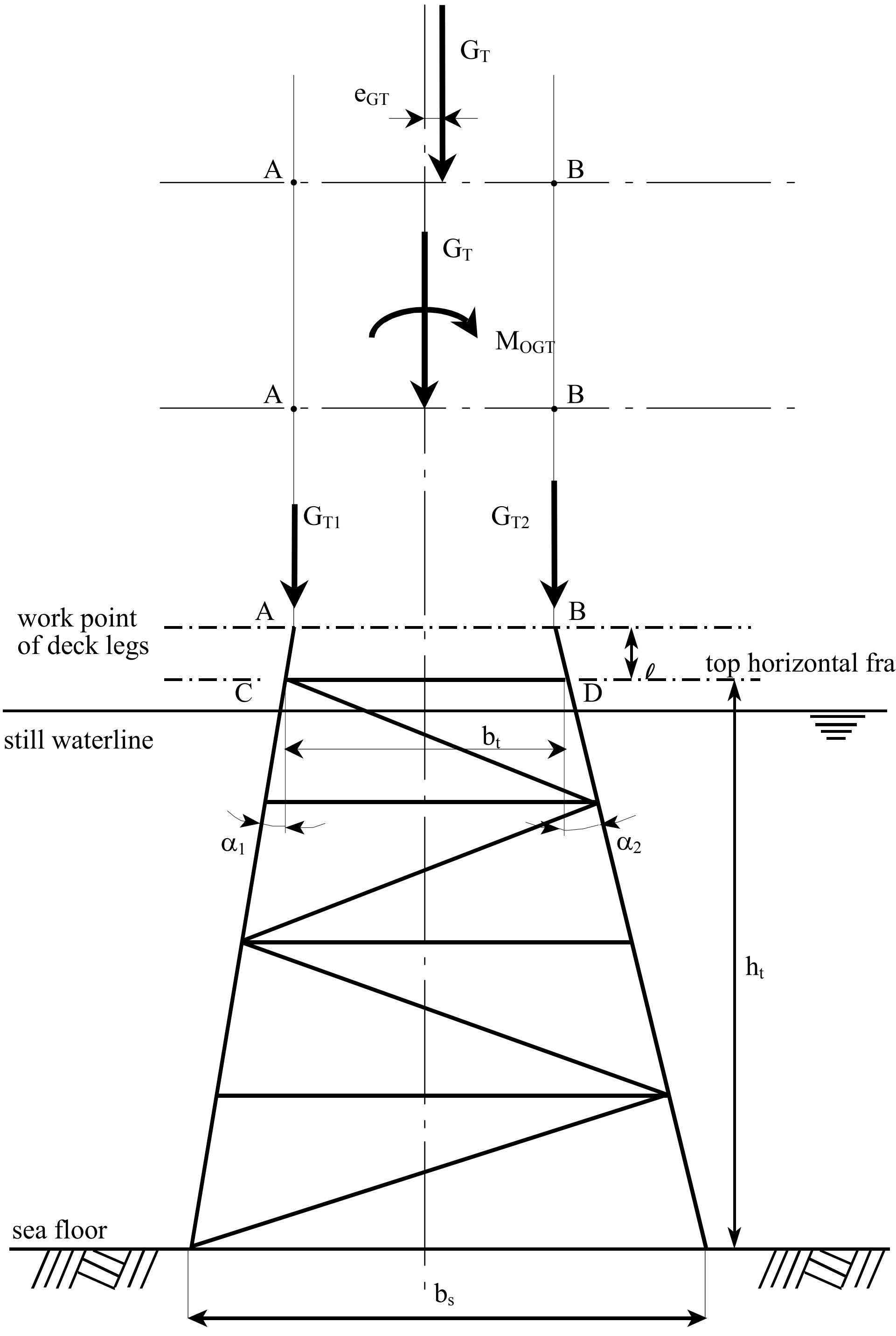

Figure 6.3-1. Permanent and variable load transfer of the superstructure to the frame

the permanent and variable loads of the superstructure will usually have an eccentric distribution, G_T does not act along the centre line of the frame and the loads at A and B will therefore not be the same.

For a global consideration of the equilibrium of the frame and the loading on the foundation the single resultant load G_T is sufficient. We can split G_T in a symmetric part and an anti-symmetric part, resulting in a symmetric load acting at the mid-point of the top brace and a moment, hence:

$$\begin{array}{ll} \text{symmetric load vertically downwards} & G_T \\ \text{moment (clockwise)} & M_{OGT} = G_T \cdot e_{GT} = \tfrac{1}{2}(G_{T2} - G_{T1}) \cdot b_t \end{array} \qquad (6.3\text{-}1)$$

For a consideration of the influence of G_T on the internal forces in the frame we need to look at the situation into a bit more detail. It is now also important where and how G_T is transferred to the frame. The load at workpoint A on the left is G_{T1} and at workpoint B on the right it is G_{T2}. For compatibility with the frame idealisation the loads at points A and B need to be transferred to points C and D, which are the joints of the main (near) vertical chord members and the top horizontal framing level [1]. This introduces a moment $\ell \cdot \tan\alpha$ in which α is a small angle (of the order of 0.1 rad ≈ 5.7°) and ℓ is a small length (of some 2 to 3 m only). Therefore, the product $\ell \tan\alpha$ is small of the second order and these moments may consequently be neglected. We may thus assume that the loads G_{T1} and G_{T2} act at the points C and D instead of at A and B. An alternative representation of the permanent and variable superstructure loads is hence:

$$\begin{array}{lll} \text{at C:} & \text{a vertical load (downwards)} & G_{T1} = (\tfrac{1}{2} - \dfrac{e_{GT}}{b_t}) \cdot G_T \\ \text{at D:} & \text{a vertical load (downwards)} & G_{T2} = (\tfrac{1}{2} + \dfrac{e_{GT}}{b_t}) \cdot G_T \end{array} \qquad (6.3\text{-}2)$$

Both global representations as well as the more detailed single load representation are shown in figure 6.3-1.

At this point it is useful to look at the individual load situation for inclined chords a bit more closely. The vertical loads G_{T1} and G_{T2} may be resolved in two ways, as shown in figure 6.3-2. It depends on the situation which one of these is more convenient for further consideration; the result will obviously be the same. How these loads are transferred into the frame and then down to the foundation depends on the framing pattern. For the pattern sketched in figure 6.3-1 load transfer on the right is illustrated in figure 6.3-3. Vertical equilibrium of joint D directly provides:

$$N_{L2} = \frac{G_{T2}}{\cos\alpha_2}$$

---

[1] It should be noted that for a jacket the workpoints A and B lie on the piles, while for a tower structure they lie on the legs. This difference is important, but for the time being no distinction is made and the (near) vertical members are simply referred to as chords.

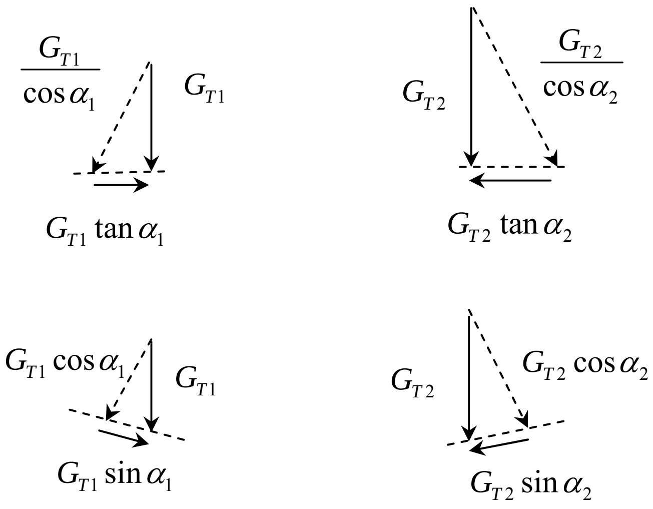

Figure 6.3-2. Two ways to resolve the vertical loads G_{T1} and

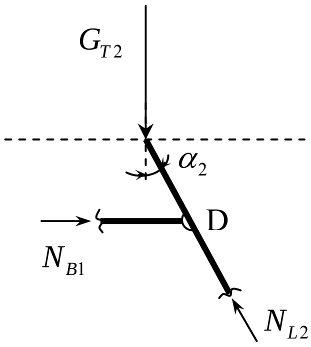

Figure 6.3-3. Load transfer for G_{T2}

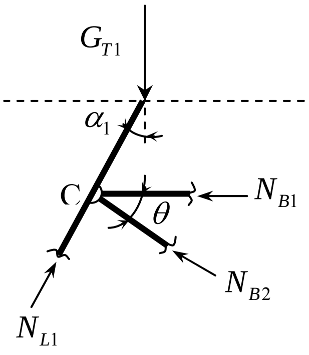

Figure 6.3-4. Load transfer for G_{T1}

while horizontal equilibrium results in:

$$N_{B1} = N_{L2} \sin \alpha_2 = G_{T2} \tan \alpha_2$$

With this information load transfer on the left can now also be solved (two unknowns and two equations), see figure 6.3-4. The analytical results involve trigonometric functions in α_1 and θ, which become rather complicated and are of no real use; however, for each particular situation N_{L1} and N_{B2} are easily calculated numerically. As $\alpha_1 << \theta$ most of G_{T1} will be transferred directly into N_{L1} with the remainder being provided by the vertical component of N_{B2}. It is stressed that for the usual frame idealisation with loads only at the joints and hinged members, the loads in the chords and braces of the frame are purely geometrically determined. They depend on the framing pattern but do not depend on member stiffness. Given the loads in the top bay the process can be continued downwards until the chord loads on the left side and on the right side are transferred to the foundation piles. This is not further discussed at this point, however.

6.3.3 Wind loads on the superstructure

The wind load on the superstructure consists of a resultant horizontal load F_W that acts at a certain height above the still water level. We can represent this load condition again in three different, but entirely equivalent ways; see figure 6.3-5. Firstly, we can model the situation as a global horizontal load F_W at a height h_W above the top horizontal framing level and a moment M_{OW} about the sea floor. This global representation is the simplest and is entirely sufficient for a consideration of the equilibrium of the frame and for the loading on the foundation. Secondly, we can model the load condition as a horizontal load F_W at the level of the workpoints A and B of the deck legs at the top of the frame, plus a moment M_{Wt} (with the subscript t for 'top') about the level of A and B. For the same reasons as in the previous section, the points A and B may be exchanged for the points C and D. Thirdly, we can represent the loading by horizontal and vertical loads (and moments, if necessary) at the joints of the (near) vertical chord members and the top horizontal brace.

Like the load G_T in the previous section, the wind loads on the superstructure are actually transferred to the frame at the workpoints of the deck legs. To determine the influence of the wind loads on the internal forces in the frame later on, the most detailed third representation is chosen. At workpoint A on the left there is a horizontal wind load component $F_{Wh,1}$ and a vertical wind load component $F_{Wv,1}$; additionally, there will generally be a moment M_1 at A. At workpoint B on the right the situation is entirely the same if the index 1 is replaced by an index 2. The loads on the left and on the right are assumed to act in the same directions, except the vertical wind load component $F_{Wv,2}$, which is opposite to $F_{Wv,1}$ because these loads are due to the wind overturning moment M_{Wt}. For unbraced deck legs the horizontal as well as the vertical components of the wind load at A and B are assumed to be equal; there is no rational basis for any other assumption. If the deck legs are braced by e.g. a diagonal member this may no longer be true; the loads at the individual workpoints will then depend on the exact configuration of the deck leg joint. However, as the joint of the diagonal brace and the deck leg will always be above the points A and B, even in this situation the vertical components of the wind load will be the same, but the horizontal components will be different. For generality, and also because the slope of the chord members is assumed to be different, the indices 1 and 2 are therefore maintained where necessary.

The following relationships between the three descriptions are obviously valid (see figure 6.3-5):

$$
\begin{aligned}
F_W &= F_{Wh,1} + F_{Wh,2} \\
M_{OW} &= F_W \cdot (h_t + h_W) = F_W \cdot (h_t + \ell + a) \approx F_W \cdot (h_t + a) \\
F_{Wv,1} &= F_{Wv,2} = F_{Wv} \\
M_{Wt} &= F_W \cdot a = \{b_t - (\alpha_1 + \alpha_2) \cdot \ell\} \cdot F_{Wv} + M_1 + M_2 \approx F_{Wv} \cdot b_t \\
M_{OW} &= M_{Wt} + F_W \cdot (h_t + \ell) \approx F_{Wv} \cdot b_t + F_W \cdot h_t
\end{aligned}
\qquad (6.3\text{-}3)
$$

As ℓ is again a small length and the moments M_1 and M_2 at the workpoints A and B are also very small, the simplifications on the right hand side are valid approximations. As in the previous section, the individual loads can again be assumed to act at the joints C and D of the chord members and the top horizontal brace instead of at A and B.

We thus have 3 equivalent representations of wind loading; a global representation:

a horizontal load (to the right) F_W

a moment about the sea floor (clockwise) $M_{OW} = F_W \cdot (h_t + h_W)$ (6.3-4)

an intermediate representation:

a horizontal load (to the right) F_W

a moment about the top of the frame (clockwise) $M_{Wt} = a \cdot F_W \approx F_{Wv} \cdot b_t$ (6.3-5)

and a detailed representation by horizontal and vertical loads:

at C:	a horizontal load (to the right)	$F_{Wh,1}$	(6.3-6)
	a vertical load (upwards)	F_{Wv}	
at D:	a horizontal load (to the right)	$F_{Wh,2}$	
	a vertical load (downwards)	F_{Wv}	

The three representations are all illustrated in figure 6.3-5.

6.3.4 Hydrodynamic loading on the frame

Hydrodynamic loads due to waves and currents have been discussed in chapter 4, sections 4.5 and 4.6. They are mostly determined using a suitable computer program to perform the laborious calculations, once preliminary member diameters have been chosen. For manual estimates during the early design stages the structure is usually idealised into an assembly of vertical cylinders, which allows numerical calculation of the hydrodynamic loading by means of spreadsheets; see section 4.6.4 and Annex D to chapter 4.

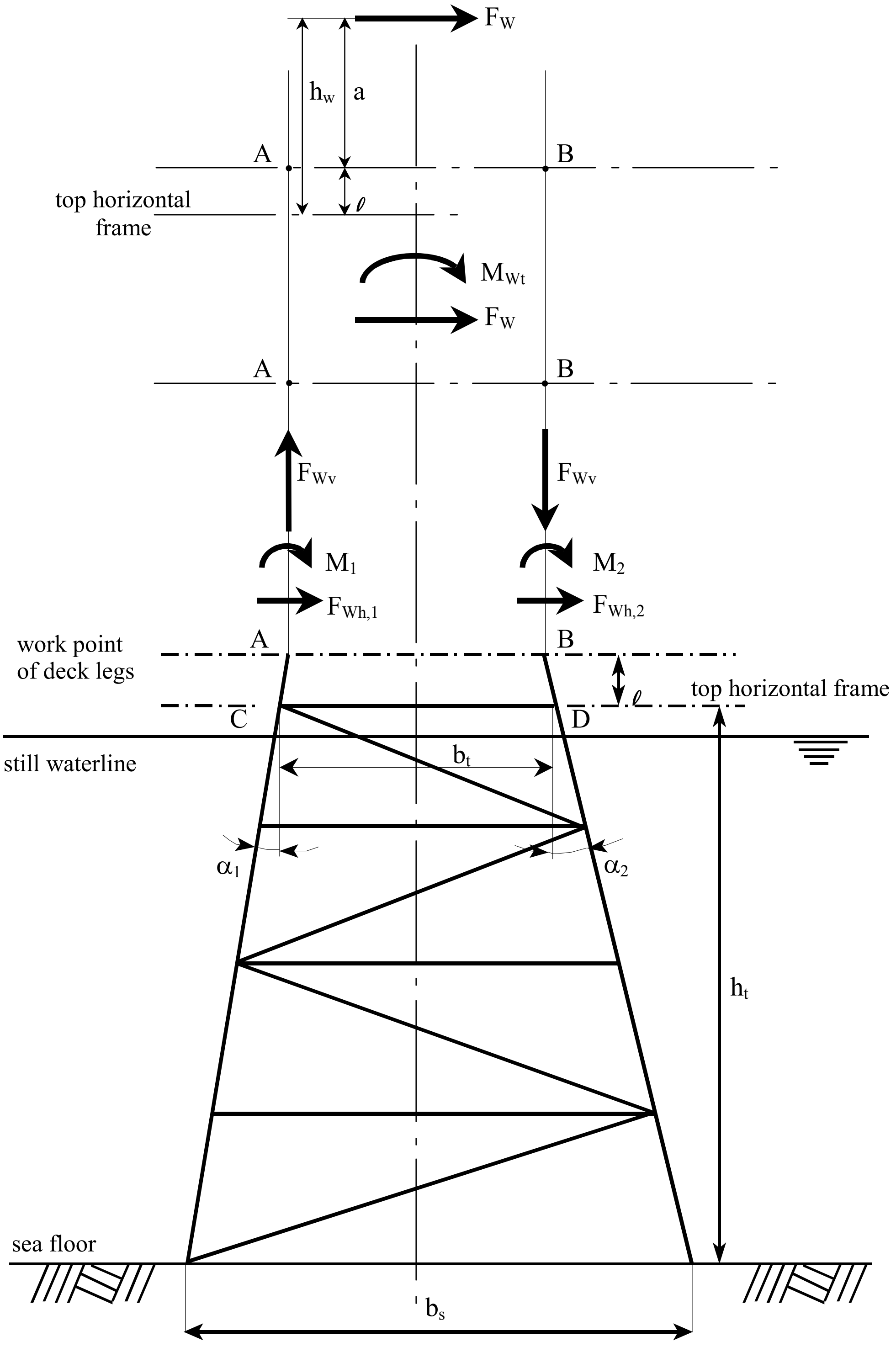

Figure 6.3-5. Transfer of wind loads on the superstructure to the frame

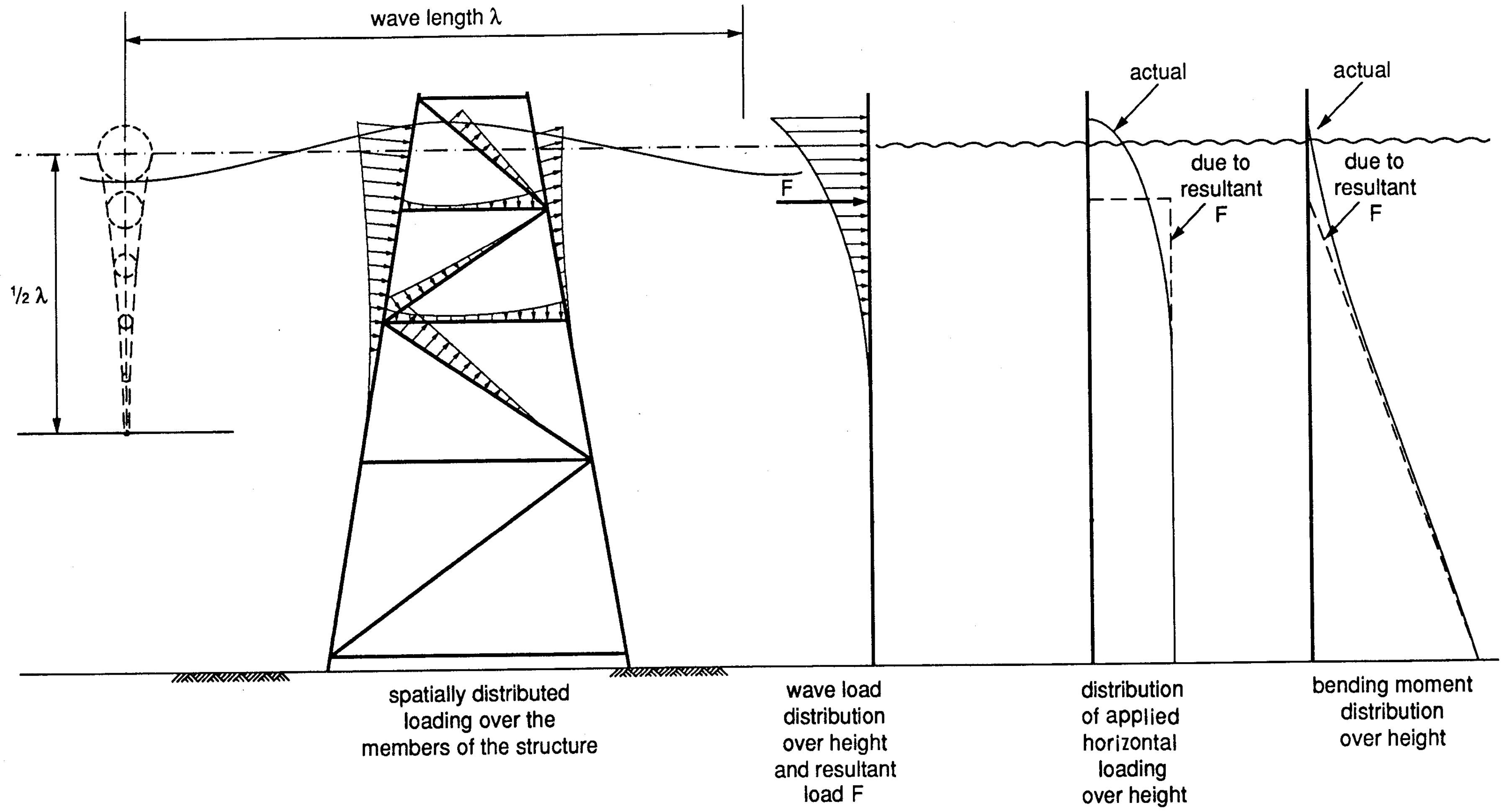
wave length λ
½ λ
F
actual
due to resultant F
actual
due to resultant F
spatially distributed loading over the members of the structure
wave load distribution over height and resultant load F
distribution of applied horizontal loading over height
bending moment distribution over height

Figure 6.3-6. Two-dimensional illustration of the spatial distribution of hydrodynamic loads on a space frame and approximate representation of the predominant horizontal loads by their resultant load F

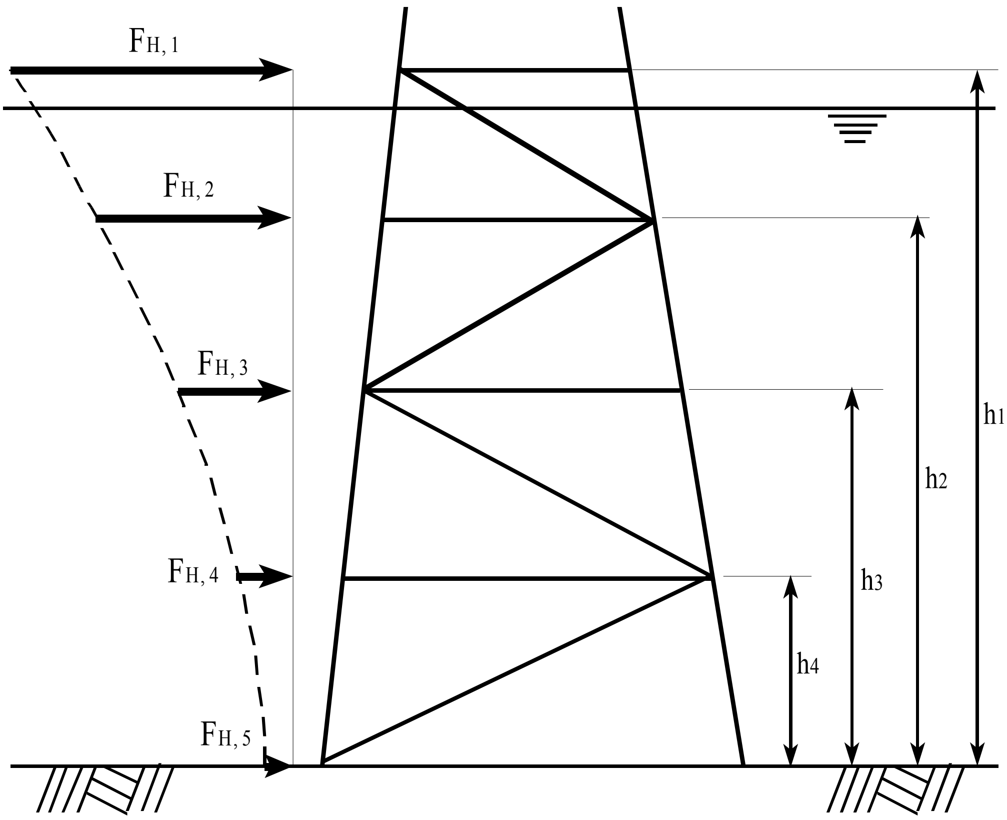

Figure 6.3-7. Application of the horizontal components of the hydrodynamic loading to the frame

In full detail the hydrodynamic loads form a system of temporally and spatially distributed loads over the elements of the space frame. Figure 6.3-6 illustrates the spatial distribution two-dimensionally for a particular point in time. We will now make 3 further simplifications. We will firstly consider the predominant horizontal components of the hydrodynamic loads only. Secondly, as we are concerned with quasi-static structural response under extreme storm loading, the time variation due to the passage of waves is disregarded. The wave is 'frozen' at the moment that it generates the maximum horizontal load and/or the maximum overturning moment on the structure. These two maxima do generally not occur at exactly the same time, but the difference for space frame structures is small. The hydrodynamic load is applied as a static design load with a magnitude equal to the design horizontal load that can be expected to occur during the structure's in-place service life, i.e. the 100 year return period wave plus current load. This is entirely adequate for foundation design and for strength and stability design of most frame members. However, one should be aware that disregarding the time variation would be unacceptable for fatigue considerations and for dynamically responding structures. One should further be aware that at the point in time during the passage of a wave at which the horizontal loads are a maximum, the vertical hydrodynamic loads are by implication a minimum. As the vertical hydrodynamic loads are the main applied loading for horizontal plan framing members, these members cannot be properly considered with the simplified loading model introduced here. The third and final simplification is that the spatially distributed horizontal loading on the individual members of the substructure is replaced by a number of horizontal point loads on the frame. This is in accordance with the macroscopic scale of the present considerations.

The total hydrodynamic loading on the support structure is divided by the number of parallel and (near) vertical frames in the wave direction considered. This results in an applied horizontal load F_H and a corresponding applied moment about the sea floor M_{OH} per frame. In accordance with the frame idealisation adopted, F_H is now applied to the frame in the form of a number of horizontal point loads at the joints, i.e. in most cases at the plan framing levels. Figure 6.3-7 shows the result. Clearly:

$$\begin{aligned} F_H &= \sum_i F_{H,i} \\ M_{OH} &= \sum_i h_i \cdot F_{H,i} \end{aligned} \tag{6.3-7}$$

In this manner all frame members will only experience axial loads. Neglect of the horizontal spatial distribution of the applied loading is of minor significance for the loads in the members of the frame under extreme storm conditions. However, depending on the number of panels in the frame the discretisation of the vertical distribution may be rather crude. This introduces some errors, of which one should again be aware. In the important wave active zone, which extends from the wave crest down to a distance of $\frac{1}{2}\lambda$ below the mean still water surface, all members are subject to distributed hydrodynamic loading between their joints. This is not represented by the proposed loading model and hence not reflected in the axial member forces in the frame idealisation. Member forces in this region should therefore be expected to be inaccurate. Below an elevation of $\frac{1}{2}\lambda$ under the still water surface wave loads do not increase any further and the manner in which the applied loading has been discretised higher up has no longer any influence. Therefore, the proposed load model will only be capable of an accurate description of the behaviour in the lower part of a frame in relatively deep water. In principle it is a rather poor representation of the actual loading situation for shallow water structures. However, *despite these shortcomings it is a very useful model to illustrate major features of the frame's structural behaviour*.

The same loading model is used in [6.3-1] in combination with graphical solution procedures using Cremona diagrams. These graphical procedures were in use from the early/mid 1970s, before the days that computers were available everywhere to solve structural engineering problems. The author of [6.3-1] and the author of this handbook were then both working for Shell in Brunei. Approximate solutions, such as those described in this chapter, were essentially the basis of hand calculations in the early days of offshore engineering. These methods were later extended, computerised and much more extensively used from the early 1980s for application in development studies and to investigate the fatigue and dynamic response of conceptual designs of deep water structures [6.3-2]. For this handbook analytical solutions are preferred over graphical solutions, because the former relate much better to the modern era with desk based computing power and spreadsheets. Also, the common skill of graphical solution methods that once existed amongst engineers is nowadays largely lost. However, whether the axial forces in the frame members are determined graphically or analytically, the results are of course the same.

6.3.5 More general modelling of hydrodynamic loads

The hydrodynamic load model discussed in the previous section is specifically intended for quasi-static structural response in extreme storm conditions. Before leaving the subject it is useful to stand back and review the modelling requirements and available options from the much broader perspective of an overall analysis methodology, rather than the narrow objective pursued here. Such a broader perspective combines considerations discussed in chapters 4, 5 and 6. A schematic decision procedure to select a particular wave load modelling option for different types of application is shown in figure 6.3-8, which has been copied from [6.3-3]. This diagram is a good and rational guide, but it should be appreciated that in a particular set of circumstances the choice may still be subject to considerable debate and may not strictly follow the guidelines given in the figure. The responsibility for the best possible option in each individual case lies with the analyst and with the analyst only.

6.3.6 Permanent and variable substructure loads

The permanent and (where relevant) variable loads of the substructure itself also act vertically, but are distributed over the substructure. Let G_S be the total permanent and variable load of the submerged substructure. The point where G_S is transferred to the foundation piles depends on the type of structure [1]. For a tower G_S is always transferred to the piles at the base, while for a jacket G_S is transferred to the piles at the top. The latter observation is explained by the fact that it is normally assumed that there is some erosion of the sea floor after installation of the structure, which undermines the original bottom support. After some time the jacket is thus assumed to hang off the piles.

In complete analogy with section 6.3.2 the permanent and variable loads of the substructure are either given as a global load condition:

---

[1] See section 5.3.4 and Annex C to chapter 5 for definitions and a discussion of jacket and tower type structures.

symmetric load vertically downwards G_S

moment (clockwise) for a tower $M_{OGS} = G_S \cdot e_{GS} = \frac{1}{2}(G_{S2} - G_{S1}) \cdot b_S$ (6.3-8)

moment (clockwise) for a jacket $M_{OGS} = G_S \cdot e_{GS} = \frac{1}{2}(G_{S2} - G_{S1}) \cdot b_t$

or as a more detailed representation by vertical loads. For a *tower* this results in:

on the left and at the sea floor (downwards) $G_{S1} = (\frac{1}{2} - \frac{e_{GS}}{b_s}) \cdot G_S$

on the right and at the sea floor (downwards) $G_{S2} = (\frac{1}{2} + \frac{e_{GS}}{b_s}) \cdot G_S$ (6.3-9)

and for a *jacket* (where any moment transfer to the top of the piles as a result of G_S is again neglected):

on the left and at the top brace at C (downwards) $G_{S1} = (\frac{1}{2} - \frac{e_{GS}}{b_t}) \cdot G_S$

on the right and at the top brace at D (downwards) $G_{S2} = (\frac{1}{2} + \frac{e_{GS}}{b_t}) \cdot G_S$ (6.3-10)

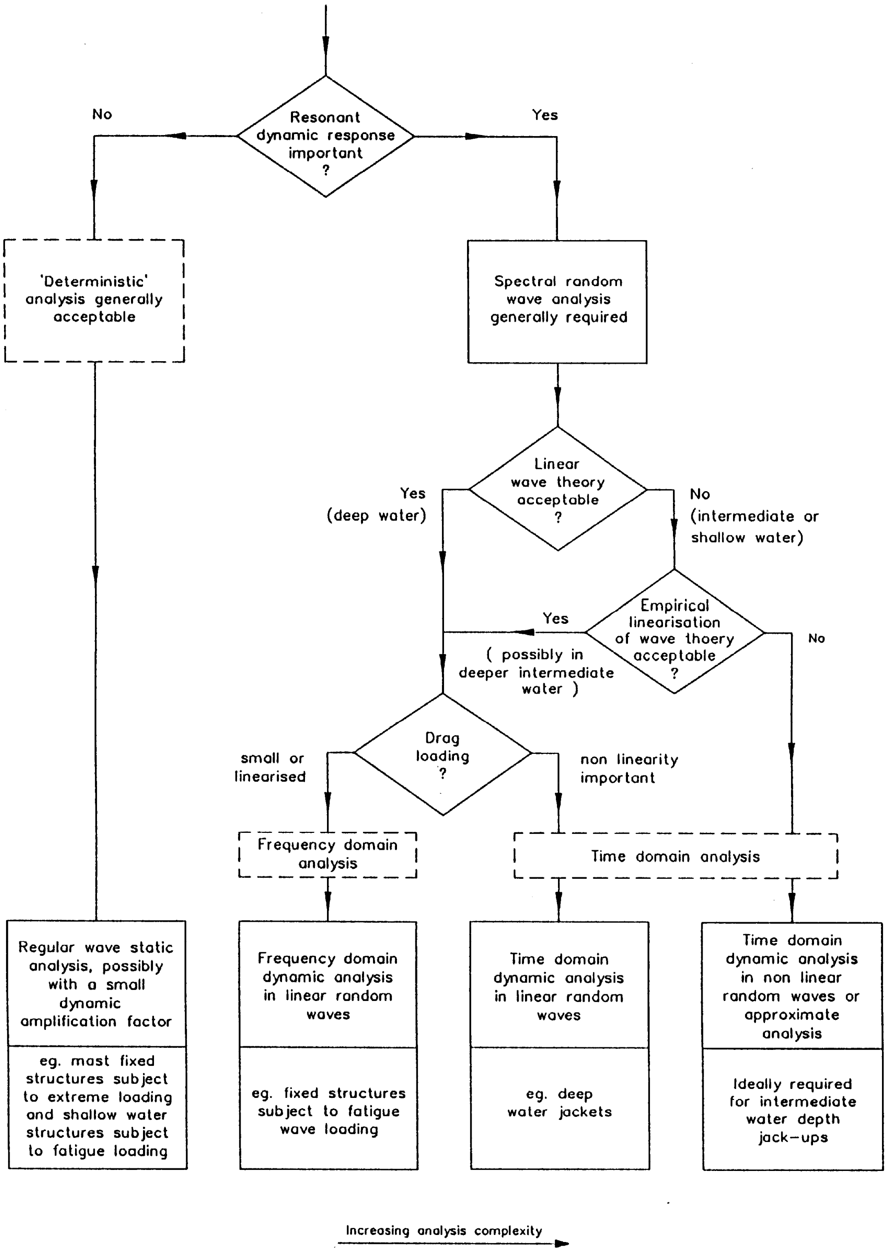
Resonant dynamic response important ?
No
Yes
'Deterministic' analysis generally acceptable
Spectral random wave analysis generally required
Linear wave theory acceptable ?
Yes (deep water)
No (intermediate or shallow water)
Empirical linearisation of wave thoery acceptable ?
Yes
(possibly in deeper intermediate water)
No
Drag loading ?
small or linearised
non linearity important
Frequency domain analysis
Time domain analysis
Regular wave static analysis, possibly with a small dynamic amplification factor
eg. most fixed structures subject to extreme loading and shallow water structures subject to fatigue loading
Frequency domain dynamic analysis in linear random waves
eg. fixed structures subject to fatigue wave loading
Time domain dynamic analysis in linear random waves
eg. deep water jackets
Time domain dynamic analysis in non linear random waves or approximate analysis
Ideally required for intermediate water depth jack-ups
Increasing analysis complexity

Figure 6.3-8. Schematic of decision procedure for the selection of a wave load modelling option for different types of application (from [6.4], figure 6.68)

6.3.7 Total applied loading in extreme storm conditions

The loads in the preceding sections are representative loads in the context of the LRFD design method discussed in section 5.6. Therefore they must be multiplied by partial load factors before they can be used as design loads. The total applied global loading on a (near) vertical frame as well as on the foundation in extreme storm conditions is thus the sum of all the global loads in sections 6.3.2 to 6.3.6, each factored by its appropriate partial load factor. Summing equations 6.3-1, 6.3-4, 6.3-7 and 6.3-8 we obtain for the (horizontal) base shear F_B and the (vertical) permanent and variable load F_V :

$$F_B = \gamma_E \cdot F_H + \gamma_E \cdot F_W = \gamma_E \cdot (F_H + F_W) \tag{6.3-11}$$

$$F_V = \gamma_G \cdot G = \gamma_G \cdot (G_T + G_S) \tag{6.3-12}$$

and for the overturning moment M_O about the sea floor,
for a *tower*:

$$\begin{aligned} M_O &= \gamma_E \cdot M_{OH} + \gamma_E \cdot M_{OW} + \gamma_G \cdot M_{OGT} + \gamma_G \cdot M_{OGS} = \\ &= \gamma_E \cdot (M_{OH} + M_{OW}) + \gamma_G \cdot \tfrac{1}{2}(G_{T2} - G_{T1}) \cdot b_t + \gamma_G \cdot \tfrac{1}{2}(G_{S2} - G_{S1}) \cdot b_s \end{aligned} \tag{6.3-13}$$

and for a *jacket*:

$$\begin{aligned} M_O &= \gamma_E \cdot M_{OH} + \gamma_E \cdot M_{OW} + \gamma_G \cdot M_{OGT} + \gamma_G \cdot M_{OGS} = \\ &= \gamma_E \cdot (M_{OH} + M_{OW}) + \gamma_G \cdot \tfrac{1}{2}(G_{T2} - G_{T1}) \cdot b_t + \gamma_G \cdot \tfrac{1}{2}(G_{S2} - G_{S1}) \cdot b_t \end{aligned} \tag{6.3-14}$$

where: F_B = total horizontal applied loading on the frame
= total horizontal applied loading on the foundation (per frame)
= base shear (per frame) [N]
F_V = total vertical applied loading on the frame [N]
F_H = hor. component of hydrodynamic loading on the substructure (per frame) [N]
F_W = horizontal wind loading on the superstructure (per frame) [N]
G = total permanent and variable loading on the frame [N]
G_T = permanent and variable loading of the superstructure (per frame) [N]
G_S = permanent and variable loading of the substructure (per frame) [N]
$G_{T1,2}$ = permanent and variable loads of the superstructure at workpoint 1 or 2 [N]
$G_{S1,2}$ = permanent and variable loads of the substructure at workpoint 1 or 2 (for a jacket) or at the sea floor (for a tower) [N]
M_O = overturning moment about the sea floor (per frame) [Nm]
M_{OH} = overt. moment due to hydrodynamic loads about the sea floor (per frame) [Nm]
M_{OW} = overt. moment due to wind loads about the sea floor (per frame) [Nm]
γ_E = partial load factor for environmental loads [-]
γ_G = partial load factor for permanent and variable loads [-]
b_t = length of the top horizontal brace [m]
b_s = length of the bottom horizontal brace at the sea floor [m]

These results show that the base shear F_B is completely unaffected by the permanent and variable loads, as was to be expected. The analogous result that the vertical load F_V ., which is applied to the frame and transmitted to the foundation does not depend on the environmental loading is only true for the simplified model adopted in this handbook; in reality environmental loading also has (small) vertical contributions. The overturning moment M_O is influenced by the environmental loading as well as the permanent and variable loading when the latter is eccentrically applied. More in particular:

- when the eccentricity is on the far side from where the waves approach the structure (positive eccentricity), i.e. when $G_{T2} + G_{S2} > G_{T1} + G_{S1}$, the overturning moment is increased;
- conversely, when the eccentricity is on the near side (negative eccentricity), i.e. when $G_{T1} + G_{S1} > G_{T2} + G_{S2}$, the overturning moment is reduced.

The principles of load transfer of vertical loads applied at the top of the frame to the chord and brace members of the frame were described at the end of section 6.3.2.

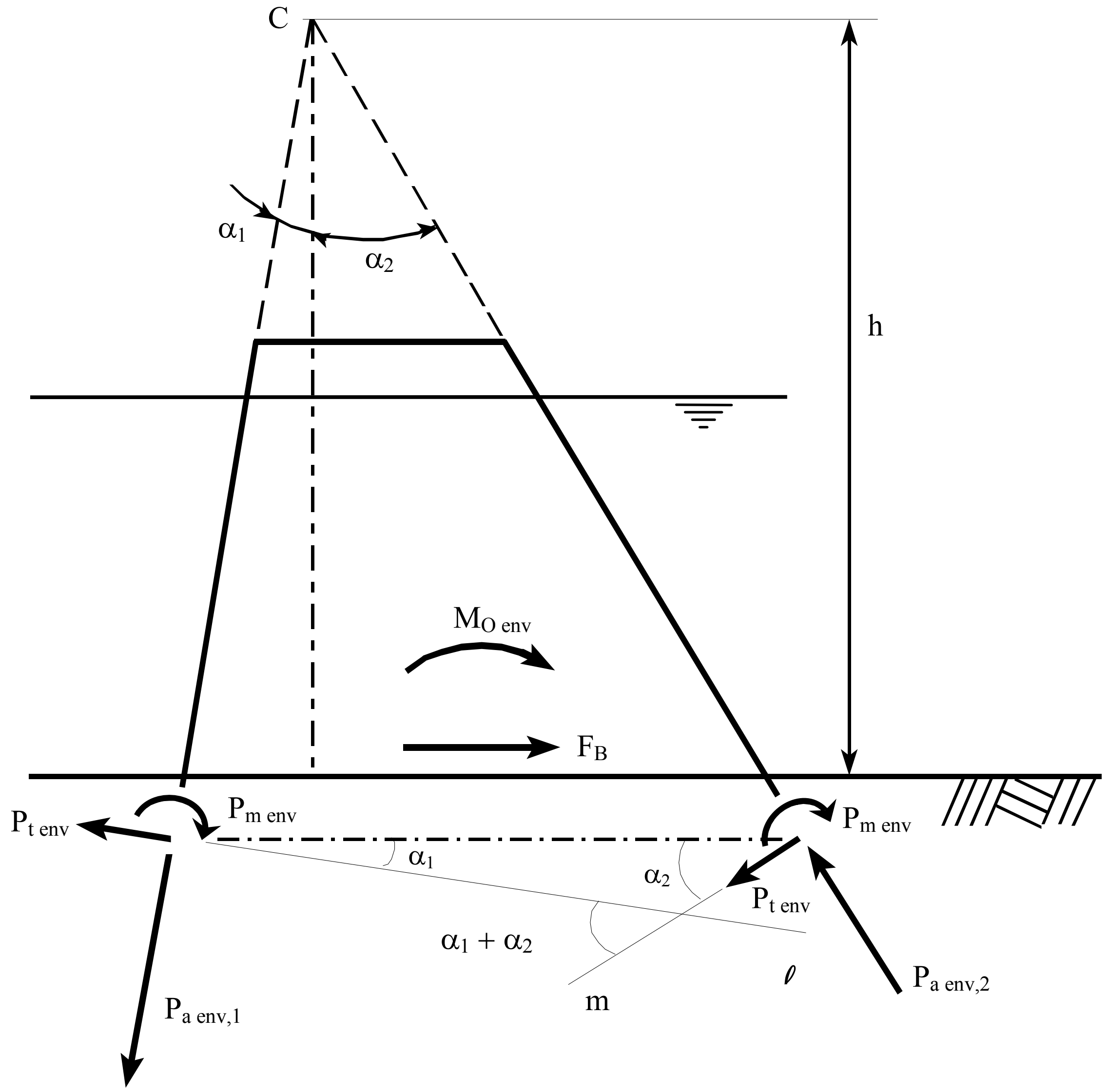

Figure 6.4-1. Support reactions at the sea floor due to environmental loading by wind, waves and current

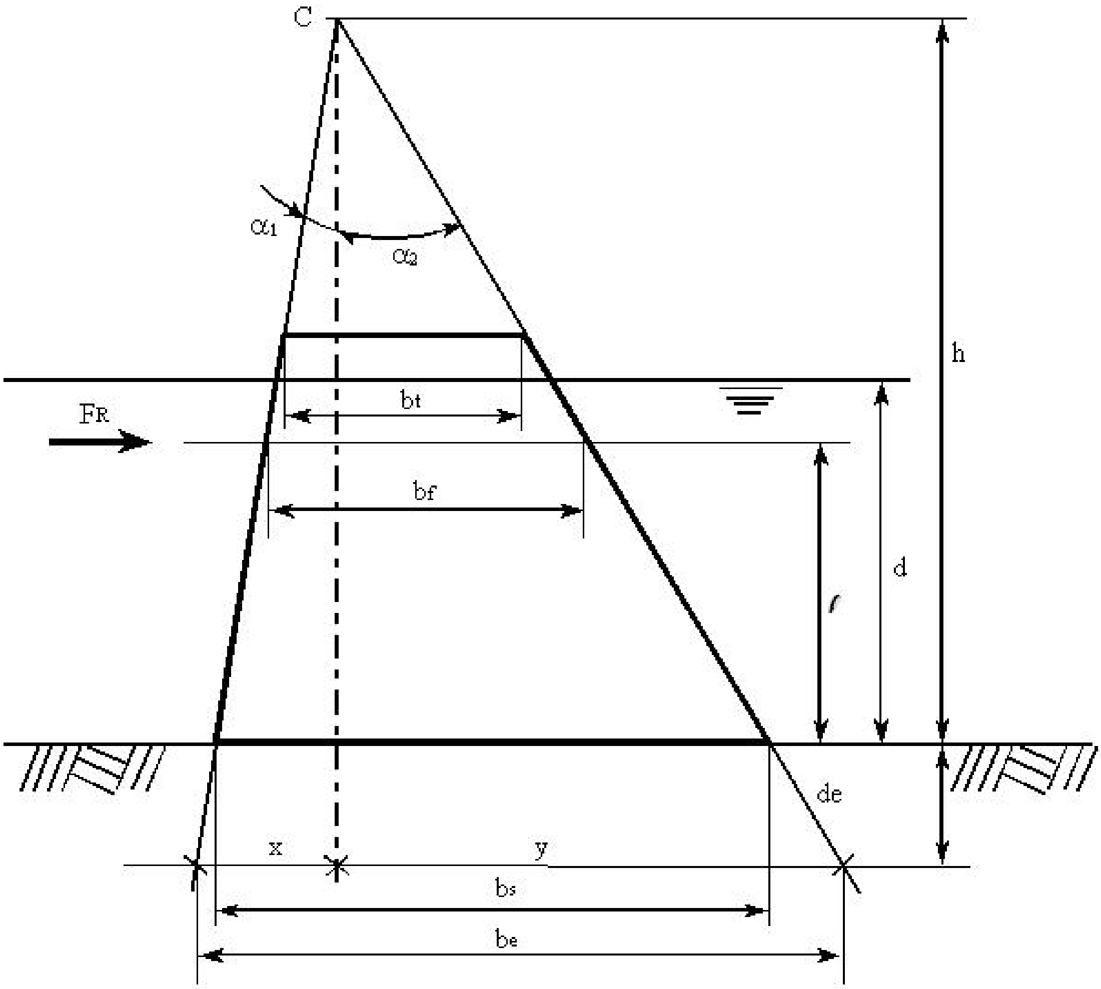

Figure 6.4-2. Geometrical relationships

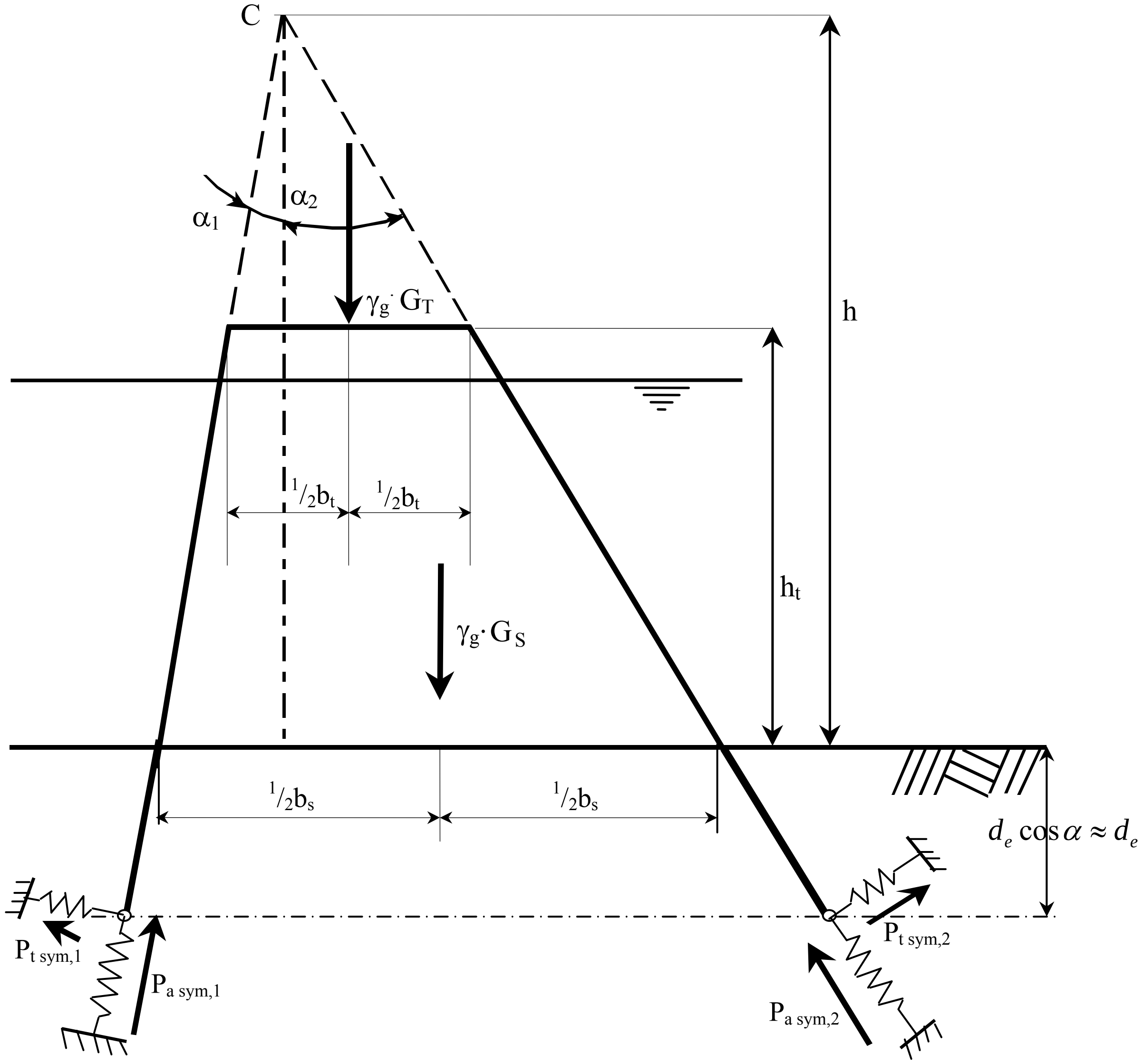

Figure 6.4-3. Support reactions at the sea floor due to symmetric part of the permanent and variable loading (tower structure)

6.4 The support reactions for the frame

6.4.1 Introduction

As noted earlier, the structural interaction between the substructure and the foundation piles is strong. Therefore these two parts of the structural system should in fact be analysed as one whole. However, this is not only inconvenient but it also becomes especially complicated as the structure is normally treated linearly while the foundation-soil behaviour is distinctly non-linear. Separate analyses of structure and foundation piles are therefore preferred and also possible. These separate analyses can give a good approximation of the behaviour, provided that the boundary conditions where the two separate parts are connected are well chosen. A natural point of separation is a cross section at the sea floor underneath the structure. The boundary conditions then consist of the forces and deformations at the top of the piles, which must match the forces and deformations at the base of the structure. For a linear analysis of the structure it is necessary to linearise the pile forces and deformations. The linearised properties for each pile are determined on the basis of the results of a separate non-linear analysis of the pile alone; see section 6.6. It is therefore very important to make the best possible estimate of the forces and moments at the top of the piles, because the linearisation will only be correct at the particular values for which the linearisation is performed. This means that, after the analyses, there is always a need to check that compatibility between structure and foundation has indeed been achieved. If this is not the case then a new linearisation should be made and the analyses should be repeated with the modified linearised properties until satisfactory agreement is obtained. This iterative procedure was already referred to in section 5.3.5 and is shown in figure 5.3-13.

6.4.2 Reactions at the sea floor

With the applied loads at the sea floor given by equations 6.3-11 to 6.3-14 we can now determine the support reactions for the frame that are provided by the foundation piles. In the interest of clarity and transparency of the overall problem, we will build up the solution by considering three separate cases: horizontal loading due to the environmental loads from wind, waves and current; vertical loading due to the symmetric part of the permanent and variable loads; and vertical loading due to the anti-symmetric part of the permanent and variable loads. The total support reactions are then assumed to be the sum of these three separate solutions. Note that strictly speaking this will not be true as pile-soil behaviour is non-linear; therefore superimposition is in fact not valid. However, for preliminary design efforts and for the educational purposes pursued here this is fully acceptable.

The three separate cases are shown in figures 6.4-1, 6.4-3 and 6.4-4, respectively. We will assume that there is one pile on either side. The piles are further assumed to be inclined with the same unequal batter angles α_1 and α_2 as the frame chord members above them. This will nearly always be so, but in some cases piles for tower structures may be installed vertically, even though the structural chord members of the frames are inclined. The results obtained hereafter do not directly apply to this latter situation, but analogous results using the same procedure as followed here can easily be derived.

The support reactions for the frame are the internal forces in the piles in a section at the sea floor just underneath the frame. In the pile cross section on either side there are 3 unknown forces, i.e. an axial force, a shear force and a moment. These forces refer to the local co-ordinate system of the pile with the $x-$axis along the centre line of the pile. For the frame an earth fixed global co-ordinate system with horizontal and vertical axes is usually chosen; its origin is normally at the sea floor. Either of these co-ordinate systems may be used; the forces in the other system can then always be derived by transformation. It depends on circumstances, and to a degree on user preference, which system is best employed.

In this section 6.4 we will work with forces in the local pile co-ordinate system. Forces at the top of the pile are always indicated by P; axial forces get a subscript $a\,(P_a)$, transverse or lateral forces a subscript $t\,(P_t)$, while moments are given a subscript $m\,(P_m)$. Horizontal and vertical forces in the global co-ordinate directions are similarly given a subscript $h\,(P_h)$ and $v\,(P_v)$, respectively.

There are a total of 6 unknowns and only 3 equilibrium equations; the problem is therefore 3 times statically indeterminate and cannot be solved without making further assumptions. When working in the local pile co-ordinate system the usual assumptions are that:

$$\begin{aligned} P_{t,1} &= P_{t,2} = P_t \\ P_{m,1} &= P_{m,2} = P_m \end{aligned} \tag{6.4-1}$$

and that there is a simple relationship between P_m and P_t, which can be expressed as:

$$P_m = d_e \cdot P_t \tag{6.4-2}$$

d_e relates to a small and fictitious distance along the pile below the sea floor. It indicates the distance to an artificial lower point of the pile, to which the sea floor reaction forces can be moved under the condition that the pile moment becomes zero, as will be discussed in section 6.6.

Note that no assumption is made about the two axial forces. Under the total applied loading these will usually be opposite in direction but not equal in magnitude. For the time being the above assumptions will just be adopted; they will be justified later, see section 6.6. They reduce the number of unknowns to 3, i.e. $P_{a,1}$ and $P_{a,2}$ and P_t, and these can readily be solved from the three equilibrium equations.

Two further observations should be made. Firstly and as noted earlier, in this section 6.4 the reaction forces are determined in the local pile co-ordinate system. The alternative option of working in the global frame co-ordinate system is an equally possible method that is often used, while adopting a slightly different set of assumptions for the pile forces at the top of the pile to make the problem statically determinate. One of these assumptions is that the internal pile moment may be neglected in the overall moment equilibrium of the substructure as a whole; $P_m = 0$ then replaces equation 6.4-2. This method will be discussed in section 6.5. Secondly, the artificial pile support model adopted here consists of a ‘dummy member’ with a hinge at a distance d_e along the pile and below the sea floor. There is also an alternative pile support model in use that employs a clamped (built-in) ‘dummy member’ instead of a hinged one; this latter ‘dummy member’ to represent the pile is built-in at a point $2d_e$ down the pile. This will be further discussed in section 6.6.

Case 1: Horizontal loading due to the environment

We will first look at the case of environmental loading only, see figure 6.4-1. To indicate that applied loads and support forces are both due to environmental loading they are given an additional subscript *env*. As the base shear F_B has no other contributions than from environmental loads $F_{B\,env} = F_B$, and as no confusion can arise we will omit the subscript *env* for F_B. Horizontal, vertical and moment equilibrium about some arbitrary point involves all 3 unknowns and makes the solution algebraically rather cumbersome. By a more intelligent use of the equilibrium equations the solution becomes a lot simpler. Therefore we will first apply moments about point C, the intersection point of the piles high above the frame. Moment equilibrium now involves $P_{t\,env}$ as the only unknown. Introducing the notation:

$$M_{O\,env} = M_{OH} + M_{OW}$$

we obtain:

$$\sum M_C = \gamma_E \cdot M_{O\,env} - \gamma_E \cdot F_B h + 2d_{e\,env} P_{t\,env} + P_{t\,env}\frac{h}{\cos\alpha_1} + P_{t\,env}\frac{h}{\cos\alpha_2} = 0$$

$$P_{t\,env}\left(\frac{h}{\cos\alpha_1} + \frac{h}{\cos\alpha_2} + 2d_{e\,env}\right) = \gamma_E \cdot (F_B\,h - M_{O\,env})$$

which results in:

$$P_{t\,env} = \frac{h\cos\alpha_1 \cdot \cos\alpha_2}{h\cos\alpha_1 + h\cos\alpha_2 + 2d_{e\,env} \cdot \cos\alpha_1 \cdot \cos\alpha_2} \cdot \gamma_E \cdot \left(F_B - \frac{M_{O\,env}}{h}\right) \qquad (6.4\text{-}3)$$

Next, equilibrium along the line m in figure 6.4-1 involves only $P_{t\,env}$ (now known) and $P_{a\,env,1}$:

$$\sum_m F = \gamma_E \cdot F_B \cos\alpha_2 - P_{t\,env}\cos(\alpha_1 + \alpha_2) - P_{a\,env,1}\sin(\alpha_1 + \alpha_2) - P_{t\,env} = 0$$

or:

$$P_{a\,env,1} = \gamma_E \cdot F_B \cdot \frac{\cos\alpha_2}{\sin(\alpha_1 + \alpha_2)} - P_{t\,env} \cdot \frac{1 + \cos(\alpha_1 + \alpha_2)}{\sin(\alpha_1 + \alpha_2)} \qquad (6.4\text{-}4)$$

Similarly, equilibrium along line ℓ results in:

$$P_{a\,env,2} = \gamma_E \cdot F_B \cdot \frac{\cos\alpha_1}{\sin(\alpha_1 + \alpha_2)} - P_{t\,env} \cdot \frac{1 + \cos(\alpha_1 + \alpha_2)}{\sin(\alpha_1 + \alpha_2)} \qquad (6.4\text{-}5)$$

The angles α_1 and α_2 are small, typically 0.1 rad or 5.7°; their sum thus remains small as well. We may therefore write $\sin\alpha \approx \alpha$, which is correct to a deviation of up to only +1.5% for $\alpha = 0.3$, and $\cos\alpha \approx 1.0$, which is slightly less accurate with an error of up to +4.7% for $\alpha = 0.3$. Using these approximations in the equations 6.4-3 to 6.4-5 we obtain:

$$\begin{aligned}
P_{t\,env} &= \frac{1}{2}\cdot\frac{h}{h+d_{e\,env}}\cdot\gamma_E\cdot\left(F_B-\frac{M_{O\,env}}{h}\right)\\
P_{m\,env} &= d_{e\,env}\cdot P_{t\,env}\\
P_{a\,env,1} &= \frac{\gamma_E\cdot F_B-2P_{t\,env}}{\alpha_1+\alpha_2}\\
P_{a\,env,2} &= \frac{\gamma_E\cdot F_B-2P_{t\,env}}{\alpha_1+\alpha_2}
\end{aligned} \tag{6.4-6}$$

For the numerator of the axial forces we can write, using $P_{t\,env}$ from equation 6.4-6:

$$\gamma_E\cdot F_B-2P_{t\,env}=\gamma_E\cdot F_B\left(1-\frac{h}{h+d_{e\,env}}\right)+\frac{\gamma_E\cdot M_{O\,env}}{h+d_{e\,env}}=\gamma_E\cdot\frac{F_B\cdot d_{e\,env}+M_{O\,env}}{h+d_{e\,env}} \tag{6.4-7}$$

With the same small angle approximation we can express α_1 and α_2 in geometrical properties of the frame as shown in figure 6.4-2:

$$\begin{aligned}
\alpha_1 &\approx \tan\alpha_1=\frac{x}{h+d_e}\\
\alpha_2 &\approx \tan\alpha_2=\frac{y}{h+d_e}\\
\alpha_1+\alpha_2 &\approx \frac{x+y}{h+d_e}=\frac{b_e}{h+d_e}
\end{aligned} \tag{6.4-8}$$

Introducing these results into 6.4-6 gives the following set of expressions:

$$\begin{aligned}
P_{t\,env} &= \frac{1}{2}\cdot\frac{h}{h+d_{e\,env}}\cdot\gamma_E\cdot\left(F_B-\frac{M_{O\,env}}{h}\right)\\
P_{m\,env} &= d_{e\,env}\cdot P_{t\,env}\\
P_{a\,env,1} &= \gamma_E\cdot\frac{M_{O\,env}+F_B\cdot d_{e\,env}}{b_e}\\
P_{a\,env,2} &= \gamma_E\cdot\frac{M_{O\,env}+F_B\cdot d_{e\,env}}{b_e}
\end{aligned} \tag{6.4-9}$$

For small angles α_1 and α_2 the results in equations 6.4-6 and 6.4-9 are alternative and equivalent formulations (but may as a result of the approximations made not provide numerically truly identical results). They show that for environmental loading only, and under the modelling assumptions and small angle approximations made, not only the lateral but also the axial pile forces are equal, despite the unequal batter angles. It is noteworthy that these results do *not* entirely satisfy the equilibrium equations in the global co-ordinate system! Using the expressions 6.4-6 it is directly shown that horizontal equilibrium is identically met:

$$\sum_{hor}F=\gamma_E\cdot F_B-2P_{t\,env}-\alpha_1 P_{a\,env,1}-\alpha_2 P_{a\,env,2}\equiv 0$$

but that vertical equilibrium is only satisfied by approximation:

$$\sum_{vert} F = \alpha_1 P_{t\,env} - P_{a\,env,1} - \alpha_2 P_{t\,env} + P_{a\,env,2} = (\alpha_1 - \alpha_2) P_{t\,env}$$

This is only identically zero for $\alpha_1 = \alpha_2$. The non-zero difference $(\alpha_1 - \alpha_2)$ involves a small error, which is the result of the modelling assumptions and the approximations made. Moment equilibrium suffers from similar small errors. These observations imply in fact that the assumptions of equations 6.4-1 and 6.4-2 are not compatible with $\alpha_1 \neq \alpha_2$, which is no great surprise. It is a slightly undesirable shortcoming due to the somewhat less strict modelling assumptions, but not uncommon for engineering models. Thus, the assumptions 6.4-1 and 6.4-2 are strictly only valid for equal batter angles, but they are applied here for unequal batter angles as well. The model is hence not fully internally consistent. This also means that slightly different ways of deriving the relationships may end up with slightly different results.

It is of some theoretical interest to develop the relationships also for $\alpha_1 = \alpha_2 = \alpha$, but without using the small angle approximation. This provides the exact expressions for the pile forces for a symmetric frame (still given the assumptions in equations 6.4-1 and 6.4-2) and can help to demonstrate that different approaches that are used later do indeed lead to the same results. The starting points for such a development are equations 6.4-3 to 6.4-5, which result from equilibrium before the small angle approximations are introduced. For $\alpha_1 = \alpha_2 = \alpha$ equation 6.4-3 results in:

$$P_{t\,env} = \frac{1}{2} \cdot \frac{h \cos\alpha}{h + d_{e\,env} \cos\alpha} \cdot \gamma_E \cdot \left(F_B - \frac{M_{O\,env}}{h} \right) \tag{6.4-10}$$

The equations 6.4-4 and 6.4-5 now become equal; substituting 6.4-10 these equations result in:

$$P_{a\,env} = \frac{1}{2} \cdot \frac{1}{\sin\alpha} \cdot \frac{1}{h + d_{e\,env} \cos\alpha} \cdot \gamma_E \cdot \left\{ M_{O\,env} \cos^2\alpha + F_B (h \sin^2\alpha + d_{e\,env} \cos\alpha) \right\} \tag{6.4-11}$$

From the geometry in figure 6.4-2 it follows that for $\alpha_1 = \alpha_2 = \alpha$:

$$b_e = 2 \tan\alpha (h + d_{e\,env} \cos\alpha) \tag{6.4-12}$$

Introducing $2 \sin\alpha (h + d_{e\,env} \cos\alpha) = b_e \cos\alpha$ we may thus rewrite equation 6.4-11 to become:

$$P_{a\,env} = \gamma_E \cdot \frac{M_{O\,env} \cos^2\alpha + F_B (h \sin^2\alpha + d_{e\,env} \cos\alpha)}{b_e \cos\alpha} \tag{6.4-13}$$

When the small angle approximation $\sin\alpha \approx \alpha$ and $\cos\alpha \approx 1.0$ is now invoked equation 6.4-10 for $P_{t\,env}$ degenerates into equation 6.4-9. Doing the same in equation 6.4-13 for $P_{a\,env}$, while further neglecting the second order term $h\alpha^2$, this equation also degenerates into equation 6.4-9.

Case 2: Symmetric part of the permanent and variable loading

The situation for a tower structure is shown in figure 6.4-3; G_T acts at the mid-point of the top brace with length b_t, while G_S is assumed to act at the mid-point of the bottom brace with length b_s. For a jacket the situation is different in that both G_T and G_S will act at the top, as discussed in section 6.3.6. Strictly speaking the loading situation is only fully symmetric for $\alpha_1 = \alpha_2$. For unequal batter angles the geometry of the frame lacks symmetry, and consequently the load situation is not truly symmetric either. However, symmetry will nonetheless be assumed hereafter.

From symmetry it immediately follows that the support reactions at pile 1 are equal to the support reactions at pile 2. Therefore $P_{a\,sym,1} = P_{a\,sym,2} = P_{a\,sym}$, which is additional to equations 6.4-1 and 6.4-2. The support conditions at the artificial hinge points at a distance $d_{e\,env} \cdot \cos\alpha \approx d_{e\,env}$ below the sea floor can be modelled by two springs, an axial spring along the pile and a lateral spring perpendicular to the pile; see figure 6.4-3. The axial spring represents P_a, the lateral spring represents P_t.

The frame is very stiff compared to the supporting sea floor, while for nearly all situations the stiffness of the axial spring is much larger than the stiffness of the lateral spring. We may therefore consider the frame to be rigid and neglect any lateral pile forces ($P_{t\,sym} \approx 0$). Test calculations using a finite element program for a real frame and real piles confirm these approximations. These statically indeterminate finite element calculations using appropriate structural stiffnesses and realistic soil conditions indicated that $P_{t\,sym} \approx 0.01 P_{a\,sym}$, which is indeed negligible. Neglecting P_t implies that P_m should also be neglected (see equation 6.4-2). Accordingly, d_e may be set to zero as well and the axial and lateral support springs for the symmetric load case may be assumed to act at the sea floor. To emulate symmetry we adopt the average of α_1 and α_2 as the batter angle:

$$\alpha = \frac{\alpha_1 + \alpha_2}{2} \tag{6.4-14}$$

Vertical equilibrium then gives:

$$2 P_{a\,sym} \cos\alpha = \gamma_G \cdot (G_T + G_S) \tag{6.4-15}$$

Adopting the above simplifications thus results in:

$$\begin{aligned} P_{t\,sym,1} &= P_{t\,sym,2} = P_{t\,sym} = 0 \\ P_{m\,sym,1} &= P_{m\,sym,2} = P_{m\,sym} = 0 \\ P_{a\,sym,1} &= P_{a\,sym,2} = P_{a\,sym} = \tfrac{1}{2} \cdot \gamma_G \cdot \frac{G_T + G_S}{\cos\alpha} \end{aligned} \tag{6.4-16}$$

Using the small angle relationship $\cos\alpha \approx 1.0$ the axial pile forces may also be approximated by:

$$P_{a\,sym} = \tfrac{1}{2} \cdot \gamma_G \cdot (G_T + G_S) \tag{6.4-17}$$

It should be noted that the horizontal components of $P_{a\,sym}$ are always equal and opposite, so that there is no net contribution from the symmetric and permanent part of the variable loading to assist in accommodating the total base shear F_B; see the discussion on shear take-out in section 6.4.5.

Case 3: Anti-symmetric part of the permanent and variable loading

The anti-symmetric case is treated in a manner, which is fully analogous to the symmetric loading case; it is shown in figure 6.4-4. From inspection it directly follows that the directions of the support reactions for a clockwise moment (positive eccentricity) are as indicated on figure 6.4-4. From symmetry it further follows that $P_{t\,asym,1} = P_{t\,asym,2} = P_{t\,asym}$ and $P_{a\,asym,1} = P_{a\,asym,2} = P_{a\,asym}$. Considering the frame again to be made symmetrical by adopting:

$$\alpha = \frac{\alpha_1 + \alpha_2}{2} \qquad (6.4\text{-}14)$$

moment equilibrium about point C gives:

$$\sum M_C = \gamma_G \cdot (M_{OGT} + M_{OGS}) - 2P_{t\,asym} \cdot \frac{h + d_e}{\cos\alpha} = 0$$

or: $$P_{t\,asym} = \tfrac{1}{2} \cdot \gamma_G \cdot (M_{OGT} + M_{OGS}) \cdot \frac{\cos\alpha}{h + d_e} = \gamma_G \cdot (M_{OGT} + M_{OGS}) \cdot \frac{\sin\alpha}{b_e} \qquad (6\text{-}4\text{-}18)$$

Moment equilibrium about point D gives similarly:

$$\sum M_D = \gamma_G \cdot (M_{OGT} + M_{OGS}) - 2P_{a\,asym} \cdot \frac{\tfrac{1}{2} b_e}{\cos\alpha} = 0$$

or: $$P_{a\,asym} = \gamma_G \cdot (M_{OGT} + M_{OGS}) \cdot \frac{\cos\alpha}{b_e} \qquad (6.4\text{-}19)$$

At the hinged supports at depth $d_e \cos\alpha \approx d_e$ below the sea floor the pile moments are zero. Moving the support springs to the sea floor provides the following final results for the anti-symmetric case:

$$\begin{aligned}
P_{t\,asym,1} &= P_{t\,asym,2} = P_{t\,asym} = \gamma_G \cdot (M_{OGT} + M_{OGS}) \cdot \frac{\sin\alpha}{b_e} \approx \gamma_G \cdot \frac{\alpha (M_{OGT} + M_{OGS})}{b_e} \\
P_{m\,asym,1} &= P_{m\,asym,2} = P_{m\,asym} = d_{e\,asym} \cdot P_{t\,asym} \\
P_{a\,asym,1} &= P_{a\,asym,2} = P_{a\,asym} = \gamma_G \cdot (M_{OGT} + M_{OGS}) \cdot \frac{\cos\alpha}{b_e} \approx \gamma_G \cdot \frac{(M_{OGT} + M_{OGS})}{b_e}
\end{aligned} \qquad (6.4\text{-}20)$$

where the approximations on the far right are again made by invoking the small angle assumption. Note that the symmetric and the anti-symmetric load cases are subject to the same internal inconsistency as the environmental loading case when $\alpha_1 \neq \alpha_2$.

As the axial pile forces are now equal and opposite, the horizontal components of $P_{a\,asym,1}$ and $P_{a\,asym,2}$ do not cancel but add. Therefore, the anti-symmetric part of the permanent and variable loading does assist in accommodating F_B by taking out shear; see once more the discussion on shear take-out in section 6.4.5.

Combined case: Support reactions for total applied loading
Summing the support reactions for the three separate load cases in equations 6.4-9, 6.4-16 and 17 and 6.4-20 we obtain the following results:

$$\alpha = \frac{\alpha_1 + \alpha_2}{2} \tag{6.4-14}$$

$$\begin{aligned}
P_{t,1} &= P_{t\,env} - P_{t\,asym} = \frac{1}{2} \cdot \frac{h}{h + d_{e\,env}} \cdot \gamma_E \cdot \left(F_B - \frac{M_{O\,env}}{h} \right) - \gamma_G \cdot \frac{\alpha (M_{OGT} + M_{OGS})}{b_e} \\
P_{t,2} &= P_{t\,env} - P_{t\,asym} = \frac{1}{2} \cdot \frac{h}{h + d_{e\,env}} \cdot \gamma_E \cdot \left(F_B - \frac{M_{O\,env}}{h} \right) - \gamma_G \cdot \frac{\alpha (M_{OGT} + M_{OGS})}{b_e}
\end{aligned} \tag{6.4-21}$$

$$P_{m,1} = P_{m,2} = P_m = P_{m\,env} - P_{m\,asym} = d_{e\,env} \cdot P_{t\,env} - d_{e\,asym} \cdot P_{t\,asym} \tag{6.4-22}$$

$$\begin{aligned}
P_{a,1} &= P_{a\,env,1} - P_{a\,sym,1} + P_{a\,asym,1} \\
&= \gamma_E \cdot \frac{M_{O\,env} + F_B \cdot d_{e\,env}}{b_e} - \tfrac{1}{2} \cdot \gamma_G \cdot (G_T + G_S) + \gamma_G \cdot \frac{(M_{OGT} + M_{OGS})}{b_e} \\
P_{a,2} &= P_{a\,env,2} + P_{a\,sym,2} + P_{a\,asym,2} \\
&= \gamma_E \cdot \frac{M_{O\,env} + F_B \cdot d_{e\,env}}{b_e} + \tfrac{1}{2} \cdot \gamma_G \cdot (G_T + G_S) + \gamma_G \cdot \frac{(M_{OGT} + M_{OGS})}{b_e}
\end{aligned} \tag{6.4-23}$$

See figures 6.4-1 to 6.4-4 for the meaning of the variables in these expressions; the variable d_e will be discussed more fully in section 6.6. The applied loading and pile forces are positive in the directions shown in the figures. Note that for positive eccentricity of the permanent and variable loads (i.e. a clockwise moment) $P_{t\,env}$ and $P_{t\,asym}$, as well as $P_{m\,env}$ and $P_{m\,asym}$, have opposite directions.

Considering the results in equations 6.4-21 to 6.4-23 we can make the following important observations:

(a) *with regard to axial pile forces*

- The contribution to P_a from environmental loading is the same for both piles. It has the obvious form of an overturning moment divided by the width of the frame at the base. However, both numerator and denominator must be replaced by an effective overturning moment and an effective width, both with respect to a lower point than the sea floor; see section 6.4.4 for a further discussion.
- The contribution from the symmetric part of the permanent and variable loading always *adds* to the force in the pile that is in *compression* due to the environmental loads (here pile 2) and always *subtracts* from the force in the pile that is in *tension* due to the environmental loads (here pile 1).

- The contribution from the anti-symmetric part of the permanent and variable loading depends on the eccentricity, in magnitude as well as in sign. For *positive* eccentricity (when $G = G_T + G_S$ acts “downstream”, in the direction of wind and waves) the axial pile forces are *increased*, both in compression and in tension. For *negative* eccentricity (when $G = G_T + G_S$ acts “upstream”, into the direction of wind and waves) they *decrease* compression as well as tension in the piles.
- The maximum axial pile forces (and hence maximum required pile penetration) occur for the most unfavourable combination of wind/wave direction and positive eccentricity of the permanent and variable loading. The most heavily loaded pile is then the “downstream” pile.

(b) with regard to lateral pile forces

- The contribution to P_t from environmental loading is also the same for both piles. However, it is not simply equal to half the base shear. There is a reduction by a component of the axial pile forces resulting from the overturning moment due to the environmental loads; this is further discussed in section 6.4.4. The factor $(h / h + d_{e\ env})$ is of little significance.
- The symmetric part of the permanent and variable loading does *not* contribute to the lateral pile forces.
- The contribution from the anti-symmetric part of the permanent and variable loading depends once more on the eccentricity, in magnitude as well as in sign. For *positive* eccentricity (when $G = G_T + G_S$ acts “downstream”, in the direction of wind and waves) the lateral forces on both piles are *reduced*. For *negative* eccentricity (when $G = G_T + G_S$ acts “upstream”, into the direction of wind and waves) they are *increased* on both piles.
- The maximum lateral pile force occurs on the “upstream” pile for negative eccentricity of the permanent and variable loading.

(c) with regard to the pile head moments

- The pile head moments are due to environmental loading and the asymmetric part of the permanent and variable loading; they are equal on both piles. For positive eccentricity of the permanent and variable loads the two contributions have opposite signs, for negative eccentricity they add. The symmetric part of the permanent and variable loading does not contribute to the pile head moments.

Normally, all wave directions with respect to the structure should be considered. Consequently, in design no benefit can be derived from an eccentric load distribution. Members in the frame as well as the pile foundation underneath the frame should always be designed for the most unfavourable combination of wave direction and load eccentricity.

The equations 6.4-14 and 6.4-21 to 6.4-23 are quite general expressions for the support reactions of the frame at the sea floor, subject to the assumptions made in their derivation. These assumptions may be summarised as follows:

- a structural model that is a two-dimensional (near) vertical frame;
- a loading model that is described in section 6.3, resulting in applied loads at the sea floor that are given by equations 6.3-11 to 6.3-14;
- all loads act in the plane of the frame;
- the frame is supported by one (equivalent) pile on either side;

- the pile supports the frame chord member concentrically and they have the same batter angle;
- the batter angles on either side are small (say $\alpha < 0.15 \text{ rad} = 8.5°$), but they do not need to be equal when some further approximation is accepted;
- the lateral pile forces, axial pile forces and pile moments at the top of the two piles, resulting from environmental loading, are equal;
- the pile moment at the top of the pile is a constant times the corresponding lateral pile force $(P_m = d_e \cdot P_t)$.

When one of these assumptions is not satisfied, the validity of the equations is no longer ensured.

One further point should be noted. In this section the reaction forces at the sea floor have been determined analytically, which results in the above expressions. However, there is no need to memorise these equations or to have them available for reference. In practical applications it is far more straightforward to use the three equilibrium conditions at the sea floor by which they have been derived. In practical applications it is therefore the *method* and the underlying reasoning that is important, rather than the analytical results achieved. Applications proceed directly numerically, which facilitates the process. The analytical procedure followed here merely serves the purpose of illustrating the method in a general manner instead of using a particular, but arbitrary numerical example. It further serves to make the relationships visible that exist between the various parameters.

6.4.3 Reactions at the sea floor for vertical chord members and vertical piles

A special case of that considered in the preceding section is the case in which there is no batter angle, i.e. $\alpha_1 = \alpha_2 = 0$. This directly impacts on expression 6.4-21 for P_t only; the other equations remain the same. However, under these conditions also $h \to \infty$, so that $M_{O\,env} / h \to 0$ and $h / h + d_{e\,env} \to 1$, while the breadth b_e should be replaced by a breadth b that is the same over the whole height of the frame. Writing further for simplicity $d_{e\,env} = d_e$ we obtain from the equations 6.4-21 to 6.4-23:

$$\begin{aligned}
P_t &= \tfrac{1}{2}\gamma_E \cdot F_B \\
P_m &= d_e \cdot \tfrac{1}{2}\gamma_E \cdot F_B \\
P_{a,1} &= \gamma_E \cdot \frac{M_{O\,env} + F_B \cdot d_e}{b} - \tfrac{1}{2} \cdot \gamma_G \cdot (G_T + G_S) + \gamma_G \cdot \frac{(M_{OGT} + M_{OGS})}{b} \\
P_{a,2} &= \gamma_E \cdot \frac{M_{O\,env} + F_B \cdot d_e}{b} + \tfrac{1}{2} \cdot \gamma_G \cdot (G_T + G_S) + \gamma_G \cdot \frac{(M_{OGT} + M_{OGS})}{b}
\end{aligned} \qquad (6.4\text{-}24)$$

The effect is, therefore, that the lateral pile forces are now indeed equal to half the base shear each. The reduction by the component of the axial pile forces due to $M_{O\,env}$, as well as the contribution from the anti-symmetric part of the permanent and variable loads disappear. This is all, of course, as expected.

Another change is more indirect and more hidden: the axial pile forces will also increase due to the fact that $b < b_e$, unless of course the width of the frame is increased over the full height. This is, however, an unnecessary and costly modification.

6.4.4 *Reactions at the sea floor due to hydrodynamic loads only*

When we disregard permanent and variable loads as well as wind loads and consider hydrodynamic loads only, the total applied loading at the sea floor reduces to a base shear of $F_B = \gamma_E \cdot F_H$ and an overturning moment of $M_O = \gamma_E \cdot M_{O\,env} = \gamma_E \cdot M_{OH}$; see equations 6.3-11 to 6.3-14. We may represent the loading situation by a single, resultant hydrodynamic load F_R equal to $F_B = \gamma_E \cdot F_H$ with an application point at a distance $\ell = M_O / F_B = M_H / F_H$ above the sea floor; see figure 6.4-2. With:

$$\begin{aligned} F_B &= F_R \\ M_{O\,env} &= \ell \cdot F_R \\ d_{e\,env} &= d_e \\ \frac{h-\ell}{h+d_e} &= \frac{b_f}{b_e} \end{aligned}$$

we obtain from the equations 6.4-21 to 6.4-23 for the pile forces due to hydrodynamic loads only:

$$\begin{aligned} P_t &= \tfrac{1}{2} F_R \cdot \frac{b_f}{b_e} \\ P_m &= d_e \cdot P_t \\ P_a &= F_R \cdot \frac{\ell + d_e}{b_e} \end{aligned} \tag{6.4-25}$$

where: F_R = resultant hydrodynamic load [N]
b_f = breadth of the frame at the application point of F_R [m]
b_e = effective breadth of the frame between the piles at a depth $d_e \cos\alpha \approx d_e$ below the sea floor [m]
d_e = P_m / P_t = a small fictitious distance along the pile below the sea floor; the reaction forces at the sea floor can be moved to this ‘effective depth’ under the condition that the pile moment becomes zero, see section 6.6 [m]
ℓ = application point of F_R above the sea floor [m]
$\ell + d_e$ = lever arm of F_R about the ‘effective depth’ d_e, giving the total effective overturning moment [m]

By considering equation 6.4-25 we can make the following important observations:

- The *lateral pile forces* due to hydrodynamic loading are equal to half the applied base shear from hydrodynamic loads (which is distributed over two piles), multiplied by a reduction factor. This is one of the main reasons (but not the only one) for having battered piles. The reduction factor is called the batter take-out factor; its magnitude in our current model is:

$$\frac{b_f}{b_e} = \frac{\text{breadth of the frame at the application point of the resultant hydrodynamic force}}{\text{effective breadth of the frame between the piles at a depth } d_e}$$

- It should be noted that the reduction factor is not solely due to the batter angle α but is a ratio of two breadths, i.e. two geometrical dimensions. Therefore, for two structures with the same top dimension and the same batter angle α, which are subject to the same force F_R but stand in different water depths, the taller structure will experience a larger reduction than the shorter structure: b_f remains the same, while b_e increases with water depth. Physically this is due to the fact that the axial pile forces increase, because with increasing water depth the arm ℓ of the overturning moment increases more rapidly than the breadth b_e. And it is the *horizontal components of the axial pile forces that contribute to the take-out of base shear*.
- In case of vertical piles the axial pile forces have no horizontal components and the lateral pile forces are thus equal to half the applied hydrodynamic load.
- The pile moments P_m at the top of the piles *add* to the overturning action due to the hydrodynamic loads. That is the reason that the total moment that must be carried by the foundation piles is somewhat larger than the overturning moment about the sea floor. For a model that assumes $P_m = d_e \cdot P_t$ the lever arm of the applied hydrodynamic loading to the effective depth d_e is $\ell + d_e > \ell$; see further section 6.6.
- The *axial pile forces* are equal to the total effective overturning moment about the effective depth divided by the effective width, both at the distance d_e below the sea floor.

For the special case described in this section there is also a graphical solution procedure, that is based on the resolution of a given force (here F_R) into three component forces acting along given lines of action (here pile 1, pile 2 and the resultant of the lateral pile forces). The method is described in Annex A.

6.4.5 Some notes on shear take-out

For quasi-statically responding structures the shear force on the foundation, the base shear, is equal to the total applied horizontal loading on the structure. This total applied horizontal load is solely due to the environment (waves, current and wind). Permanent and variable loads act vertically and can therefore not have a contribution to horizontal loading; this was already noted in section 6.3.7.

The base shear is resisted by the foundation through two complementary mechanisms:

- by the transverse (lateral) pile loads, which are perpendicular to the piles;
  this mechanism is always present;
- by the horizontal components of (a part of) the axial pile forces;
  this mechanism only manifests itself if the piles are inclined to the vertical and is called shear take-out.

For vertical piles only the first mechanism can occur. This case was briefly discussed in section 6.4.3. Shear take-out results from the horizontal components of pairs of axial pile forces. When the axial forces of a pair of piles are equal and opposite, their horizontal components do not cancel but are additive, thus opposing the applied horizontal loading. Such equal and opposite axial pile forces arise from the overturning moment, which is caused by the environmental loads (waves, current and wind) and by the anti-symmetric part of the permanent and variable loading; see case 1 and case 3 in section 6.4.2. The symmetric part of the permanent and variable loading does not produce an overturning moment; see case 2 in section 6.4.2. Consequently, the axial pile forces that are associated with the symmetric part are equal, but are not opposite in direction and thus do not have a net horizontal resultant.

Strictly speaking, the above discussion requires a symmetric structure (frame), i.e. equal batter angles. However, for a non-symmetric structure the observations remain valid with good approximation.

In summary then, shear take-out is exclusively the result of the overturning moment. In equation form this amounts to:

$$\begin{gathered} M_O = \gamma_E \cdot M_{O\,env} + \gamma_G \cdot M_{O\,asym} = \gamma_E \cdot M_{O\,env} + \gamma_G \cdot (M_{OGT} + M_{OGS}) \\ (P_{a,1})_{Mo} = (P_{a,2})_{Mo} = (P_a)_{Mo} = \gamma_E \cdot \frac{M_{O\,env} + F_B\, d_{e\,env}}{b_e} + \gamma_G \cdot \frac{M_{OGT} + M_{OGS}}{b_e} \end{gathered} \qquad (6.4\text{-}26)$$

The shear take-out is equal to $2\alpha(P_a)_{Mo}$. The remaining base shear, being $F_B - 2\alpha(P_a)_{Mo}$, is distributed over the piles as transverse (lateral) pile forces P_t.

The discussion in this entire section 6.4 focuses on a single frame with only two piles, one on each side. However, it applies equally to multiple pile foundations as addressed in section 6.5.

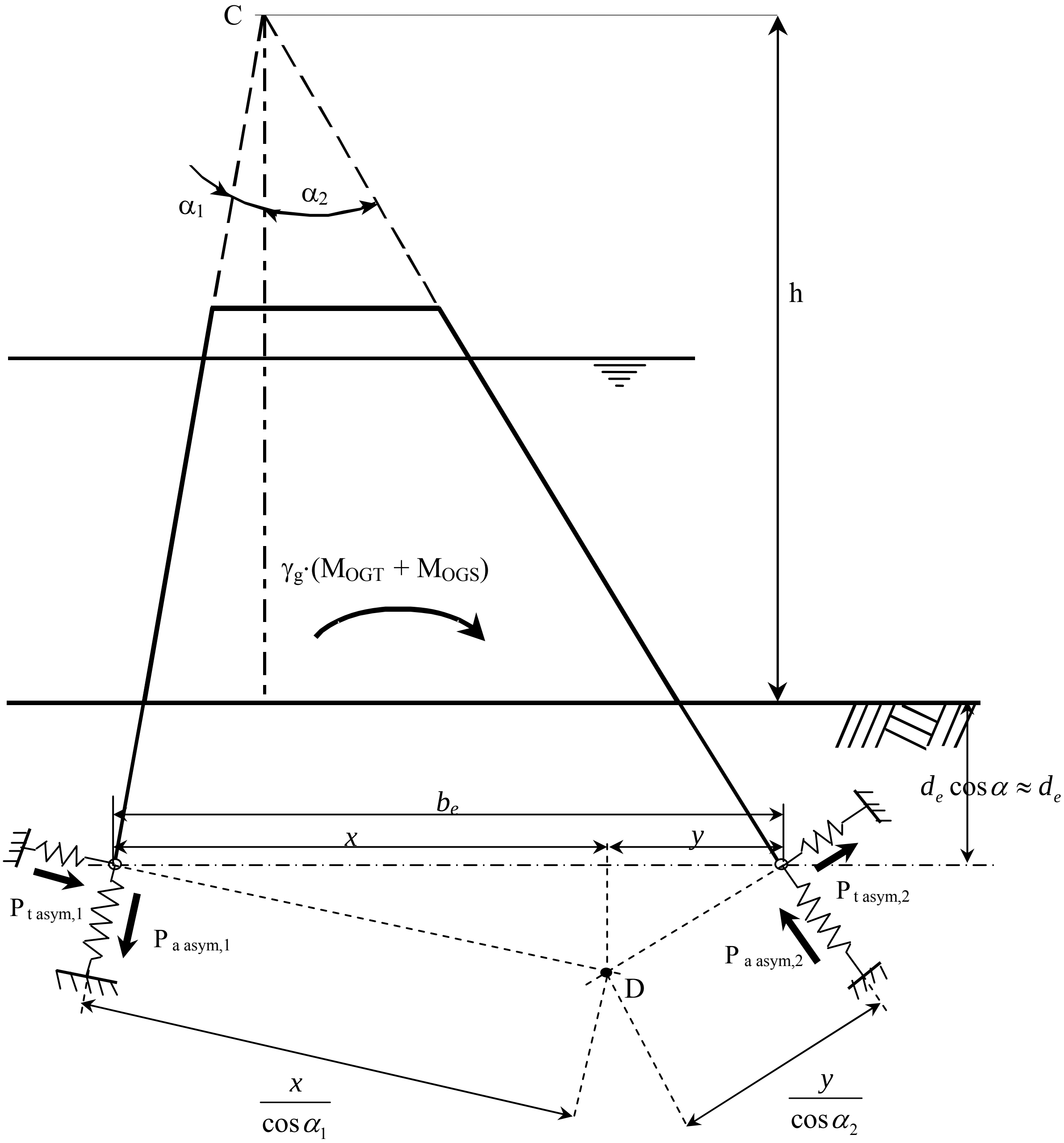

Figure 6.4-4. Support reactions at the sea floor due to the anti-symmetric part of the permanent and variable loading

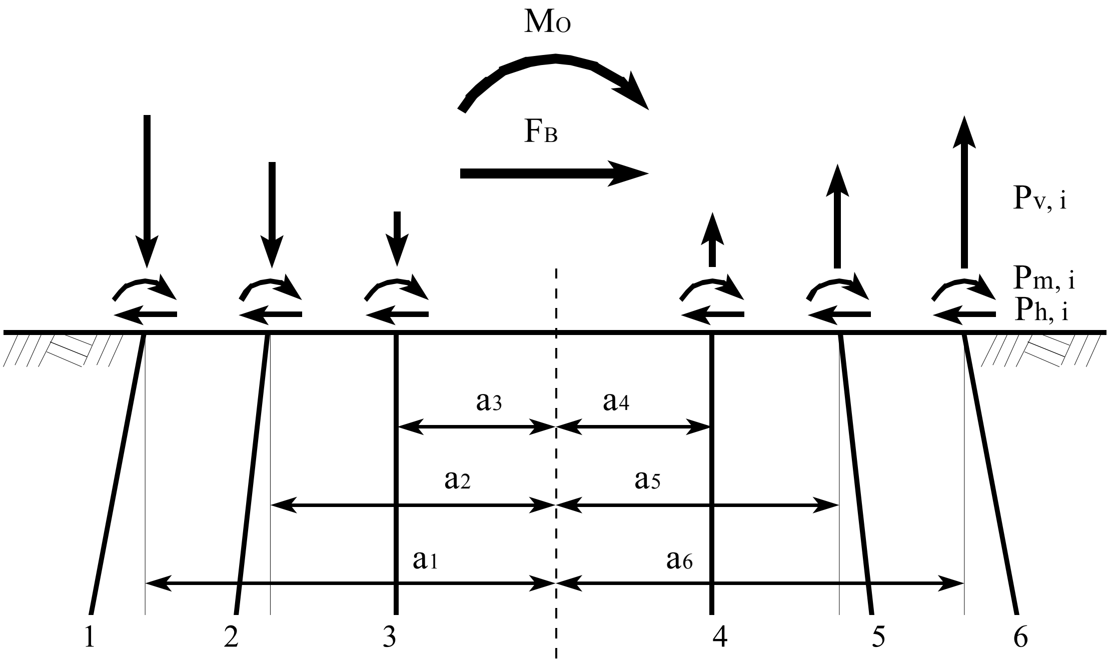

Figure 6.5-1. Multiple pile support for a frame

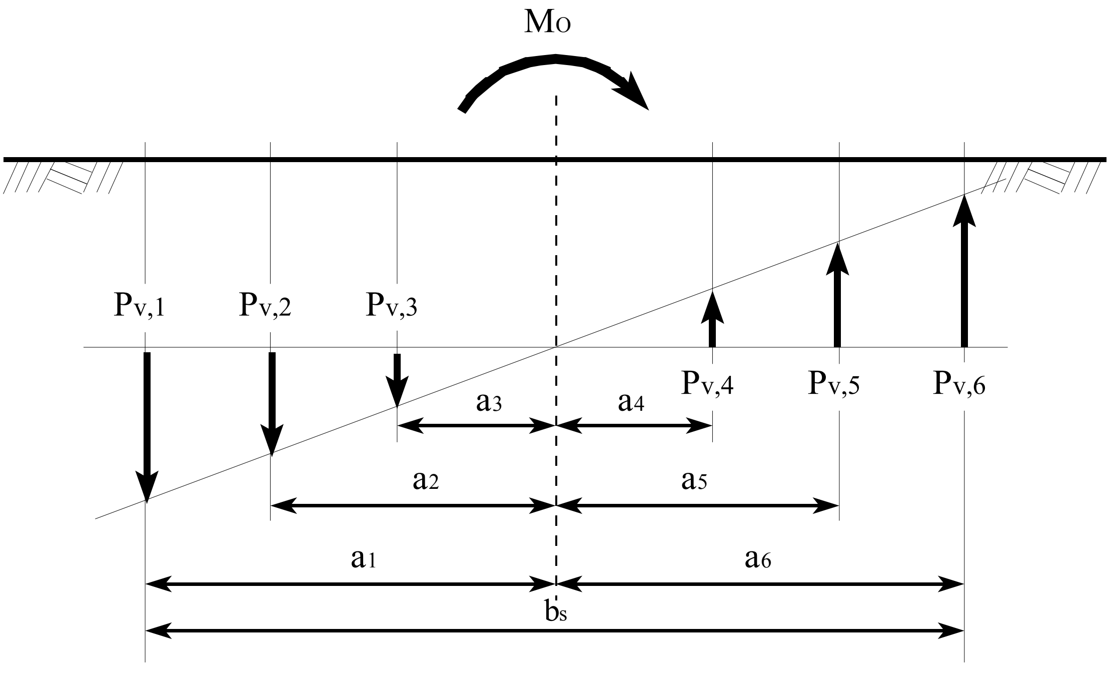

Figure 6.5-2. Vertical pile reactions due to overturning moment

6.5 Support reactions for multiple pile foundations

6.5.1 General conditions

In section 6.4 we limited the discussion to two piles, one on either side of the frame. Each pile may truly be a single pile, or represent a cluster of piles that can effectively be modelled into one equivalent pile. The latter situation is, for example, met for tower structures where the pile group around a corner leg can often be modelled by one equivalent pile generically supporting the structure at the centre of the leg. However, if a structure is supported by more than two piles that are spatially distributed the procedure described in section 6.4 cannot be followed and the results are no longer applicable. Examples of such situations are structures with more than two legs per frame, where each leg is pile supported (either with a pile through the leg or with a cluster of piles around each leg), and structures with skirt piles around the perimeter (see e.g. figure 5.5). We will now consider the more general case of multiple pile supports. However, for these cases the loading condition will need to be more restricted. There must now be no net vertical loading of the frame. Therefore, for the discussion in this section the applied loading consists of lateral environmental loads only (horizontal hydrodynamic and wind loads). The loading to be transmitted to the foundation piles is thus given by the base shear F_B (see equation 6.3-11) and the overturning moment $M_O = M_{O\,env}$ due to environmental loading (see the first term in equation 6.3-13 or 6.3-14). The permanent and variable loads constitute separate load cases and are not considered in this section.

6.5.2 Two-dimensional frame supported by multiple piles

The situation for a frame with multiple pile supports is shown in figure 6.5-1. A necessary further condition is that the piles are symmetrically positioned with respect to the centre of the frame. As the configuration of the frame above the sea floor is not relevant for the discussion the frame itself is not shown. The applied loading is F_B and M_O, both within the plane of the frame.

In contrast with the approach in section 6.4, where the pile forces were described in the local co-ordinate system of the pile (an axial pile force, a lateral pile force and a pile moment), we will now consider the global equilibrium of the frame in a global structural co-ordinate system. Therefore the pile forces are resolved into horizontal and vertical components. The sum of the horizontal components must be equal to F_B, while the sum of the vertical components must be zero. The overturning moment M_O must be balanced by the vertical components of the pile forces together with the moments in the cross sections of the individual piles. Therefore (figure 6.5-1):

$$\begin{aligned} F_B &= \sum_i P_{h,i} \\ 0 &= \sum_i P_{v,i} \\ M_O + \sum_i P_{m,i} &= \sum_i a_i P_{v,i} \end{aligned} \qquad (6.5\text{-}1)$$

For N piles there are in principle $3N$ unknowns (some of which may be zero) and only 3 equations; the problem is therefore highly statically indeterminate. However, as the moments in the piles are small compared to M_O, they may be neglected in the moment equation. This is a necessary simplification in order to make it possible to determine the pile forces. It is expressly noted though that the pile moments are only neglected when considering the global equilibrium of the frame, i.e. for equation 6.5-1. When the stresses in the individual piles are considered the bending moment in each pile is obviously very important and may definitely not be neglected. We will finally assume that the vertical pile forces $P_{v,i}$ are linearly proportional to the distance from the centre of the frame. This is not necessarily fully correct, but a very reasonable approximation. Using the vertical equilibrium and the simplified moment equilibrium equations from equation 6.5-1, and taking a 6-pile configuration to support the frame as an example, we can write (see figures 6.5-1 and 6.5-2):

$$\begin{aligned}
&a_1 = a_6 = \tfrac{1}{2} b_s \\
&a_2 = a_5 \\
&a_3 = a_4 \\
&P_{v,1} = P_{v,6} \\
&P_{v,2} = P_{v,5} = \frac{a_5}{a_6} \cdot P_{v,6} \\
&P_{v,3} = P_{v,4} = \frac{a_4}{a_6} \cdot P_{v,6} \\
&M_O = 2a_4 P_{v,4} + 2a_5 P_{v,5} + 2a_6 P_{v,6} = \left[\frac{2a_4^2 + 2a_5^2 + 2a_6^2}{a_6} \right] \cdot P_{v,6}
\end{aligned} \tag{6.5-2}$$

Defining:

$$\begin{aligned}
&I_{Pv} = 2a_4^2 + 2a_5^2 + 2a_6^2 \\
&W_{Pv} = \frac{I_{Pv}}{a_6} = \frac{2 I_{Pv}}{b_s}
\end{aligned} \tag{6.5-3}$$

where: I_{Pv} = the 'moment of inertia' of the vertical pile forces about the centre of the frame [m^2]

$\frac{1}{2} b_s$ = largest pile distance, or the distance to the 'extreme fibre' of the cross section over the foundation [m]

W_{Pv} = 'section modulus' of the cross section associated with the vertical pile forces [m]

we get from the last expression in equation 6.5-2 the simple result:

$$P_{v,6} = \frac{M_O}{W_{Pv}} \tag{6.5-4}$$

Equation 6.5-4 states that the vertical component of the axial pile force at the corner of the frame is equal to the overturning moment divided by the 'section modulus' of the cross section over the foundation. This is fully analogous to the familiar beam theory equation for the bending stress in a cross section due to pure bending. Note, however, that the two 'section moduli' are defined in a fully analogous manner but are not the same. The section modulus in beam theory is the moment of inertia of the cross sectional *area* in m^4, divided by the largest distance to the neutral axis; the unit is therefore m^3. The section modulus for the foundation reflects the moment of inertia (i.e. the sum of the squared distances to the neutral axis) of the *vertical pile forces* in m^2, again divided by the largest distance to the neutral axis. The unit of W_{Pv} is thus m^1 and not m^3.

Equation 6.5-4 is a very useful concept that can be generalised for oblique wave/wind directions and three-dimensional structures, as will be discussed in the next section.

The horizontal equilibrium equation in 6.5-1 stands on its own. There is no way to determine the individual forces $P_{h,i}$ and the only assumption that can reasonably be made is that the base shear is equally distributed over all piles:

$$P_{h,i} = \frac{F_B}{N} \tag{6.5-5}$$

Knowing both $P_{v,i}$ and $P_{h,i}$ as well as the pile batter for each pile, the pile forces $P_{a,i}$ and $P_{t,i}$ can be determined by resolving $P_{v,i}$ and $P_{h,i}$ along the axes of the pile; see figure 6.5-3:

$$\begin{aligned} P_{a,i} &= P_{v,i}\cos\alpha_i + P_{h,i}\sin\alpha_i \approx P_{v,i} + \alpha_i P_{h,i} \\ P_{t,i} &= P_{h,i}\cos\alpha_i - P_{v,i}\sin\alpha_i \approx P_{h,i} - \alpha_i P_{v,i} \end{aligned} \tag{6.5-6}$$

The expressions 6.5-6 are equally valid for piles that are in compression and piles that are in tension. Note that the angles α_i are the angles within the (near) vertical plane of the frame. As the frame itself may be inclined they are not necessarily the true batter angles.

In the method described above vertical and horizontal support forces are solved in the global structural co-ordinate system. The axial and lateral pile forces are next determined by resolving $P_{h,i}$ and $P_{v,i}$ along the local pile co-ordinate system of each pile. This is, of course, fully equivalent with the method in which the axial and lateral pile forces are determined directly in the local pile axis system. This can easily be demonstrated by applying the procedure in this section 6.5.2 to a frame with only two battered piles and comparing the results with those obtained earlier for case 1 in section 6.4.2, of course using the same assumption that the pile moments are zero (and hence also $d_e = d_{e\,env} = 0$ and $b_e = b_s$). When making this comparison somewhat superficially using equation 6.4-9 the results may initially seem to be different. However, this would be due to the implementation of the small angle approximations for $\cos\alpha$ and $\sin\alpha$ at different points in the process. To compare the results correctly the solutions 6.4-10 and 6.4-13 should be used, in which $\cos\alpha$ and $\sin\alpha$ are maintained. Introducing $d_{e\,env} = 0$, $b_e = b_s$ and the small angle approximation here the results will be found to be identical with the results from equation 6.5-6.

The above procedure in the global co-ordinate system can also be illustrated in another way using the concept of shear take-out. According to section 6.4.5 the shear take-out by inclined piles for environmental loading is:

$$\begin{aligned}\text{shear take-out} &= \sum_{i=1}^{6}\alpha_i (P_{a,i})_{Mo\,env} \approx \sum_{i=1}^{6}\alpha_i (P_{v,i}+\alpha_i P_{h,i})_{env} = \\ &= \sum_{i=1}^{6}(\alpha_i P_{v,i}+\alpha_i^{\,2} P_{h,i})_{env} \approx \sum_{i=1}^{6}(\alpha_i P_{v,i})_{env}\end{aligned} \tag{6.5-7}$$

We will henceforth drop the subscript 'env' as the whole discussion in this section concerns environmental loading only. As $P_{v,\,i}$ is linearly proportional to the distance to the centre of the frame this can be written as a function of the largest vertical pile force:

$$\begin{aligned}\text{shear take-out} &= 2\left[\alpha_1 P_{v,1}+\alpha_2 P_{v,2}+\alpha_3 P_{v,3}\right] = 2\left[\alpha_1 P_{v,6}+\alpha_2\frac{a_5}{a_6}P_{v,6}+\alpha_3\frac{a_4}{a_6}P_{v,6}\right] \\ &= 2\frac{\alpha_1 a_6+\alpha_2 a_5+\alpha_3 a_4}{a_6}\cdot P_{v,6}\end{aligned} \tag{6.5-8}$$

The net shear force is thus:

$$\text{net shear} = F_B - 2\frac{\alpha_1 a_6+\alpha_2 a_5+\alpha_3 a_4}{a_6}\cdot P_{v,6} \tag{6.5-9}$$

The lateral pile force on each of the 6 piles is then, according to section 6.4.5:

$$P_{t,\,i} = \frac{1}{6}(\text{net shear}) = \frac{1}{6}\left[F_B - 2\frac{\alpha_1 a_6+\alpha_2 a_5+\alpha_3 a_4}{a_6}\cdot P_{v,6}\right] \tag{6.5-10}$$

Using the method in the global co-ordinate system introduced in this section the solution is provided by the equations 6.5-2, 6.5-5 and 6.5-6:

$$\begin{aligned} P_{t,\,1} &= P_{h,\,1} - \alpha_1\,P_{v,\,1} = \frac{1}{6}F_B - \alpha_1 P_{v,6} \\ P_{t,\,2} &= P_{h,\,2} - \alpha_2 P_{v,\,2} = \frac{1}{6}F_B - \frac{\alpha_2 a_5}{a_6}P_{v,6} \\ P_{t,\,3} &= P_{h,\,3} - \alpha_3 P_{v,\,3} = \frac{1}{6}F_B - \frac{\alpha_3 a_4}{a_6}P_{v,6}\end{aligned} \tag{6.5-11}$$

The average of $(P_{t,\,1}+P_{t,\,2}+P_{t,\,3})$ is:

$$P_{t,\,i} = \frac{1}{3}(P_{t,\,1}+P_{t,\,2}+P_{t,\,3}) = \frac{1}{6}F_B - \frac{1}{3}\frac{\alpha_1 a_6+\alpha_2 a_5+\alpha_3 a_4}{a_6}P_{v,6} \tag{6.5-12}$$

This average is seen to be identical with that of equation 6.5-10, which demonstrates that the two procedures are indeed fully equivalent.

To conclude the discussion it is useful to review the validity of the above procedure in the global co-ordinate system; it is subject to five assumptions. These are:

- There is no net vertical loading on the frame; the applied loading on the structure is due to (horizontal) wave, current and wind loading only.
- The multiple piles supporting the frame are symmetrically positioned with respect to the centre of the frame.
- In the global moment equilibrium of the structure the individual pile moments are neglected.
- The vertical pile forces are linearly proportional to the distance from the centre of the frame.
- The horizontal pile forces are equal.

Of course, for a full determination of the pile forces the contributions from the permanent and variable loads must also be determined through separate load cases (see cases 2 and 3 of section 6.4.2) and must be added to the results obtained above. Please note that the pile forces for the symmetric and the anti-symmetric parts of the permanent and variable loading are directly given in the local pile co-ordinate system and must thus be added to P_a and P_t. Adding them to P_v and P_h and subsequently applying equation 6.5-6 to resolve them along the local pile axes would be quite wrong.

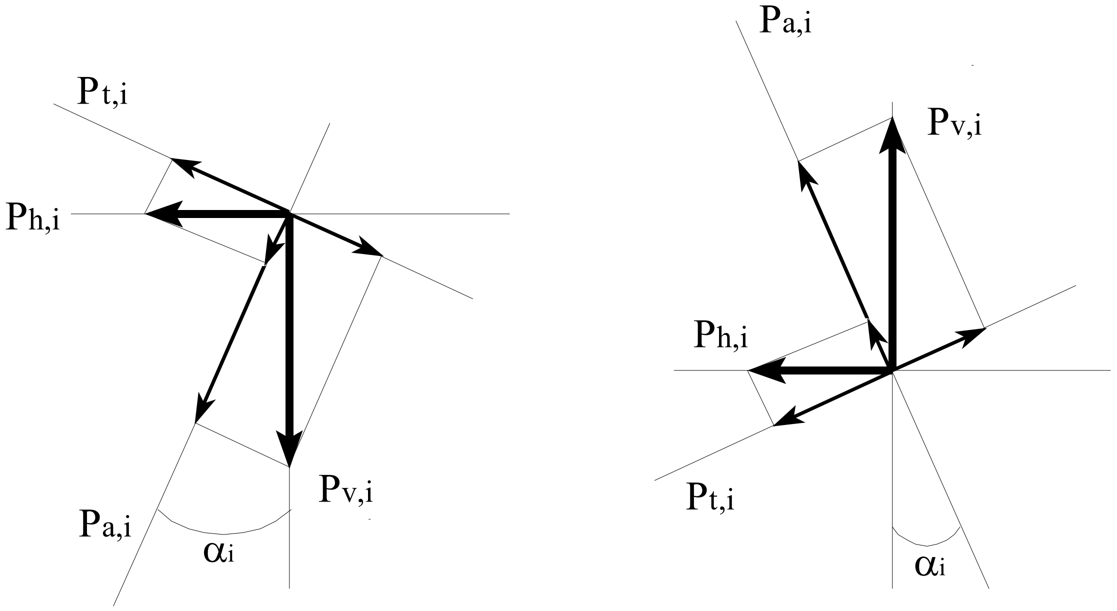

pile tension
on the left
of the frame

pile compression
on the right
of the frame

Figure 6.5-3. Resolution of horizontal and vertical pile forces into axial and lateral pile forces

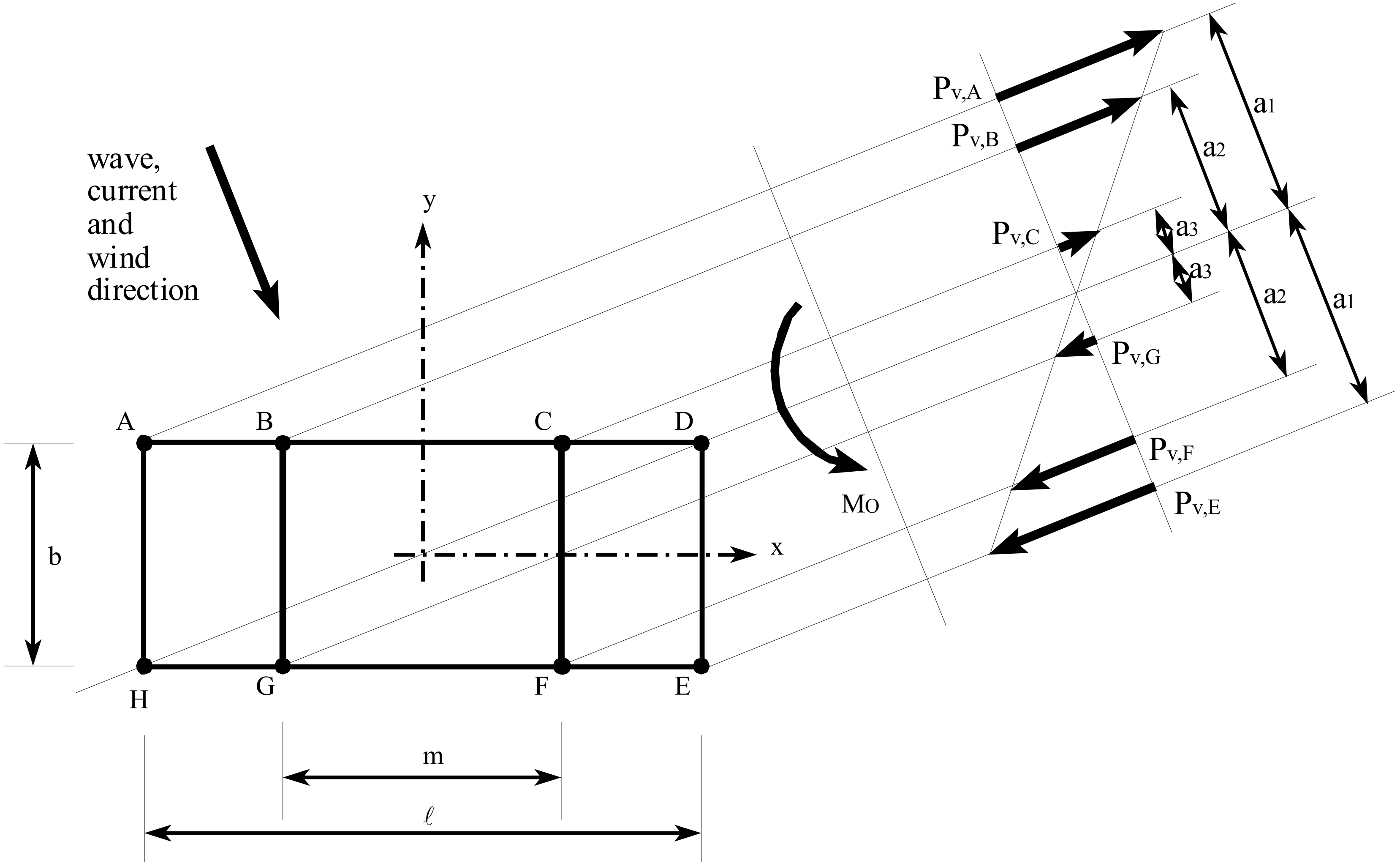

Figure 6.5-4. Multiple pile support for a structure; foundation plan for an example 8 pile structure

6.5.3 *Three-dimensional structure supported by multiple piles*

Treatment for a given direction of loading

The above result for the two-dimensional case of a (near) vertical frame can easily be extended to the three-dimensional case of an entire structure. Let figure 6.5-4 be a plan view of the foundation piles at the sea floor for an example 8-pile structure. All assumptions are the same as in the previous section, which means (among other things) that only horizontal environmental loading is considered and that the piles are symmetrically positioned; the *x*- and *y*-axes are lines of symmetry. The applied loading consists of the base shear and the overturning moment about the sea floor. Suppose now that we want tot know the pile forces for a direction of the applied loading perpendicular to the diagonal line HD. The moment vector of the overturning moment then falls along HD.

The overturning moment must make equilibrium with the moment about HD that is provided by the vertical pile forces at A to H. We do not know what the orientation of the neutral line is, but it is reasonable to assume that this will not be too far off the diagonal HD. At points A, B and C the piles are then in tension, while at points E, F and G the piles are in compression. The piles at D and H do not contribute to the moment about HD. From figure 6.5-4 we obtain:

$$
\begin{aligned}
&P_{v,B} = \frac{a_2}{a_1} \cdot P_{v,A} \\
&P_{v,C} = \frac{a_3}{a_1} \cdot P_{v,A} \\
&M_O = 2a_1 P_{v,A} + 2a_2 P_{v,B} + 2a_3 P_{v,C} = \left[\frac{2a_1^2 + 2a_2^2 + 2a_3^2}{a_1} \right] \cdot P_{v,A} = \frac{I_{Pv,HD}}{a_1} \cdot P_{v,A} \\
&P_{v,A} = \frac{M_O}{W_{Pv,HD}}
\end{aligned}
\qquad (6.5\text{-}13)
$$

where $I_{Pv,HD}$ and $W_{Pv,HD}$ are the moment of inertia for the vertical pile forces and the section modulus of the foundation, respectively, both about the line HD. This result is fully analogous to equations 6.5-2 to 6.5-4.

The vertical pile forces at corresponding points on either side of HD are equal and opposite in direction. As there is no net vertical loading on the foundation, the pile forces at D and H must also be equal and opposite; however, they will not be equal to zero as HD will not be the neutral line. To determine the vertical pile forces at D and H we must take moments about the line which is perpendicular to HD and passes through the centre of the footprint. This provides:

$$
\begin{aligned}
&P_{vA} \cdot (\ell \cos\theta - b \sin\theta) + P_{vB} \cdot (m \cos\theta - b \sin\theta) \\
&-P_{vC} \cdot (m \cos\theta + b \sin\theta) - P_{vD} \cdot \sqrt{b^2 + \ell^2} = 0
\end{aligned}
\qquad (6.5\text{-}14)
$$

from which P_{vD} can be solved.

The horizontal pile forces at A to H are once more assumed to be equal, in this case $1/8\,F_B$. Their direction is parallel to the direction of the applied loading F_B, that is perpendicular to diagonal HD. Combination of the horizontal and vertical pile forces into axial and lateral pile forces is as per equation 6.5-6; note that the angles α_i in this equation should now be the angles in a plane parallel to the plane of the overturning moment.

General treatment

A general procedure, that is fundamentally correct and very easy to apply, is to consider the moment equilibrium for an arbitrary angle of approach of waves, current and wind. Refer again to figure 6.5-4 and let the angle of the moment vector with the positive *x*-axis be θ ; the direction of waves, current and wind with the positive *x*-axis is then $360° - (90° - \theta) = \theta - 90°$. The magnitude of the overturning moment will in general be a function of the direction, which is expressed by writing $M_O(\theta)$. The moment vector is next resolved into a moment vector along the *x*-axis (overturning in the broadside direction) and a moment vector along the *y*-axis (overturning in the end-on direction). Then:

$$\begin{aligned} M_{O,x} &= M_O(\theta)\cos\theta \\ M_{O,y} &= M_O(\theta)\sin\theta \end{aligned} \tag{6.5-15}$$

Due to the moment $M_{O,x}$ the 4 piles at A, B, C and D are in tension and the 4 piles at E, F, G and H are in compression; the vertical pile forces at the 8 points are all equal. Taking $P_{vA,x}$ as an indicator:

$$\begin{aligned} I_{Pv,x} &= 2\cdot 4\cdot\left(\tfrac{1}{2}b\right)^2 = 2b^2 \\ W_{Pv,x} &= \frac{I_{Pv,x}}{\tfrac{1}{2}b} = 4b \\ P_{vA,x} &= \frac{M_{O,x}}{W_{Pv,x}} = \frac{M_O(\theta)\cdot\cos\theta}{4b} \end{aligned} \tag{6.5-16}$$

Due to the moment $M_{O,y}$ the 4 piles at A, B, H and G are in tension and the 4 piles at C, D, E and F are in compression. The vertical forces on the inner piles are m/ℓ times those on the outer piles. Taking the largest force $P_{vA,y}$ again as an indicator we get:

$$\begin{aligned} I_{Pv,y} &= 2\cdot 2\cdot\left(\tfrac{1}{2}\ell\right)^2 + 2\cdot 2\cdot\left(\tfrac{1}{2}m\right)^2 = (\ell^2 + m^2) = \ell^2\left[1+\left(\frac{m}{\ell}\right)^2\right] \\ W_{Pv,y} &= \frac{I_{Pv,y}}{\tfrac{1}{2}\ell} = 2\ell\left[1+\left(\frac{m}{\ell}\right)^2\right] \\ P_{vA,y} &= \frac{M_{O,y}}{W_{Pv,y}} = \frac{M_O(\theta)\cdot\sin\theta}{2\ell\left[1+\left(\frac{m}{\ell}\right)^2\right]} \end{aligned} \tag{6.5-17}$$

For $0 < \theta < 90°$ the largest vertical pile forces are found at the most distant corner piles at A and E. They are:

$$P_{vA}(\theta) = -P_{vE}(\theta) = P_{vA,x} + P_{vA,y} = \frac{M_O(\theta)\cdot\cos\theta}{4b} + \frac{M_O(\theta)\cdot\sin\theta}{2\ell\left[1+\left(\frac{m}{\ell}\right)^2\right]} \qquad (6.5\text{-}18)$$

The maximum vertical pile force occurs for $dP_{vA}(\theta)/d\theta = 0$, i.e. when:

$$\frac{dP_{vA}(\theta)}{d\theta} = \frac{dM_O(\theta)}{d\theta}\cdot\left[\frac{\cos\theta}{4b} + \frac{\sin\theta}{2\ell\left[1+\left(\frac{m}{\ell}\right)^2\right]}\right] + M_O(\theta)\cdot\left[-\frac{\sin\theta}{4b} + \frac{\cos\theta}{2\ell\left[1+\left(\frac{m}{\ell}\right)^2\right]}\right] = 0 \qquad (6.5\text{-}19)$$

The main variables in this equation are the factors between the large square brackets. The variation of the overturning moment with direction is usually rather mild, and it is often justified to assume that $dM_O(\theta)/d\theta \approx 0$. Thus, using this approximation, the maximum occurs for an angle θ for which:

$$\tan\theta_{\max} = \frac{4b}{2\ell\left[1+\left(\frac{m}{\ell}\right)^2\right]} \qquad (6.5\text{-}20)$$

Substituting this angle into equation 6.5-17 the maximum vertical pile force is found. The pile forces at the other points are subsequently found by summing the separate pile forces due to the moments about the x- and the y-axes for the same angle θ, with due regard to tension and compression:

$$\left|P_{vA\to H}\right| = \left|P_{vA\to H,x} \pm P_{vA\to H,y}\right| \qquad (6.5\text{-}21)$$

Thus, when the variation of the overturning moment with direction is neglected, the maximum vertical pile force occurs for the direction given by equation 6.5-19, where θ is the angle between the moment vector and the positive x-axis. This direction does *not* coincide with the diagonal HD, for which the angle would need to be:

$$\tan\theta_{HD} = \frac{b}{\ell} \qquad (6.5\text{-}22)$$

The reason for this difference is that for a general foundation plan *neither the line through the piles with the maximum vertical forces, nor the neutral line will be perpendicular to the plane of the overturning moment*, not even for a foundation plan that is symmetric about both the x- and the y-axis. This is fully analogous to the bending of an arbitrary beam section about an axis that does not coincide with one of the principal axes of the cross section.

As before, the horizontal pile forces are assumed to be equal: $F_{h,i} = \frac{1}{8}F_B$. These forces are associated with the above vertical pile forces and act in a direction parallel to F_B (perpendicular to the moment vector), i.e. in the direction $(\theta - 90°)$.

Just as the largest vertical pile forces are found at the largest distance from the line along the moment vector (i.e. at A and E as long as $0 < \theta < 90°$), the smallest forces occur at the piles closest to this line. For $0 < \theta < 90°$ this is at D and H. The vertical pile force at H is:

$$\begin{aligned} P_{vH}(\theta) &= -P_{vH,x}(\theta) + P_{vH,y}(\theta) = -P_{vA,x}(\theta) + P_{vA,y}(\theta) = \\ &= -\frac{M_O(\theta)\cdot\cos\theta}{4b} + \frac{M_O(\theta)\cdot\sin\theta}{2\ell\left[1+\left(\dfrac{m}{\ell}\right)^2\right]} \end{aligned} \tag{6.5-23}$$

The angle for which $P_{vH}(\theta) = P_{vD}(\theta) = 0$ indicates that the neutral line will fall along HD for a loading direction $\theta = \theta_{zero}$ for which:

$$\tan\theta_{zero} = \frac{2\ell\left[1+\left(\dfrac{m}{\ell}\right)^2\right]}{4b} = \frac{1}{\tan\theta_{\max}} \tag{6.5-24}$$

In other words, for an 8 pile rectangular foundation plan and for $dM_O(\theta)/d\theta \approx 0$:

> the vertical pile forces are maximum for $\theta = \theta_{\max}$ from equation 6.5-20
> and the neutral line is oriented along diagonal HD for $\theta = \theta_{zero} = 90° - \theta_{\max}$.

Special case of a 4-pile structure

Let us now specialise the case discussed above to a 4-pile structure by omitting the interior piles at B, C, F and G. When the above general method is applied to the 4-pile structure with a rectangular, footprint ADEH (see figure 6.5-4), assuming that the variation of the overturning moment with direction can be neglected, the results are:

$$\begin{aligned} P_{v,x}(\theta) &= \frac{M_O\cos\theta}{2b} \\ P_{v,y}(\theta) &= \frac{M_O\sin\theta}{2\ell} \\ P_{vA}(\theta) &= P_{v,x}(\theta) + P_{v,y}(\theta) = \frac{M_O\cos\theta}{2b} + \frac{M_O\sin\theta}{2\ell} \\ \frac{dP_{vA}(\theta)}{d\theta} &= M_O\left[-\frac{\sin\theta}{2b} + \frac{\cos\theta}{2\ell}\right] \end{aligned} \tag{6.5-25}$$

where the factor 2 in the denominator of the forces is due to the fact that the structure has two end-on and two broadside frames. The maximum vertical pile force thus occurs for:

$$\tan\theta_{\max} = \frac{2b}{2\ell} = \frac{b}{\ell} = \tan\theta_{HD} \tag{6.5-26}$$

Hence the *moment vector* for maximum vertical pile forces now *does* fall along the diagonal HD. However, for a non-rectangular foundation plan or for more than 4 piles this is no longer assured. But even in this case the *neutral line* does *not* coincide with the diagonal HD, as will be demonstrated below. Consequently, the vertical pile forces at H and D will not be zero either!

Using equation 6.5-26: $\cos\theta = \frac{\ell}{\sqrt{\ell^2 + b^2}}$ and $\sin\theta = \frac{b}{\sqrt{\ell^2 + b^2}}$ and the four vertical pile forces become:

$$\begin{aligned}
P_{vA} &= +P_{v,x} + P_{v,y} = M_O \left[\frac{\ell}{2b\sqrt{b^2+\ell^2}} + \frac{b}{2\ell\sqrt{b^2+\ell^2}} \right] = M_O \frac{\ell^2+b^2}{2b\ell\sqrt{b^2+\ell^2}} && (t) \\
P_{vE} &= -P_{v,x} - P_{v,y} = -M_O \frac{\ell^2+b^2}{2b\ell\sqrt{b^2+\ell^2}} && (c) \\
P_{vD} &= +P_{v,x} - P_{v,y} = M_O \left[\frac{\ell}{2b\sqrt{b^2+\ell^2}} - \frac{b}{2\ell\sqrt{b^2+\ell^2}} \right] = M_O \frac{\ell^2-b^2}{2b\ell\sqrt{b^2+\ell^2}} && (t \text{ or } c) \\
P_{vH} &= -P_{v,x} + P_{v,y} = -M_O \frac{\ell^2-b^2}{2b\ell\sqrt{b^2+\ell^2}} && (c \text{ or } t)
\end{aligned} \qquad (6.5\text{-}27)$$

The pile at A is in tension and the pile at E is in compression, while the piles at D and H experience either tension or compression depending on the lengths ℓ and b. The situation where $P_{vD} = P_{vH} = 0$ will only occur for $\ell = b$. Therefore, only for a square foundation plan will the neutral line also coincide with the diagonal HD. In all other cases of a 4-pile structure, the maximum vertical pile forces will be reached for a moment vector along diagonal HD, but the *neutral line will differ from HD.*

Going back to equation 6.5-25, the minimum forces occur at D and H and are equal to:

$$P_{vH}(\theta) = -P_{v,x}(\theta) + P_{v,y}(\theta) = -\frac{M_O(\theta)\cdot\cos\theta}{2b} + \frac{M_O(\theta)\cdot\sin\theta}{2\ell} \qquad (6.5\text{-}28)$$

The condition that $P_{vH}(\theta) = P_{vD}(\theta) = 0$ occurs for:

$$\tan\theta_{zero} = \frac{2\ell}{2b} = \frac{\ell}{b} = \frac{1}{\tan\theta_{\max}} \qquad (6.5\text{-}29)$$

which again shows that the direction of the neutral line is along HD for a loading direction, which is the complement of the angle for maximum pile loading.

Concluding remarks
Please note that all considerations above are based on elastic behaviour of the foundation. This is in line with the principles applied in this handbook and provides a reasonable estimate, but as the actual foundation behaviour is non-linear the true results may be different.

In concluding this description of a three-dimensional structure supported by multiple piles we should further make the same comment as made at the end of section 6.4.2. The pile forces have been determined in equation form, but in a practical application we will proceed numerically from the global equilibrium of the structure using the *method and the reasoning* described above. The analytical process followed here illustrates this method in a general manner and serves to make the relationships between the variables visible, but the analytical results obtained are of no special value.

Finally, for a full determination of the pile forces the contributions from the permanent and variable loads should not be forgotten. The pile forces resulting therefrom must be determined through separate load cases, as described by cases 2 and 3 of section 6.4.2, and must be added to the pile forces from environmental loading determined above. It should again be noted that the pile forces for the symmetric and the anti-symmetric parts of the permanent and variable loading are directly given in the local pile co-ordinate system and must thus be added to P_a and P_t. Adding them to P_v and P_h and subsequently applying equation 6.5-6 to resolve them along the local pile axes would be quite wrong.

6.5.4 Equivalence of the procedures in sections 6.4 and 6.5

Whether the pile forces are determined in the local pile co-ordinate systems of the (inclined) piles or in the global structural co-ordinate system with horizontal and vertical axes is, of course, irrelevant for the results. This was already illustrated in section 6.5.2. Full equivalence will clearly only be obtained if the underlying assumptions are also the same. This means that (1) there is no net vertical force (i.e. no permanent and variable loads); (2) there is symmetry; and (3) the internal pile moments P_m must be neglected.

In fact the option to choose between the two approaches only exists for a frame supported by two piles, one on each side. When the frame is supported by more than two piles the procedure for multiple pile supports must be used. In a practical application the pile loads for the environmental loading are therefore often best determined by calculating the horizontal and vertical support reactions. The lateral and axial pile forces for each pile can subsequently be determined by resolving the horizontal and vertical pile forces along the local pile axes. In doing so the addition to the overturning moment from the pile moments is neglected.

The pile forces due to the permanent and variable loading must be determined through separate load cases and should be added to the pile forces caused by the environmental loading.

6.6 A model for the pile support of the frame at the sea floor

6.6.1 Review of the assumptions made

To be able to solve the statically indeterminate problem of the support reactions P_a, P_t and P_m of the frame at the sea floor we have made a number of assumptions. In section 6.4.2 we assumed for the two pile support case that the *lateral* pile forces and the pile moments were equal ($P_{t,1} = P_{t,2} = P_t$ and $P_{m,1} = P_{m,2} = P_m$), while the pile moment was further assumed to be related to the lateral pile force by $P_m = d_e \cdot P_t$. These assumptions were specifically invoked for loading by environmental loads.

For the multiple pile support conditions in sections 6.5.2 and 6.5.3 we assumed that the *vertical* pile forces $P_{v,i}$ were proportional to their distance from the centre line, that all *horizontal* pile forces $P_{h,i}$ were equal and that $P_{m,i}$ could be neglected for the global equilibrium of the frame or the structure. This set of assumptions was also related to the case in which there was environmental loading only. As the problem is statically indeterminate, the real distribution of pile forces and corresponding moments at the top of the piles depends on the stiffnesses of pile and soil layers for each individual pile as well as the stiffnesses of the local frame elements connecting the piles to the frame. This can only be solved by a detailed model of the frame-pile-soil interaction and a detailed finite element analysis.

However, in the previous sections we were only looking for a simplified model, the purpose of which was no more than an adequate representation of the pile support forces for the frame in a linearised structural analysis. The same model does not need to be suitable for analysing the much more complicated non-linear behaviour of the pile itself. In this section we will explain why the assumptions made are indeed justified in nearly all cases of practical interest. It should expressly be noted though that exceptions can occur; the judgement whether a particular type of model is adequate for a particular problem can only be made by the analyst, given the purpose of his calculations and his particular set of conditions.

6.6.2 Justification of equal pile forces at the top of the piles

That pile forces at the top are assumed to be equal (with the exception of the axial forces) is based on three circumstances:

a) the piles are all equal
b) the soils around all piles are equal
c) all piles experience the same deformations (horizontal displacement and rotation) at their top.

Equal piles does not only mean that the outside diameters are equal, but that the entire make-up of the piles must be the same. That is, the combination of diameter, wall thickness and section lengths must be identical, while the pile sections must also be located at the same depths in the ground. Only then are the structural properties that are associated with the pile-soil interaction problem identical. Below a certain depth the lateral pile forces and pile moments become zero and from there on the piles are subject to axial forces only. Therefore, below this depth the situation may differ without affecting the problem. This shows that the depths of the pile tips have no relevance for the present requirement and these do not necessarily need to be the same. However, it should be recognised that the pile penetrations indirectly determine where pile sections with a particular wall thickness are located. Therefore, for non-uniform piles the pile penetrations would also need to be the same.

Soils are very inhomogeneous, not only in disposition in the ground but given a particular type of soil they are also highly variable in properties. The soil in which the piles are installed is usually layered and not uniform. Equal soils around all piles is therefore a somewhat hypothetical condition. It implies that the layering would need to be horizontal over an area exceeding the plan dimensions of the foundation, and that the soil properties within each layer are constant. These conditions will rarely be exactly satisfied. However, a site investigation to determine soil properties for foundation design is difficult, costly and limited in extent. The soil properties used for analysis are the average properties determined from laboratory tests on samples recovered from a limited number of borings, and from a limited number of cone penetrometer and/or other in-situ tests. Therefore, lack of detailed information about the soil conditions and their possible variability across the site make it entirely reasonable to assume that the piles are located in soils with the same properties; it would be highly speculative to assume anything else. No matter how detailed and refined a non-linear analysis we might wish to carry out, the input data for the pile-soil interaction problem are limited in number and quality and constrain the options for a very detailed analysis.

With regard to the deformations at the top of the piles we can make the following observations. We will assume that piles and frame are rigidly connected at the sea floor so that there is no relative horizontal and rotational movement between them. Then, as the frame is much stiffer against deformation than the piles in the soil, the lower part of the frame may be assumed to behave as a rigid body. Therefore, it may indeed be assumed that the frame imposes the same horizontal displacements and rotations on all piles.

When the three conditions stated above are satisfied, all piles are in exactly the same circumstances. They will thus behave in exactly the same manner and generate the same reaction forces from the soil. In fact these conditions would also imply full symmetry of the foundation with respect to the centreline of the frame.

The three assumptions are hence entirely reasonable and will usually be a good approximation of reality. However, in special cases they may not be acceptable. It should expressly be noted that in such situations the results presented before are *not* valid. For the sake of completeness, two other aspects warrant some further discussion. Firstly, when piles are inclined with different angles in magnitude or orientation, the conditions to which they are subjected are in fact not identical in every respect. However, as the angles are always small this difference is of secondary importance compared to the uncertainty and variability of the soil parameters and can normally be neglected. Secondly, the pile axial forces have not been considered in the foregoing; we have only referred to the effects of pile-soil interaction under lateral loading. As the pile behaves structurally as a beam column rather than as a pure beam, and as it is subject to relatively large displacements (compared to the diameter of the pile), the axial pile forces also generate secondary moments in the pile cross sections. Since the axial forces are not the same in all piles (they will even vary from compression to tension), these additional moments will be different as well. Consequently, the whole behaviour will differ somewhat from pile to pile. Strictly speaking the piles are thus *not* in exactly the same conditions and lateral pile forces and pile moments will therefore not be identical either. However, this is again a secondary effect that may be neglected in comparison to the primary effect of lateral pile behaviour.

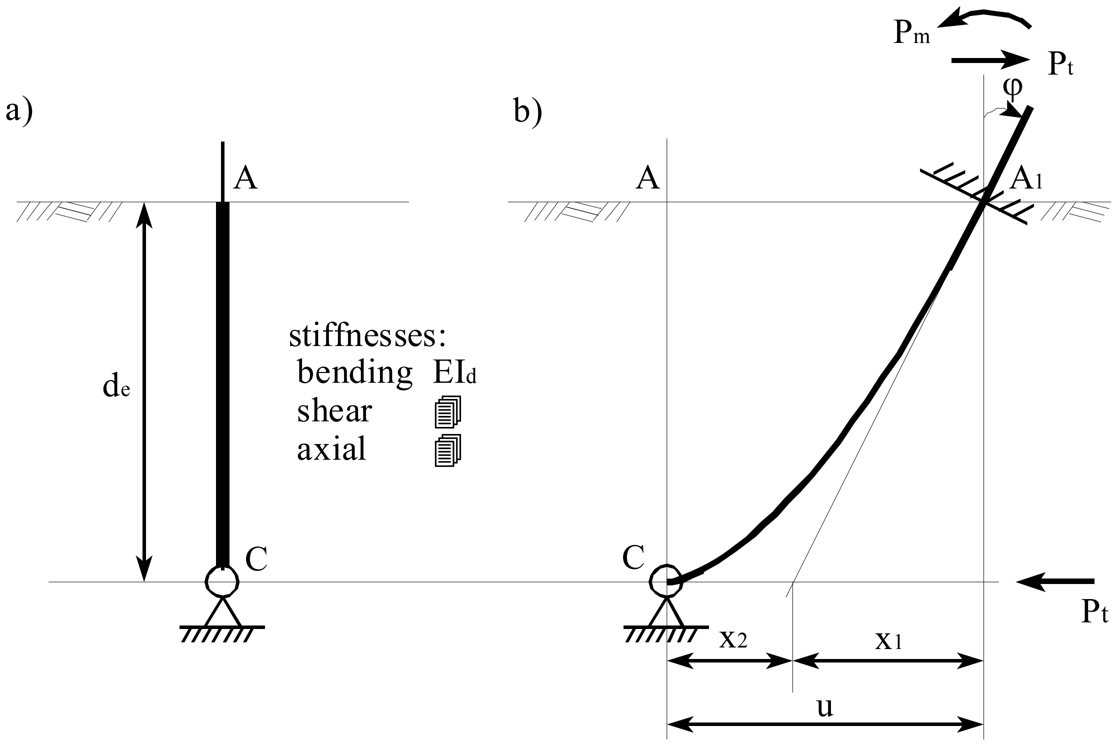

Figure 6.6-1. Representation of boundary conditions at the top of the pile by dummy member AC

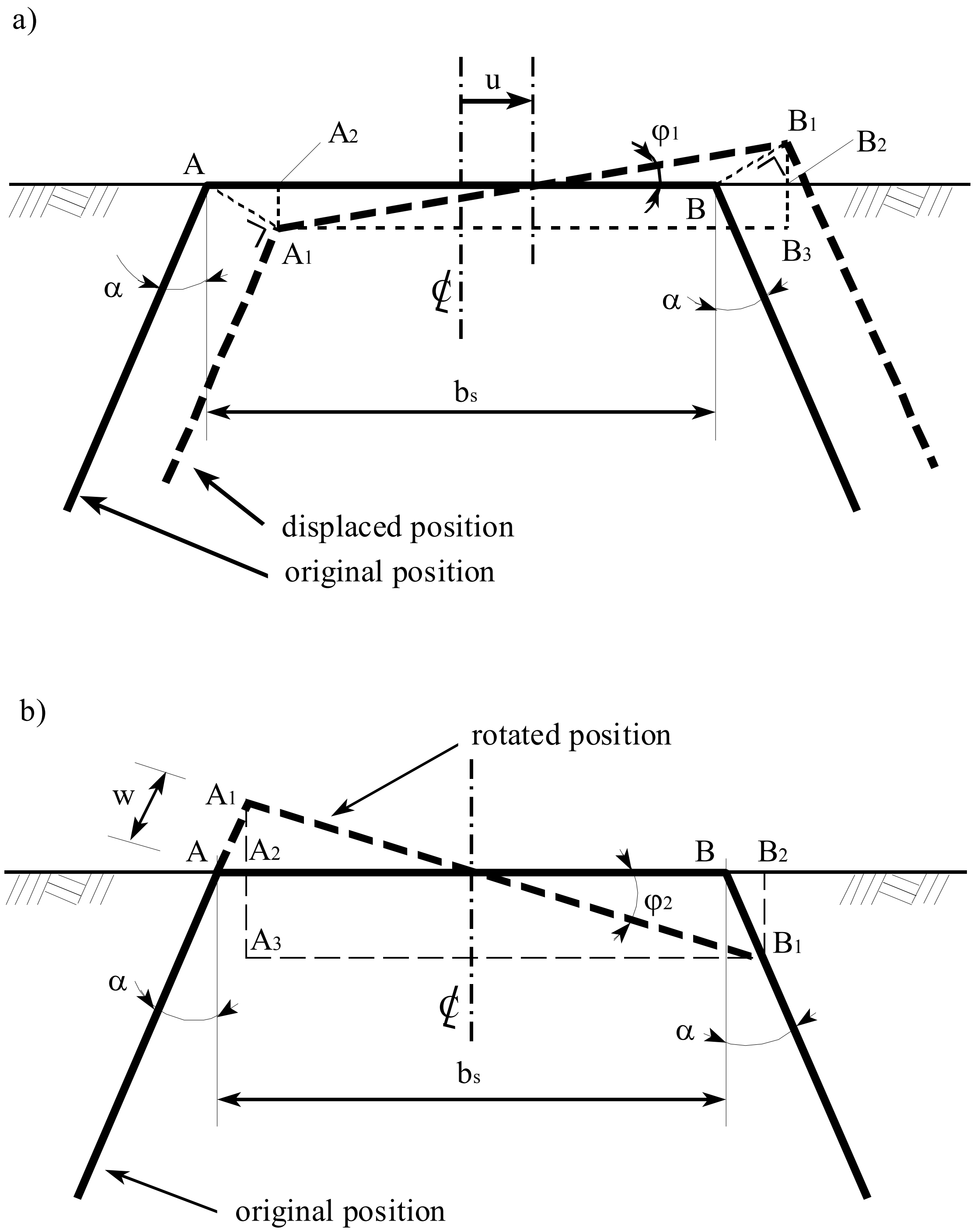

Figure 6.6-2 (a) Rotation at the top of the piles due to a rigid body displacement of the frame; the piles at A and B displace but do not change in length

(b) Rotation at the top of the piles due to a rigid body rotation of the frame; the piles at A and B become longer and shorter but do not displace

6.6.3 Relationship between pile moments and lateral pile forces

The behaviour of piles under lateral loading has been discussed in section 5.3.4; figure 5.3-9 showed an example of the deflections, moments and soil pressures along the length of the pile. The boundary conditions for the support points of the frame are the horizontal displacement u and the rotation φ at the top of the piles due to the applied loading, together with the lateral pile force P_t and the associated pile moment P_m. The lateral pile force P_t has been determined in previous sections, but the variables u, φ and P_m are as yet unknown. We have postulated that there exists a simple relationship between force and moment of the form $P_m = d_e \cdot P_t$ so that the unknown P_m may be replaced by the unknown d_e. These boundary conditions can be modelled very easily by a purely artificial member AC along the unloaded position of the pile; see figure 6.6-1a. Member AC has a length d_e and a hinge at point C. The properties that should be given to AC are a bending stiffness EI_d, while the axial and shear stiffnesses are considered to be infinitely large. EI_d is as yet unknown and needs to be determined. It should be noted that the *hypothetical or 'dummy' member* AC has no other purpose than ensuring that the correct boundary conditions at the sea floor are applied to the structural analysis of the frame.

In total we thus have 4 unknowns: u, φ, d_e and EI_d. As the problem is statically indeterminate we cannot expect to find 4 relationships between the unknowns in order to determine them all, but we need at least 3 relationships to solve the unknowns in an iterative manner. These will be determined next.

The dummy member AC must reflect the same situation at point A as the actual pile does; the deformed situation of the pile is as shown in figure 6.6-1b. In the displaced position A$_1$ we may consider the member AC to be built-in under the angle φ. At point A$_1$ the forces in a cross section of the pile are P_t and P_m. From equilibrium it follows that the forces at point C are a lateral force P_t in the opposite direction and a zero moment (there is a hinge at point C). From figure 6.6-1b it further follows that:

$$\begin{aligned} x_1 &= \varphi\, d_e \\ x_2 &= \frac{P_t d_e^3}{3EI_d} \\ u = x_1 + x_2 &= \varphi\, d_e + \frac{P_t d_e^3}{3EI_d} \end{aligned} \tag{6.6-1}$$

From this equation EI_d can be solved for each value of P_t, provided that estimates of u, φ and d_e can be made:

$$EI_d = \frac{P_t d_e^3}{3(u - \varphi\, d_e)} \tag{6.6-2}$$

This provides the first relationship between the four unknowns.

The frame is (very) stiff compared to the pile in the ground, while any structural deformation of the frame will further take place above the sea floor without affecting u and φ. Therefore, we may assume that the frame displaces and rotates as a rigid body. This allows us to estimate the rotation φ at the sea floor. The rotation has two components, as illustrated in figure 6.6-2. The batter angles of the piles are small and are assumed to be the same. Similarly, the elongation/shortening w of the piles and the rotation φ will be small. Under these conditions we can write, see figure 6.6-2:

$$\text{(a)}\qquad \begin{aligned} AA_2 &= BB_2 = u \\ A_1A_2 &= B_1B_2 \approx \alpha u \\ B_1B_3 &= B_1B_2 + B_2B_3 = B_1B_2 + A_1A_2 \approx 2\alpha u \\ \varphi_1 &\approx \frac{B_1B_3}{A_1B_3} \approx \frac{B_1B_3}{AB} \approx \frac{2\alpha u}{b_s} \end{aligned} \tag{6.6-3}$$

$$\text{(b)}\qquad \begin{aligned} AA_1 &= BB_1 = w \\ A_1A_2 &= B_1B_2 \approx w \\ A_1A_3 &= A_1A_2 + B_2B_1 \approx 2w \\ \varphi_2 &\approx \frac{A_1A_3}{A_3B_1} \approx \frac{A_1A_3}{AB} \approx \frac{2w}{b_s} \end{aligned} \tag{6.6-4}$$

$$\text{(total)}\quad \varphi = -\varphi_1 + \varphi_2 \approx \frac{2(w - \alpha u)}{b_s} \tag{6.6-5}$$

In the process we have introduced another variable in the form of the pile elongation/shortening w that must be removed. The pile elongation/shortening is due to the axial pile forces $P_{a\,env}$, which are associated with the overturning moment $M_{O\,env}$ only. At the top of the piles at points A and B these axial pile forces are largest, while at a depth L of approximately 2/3 of the pile penetration they have reduced to zero. Very approximately, we may estimate w to be equal to an elongation or shortening due to an average force of $\frac{1}{2}P_{a\,env}$ acting over the length L. Hence:

$$w \approx \frac{\frac{1}{2}P_{a\,env}}{EA/L} = \frac{P_{a\,env}L}{2EA} \tag{6.6-6}$$

This is a crude approximation, but a better estimate requires a lot more information and analysis. For the present purpose the estimate provided by equation 6.6-6 is sufficient. For a given overturning moment the axial pile forces have been determined in the preceding sections. Hence w can be estimated from equation 6.6-6 and then substituted into equation 6.6-5, thus expressing the rotation φ as a function of the unknown displacement u only. This provides the second relationship between two of the unknowns (i.e. u and φ).

The third relationship is provided by the results of a non-linear lateral pile analysis, such as shown in figure 5.3-10. The force and moment diagrams on the left hand side of figure 5.3-10 relate to a displacement $y_{top} = u$ at the head of the pile due to a lateral force $F = F_1$, while rotation of the pile head is prevented: $\theta_{top} = 0$. This constraint of the rotation is associated

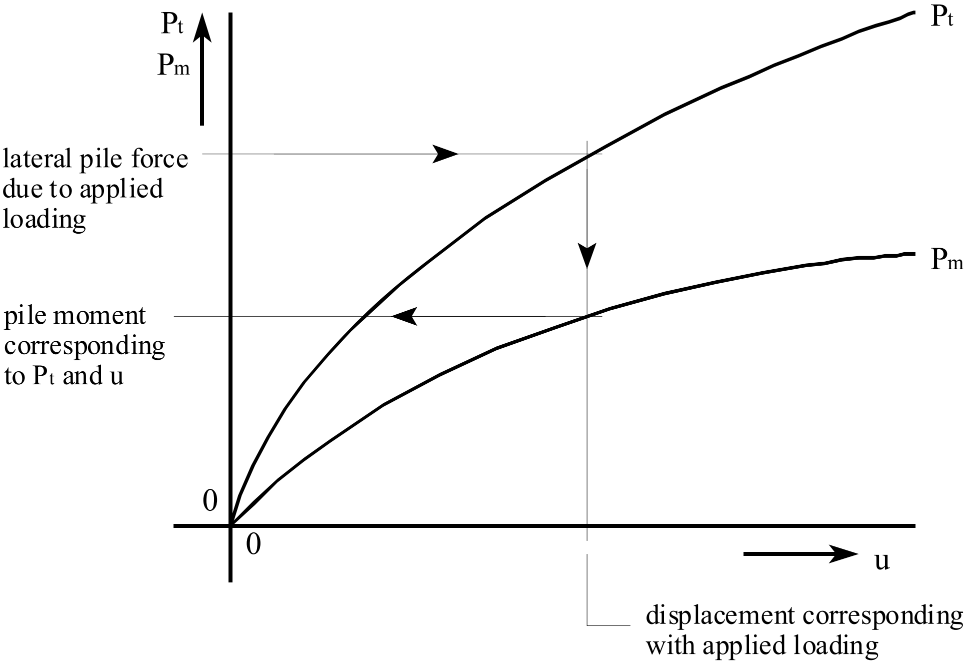

Figure 6.6-3. Lateral pile force and moment as a function of rigid body displacement u, for a compatible set of boundary conditions at the structure – foundation interface

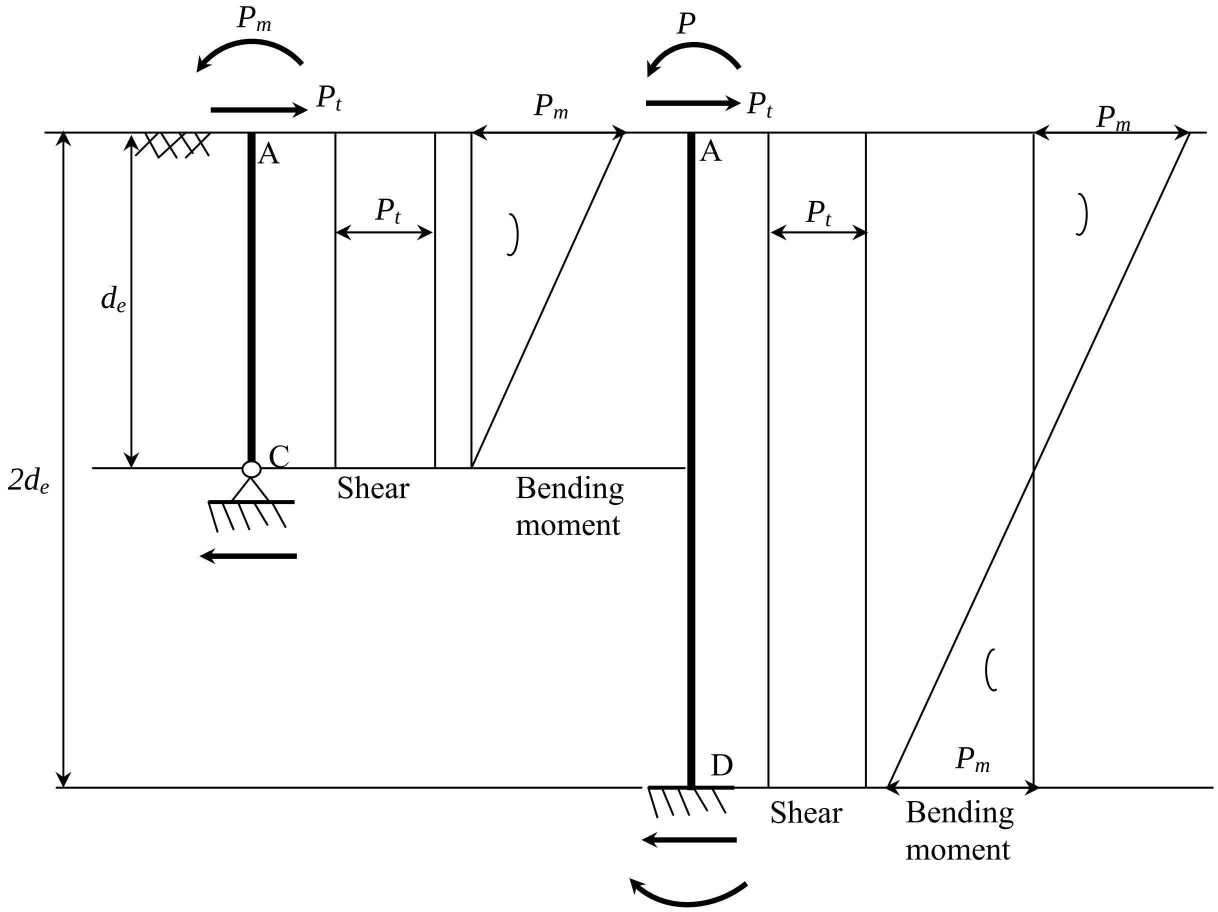

Figure 6.6-4. Representation of the boundary conditions at the top of the pile by a hinged and a clamped dummy member

with a moment $M = M_1$ at the top of the pile. However, in reality a displacement $y_{top} = u$ is accompanied by a rotation $\varphi = \varphi(u)$ of the pile head, which is given by the equations 6.6-5 and 6.6-6. This situation is presented by the force and moment diagrams on the right hand side of figure 5.3-10, which relate to a rotation $\theta_{top} = \varphi$ due to a moment $M = M_2$, while the displacement y_{top} is kept constant (in figure 5.3-10 at a value of zero). Relaxation of the rotational constraint by letting the pile head assume a rotation $\varphi = \varphi(u)$ thus corresponds with a moment $M = M_2$. To keep the pile head displacement constant this moment is accompanied by a lateral force $F = F_2$. The total loading at the top of the pile for a displacement u as well as a rotation $\varphi = \varphi(u)$ is thus a force $P_t = F_1 + F_2$ and a moment $P_m = M_1 + M_2$. It should be noted that in the process sign conventions should be carefully defined and strictly adhered to. Positive directions of rotations and moments in accordance with the right hand rule are e.g. different when working in the *yz*-plane or the *xz*-plane. Starting with a positive lateral force F_1 the displacement $y_{top} = u$ will also be positive, but the other variables M_1, $\theta_{top} = \varphi(u)$, M_2 and F_2 may all be positive or negative depending on the plane we work in and the associated sign conventions.

By performing a series of such non-linear lateral pile analyses for the right pile make-up and the given soil conditions, and increasing values of F_1 from 0 to about $\frac{1}{2} F_B$ (assuming two piles), curves of $P_{t\,env} = P_t(u)$ and $P_{m\,env} = P_m(u)$ can be constructed; see figure 6.6-3. For given applied loading, the lateral pile force P_t is known and figure 6.6-3 thus provides values of u and P_m that are associated with P_t, as well as with all the other boundary conditions for the particular structural configuration, foundation piles and soils under consideration. The length of the dummy member can then be determined from $d_e = P_m / P_t$. As u is now also known, the associated rotation φ can be determined form 6.6-5. Next EI_d is given by equation 6.6-2.

As the dummy members AC have now been determined they can be added to the structural model, after which a linear structural analysis can be completed. The structural frame analysis should obviously give the same answers for P_t and P_m as well as for u and φ as the values that resulted from the above relationships; if this is not the case something has gone wrong. Note that the foundation model is a linearised representation of the non-linear pile-soil interaction problem *around a chosen point of linearisation for a given set of conditions and assumptions*. Therefore, it is only a valid model as long as no conditions are altered. For example, for a different loading condition the foundation model has to be revised.

As introduced above, the dummy member AC is pinned at point C and has a length of d_e. An alternative representation of the same boundary conditions at the sea floor is obtained by a dummy member AD with a length of $2d_e$, which is built-in at point D; see figure 6.6-4. Either of these representations may be chosen.

Determining an appropriate foundation model for such general conditions is obviously a rather complicated and laborious process. A further simplification that may be considered is to neglect the rotation φ altogether, so that the frame is assumed to displace purely horizontally under the applied loading. The pile elongation and shortening w is then also zero, so that equations 6.6-5 and 6.6-6 vanish, while $\varphi = 0$ can be substituted into equation 6.6-2. F_2 and M_2 then also disappear and the construction of figure 6.6-3 simplifies as well, although its form remains the same. Determination of a corresponding set of values for P_t, P_m and u and the parameters d_e and EI_d of the dummy member is unaltered.

Recognising that d_e is small and that P_m is usually a rather small term in the overall moment equilibrium of the frame or the structure, d_e may alternatively be estimated much more crudely. From experience we know that at a distance of approximately 3 pile diameters below the sea floor the pile will have an inflection point; see e.g. figure 5.3-9. At this point the bending moment is zero and the inflection point could therefore conveniently serve as the hinge point C at the end of the dummy member. Thus, instead of determining the effective depth $d_e = P_m / P_t$ by calculation, it can simply be assumed to be equal to the depth of the inflection point, if a non-linear lateral pile analysis in the appropriate soil conditions and for the required magnitude of the applied loading is available. Alternatively, and even more crudely, it can just be assumed to be $d_e \approx 3D$. The additional approximations involved in such an estimate in comparison with the full and more correct modelling procedure are:

- the inflection point has a lateral displacement, so that it does not lie on the undisturbed position of the pile;
- the actual pile is subject to lateral soil pressures between the sea floor and the inflection point, while the dummy member AC is unloaded over its full length.

Using $d_e \approx 3D$ as a yardstick, the effective depth is some 3 to 10 m below the sea floor for pile diameters of 1.0 to 3.0 m. For structures in rather shallow water this is not necessarily negligibly small compared to the height of the application point of the environmental loading above the sea floor. The overturning moment may therefore be increased by some 10% due to the pile moments. The deeper the water, the smaller the contribution from P_m; in waterdepths greater than about 100 m the pile moments generally become negligibly small compared to the overturning moment.

Yet another approximate model to support the frame without any calculation is based on the fact that the pile has a few points of zero displacement along its length (see again figure 5.10 as an example). The first zero point is usually at some 6 to 8 pile diameters below the sea floor, the second at some 12 to 15 diameters. The pile deformations at and in between these points of zero displacement are very small. The pile may thus be assumed to be built-in somewhere in this region. If this model is used the structural member under the support points of the frame is the actual pile rather than the dummy member with fictitious properties. The additional approximation that the lateral soil pressures on the actual pile are not included in the frame analysis applies here as well.

6.7 The interaction between frame and piles

6.7.1 General

In section 5.3.4 we discussed different options for the configuration of the (space) frame and its foundation piles, resulting in two different types of structure: the jacket and the tower. We further noted that the structural behaviour of a jacket and a tower is markedly different as a result of differences in foundation-structure interaction. How permanent, variable and wind loads are introduced to the structure also depends on the type of structure; these loads are either applied to the frame or to the piles. For the hydrodynamic loads the type of structure is irrelevant; the hydrodynamic loads are always applied to the frame. The differences in load application with structure type were briefly mentioned in section 6.3 but not further discussed. In sections 6.4 to 6.6 we subsequently dealt with the support reactions for the frame (and conversely the loads on the foundation piles) *at the sea floor*, where the differences between a jacket and a tower have disappeared. We will now look into the interaction of foundation piles and frame and the associated differences between a tower and a jacket more closely. These differences will be illustrated further in sections 6.8 and 6.9.

In this handbook the terms ‘jacket’ and ‘tower’ will always be used in a consistent manner to distinguish two different types of structure. However, one should be aware that the terminology in the offshore industry is not so firmly established and often rather loosely used. Therefore, one should not be surprised to hear the largest steel tower structures, or even concrete structures, being referred to as ‘jackets’. In such cases the word ‘jacket’ is in fact indiscriminately used as an alternative term for a ‘structure’.

6.7.2 The tower

An example of a tower type structure is shown in figure 5.3-5. For these structures the piles are traditionally installed through short pile guides around the leg at several elevations to guide the piles down to the sea floor, after which they are driven into the ground by a pile driving hammer from above the water. When the water depth plus pile penetration exceeds the length of the original pile section a so-called add-on is welded to the pile in the field during installation and driving continues. When the pre-fabricated pile section plus one or more add-ons is equal to the full length of the pile that is to be installed, a loose follower is put on top of the pile so that driving can continue from an above water position. This is a necessity when steam hammers are used, because these can only operate from above water. The more modern, slim-line hydraulic hammers are put on top of the pile and can follow the pile through the pile guides under water, so that there is no need for a follower. The connection of the pile to the leg is made by means of a pile sleeve at the *base of the frame*; this sleeve is considerably longer than the pile guides through which the pile passes during installation, to make a proper connection possible. When the pile has been driven final penetration it ends at the top of the pile sleeve; any pile length sticking out above the top of the sleeve may be cut-off. The connection of the pile to the structure is generally achieved by cementing the annulus between the pile and the sleeve, but a mechanical connection is increasingly used as an alternative; see section 5.3.4.

In virtually all cases there are several piles clustered around each leg. The number may be as few as two and as many as e.g. six. This depends on the number of piles required for the foundation and any limitation that may be imposed by the geometrical arrangement. The distance between the piles should be as large as practically possible to avoid undue interference of the piles in the ground. If possible, centre to centre distances should be at least some 2.5 to 3 pile diameters. In any event, the piles will normally act as a pile group for which both the axial and the lateral capacity are not the same as a simple summation of the individual pile capacities. In the idealisation used in this handbook the pile group is modelled as one equivalent pile. The physical length of the pile-to-leg connection is further reduced to a point at the sea floor, while the equivalent pile is positioned at the centre of the leg, thus ignoring horizontal eccentricity.

All loads on the structure, applied above or below water, will thus be transmitted through the (near) vertical and horizontal frames to the legs, and from the bottom of the legs to the (equivalent) piles at the idealised point connection. A cross section at the sea floor creates a physical separation between the frame above and the foundation piles below this section, so that any interaction between frame and piles can only take place at these points.

The frame of a tower is subject to the following combination of applied loads and pile support forces:
- permanent and variable point loads from the superstructure as shown on figure 6.3-1;
- horizontal and vertical wind loads as shown on figure 6.3-5;
- horizontal hydrodynamic point loads as shown on figure 6.3-7;
- distributed permanent and variable loads of the submerged substructure;
- axial and lateral pile forces and pile moments at the bottom of the legs, as shown on figures 6.4-1, 6.4-3 and 6.4-4; these forces are also shown on figure 6.8-1a of the next section 6.8, where the applied loading for illustration purposes consists of a resultant hydrodynamic load only.

The legs are loaded at their top by the loads given in the equations 6.3-2, 6.3-6 and 6.3-9. The total base shear is given by equation 6.3-11 and the overturning moment by equation 6.3-13. The foundation piles representing the pile groups are subject to axial and lateral forces and a moment at the sea floor, as depicted in figures 6.4-1, 6.4-3 and 6.4-4; they are given by the equations 6.4-21 to 6.4-23. The distribution over the individual piles within the group may in the first instance be assumed to be uniform. This will generally not be very accurate but a more refined distribution can only be obtained by detailed structural modelling, taking the correct pile positions, the geometry of the structure and the stiffnesses of the various elements including soils into account. This normally requires computer modelling.

6.7.3 The jacket

An example of a jacket type structure is shown in figure 5.3-4; the main piles to support the structure run though the 4 legs of the frame. In this particular example there are two more skirt piles in sleeves between the legs. These skirt piles are very similar to the cluster piles of a tower structure and will not be considered in the discussion hereafter. Pile make-up and pile installation for the jacket are analogous to those for the tower with two differences:
- the total pile length is always equal to the pile penetration plus the height of the frame and is made up of the original pile section plus welded add-ons, there is no need for a follower;
- pile installation is of necessity done by driving with hammers from above the water, be they steam or hydraulic hammers.

The pile and the leg are concentric hollow tubular members: a tube in a tube. The only connection between them is a welded connection at the top. This connection is achieved by cutting slots (also called castellations) in the top of the leg and inserting wedges (also called

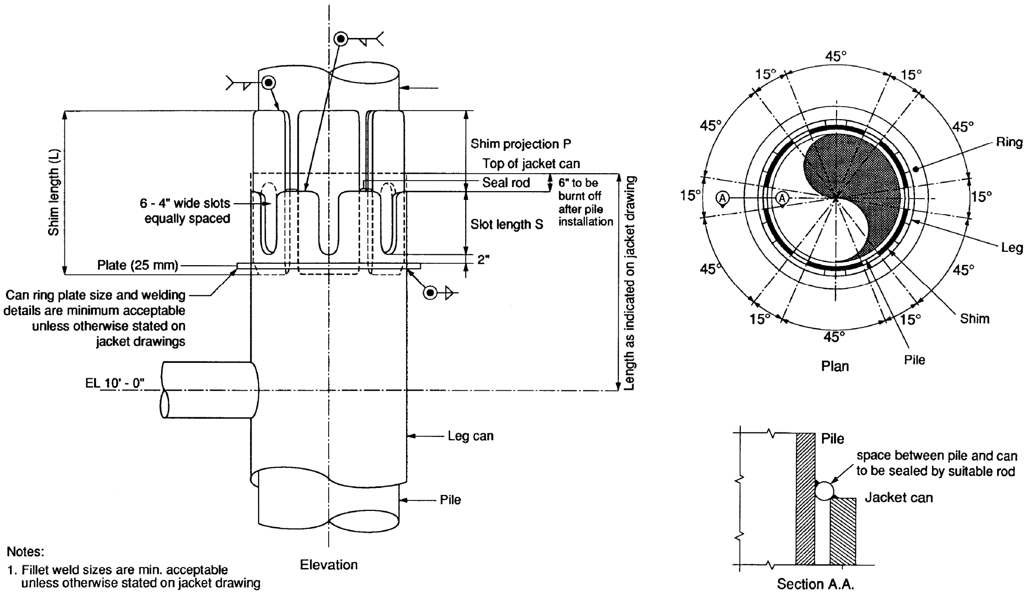
Shim length (L)
6 - 4" wide slots equally spaced
Plate (25 mm)
Can ring plate size and welding details are minimum acceptable unless otherwise stated on jacket drawings
EL 10' - 0"
Shim projection P
Top of jacket can
Seal rod
6" to be burnt off after pile installation
Slot length S
2"
Length as indicated on jacket drawing
Leg can
Pile
Elevation
45°
15°
15°
45°
45°
Ring
15°
15°
Leg
45°
45°
15°
15°
Shim
45°
Plan
Pile
A
A
Pile
space between pile and can to be sealed by suitable rod
Jacket can
Section A.A.

Notes:

1. Fillet weld sizes are min. acceptable unless otherwise stated on jacket drawing
2. Refer to jacket drawing for:
   shim length (L)
   shim thickness (t)
   shim projection (P)
   slot length (S)
   top can thickness (T)

Figure 6.7-1a. Pile to jacket connection

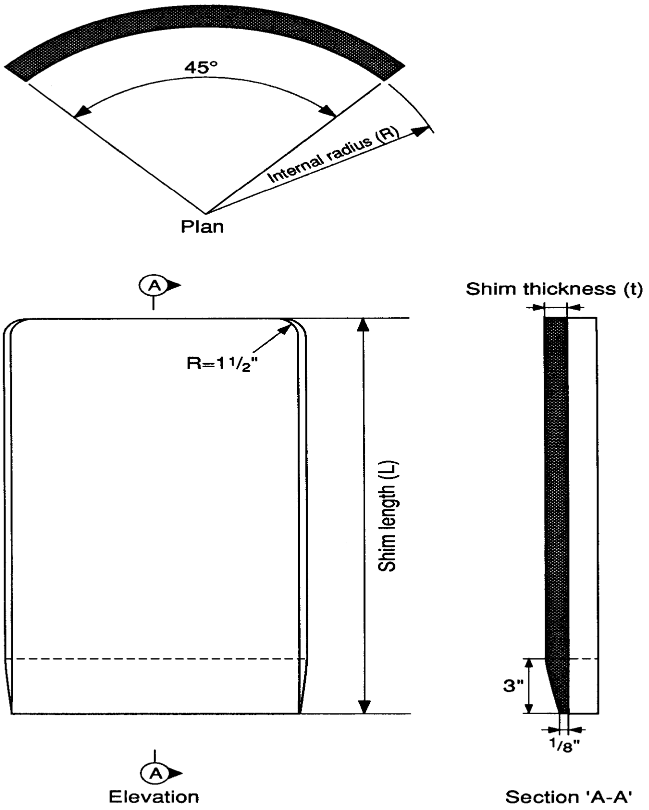

Figure 6.7-1b. Shim for pile to jacket connection

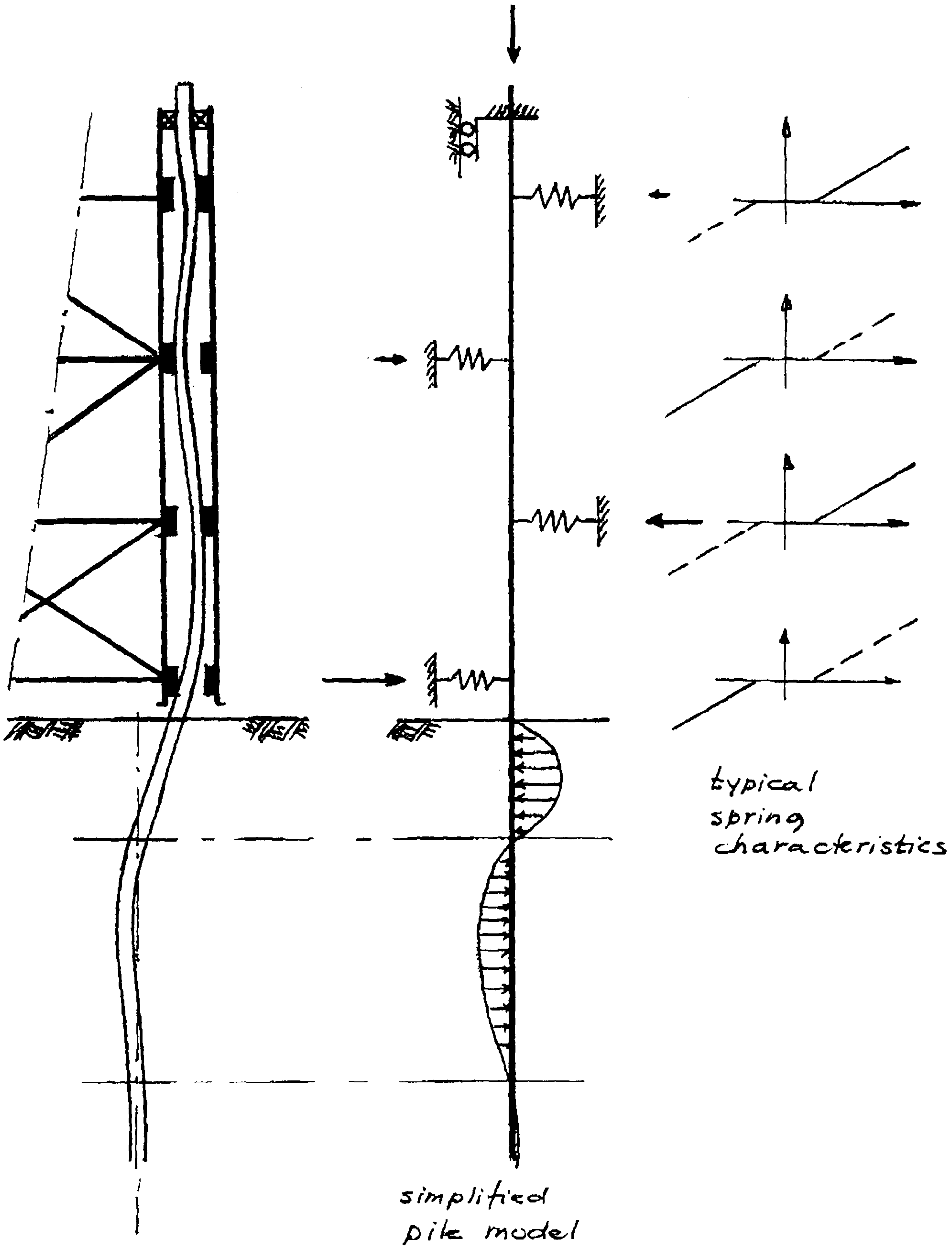

Figure 6.7-2. Two-dimensional model of the interaction between pile and jacket leg

shims) into the annulus between the pile and the leg; see figures 6.7-1a and b. Along their upper ends and sides the wedges are welded to the pile, while the leg is welded to the wedges along the slots or castellations. All these welds are fillet welds as full penetration welds are not possible in this situation. Under compressive forces the pile will of course deflect within the hollow leg and will make contact with the leg at some places. At these contact points frictional forces can develop, but these are clearly negligibly small compared to the axial force transfer that takes place at their welded connection at the top. Therefore the pile and the leg may be assumed to be free in an axial direction; they may both get longer or shorter with respect to one another without any mutual interference.

In a lateral direction the pile is very flexible in comparison with the leg. The leg has a larger diameter and is therefore much stiffer, while it is further stiffened by the braces in the frame. The points of contact between the pile and the inside of the leg are usually predetermined at the 'hard points' at the horizontal framing levels where the braces frame into the leg. This is either achieved through joint cans with a greater wall thickness and a smaller internal diameter than the rest of the leg or by insert plates that are welded to the inside of the leg. The clearances between pile and leg are thus smallest at these locations, making them the natural points of contact. At these contact points some lateral force transfer will take place, but due to the relatively low bending stiffness of the pile these forces remain rather small. The true three-dimensional situation is difficult to model and the orientation and magnitude of the contact forces are hard to determine with any degree of accuracy. In two-dimensional computer analyses the pile is often modelled as a beam column, i.e. a beam that is also subjected to compression, supported laterally by spring supports at the horizontal plan framing levels; see figure 6.7-2. The realism of such a model depends on the deformation pattern of the pile within the leg and the relative stiffnesses of pile and leg involved. The lowest two support levels experience opposite forces that are the largest of all the contact forces. We will neglect contact forces at higher elevations. The difference between the two forces at the lowest elevations is the lateral force transmitted by the frame to the pile, while the moment due to the upper force is the moment transmitted to the head of the pile. As our present considerations aim at manual or spreadsheet type calculations, we will idealise this situation further by assuming that all lateral force and moment transfer takes place at the base of the frame where the pile enters the leg. This is clearly a simplification, but a fairly realistic approximation of the real situation. It is also analogous to the assumption made for the tower where the physical length of the pile-to-leg connection was reduced to a point at the sea floor.

When the jacket is placed on the bottom of the sea and before the piles are installed the weight of the structure is supported by the sea floor. To create adequate bearing area for carrying this weight so-called mudmats are usually attached to the lowest horizontal framing level. When the piles are driven and before they are welded to the legs, the individual pile weight is similarly carried by the sea floor. After welding the two parts have become one whole. It is now common to assume that some erosion will always take place around the base of the structure, so that after some time the space frame with its mudmats is no longer supported by the sea floor and the whole structure hangs off the top of the piles. This is a more or less standard assumption for design purposes, regardless of the type of soil at the sea floor. It maximises the *compressive pile* loads, while on the other hand the *legs* are subject to some tension due to the self-weight of the jacket. Note that compression is a more onerous loading case than tension and that stability and strength considerations are of much greater concern for the smaller diameter piles than for the legs, which are not only larger in diameter but also stiffened by the frame.

Transfer of forces between frame and piles for a jacket is thus markedly different than for a tower. A cross section at the sea floor now does not make a physical separation between the frame above and the foundation piles below the section. The cross section cuts through the piles that extend to the top of the frame, so that above the cross section we have a combination of frame and piles. Note that if we look at the *frame with the piles within the legs included* the situation is exactly the same as for the tower. However, when the piles within the legs are *excluded* the situation for the frame alone is quite different.

The frame alone of a jacket structure is subject to the following combination of applied loads and pile forces:

- horizontal and vertical reaction forces at the top of the frame due to the fixed connection between pile and leg, where each pile is subjected to point loading by permanent and variable loads as well as horizontal and vertical wind loads (see figure 6.3-1 and figure 6.3-5);
- horizontal hydrodynamic point loads as shown on figure 6.3-7;
- distributed permanent and variable loads of the submerged substructure;
- axial pile forces at the top of the legs, as shown on figure 6.8-2a of the next section 6.8 (for a resultant hydrodynamic load only);
- lateral pile forces and pile moments at the bottom of the legs, as also shown on figure 6.8-2a of the next section 6.8 (for a resultant hydrodynamic load only).

The point loading on the top of the piles is given by equations 6.3-2, 6.3-6 (which are the same as for the tower) and 6.3-10 (which differs slightly from equation 6.3-9 for the tower). The reaction forces at the top of the frame depend on the geometry and stiffness of the upper frame panel and are not immediately obvious. These will be discussed further in section 6.10.

The total base shear is given by equation 6.3-11 as for the tower, while the overturning moment for the jacket is given by equation 6.3-14, which differs slightly from equation 6.3-13 for the tower in the last term. The foundation piles are subject to an axial force at the top, and a lateral force plus a moment at the sea floor. The magnitudes of these forces are again given by the equations 6.4-21 to 23, as for the tower. The axial pile forces are transmitted to the top of the frame, while the lateral pile forces and moments are transmitted to the frame at the base.

6.7.4 Hybrid structure types

Of course, variations and combinations of the two structure types are possible and do exist. An example is a substructure with so-called pin piles through the legs for a quick pinning of the structure to the sea floor during installation, supplemented by piles clustered around the legs to complete the foundation. Another example is a structure with piles through the legs, and additional skirt piles arranged along the external perimeter of the structure between the legs (see e.g. figure 5.3-4). In these hybrid cases the basic principles that apply to the jacket and to the tower remain the same, but the different support cases obviously influence one another so that the transfer of forces between legs (or other members of the frame) and foundation piles is a much more complicated problem than for the pure tower and the pure jacket. For such hybrid cases the foundation-structure interaction and the associated force transfer between frame and piles is a statically indeterminate problem that is governed by the various stiffnesses involved and must be solved by computer analysis using finite element programs and appropriate structural modelling. In this handbook we will restrict ourselves to the pure (and idealised) tower and jacket cases.

The following is a special case of a tower structure. With the development of hydraulic pile driving hammers that can follow the pile under water, the need for pile guides has largely disappeared. Therefore, the batter of the piles can now be chosen independently from the inclination of the legs. In modern structures this will often lead to *vertical pile sleeves* clustered around *inclined legs* instead of pile sleeves that are parallel with the legs. Although hydraulic hammers are capable of driving the piles under an angle as well as vertical, the latter is often preferred from a pile installation point of view. The advantage that the horizontal components of the axial pile forces contribute to balancing the applied horizontal loading (i.e. that they participate in the shear take-out) is then of course sacrificed.

A further special case is a structure that has piles through the legs with the annulus between pile and leg now grouted over the full height of the structure, instead of the welded shim connection between pile and leg at the top. Despite its initial appearance as a pile-through-leg and thus a jacket type structure, this is actually a tower structure. The grouting has transformed the pile plus leg into a composite member that behaves as one member with equivalent structural properties. The foundation support is therefore at the sea floor rather than at the top as for a jacket.

6.7.5 The internal forces and stresses in the piles

As described in section 5.3.4, the pile in the ground may be modelled as an elastic steel beam column supported by non-linear lateral and axial soil springs. The loading *on the top of the pile* has been described in detail in the preceding sections. To determine the internal forces and stresses *in the pile along its length* from the sea floor downwards the non-linear pile-soil interaction problem must be solved by performing lateral and axial pile analyses using a suitable finite element formulation.

The internal forces in the part of the pile within the jacket leg above the sea floor are usually adequately approximated by the full axial force only, as described in section 6.7.3 above.

6.8 Mechanical models for frame behaviour

6.8.1 General

Having determined the applied loading, the support reactions of the frame at the sea floor and the interaction between frame and piles, we should now establish a suitable mechanical model for the behaviour of the frame. For this purpose we will first consider the frame as a continuous beam rather than as an assembly of discrete members. In order to better illustrate the basic aspects involved we will further simplify the applied loading to hydrodynamic loading only with a single resultant horizontal load F_R and an application point at a height ℓ above the sea floor. The general support reactions at the sea floor in equations 6.4-21 to 23 then reduce to those in equation 6.4-25. We will further assume that the batter angles of legs and piles on both sides of the frame are the same.

6.8.2 A mechanical model for the tower

For the assumptions adopted in this chapter 6 and the loading condition considered here the tower frame behaves as a cantilevered vertical beam. Figure 6.8-1 shows from left to right the tower model with the applied load and the support reactions of the piles, an equivalent beam model, and the corresponding shear force and bending moment distributions over the height of the tower frame.

The tower model is a mechanical model of the real frame, represented in its simplest schematic form while retaining essential features. As long as we are considering the tower as a continuous beam, the structure above the sea floor can be condensed into a single vertical stick of the correct height. This also suffices to apply the applied load F_R at the elevation ℓ. The important features of the individual support reactions are their points of application and their orientation; these should be retained in the model. Therefore the base of the tower is represented as an additional horizontal stick of the correct width, at the ends of which the support reactions are applied. The two sticks are rigidly connected which enables the full transfer of forces from one to the other. The physical support by the pile at the sea floor in figure 6.8-1a is represented by three springs: an axial spring, a lateral spring and a rotational spring. The spring stiffnesses of these springs can be determined from non-linear pile analyses. An adequate representation of the support conditions requires general modelling by (linear or non-linear) springs for each of the 3 degrees of freedom. Standardised support conditions, such as a hinge, a roll or a clamped (built-in) support, are special cases of such general spring supports; individually or in combination these standardised supports are unable to correctly reflect the actual support conditions of the frame.

This tower model is the simplest possible, but an entirely sufficient model to schematically represent the two-dimensional frame of a tower structure with its pile foundation under the applied loading of a net resultant force. No relevant properties of the real frame and its piles have been lost. Vertical instead of battered piles are simply a special case of the model with $\alpha = 0$.

From the tower model an equivalent beam model is easily derived. This is a further condensation into an even more schematic model, which is entirely adequate from a viewpoint of equilibrium, but certain properties of the support conditions have been lost. The individual pile supports, which are retained in the tower model, are now replaced by the

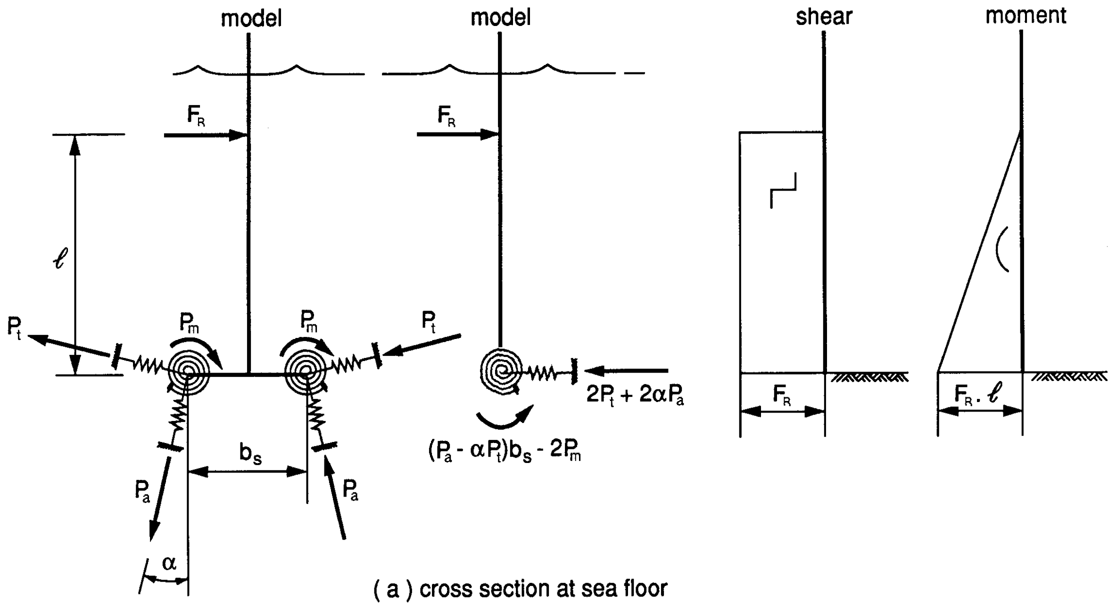

(a) cross section at sea floor

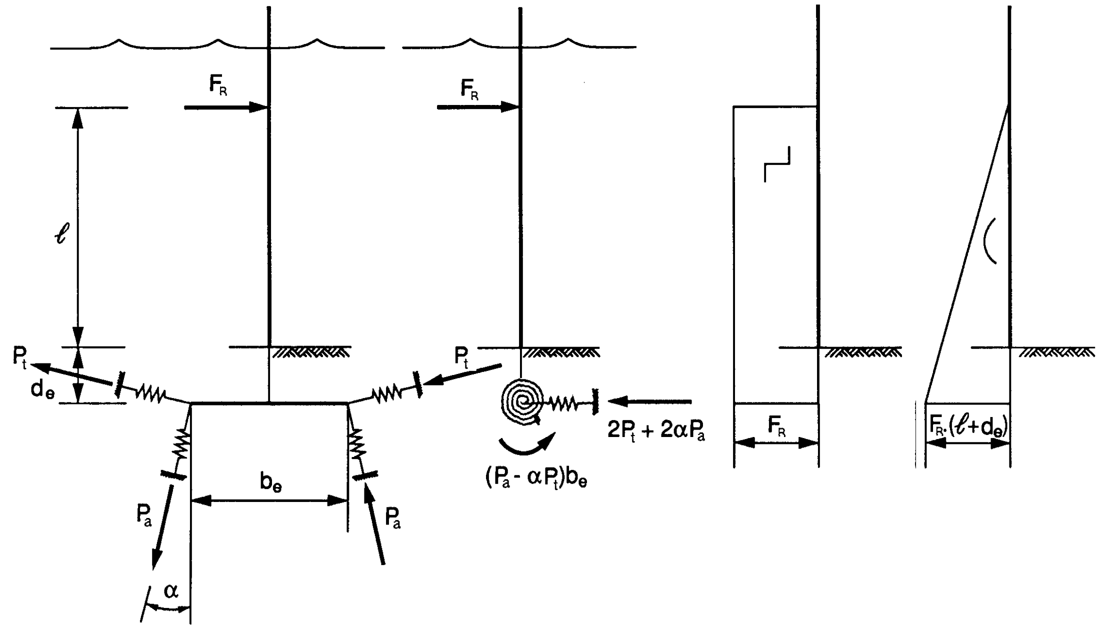

(b) cross section at hinges of dummy members

Figure 6.8-1. A schematic model of a tower frame with its associated:

-support conditions
-equivalent beam model
-shear force distribution over the height
-bending moment distribution over the height

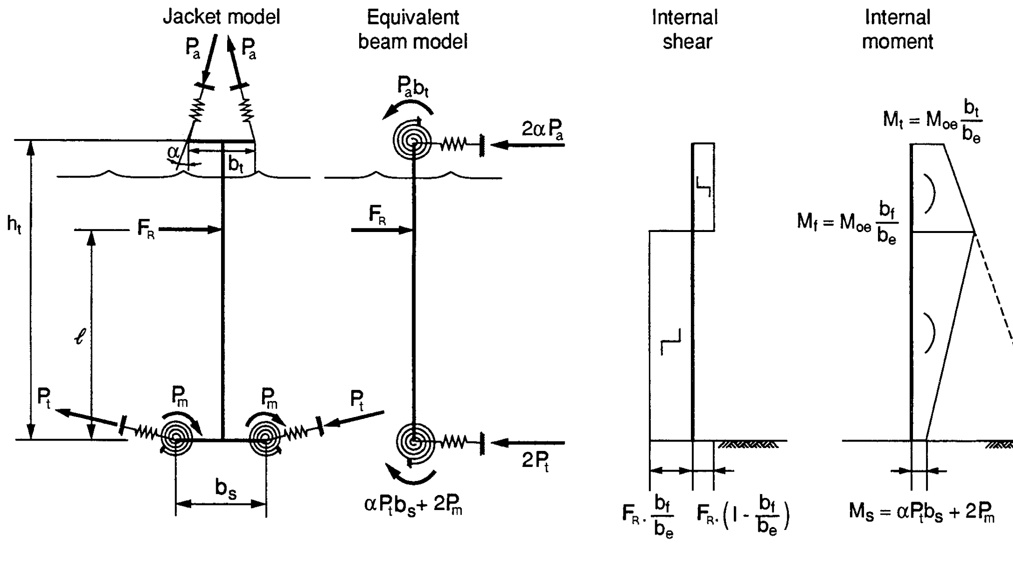

(a) cross section at sea floor

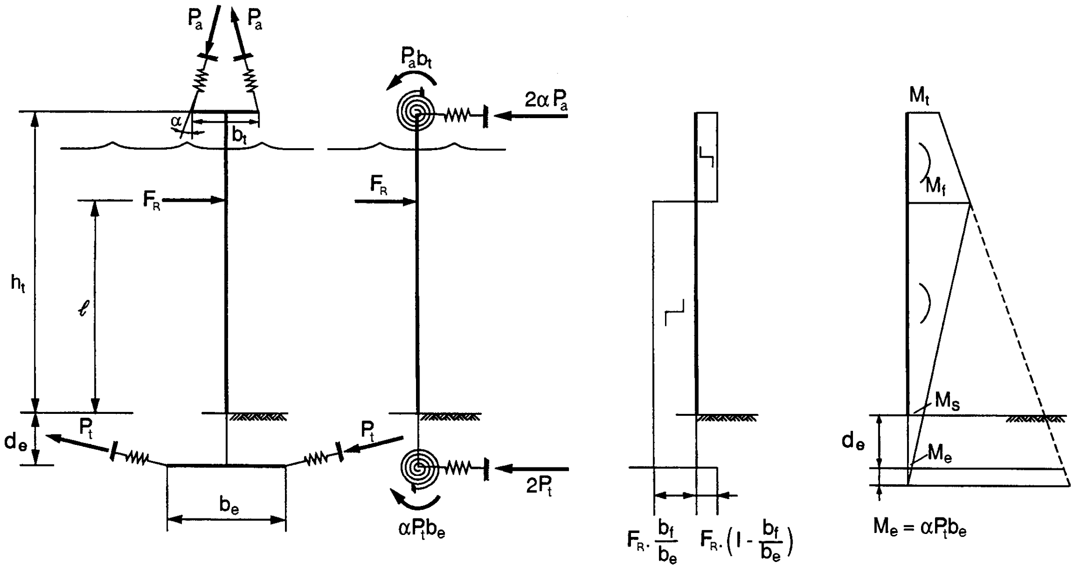

(b) cross section at hinges of dummy members

Figure 6.8-2. A schematic model of a jacket frame with its associated:

-support conditions
-equivalent beam model
-shear force distribution over the height
-bending moment distribution over the height

global foundation reactions with the associated loss of some detail. The beam is not built-in at the sea floor, but is supported by an overall lateral and an overall rotational spring at its base, as shown in figure 6.8-1a. The spring stiffnesses of these overall springs comprise the appropriately combined stiffnesses of the individual pile springs. From the beam model it is easily observed that under applied loading a tower structure experiences a non-zero (rigid body) displacement and a rotation at its base; frame deformations are further discussed in section 6.9.

From the equivalent beam model the corresponding shear force and bending moment distributions over the height of the frame follow directly from elementary applied mechanics. Above the applied load the frame is unloaded and both shear force and bending moment in the frame are therefore zero. Below the applied load the shear force is constant and equal to F_R, while the bending moment increases linearly to the sea floor to a value of $F_R \cdot \ell$.

If the support points of the frame are moved downward to a cross section at the artificial hinge points of the dummy members at a distance $d_e \cos\alpha \approx d_e$ below the sea floor the internal pile moments P_m vanish. The shear force over the height remains equal to F_R whereas the moment increases to $F_R \cdot (\ell + d_e)$. This is shown in figure 6.8-1b.

6.8.3 A mechanical model for the jacket

As we want to determine the forces in the individual legs and bracing members and the associated deformation pattern of the jacket frame, the model should represent the frame only, excluding the piles within the legs. As discussed in section 6.7.3, the jacket frame is laterally supported at its base and axially at its top, while transfer of the internal pile moment in our model also takes place at the base. The jacket model with the applied load and the support reactions of the piles, an equivalent beam model, and the corresponding shear force and bending moment distributions over the height of the jacket frame are shown from left to right in figure 6.8-2.

The jacket model is also a mechanical model of the real structure (frame only), represented in its simplest schematic form while retaining essential features. It is constructed in the same manner as the tower model, now with an additional horizontal stick of the correct width at the top of the frame to enable the axial pile forces to be applied to the frame. The lateral and rotational spring supports remain located at the base, as for the tower, but the axial spring supports are now located at the top.

From the jacket model an equivalent beam model is once more easily derived. It is markedly different from the tower equivalent beam model. Note especially the difference in the magnitude and direction of the supporting moments. While for the tower the top is a free end, for the jacket both the base and the top of the beam are spring supported by a lateral and a rotational spring, as shown in figure 6.8-2a. Under applied loading the jacket structure will therefore not only experience a non-zero (rigid body) displacement and rotation at its base, but it will additionally undergo a counter displacement and a counter rotation due to the spring support at its top; see for a further discussion of the deformation pattern section 6.9.

The corresponding shear force and bending moment distributions over the height of the frame follow once more directly from elementary applied mechanics. The part of the frame above the applied load now also experiences shear forces and bending moments in contrast to the tower case. The shear forces above and below the applied load are different in magnitude and direction. The bending moment in the jacket frame is opposite in direction to that in the tower frame. Its magnitude first increases from the top down to the point at which the applied load acts and then decreases linearly towards the base of the frame. If the support points of the frame are moved downward to a cross section at the artificial hinge points of the dummy members at a distance $d_e \cos\alpha \approx d_e$ below the sea floor the internal pile moments P_m again vanish. This is shown in figure 6.8-2b.

The overturning moment about the effective depth d_e below the sea floor is $M_{Oe} = F_R(\ell + d_e)$. From equation 6.4-25, which refers to the present loading case, we see that:

$$P_a = \frac{M_{Oe}}{b_e} \qquad (6.8\text{-}1)$$

as one would expect. The moment at the top of the frame thus is:

$$M_t = P_a \cdot b_t = M_{Oe} \cdot \frac{b_t}{b_e} \qquad (6.8\text{-}2)$$

At the application point of the applied load the moment is:

$$M_f = P_a b_t + 2\alpha P_a (h_t - \ell) = P_a \left\{ b_t + 2\alpha (h_t - \ell) \right\} = M_{Oe} \cdot \frac{b_f}{b_e} \qquad (6.8\text{-}3)$$

From thereon it decreases linearly. At the sea floor it is equal to:

$$M_s = \alpha P_t \cdot b_s + 2P_m \qquad (6.8\text{-}4)$$

while at the effective depth only the vertical components of the lateral pile forces remain:

$$M_e = \alpha P_t \cdot b_e \qquad (6.8\text{-}5)$$

The model discussed above describes the behaviour of the *frame alone*, without the piles inside the jacket legs. If we include the piles above the sea floor with the frame the situation is exactly the same as for the tower. This is demonstrated by figure 6.8-3.

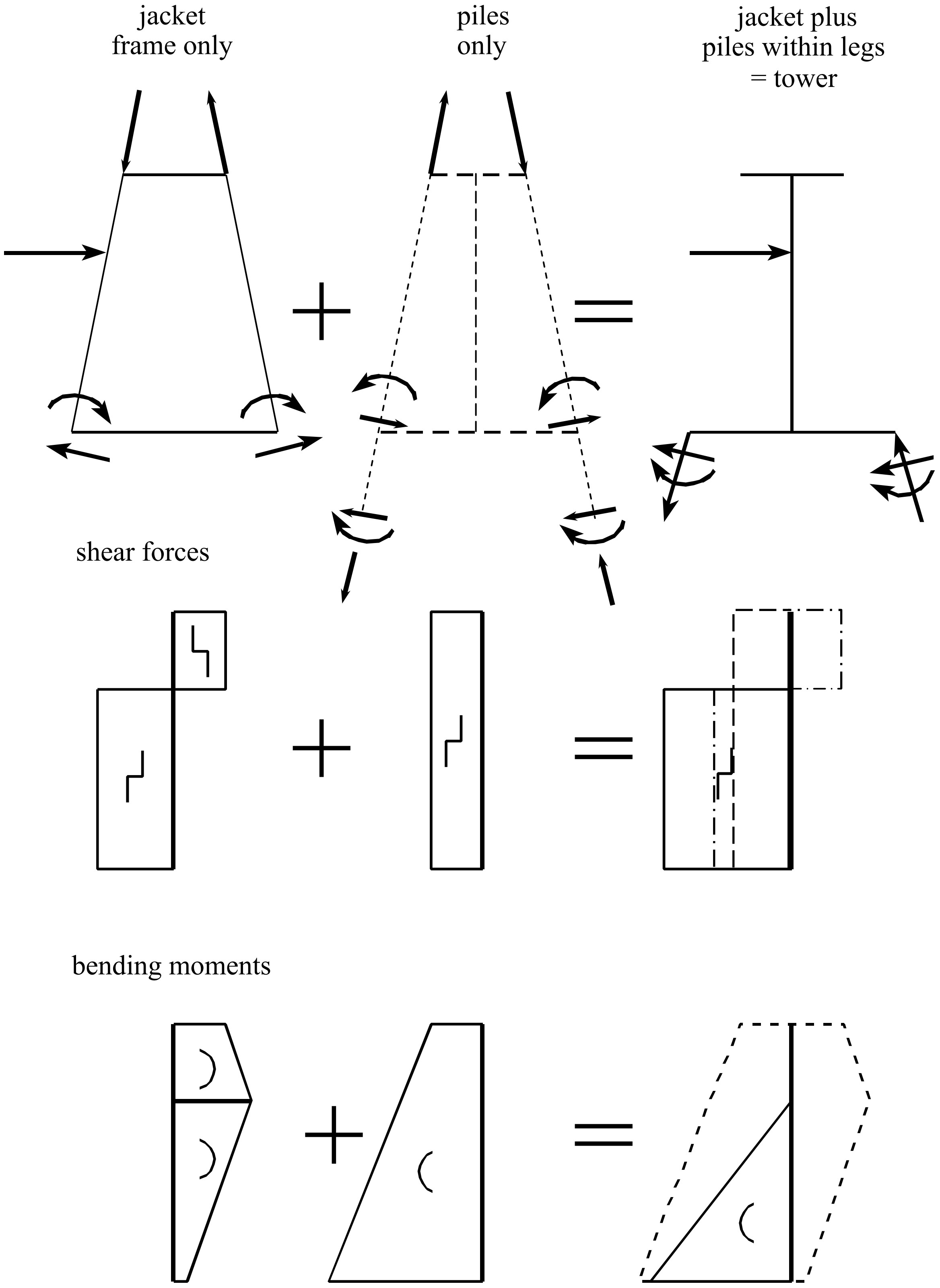

Figure 6.8-3. Jacket (frame only) plus piles within the legs is equal to a tower

a) rigid body displacement and rotation for tower and jacket

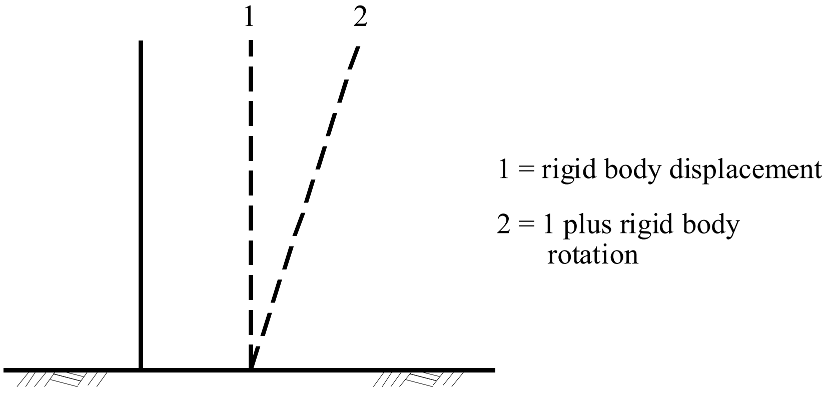

b) tower structure

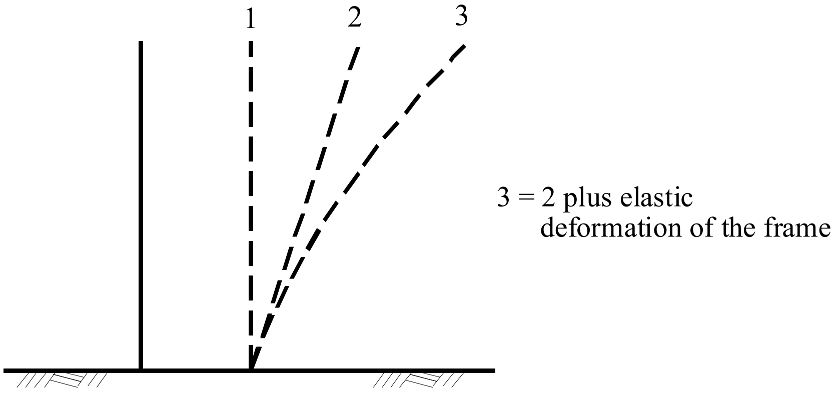

c) jacket structure

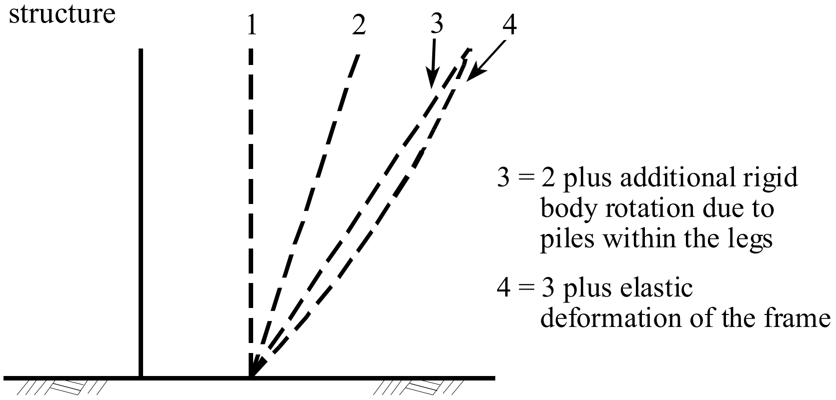
1
2
3
4
3 = 2 plus additional rigid body rotation due to piles within the legs
4 = 3 plus elastic deformation of the frame

Figure 6.9-1. Deformation of steel space frame structures

6.9 Deformations of steel space frame structures

The deformations that steel space frame structures experience are a combination of displacements and rotations of the foundation piles and deformations of the space frame itself. They are distinctly different for a tower and a jacket. To show this we will build up the deformation patterns as a summation of deformations from below and above the sea floor.

For the deformations below the sea floor we consider the structure above the ground first as a rigid body. Elastic deformations of the space frame (for a tower) and of the space frame plus the piles within the legs (for a jacket) are thus suppressed. Both structure types will then experience a rigid body displacement that is controlled by the lateral foundation spring at the sea floor, and a rigid body rotation that is controlled by the rotational foundation spring at the sea floor. As demonstrated by figure 6.8-3, these two cases are identical so that both structures experience exactly the same displacement 1 and rotation 2, see figure 6.9-1a. Due to the deformations of the foundation elements in the ground there is thus no difference between a tower and a jacket.

For the deformations above the ground we consider the two structures separately. For the tower the space frame deforms elastically as a cantilevered beam due to shear and bending, see figure 6.9-1b, where bending is normally the dominant deformation. However, for short and sturdy structures the shear deformation can be of the same order or even greater than the bending deformation. For the jacket we will let the two parts of the structure (the space frame and the piles within the jacket legs) deform individually in sequence. The frame is first held rigid, but the piles above the ground extend and compress elastically under the axial pile loads. This results in an additional rigid body rotation above the ground; see pattern 3 in figure 6.9-1c. Finally, the rigidity of the space frame is released so that the frame itself can now also deform elastically. From figure 6.8-2 we note that the frame is a beam on two supports: one at the top and one at the base. Hence it will deform with respect to pattern 3 as shown by pattern 4 in figure 6.9-1c. The deformations of a tower structure and a jacket structure are hence distinctly different.

6.10 Frame loading and sectional forces over the height of the frame

In previous sections we have discussed the global frame behaviour. We now want to determine the internal forces in the frame and for that purpose we need to consider the load application in somewhat greater detail. The internal forces are not only affected by the global loading of the frame, but also by how and where the loading is exactly applied. This was already touched upon in section 6.3-2 and illustrated by figures 6.3-2 to 4. In preparation for the determination of the individual member forces in section 6.11 we will first consider the sectional forces in cross sections over the height of the frame. We will maintain a general configuration with unequal batter angles, but we should keep in mind that this introduces slight inconsistencies in the model, as discussed in section 6.4.2.

With the mechanical model of section 6.8, the principles of the distribution of the shear force and the bending moment over the height of the frame have been shown. However, the applied loads were highly simplified to illustrate the basic features of frame behaviour. The environmental loads were represented by a single horizontal load F_R at a height ℓ above the sea floor, while the permanent and variable loads were not considered at all. A considerable improvement in the accuracy of the shear force and bending moment distribution over the height of the frame can be obtained by applying a series of point loads at the plan framing levels to represent the environmental loading, replacing the single resultant load. Furthermore, we must clearly supplement the loading with the permanent and variable loads on the frame.

The internal forces in the members of a frame are the superimposition of the forces due to hydrodynamic loading F_H, horizontal wind loading F_W, superstructure loads G_T and substructure loads G_S. Each of these four loads can be considered as a separate load case, after which the resulting internal forces can be added. This is a convenient and illustrative procedure that enhances understanding, both when using numerical finite element analyses and when using simplified manual methods. As the structural model is linear, the internal forces are simply additive. In what follows we will distinguish two instead of five different load cases, i.e. horizontal loading (due to F_H and F_W from wind, waves and current) and vertical loading (due to G_T and G_S). Furthermore, as for a tower and a jacket the load application of the vertical loads and the load transfer from the piles to the frame are different we must consider the tower and the jacket separately.

The tower frame and horizontal loading by the environment
The loads acting on a tower frame were summarised in section 6.7.2. The situation for this load case and an example frame with 4 bays is illustrated in figure 6.10-1. The horizontal load at the uppermost horizontal framing level is (see section 6.3):

$$F_1 = \gamma_E \cdot F_{H,1} + \gamma_E \cdot F_W \qquad (6.10\text{-}1)$$

At the lower elevations the horizontal loads are due to hydrodynamic loading only and are:

$$F_i = \gamma_E \cdot F_{H,i} \qquad (i \geq 2) \qquad (6.10\text{-}2)$$

The sum of the horizontal forces F_1 to F_5 is equal to the base shear that is given by equation 6.3-11 as:

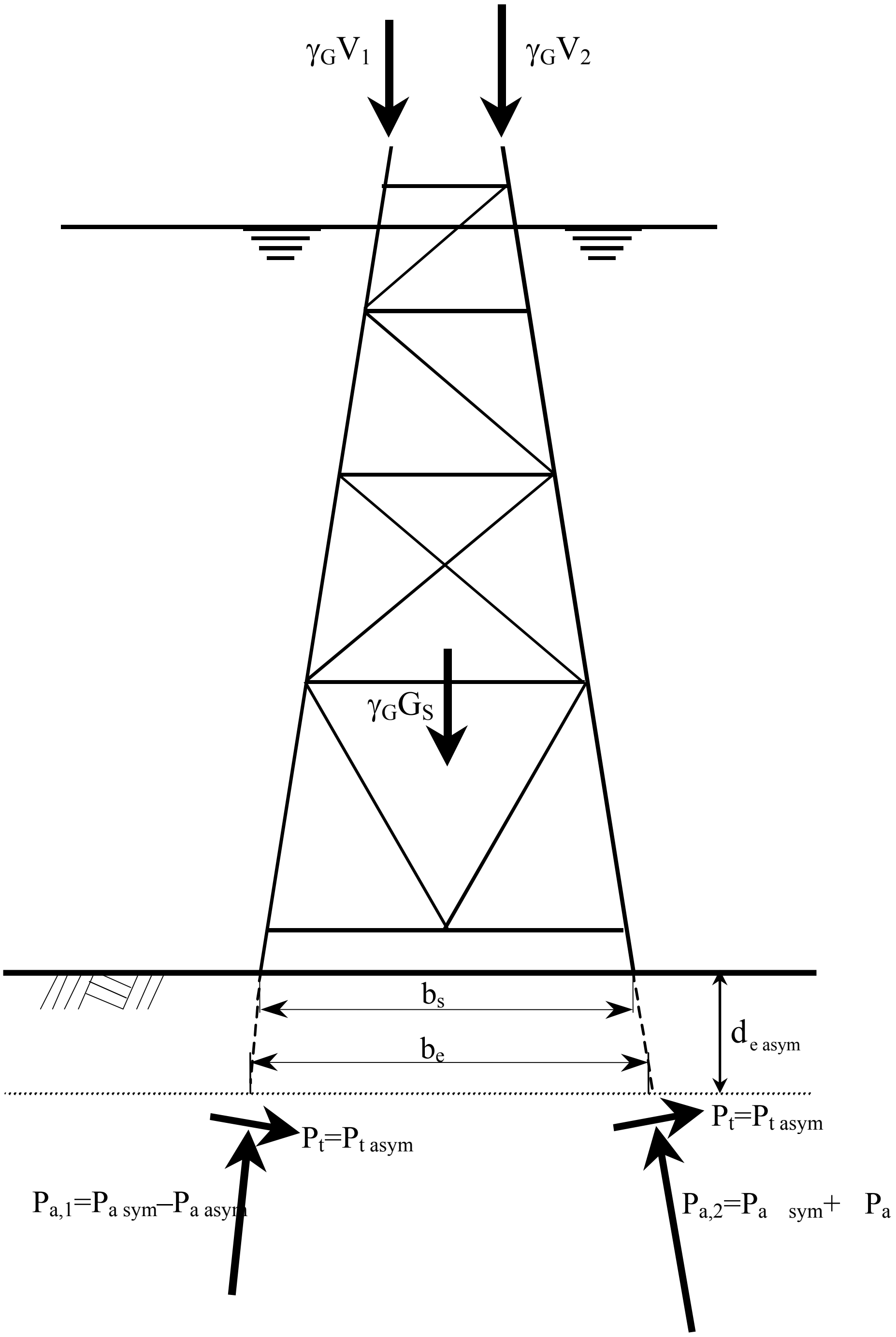

Figure 6.10-2. A tower frame subject to vertical loading

$$F_B = \gamma_E \cdot \left(F_H + F_W\right) \tag{6.10-3}$$

The overturning moment is given by equations 6.3-13 and 6.3-4 as:

$$M_O = M_{O\,env} = \gamma_E \cdot (M_{OH} + M_{OW}) = \gamma_E \cdot M_{OH} + \gamma_E \cdot F_W \cdot (h_t + h_w) \tag{6.10-4}$$

The pile forces are applied to the frame at the bottom of the legs. For the present load case these are given by case 1 of section 6.4-2; see the relevant terms in equations 6.4-21 to 23, which are:

$$\begin{aligned} P_{t,1} &= P_{t,2} = P_{t\,env} = \frac{1}{2} \cdot \frac{h}{h + d_{e\,env}} \cdot \gamma_E \cdot \left(F_B - \frac{M_{O\,env}}{h} \right) \\ P_{m,1} &= P_{m,2} = P_{m\,env} = d_{e\,env} \cdot P_{t\,env} \\ P_{a,1} &= P_{a,2} = P_{a\,env} = \gamma_E \cdot \frac{M_{O\,env} + F_B \cdot d_{e\,env}}{b_e} \end{aligned} \tag{6.10-5}$$

Without a special evaluation of the pile model (see section 6.6) $d_{e\,env}$ is not known. There are two options. We can either neglect the pile moments P_m for the global equilibrium of the frame (as we did for the multiple pile support cases in sections 6.5.2 and 6.5.3), in which case $d_{e\,env} = 0$ and the width b_e reduces to b_s, or we can use an estimate of e.g. 3 pile diameters, in which case $d_{e\,env} \approx 3D$. The axial and lateral pile forces can then be determined.

It may be verified that the sums of the horizontal and vertical loads on the frame and the associated support reactions are only identically zero if the batter angles are equal; moment equilibrium is not exactly satisfied either. See section 6.4.2 for a discussion of this slight inconsistency for $\alpha_1 \neq \alpha_2$.

The tower model, the corresponding equivalent beam model, as well as the shear force and bending moment distributions over the height of the frame due to horizontal loading are shown in figure 6.10-1. The individual member forces resulting from the shear force and the bending moment in a cross section will be determined in section 6.11.

The tower frame and vertical loading by the permanent and variable loads

The second load case is associated with vertical loads and is illustrated in figure 6.10-2. For a tower frame the topside loads are applied to the top of the legs; they are given by equation 6.3-5:

$$\begin{aligned} V_1 &= G_{T1} \\ V_2 &= G_{T2} \end{aligned} \tag{6.10-6}$$

The substructure loads G_S form a distributed load set over the entire frame; this distributed load set will manifest itself in bending moments in the individual members. Unless the permanent and variable loads of the substructure are discretised into approximate vertical component loads at the joints, the effect of G_S cannot be expressed in axial member forces like the effect of the other loads. The overall effect of G_S is, of course, reflected in the support reactions of the frame; see cases 2 and 3 of section 6.4.2.

The directions of the support reactions in figure 6.10-2 correspond with positive eccentricities of the topside and substructure loads, as consistently used in this handbook. Hence they correspond with the case that $V_2 > V_1$ and that the moments due to G_T and G_S are both clockwise. The pile forces are given by the relevant terms in equations 6.4-21 to 23:

$$\begin{aligned}
P_{t,1} &= P_{t,2} = P_{t\,asym} = -\gamma_G \cdot \frac{\alpha(M_{OGT} + M_{OGS})}{b_e} \\
P_{m,1} &= P_{m,2} = P_{m\,asym} = d_{e\,asym} \cdot P_{t\,asym} \\
P_{a,1} &= -P_{a\,sym} + P_{a\,asym} = -\tfrac{1}{2} \cdot \gamma_G \cdot (G_T + G_S) + \gamma_G \cdot \frac{(M_{OGT} + M_{OGS})}{b_e} \\
P_{a,2} &= +P_{a\,sym} + P_{a\,asym} = +\tfrac{1}{2} \cdot \gamma_G \cdot (G_T + G_S) + \gamma_G \cdot \frac{(M_{OGT} + M_{OGS})}{b_e}
\end{aligned} \tag{6.10-7}$$

A positive sign in these equations means that the direction of the force corresponds with the direction of the pile force for the horizontal load case; a negative sign means that the direction is opposite to the direction of the pile forces for the horizontal load case (see figure 6.10-1). For positive eccentricities the directions of the total pile forces are as shown on figure 6.10-2. Once the appropriate directions are established the magnitudes of the pile forces are the absolute values of the forces given by equation 6.10-7.

The above pile forces are expressed in the topside load (through G_T and M_{OGT}) and the substructure load (through G_S and M_{OGS}). They can be rewritten in terms of V_1 and V_2 at the top and G_{S1} and G_{S2} at the bottom by considering (see equations 6.3-1 and 6.3-8):

$$\begin{aligned}
G_T &= G_{T1} + G_{T2} = V_1 + V_2 \\
M_{OGT} &= \frac{1}{2}(G_{T2} - G_{T1}) \cdot b_t = \frac{1}{2}(V_2 - V_1) \cdot b_t \\
G_S &= G_{S1} + G_{S2} \\
M_{OGS} &= \frac{1}{2}(G_{S2} - G_{S1}) \cdot b_s
\end{aligned} \tag{6.10-8}$$

Substitution into equation 6.10-7 and some algebraic manipulation results in:

$$\begin{aligned}
P_{t,1} &= P_{t,2} = P_{t\,asym} = -\gamma_G \cdot \frac{1}{2} \cdot \alpha \cdot \left[(V_2 - V_1) \cdot \frac{b_t}{b_e} + (G_{S2} - G_{S1}) \cdot \frac{b_s}{b_e} \right] \\
P_{m,1} &= P_{m,2} = P_{m\,asym} = d_{e\,asym} \cdot P_{t\,asym} \\
P_{a,1} &= -\gamma_G \cdot \frac{1}{2} \cdot \left[V_1(1 + \frac{b_t}{b_e}) + V_2(1 - \frac{b_t}{b_e}) + G_{S1}(1 + \frac{b_s}{b_e}) + G_{S2}(1 - \frac{b_s}{b_e}) \right] \\
P_{a,2} &= +\gamma_G \cdot \frac{1}{2} \cdot \left[V_1(1 - \frac{b_t}{b_e}) + V_2(1 + \frac{b_t}{b_e}) + G_{S1}(1 - \frac{b_s}{b_e}) + G_{S2}(1 + \frac{b_s}{b_e}) \right]
\end{aligned} \tag{6.10-9}$$

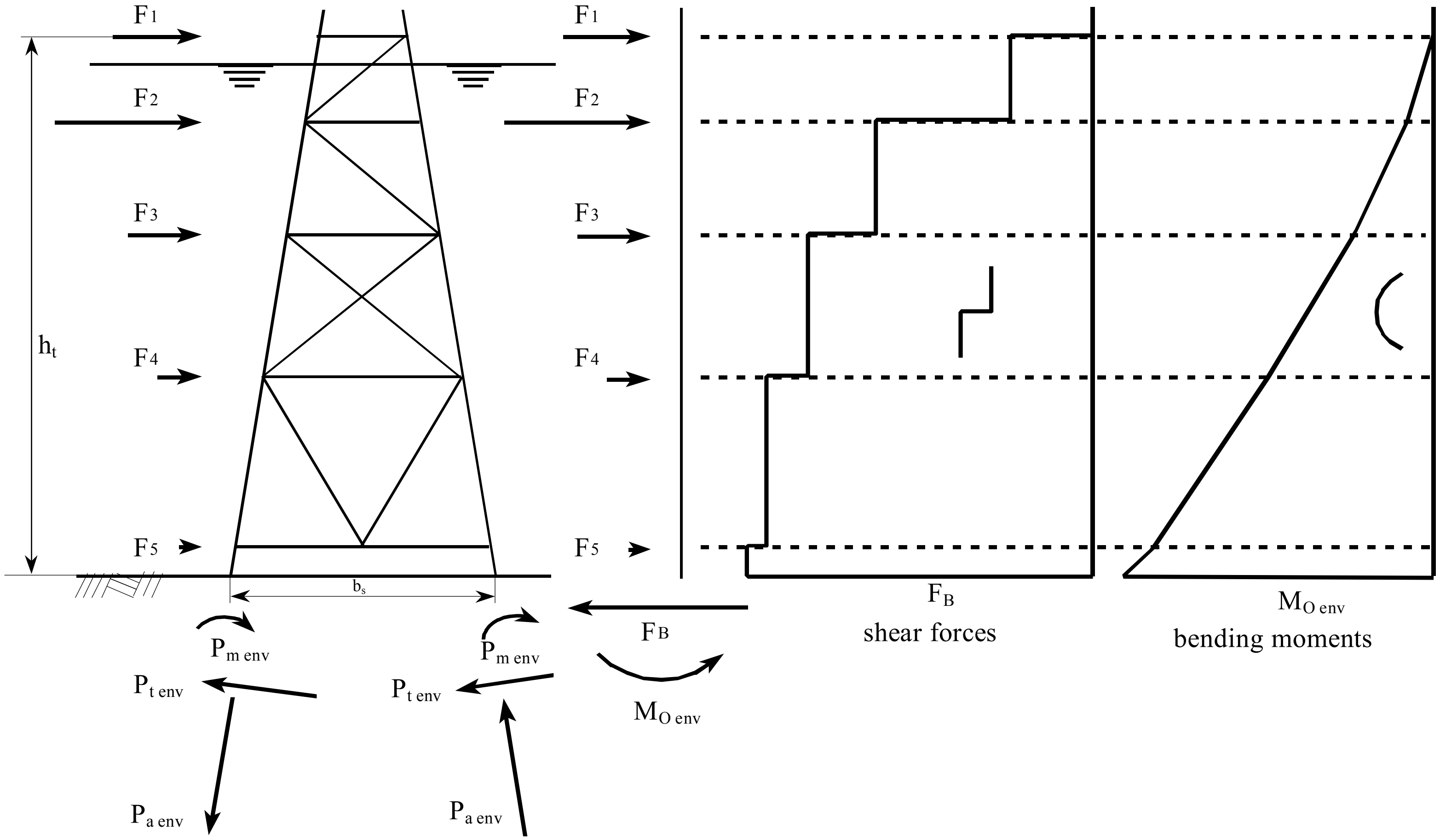

Figure 6.10-1.Tower model, equivalent beam model and sectional forces over the height of a tower frame due to horizontal loading from the environment

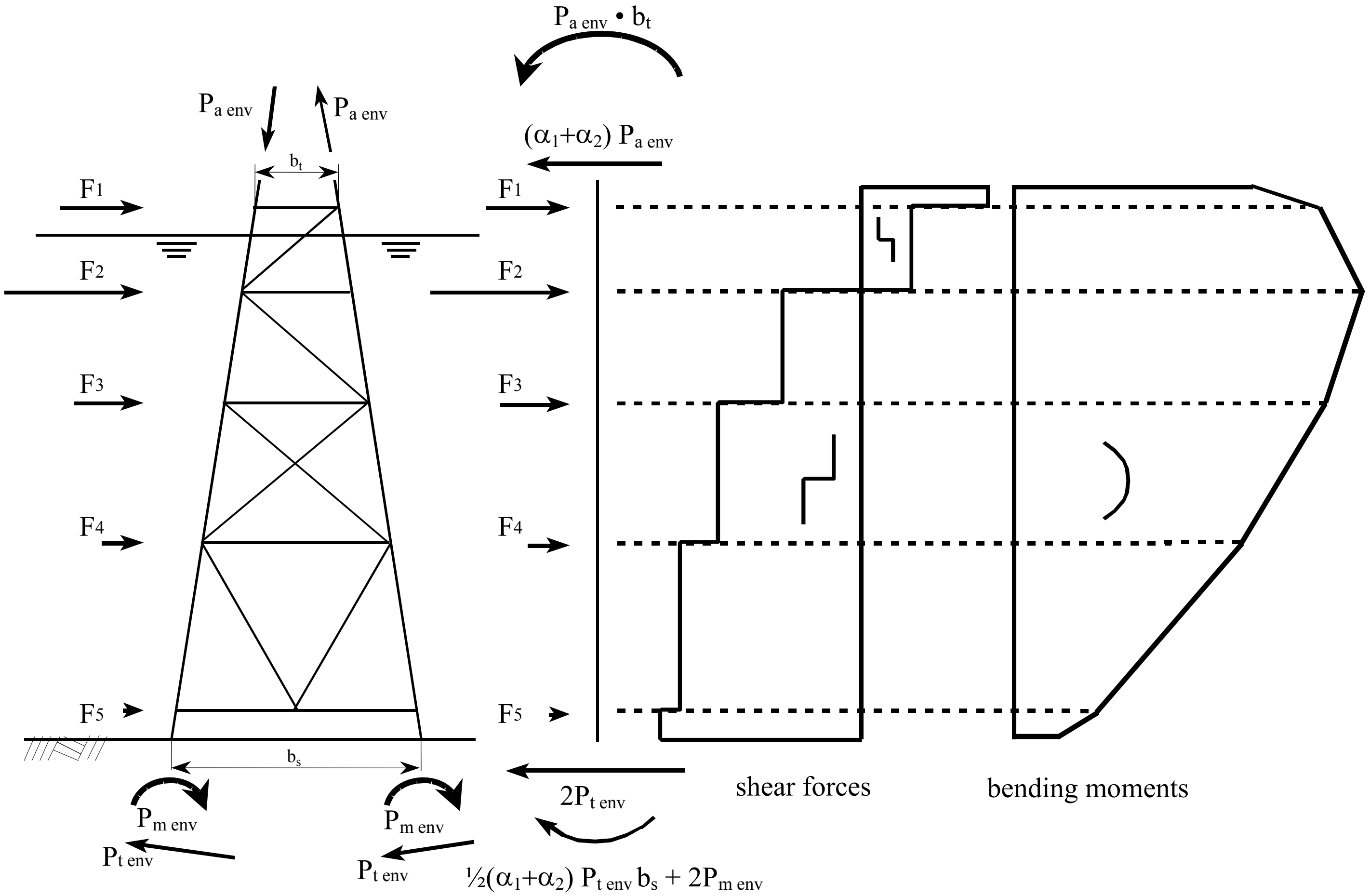

Figure 6.10-3. **Jacket model, equivalent beam model and sectional forces over the height of a jacket frame due to horizontal loading from the environment**

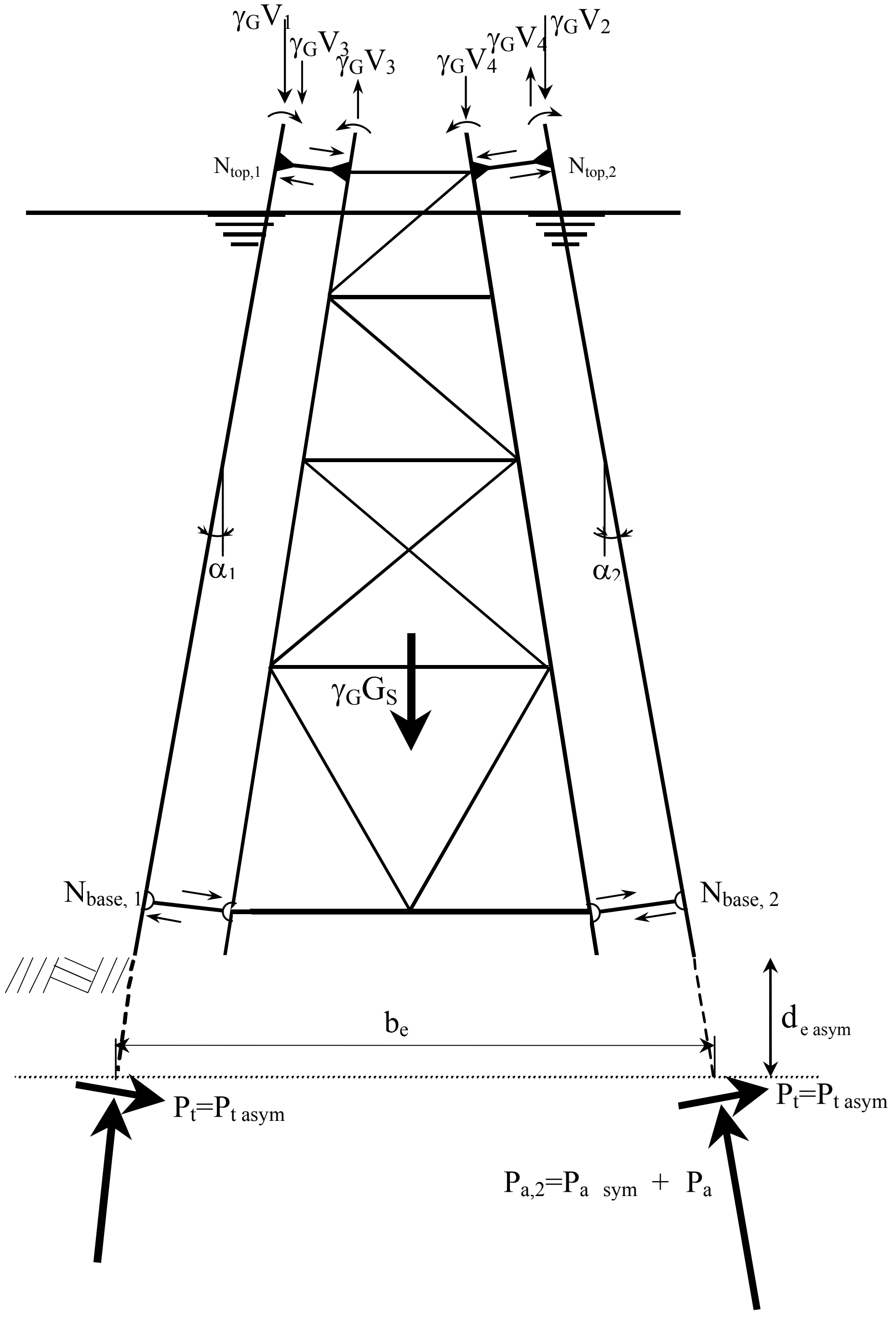

Figure 6.10-4. A jacket frame subject to vertical loading

The individual member forces due to the vertical load case will be further discussed in section 6.11.

The jacket frame and horizontal loading by the environment
When the same frame is a jacket frame instead of a tower frame, both load cases lead to markedly different results. The loads acting on a jacket frame are summarised in section 6.7.3. The horizontal load case due to environmental loading is shown in figure 6.10-3. The applied loading is identical to that for the tower frame, i.e. the equations 6.10-1 to 6.10-4 remain the same. The pile forces due to the environmental loading in equation 6.10-5 are also the same. The only difference is that the axial pile forces are now applied to the frame at the top rather than at the sea floor.

The jacket model, the equivalent beam model as well as the shear force and bending moment distributions over the height of the jacket frame and due to environmental loading are shown in figure 6.10-3; these should be compared with those in figure 6.10-1. The individual member forces resulting from the shear force and bending moment in a jacket cross section will again be determined in section 6.11.

The jacket frame and vertical loading by the permanent and variable loads
The second load case for a jacket frame when this is subjected to vertical loads is illustrated in figure 6.10-4. The loads V_1 and V_2 are now applied to the top of the piles instead of the top of the legs. This is illustrated in figure 6.10-4 by showing the piles and the legs as two parallel members. In line with previous discussions, the connection between the leg and the pile is symbolised by two short and fictitious perpendicular members. The top connection is welded and the top connecting member is hence fixed at both ends, while the bottom connecting member is hinged at both ends. The loads V_1 and V_2 are not the same in magnitude as for the tower, because the substructure frame is now assumed to hang off the top of the piles. Hence equation 6.10-6 changes into 6.10-10:

$$\begin{aligned} V_1 &= G_{T1} + G_{S1} \\ V_2 &= G_{T2} + G_{S2} \end{aligned} \qquad (6.10\text{-}10)$$

We assume again positive eccentricity or $V_2 > V_1$. The pile forces supporting the frame are governed by the global equilibrium of the system; they are exactly the same for a jacket and for a tower structure and are thus given by equation 6.10-7. The transformation into V_1 and V_2 is, however, somewhat different. For the jacket, equation 6.10-8 changes into:

$$\begin{aligned} G_T + G_S &= (G_{T1} + G_{S1}) + (G_{T2} + G_{S2}) = V_1 + V_2 \\ M_{OGT} + M_{OGS} &= \frac{1}{2}\left[(G_{T2} + G_{S2}) - (G_{T1} + G_{S1})\right] \cdot b_t = \frac{1}{2} \cdot (V_2 - V_1) \cdot b_t \end{aligned} \qquad (6\text{-}10\text{-}11)$$

When this is substituted into 6.10-7 it results in:

$$P_{t,1} = P_{t,2} = P_{t\,asym} = -\gamma_G \cdot \frac{1}{2} \cdot \alpha \cdot (V_2 - V_1) \cdot \frac{b_t}{b_e}$$

$$P_{m,1} = P_{m,2} = P_{m\,asym} = d_{e\,asym} \cdot P_{t\,asym}$$

$$P_{a,1} = -\gamma_G \cdot \frac{1}{2} \cdot \left[V_1(1 + \frac{b_t}{b_e}) + V_2(1 - \frac{b_t}{b_e}) \right] \qquad (6.10\text{-}12)$$

$$P_{a,2} = +\gamma_G \cdot \frac{1}{2} \cdot \left[V_1(1 - \frac{b_t}{b_e}) + V_2(1 + \frac{b_t}{b_e}) \right]$$

Regarding positive and negative signs the same comments as with equation 6.10-7 apply. When the directions are shown correctly, as on figure 6.10-4, the absolute values of the expressions in 6.10-12 should be taken.

The forces N_{base} in the connecting members between the piles and the legs at the bottom are directly found using the principles illustrated in figures 6.3-2 to 4:

$$N_{base,1} = P_{t\,asym} = \gamma_{G} \cdot \frac{1}{2} \cdot \alpha \cdot (V_2 - V_1) \cdot \frac{b_t}{b_e} \quad \text{(compression)}$$

$$N_{base,2} = P_{t\,asym} = \gamma_{G} \cdot \frac{1}{2} \cdot \alpha \cdot (V_2 - V_1) \cdot \frac{b_t}{b_e} \quad \text{(tension)} \qquad (6.10\text{-}13)$$

Vertical equilibrium of the pile on the left provides the balancing force V_3, which is transmitted to the top of the jacket leg. For the (assumed) direction of the force V_3 in figure 6.10-4 we get:

$$\gamma_G \cdot (V_1 + V_3) - P_{a,1} \cos\alpha_1 + P_{t\,asym} \sin\alpha_1 \approx \gamma_G \cdot (V_1 + V_3) - P_{a,1} = 0 \qquad (6.10\text{-}14)$$

The term $P_{t\,asym} \sin\alpha_1 \approx \alpha_1 P_{t\,asym}$ is of the second order in α and should be neglected. The results is:

$$V_3 = +\frac{1}{2} \cdot V_1(1 + \frac{b_t}{b_e}) + \frac{1}{2} \cdot V_2(1 - \frac{b_t}{b_e}) - V_1 = \frac{1}{2} \cdot (V_2 - V_1)(1 - \frac{b_t}{b_e}) \qquad (6.10\text{-}15)$$

As $V_2 > V_1$ the force $V_3 > 0$ and the assumed direction is thus correct.

The balancing force V_4 on the other side is found analogously:

$$\gamma_G \cdot (V_2 - V_4) - P_{a,2} \cos\alpha_2 - P_{t\,asym} \sin\alpha_2 \approx \gamma_G \cdot (V_2 - V_4) - P_{a,2} = 0 \qquad (6.10\text{-}16)$$

and: $$V_4 = +V_2 - \frac{1}{2} \cdot V_1(1 - \frac{b_t}{b_e}) - \frac{1}{2} \cdot V_2(1 + \frac{b_t}{b_e}) = \frac{1}{2} \cdot (V_2 - V_1)(1 - \frac{b_t}{b_e}) \qquad (6.10\text{-}17)$$

The sign of which confirms the direction shown. Equations 6.10-15 and 17 further show that V_4 is equal and opposite to V_3.

Finally, the forces N_{top} in the connecting members between the piles and the legs at the top can now also be determined in a similar manner as the forces N_{base}:

$$\begin{aligned} N_{top,1} &= \alpha_1 \cdot \gamma_G \cdot (V_1 + V_3) = \alpha_1 \cdot \gamma_G \cdot P_{a,1} = \alpha_1 \cdot \gamma_G \cdot \frac{1}{2} \cdot \left[V_1 (1 + \frac{b_t}{b_e}) + V_2 (1 - \frac{b_t}{b_e}) \right] \quad \text{(compression)} \\ N_{top,2} &= \alpha_2 \cdot \gamma_G \cdot (V_2 - V_4) = \alpha_2 \cdot \gamma_G \cdot P_{a,2} = \alpha_2 \cdot \gamma_G \cdot \frac{1}{2} \cdot \left[V_2 (1 + \frac{b_t}{b_e}) + V_1 (1 - \frac{b_t}{b_e}) \right] \quad \text{(compression)} \end{aligned} \qquad (6.10\text{-}18)$$

All forces on the frame are now known. A useful check is to consider vertical (unbattered) legs and piles, for which all connecting forces between frame and piles must become zero; equations 6.10-13 and 6.10-18 confirm this. Furthermore, the lateral pile forces due to the vertical loading must also be zero: $P_{t\,asym} = 0$. Equations 6.10-7, 6.10-9 and 6.10-12 all correctly show this.

For battered legs and piles the vertical loads *on the piles* thus result in a set of vertical and lateral/horizontal forces *on the frame* as shown in figure 6.10-4. These forces act at the top where the pile is connected to the leg; however, as argued before, without any significant loss of generality they may instead be assumed to act at the first horizontal framing level. The forces on the frame can be summarised as follows:

at the top joint on the left:

$$\begin{aligned} N_{top,1} &= \alpha_1 \cdot \gamma_G \cdot (V_1 + V_3) \\ &= \alpha_1 \cdot \gamma_G \cdot P_{a,1} = \alpha_1 \cdot \gamma_G \cdot \frac{1}{2} \cdot \left[V_1 (1 + \frac{b_t}{b_e}) + V_2 (1 - \frac{b_t}{b_e}) \right] \\ \gamma_G V_3 &= \tfrac{1}{2} \cdot \gamma_G \cdot (V_2 - V_1) \cdot (1 - \frac{b_t}{b_e}) \end{aligned}$$

at the bottom joint on the left:

$$N_{base,1} = \gamma_G \cdot \frac{1}{2} \cdot \alpha \cdot (V_2 - V_1) \cdot \frac{b_t}{b_e}$$

(6.10-19)

at the top joint on the right:

$$\begin{aligned} N_{top,2} &= \alpha_2 \cdot \gamma_G \cdot (V_2 - V_4) \\ &= \alpha_2 \cdot \gamma_G \cdot \frac{1}{2} \cdot \left[V_2 (1 + \frac{b_t}{b_e}) + V_1 (1 - \frac{b_t}{b_e}) \right] \\ \gamma_G V_4 &= \gamma_G \cdot \frac{1}{2} \cdot (V_2 - V_1)(1 - \frac{b_t}{b_e}) \end{aligned}$$

at the bottom joint on the right:

$$N_{base,2} = \gamma_G \cdot \frac{1}{2} \cdot \alpha \cdot (V_2 - V_1) \cdot \frac{b_t}{b_e}$$

The individual member forces due to the vertical load case will be further discussed in section 6.11.

As for the tower, the substructure load G_S still acts as a distributed load set over the entire frame, which will manifest itself in bending moments in the individual members.

Concluding remark

In the analytical form presented here the formulation of the different load cases, especially the vertical ones, appear rather complicated. However, as stated before, in a practical application it is the *methodology* that is used while working with numerical values. The procedure is then a straightforward use of elementary principles of mechanics and much simpler than it seems. The advantage of solving the problem here analytically is that the relationships between the various influences become visible.

6.11 The internal forces in the members of the frame

6.11.1 General

The final step in the two-dimensional idealisation of the in-place structural behaviour under extreme storm loading is the determination of the forces in the individual members making up the frame for a given applied loading situation. Following on from section 6.10 we will have to look separately at the internal forces due to the horizontal loading by the environment and the vertical loading from permanent and variable loading. The total internal forces are then the sum of the forces from the two load cases. Vertical loading of the frame will be looked at in section 6.11.6. We will now first consider the horizontal loading case.

Under horizontal loading the problem is characterised by a shear force and bending moment distribution over the height of the frame. This situation is illustrated in figure 6.11-1, which shows a cross section at a height z above the sea floor for a frame with a single diagonal bracing pattern. The cross section is made just above a horizontal plan framing level. The width of the frame at this point (i.e. the largest width of the panel through which the cross section cuts) is $b(z)$; the shear force and bending moment in the cross section and acting on the lower part of the frame are denoted by $S(z)$ and $M(z)$, respectively. They are often referred to as the level shear force and the level bending moment. In figure 6.11-1 they are assumed to act from left to right and clockwise, respectively. However, it should be recognised that the directions depend on whether the frame is a tower frame or a jacket frame, as well as on the elevation where the cross section is made; see figures 6.10-1 and 6.10-3. In applications the actual directions should be carefully determined.

The loading on the lower part of the frame is due to wind, wave and current action. Until now we have only considered the spatial distribution of the hydrodynamic loading in the vertical direction and discretised it into loads at the horizontal plan framing levels. However, as we are now concerned with the internal forces in the members of the frame we also need to consider its horizontal distribution. Therefore, the hydrodynamic loading $F(z)$ at the level of the cross section is shown in figure 6.11-1 as discrete loads of $\tfrac{1}{2}F(z)$ on the left leg and $\tfrac{1}{2}F(z)$ on the right leg. At the other elevations z_1 and z_2 the applied loading is similarly split over the two legs. For convenience of the discussion the explicit dependency on z will further be dropped from the notation, except where this is expressly emphasised.

The level shear force and the level bending moment have to be provided by the forces in the discrete members through which the cross-section cuts. Because of our idealisations the internal forces in the members are *axial forces* only. This reflects the principal action of the members within the frame. It implies that the members are assumed to be pin-jointed so that no moments are transferred. Furthermore, there should be no applied loading of any sort along the length of the members; all external loads are applied at the joints as shown. In the Anglo-Saxon literature such a frame is often called a truss, the distinction being that in a truss the members are connected by hinges whereas in a frame they are fully fixed to one another. However, in practical usage the exactness of the terminology cannot be relied upon.

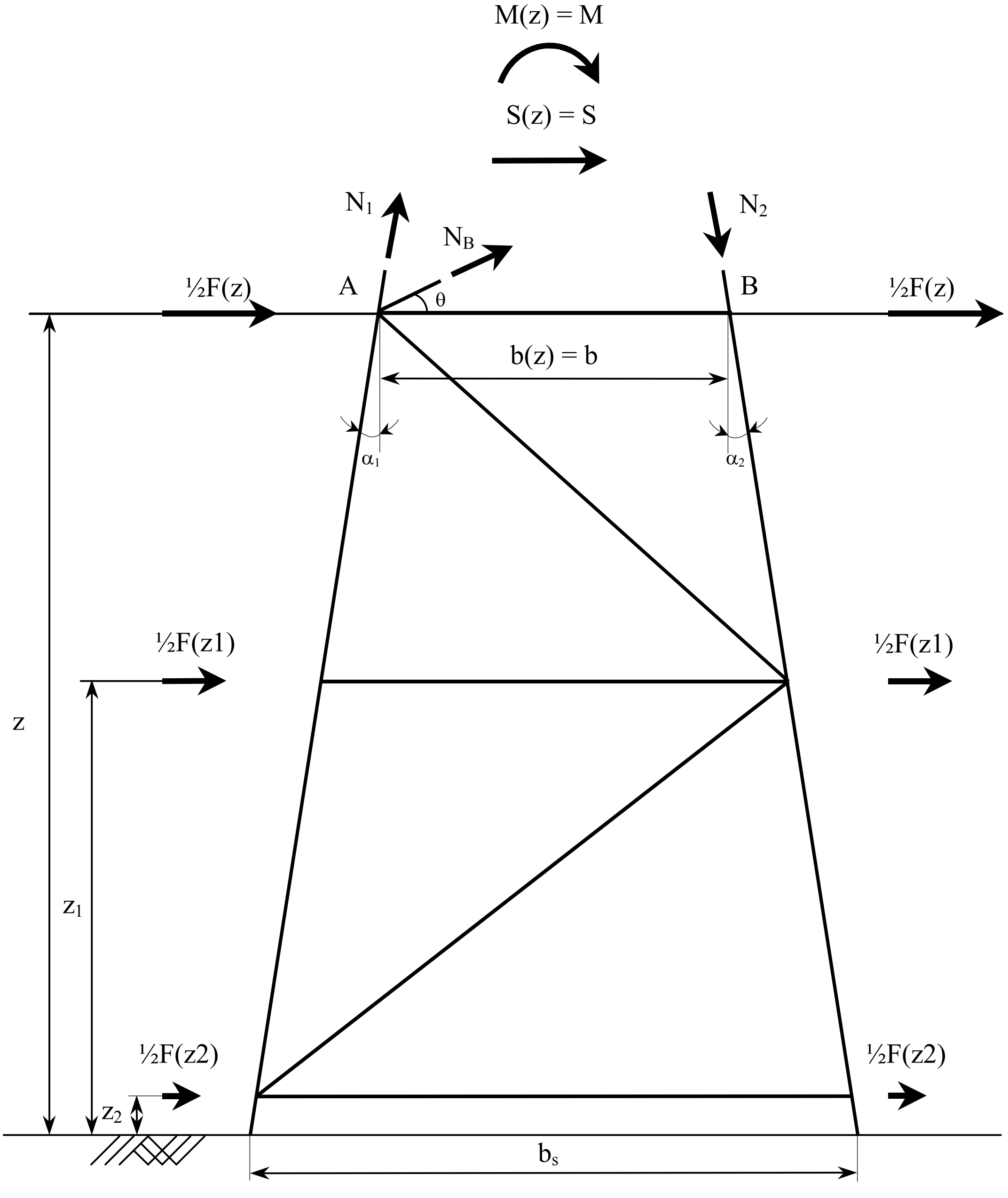

Figure 6.11-1. Internal forces in the members of a frame with single diagonal bracing

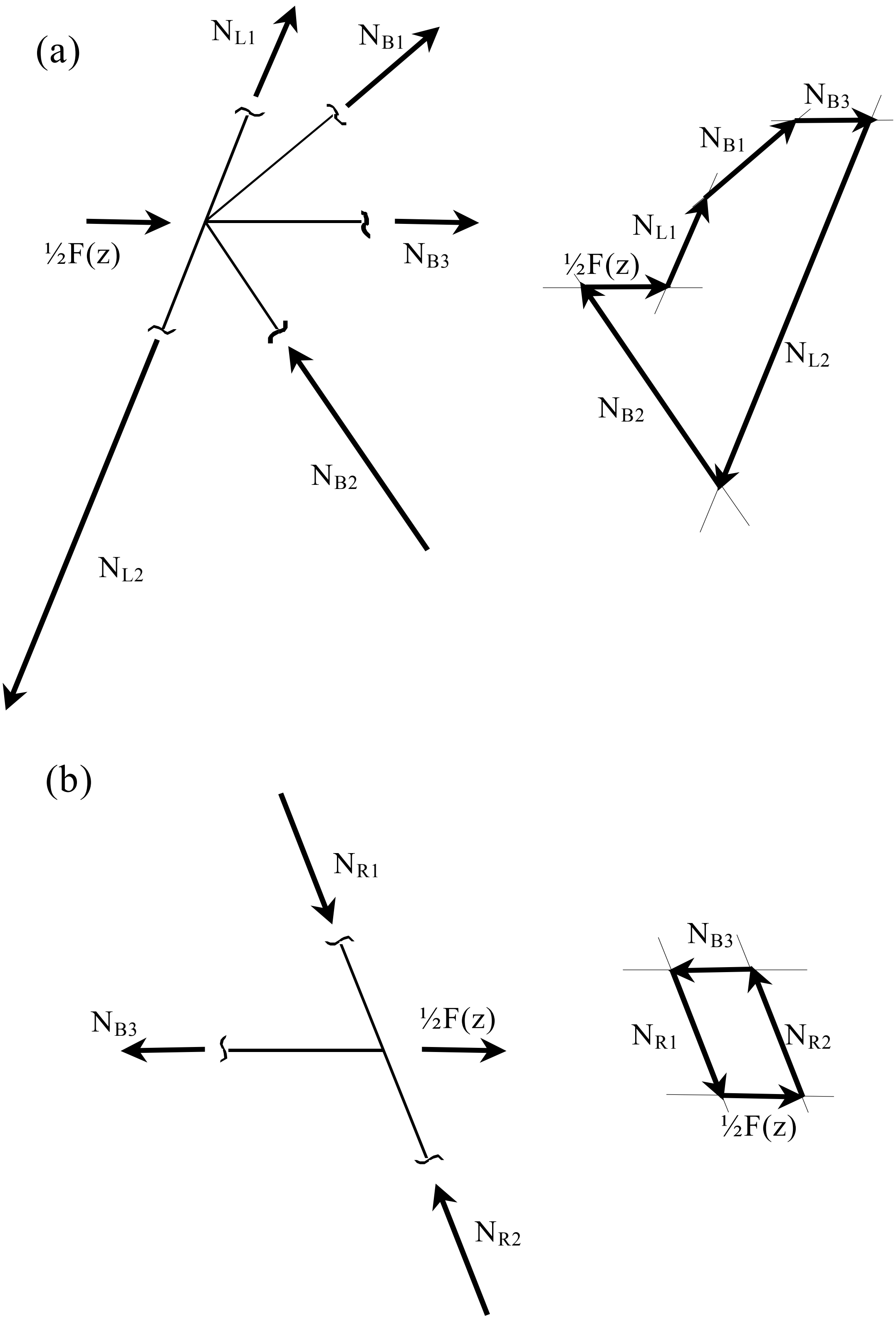

Figure 6.11-2a and b. Equilibrium of leg joints in a panel with single diagonal bracing

6.11.2 Individual leg and brace forces for diagonal bracing due to horizontal loading by the environment

The configuration of the frame shown in figure 6.11-1 has a single diagonal brace in a vertical panel. This is only one of several possibilities; other options are e.g. X-bracing or K-bracing. The equations that will be derived below depend on the configuration and are therefore valid for diagonal bracing only; for other bracing configurations they can be derived in a fully analogous manner and the result may or may not be different. However, as on other occasions it is stressed that the objective is to demonstrate the procedure rather than to derive generally applicable relationships. In practical applications it is much more straightforward to perform the procedure using numerical data. We illustrate the procedure here using a non-numerical example from which analytical formulations result. These equations have only particular value in case of an automated process for several panels and frames.

In the cross section in figure 6.11-1 there are 3 unknowns N_1, N_2 and N_B which can be solved from the 3 equations of equilibrium[1]:

$$\begin{array}{ll} \sum H = S & N_1 \sin\alpha_1 + N_2 \sin\alpha_2 + N_B \cos\theta = S \\ \sum V = 0 & N_1 \cos\alpha_1 - N_2 \cos\alpha_2 + N_B \sin\theta = 0 \\ \sum M_A = M & N_2 \cos\alpha_2 \cdot b = M \\ \sum M_B = M & (N_1 \cos\alpha_1 + N_B \sin\theta) \cdot b = M \end{array} \qquad (6.11\text{-}1)$$

The batter angles α are always small so that $\sin\alpha \approx \alpha$ and $\cos\alpha \approx 1$, but the brace angle θ is of the order of 30 to 60 degrees and $\sin\theta$ and $\cos\theta$ must therefore be retained. From the two moment equations we get:

$$\begin{array}{l} N_1 = \dfrac{M}{b} - N_B \sin\theta \\ N_2 = \dfrac{M}{b} \end{array} \qquad (6.11\text{-}2)$$

Substitution into the horizontal equation of 6.11-1 results in:

$$N_B \cos\theta - \alpha_1 N_B \sin\theta = S - \frac{(\alpha_1 + \alpha_2) M}{b}$$

or $$N_B \cos\theta \left\{ 1 - \alpha_1 \frac{\sin\theta}{\cos\theta} \right\} = S \left\{ 1 - \frac{(\alpha_1 + \alpha_2) M}{Sb} \right\} \qquad (6.11\text{-}3)$$

The brace force thus becomes:

---

[1] Actually, we are not looking at an equilibrium situation in the real sense of the word. The member forces do not counteract the level shear and level bending moment to produce equilibrium, but are the mechanism to provide $S(z)$ and $M(z)$.

$$N_B = \frac{S}{\cos\theta}\cdot\left[\left\{\frac{\cos\theta}{\cos\theta-\alpha_1\sin\theta}\right\}\cdot\left\{1-\frac{(\alpha_1+\alpha_2)M}{Sb}\right\}\right] \tag{6.11-4}$$

Substitution into the second moment equation of 6.11-1 gives for the leg force N_1:

$$N_1 = \frac{M}{b} - S\frac{\sin\theta}{\cos\theta}\cdot\left[\frac{\cos\theta}{\cos\theta-\alpha_1\sin\theta}\right]\cdot\left[1-\frac{(\alpha_1+\alpha_2)M}{Sb}\right]$$

or $$N_1 = \frac{M}{b}\left[1-\left\{\frac{\sin\theta}{\cos\theta-\alpha_1\sin\theta}\right\}\cdot\left\{\frac{Sb}{M}-(\alpha_1+\alpha_2)\right\}\right] \tag{6.11-5}$$

Consequently, the member forces are, explicitly showing the dependency on *z*:

$$\begin{aligned}
N_1(z) &= \frac{M(z)}{b(z)}\left[1-\left\{\frac{\sin\theta}{\cos\theta-\alpha_1\sin\theta}\right\}\cdot\left\{\frac{b(z)S(z)}{M(z)}-(\alpha_1+\alpha_2)\right\}\right]\\
N_2(z) &= \frac{M(z)}{b(z)}\\
N_B(z) &= \frac{S(z)}{\cos\theta}\cdot\left[\left\{\frac{\cos\theta}{\cos\theta-\alpha_1\sin\theta}\right\}\cdot\left\{1-\frac{(\alpha_1+\alpha_2)M(z)}{b(z)S(z)}\right\}\right]
\end{aligned} \tag{6.11-6}$$

These relationships have been derived for the case of a cross section through a tension brace. It can directly be verified that they are equally valid for a cross section one bay down through a compression brace, provided that α_1 and α_2 and the leg force expressions for N_1 and N_2 are interchanged. They thus express the magnitudes of these forces. Whether members are in tension or compression should therefore be determined by inspection. They have further been derived for an assumed direction of the level shear force, bending moment and member forces; see figure 6.11-1. Please note that when a different starting point is used the specific formulations (especially with regard to the signs of the various terms) may be quite different.

In a frame the shear force in a panel is mainly transmitted by the (diagonal) bracings. This is reflected in the above expression for N_B. For vertical legs $(\alpha_1=\alpha_2=0)$ there is no contribution from the horizontal components of the leg forces and the full shear force has to be transmitted by the bracing so that:

$$N_B = \frac{S}{\cos\theta} \tag{6.11-7}$$

For battered legs the brace force N_B in equation 6.11-6 is the product of three factors. The first factor reflects (as for vertical legs) that the force in the brace is considerably larger than the level shear force transmitted by the panel as a result of the brace angle. The second factor is a purely geometrical factor that is always a bit larger than 1.0 if the cross section is made as in figure 6.11-1. For typical values of $\theta \simeq 45$ degrees and $\alpha \simeq 0.10$ (5.7 deg) this factor is 1.11. The third factor is a reduction factor that is similar (but not equal) to the reduction factor for the lateral pile forces discussed earlier, as will be shown in section 6.11.5. The product of the second and the third factor between the large square brackets is the so-called *batter take-*

out factor, i.e. the total factor by which the leg forces contribute in transmitting the level shear force.

The leg forces N_1 and N_2 are clearly not equal. This is due to the fact that the vertical component of the brace force also participates in the vertical and the moment equilibrium equations. It follows that the bending moment in the section is not fully transmitted by the leg forces only, not even for zero batter and parallel legs. Equation 6.11-6 shows that the leg force N_1 is the product of two factors. The first factor is simply the moment transmitted by the cross section divided by the local distance between the legs; this factor is equal to the leg force N_2. The second factor between the large square brackets is a correction factor, which results from the discretisation of the frame into individual members (legs and braces) in a certain configuration compared to a continuous beam model. This second factor incorporates the influence of the batter angle, but it is easily verified numerically that the effect of α_1 and α_2 on the leg forces is small. We can therefore conclude that *leg batter has a very substantial influence on the brace forces, but a rather insignificant effect on the leg forces.*

We further make the following observations:

1. The expressions 6.11-6 for the leg and brace forces in a panel are equally valid for a tower and a jacket frame. However, the shear force $S(z)$ and the bending moment $M(z)$ are *not* the same for a tower and a jacket, neither in magnitude nor necessarily in direction. Consequently, the leg forces in a tower and a jacket are distinctly different, as has been noted before. However, the brace forces for a tower frame and a jacket frame are, after all, equal; see section 6.11.5.
2. For the load and structural models used in this handbook the leg and brace forces in a panel are constant over the panel height. Consequently, it does not matter at what height in the panel the cross section is made. From a structural mechanics point of view this is directly obvious, but the algebra may become rather more complicated. However, when correctly done the algebra will confirm these results.
3. Further to the previous point, the expressions have been derived for a cross section near the bottom of a panel. The calculations then involve the level shear force and the level bending moment acting on the lower part of the frame, the forces in the members above the cross section and the bottom width of the panel. We could also have made the cross section near the upper end of the same panel. If we still consider the level shear force and bending moment on the lower part of the frame, the calculations now involve the shear and moment at a different elevation z and the top width instead of the bottom width of the panel. Had we chosen to consider the level shear force and bending moment on the upper part instead of the lower part of the frame, together with the forces in the members below the cross section, then the $S(z)$ and $M(z)$ would be reversed in direction. Furthermore, the equilibrium equations for these two options are not exactly the same, e.g. the signs of the leg and brace terms in the moment equation are different. However, it is once more stressed that when the derivation is done correctly the resulting member forces will, of course, be the same.
4. Leg and brace forces can only change stepwise from panel to panel. The change in the *leg* forces is due to changes in the level bending moment as well as changes in the width of the frame, both of which are a function of elevation; see also section 6.11.4. The change in the *brace* forces is also due to a combination of factors: both the level shear force and the level bending moment change with elevation, while the brace angle is also likely to differ from panel to panel.

5. All joints must be in equilibrium. This can serve as a useful check to verify that the forces of the members that meet at a particular joint are in equilibrium, as illustrated in figure 6.11-2a and b. Figure 6.11-2b further clearly shows that the horizontal braces in a frame with diagonal bracings are loaded by half the hydrodynamic load that is applied at that level, i.e. $\frac{1}{2}F(z) = \frac{1}{2}F_i = \frac{1}{2}\gamma_E \cdot F_{H,i} \ (i \geq 2)$; see equation 6.10-2. The loading at the uppermost horizontal framing consists of hydrodynamic loading plus wind loading. Therefore the top horizontal brace is loaded by $\frac{1}{2}F_1 = \frac{1}{2}\gamma_E \cdot (F_{H,1} + F_W)$, see equation 6.10-1.
6. Verifications, such as those discussed above, are extremely useful steps in the construction of engineering models. They serve two critical purposes, i.e. firstly that assumptions made at different stages of model development are consistent instead of conflicting, and that errors are found and corrected before calculations are carried out in earnest. Secondly, they will assist the engineer in familiarising himself with his own model and improving his understanding.

6.11.3 Individual leg and brace forces for other bracing patterns due to horizontal loading by the environment

As noted, the expressions for the individual leg and brace forces depend on the framing configuration. Below we will give expressions similar to 6.11-6 for some other brace patterns without derivation. They use the same conventions as shown in figure 6.11-1 and are easily verified by the reader himself.

X-braces

In the general case of a cross section over X-braces there are 4 unknowns. Strictly speaking this is thus a statically indeterminate case that cannot be solved by equilibrium alone. If we now restrict ourselves to the case of equal batter angles α_1 and α_2, the brace angles θ_1 and θ_2 are also the same and the whole frame is symmetric about its centre line. From symmetry it follows immediately that the forces in the legs are equal and opposite and that the forces in the X-braces are also equal and opposite. It also follows that the horizontal braces in X-braced panels are unloaded, in contrast to those in a frame with a diagonal brace pattern. The resulting expressions are:

$$\begin{aligned}
N_L(z) = N_1(z) = N_2(z) &= \frac{M(z)}{b(z)}\left[1-\frac{1}{2}\cdot\left\{\frac{\sin\theta}{\cos\theta-\alpha\sin\theta}\right\}\cdot\left\{\frac{b(z)S(z)}{M(z)}-2\alpha\right\}\right] \\
N_B(z) &= \frac{1}{2}\cdot\frac{S(z)}{\cos\theta}\cdot\left[\left\{\frac{\cos\theta}{\cos\theta-\alpha\sin\theta}\right\}\cdot\left\{1-\frac{2\alpha\, M(z)}{b(z)S(z)}\right\}\right]
\end{aligned} \qquad (6.11\text{-}8)$$

These are the same as equation 6.11-6 except for the factor ½ in front of the equation for N_B and within the square brackets of the leg force. This is a result of the fact that the shear force in the cross section is now distributed over two braces instead of being carried by one diagonal.

Vertical K-braces (pointing upwards)

From a sketch of the cross section just above a horizontal plan framing level it is immediately clear that the situation is exactly the same as for X-braces, so that equation 6.11-8 is also valid for this framing pattern. However, the two bracing patterns are not identical in every respect because the horizontal braces in the frame now do carry loads.

Vertical K-braces (pointing downwards)

This situation is different from the previous cases. The braces now meet at the centre of the horizontal brace just below the cross section rather than at the leg joints. The result is:

$$\begin{aligned}
N_L(z) = N_1(z) = N_2(z) &= \frac{M(z)}{b(z)} \\
N_B(z) &= \frac{S(z)}{2\cos\theta}\cdot\left\{1-\frac{2\alpha\, M(z)}{b(z)S(z)}\right\}
\end{aligned} \qquad (6.11\text{-}9)$$

Here the horizontal braces again do carry load. For illustration, figure 6.11-3a and b show force diagrams for a leg joint in a panel with X-braces and K-braces (pointing upwards).

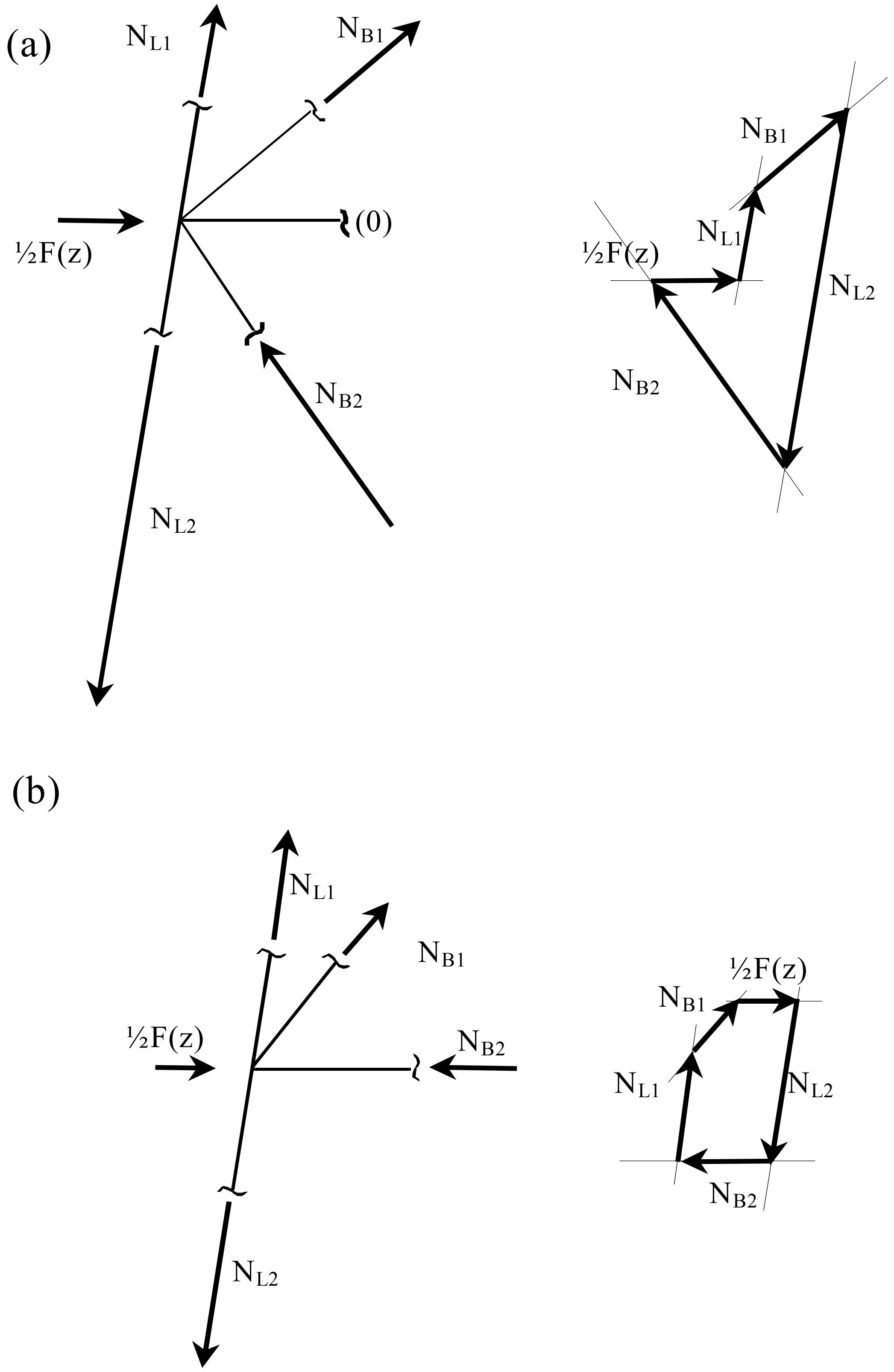

Figure 6.11-3a and b. Equilibrium of a leg joint in an X-braced and a K-braced panel

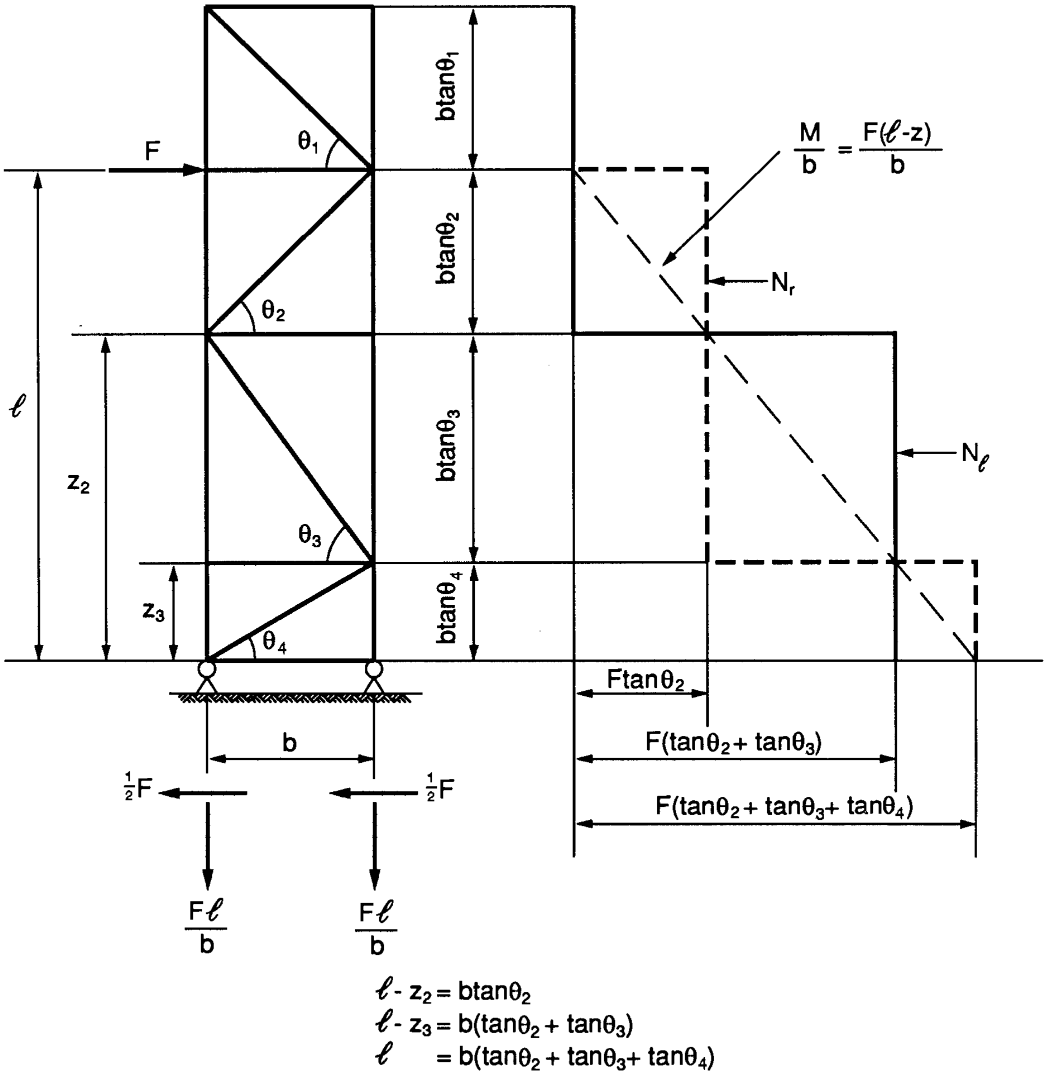

Figure 6.11-4. **Stepwise change of leg forces over the height of a tower frame (vertical legs, diagonal bracing)**

6.11.4 Further consideration of leg forces over the height of a frame due to horizontal loading by the environment

Since the frame is an assembly of discrete members the brace and leg forces can only change stepwise at the nodal points. In between horizontal plan framing levels they must remain constant, even though the bending moment in a cross section of the equivalent beam model changes in a continuous manner over the height of the panel. At first sight this appears to lead to a conflict, but this is only seemingly so. The discrete and stepwise change in the leg forces is best illustrated for a frame with vertical and parallel legs $(\alpha = 0)$ and a single resultant horizontal point load F. We will consider a tower and a jacket frame separately.

Leg forces in a tower frame

Figure 6.11-4 shows a tower frame. The member forces are most easily determined from equilibrium in a cross section of the frame, panel by panel. The frame is only loaded for $z < \ell$. The shear force $S(z) = F$ is constant; the moment $M(z) = F \cdot (\ell - z)$ is shown in the form of M/b by the sloping line on the right. Using equations 6.11-6 seems a bit formal and somewhat complicated, but produces naturally the same result as obtained from direct consideration of the cross sections. We will illustrate this below. The member forces are:

$$\begin{aligned} N_B(z) &= \frac{S(z)}{\cos\theta} = \frac{F}{\cos\theta} \\ N_1(z) &= \frac{M(z)}{b(z)} - S(z)\tan\theta = \frac{F(\ell - z)}{b} - F\tan\theta \\ N_2(z) &= \frac{M(z)}{b(z)} = \frac{F(\ell - z)}{b} \end{aligned} \tag{6.11-10}$$

where N_1 refers to the leg at the side where a diagonal brace meets the leg, and N_2 to the leg without a diagonal brace. For the individual panels and in discrete form from the top down the moment arms $(\ell - z)$ are:

$$\begin{aligned} \ell - z_1 &= 0 \\ \ell - z_2 &= b\tan\theta_2 \\ \ell - z_3 &= b(\tan\theta_2 + \tan\theta_3) \\ \ell - z_4 &= b(\tan\theta_2 + \tan\theta_3 + \tan\theta_4) \end{aligned} \tag{6.11-11}$$

By substitution we obtain for the left leg:

$$\begin{aligned} N_{L,1} &= N_{2,1} = 0 \\ N_{L,2} &= N_{1,2} = \frac{F(\ell - z_2)}{b} - F\tan\theta_2 = F(\tan\theta_2 - \tan\theta_2) = 0 \\ N_{L,3} &= N_{2,3} = \frac{F(\ell - z_3)}{b} = F(\tan\theta_2 + \tan\theta_3) \\ N_{L,4} &= N_{1,4} = \frac{F(\ell - z_4)}{b} - F\tan\theta_4 = F(\tan\theta_2 + \tan\theta_3 + \tan\theta_4 - \tan\theta_4) = F(\tan\theta_2 + \tan\theta_3) \end{aligned} \tag{6.11-12}$$

and for the right leg:

$$\begin{aligned}
N_{R,1} &= N_{1,1} = 0 \\
N_{R,2} &= N_{2,2} = \frac{F(\ell - z_2)}{b} = F\tan\theta_2 \\
N_{R,3} &= N_{1,3} = \frac{F(\ell - z_3)}{b} - F\tan\theta_3 = F(\tan\theta_2 + \tan\theta_3 - \tan\theta_3) = F\tan\theta_2 \\
N_{R,4} &= N_{2,4} = \frac{F(\ell - z_4)}{b} = F(\tan\theta_2 + \tan\theta_3 + \tan\theta_4)
\end{aligned} \qquad (6.11\text{-}13)$$

These stepwise changes of the leg forces in the left and the right leg are shown on figure 6.11-4.

Leg forces in a jacket frame

A corresponding jacket frame is shown in figure 6.11-5. The shear force is the same as for the tower frame, $S(z)=F$ for $z<\ell$, but the moment is completely different. It is opposite in sign to the tower moment and its magnitude is $M(z)=F\cdot\ell$ for $z>\ell$ and $M(z)=F\cdot\ell-F(\ell-z)=F\cdot z$ for $z<\ell$, as shown in figure 6.11-5. The equations for N_B, N_1 and N_2, as derived from equation 6.11-6, remain the same as for the tower frame but when the moment is substituted they become different (compare 6.11-10 with 6.11-14):

$$\begin{aligned}
N_B(z) &= \frac{S(z)}{\cos\theta} = \frac{F}{\cos\theta} && (z<\ell) \\
N_1(z) &= \frac{M(z)}{b(z)} = \frac{-F\ell}{b} && (z>\ell) \\
N_2(z) &= \frac{M(z)}{b(z)} = \frac{-F\ell}{b} && (z>\ell) \\
N_1(z) &= \frac{M(z)}{b(z)} - S(z)\tan\theta = \frac{-Fz}{b} - F\tan\theta && (z<\ell) \\
N_2(z) &= \frac{M(z)}{b(z)} = \frac{-Fz}{b} && (z<\ell)
\end{aligned} \qquad (6.11\text{-}14)$$

This results for the left leg in:

$$\begin{aligned}
N_{L,1} &= N_{2,1} = \frac{-F\ell}{b} = -F(\tan\theta_2 + \tan\theta_3 + \tan\theta_4) \\
N_{L,2} &= N_{1,2} = \frac{-F\,z_2}{b} - F\tan\theta_2 = -F(\tan\theta_2 + \tan\theta_3 + \tan\theta_4) \\
N_{L,3} &= N_{2,3} = \frac{-F\,z_3}{b} = -F\tan\theta_4 \\
N_{L,4} &= N_{1,4} = \frac{-F\,z_4}{b} - F\tan\theta_4 = 0 - F\tan\theta_4 = -F\tan\theta_4
\end{aligned} \qquad (6.11\text{-}15)$$

and for the right leg:

$$
\begin{aligned}
N_{R,1} &= N_{1,1} = \frac{-F\ell}{b} = -F(\tan\theta_2 + \tan\theta_3 + \tan\theta_4) \\
N_{R,2} &= N_{2,2} = \frac{-F\,z_2}{b} = -F(\tan\theta_3 + \tan\theta_4) \\
N_{R,3} &= N_{1,3} = \frac{-F\,z_3}{b} - F\tan\theta_3 = -F(\tan\theta_3 + \tan\theta_4) \\
N_{R,4} &= N_{2,4} = \frac{-F\,z_4}{b} = 0
\end{aligned}
\qquad (6.11\text{-}16)
$$

The stepwise changes for the jacket legs are clearly shown in figure 6.11-5.

In summary
As noted earlier, it is more cumbersome to use the equations 6.11-6 than to determine the leg forces directly from a cross section of the frame. The negative sign indicates that the leg forces in the jacket are opposite to those in the tower. For both types of frame the step in the leg force is equal to the external load F times the tangent of the brace angle. If the brace pattern is zigzag as chosen here, the total step at the point where the two braces meet the leg is then $F\cdot(\tan\theta_i + \tan\theta_{i+1})$ with θ_i the brace angle above and θ_{i+1} the brace angle below the cross section.

For a different brace pattern the brace forces are different than for a zigzag pattern and the stepwise changes are hence also different. For example, the brace forces in a frame with X-braces are half those of a frame with single diagonal bracing and the corresponding steps are therefore $\frac{1}{2}F\cdot\tan\theta_i$ per brace for both legs.

6.11.5 Real and apparent differences between a tower and a jacket frame

In sections 6.8 to 6.10 we have discussed the differences between a tower and a jacket structure. The distributions of the shear forces and the bending moments over the height of the two frames are markedly different, as e.g. illustrated by figures 6.10-1 and 6.10-3. This suggests that the leg and brace forces will also be different. For the leg forces this is indeed the case, but despite an appearance to the contrary the brace forces in a tower and a jacket frame are the same, as we will show.

Leg forces
The leg forces are basically equal to the bending moment in the cross section divided by the width of the panel. As for a tower and a jacket frame the moment distributions over the height of the frame are different in magnitude and direction, it immediately follows that the leg forces are also different. For applied horizontal loading from left to right, as used in this handbook, the left leg of the tower is in tension and the right leg is in compression. The bending moment in a continuous beam representation of the frame *increases* linearly towards a maximum at the base of the structure. The leg forces follow this behaviour, but due to the discrete nature of the frame they do this by stepwise increases rather than linearly. At the base the leg forces are transferred to the piles in the form of axial pile forces.

For a jacket the left leg is in compression and the right leg is in tension. The bending moment in a continuous beam representation of the frame has a non-zero value at the top. Going down, the bending moments first increase slightly, but thereafter they *decrease* linearly towards the base of the structure. The moment at the base of the frame is non-zero due to the lateral pile

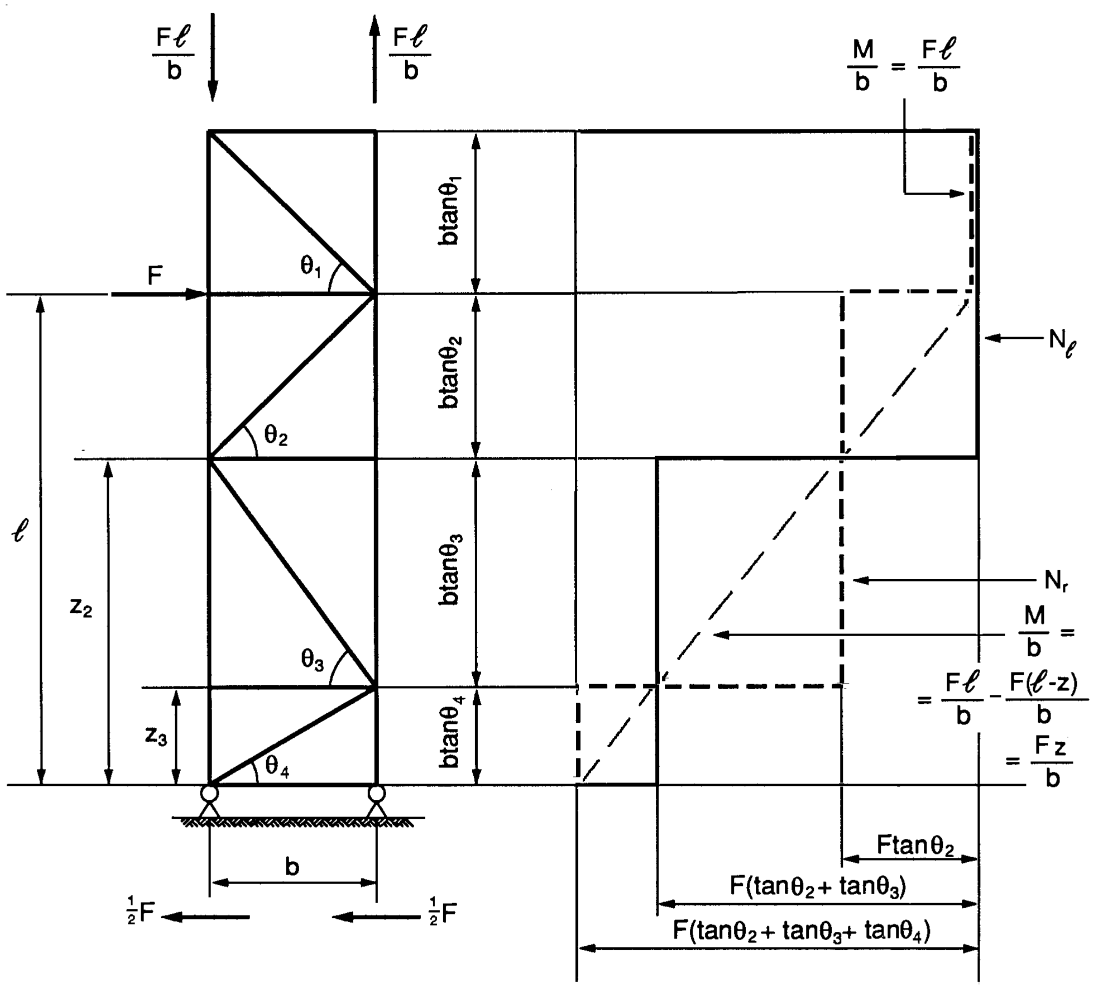

Figure 6.11-5. Stepwise change of leg forces over the height of a jacket frame (vertical legs, diagonal bracing)

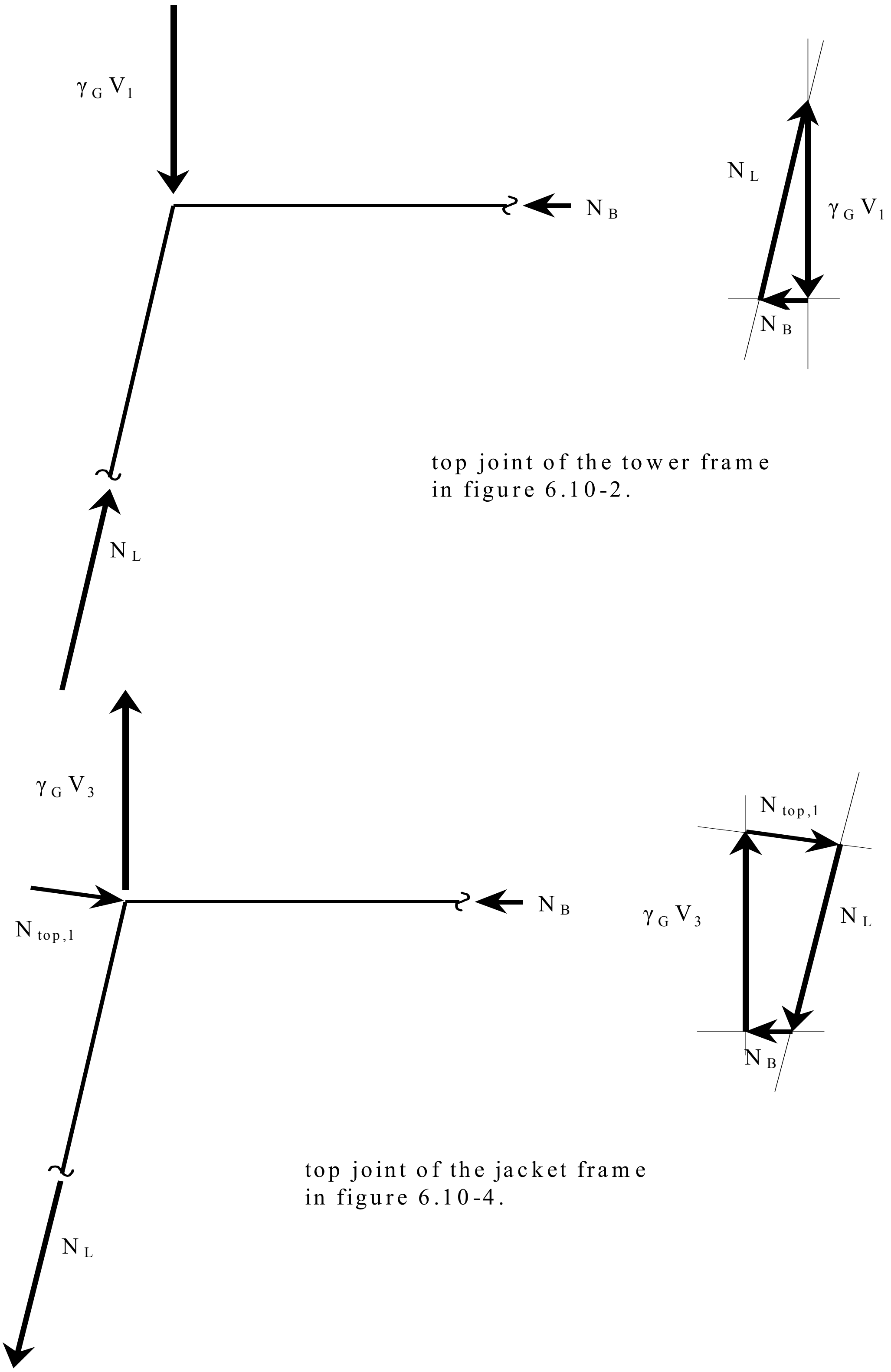

Figure 6.16.1-6. Graphical determination of member forces due to a vertical load on the frame for a joint with only two members

forces P_t and the pile moments P_m, which are both transferred to the frame at the sea floor. The leg forces again basically follow this behaviour. At the top they are equal and opposite to the axial pile forces $P_{a\,env}$, while going down they decrease stepwise. At the bottom of the leg they are zero as the legs are completely free in the axial direction at the base of the frame.

These differences in leg forces for a tower and a jacket are clearly illustrated in figures 6.11-4 and 6.11-5. The differences may be summarised as follows: tension and compression are reversed, and the forces in a tower leg increase from the top to the base, whereas the forces in a jacket leg decrease from the top to the base.

Brace forces

The first expectation probably is that the brace forces are different for a tower and a jacket. However, this is not the case as we can readily deduce from the fact that the shear force and bending moment distributions over the height are identical for a tower frame and a jacket frame when the piles and the legs are considered together, as e.g. illustrated by figure 6.8-3. It remains to be shown that the present model correctly reflects this. Using the expressions 6.11-6 for a tower and a jacket it can indeed be demonstrated that $N_B(z)$ is the same for the two types of structure. However, the algebra is a bit horrible and we will not pursue this any further.

We will make one more observation with regard to brace forces. To avoid unnecessary complications we will simplify the loading of the frame to a single horizontal point load F, applied at a height ℓ above the sea floor. We will further assume that $\alpha_1 = \alpha_2$ and illustrate the point to be made using a tower frame. Under these assumptions $S(z) = F$ and $M(z) = F \cdot (\ell - z)$ for $z < \ell$. Both these quantities are positive, i.e. they act in directions that agree with the directions indicated in figure 6.11-1. The brace force is:

$$\begin{aligned}
N_B(z) &= \frac{S(z)}{\cos\theta}\cdot\left[\left\{\frac{\cos\theta}{\cos\theta-\alpha\sin\theta}\right\}\cdot\left\{1-\frac{2\alpha\,M(z)}{b(z)S(z)}\right\}\right]\\
&= \frac{F}{\cos\theta}\cdot\left[\left\{\frac{\cos\theta}{\cos\theta-\alpha\sin\theta}\right\}\cdot\left\{1-\frac{2\alpha\,F(\ell-z)}{b(z)F}\right\}\right]\\
&= \frac{F}{\cos\theta}\cdot\left[\left\{\frac{\cos\theta}{\cos\theta-\alpha\sin\theta}\right\}\cdot\left\{\frac{b(z)-2\alpha(\ell-z)}{b(z)}\right\}\right]\\
&= \frac{F}{\cos\theta}\cdot\left[\left\{\frac{\cos\theta}{\cos\theta-\alpha\sin\theta}\right\}\cdot\left\{\frac{b_f}{b(z)}\right\}\right]
\end{aligned} \qquad (6.11\text{-}17)$$

The reduction factor in the brace force $N_B(z)$ due to the transverse components of the leg forces in the inclined legs is thus $b_f / b(z)$, which is similar (but not precisely the same) as the reduction in the lateral pile force derived in section 6.4.4. For the brace force the reduction is:

$$\frac{b_f}{b(z)} = \frac{\text{breadth of the frame at the application point of the resultant horizontal force}}{\text{largest breadth of the panel considered}}$$

while for the lateral pile force it was

$$\frac{b_f}{b_e} = \frac{\text{breadth of the frame at the application point of the resultant horizontal force}}{\text{effective breadth of the frame between the piles at a depth } d_e}$$

It is finally of interest to note that the model correctly confirms that the brace forces above the application point of the resultant load F are zero for both frames. For the tower frame this part is unloaded and $S(z) = M(z) = 0$. However, for the jacket frame both $S(z)$ and $M(z)$ are unequal to zero. For $z > \ell$ we have (see figure 6.8-2:

$$\begin{aligned} S(z) &= -F\left(1 - \frac{b_f}{b_e}\right) = -\frac{F}{b_e}(b_e - b_f) = -\frac{F}{b_e} \cdot 2\alpha(\ell + d_e) \\ M(z) &= -M_{Oe} \cdot \frac{b(z)}{b_e} = -F(\ell + d_e) \cdot \frac{b(z)}{b_e} = -\frac{F}{b_e} \cdot (\ell + d_e) \cdot b(z) \end{aligned} \qquad (6.11\text{-}18)$$

Excluding the geometrical factors the brace force $N_B(z)$ is proportional to:

$$N_B(z) \sim S(z)\left[1 - \frac{2\alpha M(z)}{b(z)S(z)}\right] = \frac{F}{b_e}\left[-2\alpha(\ell + d_e) + 2\alpha(\ell + d_e)\right] = 0 \qquad (6.11\text{-}19)$$

Therefore, also above the application point of F the tower and jacket models are completely similar: the brace forces are the same, while the leg forces remain of course different. At the side where no diagonal brace joins the leg, the leg force is $N_2 = -P_a$ while at the other side the leg force is $N_1 + N_B \sin\theta = -P_a$; as N_1 and N_B always act in the same direction the leg force $N_1 < |P_a|$.

In summary, when the piles are kept within the legs, the level shear force and the bending moment for a jacket are the same as for a tower. The brace forces are also the same, while the leg force for the tower is equal to the leg + pile force for the jacket.

6.11.6 Individual leg and brace forces due to vertical loading

In the preceding sections we have considered horizontal loading on the frame due to the environment. It remains to look at the vertical loading due to permanent and variable loading.

The vertical loads V_1 and V_2 in section 6.10 are applied locally to the top of the legs for a tower (see figure 6.10-2) or to the top of the piles for a jacket (see figure 6.10-4). In the case of a jacket these loads result in loading of the frame by V_3 and $N_{top,1}$ and V_4 and $N_{top,2}$, both at the top, and by $N_{base,1}$ and $N_{base,2}$ at the base of the frame; see figure 6.10-4.

All these loads are local point loads on a joint of the frame. When there are only 2 members joining at the joint there are only 2 unknown member forces, which can be determined from equilibrium of the joint. This can be done either by calculation or graphically; the graphical solution for this case is shown by way of example in figure 6.11-6, where the examples refer to the top joint of the tower frame in figure 6.10-2 and the top joint of the jacket frame in figure 6.10-4.

When there are more than 2 members joining at a joint the number of unknowns is greater than the number of equations (as the members are hinged moments do not provide a 3rd equation). Consequently, the force(s) in one or more of the members have to be known from other sources, or an additional assumption will have to be made. Proceeding with the example of the previous paragraph, the force in the top horizontal is known from equilibrium of the joint on the left hand side, so that the forces in the leg and the diagonal on the right hand side can now also be determined. The process can be continued downwards until we arrive at the joints at the bottom; see also figures 6.3-2 to 4 and the associated discussion in section 6.3.2.

In this manner the forces in all the frame members can be determined. The trend will be that vertical point loads at the top will become more evenly distributed through the frame, the more so the taller the frame. At the base of the tower frame the leg forces should match the support reactions in figure 6.10-2, while at the base of the jacket frame the legs should be unloaded (see figure 6.10-4).

When a joint is fixed instead of hinged, the joint is statically indeterminate and the member forces depend on the relative stiffnesses of the members. An approximate solution for this situation is described by means of the example shown in figure 6.11-7, where 3 members come together. The load V will be distributed over the leg and the diagonal brace in proportion to their axial stiffnesses and the shortening of the members; the horizontal brace will (to first order) not take up any vertical force. If the joint displaces vertically over a distance w, the leg shortening is $w\cos\alpha_2 \approx w$ while the diagonal brace shortening is $w\sin\theta$. The axial stiffness of the leg is $EA_{\ell eg}/L_{\ell eg}$, while for the diagonal brace (with subscript *db*) this is EA_{db}/L_{db}. The forces in the two members thus are:

$$\begin{aligned} F_{\ell eg} &= \frac{EA_{\ell eg}}{L_{\ell eg}} \cdot w \\ F_{db} &= \frac{EA_{db}}{L_{db}} \cdot w\sin\theta \end{aligned} \qquad (6.11\text{-}20)$$

and their ratio is:

$$\frac{F_{db}}{F_{\ell eg}} = \frac{A_{db}}{A_{\ell eg}} \cdot \frac{L_{\ell eg}}{L_{db}} \cdot \sin\theta \qquad (6.11\text{-}21)$$

If we further assume that the bottom of the panel is a rigid plane, so that the deformation is limited to the panel under consideration, the relationship between the lengths involved is:

$$L_{\ell} = \frac{L_{db}\sin\theta}{\cos\alpha_2} \approx L_{db}\sin\theta \qquad (6.11\text{-}22)$$

so that:

$$\frac{F_{db}}{F_{\ell eg}} \approx \frac{A_{db}}{A_{\ell eg}} \cdot \sin^2\theta \qquad (6.11\text{-}23)$$

With this approximate ratio the member forces can once more be determined, either computationally or graphically.

For a horizontal load H instead of a vertical load V on the same joint the situation becomes much more complex and will not be considered any further.

The permanent/variable loads of the substructure itself (G_S) comprise vertically distributed member loads, which violate the requirement that loads should only comprise of point loads on the joints. Therefore, G_S results predominantly in bending moments in all the members of the frame.

6.11.7 Total individual leg and brace loads

The total member forces are, finally, the sum of the member forces due to the horizontal loading by the environment and the member forces due to the vertical loading by the permanent/variable loads.

6.12 Examples of computer calculations

In Annexes B and C two examples of computer calculations using a finite element model are presented to illustrate the validity *and* the limitations of the results obtained with the highly idealised models developed in this handbook. The first example concerns a small three-dimensional structure in relatively shallow water for the central North Sea, the second relates to a two-dimensional frame in very deep water. Both cases are hypothetical test cases rather than real structures. They are subjected to applied wave loading only.

The two examples demonstrate that the simple and highly idealised models of steel space frame structures under wave loading correctly exhibit all features of the structural behaviour of towers and jackets. The wave loading in the idealised models is represented by a single horizontal resultant load. The analytical expressions for:

- pile forces and moments,
- level shears and moments in horizontal cross sections,
- individual member forces in the frame

are sufficiently accurate for preliminary design or assessment purposes below a depth of approximately 0.2λ under the still water surface. The accuracy rapidly decreases between an elevation of 0.2λ and the application point of the resultant load (which lies higher), and the model should not be used in the wave active zone above this application point. These inaccuracies are due to the effect of the vertically distributed wave loading in the wave active zone.

A considerable improvement can be obtained by distributing the total wave load over the height in several point loads applied at nodal points at horizontal framing levels instead of using one resultant load. The models can then be used with confidence for the purposes for which they are intended.

NOTE: This section and the associated Annexes B and C are still to be updated for improved calculations. For the structure in Annex B five point loads, one at each horizontal framing level, instead of one resultant load will then be used.

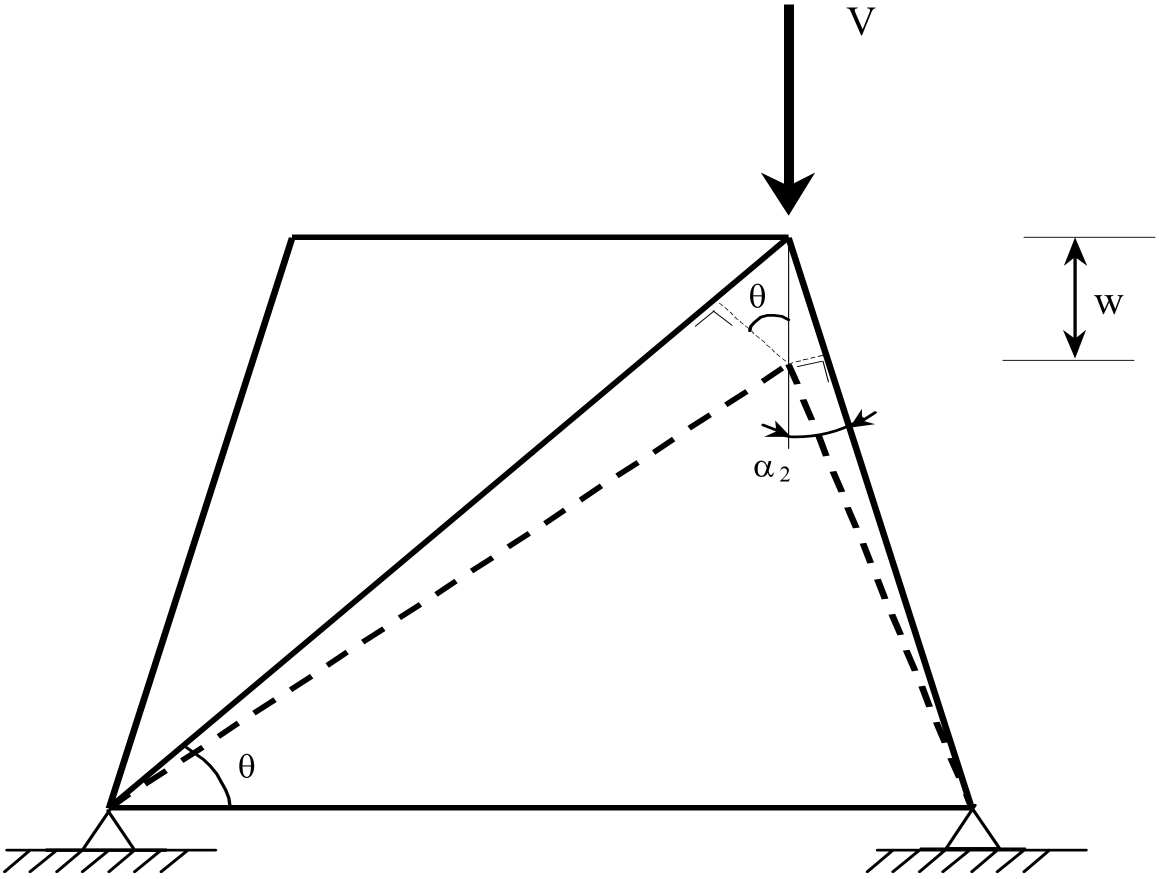

Figure 6.11-7. A statically indeterminate joint under a vertical load

6.13 References

6.3-1 Visser, W., ***The structural design of offshore jackets***; Published by the Marine Technology Directorate Limited, London; publication 94/100, 1994; ISBN 1 870553 16 0.

6.3-2 Vugts, J.H., ***Offshore structures engineering*** *– a selection of notes on some topics in the area of offshore structures engineering, based on guest lectures presented to the Norwegian Institute of Technology at Trondheim in October 1983*; Shell Internationale Petroleum Maatschappij B.V., The Hague, August 1984.

6.3-3 Barltrop, N.D.P. and Adams, A.J., ***The dynamics of fixed marine structures***; Butterworth Heinemann Ltd., London, 3rd edition 1991; ISBN 0 7506 1046 8.

Annex A – Graphical determination of axial and lateral pile reaction forces

When the internal pile moments are either neglected or have been eliminated by the introduction of the dummy members (see section 6.6) we are left with the problem of determining the axial and lateral pile reaction forces, either at the sea floor or at the artificial hinge level at a distance d_e below the sea floor. These can be determined through a graphical solution procedure as an alternative to the analytical method described in section 6.4.4. The graphical method can as easily be applied to cases with equal as with unequal pile batter angles.

The method is based on the general resolution of a given force into three component forces along known lines of action. The given force should be fully known as a vector, i.e. in magnitude and direction. The resolution is an elementary problem in applied mechanics that is solved by the procedure given below and shown in figure A.1:

- the given force F acts along line ℓ and is to be resolved into 3 forces along the lines a, b and c
- choose 2 points where the 4 lines intersect to create a construction line s: one point on ℓ (for example (ℓ, a)) and the other point where the two remaining lines cross (in this case (b, c))
- move F along ℓ to the intersection point (ℓ, a)
- resolve F along a and s into F_a and F_s
- move F_s along s to the intersection point (b, c)
- resolve F_s along b and c into F_b and F_c
- the solution is the 3 forces F_a, F_b, F_c .

For the most general case of a two-dimensional frame we have to resolve F into *four* component forces, i.e. $F_{a,1}$, $F_{a,2}$, $P_{t,1}$ and $P_{t,2}$. We must first reduce this problem with four lines of action to the previous one with three lines of action. This is done by making use of the fact that $P_{t,1}$ is assumed to be equal to $P_{t,2}$. Therefore, the resultant of $P_{t,1}$ and $P_{t,2}$ acts along the bisector of the angle between them. The various lines of action are named as follows; see figure A.2. The given force F acts along ℓ. The axial pile forces act along the piles, i.e. along line a at the left and line b at the right. The lateral pile forces act at right angles to the piles, line d at right and line e at left; their resultant acts along line c, i.e. the bisector of the angle between lines d and e. In figure A.2 the situation is pictured for equal pile batter angles ($\alpha_1 = \alpha_2$), in which case the line c is a horizontal line. However, as said before, this can easily be generalised to the case of $\alpha_1 \neq \alpha_2$ and a line c that is not horizontal. The procedure is now entirely analogous to the previous problem:

- the force F is to be resolved into 4 forces along the lines a, b, d and e
- resolve F first along a, b and c
- choose 2 intersection points of ℓ, a, b and c to construct a construction line s, i.e. one point on ℓ (e.g. (ℓ, a)) and the other point on the remaining lines (b, c)
- move F along ℓ to point (ℓ, a)

- resolve F along a and s into F_a and F_s (for clarity this is shown in figure A.2 in a separate diagram to the right)
- F_a acts along line a and is the axial pile force on the left; F_s acts along the construction line s
- move F_s along s to the intersection point (b, c)
- resolve F_s along b and c into F_b and F_c
- move F_c along c to the intersection point (d, e)
- resolve F_c along d and e into F_d and F_e
- move F_d to point (b, d) and F_e to point (a, e)
- the forces F_a, F_b, F_d and F_e are now the resolved components of F, the applied force; the pile *reaction* forces are therefore equal and opposite:
  $P_{a,1} = -F_a$, $P_{a,2} = -F_b$, $P_{t,1} = -F_e$ and $P_{t,2} = -F_d$.

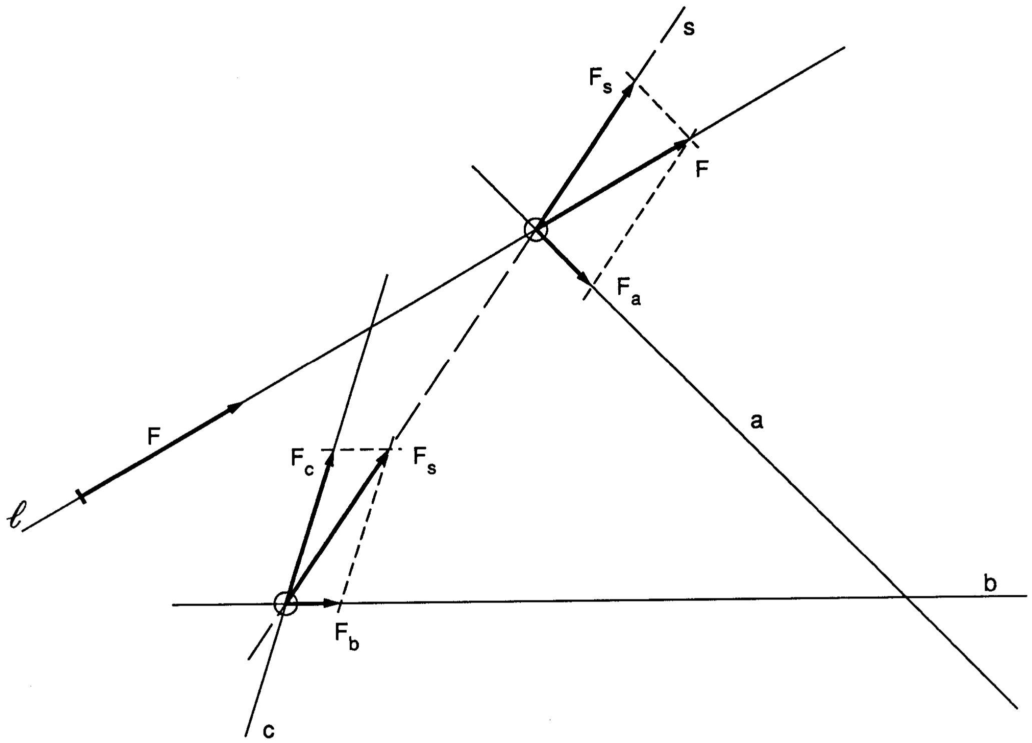

Figure A.1. The graphical resolution of a given force F into three component forces along known lines of action

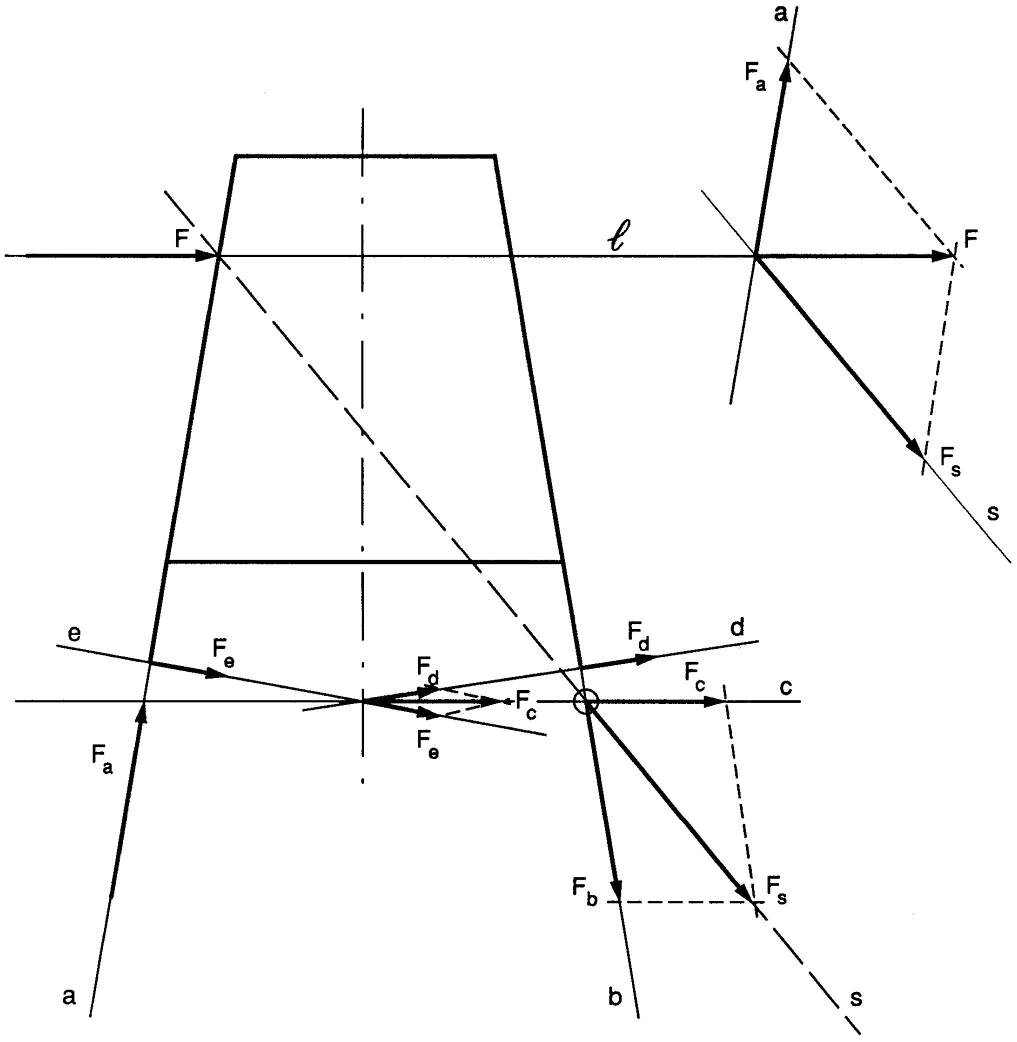

Figure A.2. Graphical determination of the axial and lateral pile reaction forces

Annex B – Example one:
A small structure for the central North Sea in 70 m waterdepth

B.1 General

We will consider a small four legged structure for the central North Sea; se figure B.1. The structure is rectangular in plan. The substructure measures 20x30 m at the top and 30x30 m at the base. Two faces are vertical and parallel, the two other faces are battered with a slope of 1:16. The height of the substructure from the sea floor to the top bracing level is 80 m. The still water depth at lowest astronomical tide (LAT) is 65 m. Allowing for tide, storm surge and reservoir compaction the mean water depth for design calculations is determined at 70 m. The horizontal plan bracings are positioned at elevations +10 m, -10 m, -30 m, -50 m and -70 m relative to MSL. The four piles, one in each corner, have a diameter of 1.22 m and a wall thickness of 0.051 m. They are driven to a penetration of 55 m below the sea floor.

The loading condition for the present calculations is wave loading only due to a wave with a height of 20.0 m and a period of 13.0 s. The wave direction is parallel to the vertical faces and hence perpendicular to the inclined faces of the structure, with the aim to look at the forces in the members of the vertical frames that have battered legs. The total horizontal wave force on the structure was calculated to be 5.16 MN and the overturning moment about the sea floor 303 MNm. We will represent this loading condition by a single resultant load that acts at an elevation of 303/5.16 = 58.7 m above the sea floor. As the total force is shared by two parallel frames the wave force per frame is 2.58 MN and the overturning moment about the sea floor is 151.5 MNm.

The substructure has been analysed with three different types of foundation:

a) with one pile through each of the four hollow tubular legs; the piles are connected to the substructure through shims at the top; case (a) refers therefore to a jacket structure;
b) with one pile through each of the four hollow tubular legs, as in the previous case, but instead of being connected through shims at the top only the piles have now been grouted to the legs over their full length; case (b) is referred to as a structure with grouted piles through the legs;
c) with one pile per corner as before, but now external to the leg and attached to the frame by a pile sleeve and a grouted connection; the sleeve extends over the height of the bottom bay; case (c) is thus a tower structure.

B.2 Member forces

The first series of calculations compares the axial member forces determined by computer analysis for a jacket frame (case a) and a tower frame (case c); see figures B.2 and B.3. All member forces have been non-dimensionalised by dividing them by the total horizontal wave force on the *whole* structure. As can be seen, the diagonal member forces are the same for both frames, but the leg forces are very different. The axial forces in the horizontal members are very small, as expected.

For the jacket, the left leg is in compression and the forces in the various bays *decrease* stepwise from 1.0 at the top to 0.0 at the bottom. The right leg is in tension and the force *decreases* stepwise from 0.83 to 0.27. The forces in the piles are shown adjacent to the legs

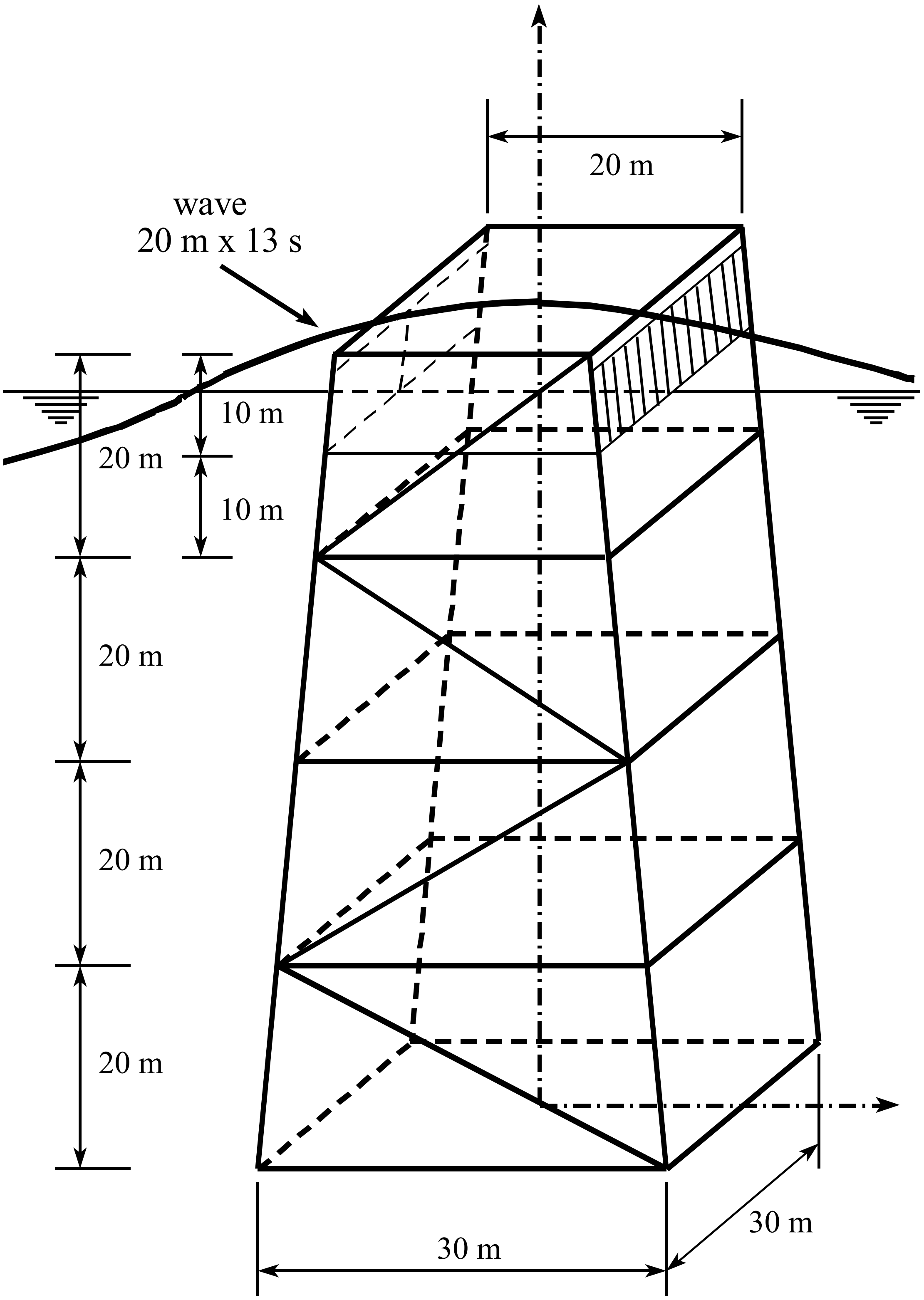

Figure B.1. A small North Sea structure in 70 m water depth

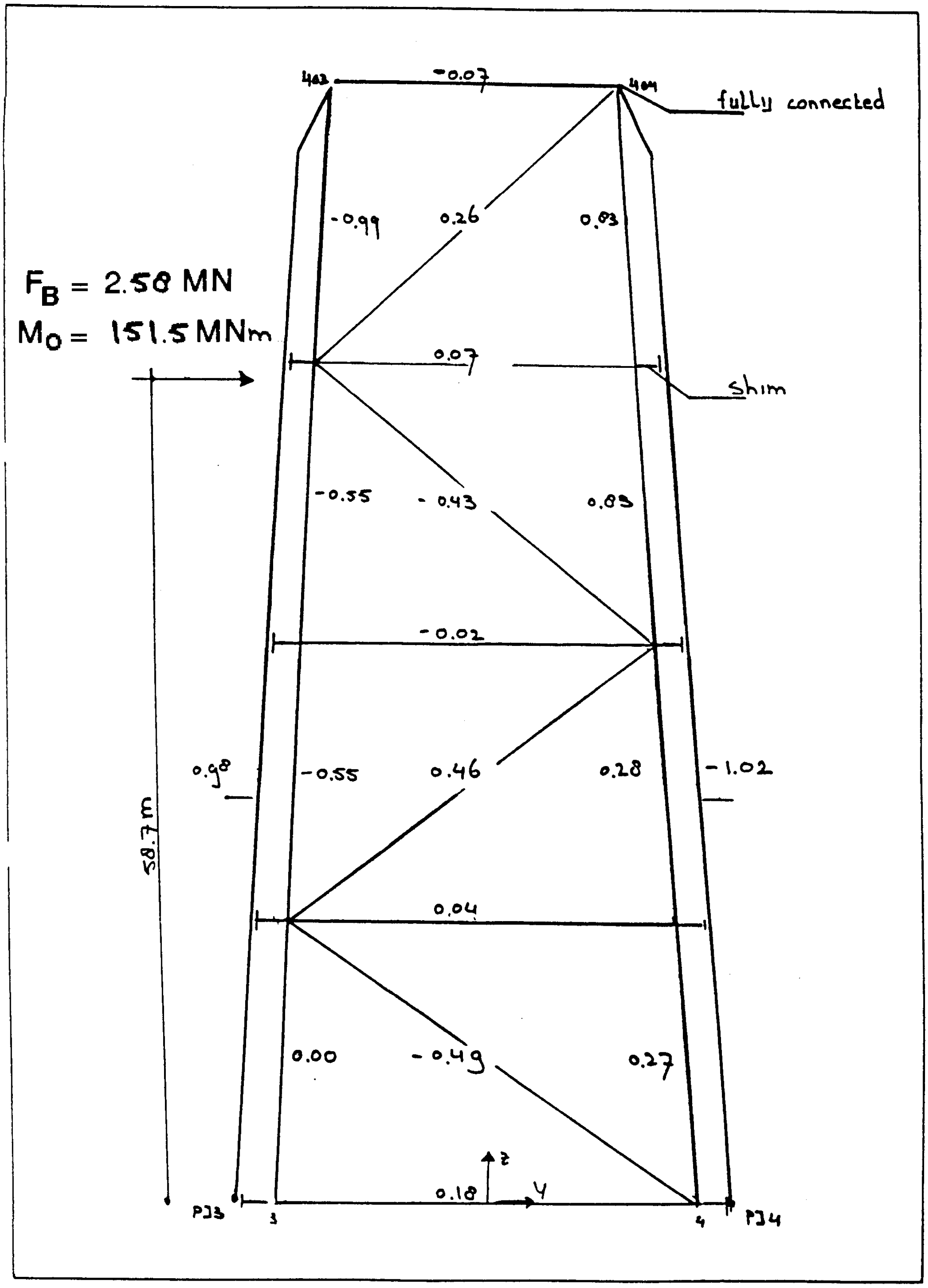

Figure B.2. Jacket frame – member forces divided by total horizontal wave load on the whole structure

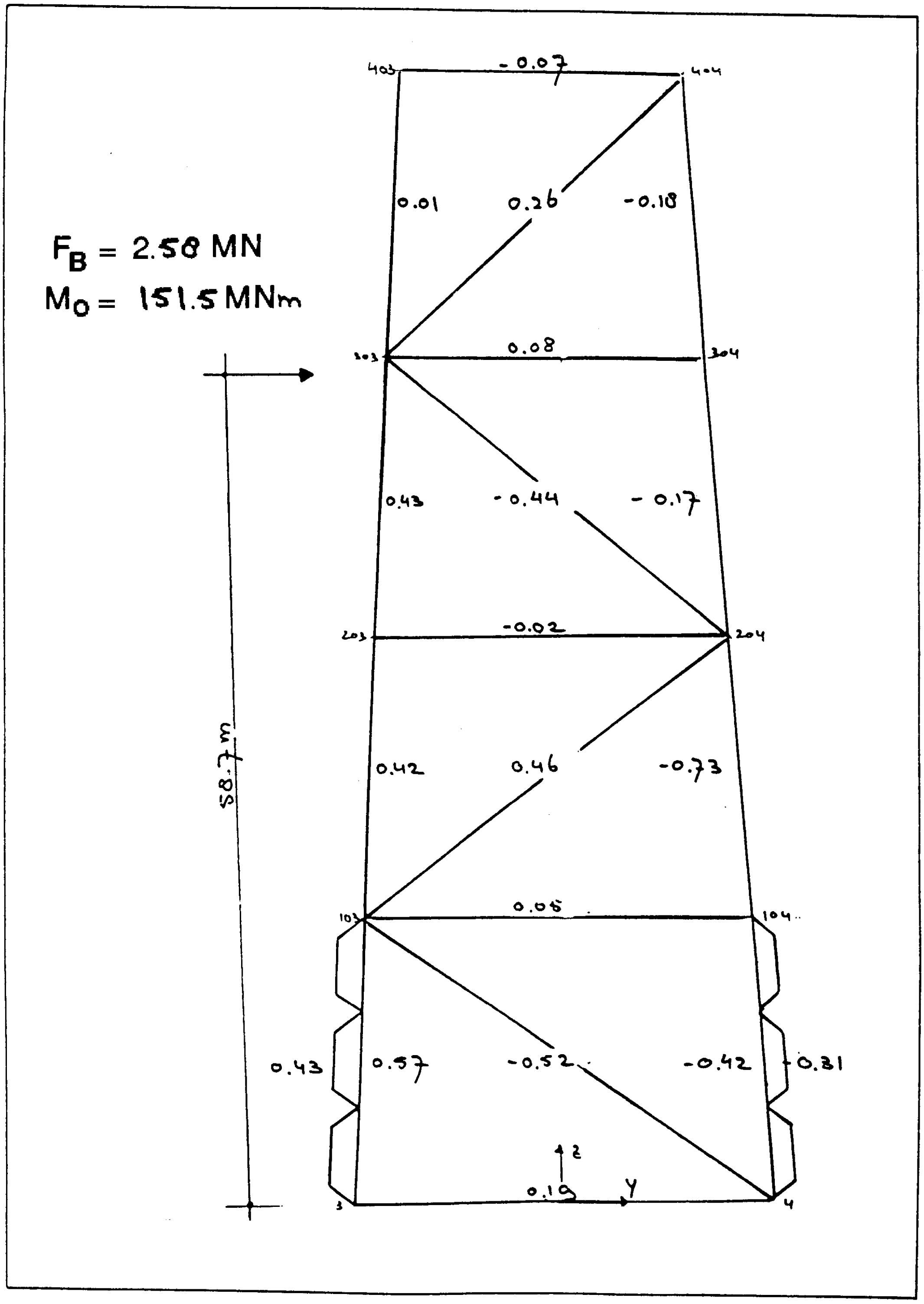

Figure B.3. Tower frame – member forces divided by total horizontal wave load on the whole structure

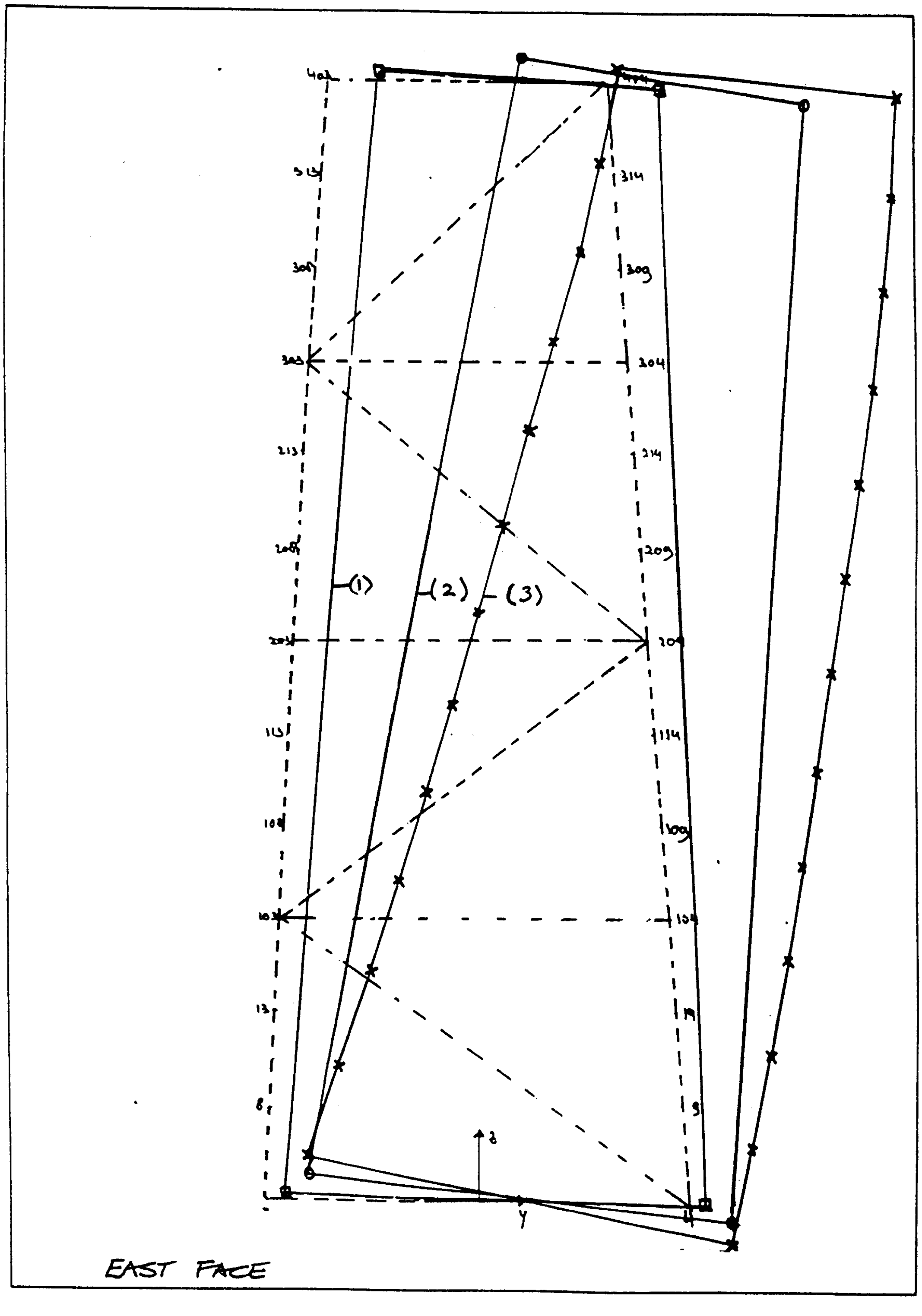

Figure B.4. Jacket deformation

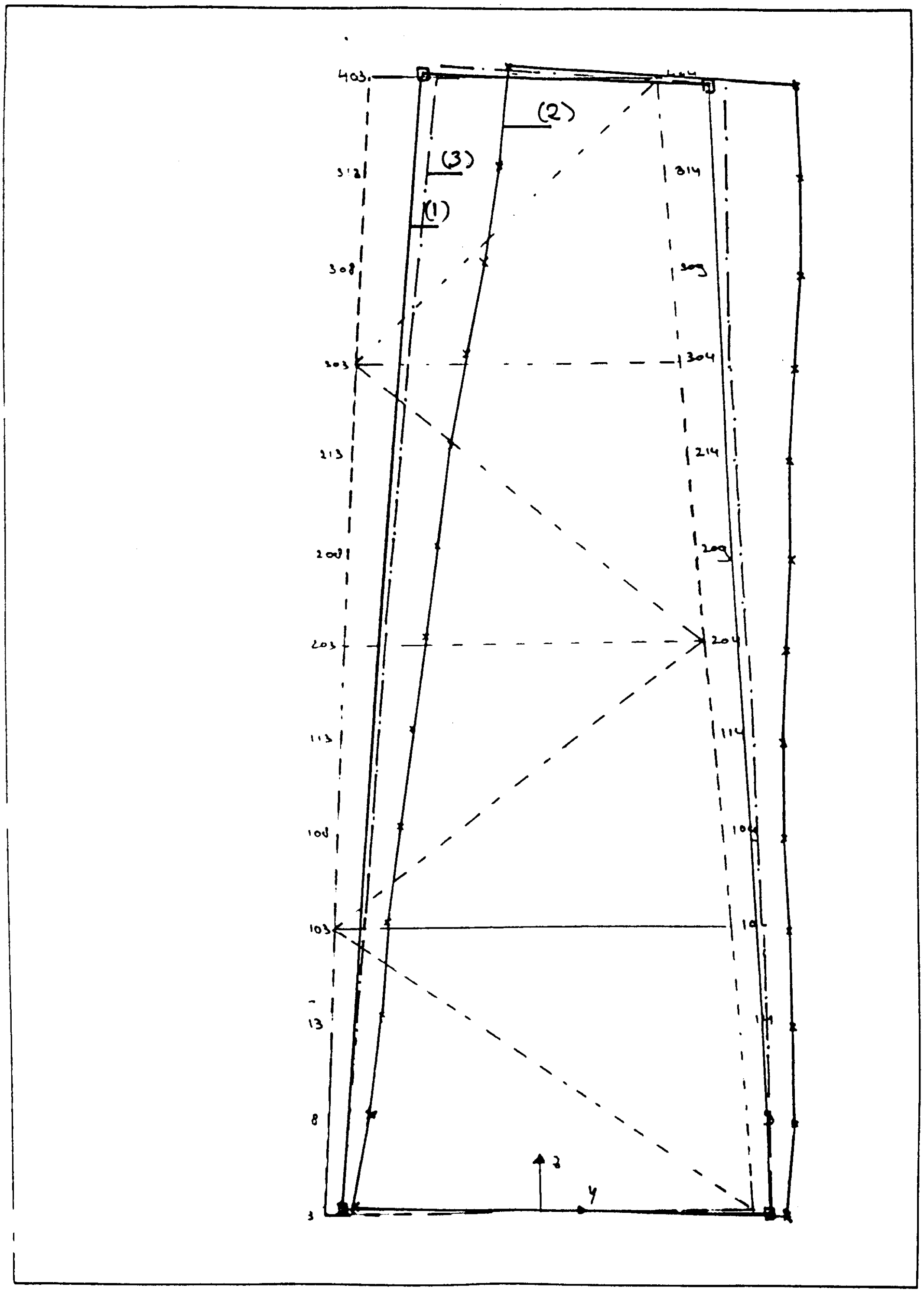

Figure B.5. Tower deformation

and are constant over the full height with a magnitude of 1.00 (0.98 and 1.02, respectively). The pile on the left is in tension and on the right it is in compression.

For the right leg the magnitude of the force is not equal to 1.0 at the top and 0.0 at the bottom due to the diagonal braces framing into the leg at these points. To verify this one should take the vertical components of the brace forces. The height of the top bay is 20.0 m, so that the angle of the brace with the horizontal is tan θ_1 = 20/(20 + 20/16) = 0.941 or θ_1 = 43.3 deg. The vertical component of the brace force is therefore 0.26 x sin θ_1 = 0.26 x 0.68 = 0.18 which is indeed equal to the shortfall in the leg force in the top bay. Similarly, the height of the bottom bay is also 20 m and the brace angle is now tan θ_3 = 20/(30 -20/16) = 0.70 or θ_3 = 34.8 deg. The vertical component is thus - 0.49 x sin θ_3 = - 0.49 x 0.57 = - 0.28, which indeed balances the + 0.27 leg force in the bottom bay.

For the tower the leg forces correspond with the expectation for a cantilevered beam, i.e. tension at the left and compression at the right. The forces now *increase* towards the base, from 0.01 to 0.57 on the left and from - 0.18 to - 0.42 on the right. The difference in the value at the top is again due to the diagonal brace (vertical component + 0.18) at the right leg. The leg forces in the bottom bay have to be combined with the pile force adjacent to the leg. On the left that results in 0.57 + 0.43 = 1.00 and on the right in - 0.42 - 0.31 = - 0.73. The shortfall in the compression on the right compared to the tension on the left is once more due to the diagonal brace coming in at this point, which is also in compression. The vertical component of the brace force is - 0.52 x 0.57 = - 0.30. Together with the (leg + pile) force on the right of - 0.73 this results in a total compressive force of -1.03.

It should expressly be noted that it is purely accidental that the total support reactions on the frame, when non-dimensionalised by the total horizontal load on the *whole* structure, have a value of approximately 1.00; this will be demonstrated later in section B.4..

B.3 Deformations

The second series of results relate to the deformations of the jacket and the tower, cases (a) and (c); see figures B.4 and B.5. For the jacket the deformation of the frame has been determined in three stages. In the first stage the frame and the piles within the legs are made infinitely stiff so that the structure above the sea floor behaves as a rigid body. The rigid body deformation reflects the displacement and the rotation of the frame at the mudline resulting from the deformation of the piles in the ground. In the second stage the high stiffness of the frame is maintained, but the piles within the legs get their real stiffness. As can be seen, the extension and shortening of the piles is a very important feature, significantly increasing the horizontal displacements and the rotation of the frame that in itself continues to displace as a rigid body. In the third and final stage the real stiffness of the frame is introduced allowing it to deform elastically. The counter-curvature due to the counteracting horizontal force and moment at the top of a jacket frame is clearly observed.

For the tower three similar but slightly different stages are shown in figure B.5. The first stage refers again to the rigid body displacement and rotation. As both frames behave as rigid bodies, the first stage deformations for the jacket and the tower are the same. In the second stage the frame members are given their true stiffnesses resulting in elastic deformation of the frame. This shows the normal pattern expected for a cantilevered beam, with some deviations in the top and bottom bays. These deviations are due to local loading and local stiffness effects. Local loading results from the vertically distributed wave load over the top part of the leg and from the pile sleeve at the bottom. To make these local patterns visible the legs between plan bracing levels have been modelled as three members in series rather than as one. As can be seen from figure B.5, the elastic deformation is larger than the rigid body deformation. The total elastic deformation of the frame is a combination of bending and shear deformation. To investigate the relative importance of each of these, shear deformation has been suppressed in stage 3 by making the braces infinitely stiff while the legs maintain their true stiffness and thus continue to deform elastically. Stage 3 therefore shows elastic deformation due to frame bending only. This demonstrates that for this structure shear deformation is much larger than bending deformation. For short and stocky beams (here $h/b \cong 3.5$) this can be expected.

Finally, in figure B.6 the total deformation patterns for all three cases (a), (b) and (c) are compared. It shows that the deformation of the jacket is much larger than that of the tower. This is mainly due to the elastic deformation (lengthening and shortening) of the piles within the jacket legs. When the piles are grouted within the legs (case b), the leg and pile together form one composite member; the structure then changes effectively into a tower and behaves accordingly. Generally speaking, therefore, a tower provides for a stiffer overall structure than a jacket, perhaps contrary to what one would at first sight expect. However, as the substructure is exactly the same in the three cases, it is of course more correct to state that the pile foundation for a jacket with its main support points at the top is more flexible than the pile foundation for a tower with its support points at the base.

These observations of the behaviour of the structure, which are based on actual computer calculations, are in full agreement with the expected behaviour as discussed for the idealised models in these notes.

B.4 Comparison of the idealised model results with computer calculations

It will be interesting to see how the calculations according to the idealised model compare quantitatively with the computer calculations. The latter results are obtained with a much more detailed model with respect to both loading (spatially distributed instead of a resultant point load) and structural representation. The idealised model treats the frame as a statically determinate assembly of members; it includes the geometry of the frame and the equilibrium of member forces per bay but ignores stiffness. The finite element model, on the other hand, performs a full stiffness analysis of the statically indeterminate frame.

It should further be appreciated that this example constitutes a severe test for the idealised model. It concerns a small structure in shallow water exposed to a wave with a 13 sec period. The corresponding (deep water) wave length is 264 m. The influence of wave action is therefore felt over the entire water depth. To represent the vertically distributed loading by a single resultant point load is thus a very crude approximation.

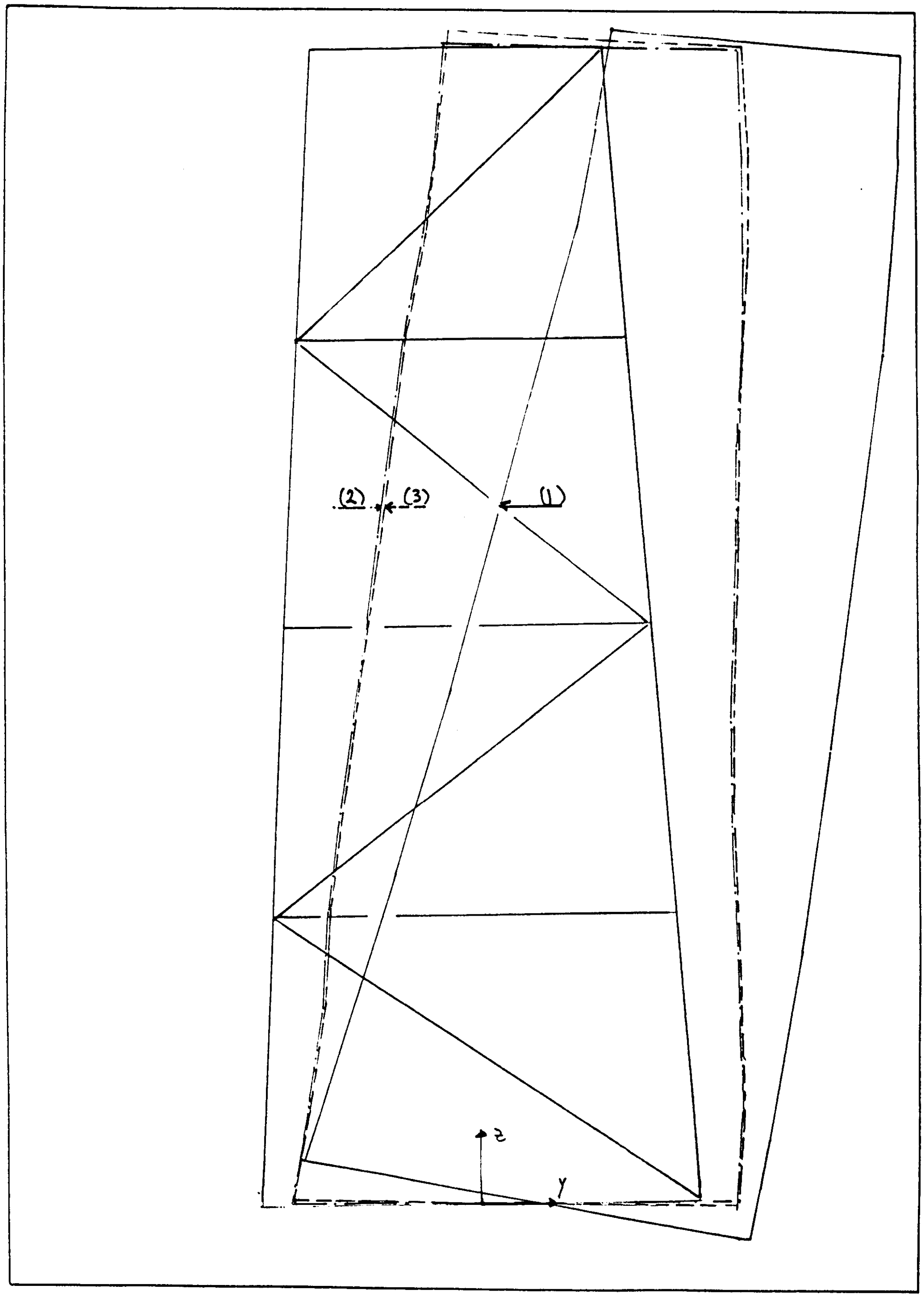

Figure B.6. Comparison of total deformation patterns for the jacket, the structure with grouted piles through the legs and the tower

- *Support reactions for the idealised model*

The following data apply to the present example for the two-dimensional frame considered:

F_B = (1/2) x 5.16 = 2.58 MN (load on one of the two parallel frames)
ℓ = 58.7 m
d_e ≈ 4 x (pile diameter) = 4 x 1.22 = 4.88 m (estimate)
b_t = 20 m
b_f = 20 + 2 x (80 - 58.7) x (1/16) = 22.66 m
b_s = 30 m
b_e = 30 + 2 x (1/16) x 4.88 = 30.61 m
$\ell + d_e$ = 58.7 + 4.88 = 63.58 m
M_O = 151.5 MNm (= 2.58 x 58.7, moment about the sea floor)
M_{Oe} = 2.58 x 63.58 = 164.04 MNm

With these data the following results are calculated.

pile forces

P_a = 164.04/30.61 = 5.36 MN
P_t = (1/2) x 2.58 x (22.66/30.61) = 0.95 MN
P_m = 4.88 x 0.95 = 4.64 MNm
P_a / F_B = 5.36/2.58 = 2.08 (compare $P_a / 2F_B$ = 1.04 with 0.98 and 1.02 in figure B.2)
P_t / F_B = 0.95/2.58 = 0.37 (i.e. 63% of F is taken up by the horizontal components of the axial pile forces)
P_m / M_O = 4.64/151.5 = 0.031
P_m / M_{Oe} = 4.64/164.04 = 0.028

equilibrium checks at the sea floor

$2P_t + 2\alpha P_a = 2 \times 0.95 + 2 \times (1/16) \times 5.36 = 2.57$ *MN (= F, correct)*

$(P_a - \alpha P_t)\, b_s - 2P_m = (5.36 - (1/16) \times 0.95) \times 30 - 2 \times 4.64 = 149.7$ *MNm* (difference with M_O of 1%)

- *The level shear force and bending moment in the idealised model*

For the *tower* $S = F_B$ = 2.58 MN and at the horizontal plan framing levels $M_i = 0$ for $z_i > \ell$ and $M_i = F.(\ell - z_i)$ for $z_i < \ell$. Therefore, from the top down:

$M_1 = M_2 = 0$;
M_3 = 2.58 x (58.7 - 40) = 48.2 MNm;
M_4 = 2.58 x (58.7 - 20) = 99.8 MNm;
M_5 = 2.58 x 58.7 = 151.5 MNm.

For the *jacket* and $z_i > \ell$,

$S = - F.(1 - b_f/b_e)$ = - 2.58 x (1 - 22.66/30.61) = - 0.67 MN and:
$M_1 = - M_t = - M_{Oe}.(b_t/b_e)$ = - 164.0 x 20/30.61 = - 107.2 MNm;
$M_2 = - M_{Oe}.(b_2/b_e)$ = - 164.0 x 22.5/30.61 = - 120.6 MNm.

For $z_i < \ell$,

$S = F.b_f / b_e = 2.58 \times 22.66/30.61 = 1.91$ MN and $M_i = -\{M_s + (M_f - M_s).(z_i/\ell)\}$. The moment $M_f = M_{Oe}.b_e/b_e = 164.0 \times 22.66/30.61 = 121.44$ MNm and the moment $M_s = \alpha S b_s + 2P_m = (1/16) \times 0.95 \times 30 + 2 \times 4.64 = 11.06$ MNm.
Then:

$$M_3 = -\{11.06 + (121.44 - 11.06) \times (40/58.7)\} = -86.28 \text{ MNm};$$
$$M_4 = -\{11.06 + (121.44 - 11.06) \times (20/58.7)\} = -48.67 \text{ MNm};$$
$$M_5 = -M_s = -11.06 \text{ MNm}.$$

- *The level shear force and bending moment in the computer model*

The level shear forces and moments are not directly known from the computer output but can be reconstructed from the member forces in figures B.2 and B.3.

For the *jacket* we then have in non-dimensional form:

bay no. from top	brace angle (deg)	hor. comp. brace force ⇒	hor. comp. leg forces ⇐	shear in frame ⇒	hor. comp. pile forces ⇒	shear in frame+piles ⇒
1	43.3	0.189	0.114	0.075	0.125	0.200
2	40.1	0.329	0.086	0.243	0.125	0.368
3	37.3	0.366	0.052	0.314	0.125	0.439
4	34.8	0.402	0.017	0.385	0.125	0.510

Similarly, for the *tower* in non-dimensional form:

bay no. from top	brace angle (deg)	hor. comp. brace force ⇒	hor. comp. leg forces ⇒	shear in frame ⇒	hor. comp. pile forces ⇒	shear in frame+piles ⇒
1	43.3	0.189	0.012	0.201	0	0.201
2	40.1	0.337	0.038	0.375	0	0.375
3	37.3	0.366	0.072	0.438	0	0.438
4	34.8	0.427	0.062	0.489	0.046	0.535

Note that the forces in figures B.2 and B.3 have been non-dimensionalised by dividing all member forces by $2F_B$. To convert the above numbers into real forces they must therefore be multiplied by 2 x 2.58 = 5.16 MN.

The moments at the plan framing levels are found from: $M_i = N_{2i}.b_i$.
Thus, from figures B.2 and B.3 and expressed in the non-dimensional leg force N_{2i}:

level	b_i (m)	jacket N_{2i}	jacket M_i (m)	tower N_{2i}	tower M_i (m)
1	20.0	0.99	19.8	0.01	0
2	22.5	0.83	18.7	0.17	3.8
3	25.0	0.55	13.8	0.43	10.8
4	27.5	0.27	7.4	0.73	20.1
5	30.0	0.00	0.0	1.00	30.0

To convert these numbers into real moments they must again be multiplied by $2F_B = 5.16$ MN.

- *Comparison of the idealised model and the computer model for level shears and moments*

Jacket (frame only):

level	bay	shear force (MN) computer model	shear force (MN) idealised model	error (%)	moment (MNm) computer model	moment (MNm) idealised model	error (%)
1					- 102.2	- 107.2	+ 4.9
	1	0.39	- 0.67	—			
2					- 96.5	- 120.6	+ 25
	2	1.25	1.91	+ 53			
3					- 71.2	- 86.3	+ 21
	3	1.62	1.91	+ 18			
4					- 38.2	- 48.7	+ 27
	4	1.99	1.91	- 4			
5					0	- 11.1	∞

Tower:

level	bay	shear force (MN) computer model	shear force (MN) idealised model	error (%)	moment (MNm) computer model	moment (MNm) idealised model	error (%)
1					0	0	—
	1	1.04	0	—			
2					19.6	0	—
	2	1.94	2.58	+ 33			
3					55.7	48.2	- 13
	3	2.26	2.58	+ 14			
4					103.7	99.8	- 4
	4	2.52	2.58	+ 2			
5					154.8	151.5	- 2

For the tower, the actual level shear force is lower than but gradually approaches the constant shear force over the height of the idealised model; for this shallow water depth the distributed

wave loading extends over the full height of the structure. The actual bending moment approaches the linear distribution in the idealised model from the upper side. This is as expected; see e.g. figure 6.4.
For the jacket case, both level shear force and bending moment for the idealised model tend to be higher in an absolute sense than for the computer model.

- *Comparison of forces in the diagonal braces for the idealised model and the computer model*

The forces in the diagonals for the idealised model are found from equation (6.11-6). Those for the computer model are taken as the average of figures B.2 and B.3. This results in the following comparison:

bay	geometrical factor $\frac{\cos\theta}{\cos\theta - \alpha\sin\theta}$	computer model (average of two figures)	equation (6.11-6) jacket	equation (6.11-6) tower	error (%)
1	1.063	+ 1.34	0.01	0	—
2	1.056	- 2.24	3.24	3.25	+ 45
3	1.050	+ 2.37	2.82	2.81	+ 19
4	1.045	- 2.61	2.49	2.48	- 5

This last table clearly indicates that the idealised model is capable of doing a good job in the lower part of the structure. The results are quite acceptable in a quantitative manner for preliminary calculations below a depth of some 0.2λ under the still water surface, which is considerably better than the theoretical depth of 0.5λ. In the present example this means below some - 50 m. In the region between - 0.2λ and the application point of the resultant force the results of the idealised model become increasingly inaccurate and above the application point they are simply not valid. This is entirely as one would expect.

Annex C – Example two:
A frame from a deep water tower structure in 750 m waterdepth

In the second example we consider the behaviour of a two-dimensional (near) vertical frame of a tower structure for a waterdepth of 750 m. This case can be expected to be much more suited to a point load representation of the wave loading. It is discussed in detail in reference [6.3]. As for the example in Annex B, we will quantitatively compare calculations according to the idealised model discussed in this chapter with computer calculations using a finite element program. The configuration of the frame is shown in figure C.1. For the first test the frame is subjected to a horizontal point load, just as for the idealised model in section 6.4.4 and Annex B. For the second test the frame is subjected to actual distributed wave loading.

Loading by a point load
For a horizontal point load figure C.2 shows the level shear force *S* divided by the total applied load. It further shows the batter take-out, i.e. the component of the level shear force taken up by the battered legs. At the sea floor the analytically calculated batter take-out is 0.64 whereas the computer calculation gives 0.63; a very good agreement indeed. In the lower part of the frame the braces therefore only need to transmit 40% or less of the applied horizontal load. It is further seen that the batter take-out increases asymptotically towards the bottom. This agrees with the analytical results for the idealised model; for a tower structure the leg force is $M(z)/b(z)$, which approaches to $F\ell/b_s$ for $z \rightarrow 0$. The difference between the analytical result and the finite element calculation in the bay immediately below the level where F is applied is due to the manner in which the load is applied in the input ($1/2\ F$ on the node in each leg) and the manner in which the computer program introduces point loads on nodes into the stiffness analysis.

The leg forces over the height of the frame are presented in figure C.3, also showing excellent agreement between the analytical and the finite element calculations. Figure C.4 compares the brace forces over the height. In the top part where there are only two legs the comparison is again very good, apart from the bay immediately below the point where the load is applied where local effects associated with the introduction of the load have an impact. Lower down where the frame has 3 and 4 legs the brace forces in one panel that are calculated by the finite element program are clearly unequal. This is due to the fact that such a panel is statically indeterminate. Proper evaluation therefore indeed requires a stiffness analysis rather than a statically determinate approximation as in the idealised model. The analytical results cannot reflect the additional complexity, but represent the *average* brace force quite successfully. The explanation for the unequal brace forces is shown in figure C.5. This figure considers the brace forces due to the combined shear deformation of a panel and the overall bending deformation of the frame as a whole.

Loading by distributed wave loading
The transfer function of the wave load for actual hydrodynamic loading is shown in figure C.6. The wave load is dominated by the forces on the 10 m diameter legs and is therefore entirely inertial, which implies that the wave force is linear. For waves with periods below about 6 seconds the wave lengths are shorter than 56 m or 5 to 6 leg diameters, so that diffraction effects have to be taken into account. This results in a substantial reduction of the total horizontal force over this part of the transfer function, as shown by figure C.6.

When the frame is subjected to actual hydrodynamic loading due to waves of several wave periods the leg and brace forces are presented in the form of transfer functions, i.e. member force divided by wave amplitude as a function of wave frequency. The results are shown in figures C.7a/b/c and C.8a/b/c. The leg force transfer functions in figures C.7a/b/c show that the analytical calculations are very good. The brace force transfer functions in figures C.8a/b/c also show very good agreement. However, these are of course subject to the same discrepancy that was noted before that the analytical calculations represent the average brace force per panel while the brace forces in the panel are in reality unequal.

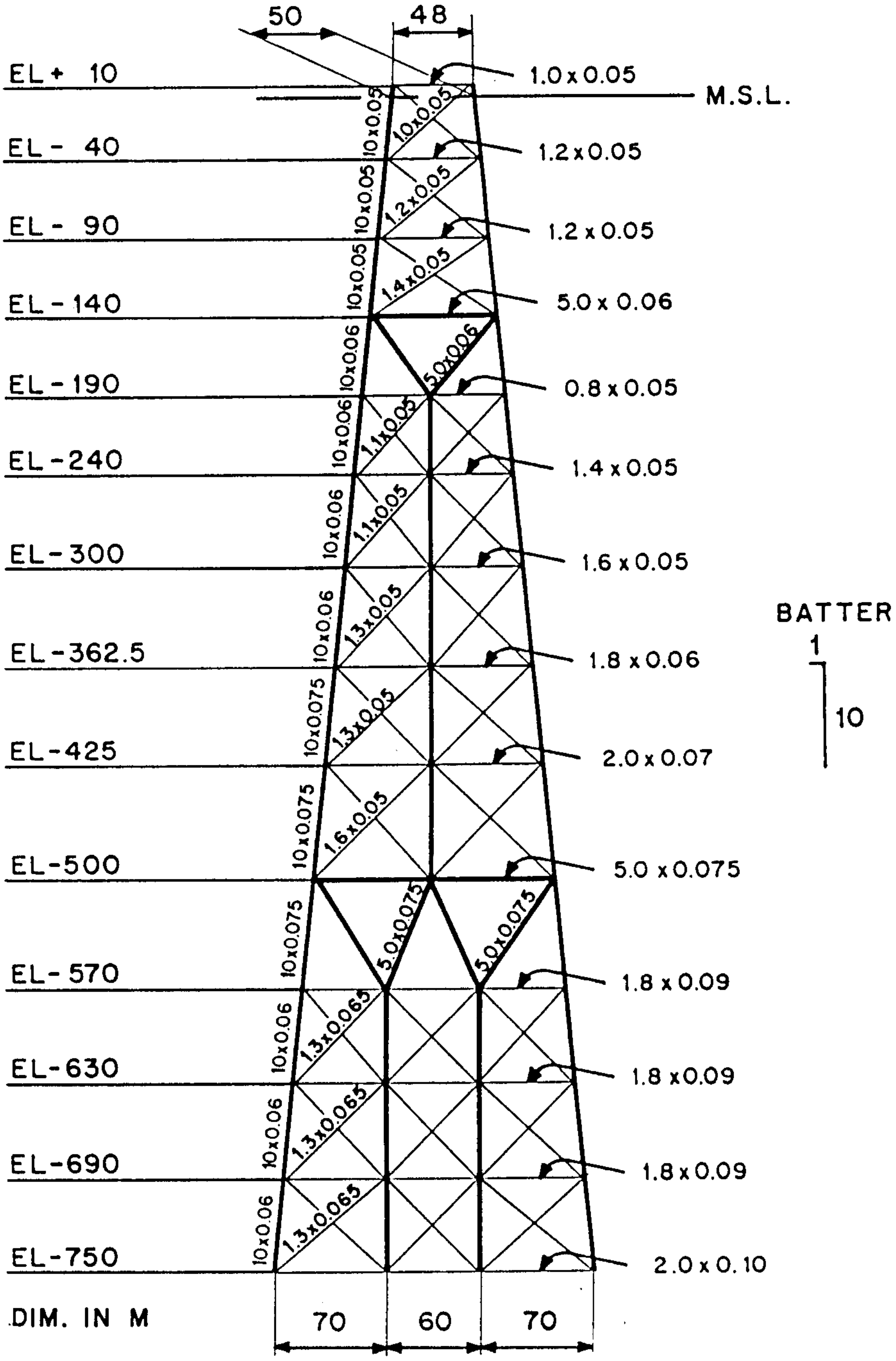

Figure C.1. A deepwater frame in 750 m water depth

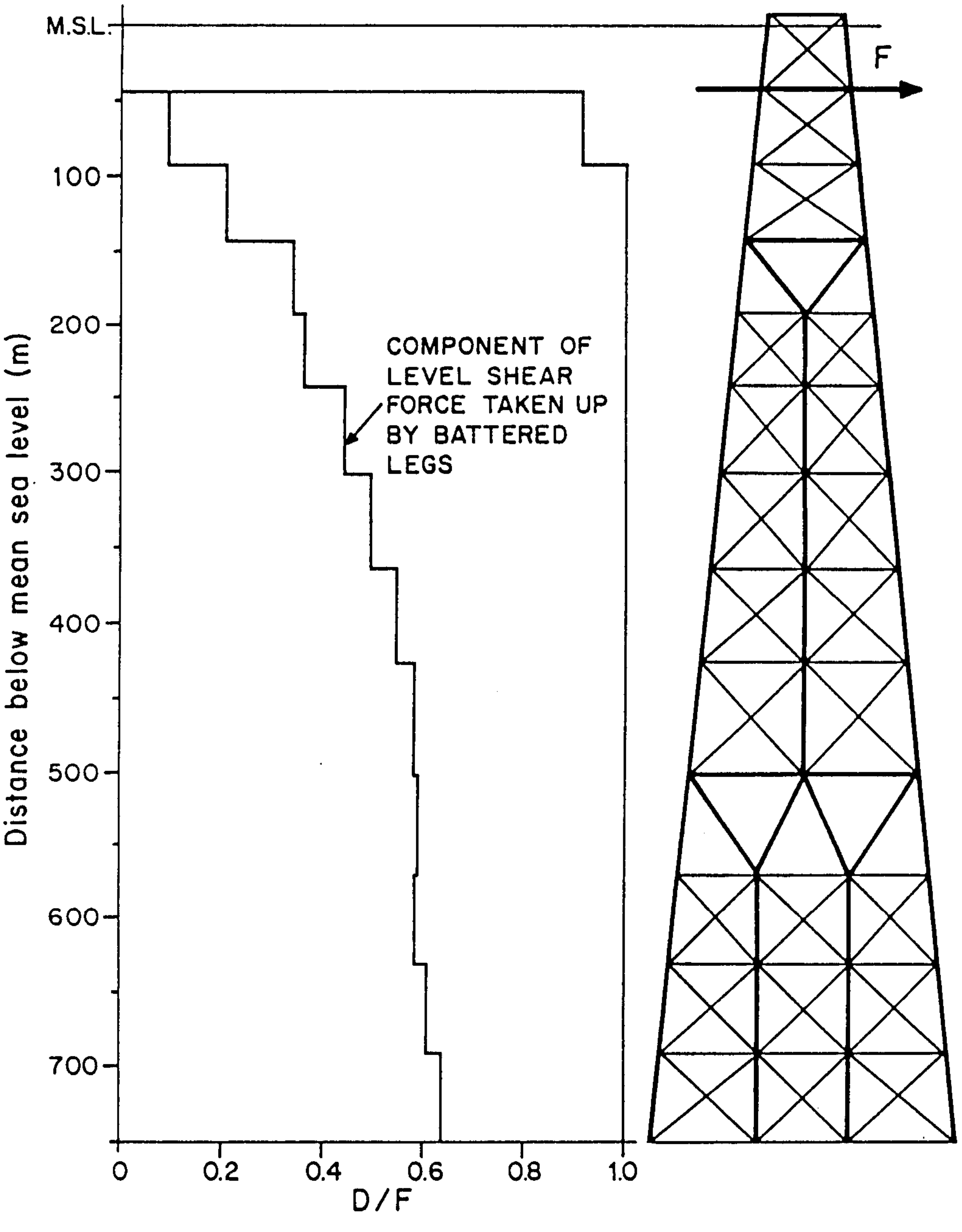

Figure C.2. Total level shear force and batter take-out over height for a horizontal point load

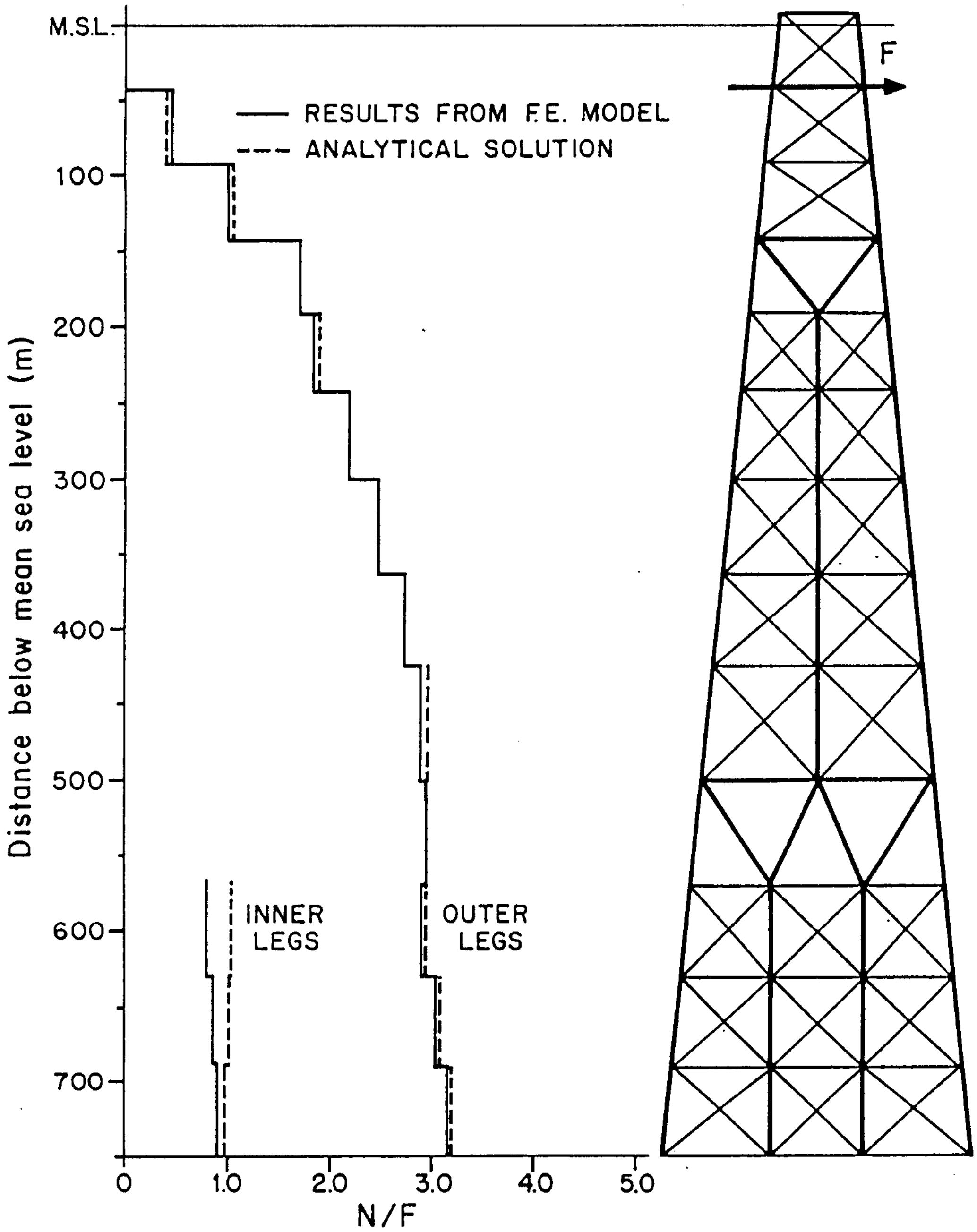

Figure C.3. Leg forces over height

Comparison of finite element model and analytical approximations for a horizontal point load

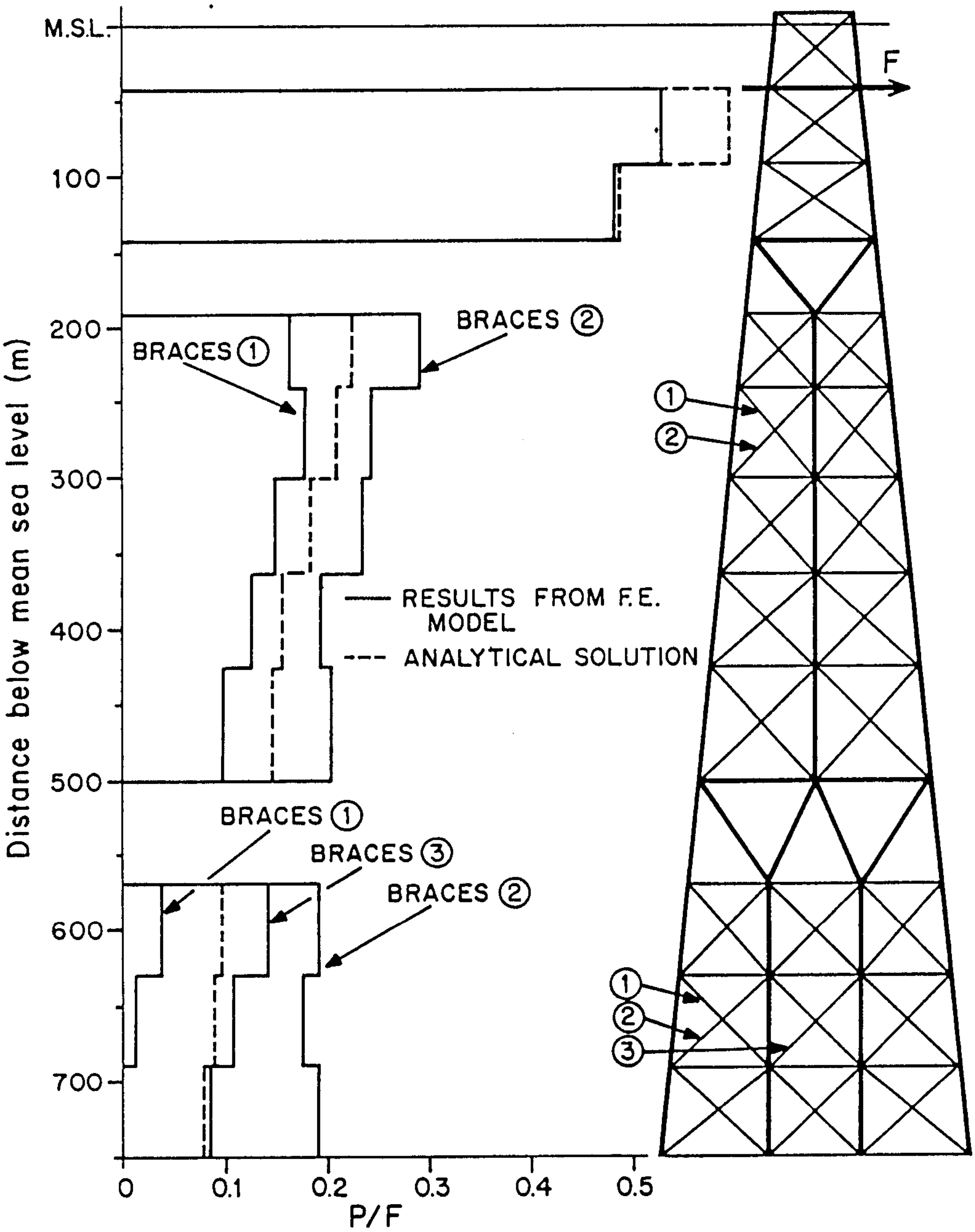

Figure C.4. Brace forces over height

Comparison of finite element model and analytical approximations for a horizontal point load

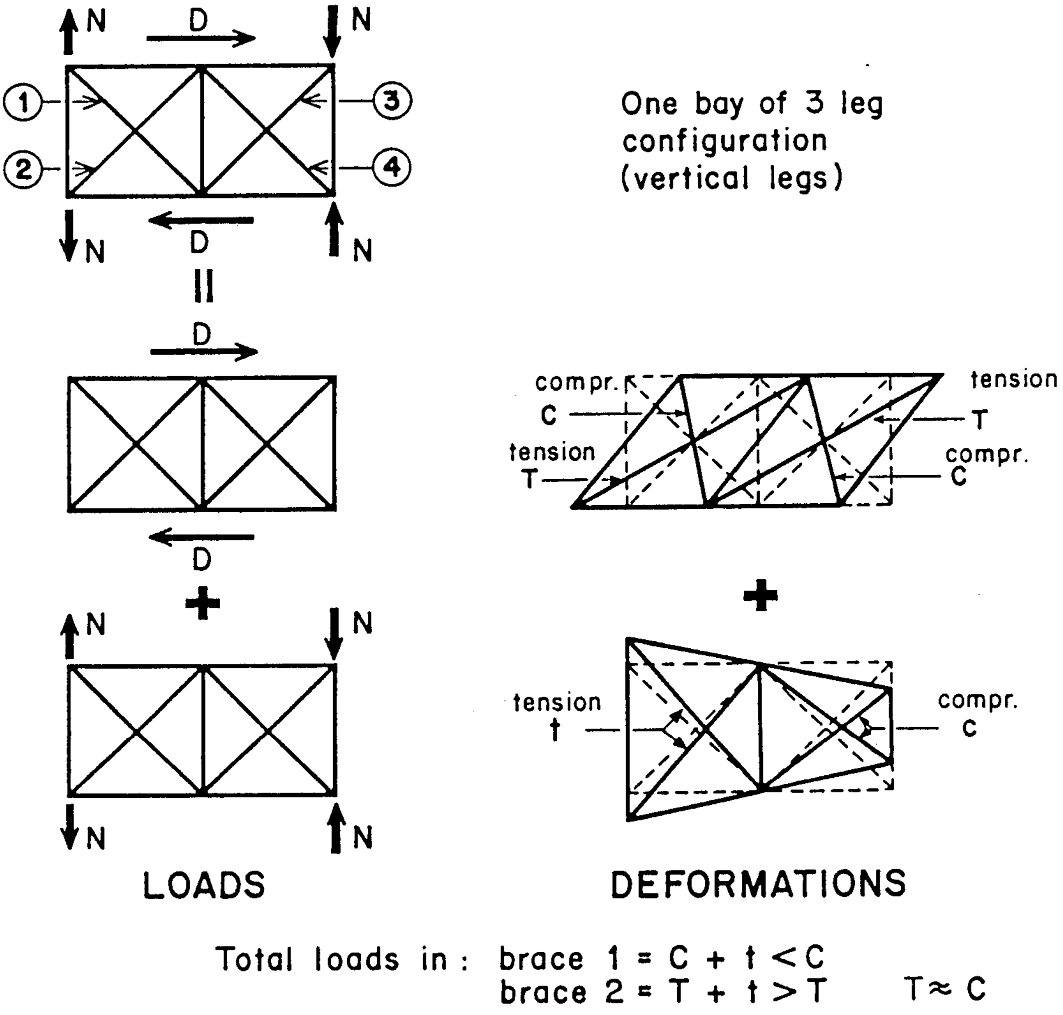

Figure C.5. Illustration of brace forces being unequal in three leg configuration

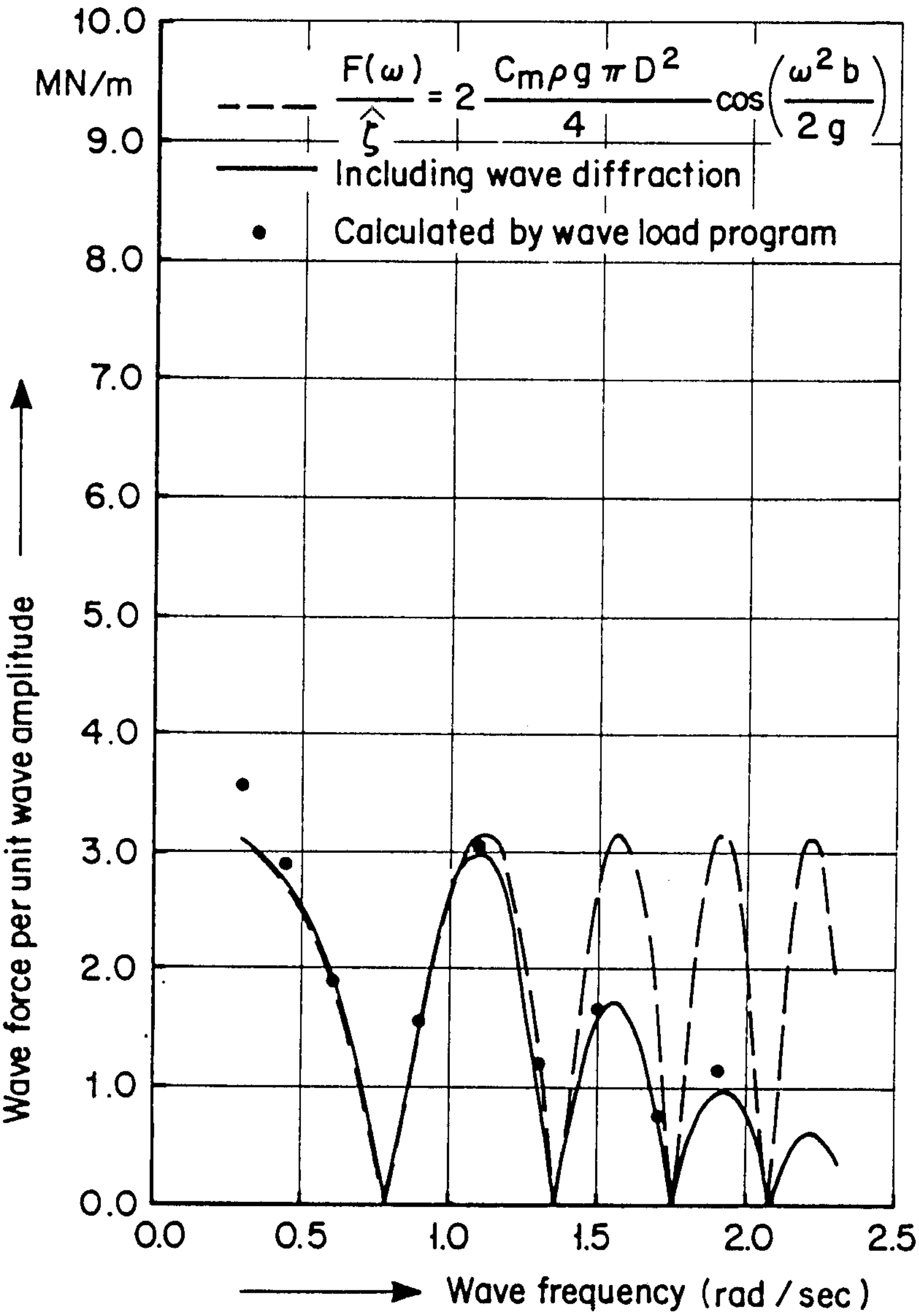

Figure C.6. Total wave force on the frame

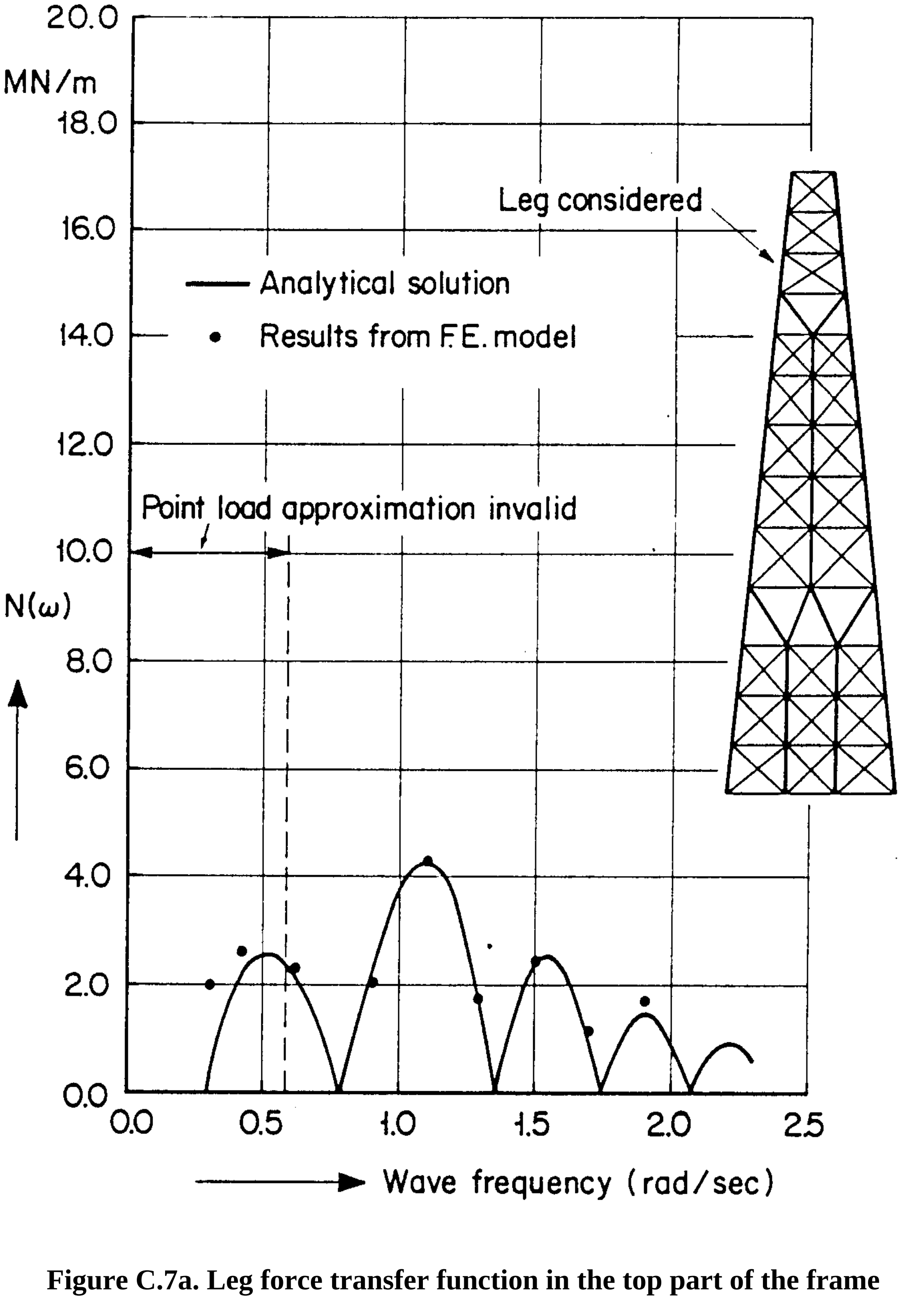

Figure C.7a. Leg force transfer function in the top part of the frame

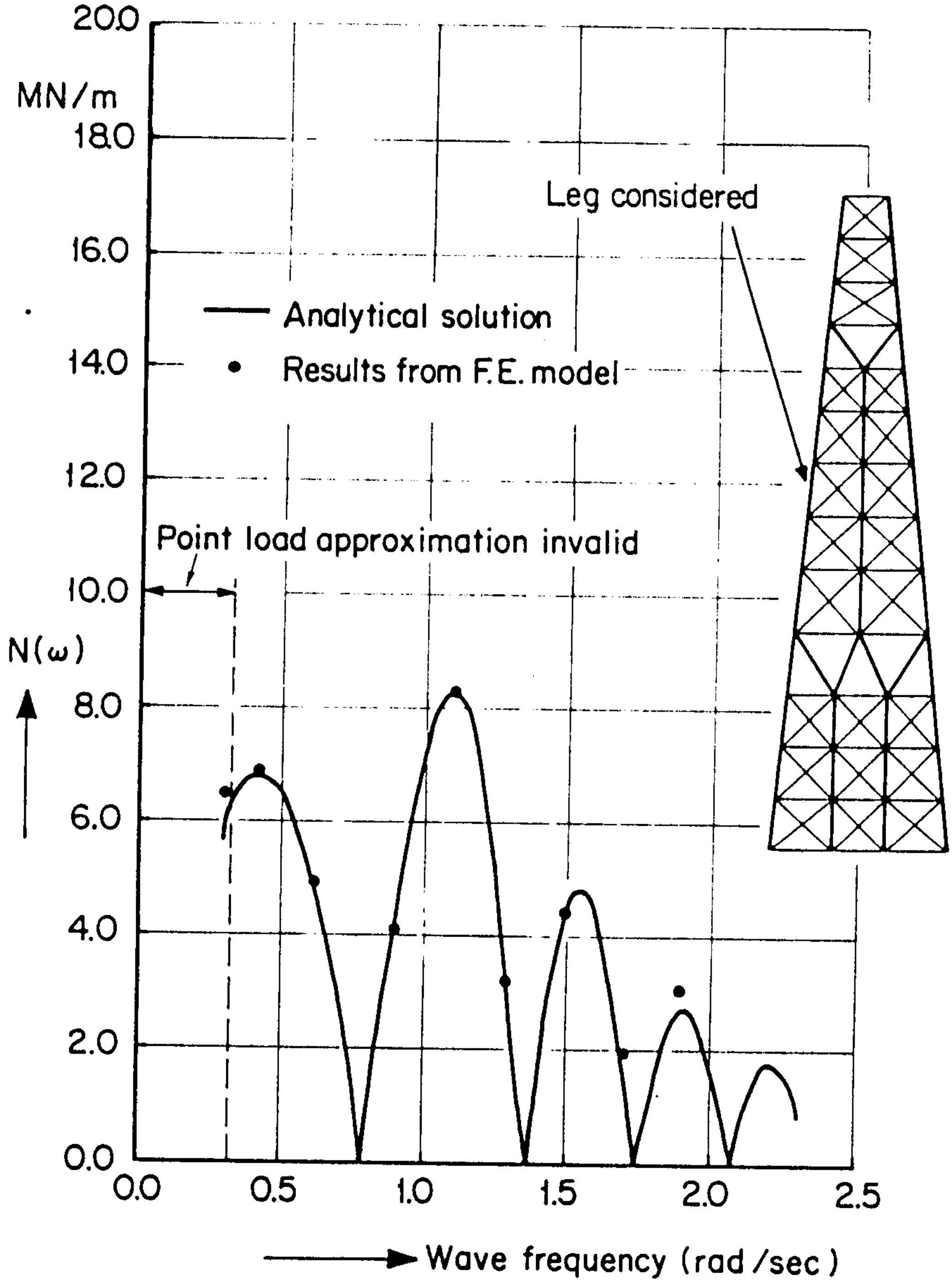

Figure C.7b. Leg force transfer function in the middle part of the frame

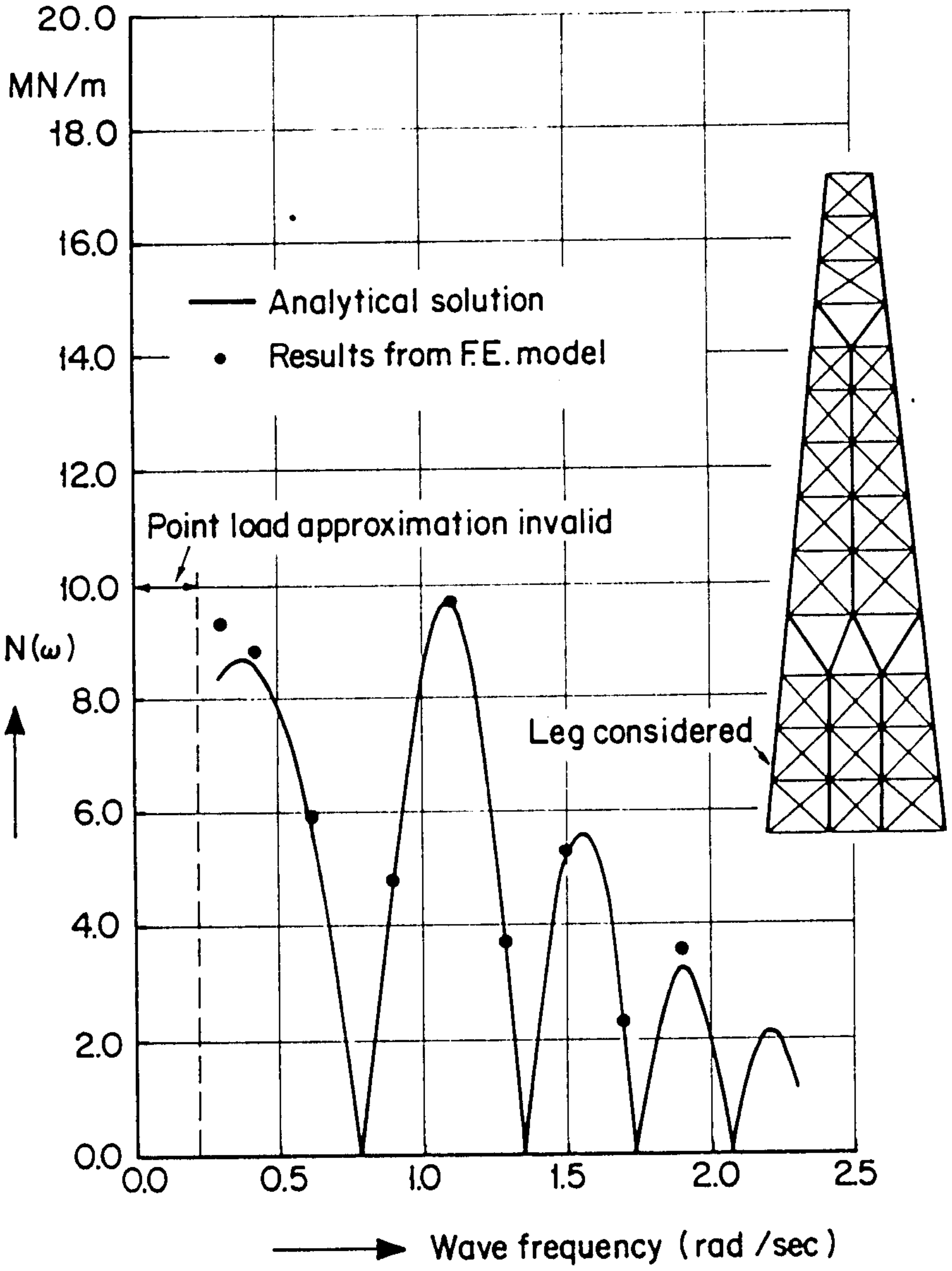

Figure C.7c. Leg force transfer function in the bottom part of the frame

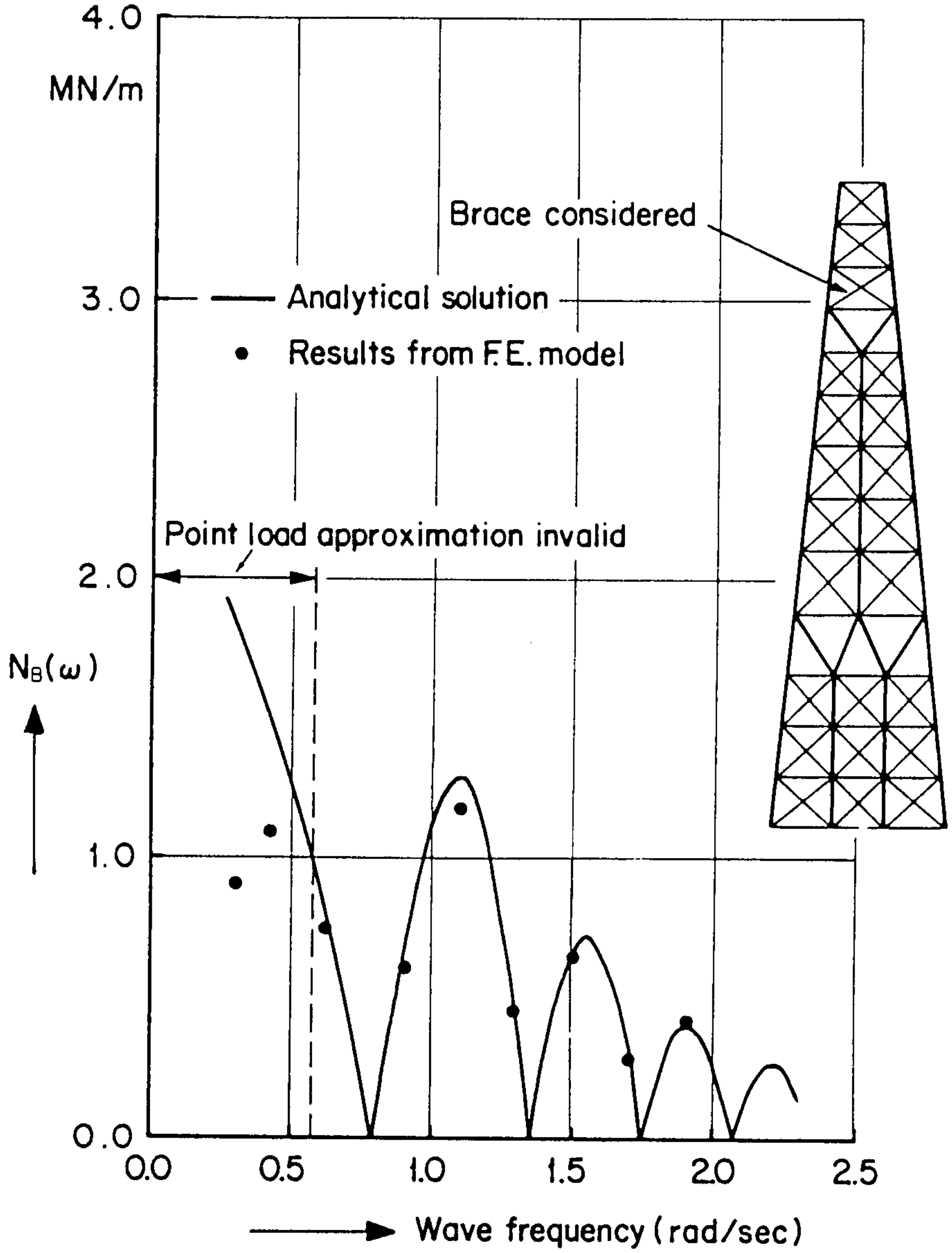

Figure C.8a. Brace force transfer function in the top part of the frame

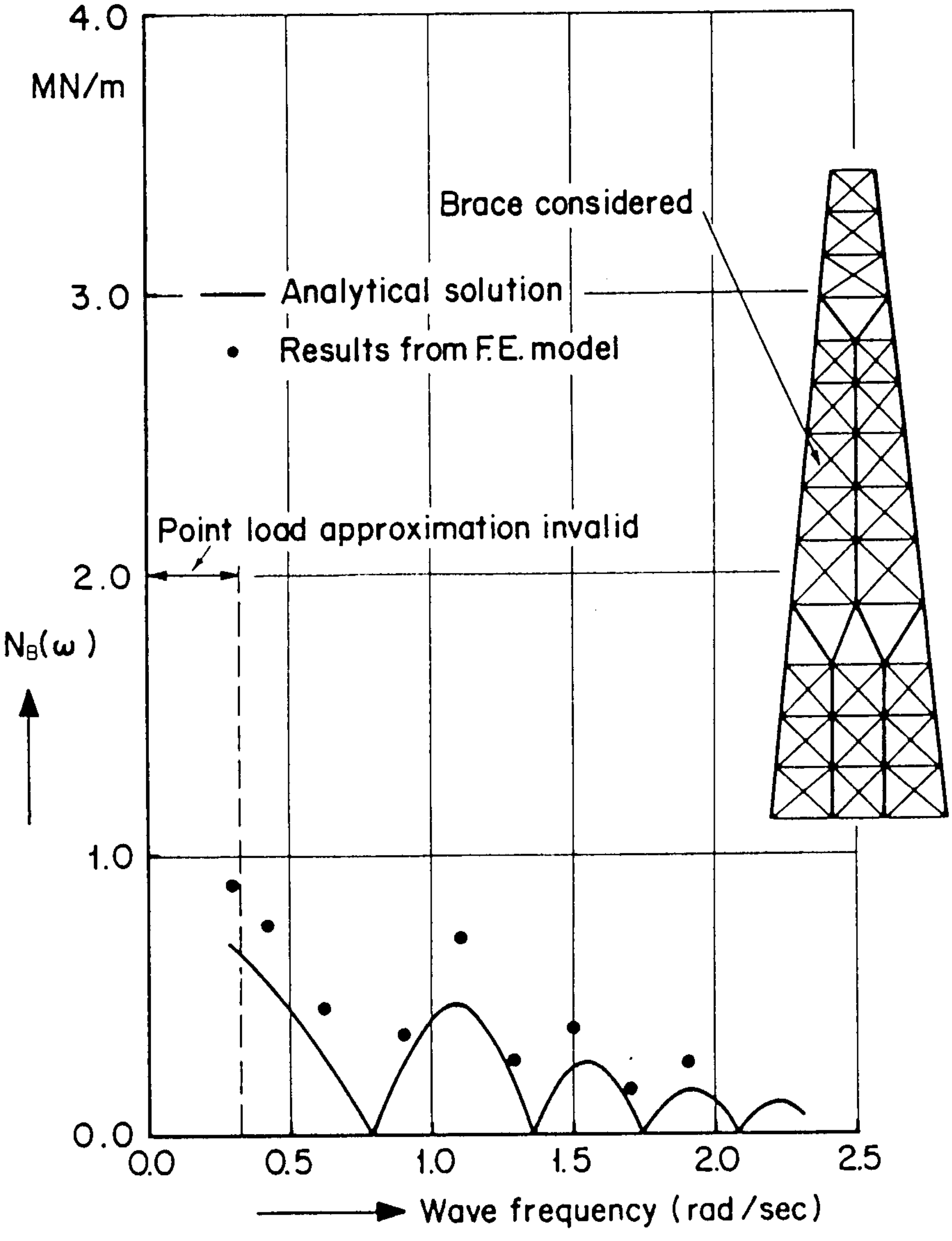

Figure C.8b. Brace force transfer function in the middle part of the frame

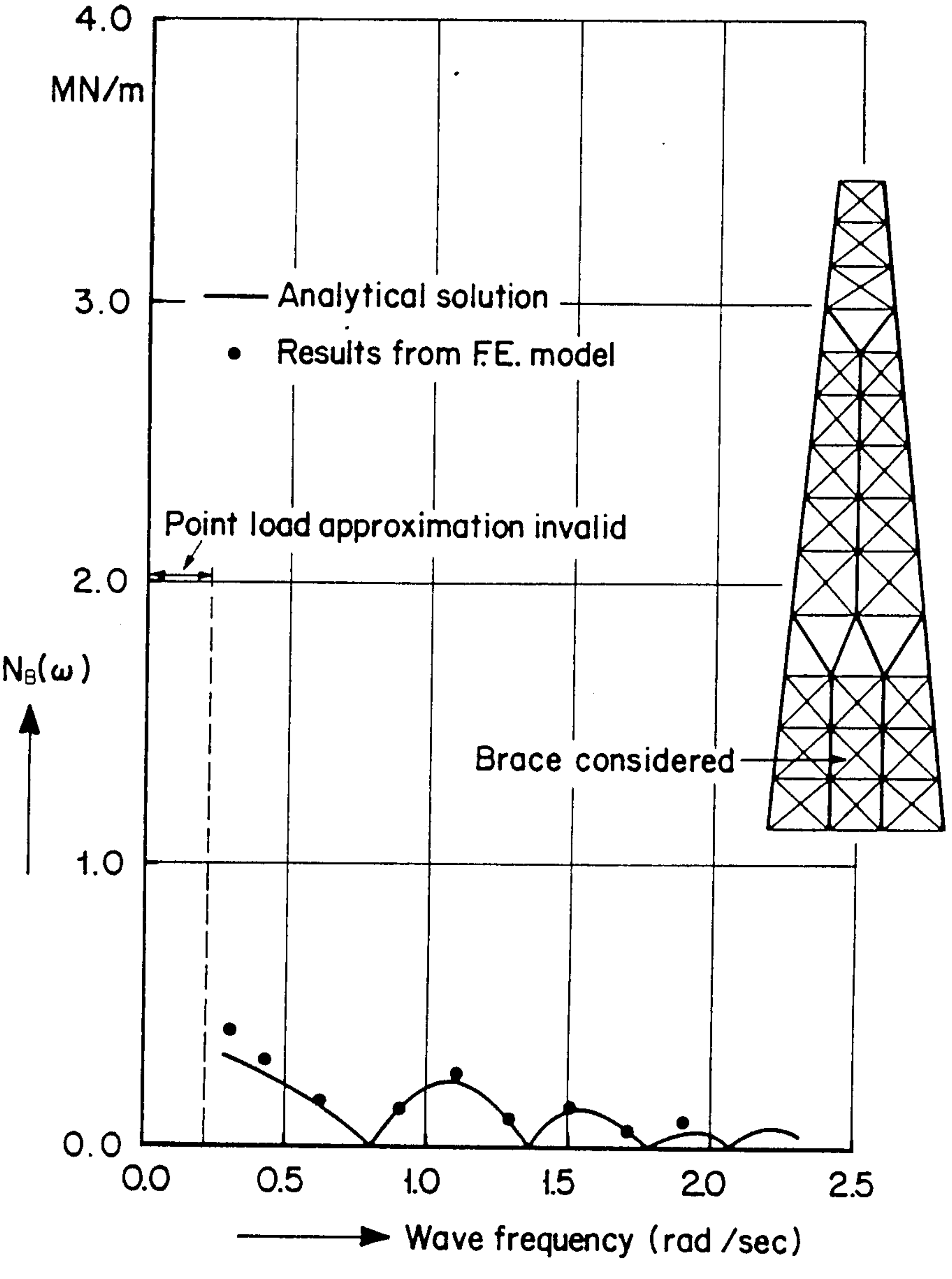

Figure C.8c. Brace force transfer function in the bottom part of the frame

Appendix A - Notations

1. Co-ordinate systems

There are four co-ordinate systems in use: a global earth fixed co-ordinate system $Oxyz$, a hydrodynamic co-ordinate system $(Oxyz)_H$, a moving co-ordinate system $(Oxyz)_F$ and a local structural co-ordinate system $O\overline{xyz}$. All four are right-handed Cartesian systems. If there is no risk of confusion the subscript or overbar may be omitted.

Global earth fixed co-ordinate system $Oxyz$
The Oxy-plane is horizontal and lies at the sea floor with Ox pointing along the longest direction of the structure (the end-on direction) and Oy along the shortest direction of the structure (the broadside direction). Oz is vertically upwards from the sea floor.

Hydrodynamic co-ordinate system $(Oxyz)_H$
The $Ox_H y_H$-plane is the undisturbed free water surface; Oz_H again points upwards. The axes are parallel with those of the global system.

Moving co-ordinate system $(Oxyz)_F$
The moving co-ordinate system is fixed to a moving floating body and translates with its constant forward speed. It will generally have its origin at the centre of gravity G of the body. $Ox_F y_F$ is horizontal with Ox_F along the longest direction of the body and pointing forward; this is also the direction of the forward speed. Oy_F points to the port side; according to the right hand rule Oz_F is then pointing upwards.

Local structural co-ordinate system $O\overline{xyz}$
Structures dealt with herein are mostly framed structures comprising components having a predominate length direction, i.e. they are assemblages of one-dimensional members (e.g. bars, beams, columns). For these members the $O\overline{x}$ axis always coincides with the longitudinal axis of the member and the plane $O\overline{yz}$ is therefore a cross section. The origin O is at the member end having the lowest global xyz co-ordinates. In nearly all cases the cross section will be symmetric with one or two axes of symmetry. The local $O\overline{y}$ axis is along the shortest and $O\overline{z}$ long the longest direction of the cross section; therefore I_{yy} will always be larger than I_{zz}. Where the two directions are equal the choice is of course irrelevant. The choice made and the positive directions selected will be clearly indicated whenever the local co-ordinate system is used. Where two-dimensional components (plates, shells) or three-dimensional components (bodies, solids) might be used the axes will be especially indicated.

2. Symbols

2.1 General notations

Symbols will be shown in italics to distinguish them from regular letters, both in equations and wherever they appear within the text; for example a is a symbol while a is a letter (in case of a one lettered word it is the definite article). A vector is underlined (e.g. $\underline{v}$) while a matrix is indicated by a bold capital (e.g. $\boldsymbol{M}$). Symbols in regular font style are scalar quantities.

Differentiation with respect to time is indicated by a dot above the symbol, e.g. $\dot{u} = {}^{du}\!/\!{}_{dt}$.
The amplitude of a harmonic function is indicated by a hat over the symbol, e.g. $F(t) = \hat{F}\sin\omega t$.

2.2 Units

Unless expressly indicated otherwise metric units and the SI system are used.

2.3 List of symbols

NOTE - Nearly all symbols used in the handbook are collected in this list(1). Only symbols that are used very locally, e.g. in connection with an external reference, are not included here.

---

(1) The current list includes symbols used up to chapter 8, inclusive. Symbols in later chapters are still to be added.

lower case

a	distance, length in general	[m]
a	half long axis of the ellipse wave orbital motion	[m]
a	offset, i.e. the distance between the intersection points of the brace centre lines with the chord centre line	[m]
a	acceleration in general	[m/s^2]
a_i	distance to a parameter at position i	[m]
a_k	coefficient of the $\cos(k\omega t)$ terms in a Fourier series expansion	[variable]
a_n	component of the water particle acceleration normal to a member	[m/s^2]
b	cross-sectional dimension perpendicular to the flow	[m]
b	half short axis of the ellipse of wave orbital motion	[m]
b	breadth in general	[m]
b_e	effective breadth of the frame between the piles at a depth d_e below the sea floor	[m]
b_f	breadth of the frame at the application point of a single resultant horizontal load F_R	[m]
b_k	coefficient of the $\sin(k\omega t)$ terms in a Fourier series expansion	[variable]
b_s	breadth of the frame at the base (the sea floor)	[m]
b_t	breadth of the frame at the top	[m]
$b(z)$	breadth of the frame at a height z above the sea floor	[m]
c	damping coefficient	[Ns/m or Nms/rad]
$c = c_i$	(intrinsic) wave celerity	[m/s]
c_{app}	apparent wave celerity with a co-existing current in an earth-fixed co-ordinate system	[m/s]
c_k	coefficient of the $\cos(k\omega t + \phi_k)$ terms in a Fourier series expansion	[variable]
d	water depth	[m]
d	brace diameter	[m]
d_e	a small fictitious distance below the sea floor; for the pile model to support the frame the internal pile moment at this 'effective depth' is zero	[m]
e	eccentricity in general; for tubular joints the distance of the intersection point of the brace centre lines to the chord centre line	[m]
e_{GS}	eccentricity of permanent and variable loads of the substructure	[m]
$f(x)$	probability density function of the variable x	[-]
f e_{GT}	eccentricity of permanent and variable loads of the superstructure	[m]
	stress due to design loads (= factored loads) (with subscripts t = axial tension, c = axial compression, b = bending stress, v = shear stress, h = hoop stress)	[N/m^2]
f	Morison hydrodynamic load per unit length	[N/m]
f_d	Morison hydrodynamic drag load per unit length	[N/m]
f_i	Morison hydrodynamic inertia load per unit length	[N/m]
f_n	undamped (cyclic) natural frequency of a one mass-spring system (or a structure in general)	[Hz]
g	gap between the braces on the chord or between the toes of the brace to chord welds	[m]
g	acceleration of gravity	[m/s^2]
h	height of the intersection point of the battered piles above the sea floor	[m]

h_t	height of top horizontal framing above the sea floor	[m]
h_W	height of application point of the wind load above top horizontal framing level	[m]
i	imaginary unit $\sqrt{-1}$	[-]
k	wave number	[m^{-1}]
k	spring stiffness	[N/m or Nm/rad]
k, n, m	counters, integer numbers (0), 1, 2, 3, ……	[-]
ℓ	distance between two (vertical) cylinders, or length of an element	[m]
ℓ	application point of F_R above the sea floor	[m]
n	number of half sine functions within buckled shape with length L; inverse of K	[-]
m	mass	[kg]
m_j	jth spectral moment	[variable]
$p(x)$	probability density function of the variable x	[-]
pdf	probability density function	[-]
$prob$	probability in general	[-]
$prob_F$	probability of failure	[-]
$prob_R$	reliability (probability of non-failure)	[-]
p-y	p-y curves(2): lateral soil resistance v. lateral pile displacement	[N/m^2 or N/m; m]
p	(factored) hydrostatic pressure	[N/m^2]
q	distributed load	[N/m]
r	radius of gyration	[m]
s	co-ordinate along an oblique axis in the horizontal plane	[m]
s	parameter in the characteristic equation for dynamic problems	[s^{-1}]
t	time	[s]
t	wall thickness	[m]
t	brace wall thickness	[m]
t-z	t-z curves(2): vertical soil frictional resistance v. vert. pile displacement	[N/m^2 or N/m; m]
t_0	time averaging interval of 1 hour for wind velocity	[s]
u	horizontal displacement of the frame at the sea floor	[m]
u_f	usage factor, utilisation ratio	[-]
u	a variable, unit in general	[variable]
u_D	demand variable	[variable]
u_S	supply variable	[variable]
$u(x,y,z;t)$	water particle velocity in waves in the x-direction	[m/s]
$u_w(x,y,z;t)$	wind gust velocity (about a certain mean) in general	[m/s]
$u_w(z;t)$	longitudinal wind gust velocity around and in the same direction as $U_w(z)$; the mean of $u_w(z;t)$ is zero	[m/s]
v	velocity in general	[m/s]
v_n	component of the water particle velocity normal to a member	[m/s]
$v(x,y,z;t)$	water particle velocity in waves in the y-direction	[m/s]
$w(x,y,z;t)$	water particle velocity in waves in the z-direction	[m/s]
w	displacement	[m]
x	displacement	[m]
x,y,z	Cartesian co-ordinates	[m]

---

(2) *p-y* and *t-z* curves may either be expressed in the form of force on the pile per unit length (N/m, the 'older' presentation) v. displacement in m, or in the form of soil pressures (N/m^2, the more recent presentation) v. displacement in m. In applying these curves users must therefore be very cautious and should carefully determine in what form the curves are provided, as well as what the requirements of a particular computer program are.

z	vertical co-ordinate	[m]

upper case

A	constant	[variable]
A	cross sectional area of a body or an element	[m^2]
A	factor in the two-parameter Pierson-Moskowitz spectrum	[$m^2(r/s)^4$]
B	constant	[variable]
B	factor in the two-parameter Pierson-Moskowitz spectrum	[$(r/s)^4$]
C	constant	[variable]
C_A	added mass coefficient	[-]
C_d	drag coefficient in Morison equation	[-]
C_m	inertia coefficient in Morison equation	[-]
D	damping force	[N]
D	demand (e.g. force, stress, displacement of a component or a structure)	[variable]
D_d	design value of the demand; design value of the internal member force	[variable]
D_{de}	equivalent diameter of an element of a vertical stick providing the same horizontal drag load as a corresponding element of a real member	[m]
D_{ie}	equivalent diameter of an element of a vertical stick providing the same horizontal inertia load as a corresponding element of a real member	[m]
D_C	characteristic value of the demand	[variable]
D_R	representative value of the demand	[variable]
D	deterministic	[-]
D	diameter	[m]
D	diameter of the chord in a tubular joint	[m]
D_{av}	average diameter ($=D_o - t = D_i + t$)	[m]
D_i	inside diameter	[m]
D_o	outside diameter	[m]
D_e	equivalent quasi-static load representing the effect of dynamic response in extreme wave conditions	[N]
$D(z)$	(wave) depth decay function	[-]
$D(\theta)$	wave directional spreading function	[-]
$D(\omega,\theta)$	wave directional spreading function	[-]
E	environmental load (in general)	[N]
E_R	representative value of environmental load (normally used in association with WSD)	[N]
E_C	characteristic value of environmental load (normally used in association with LRFD)	[N]
E	modulus of elasticity	[MPa]
EI	bending stiffness in general	[Nm^2]
EI_d	bending stiffness of the dummy member to represent a pile in the pile model	[Nm^2]
$F(x)$	distribution function of variable x (probability smaller than)	[-]
F	force, load	[N]
F_{appl}	applied load	[N]
F	characteristic strength, in stress units (with subscripts t = axial tensile strength, c = axial compressive strength, b = bending strength, v = shear strength, h = hoop strength)	[N/m^2]
F_e	Euler buckling stress	[N/m^2]
F_e'	Euler buckling stress divided by the appropriate safety factor	[N/m^2]
F_y	characteristic yield strength, in stress units	[N/m^2]
F_C	Euler buckling load	[N]
F_d	Morison drag load	[N]

F_i	Morison inertia load	[N]
F_B	total horizontal applied loading (base shear) on a frame	[N]
$F_{B\,net}$	net horizontal applied load on a frame (=F_B minus the horizontal components of the axial pile forces)	[N]
F_R	single resultant horizontal (hydrodynamic) load on a frame	[N]
F_H	horizontal component of hydrodynamic loading on the substructure (per frame)	[N]
F_V	total vertical applied loading on the frame	[N]
F_W	horizontal wind loading on the superstructure (per frame)	[N]
$F_{Wh,1,2}$	horizontal wind load at workpoint 1 or 2 (per frame)	[N]
F_{Wv}	vertical wind load component at workpoint 1 or 2 from the moment due to wind loading on the superstructure (per frame)	[N]
G	permanent load (in general)	[N]
G_R	representative value of permanent load (normally used in association with WSD)	[N]
G_C	characteristic value of permanent load (normally used in association with LRFD)	[N]
G	total permanent and variable loading of the structure (sub- and superstructure)	[N]
G_S	permanent and variable loads of the substructure	[N]
$G_{S\,1,2}$	permanent and variable loads of the substructure at workpoint 1 or 2 (for a jacket) or at the sea floor (for a tower)	[N]
G_T	permanent and variable loads of the superstructure	[N]
$G_{T\,1,2}$	permanent and variable loads of the superstructure at workpoint 1 or 2	[N]
$H(x)$	complementary distribution function of variable x (probability of exceeding)	[-]
H	wave height	[m]
H_s	significant wave height	[m]
$H_{1,2}$	horizontal force in connection between jacket leg 1,2 and pile 1,2	[N]
I	(line) moment of inertia	[m^4]
I_{Pv}	'moment of inertia' of the vertical pile forces P_v about the centre of the frame	[m^2]
$I_u(z)$	wind turbulent intensity	[-]
$\boldsymbol{K}$	stiffness matrix	[N/m, Nm/rad]
K	coefficient for the buckling length, or effective length factor, in the slenderness ratio	[-]
L	length	[m]
L	linear	[-]
L_1, L_2, L_3	exposure level	[-]
M	moment	[Nm]
M_d	overturning moment due to drag forces	[Nm]
M_i	overturning moment due to inertia forces	[Nm]
M_O	total overturning moment on a frame about the sea floor	[Nm]
M_{Oe}	effective overturning moment on a frame about the depth d_e below the sea floor	[Nm]
$M_{O\,env}$	overturning moment due to environmental loads	[Nm]
M_{OGS}	overt. mom. due to anti-symmetric part of perm. and var. substructure loading	[Nm]
M_{OGT}	overt. mom. due to anti-symmetric part of perm. and var. superstructure loading	[Nm]
M_{OH}	moment about the sea floor due to hydrodyn. loading on the substruct. (per frame)	[Nm]

M_{OW}	moment about the sea floor due to wind loading on the superstructure (per frame)	[Nm]
M_{Wt}	moment about the elevation of the workpoints due to wind loading on the superstructure (per frame)	[Nm]
$M(z)$	quasi-static level bending moment over the height of the frame	[Nm]
M	number of members in a frame	[-]
M_{min}	minimum number of members in a frame	[-]
MSL	mean sea level	[m]
N	number of nodes in a structural frame	[-]
NL	non-linear	[-]
$N_{1,2}$	leg force in leg 1 or 2	[N]
N_B	brace force	[N]
N_L	leg force	[N]
$N_{L,i}$	left leg force in i^{th} bay	[N]
$N_{R,i}$	right leg force in i^{th} bay	[N]
P	probabilistic	[-]
$P(x)$	distribution function of variable x (probability smaller than)	[-]
P	pile force at the top of the pile	[N]
P_a	axial pile force at the top of the pile	[N]
P_h	horizontal pile force at the top of the pile	[N]
P_m	moment at the top of the pile	[Nm]
P_t	transverse or lateral pile force at the top of the pile	[N]
P_v	vertical pile force at the top of the pile	[N]
Q	variable load (in general)	[N]
R	reaction force or moment	[N or Nm]
S	spring force	[N]
S	supply (resistance of a component or structure)	[variable]
S_d	design value of the supply	[variable]
S_C	characteristic value of the supply	[variable]
S_R	representative value of the supply	[variable]
$S(z)$	quasi-static level shear over the height of the frame	[N]
$S(\omega)$	wave frequency spectrum	[m^{2}s/rad]
$S(\omega,\theta)$	directional wave spectrum	[m^{2}s/rad]
SF	safety factor	[-]
T	thickness of the chord wall in a tubular joint	[m]
T	duration	[s]
T	period in general	[s]
T_i	intrinsic wave period	[s]
T_{app}	apparent wave period with a co-existing current in an earth-fixed co-ordinate system	[m/s]
T_1	average wave period based on m_0 and m_1	[s]
T_2	average wave period based on m_0 and m_2 = mean zero-crossing period	[s]
T_m	modal period of the spectrum (= T_p)	[s]
T_n	undamped natural period of a one mass-spring system (or a structure in general)	[s]
T_p	period of the peak of the spectrum	[s]
T_z	mean zero-crossing period	[s]
$V_{1,2}$	total vertical load due to permanent and variable loading plus vertical wind force at the top of leg 1,2 (for a tower) or top of pile 1,2 (for a jacket)	[N]
$V_{3,4}$	vertical force in connection between jacket leg 1,2 and pile 1,2	[N]
TD	time dependent	[-]

TI	time independent	[-]
U	a particular value of the variable u	[variable]
U_{c0}	current velocity at the still water surface	[m/s]
$U_c(z)$	current velocity as a function of distance above the sea floor	[m/s]
$U_w(x,y,z;t)$	wind velocity in general as a function of space and time	[m/s]
$U_w(z;t)$	mean wind velocity as a function of elevation and time	[m/s]
$U_w(z)$	mean wind (or steady state wind) velocity at elevation z above sea level, averaged over a particular time period (scalar quantity)	[m/s]
$U_w(10)$	mean wind velocity $U_w(z)$ at 10 m above sea level and averaged over a particular time period	[m/s]
U_{w0}	standard or reference wind velocity = sustained wind velocity, the 1 hr mean wind at $z = 10$ m above sea level	[m/s]
$U_{w,1hr}(z)$	$U_w(z)$ when averaged over 1 hour	[m/s]
$U_{w,t}(z)$	$U_w(z)$ when averaged over a period $t \leq 1$ hour	[m/s]
V	velocity in general	[m/s]
V_s	forward speed of a vessel	[m/s]
W_{Pv}	'section modulus' of the cross section over the foundation at the sea floor, in terms of the vertical pile forces	[m^1]

Vectors

$\underline{F}(t)$	vector of applied loads	[N, Nm]
$\underline{U_{wi}}(x,y,z;t)$	space and time dependent wind vector	[m/s]
$\underline{U_w}(x,y,z)$	mean wind velocity vector, constant in magnitude and direction	[m/s]
$\underline{u_w}(x,y,z;t)$	turbulent wind velocity vector around the mean; $\underline{u_w}$ varies in magnitude and direction as a function of time, the time average of $\underline{u_w}$ is by definition zero	[m/s]
$\underline{x}(t)$	vector of structural deformations	[m, rad or deg]

Greek lower case

α	exponent in the wind or current profile equation	[-]
α	numerical constant in the Pierson-Moskowitz spectrum	[-]
$\alpha_{1,2}$	slope (batter angle) of frame chord member 1 or 2	[-]
β	numerical constant in the Pierson-Moskowitz spectrum	[-]
β	ratio of brace diameter to chord diameter in a tubular joint (= d/D)	[-]
γ	ratio of chord radius to chord wall thickness in a tubular joint (= $D/2T$)	[-]
γ	ratio of brace radius to brace wall thickness in a tubular joint (= $d/2t$)	[-]
γ	peak shape parameter in the Jonswap spectrum	[-]
γ	partial factor in general	[-]
γ	overall material factor γ_S, with subscript s replaced by: t for axial tensile strength, c for axial compressive strength, b for bending strength, v for shear strength, h for hoop strength	[-]
γ_m	(true) partial material factor	[-]
γ_n	factor accounting for the importance of the type of failure and its consequences	[-]
γ_d	factor accounting for all remaining uncertainties, not accounted for by another factor	[-]
γ_D	partial factor on demand (load factor)	[-]
γ_D	partial load factor for dynamic loads D_e	[-]
γ_E	partial load factor for environmental loads	[-]
γ_G	partial load factor for permanent loads (and variable loads, if taken together)	[-]
γ_Q	partial load factor for variable loads	[-]
γ_S	partial factor on supply (resistance factor); also called overall material factor	[-]
ε	phase angle in general	[deg or rad]
ε	phase lead of the displacement of a one mass-spring system with respect to harmonic excitation	[deg or rad]
ε	spectral width parameter $0 \leq \varepsilon \leq 1$	[-]
ζ	water surface elevation	[m]
θ	angle between brace and chord in a tubular joint	[deg or rad]
θ	angle of brace with the horizontal	[deg or rad]
θ	angle of the overturning moment vector wit the positive Ox-axis; (NB: this angle is the complementary angle to the wave direction)	[deg or rad]
θ	wave direction relative to the positive $(Ox)_H$-axis	[deg or rad]
$\overline{\theta}$	mean wave direction relative to the positive $(Ox)_H$-axis	[deg or rad]
θ_c	current direction relative to the positive $(Ox)_H$ –axis	[deg or rad]
θ_s	direction of ship velocity relative to the positive x-axis	[deg or rad]
θ_w	direction of mean wind	[deg or rad]
λ	slenderness parameter (ratio) of an element	[-]
λ_E	value of the slenderness parameter at the transition of elastic buckling to yielding	[-]
$\overline{\lambda}$	relative slenderness parameter (also called non-dimensional slenderness or reduced slenderness ratio) = λ/λ_E	[-]
λ	wave length	[m]
ξ	damping ratio (non-dimensional damping coefficient)	[-]
ρ	mass density (a.o. of water)	[kg/m^3]

ρ_s	mass density of steel	[kg/m^3]
ρ_w	mass density of water	[kg/m^3]
σ	standard deviation	[variable]
σ	parameter in the Jonswap spectrum	[-]
σ_a	parameter in the Jonswap spectrum	[-]
σ_b	parameter in the Jonswap spectrum	[-]
σ	(normal) stress	[N/m^2]
σ_c	buckling stress	[N/m^2]
σ_y	yield stress	[N/m^2]
τ	ratio of brace wall thickness to chord wall thickness in a tubular joint	[-]
τ	shear stress, frictional force per unit area	[N/m^2]
	sometimes frictional force per unit length	[N/m]
φ	angle between a vertical plane through an arbitrarily inclined member and the wave direction	[deg or rad]
φ	angle of rotation at the top of the pile	[deg or rad]
φ	phase angle in general	[deg or rad]
φ	phase lag of the displacement of a one mass-spring system with respect to force harmonic excitation, or with respect to $\cos\omega_n t$ for free motions	[deg or rad]
ϕ	partial resistance factor with subscript t for axial tensile strength, c for axial compressive strength, b for bending strength, v for shear strength, h for hoop strength	[-]
ϕ_R	partial resistance factor in general (multiplication factor ≤ 1.0; inverse of γ_S)	[-]
ϕ_k	phase angle of the k^{th} component in a Fourier series expansion	[deg or rad]
ω	circular frequency in general	[rad/s]
ω_i	intrinsic wave frequency	[rad/s]
ω_{app}	apparent wave frequency with a co-existing current in an earth-fixed co-ordinate system	[rad/s]
ω_{enc}	encounter wave frequency for a ship with a forward velocity in a ship-fixed co-ordinate system	[rad/s]
ω_m	circular frequency at the mode of the spectrum	[rad/s]
ω_n	undamped (circular) natural frequency of a one mass-spring system (or a structure in general)	[rad/s]

Greek upper case

$\Phi(x,y,z;\omega,t)$	velocity potential for water waves	[m^2/s]
Ω	tuning factor, ratio of frequency of excitation to the undamped natural frequency	[-]

3. Abbreviations

API	American Petroleum Institute
DAF	Dynamic Amplification factor
FMEA	Failure Mode and Effect Analysis
FSA	Formal Safety Assessment
GBS	Gravity Base Structure
HAT	Highest Astronomical Tide
HAZOPS	HAZard and OPerability Study(-ies)
ISO	International Standards Organisation
LAT	Lowest Astronomical Tide
LRFD	Load and Resistance Factor Design
MSF	Module Support Frame
MSL	Mean Sea Level
OTC	Offshore Technology Conference
QRA	Quantitative Risk Assessment
ROV	Remotely Operated Vehicle
RP	Recommended Practice
RP	Return Period
SCF	Stress Concentration Factor
SP	Skirt Pile (a type of foundation)
SRA	Structural Reliability Assessment (or Analysis)
WSD	Working Stress Design